Lecture Notes on Introduction to Plasma Astrophysics

Matthew W. Kunz†

Department of Astrophysical Sciences, Princeton University, Peyton Hall, Princeton, NJ 08544

Princeton Plasma Physics Laboratory, PO Box 451, Princeton, NJ 08543

(compiled on 19 September 2025)

These are my lecture notes for AST521: Introduction to Plasma Astrophysics. Their creation has benefitted enormously from conservations with and lecture notes written by Steve Balbus, Telemachos Mouschovias, and Alex Schekochihin, as well as excellent texts and monographs by Braginskii (1965), Krall & Trivelpiece (1973), Hinton (1983), Helander & Sigmar (2005), and Kulsrud (2005). Note that these are a work in progress.

CONTENTS

† Email address for correspondence: mkunz@princeton.edu

PART I

Introduction to astrophysical plasmas

> We can measure the globula of matter and the spaces between them, but Space plasma itself is incomputable.
>
> Vladimir Nabokov
> *Ada, or Ardor* (1969)

I.1. What is a plasma?

Astrophysical plasmas are remarkably varied, and so it may appear difficult at first to provide a definition of just what constitutes a "plasma". Is it an ionized, conducting gas? Well, the cold, molecular phase of the interstellar medium has a degree of ionization of $\lesssim 10^{-6}$, and yet is considered a plasma. (Indeed, plenty of researchers still model this phase using ideal MHD!) Okay, so perhaps a sufficiently ionized, conducting gas (setting aside for now what is meant precisely by "sufficiently")? Well, plasmas don't necessarily have to be good conductors. Indeed, many frontier topics in plasma astrophysics involve situations in which resistivity is fundamentally important.

Clearly, any definition of a plasma must be accompanied by qualifiers, and these qualifiers are often cast in terms of dimensionless parameters that compare length and time scales. Perhaps the most important dimensionless parameter in the definition of a plasma is the *plasma parameter*,

$$\Lambda \doteq n_{\rm e} \lambda_{\rm D}^3, \tag{I.1.1}$$

where $n_{\rm e}$ is the electron number density and

$$\lambda_{\rm D} \doteq \left(\frac{T}{4\pi e^2 n_{\rm e}} \right)^{1/2} = 7.4 \left(\frac{T_{\rm eV}}{n_{\rm cm^{-3}}} \right)^{1/2} \ {\rm m} \tag{I.1.2}$$

is the Debye length, i.e., the characteristic length scale on which the Coulomb potential of an individual charged particle is exponentially attenuated ("screened") by the preferential accumulation (exclusion) of oppositely- (like-) charged particles into (from) its vicinity.[1] Thus, Λ reflects the number of electrons in a Debye sphere. Its dependence upon the temperature T suggests an alternative interpretation of Λ:

$$\Lambda = \frac{T}{4\pi e^2/\lambda_{\rm D}} \sim \frac{\text{kinetic energy}}{\text{potential energy}}. \tag{I.1.3}$$

Indeed, if the plasma is in thermodynamic equilibrium with a heat bath at temperature T, then the concentration of discrete charges follows the Boltzmann distribution,

$$n_\alpha(\boldsymbol{r}) = \overline{n_\alpha} \exp\left(-\frac{q_\alpha \Phi(\boldsymbol{r})}{T} \right), \tag{I.1.4}$$

where $\overline{n_\alpha}$ is the mean number density of species α, q_α is its electric charge, and $\Phi(\boldsymbol{r})$ is the Coulomb potential. In the limit $\Lambda \to \infty$, the distribution of charges becomes uniform, i.e., the plasma is said to be *quasi-neutral*, with equal amounts of positive and negative charge within a Debye sphere.

[1] In this course, sometimes temperature will be measured in Kelvin, and sometimes temperature will be measured in energy units (eV) after a hidden multiplication by Boltzmann's constant $k_{\rm B}$. An energy of 1 eV corresponds to a temperature of $\sim 10^4$ K (more precisely, $\simeq 1.16 \times 10^4$ K).

Debye shielding is fundamentally due to the polarization of the plasma and the associated redistribution of space charge, and is an example of how a plasma behaves as a dielectric medium. The hotter plasma, the more kinetic energy, the less bound individual electrons are to the protons. When $\Lambda \gg 1$, collective electrostatic interactions are much more important than binary particle–particle collisions, and the plasma is said to be *weakly coupled*. These are the types of plasmas that we will focus on in this course (e.g., the intracluster medium of galaxy clusters has $\Lambda \sim 10^{15}$).

Shown below is a rogue's gallery of astrophysical and space plasmas in the T–n plane, with the $\Lambda = 1$ line indicating a divide between quasi-neutral plasmas (to the left) and metals (to the right):

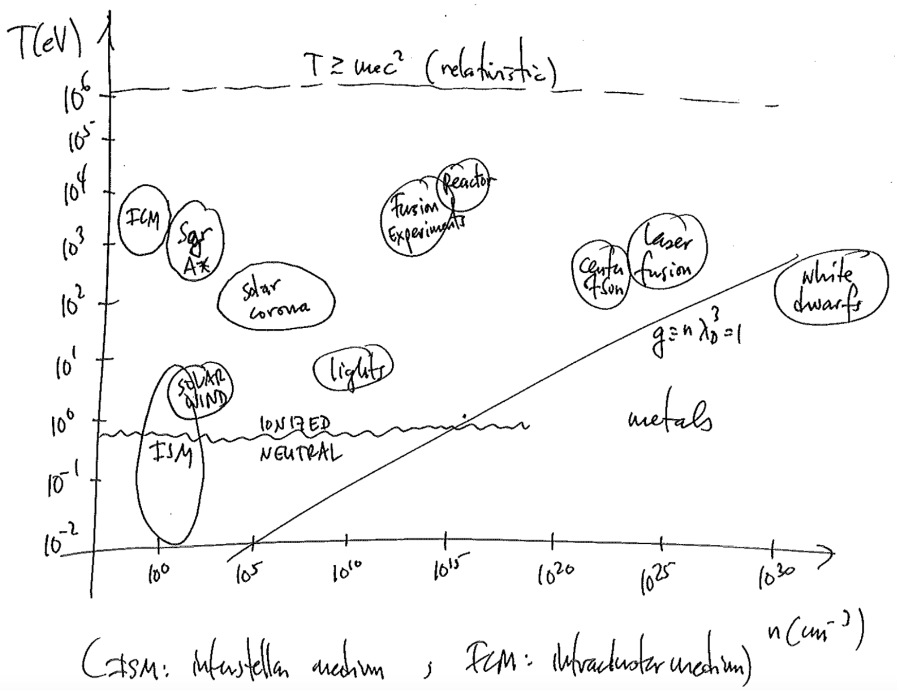

Clearly, there is a lot of parameter space here and so, to classify these plasmas further, we require additional dimensionless parameters.

I.2. Fundamental length and time scales

Another useful dividing line between different types of astrophysical and space plasmas is whether they are *collisional* or *collisionless*. In other words, is the mean free path between particle–particle collisions, $\lambda_{\rm mfp}$, larger or smaller than the macroscopic length scales of interest, L. If $\lambda_{\rm mfp} \ll L$, then the plasma is said to behave as a *fluid*, and various hydrodynamic and magnetohydrodynamic (MHD) equations can be used to describe its evolution. If, on the other hand, the mean free path is comparable to (or perhaps even larger than) the macroscopic length scales of interest, the plasma cannot be considered to be in local thermodynamic equilibrium, and the full six-dimensional phase space (3 spatial coordinates, 3 velocity coordinates) through which the constituent particles move must be retained in the description. Written in terms of the thermal speed of species α,

$$v_{{\rm th}\alpha} \doteq \left(\frac{2T_\alpha}{m_\alpha}\right)^{1/2}, \tag{I.2.1}$$

and the collision timescale τ_α, the *collisional mean free path* is

$$\lambda_{\mathrm{mfp},\alpha} \doteq v_{\mathrm{th}\alpha}\tau_\alpha. \tag{I.2.2}$$

For electron–ion collisions,

$$\tau_{\mathrm{ei}} = \frac{3\sqrt{m_\mathrm{e}}T_\mathrm{e}^{3/2}}{4\sqrt{2\pi}n_\mathrm{e}\lambda_\mathrm{e}e^4} \simeq 3.4\times10^5\left(\frac{T_\mathrm{eV}^{3/2}}{n_{\mathrm{cm}^{-3}}\lambda_\mathrm{e}}\right)\ \mathrm{s}, \tag{I.2.3}$$

where λ_e is the electron Coulomb logarithm; for ion–ion collisions,

$$\tau_{\mathrm{ii}} = \frac{3\sqrt{m_\mathrm{i}}T_\mathrm{i}^{3/2}}{4\sqrt{\pi}n_\mathrm{i}\lambda_\mathrm{i}e^4} \simeq 2.1\times10^7\left(\frac{T_\mathrm{eV}^{3/2}}{n_{\mathrm{cm}^{-3}}\lambda_\mathrm{i}}\right)\ \mathrm{s}, \tag{I.2.4}$$

where λ_i is the ion Coulomb logarithm. Note that the resulting $\lambda_{\mathrm{mfp,e}}$ and $\lambda_{\mathrm{mfp,i}}$ differ only by a factor of order unity:

$$\lambda_{\mathrm{mfp,e}} = \frac{3}{4\sqrt{\pi}}\frac{T_\mathrm{e}^2}{n_\mathrm{e}\lambda_\mathrm{e}e^4}, \quad \lambda_{\mathrm{mfp,i}} = \frac{3\sqrt{2}}{4\sqrt{\pi}}\frac{T_\mathrm{i}^2}{n_\mathrm{i}\lambda_\mathrm{i}e^4},$$

and so one often drops the species subscript on λ_{mfp}. With these definitions, it becomes clear that the plasma parameter (I.1.1) also reflects the ratio of the mean free path to the Debye length:

$$\Lambda \doteq \frac{n_\mathrm{e}\lambda_\mathrm{D}^4}{\lambda_\mathrm{D}} \sim \frac{T_\mathrm{e}^2/n_\mathrm{e}/e^4}{\lambda_\mathrm{D}} \sim \frac{\lambda_{\mathrm{mfp}}}{\lambda_\mathrm{D}}; \tag{I.2.5}$$

again, a measure of the relative importance of collective effects (λ_D) and binary collisions (λ_{mfp}).

Independent of whether a given astrophysical plasma is collisional or collisionless, nearly all such plasmas host magnetic fields, either inherited from the cosmic background in which they reside or produced *in situ* by a dynamo mechanism. There are two ways in which the strength of the magnetic field is quantified. First, the *plasma beta parameter*:

$$\beta_\alpha \doteq \frac{8\pi n_\alpha T_\alpha}{B^2}, \tag{I.2.6}$$

which reflects the relative energy densities of the thermal motions of the plasma particles and of the magnetic field. Note that

$$\beta_\alpha = \frac{2T_\alpha}{m_\alpha} \times \frac{4\pi m_\alpha n_\alpha}{B^2} = \frac{v_{\mathrm{th}\alpha}^2}{v_{\mathrm{A}\alpha}^2}, \tag{I.2.7}$$

where

$$v_{\mathrm{A}\alpha} \doteq \frac{B}{\sqrt{4\pi m_\alpha n_\alpha}} \tag{I.2.8}$$

is the *Alfvén speed* for species α.[2] Second, the *plasma magnetization*, ρ_α/L, where

$$\rho_\alpha \doteq \frac{v_{\mathrm{th}\alpha}}{\Omega_\alpha} \tag{I.2.9}$$

is the Larmor radius of species α and

$$\Omega_\alpha \equiv \frac{q_\alpha B}{m_\alpha c} \tag{I.2.10}$$

is the gyro- (or cyclotron, or Larmor) frequency. What distinguishes many astrophysical plasmas from their terrestrial laboratory counterparts is that the former can have $\beta \gg 1$

[2]Usually, a single Alfvén speed, $v_\mathrm{A} \doteq B/\sqrt{4\pi\varrho}$, is given for a plasma with mass density ϱ.

even though $\rho/L \lll 1$.[3] In other words, a magnetized astrophysical plasma need not have an energetically important magnetic field, and $\beta \gg 1$ does not preclude the magnetic field from having dynamical consequences. You've been warned.

There are two more kinetic scales worth mentioning at this point, even though they will receive relatively little notice in this course: the *plasma frequency*,

$$\omega_{\mathrm{p}\alpha} = \left(\frac{4\pi n_\alpha e^2}{m_\alpha}\right)^{1/2}, \tag{I.2.11}$$

and the *skin depth* (or *inertial length*),

$$d_\alpha \doteq \frac{c}{\omega_{\mathrm{p}\alpha}} = \left(\frac{m_\alpha c^2}{4\pi n_\alpha e^2}\right)^{1/2}. \tag{I.2.12}$$

The former is the characteristic frequency at which a plasma oscillates when one sign of charge carriers is displaced from the other sign by a small amount. Indeed, the factor $(4\pi n_\alpha e^2)$ should look familiar from the definition of the Debye length (see (I.1.2)). The latter is the characteristic scale below which the inertia of species α precludes the propagation of (certain) electromagnetic waves. For example, the ion skin depth is the scale at which the ions decouple from the electrons and any fluctuations in which the electrons are taking part (e.g., whistler waves). The following relationship between the skin depth and the Larmor radius may one day come in handy:

$$d_\alpha = \frac{v_{\mathrm{A},\alpha}}{\Omega_\alpha} = \frac{\rho_\alpha}{\beta_\alpha^{1/2}}. \tag{I.2.13}$$

I.3. Examples of astrophysical and space plasmas

	solar wind @ 1 au (earth location)	ICM @ ~100 kpc ("cooling radius")	galactic center @ 0.1 pc ("Bondi radius")	JET device (~meter)	ISM ("warm")
T	10 eV	8×10^3 eV	2×10^3 eV	10^4 eV	1 eV
n	10 cm^{-3}	5×10^{-2} cm^{-3}	100 cm^{-3}	10^{14} cm^{-3}	1 cm^{-3}
B	100 μG	1 μG	10^3 μG	3×10^4 G	5 μG

[3] The ~5 keV intracluster medium of galaxy clusters can be magnetized by a magnetic field as weak as $\sim10^{-18}$ G.

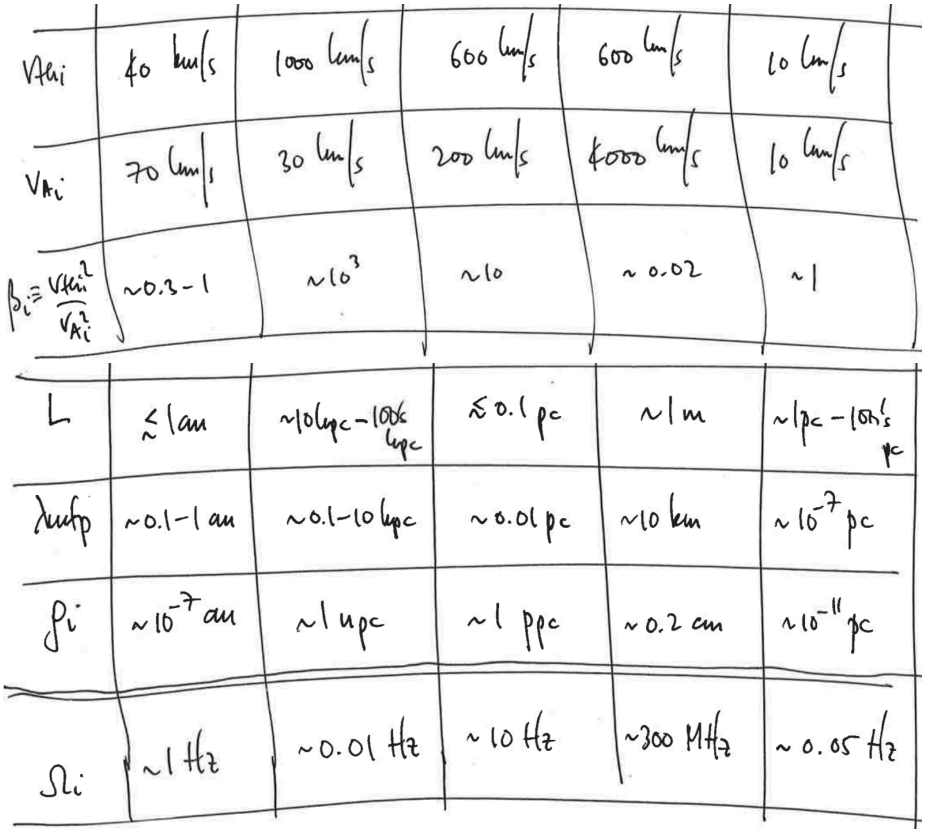

For reference, the Earth has a ∼0.5 G magnetic field.

I.4. How are plasmas measured or observed?

In class.

I.5. Debye shielding and quasi-neutrality

In § I.1, we mentioned the concept of the *Debye length* and explained its importance in the definition of a plasma. Here we derive it from first principles. This derivation starts by recalling that a large plasma parameter $\Lambda \gg 1$ implies that the kinetic energy of the plasma particles is much greater than the potential energy due to Coulomb interactions amongst binary pairs of particles. In this case, the plasma temperature T is much bigger than the Coulomb energy $e\Phi \sim e^2/\Delta r \sim e^2 n^{1/3}$, where Φ is the electrostatic potential, $\Delta r \sim n^{-1/3}$ is the typical interparticle distance, and n is the number density of the particles. Assuming a plasma in local thermodynamic equilibrium, the number density of species α' with charge $q_{\alpha'}$ sitting in the potential Φ_α of one 'central' particle of species α ought to satisfy the Boltzmann relation

$$n_{\alpha'}(\boldsymbol{r}) = \overline{n}_{\alpha'} \exp\left(-\frac{q_{\alpha'}\Phi_\alpha(\boldsymbol{r})}{T}\right) \approx \overline{n}_{\alpha'}\left(1 - \frac{q_{\alpha'}\Phi_\alpha(\boldsymbol{r})}{T}\right), \tag{I.5.1}$$

where the potential $\Phi_\alpha(\boldsymbol{r})$ depends on the distance $\boldsymbol{r}$ from the 'central' particle. To obtain the approximate equality, we have used the assumption $T \gg e\Phi_\alpha$ to Taylor expand the Boltzmann factor in its small argument. Inserting (I.5.1) into the Gauss–Poisson law for

the electric field $\boldsymbol{E} = -\boldsymbol{\nabla}\Phi_\alpha$, we have

$$\boldsymbol{\nabla}\cdot\boldsymbol{E} = -\nabla^2\Phi_\alpha = 4\pi q_\alpha\delta(\boldsymbol{r}) + 4\pi\sum_{\alpha'} q_{\alpha'}n_{\alpha'}$$
$$\approx 4\pi q_\alpha\delta(\boldsymbol{r}) + 4\pi\sum_{\alpha'} q_{\alpha'}\overline{n}_{\alpha'} - \underbrace{\left(\sum_{\alpha'}\frac{4\pi\overline{n}_{\alpha'}q_{\alpha'}^2}{T}\right)}_{\doteq\lambda_{\rm D}^{-2}}\Phi_\alpha. \tag{I.5.2}$$

The first term in (I.5.2) is the point-like charge of the 'central' particle located at $\boldsymbol{r} = \boldsymbol{0}$. The second term is the sum over all charges in the plasma, and equals zero if the plasma is overall charge-neutral (as it should be). The final term introduces the Debye length (see (I.1.2)), which is the only characteristic scale in (I.5.2). Note further that this equation has no preferred direction, and so we may exploit its spherical symmetry to recast it as follows:

$$\frac{1}{r^2}\frac{\partial}{\partial r}r^2\frac{\partial\Phi_\alpha}{\partial r} - \frac{1}{\lambda_{\rm D}^2}\Phi_\alpha = 4\pi q_\alpha\delta(\boldsymbol{r}). \tag{I.5.3}$$

The solution to this equation that asymptotes to the Coulomb potential $\Phi_\alpha \to q_\alpha/r$ as $r \to 0$ and to zero as $r \to \infty$ is

$$\boxed{\Phi_\alpha = \frac{q_\alpha}{r}\,\exp\left(-\frac{r}{\lambda_{\rm D}}\right)} \tag{I.5.4}$$

This equation states that the bare potential of the 'central' charge is exponentially attenuated ('shielded') on typical distances $\sim\lambda_{\rm D}$. This is *Debye shielding*, and the sphere of neutralizing charge accompanying the 'central' charge is referred to as the *Debye sphere* (or cloud). Debye shielding of an ion by preferential accumulation of electrons in its vicinity is sketched below:

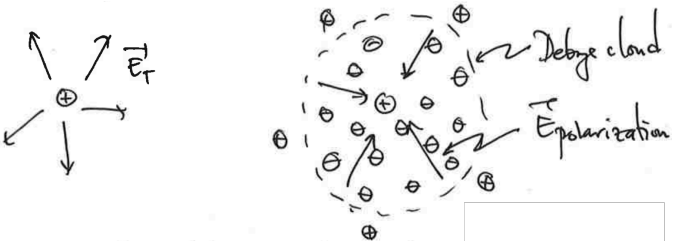

Note that the electric field due to the polarization of the plasma in response to the ion's bare Coulomb potential acts in the opposite direction to the unshielded electric field.

Now, there was nothing particularly special about the charge that we singled out as our 'central' charge. Indeed, we could have performed the above integration for any charge in the plasma. This leads us to the fundamental tenet in the statistical mechanics of a weakly coupled plasma with $\Lambda \gg 1$: every charge simultaneously hosts its own Debye sphere while being a member of another charge's Debye sphere. The key points are that, by involving a huge number of particles in the small-scale electrostatics of the plasma, these Coulomb-mediated relations (i) make the plasma 'quasi-neutral' on scales $\gg\lambda_{\rm D}$ and (ii) make collective effects in the plasma much more important than individual binary effects due to particle-particle pairings. The latter is what makes a plasma very different from a neutral gas, in which particle-particle interactions occur through hard-body collisions on scales comparable to the mean particle size.

One consequence of Debye shielding is that the electric fields that act on large scales due to the self-consistent collective interactions between $\sim\Lambda$ Debye clouds are smoothly

varying in space and time. As a result, when we write down Maxwell's equations for our quasi-neutral plasma, the fields that appear are these smooth, coarse-grained fields whose spatial structure resides far above the Debye length. Mathematically, we average the Maxwell equations over the microscopic (i.e., Debye) scales, and what remains are the collective macroscopic fields that ultimately make their way into the magnetohydrodynamics of the plasma 'fluid'.

I.6. Plasma oscillations

In the previous section, we spoke of a characteristic length scale below which particle-particle interactions are important and above which they are supplanted by collective effects between a large number of quasi-neutral Debye spheres. Is there a corresponding characteristic time scale? The answer is yes, and it may be obtained simply by dimensional analysis: take our Debye length and divide by a velocity to get time. The only velocity in our plasma thus far is the thermal speed, $v_{\mathrm{th}\alpha} = \sqrt{2T/m_\alpha}$, and so that must be it... we have obtained the *plasma frequency* of species α,

$$\omega_{\mathrm{p}\alpha} \doteq \sqrt{\frac{4\pi q_\alpha^2 n_\alpha}{m_\alpha}} \sim \frac{\lambda_{\mathrm{D}}}{v_{\mathrm{th}\alpha}}. \tag{I.6.1}$$

Of particular importance, given the smallness of the electron mass, is the electron plasma frequency ω_{pe}, which is $\sim\sqrt{m_{\mathrm{i}}/m_{\mathrm{e}}}$ larger than the ion plasma frequency and is generally the largest frequency in a weakly coupled plasma.

Fine. Dimensional analysis works. But what does this frequency actually mean? Go back to our picture of Debye shielding. That was a static picture, in that we waited long enough for the plasma to settle down into charge distributions governed by Boltzmann relations. What if we didn't wait? Surely there was some transient process whereby the particles moved around to configure themselves into these nice equilibrated Debye clouds. There was, and this transient process is referred to as a *plasma oscillation*, and it has a characteristic frequency of (you guessed it) ω_{pe}. Let's show this.

Imagine a spatially uniform, quasi-neutral plasma with well-equilibrated Debye clouds. Shift all of the electrons slightly to the right by a distance ξ, as shown in the figure below:

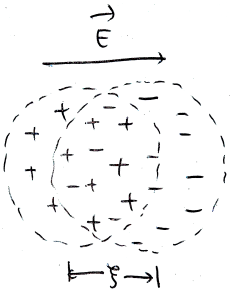

The offset between the electrons and the ions will cause an electric field pointing from the ions to the displaced electrons, given by $E = 4\pi e n_{\mathrm{e}} \xi$. The equation of motion for the electrons is then

$$m_{\mathrm{e}} \frac{\mathrm{d}^2\xi}{\mathrm{d}t^2} = -eE = -4\pi e^2 n_{\mathrm{e}} \xi = -m_{\mathrm{e}} \omega_{\mathrm{pe}}^2 \xi \quad \Longrightarrow \quad \frac{\mathrm{d}^2\xi}{\mathrm{d}t^2} = -\omega_{\mathrm{pe}}^2 \xi. \tag{I.6.2}$$

This is just the equation for a simple harmonic oscillator with frequency ω_{pe}. So, small displacements between oppositely charged species result in *plasma oscillations* (or 'Langmuir oscillations'), a collective process that occurs as the plasma attempts to

restore quasi-neutrality in response to some disturbance. Retaining the effects of electron pressure makes these oscillations propagate dispersively with a non-zero group velocity; these *Langmuir waves* have the dispersion relation $\omega^2 \approx \omega_{\rm pe}^2(1+3k^2\lambda_{\rm De}^2)$, where k is the wavenumber of the perturbation. More on that later.

I.7. Collisional relaxation and the Maxwell–Boltzmann distribution

In order for the plasma particles to move freely as plasma oscillations attempt to set up equilibrated Debye clouds, the mean free path between particle–particle collisions must be larger than the Debye length. We may estimate the former in term of the collision cross-section σ,

$$\lambda_{\rm mfp} \sim \frac{1}{n\sigma} \sim \frac{T^2}{ne^4},$$

where the cross-section $\sigma = \pi b^2$ is given by a balance between the Coulomb potential energy, $\sim e^2/b$, across some typical impact parameter b and the kinetic energy of the particles, $\sim T$. Comparing this mean free path to the Debye length (I.1.2), we find

$$\frac{\lambda_{\rm mfp}}{\lambda_{\rm D}} \sim \frac{T^2}{ne^4}\left(\frac{ne^2}{T}\right)^{1/2} \sim n\lambda_{\rm D}^3 \doteq \Lambda \gg 1.$$

Thus, a particle can travel a long distance and experience the macroscopic fields exerted by the collective electrodynamics of the plasma before being deflected by much the shorter-range, microscopic electric fields generated by another individual particle.

The scale separation between the collisional mean free path and the Debye length due to the enormity of the plasma parameter in a weakly coupled plasma says something very important about the statistical mechanics of the plasma. Because $\lambda_{\rm mfp}/\lambda_{\rm D} \sim \omega_{\rm pe}\tau_{\rm ei} \gg 1$, the particle motions are randomized and the velocity distribution of the plasma particles relaxes to a local Maxwell–Boltzmann distribution on (collisional) timescales that are much longer than the timescale on which particle correlations are established and Coulomb potentials are shielded. As a result, collisions in the plasma occur between partially equilibrated Debye clouds instead of between individual particles, the mathematical result being that the ratio $\lambda_{\rm mfp}/\lambda_{\rm D}$ is attenuated by a factor $\sim \ln\Lambda \approx$ 10–40. Thus, the logarithmic factors in the collision times (I.2.3) and (I.2.4).

Now, about this collisional relaxation. These lecture notes aren't the place to go through all the details of how collision operators are derived, but we need to establish a few facts. First, because of Debye shielding, the vast majority of scatterings that a particle experiences as it moves through a plasma are *small-angle scatterings*, with each event changing the trajectory of a particle by a small amount. These accumulate like a random walk in angle away from the original trajectory of the particle, with an average deflection angle $\langle\theta\rangle = 0$ but with a mean-square deflection angle $\langle\theta^2\rangle$ proportional to the number of scattering events. For a typical electron scattering off a sea of Debye-shielded ions of charge Ze and density n, this angle satisfies

$$\langle\theta^2\rangle \approx \frac{8\pi nLZ^2e^4}{m_{\rm e}^2v_{\rm the}^4}\ln\Lambda \tag{I.7.1}$$

after the electron has traversed a distance L. A large deflection angle, i.e. $\langle\theta^2\rangle \sim 1$, is reached once this distance

$$L \sim \frac{m_{\rm e}^2v_{\rm the}^4}{8\pi nZ^2e^4}\frac{1}{\ln\Lambda} \sim v_{\rm the}\tau_{\rm ei} \doteq \lambda_{\rm mfp,e}, \tag{I.7.2}$$

the collisional mean free path (recall the definition of the electron–ion collision time,

equation (I.2.3)). Noting that the impact parameter for a single 90-degree scattering is $\sim Ze^2/T$, we find the ratio of the cross-section for many small-angle scatterings to accumulate a 90-degree deflection, $\sigma_{\mathrm{multi},90^\circ} \sim 1/nL$ using (I.7.2), to the cross-section for a single 90-degree scattering, $\sigma_{\mathrm{single},90^\circ} = \pi b^2$ with $b \sim Ze^2/T$, is

$$\frac{\sigma_{\mathrm{multi},90^\circ}}{\sigma_{\mathrm{single},90^\circ}} \sim \ln \Lambda \gg 1. \tag{I.7.3}$$

Thus, in a weakly coupled plasma, multiple small-angle scatterings are more important than a single large-scale scattering. Visually,

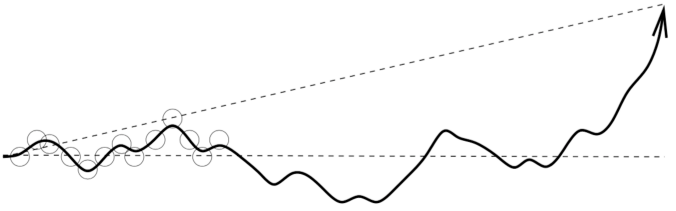

This is the physical origin of the $\ln \Lambda$ reduction in collision time mentioned in the prior paragraph.

So what do these collisions mean for treating our plasma as a fluid? If λ_{mfp} is much less than any other macroscopic scale of dynamical interest (i.e., scales on which hydrodynamics occurs), then the *velocity distribution function* $f(\boldsymbol{v})$ of the plasma – that is, the differential number of particles with velocities between $\boldsymbol{v}$ and $\boldsymbol{v} + \mathrm{d}\boldsymbol{v}$ – is well described by a Maxwell–Boltzmann distribution (often simply called a 'Maxwellian'):

$$f_{\mathrm{M}}(v) \doteq \frac{n}{\pi^{3/2} v_{\mathrm{th}}^3} \exp\left(-\frac{v^2}{v_{\mathrm{th}}^2}\right). \tag{I.7.4}$$

The factor of $\pi^{3/2} v_{\mathrm{th}}^3$ is there for normalization purposes:

$$\int \mathrm{d}^3\boldsymbol{v}\, f_{\mathrm{M}}(\boldsymbol{v}) = 4\pi \int \mathrm{d}v\, v^2 f_{\mathrm{M}}(v) = n \tag{I.7.5}$$

is the number of particles per unit volume. (Any particle distribution function should satisfy this constraint.) Note that the Maxwellian is isotropic in velocity space, depending only on the speed of the particles (rather than their vector velocity). If these particles are all co-moving with some bulk velocity $\boldsymbol{u}$, then this 'fluid' velocity is subtracted off to ensure an isotropic distribution function in that 'fluid' frame:

$$f_{\mathrm{M}}(\boldsymbol{v}) \doteq \frac{n}{\pi^{3/2} v_{\mathrm{th}}^3} \exp\left(-\frac{|\boldsymbol{v}-\boldsymbol{u}|^2}{v_{\mathrm{th}}^2}\right). \tag{I.7.6}$$

Note that the first moment of this distribution

$$\int \mathrm{d}^3\boldsymbol{v}\, \boldsymbol{v} f_{\mathrm{M}}(\boldsymbol{v}) = n\boldsymbol{u}; \tag{I.7.7}$$

and that the (mass-weighted) second moment of this distribution

$$\int \mathrm{d}^3\boldsymbol{v}\, m|\boldsymbol{v}-\boldsymbol{u}|^2 f_{\mathrm{M}}(\boldsymbol{v}) = 3p. \tag{I.7.8}$$

(Again, any velocity distribution function should satisfy these constraints.)

Different species collisionally relax to a Maxwellian at different rates (e.g., $\tau_{\mathrm{ee}} \sim \tau_{\mathrm{ei}} \sim \sqrt{m_{\mathrm{i}}/m_{\mathrm{e}}}\,\tau_{\mathrm{ii}} \sim (m_{\mathrm{i}}/m_{\mathrm{e}})\tau_{ie}$), and so each species may be described by their own

Maxwellians:

$$f_{\mathrm{M},\alpha}(\boldsymbol{v}) \doteq \frac{n_\alpha}{\pi^{3/2} v_{\mathrm{th}\alpha}^3} \exp\left(-\frac{|\boldsymbol{v}-\boldsymbol{u}_\alpha|^2}{v_{\mathrm{th}\alpha}^2}\right). \tag{I.7.9}$$

But, in the long-time limit, unless some process actively dis-equilibrates the species on a timescale comparable to or smaller than these collision times, all species will take on the *same* $\boldsymbol{u}$ and the *same* T. Their densities are, of course, the same as well, as guaranteed by quasi-neutrality (*viz.*, $\omega_{\mathrm{pe}}\tau \gg 1$ for all collision times τ).

PART II
Single-particle motion

Much of this course concerns the response of fluid elements to both imposed and self-consistently generated electromagnetic and gravitational fields. But those fluid elements are composed of charged (and neutral) particles; it would be good to know how those particles move through phase space. Now, we all know Newton's equations of motion for a particle in the presence of electric and magnetic fields:

$$\frac{\mathrm{d}\boldsymbol{r}}{\mathrm{d}t} = \boldsymbol{v}, \quad \frac{\mathrm{d}\boldsymbol{v}}{\mathrm{d}t} = \frac{q}{m}\left[\boldsymbol{E}(t,\boldsymbol{r}) + \frac{\boldsymbol{v}}{c}\times\boldsymbol{B}(t,\boldsymbol{r})\right]. \tag{II.0.10}$$

But solutions to (II.0.10) are surprisingly subtle, even in seemingly simple situations...

II.1. Particle motion in uniform electric and magnetic fields

Consider the motion of a single, charged particle. Start by decomposing the particle's position into a Larmor position $\boldsymbol{\rho}$ and a guiding-center position $\boldsymbol{R}$, *viz.*,

$$\boldsymbol{r} = \boldsymbol{\rho} + \boldsymbol{R} = -\frac{\boldsymbol{v}\times\hat{\boldsymbol{b}}}{\Omega} + \boldsymbol{R}, \tag{II.1.1}$$

where $\Omega \doteq qB/mc$ is the Larmor frequency:

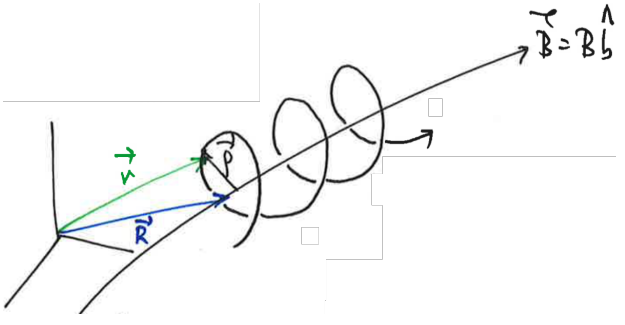

The Larmor position just oscillates around the guiding center at a rate $\dot{\vartheta} \simeq -\Omega$ (more on this later). Using this decomposition, let's begin with something relatively simple: particle motion in constant electric and magnetic fields.

Rearranging (II.1.1) and taking the time derivative,

$$\begin{aligned}\dot{\boldsymbol{R}} &= \dot{\boldsymbol{r}} - \dot{\boldsymbol{\rho}} \\ &= \boldsymbol{v} + \frac{\mathrm{d}\boldsymbol{v}}{\mathrm{d}t} \times \frac{\hat{\boldsymbol{b}}}{\Omega} \\ &= \boldsymbol{v} + \frac{q}{m}\left(\boldsymbol{E} + \frac{\boldsymbol{v}}{c} \times \boldsymbol{B}\right) \times \frac{\hat{\boldsymbol{b}}}{\Omega} \qquad \text{(using (II.0.10))} \\ &= \boldsymbol{v} + \frac{q\boldsymbol{E} \times \hat{\boldsymbol{b}}}{m\Omega} - \boldsymbol{v}_\perp \\ &= v_\parallel \hat{\boldsymbol{b}} + \frac{c\boldsymbol{E} \times \boldsymbol{B}}{B^2} \doteq v_\parallel \hat{\boldsymbol{b}} + \boldsymbol{v}_E \qquad \text{(II.1.2)} \\ &= \text{parallel streaming of the guiding center} + \text{“E cross B drift”}\end{aligned}$$

Note that the perpendicular drift is charge independent; ions and electrons drift in the same direction with the same speed. Thus, no currents are generated by this type of guiding-center drift. The physical origin of the $\boldsymbol{E} \times \boldsymbol{B}$ drift is the dependence of the gyroradius of a particle on $v_\perp$, which periodically changes due to acceleration by the perpendicular component of the electric field:

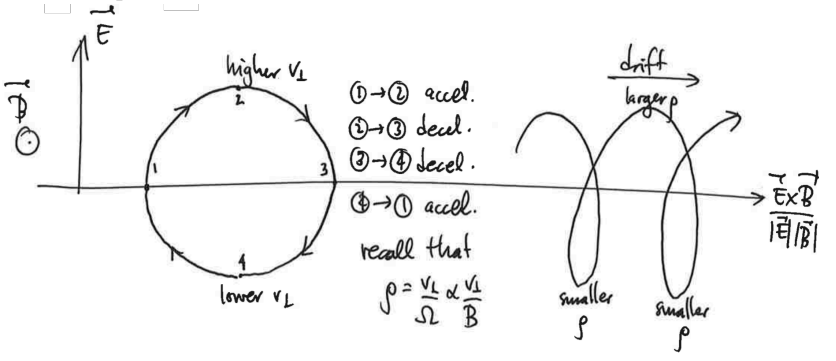

You'll see when we study ideal MHD that guiding centers $\boldsymbol{E} \times \boldsymbol{B}$ drift in order to stay on a given magnetic-field line.

For a general force $\boldsymbol{F}$, the perpendicular drift is

$$\boldsymbol{v}_F \doteq \frac{\boldsymbol{F} \times \hat{\boldsymbol{b}}}{m\Omega}, \qquad \text{(II.1.3)}$$

which is generally charge dependent and thus results in currents.

II.2. Particle motion in a non-uniform magnetic field

Next, let's keep the uniform electric field, but allow the magnetic field to vary in space. Equation (II.1.2) acquires an additional term due to gradients in the magnetic field along the particle orbit:

$$\dot{\boldsymbol{R}} = v_\parallel \hat{\boldsymbol{b}} + \boldsymbol{v}_E + \boldsymbol{v} \times \frac{\mathrm{d}}{\mathrm{d}t}\frac{\hat{\boldsymbol{b}}}{\Omega}. \qquad \text{(II.2.1)}$$

The final term in (II.2.1) includes two new drifts, which can be obtained rigorously using “guiding-center theory” (and we will, in §II.4). But they can also be obtained quite readily if you already know their names: “curvature drift” and “grad-B drift”. The former suggests

we look at the centrifugal force on a particle as it follows a curved magnetic-field line:

$$\boldsymbol{F}_{\rm c} = \frac{mv_\parallel^2}{r_{\rm c}}\hat{\boldsymbol{r}}_{\rm c}, \quad \text{where } \hat{\boldsymbol{r}}_{\rm c} = -r_{\rm c}\hat{\boldsymbol{b}}\cdot\boldsymbol{\nabla}\hat{\boldsymbol{b}} \tag{II.2.2}$$

with $r_{\rm c}$ being the radius of curvature of the field line. The unit vector $\hat{\boldsymbol{r}}_{\rm c}$ points in the direction of the curvature vector:

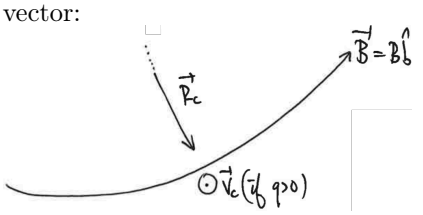

Feeding (II.2.2) into (II.1.3), we obtain the curvature drift,

$$\boldsymbol{v}_{\rm c} \doteq \frac{\boldsymbol{F}_{\rm c}\times\hat{\boldsymbol{b}}}{m\Omega} = -\frac{v_\parallel^2}{\Omega}(\hat{\boldsymbol{b}}\cdot\boldsymbol{\nabla}\hat{\boldsymbol{b}})\times\hat{\boldsymbol{b}}. \tag{II.2.3}$$

Note that it is charge dependent.

As for the "grad-B drift", imagine a magnetic dipole with moment

$$\boldsymbol{\mu} = \frac{1}{2}q\boldsymbol{r}\times\frac{\boldsymbol{v}}{c} = -\frac{1}{2}q\rho\frac{v_\perp}{c}\hat{\boldsymbol{b}} = -\frac{mv_\perp^2}{2B} \doteq -\mu\hat{\boldsymbol{b}}, \tag{II.2.4}$$

exposed to an inhomogeneous magnetic field. The force on a dipole is equal to $\boldsymbol{\nabla}(\boldsymbol{\mu}\cdot\boldsymbol{B}) = -\mu\boldsymbol{\nabla}B$, and so (using (II.1.3)), there is a drift given by

$$\boldsymbol{v}_{\nabla B} \doteq \frac{-\mu\boldsymbol{\nabla}B\times\hat{\boldsymbol{b}}}{m\Omega} = \frac{v_\perp^2}{2\Omega}\hat{\boldsymbol{b}}\times\boldsymbol{\nabla}\ln B. \tag{II.2.5}$$

This drift results from the increase (decrease) in the gyroradius of a particle as the particle enters a region of decreased (increased) magnetic-field strength:

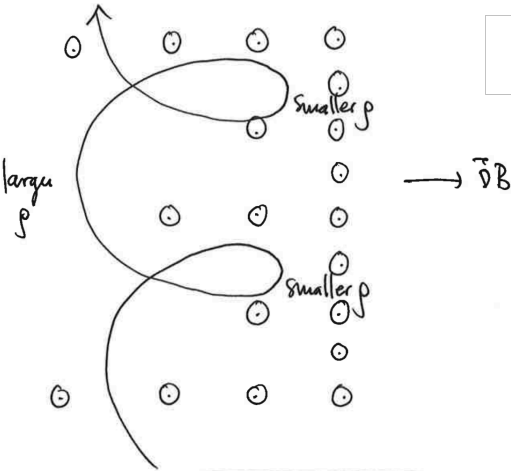

The grad-B drift is also charge dependent.

Note that, in a force-free field configuration with $\boldsymbol{\nabla}\times\boldsymbol{B} \parallel \boldsymbol{B}$, we have $\hat{\boldsymbol{b}}\cdot\boldsymbol{\nabla}\hat{\boldsymbol{b}} = \boldsymbol{\nabla}_\perp \ln B$. Thus, from (II.2.3) and (II.2.5),

$$\boldsymbol{v}_{\rm curv} + \boldsymbol{v}_{\nabla B} = \frac{v_\parallel^2 + v_\perp^2/2}{\Omega}\,\hat{\boldsymbol{b}}\times\boldsymbol{\nabla}\ln B.$$

Averaged over all particles, these drifts are $\sim v_{\rm th}(\rho/\ell_B)$, which is typically (very!) subthermal. We'll come back to this point when discussing MHD.

II.3. Particle motion in a time-dependent electric field

If $\boldsymbol{E}$ has some explicit time dependence, then there is yet another drift called "polarization drift", which can be thought of as being due to an inertial force $-m\,\mathrm{d}\boldsymbol{v}_E/\mathrm{d}t$ on the guiding center:

$$\boldsymbol{v}_{\rm pol} \doteq -\frac{\mathrm{d}\boldsymbol{v}_E}{\mathrm{d}t}\times\frac{\hat{\boldsymbol{b}}}{\Omega} = \frac{1}{\Omega}\frac{c}{B}\frac{\partial \boldsymbol{E}_\perp}{\partial t}. \tag{II.3.1}$$

If an electric field is suddenly switched on in a plasma, the ions will drift faster than the electrons (!), thus polarizing the plasma. The idea here is that, if the electric field varies as the particle navigates its gyro-orbit and does not average to zero, the result is a net shift of the guiding center in the direction of $\partial\boldsymbol{E}_\perp/\partial t$ for positive charges and in the opposite direction for negative charges. The simplest way to picture this is to consider switching on a linearly increasing perpendicular electric field at $t = 0$:

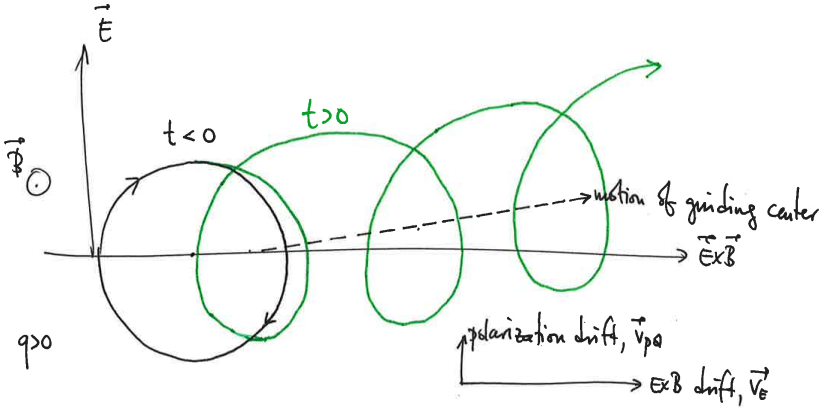

Because the ions and electrons have different signs of polarization drift, there is a current produced:

$$\boldsymbol{j}_{\rm pol} = \varrho\Big(\frac{c}{B}\Big)^2\frac{\partial\boldsymbol{E}_\perp}{\partial t}, \tag{II.3.2}$$

where $\varrho \doteq m_{\rm i}n_{\rm i} + m_{\rm e}n_{\rm e}$ is the mass density. This current is dominated by the heavier species (ions), since that species has a larger gyro-period and thus is displaced by a much larger distance by the changing electric field during each orbit. By analogy with standard electrodynamics in dielectric media, in which[4]

$$\boldsymbol{j}_{\rm pol} = \frac{\varepsilon}{4\pi}\frac{\partial\boldsymbol{E}}{\partial t},$$

we see that the effective permittivity $\varepsilon = (c/v_{\rm A})^2$, where $v_{\rm A} \doteq B/\sqrt{4\pi\varrho}$ is the Alfvén speed. (Polarization current is tied to the propagation of Alfvén waves.) Since we often have $c/v_{\rm A} \gg 1$, most plasmas have $\varepsilon \gg 1$, i.e., they behave as strongly polarizable media.

[4]Because of the standard undergraduate training in electromagnetism, you may not be familiar with dielectrics in Gaussian units. If that's true, then note the following conventions: $\boldsymbol{D} = \boldsymbol{E} + 4\pi\boldsymbol{P} \doteq \varepsilon\boldsymbol{E} \doteq (1 + 4\pi\chi_{\rm e})\boldsymbol{E}$.

II.4. Guiding-center theory

There is a systematic way of deriving drifts that are due to the non-constantly of forces along a particle's orbit, so long as these forces vary slowly. By that, we mean that the length scales (ℓ) and time scales (τ) over which the forces vary are long compared to ρ and Ω^{-1}, respectively:

$$\frac{\rho}{\ell} \ll 1, \quad (\Omega\tau)^{-1} \ll 1.$$

To enact this scale hierarchy, we introduce a small parameter,

$$\epsilon \doteq \frac{\rho}{\ell} \sim (\Omega\tau)^{-1},$$

and expand (II.0.10) in powers of ϵ. Not surprisingly, we will find a fast gyromotion and a slow guiding-center motion.

Start by writing $\boldsymbol{R} \doteq \boldsymbol{r} - \boldsymbol{\rho}$ as before, but now with the Larmor vector defined by

$$\boldsymbol{\rho} = -\frac{(\boldsymbol{v} - \boldsymbol{v}_E) \times \hat{\boldsymbol{b}}}{\Omega}. \tag{II.4.1}$$

The reason for separating out $\boldsymbol{v}_E$ from the other drifts is that the $\boldsymbol{E} \times \boldsymbol{B}$ is *not* small in ϵ. (Indeed, this is why $\boldsymbol{E} \times \boldsymbol{B}$ motion plays such a prominent role in MHD.) For ease of notation, write

$$\boldsymbol{w} \doteq \boldsymbol{v} - \boldsymbol{v}_E, \tag{II.4.2}$$

so that $\boldsymbol{\rho} = -\boldsymbol{w} \times \hat{\boldsymbol{b}}/\Omega$. Now, we know that the directions parallel ($\|$) and perpendicular ($\perp$) to the magnetic field behave differently (certainly in the $\epsilon \ll 1$ limit), so write

$$\boldsymbol{w} = v_\| \hat{\boldsymbol{b}} + \boldsymbol{w}_\perp = v_\| \hat{\boldsymbol{b}} + w_\perp \big(\hat{\boldsymbol{e}}_1 \cos\vartheta + \hat{\boldsymbol{e}}_2 \sin\vartheta\big), \tag{II.4.3}$$

where ϑ is the gyrophase:

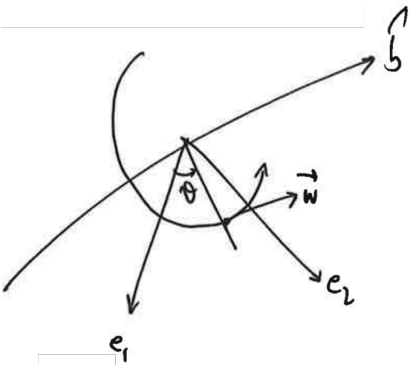

The coordinates $(\hat{\boldsymbol{e}}_1, \hat{\boldsymbol{e}}_2, \hat{\boldsymbol{b}})$ are functions of $(t, \boldsymbol{r})$ as the particle sweeps around the changing, inhomogeneous magnetic field. What follows is a gradual shift of the particle coordinates from $(\boldsymbol{r}, \boldsymbol{v})$ to $(\boldsymbol{R}, v_\|, w_\perp, \vartheta)$.

Let us first examine the motion of the guiding-center position, which follows from (II.0.10) and (II.4.1):

$$\dot{\boldsymbol{R}} = \dot{\boldsymbol{r}} - \dot{\boldsymbol{\rho}} = \underbrace{v_\| \hat{\boldsymbol{b}}}_{⓪} + \underbrace{\boldsymbol{v}_E}_{⓪} \underbrace{- \frac{\mathrm{d}\boldsymbol{v}_E}{\mathrm{d}t} \times \frac{\hat{\boldsymbol{b}}}{\Omega}}_{①} + \underbrace{\boldsymbol{w} \times \frac{\mathrm{d}}{\mathrm{d}t} \frac{\hat{\boldsymbol{b}}}{\Omega}}_{①}. \tag{II.4.4}$$

The order in ϵ of each term (relative to v_{th}) has been noted. To leading order, there is

parallel streaming and the $\boldsymbol{E}\times\boldsymbol{B}$ drift. The next-order terms are those dependent upon spatiotemporal changes in the electromagnetic fields along the particle's trajectory.

Next, the evolution of the parallel velocity:

$$\dot{v}_\parallel = \frac{\mathrm{d}}{\mathrm{d}t}(\boldsymbol{v}\cdot\hat{\boldsymbol{b}}) = \underbrace{\frac{q}{m}E_\parallel}_{\textcircled{-1}} + \underbrace{(\boldsymbol{v}_E+\boldsymbol{w})\cdot\frac{\mathrm{d}\hat{\boldsymbol{b}}}{\mathrm{d}t}}_{\textcircled{0}},$$

where the ordering is given relative to v_{th}/τ. That $\mathcal{O}(\epsilon^{-1})$ term is a problem; it says that $E_\parallel$ accelerates particles along field lines on the timescale of a Larmor gyration. Since ions and electrons are accelerated in opposite directions, this would lead to a rapid charge separation, ultimately violating our assumption of slowly varying fields. $E_\parallel$ must be $\mathcal{O}(\epsilon)$:

$$\dot{v}_\parallel = \frac{\mathrm{d}}{\mathrm{d}t}(\boldsymbol{v}\cdot\hat{\boldsymbol{b}}) = \underbrace{\frac{q}{m}E_\parallel}_{\textcircled{0}} + \underbrace{(\boldsymbol{v}_E+\boldsymbol{w})\cdot\frac{\mathrm{d}\hat{\boldsymbol{b}}}{\mathrm{d}t}}_{\textcircled{0}}. \tag{II.4.5}$$

Following similar steps, one can also show that

$$\dot{w}_\perp = -\hat{\boldsymbol{e}}_\perp\cdot\left(\underbrace{v_\parallel\frac{\mathrm{d}\hat{\boldsymbol{b}}}{\mathrm{d}t}}_{\textcircled{0}} + \underbrace{\frac{\mathrm{d}\boldsymbol{v}_E}{\mathrm{d}t}}_{\textcircled{0}}\right). \tag{II.4.6}$$

All these terms have clean physical interpretations. Parallel electric fields accelerate particles along field lines; the plane of the perpendicular drifts tilts as the particles stream along a varying $\hat{\boldsymbol{b}}$; and parallel motion can become perpendicular motion if $\hat{\boldsymbol{b}}$ changes along the orbit.

It's a bit more work to show that

$$\dot{\vartheta} = \underbrace{-\Omega}_{\textcircled{-1}} \underbrace{-\hat{\boldsymbol{e}}_2\cdot\frac{\mathrm{d}\hat{\boldsymbol{e}}_1}{\mathrm{d}t}}_{\textcircled{0}} \underbrace{-\frac{\boldsymbol{w}_\perp\times\hat{\boldsymbol{b}}}{w_\perp^2}\cdot\left(v_\parallel\frac{\mathrm{d}\hat{\boldsymbol{b}}}{\mathrm{d}t}+\frac{\mathrm{d}\boldsymbol{v}_E}{\mathrm{d}t}\right)}_{\textcircled{0}}, \tag{II.4.7}$$

and so I'll show you the steps. (It should be obvious that the dominant term is $-\Omega$, i.e., $\dot{\vartheta} = -\Omega + \mathcal{O}(\epsilon^0) + \dots$) Here are those steps:

$$\begin{aligned}\frac{\mathrm{d}\boldsymbol{w}_\perp}{\mathrm{d}t} &= \frac{\mathrm{d}w_\perp}{\mathrm{d}t}\hat{\boldsymbol{e}}_\perp + w_\perp\left(\frac{\mathrm{d}\hat{\boldsymbol{e}}_1}{\mathrm{d}t}\cos\vartheta + \frac{\mathrm{d}\hat{\boldsymbol{e}}_2}{\mathrm{d}t}\sin\vartheta\right) + \underbrace{w_\perp(-\hat{\boldsymbol{e}}_1\sin\vartheta+\hat{\boldsymbol{e}}_2\cos\vartheta)\,\dot{\vartheta}}_{=-\boldsymbol{w}_\perp\times\hat{\boldsymbol{b}}} \\ &= -\hat{\boldsymbol{e}}_\perp\hat{\boldsymbol{e}}_\perp\cdot\left(v_\parallel\frac{\mathrm{d}\hat{\boldsymbol{b}}}{\mathrm{d}t}+\frac{\mathrm{d}\boldsymbol{v}_E}{\mathrm{d}t}\right) + w_\perp\left(\frac{\mathrm{d}\hat{\boldsymbol{e}}_1}{\mathrm{d}t}\cos\vartheta+\frac{\mathrm{d}\hat{\boldsymbol{e}}_2}{\mathrm{d}t}\sin\vartheta\right) - (\boldsymbol{w}_\perp\times\hat{\boldsymbol{b}})\,\dot{\vartheta}\end{aligned}$$

$$\implies \quad -\frac{\boldsymbol{w}_\perp \times \hat{\boldsymbol{b}}}{w_\perp^2}\cdot\frac{\mathrm{d}\boldsymbol{w}_\perp}{\mathrm{d}t} = \cancelto{0}{\frac{(\boldsymbol{w}_\perp \times \hat{\boldsymbol{b}})\cdot\hat{\boldsymbol{e}}_\perp\hat{\boldsymbol{e}}_\perp}{w_\perp^2}\cdot\left(v_\parallel\frac{\mathrm{d}\hat{\boldsymbol{b}}}{\mathrm{d}t}+\frac{\mathrm{d}\boldsymbol{v}_E}{\mathrm{d}t}\right)} + \underbrace{\left(-\hat{\boldsymbol{e}}_1\cdot\frac{\mathrm{d}\hat{\boldsymbol{e}}_2}{\mathrm{d}t}\sin^2\vartheta + \hat{\boldsymbol{e}}_2\cdot\frac{\mathrm{d}\hat{\boldsymbol{e}}_1}{\mathrm{d}t}\cos^2\vartheta\right)}_{\text{since } \hat{\boldsymbol{e}}_1\cdot\mathrm{d}\hat{\boldsymbol{e}}_1/\mathrm{d}t = \hat{\boldsymbol{e}}_2\cdot\mathrm{d}\hat{\boldsymbol{e}}_2/\mathrm{d}t = 0} + \dot{\vartheta}$$

$$\begin{aligned}\implies \quad \dot{\vartheta} &= -\frac{\boldsymbol{w}_\perp \times \hat{\boldsymbol{b}}}{w_\perp^2}\cdot\frac{\mathrm{d}\boldsymbol{w}_\perp}{\mathrm{d}t} - \hat{\boldsymbol{e}}_2\cdot\frac{\mathrm{d}\hat{\boldsymbol{e}}_1}{\mathrm{d}t} \qquad (\text{since } -\hat{\boldsymbol{e}}_1\cdot\mathrm{d}\hat{\boldsymbol{e}}_2/\mathrm{d}t = \hat{\boldsymbol{e}}_2\cdot\mathrm{d}\hat{\boldsymbol{e}}_1/\mathrm{d}t)\\ &= -\Omega - \hat{\boldsymbol{e}}_2\cdot\frac{\mathrm{d}\hat{\boldsymbol{e}}_1}{\mathrm{d}t} - \frac{\boldsymbol{w}_\perp \times \hat{\boldsymbol{b}}}{w_\perp^2}\cdot\left(v_\parallel\frac{\mathrm{d}\hat{\boldsymbol{b}}}{\mathrm{d}t}+\frac{\mathrm{d}\boldsymbol{v}_E}{\mathrm{d}t}\right).\end{aligned}$$

So, we now have the evolution of $(\boldsymbol{R}, v_\parallel, w_\perp, \vartheta)$, but it's given in terms of $(\boldsymbol{r}, \boldsymbol{v})$. To proceed, we must write the latter in terms of the former.

To do that, we Taylor expand about the guiding-center position; e.g.,

$$\hat{\boldsymbol{b}}(t,\boldsymbol{r}) = \hat{\boldsymbol{b}}(t,\boldsymbol{R}) - \frac{\boldsymbol{w}_\perp \times \hat{\boldsymbol{b}}}{\Omega}\cdot\boldsymbol{\nabla}\hat{\boldsymbol{b}}(t,\boldsymbol{R}) + \ldots \tag{II.4.8}$$

Also,

$$\begin{aligned}\left.\frac{\mathrm{d}}{\mathrm{d}t}\right|_{\boldsymbol{r},\boldsymbol{v}} &= \left.\frac{\partial}{\partial t}\right|_{\boldsymbol{R},v_\parallel,w_\perp,\vartheta} + \dot{\boldsymbol{R}}\cdot\left.\frac{\partial}{\partial \boldsymbol{R}}\right|_{t,v_\parallel,w_\perp,\vartheta} + \dot{v}_\parallel\left.\frac{\partial}{\partial v_\parallel}\right|_{t,\boldsymbol{R},w_\perp,\vartheta} + \dot{w}_\perp\left.\frac{\partial}{\partial w_\perp}\right|_{t,\boldsymbol{R},v_\parallel,\vartheta}\\ &\quad + \dot{\vartheta}\left.\frac{\partial}{\partial\vartheta}\right|_{t,\boldsymbol{R},v_\parallel,w_\perp}.\end{aligned} \tag{II.4.9}$$

Henceforth, I'll be suppressing the argument $(t, \boldsymbol{R})$ on $\hat{\boldsymbol{b}}$ and $\boldsymbol{v}_E$ and the what's-held-fixed labels on the partial derivatives. Using (II.4.8) and (II.4.9), we must evaluate our $(\mathrm{d}/\mathrm{d}t)(\boldsymbol{R}, v_\parallel, w_\perp, \vartheta)$ order by order in ϵ.

At $\mathcal{O}(\epsilon^{-1})$, we have $\dot{\vartheta} = -\Omega$, i.e, Larmor gyration. At $\mathcal{O}(\epsilon^0)$, $\dot{\boldsymbol{R}} = v_\parallel\hat{\boldsymbol{b}} + \boldsymbol{v}_E$, which is the same as guiding-center motion in constant fields. Next, work on $\dot{v}_\parallel$ and $\dot{w}_\perp$. Begin by noticing that

$$\dot{\vartheta}\frac{\partial}{\partial\vartheta} = -\Omega\frac{\partial}{\partial\vartheta} + \mathcal{O}(\epsilon^0)$$

is the biggest term in $\mathrm{d}/\mathrm{d}t$ (see (II.4.9)). Thus,

$$\frac{\mathrm{d}\hat{\boldsymbol{b}}}{\mathrm{d}t} = \left(\frac{\partial}{\partial t} + v_\parallel\hat{\boldsymbol{b}}\cdot\boldsymbol{\nabla} + \boldsymbol{v}_E\cdot\boldsymbol{\nabla}\right)\hat{\boldsymbol{b}} + \Omega\frac{\partial}{\partial\vartheta}\left(\frac{\boldsymbol{w}_\perp \times \hat{\boldsymbol{b}}}{\Omega}\right)\cdot\boldsymbol{\nabla}\hat{\boldsymbol{b}} + \mathcal{O}(\epsilon), \tag{II.4.10}$$

$$\frac{\mathrm{d}\boldsymbol{v}_E}{\mathrm{d}t} = \left(\frac{\partial}{\partial t} + v_\parallel\hat{\boldsymbol{b}}\cdot\boldsymbol{\nabla} + \boldsymbol{v}_E\cdot\boldsymbol{\nabla}\right)\boldsymbol{v}_E + \underbrace{\Omega\frac{\partial}{\partial\vartheta}\left(\frac{\boldsymbol{w}_\perp \times \hat{\boldsymbol{b}}}{\Omega}\right)}_{=\boldsymbol{w}_\perp}\cdot\boldsymbol{\nabla}\boldsymbol{v}_E + \mathcal{O}(\epsilon), \tag{II.4.11}$$

where (to remind you) $\hat{\boldsymbol{b}}$ and $\boldsymbol{v}_E$ are functions of $(t, \boldsymbol{R})$. (The difference between, say, $\hat{\boldsymbol{b}}(t,\boldsymbol{r})$ and $\hat{\boldsymbol{b}}(t,\boldsymbol{R})$ can be packed into the omitted $\mathcal{O}(\epsilon)$ terms.) Using (II.4.10) and

(II.4.11) in the evolution equations (II.4.5) and (II.4.6) for $v_\parallel$ and $w_\perp$, respectively, gives

$$\frac{\mathrm{d}v_\parallel}{\mathrm{d}t} = \frac{qE_\parallel}{m} + \left(\boldsymbol{v}_E + \boldsymbol{w}\right)\cdot\left(\frac{\mathrm{D}\hat{\boldsymbol{b}}}{\mathrm{D}t} + \boldsymbol{w}_\perp\cdot\boldsymbol{\nabla}_\perp\hat{\boldsymbol{b}}\right), \tag{II.4.12}$$

$$\frac{\mathrm{d}w_\perp}{\mathrm{d}t} = -\hat{\boldsymbol{e}}_\perp\cdot\left[\left(\frac{\mathrm{D}}{\mathrm{D}t} + \boldsymbol{w}_\perp\cdot\boldsymbol{\nabla}_\perp\right)\left(v_\parallel\hat{\boldsymbol{b}} + \boldsymbol{v}_E\right)\right], \tag{II.4.13}$$

where

$$\frac{\mathrm{D}}{\mathrm{D}t} \doteq \frac{\partial}{\partial t} + \left(v_\parallel\hat{\boldsymbol{b}} + \boldsymbol{v}_E\right)\cdot\boldsymbol{\nabla} \tag{II.4.14}$$

is the Lagrangian time derivative in the parallel-streaming and $\boldsymbol{E}\times\boldsymbol{B}$-drifting frame. (Remember – partial derivatives are with respect to the $(t, \boldsymbol{R}, v_\parallel, w_\perp, \vartheta)$ coordinates.) In (II.4.12) and (II.4.13) we find a mix of terms that are independent of ϑ and dependent upon ϑ. For example, grouping such terms in (II.4.12),

$$\frac{\mathrm{d}v_\parallel}{\mathrm{d}t} = \left\{\frac{qE_\parallel}{m} + \boldsymbol{v}_E\cdot\frac{\mathrm{D}\hat{\boldsymbol{b}}}{\mathrm{D}t}\right\} + \left\{\boldsymbol{w}\cdot\left(\frac{\mathrm{D}\hat{\boldsymbol{b}}}{\mathrm{D}t} + \boldsymbol{w}_\perp\cdot\boldsymbol{\nabla}_\perp\hat{\boldsymbol{b}}\right) + \boldsymbol{w}_\perp\boldsymbol{v}_E : \boldsymbol{\nabla}_\perp\hat{\boldsymbol{b}}\right\}. \tag{II.4.15}$$

To separate the two groups, we introduce the gyro-averaging procedure

$$\left\langle \ldots \right\rangle_{\boldsymbol{R}} \doteq \frac{1}{2\pi}\oint \mathrm{d}\vartheta\,(\ldots), \tag{II.4.16}$$

where the gyrophase integral is taken at fixed $\boldsymbol{R}$. The following identities are useful:

$$\langle\boldsymbol{w}\rangle_{\boldsymbol{R}} = w_\parallel\hat{\boldsymbol{b}}, \quad \langle\boldsymbol{w}\boldsymbol{w}\rangle_{\boldsymbol{R}} = w_\parallel^2\,\hat{\boldsymbol{b}}\hat{\boldsymbol{b}} + \frac{w_\perp^2}{2}(\boldsymbol{I} - \hat{\boldsymbol{b}}\hat{\boldsymbol{b}}). \tag{II.4.17}$$

Applying the gyro-average to (II.4.15) and using these identities yields

$$\left\langle\dot{v}_\parallel\right\rangle_{\boldsymbol{R}} = \left\{\frac{qE_\parallel}{m} + \boldsymbol{v}_E\cdot\frac{\mathrm{D}\hat{\boldsymbol{b}}}{\mathrm{D}t}\right\} + \underbrace{\left\{\frac{w_\perp^2}{2}\,(\boldsymbol{I} - \hat{\boldsymbol{b}}\hat{\boldsymbol{b}}) : \boldsymbol{\nabla}_\perp\hat{\boldsymbol{b}}\right\}}_{= -\hat{\boldsymbol{b}}\cdot\boldsymbol{\nabla}\ln B}$$

$$\boxed{\left\langle\dot{v}_\parallel\right\rangle_{\boldsymbol{R}} = \frac{qE_\parallel}{m} + \boldsymbol{v}_E\cdot\frac{\mathrm{D}\hat{\boldsymbol{b}}}{\mathrm{D}t} - \frac{w_\perp^2}{2B}\,\hat{\boldsymbol{b}}\cdot\boldsymbol{\nabla}B} \tag{II.4.18}$$

So, guiding-center acceleration along field lines is driven by (1) parallel electric fields, (2) a fictitious force that accounts for boosting to the non-inertial frame of a varying $\boldsymbol{v}_E$, and (3) mirroring forces by parallel gradients in the magnetic-field strength. The interpretation of the second term is aided by noting that

$$\boldsymbol{v}_E\cdot\frac{\mathrm{D}\hat{\boldsymbol{b}}}{\mathrm{D}t} = -\frac{\mathrm{D}\boldsymbol{v}_E}{\mathrm{D}t}\cdot\hat{\boldsymbol{b}},$$

since $\boldsymbol{v}_E\cdot\hat{\boldsymbol{b}} = 0$. In the third term, you should recognize the combination $w_\perp^2/2B$.

Doing the same for $w_\perp\ldots$

$$\begin{aligned}\frac{\mathrm{d}w_\perp}{\mathrm{d}t} = &-(\hat{\boldsymbol{e}}_1\cos\vartheta + \hat{\boldsymbol{e}}_2\sin\vartheta)\cdot\left(v_\parallel\frac{\mathrm{D}\hat{\boldsymbol{b}}}{\mathrm{D}t} + \frac{\mathrm{D}\boldsymbol{v}_E}{\mathrm{D}t}\right)\\ &-(\hat{\boldsymbol{e}}_1\cos\vartheta + \hat{\boldsymbol{e}}_2\sin\vartheta)\cdot\left(v_\parallel\boldsymbol{w}_\perp\cdot\boldsymbol{\nabla}_\perp\hat{\boldsymbol{b}} + \boldsymbol{w}_\perp\cdot\boldsymbol{\nabla}_\perp\boldsymbol{v}_E\right)\end{aligned}$$

$$\begin{aligned}\implies \quad \langle \dot{w}_\perp \rangle_{\boldsymbol{R}} &= -\big(\langle \cos\vartheta \boldsymbol{w}_\perp \rangle_{\boldsymbol{R}} \cdot \boldsymbol{\nabla}_\perp v_\parallel \hat{\boldsymbol{b}}\big)\cdot \hat{\boldsymbol{e}}_1 - \big(\langle \cos\vartheta \boldsymbol{w}_\perp \rangle_{\boldsymbol{R}} \cdot \boldsymbol{\nabla}_\perp \boldsymbol{v}_E\big)\cdot \hat{\boldsymbol{e}}_1 \\ &\quad - \big(\langle \sin\vartheta \boldsymbol{w}_\perp \rangle_{\boldsymbol{R}} \cdot \boldsymbol{\nabla}_\perp v_\parallel \hat{\boldsymbol{b}}\big)\cdot \hat{\boldsymbol{e}}_2 - \big(\langle \sin\vartheta \boldsymbol{w}_\perp \rangle_{\boldsymbol{R}} \cdot \boldsymbol{\nabla}_\perp \boldsymbol{v}_E\big)\cdot \hat{\boldsymbol{e}}_2 \\ &= -\frac{w_\perp}{2}\hat{\boldsymbol{e}}_1\hat{\boldsymbol{e}}_1 : \boldsymbol{\nabla}_\perp v_\parallel \hat{\boldsymbol{b}} - \frac{w_\perp}{2}\hat{\boldsymbol{e}}_1\hat{\boldsymbol{e}}_1 : \boldsymbol{\nabla}_\perp \boldsymbol{v}_E \\ &\quad - \frac{w_\perp}{2}\hat{\boldsymbol{e}}_2\hat{\boldsymbol{e}}_2 : \boldsymbol{\nabla}_\perp v_\parallel \hat{\boldsymbol{b}} - \frac{w_\perp}{2}\hat{\boldsymbol{e}}_2\hat{\boldsymbol{e}}_2 : \boldsymbol{\nabla}_\perp \boldsymbol{v}_E \\ &= -\frac{w_\perp}{2}(\boldsymbol{I} - \hat{\boldsymbol{b}}\hat{\boldsymbol{b}}) : \boldsymbol{\nabla} v_\parallel \hat{\boldsymbol{b}} - \frac{w_\perp}{2}(\boldsymbol{I} - \hat{\boldsymbol{b}}\hat{\boldsymbol{b}}) : \boldsymbol{\nabla}\boldsymbol{v}_E\end{aligned}$$

$$\boxed{\langle \dot{w}_\perp \rangle_{\boldsymbol{R}} = \frac{v_\parallel w_\perp}{2B}\hat{\boldsymbol{b}}\cdot\boldsymbol{\nabla}B - \frac{w_\perp}{2}(\boldsymbol{I} - \hat{\boldsymbol{b}}\hat{\boldsymbol{b}}) : \boldsymbol{\nabla}\boldsymbol{v}_E} \tag{II.4.19}$$

And, in a similar manner,

$$\boxed{\langle \dot{\vartheta} \rangle_{\boldsymbol{R}} = -\Omega - \hat{\boldsymbol{e}}_2 \cdot \frac{\mathrm{D}\hat{\boldsymbol{e}}_1}{\mathrm{D}t} - \frac{v_\parallel}{2}\hat{\boldsymbol{b}}\cdot\boldsymbol{\nabla}\times\big(v_\parallel\hat{\boldsymbol{b}} + \boldsymbol{v}_E\big)} \tag{II.4.20}$$

But this one doesn't really matter – we'll only ever need the leading-order $\dot{\vartheta} = -\Omega$.

We can also go back and compute the $\mathcal{O}(\epsilon)$ terms in $\dot{\boldsymbol{R}}$ (see (II.4.4)), in order to see the appearance of inhomogeneities in the evolution of the guiding center:

$$\begin{aligned}\langle \dot{\boldsymbol{R}} \rangle_{\boldsymbol{R}} &= v_\parallel\hat{\boldsymbol{b}} + \boldsymbol{v}_E - \left\langle \frac{\mathrm{d}\boldsymbol{v}_E}{\mathrm{d}t}\times\frac{\hat{\boldsymbol{b}}}{\Omega}\right\rangle_{\boldsymbol{R}} + \left\langle \boldsymbol{w}\times\frac{\mathrm{d}}{\mathrm{d}t}\frac{\hat{\boldsymbol{b}}}{\Omega}\right\rangle_{\boldsymbol{R}} \\ &= v_\parallel\hat{\boldsymbol{b}} + \boldsymbol{v}_E - \frac{\mathrm{D}\boldsymbol{v}_E}{\mathrm{D}t}\times\frac{\hat{\boldsymbol{b}}}{\Omega} + v_\parallel\frac{\hat{\boldsymbol{b}}}{\Omega}\times\frac{\mathrm{D}\hat{\boldsymbol{b}}}{\mathrm{D}t} + \left\langle \boldsymbol{w}_\perp\times\left(\boldsymbol{w}_\perp\cdot\boldsymbol{\nabla}_\perp\frac{\hat{\boldsymbol{b}}}{\Omega}\right)\right\rangle_{\boldsymbol{R}} \\ &= v_\parallel\hat{\boldsymbol{b}} + \boldsymbol{v}_E - \frac{\mathrm{D}\boldsymbol{v}_E}{\mathrm{D}t}\times\frac{\hat{\boldsymbol{b}}}{\Omega} + v_\parallel\frac{\hat{\boldsymbol{b}}}{\Omega}\times\frac{\mathrm{D}\hat{\boldsymbol{b}}}{\mathrm{D}t} \\ &\quad + \frac{w_\perp^2}{2}\left[\hat{\boldsymbol{e}}_1\times\left(\hat{\boldsymbol{e}}_1\cdot\boldsymbol{\nabla}\frac{\hat{\boldsymbol{b}}}{\Omega}\right) + \hat{\boldsymbol{e}}_2\times\left(\hat{\boldsymbol{e}}_2\cdot\boldsymbol{\nabla}\frac{\hat{\boldsymbol{b}}}{\Omega}\right)\right]\end{aligned}$$

$$\boxed{\langle \dot{\boldsymbol{R}} \rangle_{\boldsymbol{R}} = \left[v_\parallel + \frac{w_\perp^2}{2\Omega}\hat{\boldsymbol{b}}\cdot(\boldsymbol{\nabla}\times\hat{\boldsymbol{b}})\right]\hat{\boldsymbol{b}} + \boldsymbol{v}_E + \frac{w_\perp^2}{2\Omega}\hat{\boldsymbol{b}}\times\boldsymbol{\nabla}\ln B + \frac{\hat{\boldsymbol{b}}}{\Omega}\times\left(v_\parallel\frac{\mathrm{D}\hat{\boldsymbol{b}}}{\mathrm{D}t} + \frac{\mathrm{D}\boldsymbol{v}_E}{\mathrm{D}t}\right)} \tag{II.4.21}$$

Again, every $\hat{\boldsymbol{b}}$ and $\boldsymbol{v}_E$ in these formulae are evaluated at $(t, \boldsymbol{R})$. From left to right, we have (1) parallel streaming (including an $\mathcal{O}(\epsilon)$ correction to the parallel velocity), (2) $\boldsymbol{E}\times\boldsymbol{B}$ drift, (3) grad-B drift, (4) curvature drift, and (5) polarization drift. We'll return to II.4.18, (II.4.20), and (II.4.21) when we introduce gyrokinetics.

II.5. First adiabatic invariant

The equation for $\langle \dot{w}_\perp \rangle_{\boldsymbol{R}}$, (II.4.19), implies something special. Note that

$$
\begin{aligned}
(\boldsymbol{I} - \hat{\boldsymbol{b}}\hat{\boldsymbol{b}}) : \boldsymbol{\nabla} \boldsymbol{v}_E &= \underbrace{\boldsymbol{\nabla} \cdot \left(\frac{c\boldsymbol{E} \times \hat{\boldsymbol{b}}}{B} \right)}_{\text{use Faraday's law}} - \hat{\boldsymbol{b}} \cdot \left(\hat{\boldsymbol{b}} \cdot \boldsymbol{\nabla} \frac{c\boldsymbol{E} \times \hat{\boldsymbol{b}}}{B} \right) \\
&= -\frac{\partial \ln B}{\partial t} \underbrace{- c\boldsymbol{E} \cdot \left(\boldsymbol{\nabla} \times \frac{\hat{\boldsymbol{b}}}{B} \right) - \hat{\boldsymbol{b}} \cdot \left(\hat{\boldsymbol{b}} \cdot \boldsymbol{\nabla} \frac{c\boldsymbol{E} \times \hat{\boldsymbol{b}}}{B} \right)}_{\text{user vector identities to expand}} \\
&= -\frac{\partial \ln B}{\partial t} - \frac{c\boldsymbol{E} \cdot (\boldsymbol{\nabla} \times \hat{\boldsymbol{b}})}{B} \underbrace{- \frac{c\boldsymbol{E} \cdot (\hat{\boldsymbol{b}} \times \boldsymbol{\nabla} \ln B)}{B} - \frac{c\hat{\boldsymbol{b}}\hat{\boldsymbol{b}} : \boldsymbol{\nabla}(\boldsymbol{E} \times \hat{\boldsymbol{b}})}{B}}_{\text{use vector identities to rearrange}} \\
&= -\frac{\partial \ln B}{\partial t} - \underbrace{\frac{c\boldsymbol{E} \cdot (\boldsymbol{\nabla} \times \hat{\boldsymbol{b}})}{B}}_{\substack{\text{write} \\ \boldsymbol{E} = \boldsymbol{E}_\parallel \hat{\boldsymbol{b}} + \boldsymbol{E}_\perp}} - \underbrace{\frac{c\boldsymbol{E} \times \hat{\boldsymbol{b}}}{B}}_{= \boldsymbol{v}_E} \cdot \boldsymbol{\nabla} \ln B + \frac{c\boldsymbol{E}_\perp \cdot (\boldsymbol{\nabla} \times \hat{\boldsymbol{b}})}{B} \\
&= -\frac{\partial \ln B}{\partial t} - \underbrace{\frac{cE_\parallel \hat{\boldsymbol{b}} \cdot (\boldsymbol{\nabla} \times \hat{\boldsymbol{b}})}{B}}_{\substack{\text{is } \mathcal{O}(\epsilon) \text{ relative} \\ \text{to other terms}}} - \boldsymbol{v}_E \cdot \boldsymbol{\nabla} \ln B = -\frac{\partial \ln B}{\partial t} - \boldsymbol{v}_E \cdot \boldsymbol{\nabla} \ln B + \mathcal{O}(\epsilon).
\end{aligned}
$$

And so (II.4.19) becomes

$$
\begin{aligned}
\langle \dot{w}_\perp \rangle_{\boldsymbol{R}} &= \frac{v_\parallel w_\perp}{2} \hat{\boldsymbol{b}} \cdot \boldsymbol{\nabla} \ln B - \frac{w_\perp}{2} \left(-\frac{\partial \ln B}{\partial t} - \boldsymbol{v}_E \cdot \boldsymbol{\nabla} \ln B \right) + \mathcal{O}(\epsilon) \\
&= \frac{w_\perp}{2} \left(\frac{\partial}{\partial t} + v_\parallel \hat{\boldsymbol{b}} \cdot \boldsymbol{\nabla} + \boldsymbol{v}_E \cdot \boldsymbol{\nabla} \right) \ln B + \mathcal{O}(\epsilon) \\
&= \frac{w_\perp}{2} \frac{\mathrm{D} \ln B}{\mathrm{D}t} + \mathcal{O}(\epsilon),
\end{aligned}
$$

which implies

$$
\boxed{\langle \dot{\mu} \rangle_{\boldsymbol{R}} = \mathcal{O}(\epsilon)} \tag{II.5.1}
$$

where $\mu \doteq m w_\perp^2 / 2B(t, \boldsymbol{R})$. In words, the magnetic moment μ is constant on the time and length scales of the field variation. Its constancy is telling us that, on these time and length scales, ϑ is an ignorable coordinate. (This property forms the basis of gyrokinetics.) More fundamentally, μ conservation is telling us that plasmas are "diamagnetic", that is, all particle-generated fluxes add to reduce the ambient field. The total change in B is proportional to the change in the perpendicular kinetic energy of the particle. The greater the plasma thermal energy, the more it excludes the magnetic field.

For a fluid element containing an ensemble of magnetized particles, μ conservation implies that the thermal pressure perpendicular to the local magnetic field of that fluid element $p_\perp \doteq \langle m w_\perp^2 / 2 \rangle \propto nB$, where the angle brackets $\langle \cdot \rangle$ denote the ensemble average. We'll revisit this important point in §§II.9 and XIV.

II.6. Adiabatic invariance

μ is one of several adiabatic invariants, which are related to the exactly conserved Poincaré invariants of classical mechanics. Adiabatic invariance is one of the most important concepts in the plasma physics of weakly collisional plasmas. The invariants emerge from the periodic motion induced by the magnetic field, and derive from the Hamiltonian action $\oint \wp \cdot \mathrm{d}\boldsymbol{q}$ around a loop representing nearly periodic motion. μ is the "first adiabatic invariant" of plasma physics; the corresponding periodic motion is obviously the gyromotion of a particle about a magnetic field. The canonical momentum $\wp$ in this case is the particle' angular momentum, $mv_\perp\rho$; the angular variable ϑ is the q, the conjugate coordinate. If the particle's orbit changes slowly, either because $\partial_t \ln B \ll \Omega$ or because the particle is drifting slowly into a region of varying field strength and/or geometry, then the action changes very little.[5] You might see a "simple" derivation of μ conservation in some textbooks, rather different from the guiding-center-theory approach we've taken above. It runs something like this:

$$\begin{aligned}(\Delta\mu \text{ in one orbit}) &= \frac{\Delta(mw_\perp^2/2)}{B} - \mu\frac{\Delta B}{B} = \frac{1}{B}\int_0^{2\pi/\Omega} \mathrm{d}t\,\frac{\mathrm{d}}{\mathrm{d}t}\left(\frac{1}{2}mw_\perp^2\right) - \mu\frac{\Delta B}{B}\\ &= \frac{1}{B}\int_0^{2\pi/\Omega} \mathrm{d}t\, q\boldsymbol{w}_\perp\cdot\boldsymbol{E}_\perp - \mu\frac{\Delta B}{B}\\ &= \frac{q}{B}\oint \mathrm{d}\boldsymbol{\ell}_\perp\cdot\boldsymbol{E}_\perp - \mu\frac{\Delta B}{B}\\ &= \mu\frac{\Delta B}{B} - \mu\frac{\Delta B}{B} = 0.\end{aligned}$$

The idea is that the electric field associated with the change in the magnetic field accelerates the particle, increasing its perpendicular energy in such a way that μ is conserved.

A nice example of adiabatic invariance at work is magnetic mirroring. Imagine a magnetized particle trapped inside the potential well of a static magnetic bottle:

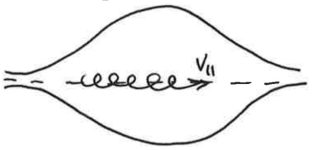

The energy of the particle is conserved,

$$\varepsilon = \frac{1}{2}mv_\parallel^2 + \frac{1}{2}mv_\perp^2 = \text{const},$$

as is its magnetic moment, $\mu = \text{const}$. Thus, as the particle moves from its initial position where the magnetic-field strength is B_0 into a region where the field strength is B, its parallel velocity, initially $v_{\parallel 0}$, must adjust according to these constraints:

$$\frac{1}{2}mv_{\parallel 0}^2 + \mu B_0 = \frac{1}{2}mv_\parallel^2 + \mu B = \varepsilon \quad\Longrightarrow\quad v_\parallel = \pm\sqrt{\frac{2}{m}(\varepsilon - \mu B)} \tag{II.6.1}$$

With ε and μ constant, this establishes a relationship between the parallel velocity of the particle and the local magnetic-field strength (at the particle's gyro-center): if B

[5] How little? Kruskal (1958, 1962) and Northrop (1963*b*) showed that μ is conserved "to all orders", meaning that, if μ can be written as an expansion in the small parameter ϵ, $\mu = \mu_0 + \epsilon\mu_1 + \epsilon^2\mu_2 + \ldots$, then $\Delta\mu \doteq \mu - \mu_0 = c_1\exp(-c_2/\epsilon)$, where c_1 and c_2 are positive constants of order unity.

increases in the particle's frame, $v_\perp$ must increase by μ conservation, and $v_\parallel$ must then decrease by energy conservation. If the particle encounters a strong enough magnetic field that $v_\parallel \to 0$, the particle is said to "reflect" off of the strong-field region. The criterion for reflection is (II.6.1) with $v_\parallel = 0$:

$$\frac{1}{2}mv_{\parallel 0}^2 + \mu(B_0 - B) = 0 \quad \Longrightarrow \quad \frac{v_{\parallel 0}}{v_{\perp 0}} \leqslant \sqrt{\frac{B}{B_0} - 1} \text{ for confinement} \tag{II.6.2}$$

This defines a critical pitch angle separated particles that are trapped inside the magnetic bottle from those that can escape (the "loss cone"):

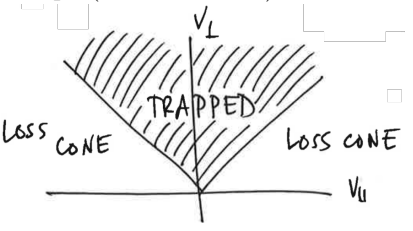

Collisions, which break μ, would of course promote the leakage of particles out of the trapped region.

Now, what if the ends of the mirror were to move slowly?

II.7. Second adiabatic invariant

Imagine a charged particle confined in a square-well potential:

Assume that the bounce time (i.e., the time required for the particle to transit the mirror, bounce, and return to its starting point) is much less than the time over which the ends of the mirror move. There will be an approximately conserved quantity,

$$\mathcal{J} \doteq \oint \mathrm{d}s\, mv_\parallel, \tag{II.7.1}$$

associated with the periodic bounce motion of the guiding center in the evolving mirror. This integral – the second adiabatic invariant – is taken over the "bounce orbit" of the guiding center, with the differential $\mathrm{d}s$ oriented along the local magnetic-field direction and the limits being the turning points of the bounce orbit.[6] For example, if the mirror shrinks adiabatically, then $v_\parallel$ increases.[7] Proving this is more involved, and $\mathcal{J}$ is typically a less robust invariant than μ (although it is of crucial importance for the persistence of the van Allen belts, by ensuring that precessing particles trapped in the Earth's magnetic field return to their native field line after circumnavigating the Earth). If you're interested in the finer details, consult Northrop (1963*a*, pg. 294).

[6]The canonical momentum here is technically $mv_\parallel + eA_\parallel/c$, but the latter (vector-potential) term representing the momentum associated with the electromagnetic field, once integrated over the bounce orbit, equals the total amount of magnetic flux enclosed by the orbit ($= 0$).

[7]Note that both μ and $\mathcal{J}$ are of the form (energy)/(frequency). This is the general form of an adiabatic invariant. Think of $E/\omega = \hbar$ (Einstein) or $\oint p\,\mathrm{d}q = nh$ (Sommerfeld). Einstein, at the Solray conference in 1911, said that this is the general form of an adiabatic invariant, and that this is what ought to be quantized.

II.8. Third adiabatic invariant

There is yet another adiabatic invariant associated with the periodic motion of charged particles in a magnetic field, but it often receives much less attention than the first two because of its lesser utility. The reason is because the associated periodic motion is not as general as, say, a particle gyrating about a field line. In this case, the approximately conserved quantity

$$\mathcal{K} \doteq \oint \mathrm{d}\ell\, \wp_\phi \simeq e \oint \mathrm{d}\ell\, A_\phi = e\Phi \tag{II.8.1}$$

is the magnetic flux enclosed within a periodic orbit caused by cross-field drifts. (The drift velocity v_ϕ is typically small compared to eA_ϕ, thus the "$\simeq$" in (II.8.1).) If the particle orbit also involves bouncing between two turning points in a magnetic mirror, then the periodic orbit associated with the drift motion is to be evaluated at the "bounce center" (just as $\mathcal{J}$ is to be evaluated using an orbit of the guiding center). As with all adiabatic invariants, there is a comparison of time scales that must be done; here, it is between the time scale on which the magnetic field varies and the period of the drift orbit. In the Earth's inner magnetosphere, the time for trapped particles with energies of ∼MeV to circumnavigate the Earth via their cross-field drifts is ∼1 hr, and so any geomagnetic storms would interfere with $\mathcal{K}$ conservation. Again, the separation of time scales and field geometry required for $\mathcal{K}$ conservation is not particularly general, but it is important to bear in mind that particles like to keep the total magnetic flux constant within both their gyro-orbits (μ conservation) and their drift orbits ($\mathcal{K}$ conservation).

II.9. Application: Magnetic pumping

Imagine a stationary, uniform, magnetically confined plasma whose thermal pressure p_0 is initially isotropic, i.e., $p_\perp(0) = p_\parallel(0) = p_0$, where $p_\perp \doteq \langle mv_\perp^2/2\rangle$ is the perpendicular pressure and $p_\parallel \doteq \langle mv_\parallel^2\rangle$ is the parallel pressure. (Again, the angle brackets $\langle\,\cdot\,\rangle$ denote an ensemble average over all the particle constituting the plasma. Note that $3p \doteq \langle mv^2\rangle = p_\parallel + 2p_\perp$.) Take the magnetic field to be uniform with strength B_0.

Slowly increase the strength of this field from B_0 to B_1. "Slowly" here means that the rate of increase is slow compared with the gyro-frequency of the trapped particles but fast compared with the rate at which collisions establish isotropy of the particle distribution function. Then, by adiabatic invariance, we have $p_\perp = (B_1/B_0)p_0$ and $p_\parallel = p_0$. Now, wait. Eventually, energy-conserving Coulomb collisions will isotropize the temperature, so that $p_\perp = p_\parallel = (1 + 2B_1/B_0)(p_0/3)$. Once the system is well equilibrated, decrease the magnetic-field strength back to its initial value, B_0, again at a rate that is slow compared to the gyro-frequency of the trapped particles but fast compared with the collision frequency. Then $p_\perp = (B_0/B_1)(1+2B_1/B_0)(p_0/3)$ and $p_\parallel = (1+2B_1/B_0)(p_0/3)$. Again, wait long enough for the temperatures to equilibrate. The final isotropic pressure is given by

$$p = \left[\frac{2 + 5(B_1/B_0) + 2(B_1/B_0)^2}{9(B_1/B_0)}\right] p_0.$$

For $B_1 = 2B_0$, this is an ≃11% increase in the thermal energy of the plasma. Repeating this cycle 7 times more than doubles the thermal energy!

Questions to ponder: Where did this thermal energy come from? If you had increased/decreased the field strength on a time scale much longer than the collisional equilibration time, how would p have changed? Suppose this plasma were instead confined

in a magnetic mirror reminiscent of that drawn in §II.7, whose length decreases and then increases by a factor of 2 in each cycle. Then what?

II.10. Summary of single-particle drifts and their currents

Here is a summary of the single-particle guiding-center drifts that we've discussed:

$$\boldsymbol{v}_E = \frac{c}{B}\boldsymbol{E}\times\hat{\boldsymbol{b}}, \quad \boldsymbol{v}_{\nabla B} = \frac{w_\perp^2}{2\Omega}\hat{\boldsymbol{b}}\times\boldsymbol{\nabla}\ln B, \quad \boldsymbol{v}_{\rm c} = \frac{v_\parallel^2}{\Omega}\hat{\boldsymbol{b}}\times(\hat{\boldsymbol{b}}\cdot\boldsymbol{\nabla}\hat{\boldsymbol{b}}), \quad \boldsymbol{v}_{\rm pol} = \frac{1}{\Omega}\frac{c}{B}\frac{\partial \boldsymbol{E}_\perp}{\partial t},$$

where the latter two are part of the more general "acceleration" drift,

$$\frac{\hat{\boldsymbol{b}}}{\Omega}\times\frac{\mathrm{D}}{\mathrm{D}t}(v_\parallel\hat{\boldsymbol{b}}+\boldsymbol{v}_E).$$

Note that these are all perpendicular to the magnetic field. Later in these notes, we will make a connection between the single-particle drifts and the magnetohydrodynamic equations. For that, we actually need one more "drift" – the *diamagnetic flow* – and something called the *magnetization current*. These contributions, neither of which are associated with true particle drifts, are discussed in the next two sections. But first it will help to compute the currents associated with the particle drifts and include them here. As we have already emphasized, the $\boldsymbol{E}\times\boldsymbol{B}$ drift is species independent, and thus contributes no current in a quasi-neutral plasma. What about the others?

To compute the perpendicular currents associated with the particle drifts, $\boldsymbol{j}_{\perp,\rm dr}$, we imagine a plasma whose particles' velocities are distributed according to a distribution function $f_\alpha(\boldsymbol{v})$ for each species α. The perpendicular current is then obtained by affixing a species label α to the drifts we computed, multiplying each of them by q_α, summing over species, and integrating over the velocity space after weighting each drift by f_α, *viz.*

$$\begin{aligned}
\boldsymbol{j}_{\perp,\rm dr} &= \sum_\alpha q_\alpha \int \mathrm{d}\boldsymbol{v}\, \boldsymbol{v}_{{\rm dr},\alpha} f_\alpha \\
&= \sum_\alpha q_\alpha \int \mathrm{d}\boldsymbol{v} \left[\frac{w_\perp^2}{2\Omega_\alpha}\hat{\boldsymbol{b}}\times\boldsymbol{\nabla}\ln B + \frac{\hat{\boldsymbol{b}}}{\Omega_\alpha}\times\frac{\mathrm{D}}{\mathrm{D}t}(v_\parallel\hat{\boldsymbol{b}}+\boldsymbol{v}_{\rm E})\right] f_\alpha \\
&= \frac{c}{B}\hat{\boldsymbol{b}}\times\boldsymbol{\nabla}\ln B\sum_\alpha\int \mathrm{d}\boldsymbol{v}\,\frac{1}{2}m_\alpha w_\perp^2 f_\alpha + \frac{c}{B}\hat{\boldsymbol{b}}\times(\hat{\boldsymbol{b}}\cdot\boldsymbol{\nabla}\hat{\boldsymbol{b}})\sum_\alpha\int \mathrm{d}\boldsymbol{v}\, m_\alpha v_\parallel^2 f_\alpha \\
&\quad + \frac{c}{B}\hat{\boldsymbol{b}}\times\left(\frac{\partial\hat{\boldsymbol{b}}}{\partial t}+\boldsymbol{v}_E\cdot\boldsymbol{\nabla}\hat{\boldsymbol{b}}+\hat{\boldsymbol{b}}\cdot\boldsymbol{\nabla}\boldsymbol{v}_E\right)\sum_\alpha\int \mathrm{d}\boldsymbol{v}\, m_\alpha v_\parallel f_\alpha \\
&\quad + \frac{c}{B}\hat{\boldsymbol{b}}\times\left(\frac{\partial\boldsymbol{v}_E}{\partial t}+\boldsymbol{v}_E\cdot\boldsymbol{\nabla}\boldsymbol{v}_E\right)\sum_\alpha\int \mathrm{d}\boldsymbol{v}\, m_\alpha f_\alpha. \qquad \text{(II.10.1)}
\end{aligned}$$

Each of the above integrals over the distribution function f_α have a name: $\int \mathrm{d}\boldsymbol{v}\, m_\alpha f_\alpha = m_\alpha n_\alpha$ is the mass density, $\int \mathrm{d}\boldsymbol{v}\, m_\alpha v_\parallel f_\alpha = m_\alpha n_\alpha u_{\parallel\alpha}$ is the parallel component of the bulk momentum density, and

$$\int \mathrm{d}\boldsymbol{v}\,\frac{1}{2}m_\alpha w_\perp^2 f_\alpha = p_{\perp\alpha}, \quad \int \mathrm{d}\boldsymbol{v}\, m_\alpha v_\parallel^2 f_\alpha = p_{\parallel\alpha} + m_\alpha n_\alpha u_{\parallel\alpha}^2$$

are measures of the particle energies perpendicular and parallel to the magnetic-field direction. Namely, $p_{\perp\alpha}$ ($p_{\parallel\alpha}$) measures the energetic content of the random ("thermal") motions of the particles of species α in the direction perpendicular (parallel) to the local

magnetic field. Substituting these expressions into (II.10.1) yields

$$\frac{B}{c}\boldsymbol{j}_{\perp,\mathrm{dr}} = \sum_\alpha p_{\perp\alpha}\hat{\boldsymbol{b}}\times\boldsymbol{\nabla}\ln B + \sum_\alpha\Big(p_{\parallel\alpha}+m_\alpha n_\alpha u_{\parallel\alpha}^2\Big)\hat{\boldsymbol{b}}\times(\hat{\boldsymbol{b}}\cdot\boldsymbol{\nabla}\hat{\boldsymbol{b}}) + \sum_\alpha m_\alpha n_\alpha\hat{\boldsymbol{b}}\times\left[u_{\parallel\alpha}\frac{\partial\hat{\boldsymbol{b}}}{\partial t}+u_{\parallel\alpha}\boldsymbol{v}_E\cdot\boldsymbol{\nabla}\hat{\boldsymbol{b}}+u_{\parallel\alpha}\hat{\boldsymbol{b}}\cdot\boldsymbol{\nabla}\boldsymbol{v}_E+\frac{\partial\boldsymbol{v}_E}{\partial t}+\boldsymbol{v}_E\cdot\boldsymbol{\nabla}\boldsymbol{v}_E\right]. \tag{II.10.2}$$

This may be further simplified using $\hat{\boldsymbol{b}}\times\hat{\boldsymbol{b}}=0$ and writing

$$\frac{\mathrm{d}}{\mathrm{d}t_\alpha}\doteq\frac{\partial}{\partial t}+\boldsymbol{u}_\alpha\cdot\boldsymbol{\nabla},\quad\text{where }\boldsymbol{u}_\alpha\doteq u_{\parallel\alpha}\hat{\boldsymbol{b}}+\boldsymbol{v}_{\mathrm{E}}. \tag{II.10.3}$$

The result is that

$$\frac{B}{c}\boldsymbol{j}_{\perp,\mathrm{dr}} = \sum_\alpha p_{\perp\alpha}\hat{\boldsymbol{b}}\times\boldsymbol{\nabla}\ln B+\sum_\alpha p_{\parallel\alpha}\hat{\boldsymbol{b}}\times(\hat{\boldsymbol{b}}\cdot\boldsymbol{\nabla}\hat{\boldsymbol{b}})+\sum_\alpha m_\alpha n_\alpha\hat{\boldsymbol{b}}\times\frac{\mathrm{d}\boldsymbol{u}_\alpha}{\mathrm{d}t_\alpha}. \tag{II.10.4}$$

So there are currents associated with the grad-B drift, the curvature drift, and the acceleration drifts (which include the polarization drift). We'll return to this formula in §II.12 after discussing the magnetization current.

II.11. Magnetization current

Plasmas are diamagnetic, a fact we pointed out when discussing μ conservation: the greater the plasma (perpendicular) thermal energy, the more it excludes the magnetic field. There is a macroscopic current, not caused by single-particle drifts, associated with this property. Essentially, because a magnetized plasma may be thought of as being composed of magnetic dipoles, each of which being associated with a gyro-orbiting particle, a plasma may be considered as a magnetic material. From basic electromagnetism, the current of a magnetic material in which the magnetization is non-uniform is given by $\boldsymbol{j}_M=c\boldsymbol{\nabla}\times\boldsymbol{M}$, where $\boldsymbol{M}$ is the magnetization per unit volume due to these magnetic dipoles. The latter may be obtained by integrating up all the magnetic moments of each of the particles, $-\mu\hat{\boldsymbol{b}}$ (see (II.2.4)), weighted by the particle distribution function:

$$\boldsymbol{M}=-\hat{\boldsymbol{b}}\sum_\alpha\int\mathrm{d}\boldsymbol{v}\,\mu_\alpha f_\alpha=-\frac{\hat{\boldsymbol{b}}}{B}\sum_\alpha\int\mathrm{d}\boldsymbol{v}\,\frac{1}{2}m_\alpha w_\perp^2 f_\alpha=-\frac{\hat{\boldsymbol{b}}}{B}\sum_\alpha p_{\perp\alpha}. \tag{II.11.1}$$

The resulting current is

$$\boldsymbol{j}_M=c\boldsymbol{\nabla}\times\boldsymbol{M}=-c\boldsymbol{\nabla}\times\left(\frac{\hat{\boldsymbol{b}}}{B}\sum_\alpha p_{\perp\alpha}\right). \tag{II.11.2}$$

The figure below illustrates the origin of this current. In this example, there are more ions gyrating about the (uniform) magnetic field in the center of the plasma than near the edge, and so there is a density (and thus pressure) gradient pointing inwards (indicated by the blue arrows). Therefore, there are more particles whose field-perpendicular velocities are oriented clockwise along the red dashed line than there are particles whose velocities are oriented counter-clockwise. The difference results in a current that flows as indicated, in the $\hat{\boldsymbol{b}}\times\boldsymbol{\nabla}n$ direction. A similar effect occurs if the density of guiding centers is uniform but the particles' perpendicular velocities are larger in some region of space than they are elsewhere. Alternatively, one may think of the magnetization current in terms of diamagnetism: if the perpendicular thermal energy of the particles is larger in one region

than in another, the ability of the plasma to exclude magnetic fields is inhomogeneous. This produces a current.

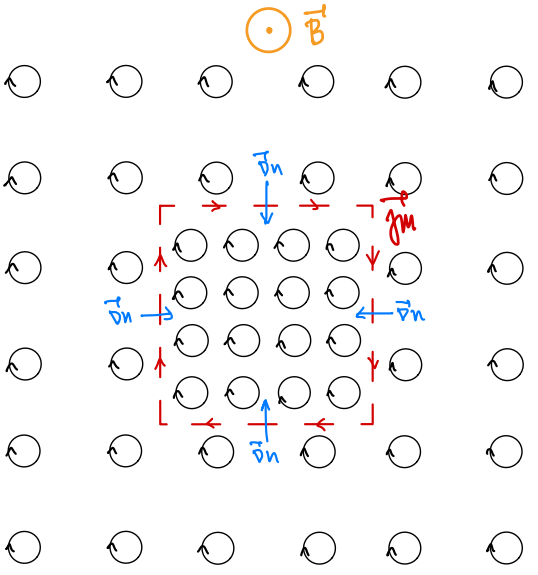

II.12. Total plasma current and the diamagnetic flow

Let us add up all the perpendicular currents we have discussed thus far:

$$\begin{aligned}\boldsymbol{j}_\perp &= \boldsymbol{j}_M + \boldsymbol{j}_{\perp,\mathrm{dr}} \\ &= -c\boldsymbol{\nabla}\times\left(\frac{\hat{\boldsymbol{b}}}{B}\sum_\alpha p_{\perp\alpha}\right) + \frac{c}{B}\sum_\alpha p_{\perp\alpha}\hat{\boldsymbol{b}}\times\boldsymbol{\nabla}\ln B + \frac{c}{B}\sum_\alpha p_{\parallel\alpha}\hat{\boldsymbol{b}}\times(\hat{\boldsymbol{b}}\cdot\boldsymbol{\nabla}\hat{\boldsymbol{b}}) \\ &\quad + \frac{c}{B}\sum_\alpha m_\alpha n_\alpha \hat{\boldsymbol{b}}\times\frac{\mathrm{d}\boldsymbol{u}_\alpha}{\mathrm{d}t_\alpha}. \end{aligned} \tag{II.12.1}$$

The first two terms may be combined to yield

$$\frac{B}{c}\boldsymbol{j}_\perp = -\boldsymbol{\nabla}\times\left(\hat{\boldsymbol{b}}\sum_\alpha p_{\perp\alpha}\right) + \sum_\alpha p_{\parallel\alpha}\hat{\boldsymbol{b}}\times(\hat{\boldsymbol{b}}\cdot\boldsymbol{\nabla}\hat{\boldsymbol{b}}) + \sum_\alpha m_\alpha n_\alpha \hat{\boldsymbol{b}}\times\frac{\mathrm{d}\boldsymbol{u}_\alpha}{\mathrm{d}t_\alpha}. \tag{II.12.2}$$

This next step will be made clearer later in the course, but for now let use simply introduce the tensor

$$\boldsymbol{P}_\alpha = p_{\perp\alpha}(\boldsymbol{I} - \hat{\boldsymbol{b}}\hat{\boldsymbol{b}}) + p_{\parallel\alpha}\hat{\boldsymbol{b}}\hat{\boldsymbol{b}}, \tag{II.12.3}$$

where $\boldsymbol{I}$ is the unit dyadic. (This is the form of the thermal pressure tensor in a magnetized plasma.) Noting that $\boldsymbol{\nabla}\times\hat{\boldsymbol{b}} - \hat{\boldsymbol{b}}\cdot(\hat{\boldsymbol{b}}\cdot\boldsymbol{\nabla}\hat{\boldsymbol{b}}) = \hat{\boldsymbol{b}}\hat{\boldsymbol{b}}\cdot(\boldsymbol{\nabla}\times\hat{\boldsymbol{b}})$ is parallel to $\hat{\boldsymbol{b}}$, equation (II.12.2) becomes simply

$$\frac{B}{c}\boldsymbol{j}_\perp = \hat{\boldsymbol{b}}\times\sum_\alpha\left(\boldsymbol{\nabla}\cdot\boldsymbol{P}_\alpha + m_\alpha n_\alpha\frac{\mathrm{d}\boldsymbol{u}_\alpha}{\mathrm{d}t_\alpha}\right). \tag{II.12.4}$$

Taking $\hat{\boldsymbol{b}}\times$ (II.12.4) and using the vector identity $\hat{\boldsymbol{b}}\times(\hat{\boldsymbol{b}}\times\boldsymbol{A}) = -\boldsymbol{A}_\perp$, we obtain

$$\sum_\alpha\left(m_\alpha n_\alpha\frac{\mathrm{d}\boldsymbol{u}_\alpha}{\mathrm{d}t_\alpha} + \boldsymbol{\nabla}\cdot\boldsymbol{P}_\alpha\right)_\perp = \frac{\boldsymbol{j}\times\boldsymbol{B}}{c}. \tag{II.12.5}$$

If this looks familiar to you, congratulations! You know MHD, and now you see how single-particle drifts and magnetization current fit into the MHD description. If it doesn't look familiar to you, then you just wait... patience is a virtue.

In the meantime, let me just point out that the quantity

$$\boldsymbol{u}_{\mathrm{dia},\alpha} \doteq \frac{\hat{\boldsymbol{b}}}{\Omega_\alpha} \times \frac{\boldsymbol{\nabla}\cdot\boldsymbol{P}_\alpha}{m_\alpha n_\alpha} \tag{II.12.6}$$

that appears implicitly in (II.12.4) has a name – it is referred to as the *diamagnetic flow velocity* of species α.[8] It is *not* a particle drift, but rather refers to net flux of gyrating particles passing through a reference surface due to an inhomogeneous distribution of guiding centers. The diamagnetic flow is explored further in HW01.

We'll return to (II.12.5) and all these drifts later in the course when we discuss MHD waves, the Braginskii-MHD equations, and gyrokinetics.

PART III
Overview of kinetic theory

> How dare we speak of the laws of chance? Is not chance the antithesis of all law?
>
> Joseph Bertrand
> *Calcul des probabilités* (1889)

III.1. Why a statistical description?

If you read Part II, then you might think plasma physics is solved. At any time, compute the electromagnetic fields produced by the charged particles, and then use these fields to evolve the particle phase-space positions using (II.0.10), or perhaps to evolve the guiding-center phase-space positions using (II.4.18)–(II.4.21). Done. Well, not quite. First, there are simply too many particles to follow in a real plasma. There are $\sim 10^{28}$ particles in this room alone. One data dump of $\boldsymbol{r}$ and $\boldsymbol{v}$ for all of these particles would be $\sim 5 \times 10^{17}$ TB (!!!) Secondly, we're not really all that interested in every single particle; we usually want bulk information, like density, momentum, pressure, heat flux, etc. Thirdly, and perhaps most importantly, a many-body system like a plasma is chaotic. Even if we could solve all phase-space trajectories of all the particles given some initial conditions, we would have to admit that those initial conditions are completely arbitrary, and that infinitesimal changes to those initial conditions will yield microscopically different results. It'd be a shame if that mattered, wouldn't it?

This is where a statistical approach comes in handy: What is the probability that a particle will have position $\boldsymbol{r}$ and velocity $\boldsymbol{v}$ in some six-dimensional phase-space interval $\mathrm{d}^3\boldsymbol{r}\mathrm{d}^3\boldsymbol{v}$? How does this probability evolve? Under what conditions is this probabilistic evolution accurate enough to yield meaningful predictions for a single realization of the system? Answering these questions is the job of *kinetic theory*. Think about flipping a coin. We all know that the odds of getting heads is 50%. But those are the *odds* – not very useful is you're betting your career on a single coin toss. Or even two coin tosses,

[8] I am deliberately *not* calling it the "diamagnetic drift velocity", as some are wont to do. Nothing is actually drifting, so this moniker makes no sense! Later in this course, we will show that the diamagnetic flow is what one obtains when Taylor-expanding an equilibrium distribution $f(\mathcal{E}, \mu, \boldsymbol{R})$ that is a function of the particle energy $\mathcal{E}$, magnetic moment μ, and guiding-position $\boldsymbol{R}$ about the particle position $\boldsymbol{r} \doteq \boldsymbol{R} + \boldsymbol{\rho}$ and computing its first velocity-space moment.

or ten. But perhaps very useful if you flip the coin 10^{28} times and make a wager on the percentage of tosses that came up heads. Or, if you're rich and have 10^{28} coins lying around, you could flip them all at the same time and count the number of heads as a fraction of the total. Why kinetic theory works as a predictive theory is that, statistically, there is no difference between running, say, a particle-in-cell code with 100 particles per cell many, many, many times each with different initial conditions randomly sampled from some prescribed distribution, and running the same code just once with 10^{28} particles per cell and a single realization of the initial conditions. The statistics you learn from the first experiment should be an accurate representation of the actual results in the second experiment.

The trick is actually building a rigorous, predictive kinetic theory of plasmas. In this Part III, I'll sketch how one is built, highlighting its assumptions. If you're left wanting more, you can find my AST554 notes here.

III.2. The Klimontovich equation as a microscopic description of a plasma

A complete description of a plasma would emerge if one were to have knowledge of all the coordinates and momenta of all of the constituent particles, as well as the electromagnetic fields in which they move and which they self-consistently produce. We've already discussed why such a description would be untenable with which to work, but let us nevertheless adopt this microscopic standpoint and see where it leads.

Start by defining the function

$$F_\alpha(t,\boldsymbol{r},\boldsymbol{v}) = \sum_{i=1}^{N_\alpha} \delta(\boldsymbol{r}-\boldsymbol{R}_{\alpha i}(t))\delta(\boldsymbol{v}-\boldsymbol{V}_{\alpha i}(t)), \tag{III.2.1}$$

which completely specifies the positions $\boldsymbol{R}_{\alpha i}(t)$ and velocities $\boldsymbol{V}_{\alpha i}(t)$ of N_α particles of species α as functions of time. Note that

$$\lim_{\mathrm{d}\boldsymbol{r}\mathrm{d}\boldsymbol{v}\to 0} \int \mathrm{d}\boldsymbol{r}\mathrm{d}\boldsymbol{v}\, F_\alpha(t,\boldsymbol{r},\boldsymbol{v})$$

is either unity or zero, depending upon whether there is a particle at $(\boldsymbol{r},\boldsymbol{v})$ at time t, so that

$$\int \mathrm{d}\boldsymbol{r}\mathrm{d}\boldsymbol{v}\, F_\alpha(t,\boldsymbol{r},\boldsymbol{v}) = N_\alpha. \tag{III.2.2}$$

Thus, the microscopic state of the plasma at any time t would be known if one were to know $\boldsymbol{R}_{\alpha i}$ and $\boldsymbol{V}_{\alpha i}$ at $t=0$ and their temporal evolution. Hamilton's equations of motion provide us with the latter:

$$\frac{\mathrm{d}\boldsymbol{R}_{\alpha i}}{\mathrm{d}t} = \boldsymbol{V}_{\alpha i} \qquad \text{and} \qquad \frac{\mathrm{d}\boldsymbol{V}_{\alpha i}}{\mathrm{d}t} = \frac{q_\alpha}{m_\alpha}\left(\boldsymbol{E}_\mathrm{m} + \frac{\boldsymbol{V}_{\alpha i}}{c}\times\boldsymbol{B}_\mathrm{m}\right), \tag{III.2.3}$$

where q_α and m_α are the charge and mass of species α, and

$$\boldsymbol{E}_\mathrm{m} = \boldsymbol{E}_\mathrm{m}(t,\boldsymbol{R}_{\alpha i}(t)) \qquad \text{and} \qquad \boldsymbol{B}_\mathrm{m} = \boldsymbol{B}_\mathrm{m}(t,\boldsymbol{R}_{\alpha i}(t)) \tag{III.2.4}$$

are the "microphysical" electric and magnetic fields evaluated at the particle position $\boldsymbol{R}_{\alpha i}$ at time t. The adjective "microphysical" here is meant to indicate that $\boldsymbol{E}_\mathrm{m}$ and $\boldsymbol{B}_\mathrm{m}$ are the fields self-consistently generated by the particles themselves. These satisfy Maxwell's

equations:

$$\boldsymbol{\nabla}\times\boldsymbol{E}_{\rm m}=-\frac{1}{c}\frac{\partial\boldsymbol{B}_{\rm m}}{\partial t}, \tag{III.2.5}$$

$$\boldsymbol{\nabla}\times\boldsymbol{B}_{\rm m}=\frac{1}{c}\frac{\partial\boldsymbol{E}_{\rm m}}{\partial t}+\frac{4\pi}{c}\sum_{\alpha}q_\alpha\int{\rm d}\boldsymbol{v}\,\boldsymbol{v}F_\alpha(t,\boldsymbol{r},\boldsymbol{v}), \tag{III.2.6}$$

$$\boldsymbol{\nabla}\cdot\boldsymbol{E}_{\rm m}=4\pi\sum_{\alpha}q_\alpha\int{\rm d}\boldsymbol{v}\,F_\alpha(t,\boldsymbol{r},\boldsymbol{v}), \tag{III.2.7}$$

$$\boldsymbol{\nabla}\cdot\boldsymbol{B}_{\rm m}=0. \tag{III.2.8}$$

Because Maxwell's equations are linear, we can add to these fields any that may be externally imposed: $\boldsymbol{E}_{\rm m}\to\boldsymbol{E}_{\rm m}+\boldsymbol{E}_{\rm ext}$ and $\boldsymbol{B}_{\rm m}\to\boldsymbol{B}_{\rm m}+\boldsymbol{B}_{\rm ext}$. This will be useful for describing magnetized plasmas threaded by an external magnetic field. Before we proceed any further, two things are worth noting:

(1) The electric and magnetic fields in (III.2.3) omit the contribution from particle (αi). In other words, a particle does not interact electromagnetically with itself.

(2) Writing $(\boldsymbol{r},\boldsymbol{v})$ and ${\rm d}\boldsymbol{r}{\rm d}\boldsymbol{v}$ all the time is exhausting. Denote $\boldsymbol{x}=(\boldsymbol{r},\boldsymbol{v})$ and ${\rm d}\boldsymbol{x}={\rm d}\boldsymbol{r}{\rm d}\boldsymbol{v}$, i.e., $\boldsymbol{x}$ is the phase-space coordinate and ${\rm d}\boldsymbol{x}$ is a small volume of phase space. Likewise, $\boldsymbol{X}_{\alpha i}=(\boldsymbol{R}_{\alpha i},\boldsymbol{V}_{\alpha i})$.

Now, let us consider how $F_\alpha(t,\boldsymbol{x})\doteq F_\alpha(t,\boldsymbol{r},\boldsymbol{v})$ evolves:[9]

$$\begin{aligned}
\frac{\partial F_\alpha}{\partial t}&=\frac{\partial}{\partial t}\sum_{i=1}^{N_\alpha}\delta(\boldsymbol{x}-\boldsymbol{X}_{\alpha i}(t))\\
&=\sum_{i=1}^{N_\alpha}\frac{{\rm d}\boldsymbol{X}_{\alpha i}}{{\rm d}t}\cdot\frac{\partial}{\partial\boldsymbol{X}_{\alpha i}}\,\delta(\boldsymbol{x}-\boldsymbol{X}_{\alpha i}(t))\\
&=-\sum_{i=1}^{N_\alpha}\frac{{\rm d}\boldsymbol{X}_{\alpha i}}{{\rm d}t}\cdot\frac{\partial}{\partial\boldsymbol{x}}\,\delta(\boldsymbol{x}-\boldsymbol{X}_{\alpha i}(t))\\
&=-\sum_{i=1}^{N_\alpha}\left\{\boldsymbol{V}_{\alpha i}\cdot\boldsymbol{\nabla}+\frac{q_\alpha}{m_\alpha}\left[\boldsymbol{E}_{\rm m}(t,\boldsymbol{R}_{\alpha i}(t))+\frac{\boldsymbol{V}_{\alpha i}}{c}\times\boldsymbol{B}_{\rm m}(t,\boldsymbol{R}_{\alpha i}(t))\right]\cdot\frac{\partial}{\partial\boldsymbol{v}}\right\}\delta(\boldsymbol{x}-\boldsymbol{X}_{\alpha i}(t))\\
&=-\sum_{i=1}^{N_\alpha}\left\{\boldsymbol{v}\cdot\boldsymbol{\nabla}+\frac{q_\alpha}{m_\alpha}\left[\boldsymbol{E}_{\rm m}(t,\boldsymbol{r})+\frac{\boldsymbol{v}}{c}\times\boldsymbol{B}_{\rm m}(t,\boldsymbol{r})\right]\cdot\frac{\partial}{\partial\boldsymbol{v}}\right\}\delta(\boldsymbol{x}-\boldsymbol{X}_{\alpha i}(t))\\
&=-\left\{\boldsymbol{v}\cdot\boldsymbol{\nabla}+\frac{q_\alpha}{m_\alpha}\left[\boldsymbol{E}_{\rm m}(t,\boldsymbol{r})+\frac{\boldsymbol{v}}{c}\times\boldsymbol{B}_{\rm m}(t,\boldsymbol{r})\right]\cdot\frac{\partial}{\partial\boldsymbol{v}}\right\}\sum_{i=1}^{N_\alpha}\delta(\boldsymbol{x}-\boldsymbol{X}_{\alpha i}(t))\\
&=-\left\{\boldsymbol{v}\cdot\boldsymbol{\nabla}+\frac{q_\alpha}{m_\alpha}\left[\boldsymbol{E}_{\rm m}(t,\boldsymbol{r})+\frac{\boldsymbol{v}}{c}\times\boldsymbol{B}_{\rm m}(t,\boldsymbol{r})\right]\cdot\frac{\partial}{\partial\boldsymbol{v}}\right\}F_\alpha(\boldsymbol{t},\boldsymbol{x})
\end{aligned}$$

$$\Longrightarrow\quad\boxed{\left[\frac{\partial}{\partial t}+\boldsymbol{v}\cdot\boldsymbol{\nabla}+\frac{q_\alpha}{m_\alpha}\left(\boldsymbol{E}_{\rm m}+\frac{\boldsymbol{v}}{c}\times\boldsymbol{B}_{\rm m}\right)\cdot\frac{\partial}{\partial\boldsymbol{v}}\right]F_\alpha(t,\boldsymbol{x})=0} \tag{III.2.9}$$

Equation (III.2.9) is called the *Klimontovich equation*. While it is equivalent to phase-

[9] Do you understand each of these steps? Namely, ask yourself: what if ${\rm d}\boldsymbol{X}_{\alpha i}/{\rm d}t$ involved a drag force $\propto\boldsymbol{V}_{\alpha i}$? Because the property $X(t)\delta(x-X(t))=x\delta(x-X(t))$ does *not* imply that $X(t)\delta'(x-X(t))=x\delta'(x-X(t))$, what is required of ${\rm d}\boldsymbol{X}_{\alpha i}/{\rm d}t$ for the following to hold?

space conservation, it is *not* a statistical equation. With proper initial conditions, it is completely deterministic. Together with Maxwell's equations (III.2.5)–(III.2.8), the densities and fields are determined for all time.

The Klimontovich equation (III.2.9) can be thought of as expressing the incompressibility of the substance $F_\alpha(t, \boldsymbol{x})$ as it moves in phase space: $\mathrm{D}F_\alpha/\mathrm{D}t = 0$, where $\mathrm{D}/\mathrm{D}t$ is the phase-space Lagrangian (i.e., comoving) derivative. Nicholson (1983) writes, "is it any wonder that a point particle is incompressible?" Phase-space trajectories that follow the characteristics of (III.2.9) and start from an interval $\mathrm{d}\boldsymbol{x}$ where $F_\alpha = 0$ will carry that null information along with them. Likewise with intervals where $\lim_{\mathrm{d}\boldsymbol{x}\to 0} \int \mathrm{d}\boldsymbol{x}\, F_\alpha(\boldsymbol{x}) = 1$. Thus, the phase space is populated in a very choppy way. For that reason, as well as the simple fact that, despite some mathematics, we haven't actually simplified anything, the Klimontovich equation as a description of the plasma is not worth much practical use. One has simply replaced $6N$ equations for each particle with a single equation having $6N$ dimensions. However, this kind of treatment can form the basis of a *statistical* description of the plasma. But, for that, we need some kind of averaging process...

III.3. The Liouville ("Leé-ooo-ville") distribution

Wandering aimlessly around PPPL one day, you stumble curiously upon a plasma lab, equipped with a big green button with "START" written on it, a big red button with "STOP" written on it, and a bucket labelled "initial conditions" sitting mysteriously over in the corner. Never one to mind your own business, you walk over to the bucket, reach inside, and, from the many, many sealed envelopes you feel, select one. Inside this envelope you find a list specifying the positions and velocities of all the plasma particles that are to comprise the initial conditions for your experiment. Being the intellectually curious experimentalist that you are, you follow the instructions in the envelope and put all the particles exactly where they should be and press the green button. Particles whizz about you in a beautiful dance of plasma motion. Satisfied, you press the red button. Never one to let a good experiment go to waste, you commence with writing down the final positions and velocities of every single particle into your log book. Well, that was fun... let's do it again. Reach into the bucket, pull out an envelope, follow the instructions, press "START", press "STOP", record. You note that, with the different initial conditions, you obtained a different result. This is getting interesting. Do it again. And again. And again. And again. After a while you grow tired of this business and decide that, whatever might happen on the next experiment, it can't be all that different from all the experiments you've already run. Besides, these lists are getting quite long. So you decide to average the results from all the experiments you've done, trash your overflowing log book in favor of data from the average you've calculated, and hope that, whatever might happen in a future experiment that you'd rather not run, this average should be a good enough description. So you leave the room, walk down to greet your fellow graduate students at the water cooler, and, full of pride, relay to them all you've accomplished today. An aspiring theory student responds, "That seems like a lot of work just to get an average. Say, did you happen to notice any additional information written on the side of the bucket?" She accompanies you back to the lab to check. Sure enough, there on the side of the bucket, in fine print, is a formula describing the distribution of initial conditions inside the bucket. Your clever friend says, "Ha! All that work! All you needed was this information about the statistics of the initial conditions and then you would've only had to run the experiment once – on the statistics."

What your friend is advocating is the approach of kinetic theory. If we knew the probability of these particles being somewhere, with some velocities, at some time, then,

equipped with the Klimontovich equation, perhaps we could calculate the probability of these particles being somewhere, with some velocities, at some future time. Let's see where this line of thought leads. Introduce the distribution function P_N of the coordinates and momenta of all of the $N \doteq \sum_\alpha N_\alpha$ particles in the system. Specifically,

$$P_N \prod_\alpha \mathrm{d}\boldsymbol{X}_{\alpha 1}\mathrm{d}\boldsymbol{X}_{\alpha 2}\ldots\mathrm{d}\boldsymbol{X}_{\alpha N_\alpha}$$

gives the probability that, at time t, the phase-space coordinates of the particles of species α have the values $\boldsymbol{X}_{\alpha 1}$, $\boldsymbol{X}_{\alpha 2}$, …, $\boldsymbol{X}_{\alpha N_\alpha}$ in the range $\mathrm{d}\boldsymbol{X}_{\alpha 1}\mathrm{d}\boldsymbol{X}_{\alpha 2}\ldots\mathrm{d}\boldsymbol{X}_{\alpha N_\alpha}$. This $6N$-dimensional phase space is sometimes called the "Γ space". The actual microscopic state in any one realization of the plasma is expressed in the Γ space by a point $\{\boldsymbol{X}_{\alpha i}\}$. Before proceeding, let me flag a few important points (see also §2.1.B of Ichimaru (2004) and §7.2 of Krall & Trivelpiece (1973)):

(1) The system points $\{\boldsymbol{X}_{\alpha i}\}$ do not interact with one another and so P_N satisfies a continuity equation of the Liouville kind:

$$\frac{\mathrm{D}P_N}{\mathrm{D}t} \doteq \frac{\partial P_N}{\partial t} + \sum_\alpha \sum_{i=1}^{N_\alpha} \frac{\mathrm{d}\boldsymbol{X}_{\alpha i}}{\mathrm{d}t}\cdot\frac{\partial P_N}{\partial \boldsymbol{X}_{\alpha i}} = 0; \tag{III.3.1}$$

i.e., the probability density is conserved along a characteristic trajectory in phase space.

(2) Because P_N is a probability, we have

$$\int \prod_\alpha \mathrm{d}\boldsymbol{X}_{\alpha 1}\mathrm{d}\boldsymbol{X}_{\alpha 2}\ldots\mathrm{d}\boldsymbol{X}_{\alpha N_\alpha}\, P_N \doteq \int \mathrm{d}\boldsymbol{X}_{\mathrm{all}}\, P_N = 1,$$

where I've introduced the shorthand $\mathrm{d}\boldsymbol{X}_{\mathrm{all}}$ to indicate integration over all of the Γ space (including all species).

(3) In thermodynamic equilibrium, P_N equals the Gibbs distribution

$$D_N \doteq \frac{1}{\mathcal{Z}}\exp\left(-\frac{\mathcal{H}}{T}\right), \tag{III.3.2}$$

where $\mathcal{H} = \mathcal{H}(\Gamma)$ is the Hamiltonian (kinetic plus potential energy), T is the (species-independent!) equilibrium temperature (in energy units), and

$$\mathcal{Z} \doteq \int \prod_\alpha \mathrm{d}\boldsymbol{X}_{\alpha 1}\ldots\mathrm{d}\boldsymbol{X}_{\alpha N_\alpha}\, \exp\left(-\frac{\mathcal{H}}{T}\right) \tag{III.3.3}$$

is the partition function. We will often be concerned with non-equilibrium systems, and so we will need to know how P_N evolves in time from a given starting distribution $P_N(0)$.

(4) Returning to the story at the beginning of this section, it is profitable to think of P_N in the statistical-mechanics ensemble sense: imagine $\mathcal{N}$ replicas of our plasma, all macroscopically identical but microscopically different, with the system points $\{\boldsymbol{X}_{\alpha i}\}$ scattered over the Γ space. Then P_N can be defined from

$$P_N \prod_\alpha \mathrm{d}\boldsymbol{X}_{\alpha 1}\mathrm{d}\boldsymbol{X}_{\alpha 2}\ldots\mathrm{d}\boldsymbol{X}_{\alpha N_\alpha} \doteq \lim_{\mathcal{N}\to\infty}\frac{\mathcal{N}_s}{\mathcal{N}}, \tag{III.3.4}$$

where $\mathcal{N}_s$ is the number of those system points contained in an infinitesimal volume $\prod_\alpha \mathrm{d}\boldsymbol{X}_{\alpha 1}\ldots\mathrm{d}\boldsymbol{X}_{\alpha N_\alpha}$ in the Γ space around $\{\boldsymbol{X}_{\alpha i}\}$. (Why can we do this for a

plasma? Hint: think about the accuracy of using a statistical description of an N-body system to describe any one realization of the system. What happens to the model's predictive power when N is not very large?)

III.4. Reduced distribution functions

With a probability distribution in hand, we can perform an ensemble average over all these realizations of the plasma. Each one of these realizations is deterministic, but the system is stochastic between different realizations. Averaging amongst all these different realizations will turn our spiky "fine-grained" F_α into the smooth "coarse-grained" distribution. For example,

$$\int \mathrm{d}\boldsymbol{X}_{\alpha 2} \ldots \mathrm{d}\boldsymbol{X}_{\alpha N_\alpha} \prod_\beta \mathrm{d}\boldsymbol{X}_{\beta 1} \mathrm{d}\boldsymbol{X}_{\beta 2} \ldots \mathrm{d}\boldsymbol{X}_{\beta N_\beta} \, P_N$$

is the joint probability that particle $\alpha 1$ has coordinates in $(\boldsymbol{X}_{\alpha 1})$ to $(\boldsymbol{X}_{\alpha 1} + \mathrm{d}\boldsymbol{X}_{\alpha 1})$ *irrespective* of the coordinates of particles $\alpha 2$, …, αN_α, $\beta 1$, $\beta 2$, …, βN_β, etc. This *reduced distribution function* is called the *one-particle distribution function*. It can be normalized to one's tastes. I choose the following:[10]

$$f_\alpha(t, \boldsymbol{x}) \doteq N_\alpha \int \mathrm{d}\boldsymbol{X}_{\alpha 2} \ldots \mathrm{d}\boldsymbol{X}_{\alpha N_\alpha} \prod_\beta \mathrm{d}\boldsymbol{X}_{\beta 1} \mathrm{d}\boldsymbol{X}_{\beta 2} \ldots \mathrm{d}\boldsymbol{X}_{\beta N_\beta} \, P_N, \tag{III.4.1}$$

The operative word here is "irrespective". Of course the probability of, say, an electron being at some phase-space position $\boldsymbol{x}$ is impacted by an ion being nearby at $\boldsymbol{x}' \approx \boldsymbol{x}$, but this information is not is f_α. The influence of a near neighbor on the distribution of a particle is contained in a less reduced description, e.g., the *two-particle distribution function*:

$$f_{\alpha\beta}(t, \boldsymbol{x}, \boldsymbol{x}') \doteq N_\alpha N_\beta \int \mathrm{d}\boldsymbol{X}_{\alpha 2} \ldots \mathrm{d}\boldsymbol{X}_{\alpha N_\alpha} \mathrm{d}\boldsymbol{X}_{\beta 2} \ldots \mathrm{d}\boldsymbol{X}_{\beta N_\beta} \prod_\gamma \mathrm{d}\boldsymbol{X}_{\gamma 1} \mathrm{d}\boldsymbol{X}_{\gamma 2} \ldots \mathrm{d}\boldsymbol{X}_{\gamma N_\gamma} \, P_N. \tag{III.4.2}$$

Then $f_{\alpha\beta}(t, \boldsymbol{x}, \boldsymbol{x}')\mathrm{d}\boldsymbol{x}\mathrm{d}\boldsymbol{x}'/N_\alpha N_\beta$ is the joint probability that particle $\alpha 1$ is at $\boldsymbol{x}$ in interval $\mathrm{d}\boldsymbol{x}$ *and* particle $\beta 1$ is at $\boldsymbol{x}'$ in interval $\mathrm{d}\boldsymbol{x}'$, irrespective of all other particles.

Note three things:

(1) The species labels α and β could refer to the same type of particle ($\alpha = \beta$), in which case $\beta 1 \to \alpha 2$. (Particles are indistinguishable amongst a species, and so the exact numerical indices do not matter.) In this case, $N_\beta \to N_\alpha - 1$.

(2) The two-particle distribution function $f_{\alpha\beta}$ is still a reduced distribution, but, as opposed to the one-particle distribution function f_α, it contains some information about two-body interactions. If the particles do not interact, then $f_{\alpha\beta} = f_\alpha f_\beta$, the product of one-particle distribution functions… simple.

(3) One could of course generalize this process. For example, the three-particle distri-

[10] The reason for the N_α is so that $\int \mathrm{d}\boldsymbol{v} \, f_\alpha(t, \boldsymbol{x})$ is the number density n_α, a customary normalization for the one-particle distribution function. Others might introduce a prefactor $\mathcal{V}$ for volume, which makes $\int \mathrm{d}\boldsymbol{v} \, f_\alpha(t, \boldsymbol{x})$ equal to the fraction of the mean number density $\overline{n}_\alpha \doteq N_\alpha/\mathcal{V}$ in that volume.

bution function is

$$f_{\alpha\beta\gamma} \doteq N_\alpha N_\beta N_\gamma \int \frac{\mathrm{d}\boldsymbol{X}_{\mathrm{all}}}{\mathrm{d}\boldsymbol{X}_{\alpha 1}\mathrm{d}\boldsymbol{X}_{\beta 1}\mathrm{d}\boldsymbol{X}_{\gamma 1}}\, P_N; \tag{III.4.3}$$

the four-particle distribution function is

$$f_{\alpha\beta\gamma\delta} \doteq N_\alpha N_\beta N_\gamma N_\delta \int \frac{\mathrm{d}\boldsymbol{X}_{\mathrm{all}}}{\mathrm{d}\boldsymbol{X}_{\alpha 1}\mathrm{d}\boldsymbol{X}_{\beta 1}\mathrm{d}\boldsymbol{X}_{\gamma 1}\mathrm{d}\boldsymbol{X}_{\delta 1}}\, P_N;$$

and so on.

We combine this machinery with the Klimontovich distribution (III.2.1) as follows.

Each term in $F_\alpha = \sum_i \delta(\boldsymbol{x} - \boldsymbol{X}_{\alpha i})$ describes the location of a particle in terms of its initial conditions, and P_N describes the probability of a particle having a certain set of initial conditions, and so the reduced descriptions of P_N can be expressed in terms of the averages of products of F_α over all possible initial conditions. These averages are defined by

$$\langle G(F_\alpha, F_\beta, \ldots, F_\gamma)\rangle \doteq \int \mathrm{d}\boldsymbol{X}_{\mathrm{all}}\, P_N\, G(F_\alpha, F_\beta, \ldots, F_\gamma). \tag{III.4.4}$$

Let's put this to work.

III.5. Towards the Vlasov equation

Integrate the Klimontovich distribution (III.2.1) over the Liouville distribution (see (III.4.4)):

$$\begin{aligned}
\langle F_\alpha(t,\boldsymbol{x})\rangle &\doteq \sum_{i=1}^{N_\alpha} \int \mathrm{d}\boldsymbol{X}_{\mathrm{all}}\, P_N\, \delta(\boldsymbol{x} - \boldsymbol{X}_{\alpha i}(t)) \\
&= N_\alpha \int \mathrm{d}\boldsymbol{X}_{\mathrm{all}}\, P_N\, \delta(\boldsymbol{x} - \boldsymbol{X}_{\alpha 1}(t)) \quad \text{(particles are indistinguishable)} \\
&= N_\alpha \int \mathrm{d}\boldsymbol{X}_{\alpha 2} \ldots \mathrm{d}\boldsymbol{X}_{\alpha N_\alpha} \prod_\beta \mathrm{d}\boldsymbol{X}_{\beta 1}\mathrm{d}\boldsymbol{X}_{\beta 2} \ldots \mathrm{d}\boldsymbol{X}_{\beta N_\beta}\, P_N \\
&\doteq f_\alpha(t,\boldsymbol{x}) \quad \text{(def'n of one-particle distribution function, (III.4.1))}.
\end{aligned} \tag{III.5.1}$$

Similarly, the average electromagnetic fields are obtained by averaging the microscopic fields $\boldsymbol{E}_{\mathrm{m}}$ and $\boldsymbol{B}_{\mathrm{m}}$, which depend upon the positions of the (point-like) particles, over the probable locations of all of the particles:

$$\boldsymbol{E} \doteq \langle \boldsymbol{E}_{\mathrm{m}}\rangle = \int \mathrm{d}\boldsymbol{X}_{\mathrm{all}}\, P_N\, \boldsymbol{E}_{\mathrm{m}} \qquad \text{and} \qquad \boldsymbol{B} \doteq \langle \boldsymbol{B}_{\mathrm{m}}\rangle = \int \mathrm{d}\boldsymbol{X}_{\mathrm{all}}\, P_N\, \boldsymbol{B}_{\mathrm{m}}. \tag{III.5.2}$$

Using (III.5.1) and (III.5.2) in the Maxwell equations (III.2.5)–(III.2.8) gives

$$\boldsymbol{\nabla} \times \boldsymbol{E} = -\frac{1}{c}\frac{\partial \boldsymbol{B}}{\partial t}, \tag{III.5.3}$$

$$\boldsymbol{\nabla} \times \boldsymbol{B} = \frac{1}{c}\frac{\partial \boldsymbol{E}}{\partial t} + \frac{4\pi}{c}\sum_\alpha q_\alpha \int \mathrm{d}\boldsymbol{v}\, \boldsymbol{v} f_\alpha(t,\boldsymbol{r},\boldsymbol{v}), \tag{III.5.4}$$

$$\boldsymbol{\nabla} \cdot \boldsymbol{E} = 4\pi \sum_\alpha q_\alpha \int \mathrm{d}\boldsymbol{v}\, f_\alpha(t,\boldsymbol{r},\boldsymbol{v}), \tag{III.5.5}$$

$$\boldsymbol{\nabla} \cdot \boldsymbol{B} = 0. \tag{III.5.6}$$

Simple. This is because Maxwell's equations are linear.

The difficulty is that the Klimontovich equation (III.2.9) is *not*. It has a quadratic nonlinearity, which it what makes it so hard to solve. Let's see that. The integral of (III.2.9) over the Liouville distribution is

$$\frac{\partial}{\partial t}\langle F_\alpha\rangle + \boldsymbol{v}\cdot\boldsymbol{\nabla}\langle F_\alpha\rangle + \left\langle \frac{q_\alpha}{m_\alpha}\left(\boldsymbol{E}_\mathrm{m} + \frac{\boldsymbol{v}}{c}\times\boldsymbol{B}_\mathrm{m}\right)\cdot\frac{\partial F_\alpha}{\partial \boldsymbol{v}}\right\rangle = 0. \tag{III.5.7}$$

The first two terms in (III.5.7) involve only the one-particle distribution function f_α (see (III.5.1)). The third and final term can be manipulated further by decomposing the microscopic electromagnetic fields into their mean and fluctuating parts:

$$\boldsymbol{E}_\mathrm{m} = \langle \boldsymbol{E}_\mathrm{m}\rangle + \delta\boldsymbol{E} \doteq \boldsymbol{E} + \delta\boldsymbol{E} \qquad \text{and} \qquad \boldsymbol{B}_\mathrm{m} = \langle \boldsymbol{B}_\mathrm{m}\rangle + \delta\boldsymbol{B} \doteq \boldsymbol{B} + \delta\boldsymbol{B}. \tag{III.5.8}$$

The fields $\boldsymbol{E}$ and $\boldsymbol{B}$ are smooth and coarse-grained; they are the "macroscopic" fields obtained by averaging the microscopic fields over all possible positions of the plasma particles, weighted by the Liouville distribution. The remainders, $\delta\boldsymbol{E}$ and $\delta\boldsymbol{B}$, are spiky and fine-grained; they capture the influence of the discrete nature of the particles on the electromagnetic fields. Using (III.5.8) in the Klimontovich equation (III.5.7) and likewise writing $F_\alpha = f_\alpha + \delta F_\alpha$, we obtain

$$\boxed{\left[\frac{\partial}{\partial t} + \boldsymbol{v}\cdot\boldsymbol{\nabla} + \frac{q_\alpha}{m_\alpha}\left(\boldsymbol{E} + \frac{\boldsymbol{v}}{c}\times\boldsymbol{B}\right)\cdot\frac{\partial}{\partial \boldsymbol{v}}\right] f_\alpha(t,\boldsymbol{x}) = -\left\langle \frac{q_\alpha}{m_\alpha}\left(\delta\boldsymbol{E} + \frac{\boldsymbol{v}}{c}\times\delta\boldsymbol{B}\right)\cdot\frac{\partial \delta F_\alpha}{\partial \boldsymbol{v}}\right\rangle} \tag{III.5.9}$$

If there are externally imposed electric and magnetic fields, they can be added to $\boldsymbol{E}$ and $\boldsymbol{B}$, respectively.

III.6. The BBGKY hierarchy

At this point, some derivations discuss the size of the right-hand side of (III.5.9) versus its left-hand side, the latter of which might look familiar to you. Let's postpone that for now and just see if we can obtain a general set of equations describing the statistical mechanics of a plasma. **The details of what follows in this section constitutes optional material.**

Let us concern ourselves with non-relativistic plasmas, such that the microscopic magnetic field can be dropped and the Coulomb potential gives an electrostatic field

$$\boldsymbol{E}_\mathrm{m} = -\frac{\partial}{\partial \boldsymbol{r}}\sum_\alpha q_\alpha \int \mathrm{d}\boldsymbol{x}'\,\frac{F_\alpha(t,\boldsymbol{x}')}{|\boldsymbol{r}-\boldsymbol{r}'|}. \tag{III.6.1}$$

Thus, $\delta\boldsymbol{B} = 0$, $\boldsymbol{B} = \boldsymbol{B}_\mathrm{ext}$, and

$$\delta\boldsymbol{E} = -\frac{\partial}{\partial \boldsymbol{r}}\sum_\alpha q_\alpha \int \mathrm{d}\boldsymbol{x}'\,\frac{\delta F_\alpha(t,\boldsymbol{x}')}{|\boldsymbol{r}-\boldsymbol{r}'|}. \tag{III.6.2}$$

In this case,

$$\boldsymbol{E} = \boldsymbol{E}_\mathrm{ext} + \langle \boldsymbol{E}_\mathrm{m}\rangle = \boldsymbol{E}_\mathrm{ext} - \frac{\partial}{\partial \boldsymbol{r}}\sum_\alpha q_\alpha \int \mathrm{d}\boldsymbol{x}'\,\frac{f_\alpha(t,\boldsymbol{x}')}{|\boldsymbol{r}-\boldsymbol{r}'|}. \tag{III.6.3}$$

Then, using (III.5.9), the equation governing the one-particle distribution function is

$$\left[\frac{\partial}{\partial t} + \boldsymbol{v}\cdot\boldsymbol{\nabla} + \frac{q_\alpha}{m_\alpha}\left(\boldsymbol{E} + \frac{\boldsymbol{v}}{c}\times\boldsymbol{B}\right)\cdot\frac{\partial}{\partial \boldsymbol{v}}\right] f_\alpha(t,\boldsymbol{x}) = \left\langle \frac{\partial}{\partial \boldsymbol{r}}\sum_\beta \frac{q_\alpha q_\beta}{m_\alpha}\int \mathrm{d}\boldsymbol{x}'\,\frac{\delta F_\beta(t,\boldsymbol{x}')}{|\boldsymbol{r}-\boldsymbol{r}'|}\cdot\frac{\partial}{\partial \boldsymbol{v}}\delta F_\alpha(t,\boldsymbol{x})\right\rangle. \tag{III.6.4}$$

Recall that, on scales $L \gtrsim \lambda_{\rm D}$, individual particle particles are shielded and what remains are fields due to the collective action of a large number of particles. Also recall that the Coulomb potential is long-range, and so the fields decay on distances long compared to the interparticle spacing ($\lambda_{\rm D} \gg \delta r$). This gives collective behavior: interaction of particles with the mean ("macroscopic") fields generated by all other particles. This means that the entire left-hand side of (III.6.4) consists of terms that vary smoothly in phase space, since it's entirely insensitive to the discrete nature of the plasma. The right-hand side, by contrast, is very sensitive, and is ultimately responsible for collisional effects. Note that it is quadratic in δF. To solve this equation, we must write $\langle \delta F_\beta \delta F_\alpha \rangle$ in terms of f_α.

First, rearrange (III.6.4) to obtain

$$\begin{aligned}\dot{f}_\alpha(t,\boldsymbol{x}) &\doteq \left[\frac{\partial}{\partial t} + \boldsymbol{v}\cdot\boldsymbol{\nabla} + \frac{q_\alpha}{m_\alpha}\left(\boldsymbol{E} + \frac{\boldsymbol{v}}{c}\times\boldsymbol{B}\right)\cdot\frac{\partial}{\partial \boldsymbol{v}}\right] f_\alpha(t,\boldsymbol{x}) \\ &= \sum_\beta \frac{q_\alpha q_\beta}{m_\alpha}\int \mathrm{d}\boldsymbol{x}'\,\frac{\partial}{\partial \boldsymbol{r}}\frac{1}{|\boldsymbol{r}-\boldsymbol{r}'|}\cdot\frac{\partial}{\partial \boldsymbol{v}}\big\langle \delta F_\alpha(t,\boldsymbol{x})\delta F_\beta(t,\boldsymbol{x}')\big\rangle. \qquad \text{(III.6.5)}\end{aligned}$$

Next, write

$$\begin{aligned}\big\langle \delta F_\alpha(t,\boldsymbol{x})\delta F_\beta(t,\boldsymbol{x}')\big\rangle &= \big\langle (F_\alpha - f_\alpha)(F_\beta - f_\beta)\big\rangle \\ &= \big\langle F_\alpha F_\beta\big\rangle - \big\langle f_\alpha F_\beta\big\rangle - \big\langle F_\alpha f_\beta\big\rangle + \big\langle f_\alpha f_\beta\big\rangle \\ &= \big\langle F_\alpha F_\beta\big\rangle - f_\alpha f_\beta - f_\alpha f_\beta + f_\alpha f_\beta \\ &= \big\langle F_\alpha(t,\boldsymbol{x})F_\beta(t,\boldsymbol{x}')\big\rangle - f_\alpha(t,\boldsymbol{x})f_\beta(t,\boldsymbol{x}'). \qquad \text{(III.6.6)}\end{aligned}$$

We must calculate the correlation $\langle F_\alpha F_\beta\rangle$ in (III.6.6) using the Klimontovich distributions $F_\alpha(t,\boldsymbol{x}) = \sum_{i=1}^{N_\alpha}\delta(\boldsymbol{x}-\boldsymbol{X}_{\alpha i}(t))$ and $F_\beta(t,\boldsymbol{x}') = \sum_{j=1}^{N_\beta}\delta(\boldsymbol{x}'-\boldsymbol{X}_{\beta j}(t))$. To do so, first split up the sums into like-particle and unlike-particle pieces:

$$\begin{aligned}\big\langle F_\alpha(t,\boldsymbol{x})F_\beta(t,\boldsymbol{x}')\big\rangle &= \int \mathrm{d}\boldsymbol{X}_{\rm all}\sum_{i=1}^{N_\alpha}\sum_{j=1}^{N_\beta} P_N\,\delta(\boldsymbol{x}-\boldsymbol{X}_{\alpha i}(t))\delta(\boldsymbol{x}'-\boldsymbol{X}_{\beta j}(t)) \\ &= \delta_{\alpha\beta}\int \mathrm{d}\boldsymbol{X}_{\rm all}\sum_{i=1}^{N_\alpha}\sum_{j=1}^{N_\alpha} P_N\,\delta(\boldsymbol{x}-\boldsymbol{X}_{\alpha i}(t))\delta(\boldsymbol{x}'-\boldsymbol{X}_{\alpha j}(t)) \\ &\quad + (1-\delta_{\alpha\beta})\int \mathrm{d}\boldsymbol{X}_{\rm all}\sum_{i=1}^{N_\alpha}\sum_{j=1}^{N_\beta} P_N\,\delta(\boldsymbol{x}-\boldsymbol{X}_{\alpha i}(t))\delta(\boldsymbol{x}'-\boldsymbol{X}_{\beta j}(t)).\end{aligned} \qquad \text{(III.6.7)}$$

Next, separate out $i = j$ in the like-particle piece:

$$\begin{aligned}\big\langle F_\alpha(t,\boldsymbol{x})F_\beta(t,\boldsymbol{x}')\big\rangle &= \delta_{\alpha\beta}\left[\int \mathrm{d}\boldsymbol{X}_{\rm all}\sum_{i=1}^{N_\alpha} P_N\,\delta(\boldsymbol{x}-\boldsymbol{X}_{\alpha i}(t))\delta(\boldsymbol{x}'-\boldsymbol{x})\right. \\ &\qquad \left. + \sum_{i=1}^{N_\alpha}\sum_{j\neq i}^{N_\alpha}\int \mathrm{d}\boldsymbol{X}_{\rm all}\,P_N\,\delta(\boldsymbol{x}-\boldsymbol{X}_{\alpha i}(t))\delta(\boldsymbol{x}'-\boldsymbol{X}_{\alpha j}(t))\right] \\ &\quad + (1-\delta_{\alpha\beta})\int \mathrm{d}\boldsymbol{X}_{\rm all}\sum_{i=1}^{N_\alpha}\sum_{j=1}^{N_\beta} P_N\,\delta(\boldsymbol{x}-\boldsymbol{X}_{\alpha i}(t))\delta(\boldsymbol{x}'-\boldsymbol{X}_{\beta j}(t)).\end{aligned} \qquad \text{(III.6.8)}$$

Now use the indistinguishability of particles and the definitions of the one- and two-

particle distribution functions (see (III.4.1) and (III.4.2)) to find

$$\begin{aligned}\left\langle F_\alpha(t,\boldsymbol{x})F_\beta(t,\boldsymbol{x}')\right\rangle &= \delta_{\alpha\beta}\left[\delta(\boldsymbol{x}'-\boldsymbol{x})f_\alpha(t,\boldsymbol{x}) + \left(\frac{N_\alpha-1}{N_\alpha}\right)f_{\alpha\alpha}(t,\boldsymbol{x},\boldsymbol{x}')\right] \\ &\quad + (1-\delta_{\alpha\beta})f_{\alpha\beta}(t,\boldsymbol{x},\boldsymbol{x}') \\ &= \delta_{\alpha\beta}\delta(\boldsymbol{x}-\boldsymbol{x}')f_\alpha(t,\boldsymbol{x}) + f_{\alpha\beta}(t,\boldsymbol{x},\boldsymbol{x}') + \mathcal{O}\left(\frac{1}{N_\alpha}\right). \qquad \text{(III.6.9)}\end{aligned}$$

Substituting (III.6.9) into (III.6.5) and dropping the $\mathcal{O}(1/N_\alpha)$ term, we see that the first term $\propto\delta_{\alpha\beta}\delta(\boldsymbol{x}-\boldsymbol{x}')$ vanishes. This is because

$$\int \mathrm{d}\boldsymbol{r}'\,\delta(\boldsymbol{r}-\boldsymbol{r}')\frac{\partial}{\partial\boldsymbol{r}}\frac{1}{|\boldsymbol{r}-\boldsymbol{r}'|} = 0;$$

i.e., no self-interaction with the Coulomb force. Thus, equation (III.6.5) becomes

$$\dot{f}_\alpha = -\sum_\beta \frac{q_\alpha q_\beta}{m_\alpha}\int \mathrm{d}\boldsymbol{x}'\,\frac{\partial}{\partial\boldsymbol{r}}\frac{1}{|\boldsymbol{r}-\boldsymbol{r}'|}\cdot\frac{\partial}{\partial\boldsymbol{v}}\left[f_\alpha(t,\boldsymbol{x})f_\beta(t,\boldsymbol{x}') - f_{\alpha\beta}(t,\boldsymbol{x},\boldsymbol{x}')\right]. \qquad \text{(III.6.10)}$$

At this point, it's worth reiterating the definitions of f_α and $f_{\alpha\beta}$. f_α is the one-particle distribution function – the probability that a particle of species α has phase-space position $\boldsymbol{x}$ at time t in the interval $\mathrm{d}\boldsymbol{x}$ *regardless* of all other particles. No particle–particle interactions are encoded in f_α. $f_{\alpha\beta}$, on the other hand, is the joint probability that a particle of species α has phase-space position $\boldsymbol{x}$ at time t *and* a particle of species β has phase-space position $\boldsymbol{x}'$ at time t, *regardless* of all other particles. Now, suppose all particles were truly uncorrelated (i.e., no collisions). Then $f_{\alpha\beta}(t,\boldsymbol{x},\boldsymbol{x}') = f_\alpha(t,\boldsymbol{x})f_\beta(t,\boldsymbol{x}')$, and the right-hand side of (III.6.10) would vanish. This would return the Vlasov equation, $\dot{f}_\alpha = 0$. This suggests that we introduce some function, say, $g_{\alpha\beta}(t,\boldsymbol{x},\boldsymbol{x}')$, which captures their difference:

$$f_{\alpha\beta} = f_\alpha f_\beta + g_{\alpha\beta}. \qquad \text{(III.6.11)}$$

This is the first step in what is known as the *Mayer cluster (or cumulant) expansion*. It splits the statistically independent pieces of $f_{\alpha\beta}$, which have multiplicative probabilities, apart from the statistically dependent piece. It's almost always useful to split off the piece of a joint probability distribution that corresponds to uncorrelated events. Nicholson (1983) on page 54 of his textbook has a cute analogy concerning correlated and uncorrelated coin tosses and die rolls. I prefer Yahtzee: the difference between rolling each die separately versus putting them all in the can and shaking them all and rolling them all out at the same time, so that their mutual collisions influence which side of each die faces up when the system comes to rest.

So, now we have from (III.6.10) and (III.6.11) that

$$\boxed{\dot{f}_\alpha = \sum_\beta \frac{q_\alpha q_\beta}{m_\alpha}\int \mathrm{d}\boldsymbol{x}'\,\frac{\partial}{\partial\boldsymbol{r}}\frac{1}{|\boldsymbol{r}-\boldsymbol{r}'|}\cdot\frac{\partial}{\partial\boldsymbol{v}}g_{\alpha\beta}(t,\boldsymbol{x},\boldsymbol{x}')} \qquad \text{(III.6.12)}$$

This is the first step in what is known as the *BBGKY hierarchy* (Bogoliubov, Born, Green, Kirkwood, Yvon; 1935–1949): the evolution of the one-particle distribution depends on correlations between two particles.

Let us proceed to find an equation for how the two-particle correlation $g_{\alpha\beta}$ evolves:

$$\begin{aligned}\frac{\partial}{\partial t}g_{\alpha\beta}(t,\boldsymbol{x},\boldsymbol{x}') &= \frac{\partial}{\partial t}\big[f_{\alpha\beta}(t,\boldsymbol{x},\boldsymbol{x}') - f_\alpha(t,\boldsymbol{x})f_\beta(t,\boldsymbol{x}')\big]\\ &= \frac{\partial}{\partial t}\big[\big\langle F_\alpha(t,\boldsymbol{x})F_\beta(t,\boldsymbol{x}')\big\rangle - \delta_{\alpha\beta}\delta(\boldsymbol{x}-\boldsymbol{x}')\,f_\alpha(t,\boldsymbol{x}) - f_\alpha(t,\boldsymbol{x})f_\beta(t,\boldsymbol{x}')\big]\\ &= \Big\langle \frac{\partial F_\alpha(t,\boldsymbol{x})}{\partial t}F_\beta(t,\boldsymbol{x}') + F_\alpha(t,\boldsymbol{x})\frac{\partial F_\beta(t,\boldsymbol{x}')}{\partial t} - \delta_{\alpha\beta}\delta(\boldsymbol{x}-\boldsymbol{x}')\frac{\partial f_\alpha(t,\boldsymbol{x})}{\partial t}\\ &\quad - \frac{\partial f_\alpha(t,\boldsymbol{x})}{\partial t}f_\beta(t,\boldsymbol{x}') - f_\alpha(t,\boldsymbol{x})\frac{\partial f_\beta(t,\boldsymbol{x}')}{\partial t}\Big\rangle. \qquad \text{(III.6.13)}\end{aligned}$$

Using the Klimontovich equation (III.2.9) and the kinetic equation for the one-particle distribution function (III.6.12), and defining

$$\begin{aligned}\boldsymbol{a} &\doteq \frac{q_\alpha}{m_\alpha}\left[\boldsymbol{E}(t,\boldsymbol{r}) + \frac{\boldsymbol{v}}{c}\times\boldsymbol{B}(t,\boldsymbol{r})\right],\\ \boldsymbol{a}' &\doteq \frac{q_\beta}{m_\beta}\left[\boldsymbol{E}(t,\boldsymbol{r}') + \frac{\boldsymbol{v}'}{c}\times\boldsymbol{B}(t,\boldsymbol{r}')\right],\end{aligned}$$

equation (III.6.13) becomes

$$\begin{aligned}&\frac{\partial g_{\alpha\beta}(t,\boldsymbol{x},\boldsymbol{x}')}{\partial t}\\ &= \Big\langle\Big[-\boldsymbol{v}\cdot\boldsymbol{\nabla}F_\alpha(t,\boldsymbol{x}) - \boldsymbol{a}\cdot\frac{\partial F_\alpha(t,\boldsymbol{x})}{\partial\boldsymbol{v}} - \frac{q_\alpha}{m_\alpha}\delta\boldsymbol{E}(t,\boldsymbol{r})\cdot\frac{\partial F_\alpha(t,\boldsymbol{x})}{\partial\boldsymbol{v}}\Big]F_\beta(t,\boldsymbol{x}')\\ &+ F_\alpha(t,\boldsymbol{x})\Big[-\boldsymbol{v}'\cdot\boldsymbol{\nabla}'F_\beta(t,\boldsymbol{x}') - \boldsymbol{a}'\cdot\frac{\partial F_\beta(t,\boldsymbol{x}')}{\partial\boldsymbol{v}'} - \frac{q_\beta}{m_\beta}\delta\boldsymbol{E}(t,\boldsymbol{r}')\cdot\frac{\partial F_\beta(t,\boldsymbol{x}')}{\partial\boldsymbol{v}'}\Big]\\ &- \delta_{\alpha\beta}\delta(\boldsymbol{x}-\boldsymbol{x}')\Big[-\boldsymbol{v}\cdot\boldsymbol{\nabla}f_\alpha(t,\boldsymbol{x}) - \boldsymbol{a}\cdot\frac{\partial f_\alpha(t,\boldsymbol{x})}{\partial\boldsymbol{v}}\\ &\qquad + \sum_\gamma\frac{q_\alpha q_\gamma}{m_\alpha}\int\mathrm{d}\boldsymbol{x}''\,\frac{\partial}{\partial\boldsymbol{r}}\frac{1}{|\boldsymbol{r}-\boldsymbol{r}''|}\cdot\frac{\partial g_{\alpha\gamma}(t,\boldsymbol{x},\boldsymbol{x}'')}{\partial\boldsymbol{v}}\Big]\\ &- \Big[-\boldsymbol{v}\cdot\boldsymbol{\nabla}f_\alpha(t,\boldsymbol{x}) - \boldsymbol{a}\cdot\frac{\partial f_\alpha(t,\boldsymbol{x})}{\partial\boldsymbol{v}}\\ &\quad + \sum_\gamma\frac{q_\alpha q_\gamma}{m_\alpha}\int\mathrm{d}\boldsymbol{x}''\,\frac{\partial}{\partial\boldsymbol{r}}\frac{1}{|\boldsymbol{r}-\boldsymbol{r}''|}\cdot\frac{\partial g_{\alpha\gamma}(t,\boldsymbol{x},\boldsymbol{x}'')}{\partial\boldsymbol{v}}\Big]f_\beta(t,\boldsymbol{x}')\\ &- f_\alpha(t,\boldsymbol{x})\Big[-\boldsymbol{v}'\cdot\boldsymbol{\nabla}'f_\beta(t,\boldsymbol{x}') - \boldsymbol{a}'\cdot\frac{\partial f_\beta(t,\boldsymbol{x}')}{\partial\boldsymbol{v}'}\\ &\qquad + \sum_\gamma\frac{q_\beta q_\gamma}{m_\beta}\int\mathrm{d}\boldsymbol{x}''\,\frac{\partial}{\partial\boldsymbol{r}'}\frac{1}{|\boldsymbol{r}'-\boldsymbol{r}''|}\cdot\frac{\partial g_{\beta\gamma}(t,\boldsymbol{x}',\boldsymbol{x}'')}{\partial\boldsymbol{v}'}\Big]\Big\rangle. \qquad \text{(III.6.14)}\end{aligned}$$

Using (III.6.9) with $f_{\alpha\beta} = f_\alpha f_\beta + g_{\alpha\beta}$ (see (III.6.11)) in (III.6.14) gives

$$\big\langle F_\alpha(t,\boldsymbol{x})F_\beta(t,\boldsymbol{x}')\big\rangle = f_\alpha(t,\boldsymbol{x})f_\beta(t,\boldsymbol{x}') + g_{\alpha\beta}(t,\boldsymbol{x},\boldsymbol{x}') + \delta_{\alpha\beta}\delta(\boldsymbol{x}-\boldsymbol{x}')f_\alpha(t,\boldsymbol{x});$$

substituting this into (III.6.14) eliminates a lot of terms! Suppressing the time argument

for economy of notation,

$$\begin{aligned}\frac{\partial g_{\alpha\beta}(\boldsymbol{x},\boldsymbol{x}')}{\partial t} &= -\frac{q_\alpha}{m_\alpha}\left\langle \delta\boldsymbol{E}(\boldsymbol{r})\cdot\frac{\partial F_\alpha(\boldsymbol{x})}{\partial \boldsymbol{v}}\,F_\beta(\boldsymbol{x}')\right\rangle - \frac{q_\beta}{m_\beta}\left\langle F_\alpha(\boldsymbol{x})\,\delta\boldsymbol{E}(\boldsymbol{r}')\cdot\frac{\partial F_\beta(\boldsymbol{x}')}{\partial \boldsymbol{v}'}\right\rangle \\ &\quad - \left(\boldsymbol{v}\cdot\boldsymbol{\nabla}+\boldsymbol{a}\cdot\frac{\partial}{\partial\boldsymbol{v}}+\boldsymbol{v}'\cdot\boldsymbol{\nabla}'+\boldsymbol{a}'\cdot\frac{\partial}{\partial\boldsymbol{v}'}\right) g_{\alpha\beta}(\boldsymbol{x},\boldsymbol{x}') \\ &\quad - f_\beta(\boldsymbol{x}')\sum_\gamma \frac{q_\alpha q_\gamma}{m_\alpha}\int \mathrm{d}\boldsymbol{x}''\,\frac{\partial}{\partial\boldsymbol{r}}\frac{1}{|\boldsymbol{r}-\boldsymbol{r}''|}\cdot\frac{\partial g_{\alpha\gamma}(\boldsymbol{x},\boldsymbol{x}'')}{\partial\boldsymbol{v}} \\ &\quad - f_\alpha(\boldsymbol{x})\sum_\gamma \frac{q_\beta q_\gamma}{m_\beta}\int \mathrm{d}\boldsymbol{x}''\,\frac{\partial}{\partial\boldsymbol{r}'}\frac{1}{|\boldsymbol{r}'-\boldsymbol{r}''|}\cdot\frac{\partial g_{\beta\gamma}(\boldsymbol{x}',\boldsymbol{x}'')}{\partial\boldsymbol{v}'} \\ &\quad - \delta_{\alpha\beta}\delta(\boldsymbol{x}-\boldsymbol{x}')\sum_\gamma \frac{q_\alpha q_\gamma}{m_\alpha}\int \mathrm{d}\boldsymbol{x}''\,\frac{\partial}{\partial\boldsymbol{r}}\frac{1}{|\boldsymbol{r}-\boldsymbol{r}''|}\cdot\frac{\partial g_{\alpha\gamma}(\boldsymbol{x},\boldsymbol{x}'')}{\partial\boldsymbol{v}}, \end{aligned} \tag{III.6.15}$$

where the following identity has been used:

$$\left(\boldsymbol{v}\cdot\boldsymbol{\nabla}+\boldsymbol{a}\cdot\frac{\partial}{\partial\boldsymbol{v}}+\boldsymbol{v}'\cdot\boldsymbol{\nabla}'+\boldsymbol{a}'\cdot\frac{\partial}{\partial\boldsymbol{v}'}\right)\delta_{\alpha\beta}\delta(\boldsymbol{x}-\boldsymbol{x}')=0.$$

Writing

$$\delta\boldsymbol{E}(\boldsymbol{r}) = -\frac{\partial}{\partial\boldsymbol{r}}\sum_\gamma q_\gamma\int \mathrm{d}\boldsymbol{x}''\,\frac{\delta F_\gamma(\boldsymbol{x}'')}{|\boldsymbol{r}-\boldsymbol{r}''|},$$

$$\delta\boldsymbol{E}(\boldsymbol{r}') = -\frac{\partial}{\partial\boldsymbol{r}'}\sum_\gamma q_\gamma\int \mathrm{d}\boldsymbol{x}''\,\frac{\delta F_\gamma(\boldsymbol{x}'')}{|\boldsymbol{r}'-\boldsymbol{r}''|},$$

equation (III.6.15) becomes

$$\begin{aligned}&\left[\frac{\partial}{\partial t}+\boldsymbol{v}\cdot\boldsymbol{\nabla}+\boldsymbol{a}\cdot\frac{\partial}{\partial\boldsymbol{v}}+\boldsymbol{v}'\cdot\boldsymbol{\nabla}'+\boldsymbol{a}'\cdot\frac{\partial}{\partial\boldsymbol{v}'}\right] g_{\alpha\beta}(\boldsymbol{x},\boldsymbol{x}') \\ &\quad = \sum_\gamma \frac{q_\alpha q_\gamma}{m_\alpha}\int \mathrm{d}\boldsymbol{x}''\,\frac{\partial}{\partial\boldsymbol{r}}\frac{1}{|\boldsymbol{r}-\boldsymbol{r}''|}\cdot\frac{\partial}{\partial\boldsymbol{v}}\big\langle F_\alpha(\boldsymbol{x})F_\beta(\boldsymbol{x}')\delta F_\gamma(\boldsymbol{x}'')\big\rangle \\ &\quad + \sum_\gamma \frac{q_\beta q_\gamma}{m_\beta}\int \mathrm{d}\boldsymbol{x}''\,\frac{\partial}{\partial\boldsymbol{r}'}\frac{1}{|\boldsymbol{r}'-\boldsymbol{r}''|}\cdot\frac{\partial}{\partial\boldsymbol{v}'}\big\langle F_\alpha(\boldsymbol{x})F_\beta(\boldsymbol{x}')\delta F_\gamma(\boldsymbol{x}'')\big\rangle \\ &\quad - f_\beta(\boldsymbol{x}')\sum_\gamma \frac{q_\alpha q_\gamma}{m_\alpha}\int \mathrm{d}\boldsymbol{x}''\,\frac{\partial}{\partial\boldsymbol{r}}\frac{1}{|\boldsymbol{r}-\boldsymbol{r}''|}\cdot\frac{\partial g_{\alpha\gamma}(\boldsymbol{x},\boldsymbol{x}'')}{\partial\boldsymbol{v}} \\ &\quad - f_\alpha(\boldsymbol{x})\sum_\gamma \frac{q_\beta q_\gamma}{m_\beta}\int \mathrm{d}\boldsymbol{x}''\,\frac{\partial}{\partial\boldsymbol{r}'}\frac{1}{|\boldsymbol{r}'-\boldsymbol{r}''|}\cdot\frac{\partial g_{\beta\gamma}(\boldsymbol{x}',\boldsymbol{x}'')}{\partial\boldsymbol{v}'} \\ &\quad - \delta_{\alpha\beta}\delta(\boldsymbol{x}-\boldsymbol{x}')\sum_\gamma \frac{q_\alpha q_\gamma}{m_\alpha}\int \mathrm{d}\boldsymbol{x}''\,\frac{\partial}{\partial\boldsymbol{r}}\frac{1}{|\boldsymbol{r}-\boldsymbol{r}''|}\cdot\frac{\partial g_{\alpha\gamma}(\boldsymbol{x},\boldsymbol{x}'')}{\partial\boldsymbol{v}}. \end{aligned} \tag{III.6.16}$$

Things are starting to look better.

Note the appearance in (III.6.16) of the triple correlation $\langle F_\alpha F_\beta\,\delta F_\gamma\rangle$. Following a similar calculation that led to (III.6.9) for $\langle F_\alpha F_\beta\rangle$ gives

$$\begin{aligned}\big\langle F_\alpha(\boldsymbol{x})F_\beta(\boldsymbol{x}')F_\gamma(\boldsymbol{x}'')\big\rangle &= f_{\alpha\beta\gamma}(\boldsymbol{x},\boldsymbol{x}',\boldsymbol{x}'') \\ &\quad + \delta_{\alpha\beta}\delta(\boldsymbol{x}-\boldsymbol{x}')\,f_{\alpha\gamma}(\boldsymbol{x},\boldsymbol{x}'') + \delta_{\alpha\gamma}\delta(\boldsymbol{x}-\boldsymbol{x}'')\,f_{\alpha\beta}(\boldsymbol{x},\boldsymbol{x}') + \delta_{\beta\gamma}\delta(\boldsymbol{x}'-\boldsymbol{x}'')\,f_{\alpha\gamma}(\boldsymbol{x},\boldsymbol{x}'') \\ &\quad + \delta_{\alpha\beta}\delta_{\beta\gamma}\delta(\boldsymbol{x}-\boldsymbol{x}')\delta(\boldsymbol{x}'-\boldsymbol{x}'')f_\alpha(\boldsymbol{x}), \end{aligned} \tag{III.6.17}$$

so that

$$\begin{aligned}\big\langle F_\alpha(\boldsymbol{x})F_\beta(\boldsymbol{x}')\delta F_\gamma(\boldsymbol{x}'')\big\rangle &= f_{\alpha\beta\gamma}(\boldsymbol{x},\boldsymbol{x}',\boldsymbol{x}'') - f_{\alpha\beta}(\boldsymbol{x},\boldsymbol{x}')f_\gamma(\boldsymbol{x}'')\\ &+ \delta_{\alpha\beta}\delta(\boldsymbol{x}-\boldsymbol{x}')\big[f_{\alpha\gamma}(\boldsymbol{x},\boldsymbol{x}'') - f_\alpha(\boldsymbol{x})f_\gamma(\boldsymbol{x}'')\big] + \delta_{\alpha\gamma}\delta(\boldsymbol{x}-\boldsymbol{x}'')f_{\alpha\beta}(\boldsymbol{x},\boldsymbol{x}')\\ &+ \delta_{\beta\gamma}\delta(\boldsymbol{x}'-\boldsymbol{x}'')f_{\alpha\gamma}(\boldsymbol{x},\boldsymbol{x}'') + \delta_{\alpha\beta}\delta_{\beta\gamma}\delta(\boldsymbol{x}-\boldsymbol{x}')\delta(\boldsymbol{x}'-\boldsymbol{x}'')f_\alpha(\boldsymbol{x}). \qquad \text{(III.6.18)}\end{aligned}$$

To make further progress, write the three-particle distribution function $f_{\alpha\beta\gamma}$ using the Mayer cluster expansion,

$$\begin{aligned}f_{\alpha\beta\gamma}(\boldsymbol{x},\boldsymbol{x}',\boldsymbol{x}'') &= f_\alpha(\boldsymbol{x})f_\beta(\boldsymbol{x}')f_\gamma(\boldsymbol{x}'')\\ &+ f_\alpha(\boldsymbol{x})g_{\beta\gamma}(\boldsymbol{x}',\boldsymbol{x}'') + f_\beta(\boldsymbol{x}')g_{\alpha\gamma}(\boldsymbol{x},\boldsymbol{x}'') + f_\gamma(\boldsymbol{x}'')g_{\alpha\beta}(\boldsymbol{x},\boldsymbol{x}')\\ &+ h_{\alpha\beta\gamma}(\boldsymbol{x},\boldsymbol{x}',\boldsymbol{x}''), \qquad \text{(III.6.19)}\end{aligned}$$

where $h_{\alpha\beta\gamma}$ is the three-particle correlation function. Using (III.6.19) alongside $f_{\alpha\beta} = f_\alpha f_\beta + g_{\alpha\beta}$ (see (III.6.11)), equation (III.6.18) becomes

$$\begin{aligned}&\big\langle F_\alpha(\boldsymbol{x})F_\beta(\boldsymbol{x}')\delta F_\gamma(\boldsymbol{x}'')\big\rangle = f_\alpha(\boldsymbol{x})g_{\beta\gamma}(\boldsymbol{x}',\boldsymbol{x}'') + f_\beta(\boldsymbol{x}')g_{\alpha\gamma}(\boldsymbol{x},\boldsymbol{x}'')\\ &+ \delta_{\beta\gamma}\delta(\boldsymbol{x}'-\boldsymbol{x}'')\big[f_\alpha(\boldsymbol{x})f_\gamma(\boldsymbol{x}'') + g_{\alpha\gamma}(\boldsymbol{x},\boldsymbol{x}'')\big] + \delta_{\alpha\gamma}\delta(\boldsymbol{x}-\boldsymbol{x}'')\big[f_\alpha(\boldsymbol{x})f_\beta(\boldsymbol{x}') + g_{\alpha\beta}(\boldsymbol{x},\boldsymbol{x}')\big]\\ &+ \delta_{\alpha\beta}\delta(\boldsymbol{x}-\boldsymbol{x}')\big[\delta_{\beta\gamma}\delta(\boldsymbol{x}'-\boldsymbol{x}'')f_\alpha(\boldsymbol{x}) + g_{\alpha\gamma}(\boldsymbol{x},\boldsymbol{x}'')\big] + h_{\alpha\beta\gamma}(\boldsymbol{x},\boldsymbol{x}',\boldsymbol{x}''). \qquad \text{(III.6.20)}\end{aligned}$$

Plugging (III.6.20) back into (III.6.16) gives, after much simplification,

$$\begin{aligned}&\left(\frac{\partial}{\partial t} + \boldsymbol{v}\cdot\boldsymbol{\nabla} + \boldsymbol{a}\cdot\frac{\partial}{\partial\boldsymbol{v}} + \boldsymbol{v}'\cdot\boldsymbol{\nabla}' + \boldsymbol{a}'\cdot\frac{\partial}{\partial\boldsymbol{v}'}\right)g_{\alpha\beta}(t,\boldsymbol{x},\boldsymbol{x}')\\ &\quad - \sum_\gamma \frac{q_\alpha q_\gamma}{m_\alpha}\int \mathrm{d}\boldsymbol{x}''\,\frac{\partial}{\partial\boldsymbol{r}}\frac{1}{|\boldsymbol{r}-\boldsymbol{r}''|}\cdot\frac{\partial f_\alpha(t,\boldsymbol{x})}{\partial\boldsymbol{v}}\,g_{\beta\gamma}(t,\boldsymbol{x}',\boldsymbol{x}'')\\ &\quad - \sum_\gamma \frac{q_\beta q_\gamma}{m_\beta}\int \mathrm{d}\boldsymbol{x}''\,\frac{\partial}{\partial\boldsymbol{r}'}\frac{1}{|\boldsymbol{r}'-\boldsymbol{r}''|}\cdot\frac{\partial f_\beta(t,\boldsymbol{x}')}{\partial\boldsymbol{v}'}\,g_{\alpha\gamma}(t,\boldsymbol{x},\boldsymbol{x}'')\\ &\quad = \frac{\partial}{\partial\boldsymbol{r}}\frac{q_\alpha q_\beta}{|\boldsymbol{r}-\boldsymbol{r}'|}\cdot\left(\frac{1}{m_\alpha}\frac{\partial}{\partial\boldsymbol{v}} - \frac{1}{m_\beta}\frac{\partial}{\partial\boldsymbol{v}'}\right)\Big[f_\alpha(t,\boldsymbol{x})f_\beta(t,\boldsymbol{x}') + g_{\alpha\beta}(t,\boldsymbol{x},\boldsymbol{x}')\Big]\\ &\quad + \sum_\gamma q_\gamma\int \mathrm{d}\boldsymbol{x}''\left(\frac{1}{m_\alpha}\frac{\partial}{\partial\boldsymbol{r}}\frac{q_\alpha}{|\boldsymbol{r}-\boldsymbol{r}''|}\cdot\frac{\partial}{\partial\boldsymbol{v}} + \frac{1}{m_\beta}\frac{\partial}{\partial\boldsymbol{r}'}\frac{q_\beta}{|\boldsymbol{r}'-\boldsymbol{r}''|}\cdot\frac{\partial}{\partial\boldsymbol{v}'}\right)h_{\alpha\beta\gamma}(t,\boldsymbol{x},\boldsymbol{x}',\boldsymbol{x}'')\\ &\quad + \text{ self-interaction terms that vanish.} \qquad \text{(III.6.21)}\end{aligned}$$

Ugh! The evolution of $g_{\alpha\beta}$ depends on $h_{\alpha\beta\gamma}$!

We could keep going, but the set of equations we'll get is just as difficult to solve than the original Klimontovich equation. We must break the hierarchy at some point, in order to obtain a closed system of equations.

III.7. Closing the chain of statistical equations

There is a natural small parameter in a weakly coupled plasma:

$$\Lambda^{-1} \doteq (n\lambda_{\mathrm{D}}^3)^{-1} \lll 1; \qquad \text{(III.7.1)}$$

i.e., there are many particles in a Debye sphere. Recall that this also means that the average potential energy of the plasma is small compared to the average kinetic energy. To the extent that the potential energy due to interactions can be neglected, the plasma behaves like an ideal gas; thus, Λ^{-1} measures the size of departures of the thermodynamic properties of the plasma from those of an ideal gas.

Before explaining what this means for our BBGKY hierarchy, let us compare this situation with that of a gas of neutral particles. In that situation, the range of the interaction force r_0 is much smaller than the mean spacing δr of the particles $\sim n^{-1/3}$. Then it makes sense to expand particle correlations in the small parameter nr_0^3, and thus neglect the triple correlation. In other words, particle–particle collisions are sufficiently rare due to the small cross section that three-body collisions are much rarer than two-body collisions, with the presence of a third body affecting the collision between two bodies at an asymptotically small level. In a plasma, by contrast, $r_0 \approx \lambda_{\rm D} \gg n^{-1/3}$ implies $nr_0^3 \gg 1$. This is because Debye screening limits the range of the interaction potential, but to a value that is still large compared to the average interparticle separation (i.e., the Coulomb force is long range compared to the scattering force of direct two-body collisions, but has its long range attenuated by Debye screening). However, this does not mean that three-body interactions are more important than two-body interactions, despite $nr_0^3 \gg 1$ for a plasma. This is because, even though a charged particle is interacting with all the particles in its Debye sphere and thus undergoes $\sim\Lambda$ simultaneous Coulomb collisions, such collisions are *weak*, in the sence that the effect of, say, particle A on particle B's orbit is small enough that the collision between particle B and another particle C is practically unaffected. This is because collisions in an ionized plasma result in small-angle (rather than large-angle) deflections. Another way of saying this is that the joint distribution $f_{\alpha\beta}$ of two particles in a small volume ($n^{-1} \ll \mathcal{V} \ll \lambda_{\rm D}^3$) is determined by the many particles outside of the volume rather than by the separation of the two particles from one another; i.e., $f_{\alpha\beta} \approx f_\alpha f_\beta$. We will prove this explicitly in due course, but for now we use these arguments to order

$$\begin{aligned} f_\alpha &\sim \mathcal{O}(1), \\ g_{\alpha\beta} &\sim \mathcal{O}(\Lambda^{-1}), \\ h_{\alpha\beta\gamma} &\sim \mathcal{O}(\Lambda^{-2}), \\ &\dots \end{aligned}$$

Thus, the BBGKY hierarchy can be truncated by dropping, say, three-body interactions ($h_{\alpha\beta\gamma} \to 0$). In this case, our closed set of kinetic equations is:

$$\left(\frac{\partial}{\partial t} + \boldsymbol{v}\cdot\boldsymbol{\nabla} + \boldsymbol{a}\cdot\frac{\partial}{\partial \boldsymbol{v}}\right) f_\alpha(t,\boldsymbol{x}) = \sum_\beta \frac{q_\alpha q_\beta}{m_\alpha}\int \mathrm{d}\boldsymbol{x}'\, \frac{\partial}{\partial \boldsymbol{r}}\frac{1}{|\boldsymbol{r}-\boldsymbol{r}'|}\cdot\frac{\partial g_{\alpha\beta}(t,\boldsymbol{x},\boldsymbol{x}')}{\partial \boldsymbol{v}}, \quad \text{(III.7.2)}$$

$$\begin{aligned} &\left(\frac{\partial}{\partial t} + \boldsymbol{v}\cdot\boldsymbol{\nabla} + \boldsymbol{a}\cdot\frac{\partial}{\partial \boldsymbol{v}} + \boldsymbol{v}'\cdot\boldsymbol{\nabla}' + \boldsymbol{a}'\cdot\frac{\partial}{\partial \boldsymbol{v}'}\right) g_{\alpha\beta}(t,\boldsymbol{x},\boldsymbol{x}') \\ &\quad - \sum_\gamma \frac{q_\alpha q_\gamma}{m_\alpha}\int \mathrm{d}\boldsymbol{x}''\, \frac{\partial}{\partial \boldsymbol{r}}\frac{1}{|\boldsymbol{r}-\boldsymbol{r}''|}\cdot\frac{\partial f_\alpha(t,\boldsymbol{x})}{\partial \boldsymbol{v}}\, g_{\beta\gamma}(t,\boldsymbol{x}',\boldsymbol{x}'') \\ &\quad - \sum_\gamma \frac{q_\beta q_\gamma}{m_\beta}\int \mathrm{d}\boldsymbol{x}''\, \frac{\partial}{\partial \boldsymbol{r}'}\frac{1}{|\boldsymbol{r}'-\boldsymbol{r}''|}\cdot\frac{\partial f_\beta(t,\boldsymbol{x}')}{\partial \boldsymbol{v}'}\, g_{\alpha\gamma}(t,\boldsymbol{x},\boldsymbol{x}'') \\ &\quad = \frac{\partial}{\partial \boldsymbol{r}}\frac{q_\alpha q_\beta}{|\boldsymbol{r}-\boldsymbol{r}'|}\cdot\left(\frac{1}{m_\alpha}\frac{\partial}{\partial \boldsymbol{v}} - \frac{1}{m_\beta}\frac{\partial}{\partial \boldsymbol{v}'}\right)\Big[f_\alpha(t,\boldsymbol{x})f_\beta(t,\boldsymbol{x}') + g_{\alpha\beta}(t,\boldsymbol{x},\boldsymbol{x}')\Big], \end{aligned} \quad \text{(III.7.3)}$$

where

$$\boldsymbol{a} \doteq \frac{q_\alpha}{m_\alpha}\left[\boldsymbol{E}(t,\boldsymbol{r}) + \frac{\boldsymbol{v}}{c}\times\boldsymbol{B}(t,\boldsymbol{r})\right],$$
$$\boldsymbol{a}' \doteq \frac{q_\beta}{m_\beta}\left[\boldsymbol{E}(t,\boldsymbol{r}') + \frac{\boldsymbol{v}'}{c}\times\boldsymbol{B}(t,\boldsymbol{r}')\right],$$
$$\boldsymbol{E}(t,\boldsymbol{r}) = \boldsymbol{E}_{\rm ext}(t,\boldsymbol{r}) - \frac{\partial}{\partial\boldsymbol{r}}\sum_\gamma q_\gamma\int \mathrm{d}\boldsymbol{x}''\,\frac{f_\gamma(t,\boldsymbol{x}'')}{|\boldsymbol{r}-\boldsymbol{r}''|},$$
$$\boldsymbol{B}(t,\boldsymbol{r}) = \boldsymbol{B}_{\rm ext}(t,\boldsymbol{r}).$$

Physical description of each term in (III.7.3):

(1) RHS term $\propto f_\alpha f_\beta$: establishes a two-particle correlation between initially uncorrelated particles α and β caused by a binary Coulomb interaction.

(2) RHS term $\propto g_{\alpha\beta}$: drives changes to an existing two-particle correlation caused by a binary Coulomb interaction between α and β.

(3) LHS first term $\propto \dot{g}_{\alpha\beta}$: conservatively advects the two-particle correlation $g_{\alpha\beta}$ through phase space; the $\boldsymbol{a}\cdot\partial/\partial\boldsymbol{v}$ and $\boldsymbol{a}'\cdot\partial/\partial\boldsymbol{v}'$ terms represent the effect of the mean field on the two-particle correlation.

(4) LHS second term $\propto f_\alpha g_{\beta\gamma}$: modifies correlations between α and β, due to Coulomb interactions between particle α and all other particles γ in the bath that are correlated with β. This is an important *shielding* term, in which a typical particle in the bath both mediates and modifies the correlation between particles α and β.

(5) LHS third term $\propto f_\beta g_{\alpha\gamma}$: modifies correlations between α and β, due to Coulomb interactions between particle β and all other particles γ in the bath that are correlated with α. This is another important shielding term.

III.8. The Vlasov equation

Solutions to (III.7.3) are difficult to come by. If you take AST554: Irreversible Processes in Plasmas, you'll learn how to obtain one very important solution, called the Balescu–Lenard equation. But for now, let us drop two-particle correlations ($g_{\alpha\beta}\to 0$) to find the *Vlasov equation*:

$$\boxed{\dot{f}_\alpha \doteq \left[\frac{\partial}{\partial t} + \boldsymbol{v}\cdot\boldsymbol{\nabla} + \frac{q_\alpha}{m_\alpha}\left(\boldsymbol{E}+\frac{\boldsymbol{v}}{c}\times\boldsymbol{B}\right)\cdot\frac{\partial}{\partial\boldsymbol{v}}\right]f_\alpha(t,\boldsymbol{x}) = 0} \tag{III.8.1}$$

Thus, the one-particle distribution function f_α is our old familiar friend, customarily referred to as *the* distribution function of the plasma. The assumption here is that the phase densities at different points in 6D phase space are completely independent (but for collective interactions via electromagnetic fields). Let us use (III.7.3) to see whether this is a good assumption.

First, by ordering $\partial/\partial\boldsymbol{v}\sim v_{\rm th}^{-1}$ and $|\boldsymbol{r}-\boldsymbol{r}'|\sim\lambda_{\rm D}$, we find that the "collision operator" on the right-hand side of (III.7.2) satisfies

$$\left(\frac{\partial f}{\partial t}\right)_{\rm c} \sim \frac{q^2}{m}v_{\rm th}^3\frac{\lambda_{\rm D}}{v_{\rm th}}g \sim \frac{v_{\rm th}^3}{n}\omega_{\rm p}g.$$

Second, adopting $f\sim nv_{\rm th}^{-3}$ and $\partial g/\partial t\sim\omega_{\rm p}g$, where $\omega_{\rm p}$ is the plasma frequency, equation

(III.7.3) implies

$$\omega_{\rm p} g \sim \frac{q^2}{\lambda_{\rm D}^2}\frac{f^2}{m v_{\rm th}} \sim \frac{q^2}{\lambda_{\rm D}^2}\frac{f}{m v_{\rm th}}\frac{n}{v_{\rm th}^3} \sim \frac{\omega_{\rm p}}{\lambda_{\rm D}^3}\frac{1}{v_{\rm th}^3} f.$$

Thus,

$$\left(\frac{\partial f}{\partial t}\right)_{\rm c} \sim \frac{1}{n\lambda_{\rm D}^3}\,\omega_{\rm p} f = \frac{1}{\Lambda}\omega_{\rm p} f \lll \omega_{\rm p} f. \tag{III.8.2}$$

As $\Lambda \to \infty$, we obtain the Vlasov equation.

Before we do anything with the Vlasov equation, a comment is in order. Consider the following excerpt from page 38 of Ichimaru (2004):

> It is interesting to note a formal similarity between the Vlasov equation and the Klimontovich equation... Yet it is quite important also to note the fundamental difference in the physical contents between the two equations: while the Klimontovich equation deals with the microscopic distribution function, containing all the fine structures arising from the individuality of the particles, the Vlasov equation is concerned with a coarse-grained distribution function obtained from a statistical average of the microscopic distribution function. The fluctuations due to discreteness of the particles have not been retained in the Vlasov equation.

In the next section, I offer a few abbreviated words on these "fluctuations due to discreteness of the particles" – i.e., Coulomb collisions.

III.9. A brief primer on collisions and irreversibility

First, take another look at the Vlasov equation (III.8.1), rewritten here:

$$\dot{f}_\alpha(t,\boldsymbol{x}) \doteq \left[\frac{\partial}{\partial t} + \boldsymbol{v}\cdot\boldsymbol{\nabla} + \frac{q_\alpha}{m_\alpha}\left(\boldsymbol{E} + \frac{\boldsymbol{v}}{c}\times\boldsymbol{B}\right)\cdot\frac{\partial}{\partial \boldsymbol{v}}\right] f_\alpha(t,\boldsymbol{x}) = 0. \tag{III.9.1}$$

Note that setting $t \to t' \doteq -t$, $\boldsymbol{r} \to \boldsymbol{r}' \doteq \boldsymbol{r}$, $\boldsymbol{v} \to \boldsymbol{v}' \doteq -\boldsymbol{v}$, $f_\alpha \to f'_\alpha \doteq f_\alpha(-t,\boldsymbol{r},-\boldsymbol{v})$, $\boldsymbol{E} \to \boldsymbol{E}' \doteq \boldsymbol{E}(-t,\boldsymbol{r})$, and $\boldsymbol{B} \to \boldsymbol{B}' \doteq -\boldsymbol{B}(-t,\boldsymbol{r})$ in (III.9.1) changes nothing:

$$\left[\frac{\partial}{\partial t'} + \boldsymbol{v}'\cdot\boldsymbol{\nabla}' + \frac{q_\alpha}{m_\alpha}\left(\boldsymbol{E}' + \frac{\boldsymbol{v}'}{c}\times\boldsymbol{B}'\right)\cdot\frac{\partial}{\partial \boldsymbol{v}'}\right] f'_\alpha(t',\boldsymbol{x}') = 0.$$

Thus, the Vlasov–Maxwell set of equations is *time-reversible*. All information about the phase-space fluid elements is preserved for all time.

Next, calculate the evolution of the entropy,

$$\mathcal{S} \doteq -\sum_\alpha \int {\rm d}\boldsymbol{x}\, f_\alpha(t,\boldsymbol{x}) \ln f_\alpha(t,\boldsymbol{x}), \tag{III.9.2}$$

in a Vlasov plasma:

$$\dot{\mathcal{S}} = -\sum_\alpha \int {\rm d}\boldsymbol{x}\, \dot{f}_\alpha\big(1+\ln f_\alpha\big) = 0. \tag{III.9.3}$$

Entropy is constant. What a comforting thought.

Of course, these things aren't generally true. The world is not time-reversible, no matter how much we wish it to be so. In dropping

$$-\left\langle \frac{q_\alpha}{m_\alpha}\left(\delta\boldsymbol{E} + \frac{\boldsymbol{v}}{c}\times\delta\boldsymbol{B}\right)\cdot\frac{\partial \delta F_\alpha}{\partial \boldsymbol{v}}\right\rangle$$

from the right-hand side of the Liouville-averaged Klimontovich equation (see (III.5.9)), we have lost entropy-increasing collisional dissipation and irreversibility. It's actually a lot

of work to (rigorously or not) derive the appropriate collision operator, Balescu–Lenard (Balescu 1960; Lenard 1960) or Landau (Landau 1937), and so I'll simply write down the latter, as if it's entirely obvious from whence it came:

$$C[f_\alpha] = \sum_\beta \frac{2\pi q_\alpha^2 q_\beta^2 \ln\lambda_{\alpha\beta}}{m_\alpha} \frac{\partial}{\partial \boldsymbol{v}} \cdot \int \mathrm{d}\boldsymbol{v}' \, \boldsymbol{U}(\boldsymbol{v}-\boldsymbol{v}') \cdot \left(\frac{1}{m_\alpha}\frac{\partial}{\partial \boldsymbol{v}} - \frac{1}{m_\beta}\frac{\partial}{\partial \boldsymbol{v}'} \right) f_\alpha(\boldsymbol{v}) f_\beta(\boldsymbol{v}'), \tag{III.9.4}$$

where $\boldsymbol{U}(\boldsymbol{u}) \doteq (u^2\boldsymbol{I} - \boldsymbol{u}\boldsymbol{u})/u^3$ and $\ln\lambda_{\alpha\beta}$ is the Coulomb logarithm (see the NRL plasma formulary). If you want to know all the nitty-gritty details, I have detailed lecture notes, or you could just take AST554. But, in the meantime, here are some properties that any rigorously derived collision operator ought to satisfy:

- If $f_\alpha \geqslant 0$ at $t = 0$, then $f_\alpha \geqslant 0$ for all time t.
- Particle number is conserved:

$$\int \mathrm{d}\boldsymbol{v} \, C[f_\alpha] = 0 \quad \text{for each } \alpha.$$

- Total momentum is conserved:

$$\sum_\alpha \int \mathrm{d}\boldsymbol{v} \, m_\alpha \boldsymbol{v} \, C[f_\alpha] = 0.$$

  (NB: momentum of each individual species is *not* conserved. Newton would have a problem with that.)

- Total kinetic energy is conserved:

$$\sum_\alpha \int \mathrm{d}\boldsymbol{v} \, \frac{1}{2} m_\alpha v^2 \, C[f_\alpha] = 0.$$

  (NB: again, this holds only for the entire plasma, not each species by itself.)

- The entropy $\mathcal{S}$ (see (III.9.2)) can either increase or remain constant under the action of the collision operator. It *cannot* decrease!
- Maxwell distributions for all species with equal temperatures and mean velocities are a time-independent solution:

$$f_{\mathrm{M},\alpha} = \frac{n_\alpha}{\pi^{3/2} v_{\mathrm{th}\alpha}^3} \exp\left(-\frac{|\boldsymbol{v}-\boldsymbol{u}|^2}{v_{\mathrm{th}\alpha}^2} \right), \quad v_{\mathrm{th}\alpha}^2 \doteq \frac{2T}{m_\alpha}$$

  with the same temperature T and mean velocity $\boldsymbol{u}$ for all α.

- As $t \to \infty$, any f_α satisfying $f_\alpha \geqslant 0$ approaches a Maxwell distribution with equal temperatures and mean velocities for all species.

It's left as an exercise to the reader to show that (III.9.4) satisfies all of these properties.

In practice, the Balescu–Lenard and Landau collision operators are rarely used. When collision aren't simply thrown out altogether, various simplified operators are chosen, mostly based on their analytical and/or numerical tractability, but also because some of them can be obtained rigorously as certain limits of the full Landau operator. Here are just a few, which are provided mainly so that you recognize them if they ever cross into

your future light cone:

Bhatnagar–Gross–Krook (BGK): $C[f_\alpha] = -\nu(f_\alpha - f_{\mathrm{M},\alpha})$

Lenard–Bernstein: $C[f_\alpha] = \nu \dfrac{\partial}{\partial \boldsymbol{v}} \cdot \Bigg[\underbrace{(\boldsymbol{v}-\boldsymbol{u}) f_\alpha}_{\text{drag}} + \underbrace{\dfrac{v_{\mathrm{th}\alpha}^2}{2} \dfrac{\partial f_\alpha}{\partial \boldsymbol{v}}}_{\text{diffusion}} \Bigg]$

Lorentz: $C[f_\alpha] = \nu \mathcal{L}[f_\alpha]$

$$\text{where } \mathcal{L} \doteq \underbrace{\frac{1}{2}\left[\frac{\partial}{\partial \xi}(1-\xi^2)\frac{\partial}{\partial \xi} + \frac{1}{1-\xi^2}\frac{\partial}{\partial \phi_v^2}\right]}_{\text{velocity pitch-angle diffusion; } \xi \doteq \cos\theta_v}$$

Fokker–Planck: $$C[f_\alpha] = \underbrace{-\frac{\partial}{\partial \boldsymbol{v}} \cdot \left[\boldsymbol{A}_\alpha(\boldsymbol{v}) f_\alpha\right]}_{\text{drag}} + \underbrace{\frac{1}{2}\frac{\partial}{\partial \boldsymbol{v}}\frac{\partial}{\partial \boldsymbol{v}} : \left[\boldsymbol{B}_\alpha(\boldsymbol{v}) f_\alpha\right]}_{\text{diffusion}} .$$

The velocity-dependent Fokker–Planck coefficients $\boldsymbol{A}_\alpha$ and $\boldsymbol{B}_\alpha$ are related to the "jump moments" $\langle \Delta \boldsymbol{v} \rangle$ and $\langle \Delta \boldsymbol{v} \Delta \boldsymbol{v} \rangle$, which are expectation values for changes and correlations in particle velocities over a short (but not too short – there is a Markov assumption involved) interval of time.

III.10. Moments of the kinetic equation

Accepting that there *is* a collision operator – whatever it is – one may proceed to take moments of the kinetic equation to obtain "fluid" equations, with which you are undoubtedly more familiar. Start with the Vlasov–Landau equation, repeated here for convenience:

$$\dot{f}_\alpha \doteq \frac{\partial f_\alpha}{\partial t} + \boldsymbol{v} \cdot \boldsymbol{\nabla} f_\alpha + \frac{q_\alpha}{m_\alpha}\left(\boldsymbol{E} + \frac{\boldsymbol{v}}{c} \times \boldsymbol{B}\right) \cdot \frac{\partial f_\alpha}{\partial \boldsymbol{v}} = C[f_\alpha].$$

We could of course add additional forces on the charged particles, such as that due to gravity, $m_\alpha \boldsymbol{g}$. Since we'll use quasi-neutrality to eliminate $\boldsymbol{E}$ at some point, let's do that:

$$\dot{f}_\alpha \doteq \frac{\partial f_\alpha}{\partial t} + \boldsymbol{v} \cdot \boldsymbol{\nabla} f_\alpha + \left[\frac{q_\alpha}{m_\alpha}\left(\boldsymbol{E} + \frac{\boldsymbol{v}}{c} \times \boldsymbol{B}\right) + \boldsymbol{g}\right] \cdot \frac{\partial f_\alpha}{\partial \boldsymbol{v}} = C[f_\alpha]. \tag{III.10.1}$$

Now, $\boldsymbol{v}$ contains both thermal and mean velocities. It is useful to split them apart (e.g., because they might have very different magnitudes):

$$\boldsymbol{w} \doteq \boldsymbol{v} - \boldsymbol{u}_\alpha(t, \boldsymbol{r}), \tag{III.10.2}$$

where

$$\boldsymbol{u}_\alpha(t, \boldsymbol{r}) \doteq \frac{1}{n_\alpha} \int \mathrm{d}\boldsymbol{v}\, \boldsymbol{v} f_\alpha, \quad n_\alpha(t, \boldsymbol{r}) \doteq \int \mathrm{d}\boldsymbol{v}\, f_\alpha. \tag{III.10.3}$$

Enacting this transformation of variables, $f_\alpha(t, \boldsymbol{r}, \boldsymbol{v}) \to f_\alpha(t, \boldsymbol{r}, \boldsymbol{w})$, through the use of

$$\left.\frac{\partial}{\partial t}\right|_{\boldsymbol{v}} = \left.\frac{\partial}{\partial t}\right|_{\boldsymbol{w}} + \left.\frac{\partial \boldsymbol{w}}{\partial t}\right|_{\boldsymbol{v}} \cdot \frac{\partial}{\partial \boldsymbol{w}} = \left.\frac{\partial}{\partial t}\right|_{\boldsymbol{w}} - \frac{\partial \boldsymbol{u}_\alpha}{\partial t} \cdot \frac{\partial}{\partial \boldsymbol{w}}, \tag{III.10.4}$$

$$\left.\frac{\partial}{\partial \boldsymbol{r}}\right|_{\boldsymbol{v}} = \left.\frac{\partial}{\partial \boldsymbol{r}}\right|_{\boldsymbol{w}} + \left.\frac{\partial \boldsymbol{w}}{\partial \boldsymbol{r}}\right|_{\boldsymbol{v}} \cdot \frac{\partial}{\partial \boldsymbol{w}} = \left.\frac{\partial}{\partial \boldsymbol{r}}\right|_{\boldsymbol{w}} - \frac{\partial \boldsymbol{u}_\alpha}{\partial \boldsymbol{r}} \cdot \frac{\partial}{\partial \boldsymbol{w}}, \tag{III.10.5}$$

equation (III.10.1) becomes

$$\frac{\mathrm{D}f_\alpha}{\mathrm{D}t_\alpha} + \boldsymbol{w}\cdot\boldsymbol{\nabla}f_\alpha + \Bigg[\underbrace{\frac{q_\alpha}{m_\alpha}\left(\boldsymbol{E}+\frac{\boldsymbol{u}_\alpha}{c}\times\boldsymbol{B}\right)+\boldsymbol{g}-\frac{\mathrm{D}\boldsymbol{u}_\alpha}{\mathrm{D}t_\alpha}}_{\doteq\,\boldsymbol{a}_\alpha(t,\boldsymbol{r})} + \frac{q_\alpha}{m_\alpha}\left(\frac{\boldsymbol{w}}{c}\times\boldsymbol{B}\right) - \boldsymbol{w}\cdot\boldsymbol{\nabla}\boldsymbol{u}_\alpha\Bigg]\cdot\frac{\partial f_\alpha}{\partial\boldsymbol{w}}$$
$$= C[f_\alpha], \tag{III.10.6}$$

where

$$\frac{\mathrm{D}}{\mathrm{D}t_\alpha} \doteq \frac{\partial}{\partial t} + \boldsymbol{u}_\alpha\cdot\boldsymbol{\nabla} \tag{III.10.7}$$

is the Lagrangian time derivative taken in the frame comoving with the mean velocity $\boldsymbol{u}_\alpha$ of species α. The additional acceleration terms in (III.10.6) that result from the frame transformation, *viz.* $\mathrm{D}\boldsymbol{u}_\alpha/\mathrm{D}t_\alpha$ and $\boldsymbol{w}\cdot\boldsymbol{\nabla}\boldsymbol{u}_\alpha$, are the result of boosting to a time- and space-dependent frame. The former term is fairly self-explanatory – particles must be accelerated so as to continue residing in the "fluid element" they comprise, which is itself being accelerated by various (magneto)hydrodynamic forces that result in $\mathrm{D}\boldsymbol{u}_\alpha/\mathrm{D}t_\alpha$– but the latter deserves some discussion. Imagine you are trying to walk at constant velocity $\boldsymbol{w} = w\hat{\boldsymbol{x}}$ across several layers of differentially moving conveyor belts with velocities $\boldsymbol{u} = u(x)\hat{\boldsymbol{y}}$, as in the figure below. In your frame (and the frame of the conveyor belts), your velocity will always be $w\hat{\boldsymbol{x}}$. But, in the lab frame, your velocity will include the velocity of the conveyor belts. This means that, extra time you step onto a new conveyor belt that has some velocity oriented in the y direction that is different from that of the last conveyor belt, you will be accelerating in the lab frame. That is, your velocity in the lab frame will change over an interval of time from one conveyor belt to the next. Mathematically, the figure below corresponds to an acceleration $w\Delta u_y/\Delta x$ every time you step from one conveyor belt at position x with velocity $u\hat{\boldsymbol{y}}$ to another conveyor belt at position $x+\Delta x$ with velocity $(u+\Delta u)\hat{\boldsymbol{y}}$. The difference between these two points of view is enacted by adding $-\boldsymbol{w}\cdot\boldsymbol{\nabla}\boldsymbol{u}_\alpha$ to the acceleration term of (III.10.6).

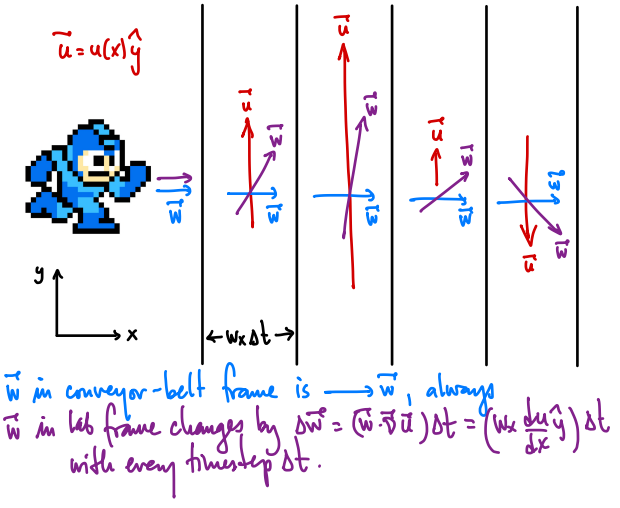

Next, take those moments:

$$\int \mathrm{d}\boldsymbol{w}\,(\text{III.10.6}): \quad \frac{\mathrm{D}}{\mathrm{D}t_\alpha}\cancelto{n_\alpha}{\int \mathrm{d}\boldsymbol{w}\, f_\alpha} + \cancelto{0}{\int \mathrm{d}\boldsymbol{w}\,\boldsymbol{w}\cdot\boldsymbol{\nabla} f_\alpha} + \boldsymbol{a}_\alpha \cdot \cancelto{0}{\int \mathrm{d}\boldsymbol{w}\,\frac{\partial f_\alpha}{\partial \boldsymbol{w}}}$$
$$+ \frac{q_\alpha}{m_\alpha}\cancelto{0}{\int \mathrm{d}\boldsymbol{w}\left(\frac{\boldsymbol{w}}{c}\times\boldsymbol{B}\right)\cdot\frac{\partial f_\alpha}{\partial \boldsymbol{w}}} - \underbrace{\int \mathrm{d}\boldsymbol{w}\,(\boldsymbol{w}\cdot\boldsymbol{\nabla}\boldsymbol{u}_\alpha)\cdot\frac{\partial f_\alpha}{\partial \boldsymbol{w}}}_{\overset{\text{bp}}{=} -(\boldsymbol{\nabla}\cdot\boldsymbol{u}_\alpha)\cancelto{n_\alpha}{\int \mathrm{d}\boldsymbol{w}\, f_\alpha}}$$
$$= \cancelto{0}{\int \mathrm{d}\boldsymbol{w} C[f_\alpha]}$$

$$\implies \boxed{\frac{\mathrm{D}n_\alpha}{\mathrm{D}t_\alpha} + n_\alpha \boldsymbol{\nabla}\cdot\boldsymbol{u}_\alpha = 0} \quad \text{(continuity equation for species } \alpha) \tag{III.10.8}$$

$$\int \mathrm{d}\boldsymbol{w}\, m_\alpha \boldsymbol{w}(\text{III.10.6}): \quad \frac{\mathrm{D}}{\mathrm{D}t_\alpha}\cancelto{0}{\int \mathrm{d}\boldsymbol{w}\, m_\alpha \boldsymbol{w} f_\alpha} + \int \mathrm{d}\boldsymbol{w}\, m_\alpha \boldsymbol{w}\boldsymbol{w}\cdot\boldsymbol{\nabla} f_\alpha + m_\alpha \boldsymbol{a}_\alpha \cdot \underbrace{\int \mathrm{d}\boldsymbol{w}\,\boldsymbol{w}\frac{\partial f_\alpha}{\partial \boldsymbol{w}}}_{\overset{\text{bp}}{=} -n_\alpha \boldsymbol{I}}$$
$$+ q_\alpha \cancelto{0}{\int \mathrm{d}\boldsymbol{w}\,\boldsymbol{w}\left(\frac{\boldsymbol{w}}{c}\times\boldsymbol{B}\right)\cdot\frac{\partial f_\alpha}{\partial \boldsymbol{w}}} - \cancelto{0}{\int \mathrm{d}\boldsymbol{w}\, m_\alpha \boldsymbol{w}(\boldsymbol{w}\cdot\boldsymbol{\nabla}\boldsymbol{u}_\alpha)\cdot\frac{\partial f_\alpha}{\partial \boldsymbol{w}}}$$
$$= \int \mathrm{d}\boldsymbol{w}\, m_\alpha \boldsymbol{w} C[f_\alpha]$$

$$\implies \boxed{\boldsymbol{\nabla}\cdot\boldsymbol{P}_\alpha - m_\alpha n_\alpha \boldsymbol{a}_\alpha = \int \mathrm{d}\boldsymbol{w}\, m_\alpha \boldsymbol{w} C[f_\alpha] \doteq \boldsymbol{R}_\alpha} \quad \text{(force equation for species } \alpha) \tag{III.10.9}$$

where

$$\boxed{\boldsymbol{P}_\alpha \doteq \int \mathrm{d}\boldsymbol{w}\, m_\alpha \boldsymbol{w}\boldsymbol{w} f_\alpha} \tag{III.10.10}$$

is the thermal pressure tensor of species α and $\boldsymbol{R}_\alpha$ is the friction force on species α (recall Newton's third law, $\sum_\alpha \boldsymbol{R}_\alpha = 0$). Equation (III.10.9) may of course be rewritten in the following, perhaps more familiar, form:

$$m_\alpha n_\alpha \frac{\mathrm{D}\boldsymbol{u}_\alpha}{\mathrm{D}t_\alpha} = q_\alpha n_\alpha\left(\boldsymbol{E} + \frac{\boldsymbol{u}_\alpha}{c}\times\boldsymbol{B}\right) + m_\alpha n_\alpha \boldsymbol{g} - \boldsymbol{\nabla}\cdot\boldsymbol{P}_\alpha + \boldsymbol{R}_\alpha. \tag{III.10.11}$$

If we sum (III.10.11) over species, the electric-field term vanishes by quasineutrality, $\sum_\alpha q_\alpha n_\alpha = 0$. Then, defining the total mass density $\varrho \doteq \sum_\alpha m_\alpha n_\alpha$ and the mean center-of-mass velocity $\boldsymbol{u} \doteq \varrho^{-1}\sum_\alpha m_\alpha n_\alpha \boldsymbol{u}_\alpha$, equation (III.10.11) implies

$$\varrho\left(\frac{\partial}{\partial t} + \boldsymbol{u}\cdot\boldsymbol{\nabla}\right)\boldsymbol{u} = \frac{\boldsymbol{j}}{c}\times\boldsymbol{B} + \varrho\boldsymbol{g} - \boldsymbol{\nabla}\cdot(\boldsymbol{P} + \boldsymbol{D}), \tag{III.10.12}$$

where

$$\boldsymbol{j} = \sum_\alpha q_\alpha n_\alpha \boldsymbol{u}_\alpha \tag{III.10.13}$$

is the current density, $\boldsymbol{P} \doteq \sum_\alpha \boldsymbol{P}_\alpha$ is the total pressure tensor, and

$$\boldsymbol{D} \doteq \sum_\alpha m_\alpha n_\alpha \Delta\boldsymbol{u}_\alpha \Delta\boldsymbol{u}_\alpha \tag{III.10.14}$$

is a tensor composed of species drifts relative to the center-of-mass velocity,

$$\Delta\boldsymbol{u}_\alpha \doteq \boldsymbol{u}_\alpha - \boldsymbol{u}. \tag{III.10.15}$$

(Note that $\sum_\alpha m_\alpha n_\alpha \Delta\boldsymbol{u}_\alpha = 0$, by definition.) Returning to those moments...

$$\begin{aligned}
\int \mathrm{d}\boldsymbol{w}\, m_\alpha w_i w_j (\text{III.10.6}) : \quad & \frac{\mathrm{D}}{\mathrm{D}t_\alpha} \underbrace{\int \mathrm{d}\boldsymbol{w}\, m_\alpha w_i w_j}_{= P_{\alpha,ij}} + \int \mathrm{d}\boldsymbol{w}\, m_\alpha w_i w_j \boldsymbol{w}\cdot\boldsymbol{\nabla} f_\alpha \\
& + m_\alpha a_{\alpha,k} \cancelto{0}{\int \mathrm{d}\boldsymbol{w}\, w_i w_j \frac{\partial f_\alpha}{\partial w_k}} \\
& + \underbrace{\int \mathrm{d}\boldsymbol{w}\, q_\alpha w_i w_j \left(\frac{\boldsymbol{w}}{c}\times\boldsymbol{B}\right)\cdot\frac{\partial f_\alpha}{\partial \boldsymbol{w}}}_{\overset{\text{bp}}{=} -\int \mathrm{d}\boldsymbol{w}\, q_\alpha \left[w_i\left(\frac{\boldsymbol{w}}{c}\times\boldsymbol{B}\right)_j + \left(\frac{\boldsymbol{w}}{c}\times\boldsymbol{B}\right)_i w_j\right] f_\alpha} \\
& \qquad = -\frac{q_\alpha}{m_\alpha}\left(\frac{\boldsymbol{P}_\alpha}{c}\times\boldsymbol{B}\right)_{ij} - \frac{q_\alpha}{m_\alpha}\left(\frac{\boldsymbol{P}_\alpha}{c}\times\boldsymbol{B}\right)_{ji} \\
& - \underbrace{\int \mathrm{d}\boldsymbol{w}\, m_\alpha w_i w_j (\boldsymbol{w}\cdot\boldsymbol{\nabla} u_{\alpha,\ell}) \frac{\partial f_\alpha}{\partial w_\ell}}_{\overset{\text{bp}}{=} -\int \mathrm{d}\boldsymbol{w}\, m_\alpha \left[w_i(\boldsymbol{w}\cdot\boldsymbol{\nabla}u_{\alpha,j}) + (\boldsymbol{w}\cdot\boldsymbol{\nabla}u_{\alpha,i}) w_j + w_i w_j (\boldsymbol{\nabla}\cdot\boldsymbol{u}_\alpha)\right] f_\alpha} \\
& \qquad = -(\boldsymbol{P}_\alpha\cdot\boldsymbol{\nabla}\boldsymbol{u}_\alpha)_{ij} - (\boldsymbol{P}_\alpha\cdot\boldsymbol{\nabla}\boldsymbol{u}_\alpha)_{ji} - \boldsymbol{P}_\alpha(\boldsymbol{\nabla}\cdot\boldsymbol{u}_\alpha) \\
& = \int \mathrm{d}\boldsymbol{w}\, m_\alpha w_i w_j C[f_\alpha].
\end{aligned} \tag{III.10.16}$$

Define the heat flux tensor for species α:

$$\boldsymbol{Q}_\alpha \doteq \int \mathrm{d}\boldsymbol{w}\, m_\alpha \boldsymbol{w}\boldsymbol{w}\boldsymbol{w} f_\alpha. \tag{III.10.17}$$

Then, equation (III.10.16) becomes

$$\begin{aligned}
& \frac{\mathrm{D}\boldsymbol{P}_\alpha}{\mathrm{D}t_\alpha} + \boldsymbol{\nabla}\cdot\boldsymbol{Q}_\alpha + \frac{q_\alpha}{m_\alpha}\left[\left(\frac{\boldsymbol{P}_\alpha}{c}\times\boldsymbol{B}\right) + \left(\frac{\boldsymbol{P}_\alpha}{c}\times\boldsymbol{B}\right)^T\right] + \left[(\boldsymbol{P}_\alpha\cdot\boldsymbol{\nabla}\boldsymbol{u}_\alpha) + (\boldsymbol{P}_\alpha\cdot\boldsymbol{\nabla}\boldsymbol{u}_\alpha)^T\right] \\
& \quad + \boldsymbol{P}_\alpha(\boldsymbol{\nabla}\cdot\boldsymbol{u}_\alpha) = \int \mathrm{d}\boldsymbol{w}\, m_\alpha \boldsymbol{w}\boldsymbol{w} C[f_\alpha],
\end{aligned} \tag{III.10.18}$$

where the superscript T denotes the transpose. In component form, (III.10.18) reads

$$\begin{aligned}
& \frac{\mathrm{D}P_{\alpha,ij}}{\mathrm{D}t_\alpha} + (\boldsymbol{\nabla}\cdot\boldsymbol{Q}_\alpha)_{ij} + \frac{q_\alpha}{m_\alpha}\left(\epsilon_{jk\ell}P_{\alpha,ik}B_\ell + \epsilon_{ik\ell}P_{\alpha,jk}B_\ell\right) \\
& \quad + \left(\delta_{i\ell}P_{\alpha,jk} + \delta_{j\ell}P_{\alpha,ik} + \delta_{k\ell}P_{\alpha,ij}\right)\frac{\partial u_{\alpha,\ell}}{\partial r_k} = \int \mathrm{d}\boldsymbol{w}\, m_\alpha w_i w_j C[f_\alpha].
\end{aligned} \tag{III.10.19}$$

Usually the trace of this equation is taken, with

$$p_\alpha \doteq \frac{1}{3}\mathrm{tr}\,\boldsymbol{P}_\alpha. \tag{III.10.20}$$

Then (III.10.18) provides an evolutionary equation for the internal energy:

$$\frac{3}{2}\frac{\mathrm{D}p_\alpha}{\mathrm{D}t_\alpha} + \boldsymbol{\nabla}\cdot\boldsymbol{q}_\alpha + \boldsymbol{P}_\alpha : \boldsymbol{\nabla}\boldsymbol{u}_\alpha + \frac{3}{2}p_\alpha \boldsymbol{\nabla}\cdot\boldsymbol{u}_\alpha = Q_\alpha, \tag{III.10.21}$$

where

$$\boldsymbol{q}_\alpha \doteq \int \mathrm{d}\boldsymbol{w}\, \frac{1}{2} m_\alpha w^2 \boldsymbol{w} f_\alpha \tag{III.10.22}$$

is the conductive heat flux of species α and

$$Q_\alpha \doteq \int \mathrm{d}\boldsymbol{w}\, \frac{1}{2} m_\alpha w^2 C[f_\alpha] \tag{III.10.23}$$

is the collisional energy exchange. Further writing

$$\boxed{\boldsymbol{P}_\alpha \doteq p_\alpha \boldsymbol{I} + \boldsymbol{\Pi}_\alpha,} \tag{III.10.24}$$

where $\boldsymbol{\Pi}_\alpha$ is the viscous stress tensor of species α and using (III.10.8) to replace $\boldsymbol{\nabla}\cdot\boldsymbol{u}_\alpha$ in (III.10.21) by $\mathrm{d}\ln n_\alpha/\mathrm{d}t$, the internal energy equation (III.10.21) provides an equation for the hydrodynamic entropy:

$$\boxed{\frac{3}{2}p_\alpha \frac{\mathrm{D}}{\mathrm{D}t_\alpha}\ln\frac{p_\alpha}{n_\alpha^{5/3}} = -\boldsymbol{\nabla}\cdot\boldsymbol{q}_\alpha - \boldsymbol{\Pi}_\alpha : \boldsymbol{\nabla}\boldsymbol{u}_\alpha + Q_\alpha} \tag{III.10.25}$$

Finally, using (III.10.24), the force equation (III.10.11) becomes

$$\boxed{m_\alpha n_\alpha \frac{\mathrm{D}\boldsymbol{u}_\alpha}{\mathrm{D}t_\alpha} = q_\alpha n_\alpha\left(\boldsymbol{E} + \frac{\boldsymbol{u}_\alpha}{c}\times\boldsymbol{B}\right) + m_\alpha n_\alpha \boldsymbol{g} - \boldsymbol{\nabla}p_\alpha - \boldsymbol{\nabla}\cdot\boldsymbol{\Pi}_\alpha + \boldsymbol{R}_\alpha} \tag{III.10.26}$$

Clearly, to close the system of hydrodynamic equations (viz., (III.10.8), (III.10.25), and (III.10.26)), we require $(\boldsymbol{\Pi}_\alpha, \boldsymbol{q}_\alpha, \boldsymbol{R}_\alpha, Q_\alpha)$ expressed in terms of the lower "fluid" moments $(n_\alpha, \boldsymbol{u}_\alpha, p_\alpha)$. This is the purpose of what is called the *Chapman–Enskog expansion*, which is only possible when the collisional mean free path is much smaller than the lengthscales of interest (e.g., gradient scales) so that the distribution function f_α is nearly Maxwellian. This will give a tractable kinetic equation, without time variation, which will close the moment equations and allow evolution on a slow timescale. The result is *magnetohydrodynamics*.

PART IV
Ideal hydrodynamics

Unfortunately, fluid dynamics has all but disappeared from the US undergraduate curriculum, as physics departments have made way for quantum mechanics and condensed matter.[11] This is a shame – yes, it's classical physics and thus draws less 'oohs' and 'aahs' from the student (and professorial, for that matter) crowd. But there are many good reasons to study it. First, it forms the bedrock of fascinating and modern topics like non-equilibrium statistical mechanics, including the kinetic theory of gases and particles. Second, it is mathematically rich without being physically opaque. The more you really understand the mathematics, the more you really understand physically what is going

[11] An excellent textbook from which to learn elementary fluid dynamics is Acheson's *Elementary Fluid Dynamics*. It provides an engaging mix of history, physical insight, and transparent mathematics. I recommend it.

on; the same cannot be said for many branches of modern physics. Third, nonlinear dynamics and chaos, burgeoning fields in their own right, are central to arguably the most important unsolved problem in classical physics: fluid turbulence. Solve that, and your solution would have immediate impact and practical benefits to society. Finally, follow in the footsteps of greatness: on Feynman's chalkboard at the time of his death was the remit 'to learn . . . nonlinear classical hydro'. With that, let's begin.

IV.1. The equations of ideal hydrodynamics

The equations of hydrodynamics and MHD may be obtained rigorously by taking velocity-space moments of the Boltzmann and Vlasov–Landau kinetic equations, as in §III.10. But they may be alternatively derived by using things every physicist should know: mass is conserved, Newton's second law (force equals mass times acceleration), and the first law of thermodynamics (energy is conserved).

IV.1.1. *Mass is conserved: The continuity equation*

We describe our gaseous fluid by a mass density ϱ, which in general is a function of time t and position $\boldsymbol{r}$.[12] Imagine an arbitrary fixed volume $\mathcal{V}$ enclosing some of that fluid. The mass inside of the volume is simply

$$M = \int_{\mathcal{V}} \mathrm{d}V\, \varrho. \tag{IV.1.1}$$

Now let's mathematize our intuition: within this fixed volume, the only way the enclosed mass can change is by material flowing in or out of its surface $\mathcal{S}$:

$$\frac{\mathrm{d}M}{\mathrm{d}t} \doteq \int_{\mathcal{V}} \mathrm{d}V\, \frac{\partial \varrho}{\partial t} = -\int_{\mathcal{S}} \mathrm{d}\boldsymbol{S}\cdot\varrho\boldsymbol{u}, \tag{IV.1.2}$$

where $\boldsymbol{u}$ is the flow velocity.

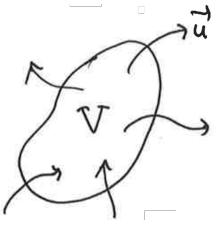

Gauss' theorem may be applied to rewrite the right-hand side of this equation as follows:

$$\int_{\mathcal{S}} \mathrm{d}\boldsymbol{S}\cdot\varrho\boldsymbol{u} = \int_{\mathcal{V}} \mathrm{d}V\, \boldsymbol{\nabla}\cdot(\varrho\boldsymbol{u}). \tag{IV.1.3}$$

Because the volume under consideration is arbitrary, the integrands of the volume integrals in (IV.1.2) and (IV.1.3) must be the same. Therefore,

$$\boxed{\frac{\partial \varrho}{\partial t} + \boldsymbol{\nabla}\cdot(\varrho\boldsymbol{u}) = 0} \tag{IV.1.4}$$

This is the *continuity equation*; it's the differential form of mass conservation.

[12] Here I denote the mass density by ϱ to avoid confusion with the Larmor radius ρ. But, given that ρ is standard notation in hydrodynamics for the mass density, and ρ is standard notation in plasma physics for the Larmor radius, you should learn to tell the difference based on the context.

Exercise. Go to the bathroom and turn on the sink slowly to get a nice, laminar stream flowing down from the faucet. Go on, I'll wait. If you followed instructions, then you'll see that the stream becomes more narrow as it descends. Knowing that the density of water is very nearly constant, use the continuity equation to show that the cross-sectional area of the stream $A(z)$ as a function of distance from the faucet z is

$$A(z) = \frac{A_0}{\sqrt{1 + 2gz/v_0^2}},$$

where A_0 is the cross-sectional area of the stream upon exiting the faucet with velocity v_0 and g is the gravitational acceleration. If you turn the faucet to make the water flow faster, what happens to the tapering of the stream?

IV.1.2. *Newton's second law: The momentum equation*

So far we have an equation for the evolution of the mass density ϱ expressed in terms of the fluid velocity $\boldsymbol{u}$. How does the latter evolve? Newton's second law provides the answer: simply add up the accelerations, divide by the mass (density), and you've got the time rate of change of the velocity. But there is a subtlety here: there is a difference between the time rate of change of the velocity in the lab frame and the time rate of change of the velocity in the fluid frame. So which time derivative of $\boldsymbol{u}$ do we take? The key is in how the accelerations are expressed. Are these accelerations acting on a fixed point in space, or are they acting on an element of our fluid? It is much easier (and more physical) to think of these accelerations in the latter sense: given a deformable patch of the fluid – large enough in extent to contain a very large number of atoms but small enough that all the macroscopic variables such as density, velocity, and pressure have a unique value over the dimensions of the patch – what forces are acting on that patch? These are relatively simple to catalog, and we will do so in short order. But first, let's answer our original question: which time derivative of $\boldsymbol{u}$ do we take? Since we have committed to expressing the forces in the frame of the fluid element, the acceleration must likewise be expressed in this frame. The acceleration is *not*

$$\frac{\partial \boldsymbol{u}}{\partial t}. \tag{IV.1.5}$$

Remember what a partial derivative means: something is being fixed! Here, it is the instantaneous position $\boldsymbol{r}$ of the fluid element. Equation (IV.1.5) is the answer to the question, 'how does the fluid velocity evolve at a fixed point in space?' Instead, we wish to fix our sights on the fluid element itself, which is moving. The acceleration we calculate must account for this frame transformation:

$$\boldsymbol{a} = \frac{\partial \boldsymbol{u}}{\partial t} + \frac{\mathrm{d}\boldsymbol{r}}{\mathrm{d}t} \cdot \boldsymbol{\nabla} \boldsymbol{u}, \tag{IV.1.6}$$

where $\mathrm{d}\boldsymbol{r}/\mathrm{d}t$ is the rate of change of the position of the fluid element, i.e., the velocity $\boldsymbol{u}(t, \boldsymbol{r})$. This combination of derivatives is so important that it has its own notation:

$$\frac{\mathrm{D}}{\mathrm{D}t} \doteq \frac{\partial}{\partial t} + \boldsymbol{u} \cdot \boldsymbol{\nabla}. \tag{IV.1.7}$$

It is variously referred to as the *Lagrangian derivative*, or comoving derivative, or convective derivative. By contrast, the expression given by (IV.1.5) is the *Eulerian deriative.* Note that the continuity equation (IV.1.4) may be expressed using the Lagrangian derivative as

$$\frac{\mathrm{D} \ln \varrho}{\mathrm{D}t} = -\boldsymbol{\nabla} \cdot \boldsymbol{u}, \tag{IV.1.8}$$

which states that incompressible flow corresponds to $\boldsymbol{\nabla}\cdot\boldsymbol{u}=0$.

So, given some force $\boldsymbol{F}$ per unit volume that is acting on our fluid element, we now know how the fluid velocity evolves: force (per unit volume) equals mass (per unit volume) times acceleration (in the frame of the fluid element):

$$\boldsymbol{F}=\varrho\frac{\mathrm{D}\boldsymbol{u}}{\mathrm{D}t}. \tag{IV.1.9}$$

Now we need only catalog the relevant forces. This could be, say, gravity: $\varrho\boldsymbol{g}=-\varrho\boldsymbol{\nabla}\Phi$. Or, if the fluid element is conducting, electromagnetic forces (which we'll get to later in the course). But the most deserving of discussion at this point is the pressure force due to the internal thermal motions of the particles comprising the gas. For an ideal gas, the equation of state is

$$P=\frac{\varrho k_{\mathrm{B}}T}{m}\doteq\varrho C^2, \tag{IV.1.10}$$

where T is the temperature in Kelvin, k_{B} is the Boltzmann constant, m is the mass per particle, and C is the speed of sound in an isothermal gas. Plasma physicists often drop Boltzmann's constant and register temperature in energy units (e.g., eV), and I will henceforth do the same in these notes. How does gas pressure due to microscopic particle motions exert a macroscopic force on a fluid element? First, the pressure must be spatially non-uniform: there must be more or less energetic content in the thermal motions of the particles in one region versus another, whether it be because the gas temperature varies in space or because there are more particles in one location as opposed to another. For example, the pressure force in the x direction in a slab of thickness $\mathrm{d}x$ and cross-sectional area $\mathrm{d}y\,\mathrm{d}z$ is

$$\big[P(t,x-\mathrm{d}x/2,y,z)-P(t,x+\mathrm{d}x/2,y,z)\big]\mathrm{d}y\,\mathrm{d}z=-\frac{\partial P}{\partial x}\,\mathrm{d}V. \tag{IV.1.11}$$

Unless the thermal motions of the particles are not sufficiently randomized to be isotropic (e.g., if the collisional mean free path of the plasma is so long that inter-particle collisions cannot drive the system quickly enough towards local thermodynamic equilibrium), there is nothing particularly special about the x direction, and so the pressure force force acting on some differential volume $\mathrm{d}V$ is just $-\boldsymbol{\nabla}P\,\mathrm{d}V$.

Assembling the lessons we've learned here, we have the following force equation for our fluid:

$$\boxed{\varrho\frac{\mathrm{D}\boldsymbol{u}}{\mathrm{D}t}\doteq\varrho\left(\frac{\partial}{\partial t}+\boldsymbol{u}\cdot\boldsymbol{\nabla}\right)\boldsymbol{u}=-\boldsymbol{\nabla}P-\varrho\boldsymbol{\nabla}\Phi} \tag{IV.1.12}$$

This equation is colloquially known as the *momentum equation*, even though it evolves the fluid velocity rather than its momentum density. To obtain an equation for the latter, the continuity equation (IV.1.4) may be used to move the mass density into the time and space derivatives:

$$\begin{aligned}\frac{\partial(\varrho\boldsymbol{u})}{\partial t}+\boldsymbol{\nabla}\cdot(\varrho\boldsymbol{u}\boldsymbol{u})&=\frac{\partial\varrho}{\partial t}\boldsymbol{u}+\varrho\frac{\partial\boldsymbol{u}}{\partial t}+\varrho\boldsymbol{u}\cdot\boldsymbol{\nabla}\boldsymbol{u}+\boldsymbol{\nabla}\cdot(\varrho\boldsymbol{u})\boldsymbol{u}\\&=\left[\frac{\partial\varrho}{\partial t}+\boldsymbol{\nabla}\cdot(\varrho\boldsymbol{u})\right]\boldsymbol{u}+\varrho\left(\frac{\partial}{\partial t}+\boldsymbol{u}\cdot\boldsymbol{\nabla}\right)\boldsymbol{u}\\&=\left[\quad 0\quad\right]\boldsymbol{u}+\varrho\frac{\mathrm{D}\boldsymbol{u}}{\mathrm{D}t}=\boldsymbol{F}.\end{aligned} \tag{IV.1.13}$$

Thus, an equation for the momentum density:

$$\boxed{\frac{\partial(\varrho \boldsymbol{u})}{\partial t} + \boldsymbol{\nabla}\cdot(\varrho \boldsymbol{u}\boldsymbol{u}) = -\boldsymbol{\nabla} P - \varrho \boldsymbol{\nabla}\Phi} \tag{IV.1.14}$$

This form is particularly useful for deriving an evolution equation for the kinetic energy density. Dotting (IV.1.14) with $\boldsymbol{u}$ and grouping terms,

$$\frac{\partial}{\partial t}\left(\frac{1}{2}\varrho u^2\right) + \boldsymbol{\nabla}\cdot\left(\frac{1}{2}\varrho u^2 \boldsymbol{u}\right) = -\boldsymbol{u}\cdot\boldsymbol{\nabla} P - \varrho \boldsymbol{u}\cdot\boldsymbol{\nabla}\Phi, \tag{IV.1.15}$$

which is a statement that the kinetic energy of a fluid element changes as work is done by the forces.

Now, how to we know the pressure P? There's an equation for that...

IV.1.3. *First law of thermodynamics: The internal energy equation*

There are several ways to go about obtaining an evolution equation for the pressure. One way is to introduce the *internal energy*,

$$e \doteq \frac{P}{\gamma - 1} \tag{IV.1.16}$$

and use the first law of thermodynamics to argue that e is conserved but for $P\,\mathrm{d}V$ work:

$$\boxed{\frac{\partial e}{\partial t} + \boldsymbol{\nabla}\cdot(e\boldsymbol{u}) = -P\boldsymbol{\nabla}\cdot\boldsymbol{u}} \tag{IV.1.17}$$

This is the *internal energy* equation.

Equation (IV.1.17) may be used to derive a total (kinetic + internal + potential) energy equation for the fluid as follows. Do (IV.1.15) + (IV.1.17):

$$\begin{aligned}\frac{\partial}{\partial t}\left(\frac{1}{2}\varrho u^2 + e\right) + \boldsymbol{\nabla}\cdot\left[\left(\frac{1}{2}\varrho u^2 + e\right)\boldsymbol{u}\right] &= -\boldsymbol{\nabla}\cdot(P\boldsymbol{u}) - \varrho\boldsymbol{u}\cdot\boldsymbol{\nabla}\Phi, \\ &= -(\gamma-1)\boldsymbol{\nabla}\cdot(e\boldsymbol{u}) - \varrho\boldsymbol{u}\cdot\boldsymbol{\nabla}\Phi\end{aligned}$$

$$\implies \quad \frac{\partial}{\partial t}\left(\frac{1}{2}\varrho u^2 + e\right) + \boldsymbol{\nabla}\cdot\left[\left(\frac{1}{2}\varrho u^2 + \gamma e\right)\boldsymbol{u}\right] = -\varrho\boldsymbol{u}\cdot\boldsymbol{\nabla}\Phi. \tag{IV.1.18}$$

Now use the continuity equation (IV.1.4) to write

$$\frac{\partial(\varrho\Phi)}{\partial t} + \boldsymbol{\nabla}\cdot(\varrho\Phi\boldsymbol{u}) = \varrho\boldsymbol{u}\cdot\boldsymbol{\nabla}\Phi + \varrho\frac{\partial\Phi}{\partial t}. \tag{IV.1.19}$$

Adding this equation to (IV.1.18) yields the desired result:

$$\boxed{\frac{\partial}{\partial t}\left(\frac{1}{2}\varrho u^2 + e + \varrho\Phi\right) + \boldsymbol{\nabla}\cdot\left[\left(\frac{1}{2}\varrho u^2 + \gamma e + \varrho\Phi\right)\boldsymbol{u}\right] = \varrho\frac{\partial\Phi}{\partial t}} \tag{IV.1.20}$$

The first term in parentheses under the time derivative is sometimes denoted by $\mathcal{E}$.

Yet another way of expressing the internal energy equation (IV.1.17) is to write $e = \varrho T/m(\gamma-1)$ and use the continuity equation (IV.1.4) to eliminate the derivatives of the mass density. The result is

$$\frac{\mathrm{D}\ln T}{\mathrm{D}t} = -(\gamma-1)\boldsymbol{\nabla}\cdot\boldsymbol{u}, \tag{IV.1.21}$$

which states that the temperature of a fluid element is constant in an incompressible

fluid (*viz.*, one with $\boldsymbol{\nabla}\cdot\boldsymbol{u}=0$). If this seems intuitively unfamiliar to you, consider this: the hydrodynamic entropy of a fluid element is given by

$$s \doteq \frac{1}{\gamma-1}\ln P\varrho^{-\gamma} = \frac{1}{\gamma-1}\ln T\varrho^{1-\gamma}. \tag{IV.1.22}$$

Taking the Lagrangian time derivative of the entropy along the path of a fluid element yields

$$\frac{\mathrm{D}s}{\mathrm{D}t} = \frac{\mathrm{D}\ln T}{\mathrm{D}t} - (\gamma-1)\frac{\mathrm{D}\ln\varrho}{\mathrm{D}t}. \tag{IV.1.23}$$

It is then just a short trip back to (IV.1.8) to see that (IV.1.21) is, in fact, the second law of thermodynamics – entropy is conserved in the absence of sources or dissipative sinks:

$$\boxed{\frac{\mathrm{D}s}{\mathrm{D}t}=0} \tag{IV.1.24}$$

In this sense, fluid elements in ideal hydrodynamics are thermodynamically isolated from one another.

Note that when we wrote down our hydrodynamic equations for a scalar pressure (see (IV.1.14) and (IV.1.17)) and didn't affix any species labels to any quantities, we were implicitly assuming that our hydrodynamics occurs on time scales much longer than the collisional equilibration times, so that all species can be well described by local Maxwellians with the same density, fluid velocity, and temperature. Not all astrophysical systems are so cooperative, and anisotropic pressures, velocity drifts between species, and dis-equilibration of species temperatures can often be the norm. Hydrodynamics (and magnetohydrodynamics) are fairly simple, but do not let their simplicity lure you into using them when it's not appropriate to do so – a hard-earned lesson for many astrophysicists.

IV.2. Summary: Adiabatic equations of hydrodynamics

The adiabatic equations of hydrodynamics, written in conservative form, are:

$$\frac{\partial\varrho}{\partial t} + \boldsymbol{\nabla}\cdot(\varrho\boldsymbol{u}) = 0, \tag{IV.2.1a}$$

$$\frac{\partial(\varrho\boldsymbol{u})}{\partial t} + \boldsymbol{\nabla}\cdot(\varrho\boldsymbol{u}\boldsymbol{u}) = -\boldsymbol{\nabla}P - \varrho\boldsymbol{\nabla}\Phi, \tag{IV.2.1b}$$

$$\frac{\partial e}{\partial t} + \boldsymbol{\nabla}\cdot(e\boldsymbol{u}) = -P\boldsymbol{\nabla}\cdot\boldsymbol{u}. \tag{IV.2.1c}$$

The left-hand sides of these equations express advection of, respectively, the mass density, the momentum density, and the internal energy density by the fluid velocity; the right-hand sides represents sources and sinks. If we instead write these equations in terms of the density, fluid velocity, and entropy and make use of the Lagrangian derivative (IV.1.7), we have

$$\frac{\mathrm{D}\varrho}{\mathrm{D}t} = -\varrho\boldsymbol{\nabla}\cdot\boldsymbol{u}, \tag{IV.2.2a}$$

$$\frac{\mathrm{D}\boldsymbol{u}}{\mathrm{D}t} = -\frac{1}{\varrho}\boldsymbol{\nabla}P - \boldsymbol{\nabla}\Phi, \tag{IV.2.2b}$$

$$\frac{\mathrm{D}s}{\mathrm{D}t} = 0, \tag{IV.2.2c}$$

where $s \doteq (\gamma-1)^{-1}\ln P\varrho^{-\gamma}$. The limit $\gamma\to\infty$, often of utility for describing liquids, corresponds to $\mathrm{D}\varrho/\mathrm{D}t=0$, i.e., incompressibility.

IV.3. Mathematical matters

IV.3.1. *Vector identities*

As a start to this section, let me advise you to brush up on your vector calculus...

$$\begin{aligned}
\boldsymbol{A}\cdot(\boldsymbol{B}\times\boldsymbol{C}) &= \boldsymbol{B}\cdot(\boldsymbol{C}\times\boldsymbol{A}) = \boldsymbol{C}\cdot(\boldsymbol{A}\times\boldsymbol{B}),\\
\boldsymbol{A}\times(\boldsymbol{B}\times\boldsymbol{C}) &= \boldsymbol{B}(\boldsymbol{A}\cdot\boldsymbol{C}) - \boldsymbol{C}(\boldsymbol{A}\cdot\boldsymbol{B}),\\
\boldsymbol{\nabla}\cdot(\boldsymbol{A}\times\boldsymbol{B}) &= \boldsymbol{B}\cdot(\boldsymbol{\nabla}\times\boldsymbol{A}) - \boldsymbol{A}\cdot(\boldsymbol{\nabla}\times\boldsymbol{B}),\\
\boldsymbol{\nabla}\times(\boldsymbol{A}\times\boldsymbol{B}) &= (\boldsymbol{B}\cdot\boldsymbol{\nabla})\boldsymbol{A} - (\boldsymbol{A}\cdot\boldsymbol{\nabla})\boldsymbol{B} - \boldsymbol{B}(\boldsymbol{\nabla}\cdot\boldsymbol{A}) + \boldsymbol{A}(\boldsymbol{\nabla}\cdot\boldsymbol{B}),\\
\boldsymbol{A}\times(\boldsymbol{\nabla}\times\boldsymbol{B}) + \boldsymbol{B}\times(\boldsymbol{\nabla}\times\boldsymbol{A}) &= \boldsymbol{\nabla}(\boldsymbol{A}\cdot\boldsymbol{B}) - (\boldsymbol{A}\cdot\boldsymbol{\nabla})\boldsymbol{B} - (\boldsymbol{B}\cdot\boldsymbol{\nabla})\boldsymbol{A},\\
&\ldots
\end{aligned}$$

Fluid dynamics is full of these things, and you should either (i) commit them to memory, (ii) carry your NRL formulary with you everywhere, or (iii) know how to quickly derive them using things like

$$\epsilon_{kij}\epsilon_{k\ell m} = \delta_{i\ell}\delta_{jm} - \delta_{im}\delta_{j\ell},$$

where δ_{ij} is the Kronecker delta and ϵ_{ijk} is the Levi–Civita symbol.

IV.3.2. *Leibniz's rule and the Lagrangian derivative of integrals*

In the proofs of many conservation laws, a Lagrangian time derivative is taken of a surface or volume integral whose integration limits are time-dependent. In this case, $\mathrm{D}/\mathrm{D}t$ does *not* commute with the integral sign. The trick to dealing with these situations is related to Leibniz's rule:

$$\frac{\mathrm{d}}{\mathrm{d}t}\int_{a(t)}^{b(t)}\mathrm{d}x\,f(t,x) = \int_{a(t)}^{b(t)}\mathrm{d}x\,\frac{\partial}{\partial t}f(t,x) + f(t,b(t))\frac{\mathrm{d}b}{\mathrm{d}t} - f(t,a(t))\frac{\mathrm{d}a}{\mathrm{d}t}. \tag{IV.3.1}$$

In three dimensions, if we're taking the time derivative of a volume integral whose integration limits $\mathcal{V}(t)$ are time-dependent, the generalization of the above is

$$\frac{\mathrm{d}}{\mathrm{d}t}\int_{\mathcal{V}(t)}\mathrm{d}\mathcal{V}\,f(t,\boldsymbol{r}) = \int_{\mathcal{V}(t)}\mathrm{d}\mathcal{V}\,\frac{\partial}{\partial t}f(t,\boldsymbol{r}) + \oint_{\partial\mathcal{V}(t)}\mathrm{d}\boldsymbol{\mathcal{S}}\cdot\big[f(t,\boldsymbol{r})\boldsymbol{u}_\mathrm{b}(t,\boldsymbol{r})\big], \tag{IV.3.2}$$

where $\boldsymbol{u}_\mathrm{b}$ is the velocity of the bounding surface $\partial\mathcal{V}(t)$. This is known as the Reynolds transport theorem. In words, the time rate-of-change of a quantity positioned within a moving volume is a combination of the lab-frame rate-of-change of that quantity (i.e., the time derivative at fixed position $\boldsymbol{r}$ – note the partial derivative) and how much of that quantity flowed through the surface. When the velocity of the bounding surface equals the fluid velocity, $\boldsymbol{u}_\mathrm{b}=\boldsymbol{u}(t,\boldsymbol{r})$, so that each moving volume corresponds to that of a fluid element, we may replace $\mathrm{d}/\mathrm{d}t$ in (IV.3.2) with the Lagrangian derivative $\mathrm{D}/\mathrm{D}t$:

$$\boxed{\frac{\mathrm{D}}{\mathrm{D}t}\int_{\mathcal{V}(t)}\mathrm{d}\mathcal{V}\,f(t,\boldsymbol{r}) = \int_{\mathcal{V}(t)}\mathrm{d}\mathcal{V}\,\frac{\partial}{\partial t}f(t,\boldsymbol{r}) + \oint_{\partial\mathcal{V}(t)}\mathrm{d}\boldsymbol{\mathcal{S}}\cdot\big[f(t,\boldsymbol{r})\boldsymbol{u}(t,\boldsymbol{r})\big]} \tag{IV.3.3}$$

You've already encountered an example of this – mass conservation, in which the volume was a "material volume" moving with the fluid element itself:

$$0 = \frac{\mathrm{D}M}{\mathrm{D}t} \doteq \frac{\mathrm{D}}{\mathrm{D}t}\int_{\mathcal{V}(t)}\mathrm{d}\mathcal{V}\,\rho = \int_{\mathcal{V}(t)}\mathrm{d}\mathcal{V}\,\frac{\partial\rho}{\partial t} + \oint_{\partial\mathcal{V}(t)}\mathrm{d}\boldsymbol{\mathcal{S}}\cdot(\rho\boldsymbol{u}).$$

Using the divergence theorem on the final (surface-integral) term gives

$$0 = \int_{\mathcal{V}(t)} \mathrm{d}\mathcal{V} \left[\frac{\partial \rho}{\partial t} + \boldsymbol{\nabla} \cdot (\rho \boldsymbol{u}) \right],$$

which provides us with our continuity equation.

A similar rule to (IV.3.3) is needed for time derivatives of surface integrals whose integration limits $\mathcal{S}(t)$ are time-dependent. For a vector field $\boldsymbol{F} = \boldsymbol{F}(t, \boldsymbol{r})$ and a bounding surface $\mathcal{S}(t)$ whose contour $\partial\mathcal{S}(t)$ moves with the fluid velocity $\boldsymbol{u} = \boldsymbol{u}(t, \boldsymbol{r})$, this is given by

$$\boxed{\frac{\mathrm{D}}{\mathrm{D}t} \int_{\mathcal{S}(t)} \mathrm{d}\boldsymbol{\mathcal{S}} \cdot \boldsymbol{F} = \int_{\mathcal{S}(t)} \mathrm{d}\boldsymbol{\mathcal{S}} \cdot \left[\frac{\partial \boldsymbol{F}}{\partial t} + (\boldsymbol{\nabla} \cdot \boldsymbol{F}) \boldsymbol{u} \right] - \oint_{\partial\mathcal{S}(t)} \mathrm{d}\boldsymbol{\ell} \cdot (\boldsymbol{u} \times \boldsymbol{F})} \tag{IV.3.4}$$

(By convention, the contour is taken in the counter-clockwise direction.) Note that $-\mathrm{d}\boldsymbol{\ell} \cdot (\boldsymbol{u} \times \boldsymbol{F}) = \boldsymbol{F} \cdot (\boldsymbol{u} \times \mathrm{d}\boldsymbol{\ell})$. In words, the comoving change of the differential surface element $\mathrm{d}\boldsymbol{\mathcal{S}}$ equals the amount of area swept out in a time $\mathrm{d}t$ via the advection of a differential line element $\mathrm{d}\boldsymbol{\ell}$ on $\partial\mathcal{S}$ by a distance $\boldsymbol{u}\,\mathrm{d}t$:

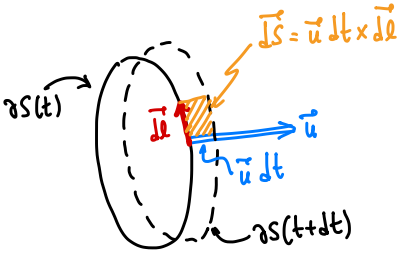

Equation (IV.3.4) can be used to prove conservation of magnetic flux (§V.1.2) and conservation of fluid vorticity (§IV.4).

IV.3.3. $\boldsymbol{u} \cdot \boldsymbol{\nabla} \boldsymbol{u}$ *and curvilinear coordinates*

Finally, the nonlinear combination $\boldsymbol{u} \cdot \boldsymbol{\nabla} \boldsymbol{u}$ that features prominently in the Lagrangian time derivative can be complicated, particularly in curvilinear coordinates where the gradient operator within it acts on the unit vectors within $\boldsymbol{u}$. For example, in cylindrical coordinates (R, φ, Z),

$$\begin{aligned} \boldsymbol{u} \cdot \boldsymbol{\nabla} \boldsymbol{u} &= \boldsymbol{u} \cdot \boldsymbol{\nabla} \big(u_R \hat{\boldsymbol{R}} + u_\varphi \hat{\boldsymbol{\varphi}} + u_Z \hat{\boldsymbol{Z}} \big) \\ &= (\boldsymbol{u} \cdot \boldsymbol{\nabla} u_R) \hat{\boldsymbol{R}} + (\boldsymbol{u} \cdot \boldsymbol{\nabla} u_\varphi) \hat{\boldsymbol{\varphi}} + (\boldsymbol{u} \cdot \boldsymbol{\nabla} u_Z) \hat{\boldsymbol{Z}} + \frac{u_\varphi^2}{R} \frac{\partial \hat{\boldsymbol{\varphi}}}{\partial \varphi} + \frac{u_R u_\varphi}{R} \frac{\partial \hat{\boldsymbol{R}}}{\partial \varphi} \\ &= (\boldsymbol{u} \cdot \boldsymbol{\nabla} u_i) \hat{\boldsymbol{e}}_i - \frac{u_\varphi^2}{R} \hat{\boldsymbol{R}} + \frac{u_R u_\varphi}{R} \hat{\boldsymbol{\varphi}}, \end{aligned} \tag{IV.3.5}$$

where, to obtain the final equality, we have used $\partial\hat{\boldsymbol{\varphi}}/\partial\varphi = -\hat{\boldsymbol{R}}$ and $\partial\hat{\boldsymbol{R}}/\partial\varphi = \hat{\boldsymbol{\varphi}}$; summation over the repeated index i is implied in the first term in the final line. A similar calculation in spherical coordinates (r, ϑ, φ) yields

$$\begin{aligned} \boldsymbol{u} \cdot \boldsymbol{\nabla} \boldsymbol{u} &= \left(u_r \frac{\partial}{\partial r} + \frac{u_\vartheta}{r} \frac{\partial}{\partial \vartheta} + \frac{u_\varphi}{r \sin\vartheta} \frac{\partial}{\partial \varphi} \right) \left(u_r \hat{\boldsymbol{r}} + u_\vartheta \hat{\boldsymbol{\vartheta}} + u_\varphi \hat{\boldsymbol{\varphi}} \right) \\ &= (\boldsymbol{u} \cdot \boldsymbol{\nabla} u_i) \hat{\boldsymbol{e}}_i - \frac{u_\vartheta^2 + u_\varphi^2}{r} \hat{\boldsymbol{r}} + \left(\frac{u_r u_\vartheta}{r} - \frac{u_\varphi^2 \cot\vartheta}{r} \right) \hat{\boldsymbol{\vartheta}} + \left(\frac{u_\vartheta u_\varphi \cot\vartheta}{r} + \frac{u_r u_\varphi}{r} \right) \hat{\boldsymbol{\varphi}} \end{aligned} \tag{IV.3.6}$$

The last two terms in the cylindrical $\boldsymbol{u}\cdot\boldsymbol{\nabla}\boldsymbol{u}$, equation (IV.3.5), might look familiar to you from working in rotating frames. Indeed, let us write $\boldsymbol{u} = \boldsymbol{v} + R\Omega(R,Z)\hat{\boldsymbol{\varphi}}$, where Ω is an angular velocity, and substitute this decomposition into (IV.3.5):

$$\begin{aligned}\boldsymbol{u}\cdot\boldsymbol{\nabla}\boldsymbol{u} &= \left[(\boldsymbol{v}+R\Omega\hat{\boldsymbol{\varphi}})\cdot\boldsymbol{\nabla}v_i\right]\hat{\boldsymbol{e}}_i + \left[(\boldsymbol{v}+R\Omega\hat{\boldsymbol{\varphi}})\cdot\boldsymbol{\nabla}(R\Omega)\right]\hat{\boldsymbol{\varphi}} \\ &\quad - \frac{(v_\varphi+R\Omega)^2}{R}\hat{\boldsymbol{R}} + \frac{v_R(v_\varphi+R\Omega)}{R}\hat{\boldsymbol{\varphi}} \\ &= \left[\left(\boldsymbol{v}\cdot\boldsymbol{\nabla} + \Omega\frac{\partial}{\partial\vartheta}\right)v_i\right]\hat{\boldsymbol{e}}_i + \left[2\Omega\hat{\boldsymbol{z}}\times\boldsymbol{v} - R\Omega^2\hat{\boldsymbol{R}} + R\hat{\boldsymbol{\varphi}}(\boldsymbol{v}\cdot\boldsymbol{\nabla})\Omega\right] \\ &\quad + \left[\frac{v_R v_\varphi}{R}\hat{\boldsymbol{\varphi}} - \frac{v_\varphi^2}{R}\hat{\boldsymbol{R}}\right]. \end{aligned} \tag{IV.3.7}$$

Each of these terms has a straightforward physical interpretation. The first term in brackets represents advection by the flow and the rotation. The second term in brackets contains the Coriolis force, the centrifugal force, and 'tidal' terms due to the differential rotation, in that order. (The 'tidal' terms can be thought of the fictitious acceleration required for a fluid element to maintain its presence in the local rotating frame as it is displaced radially or vertically. They come from Taylor expanding the angular velocity about a point in the disk.) The third and final term is brackets are curvature terms due to the cylindrical geometry.

Exercise: Show that the $R\varphi$-component in cylindrical coordinates of the rate-of-strain tensor

$$W_{ij} \doteq \frac{\partial u_i}{\partial x_j} + \frac{\partial u_j}{\partial x_i} - \frac{2}{3}\delta_{ij}\frac{\partial u_k}{\partial x_k}$$

is given by

$$W_{R\varphi} = \frac{1}{R}\frac{\partial u_R}{\partial\varphi} + R\frac{\partial}{\partial R}\frac{u_\varphi}{R}.$$

Hint: $\partial u_i/\partial x_j = [(\hat{\boldsymbol{e}}_j\cdot\boldsymbol{\nabla})\boldsymbol{u}]\cdot\hat{\boldsymbol{e}}_i$ is coordinate invariant.

IV.4. Vorticity and Kelvin's circulation theorem

With some vector identities in hand, let's take the curl of the force equation (IV.2.2*b*):

$$\boldsymbol{\nabla}\times\left(\frac{\mathrm{D}\boldsymbol{u}}{\mathrm{D}t} = -\frac{1}{\rho}\boldsymbol{\nabla}P - \boldsymbol{\nabla}\Phi\right).$$

The potential term vanishes, since the curl of a gradient is zero. Likewise, the pressure term becomes

$$-\boldsymbol{\nabla}\frac{1}{\rho}\times\boldsymbol{\nabla}P = \frac{1}{\rho^2}\boldsymbol{\nabla}\rho\times\boldsymbol{\nabla}P.$$

As for the left-hand side, the gradient operator commutes with $\partial/\partial t$, but not with $\boldsymbol{u}\cdot\boldsymbol{\nabla}$. Instead,

$$\boldsymbol{\nabla}\times\left[(\boldsymbol{u}\cdot\boldsymbol{\nabla})\boldsymbol{u}\right] = \boldsymbol{\nabla}\times\left[\frac{1}{2}\boldsymbol{\nabla}u^2 - \boldsymbol{u}\times(\boldsymbol{\nabla}\times\boldsymbol{u})\right] = -\boldsymbol{\nabla}\times(\boldsymbol{u}\times\boldsymbol{\omega}),$$

where

$$\boldsymbol{\omega} \doteq \boldsymbol{\nabla}\times\boldsymbol{u} \tag{IV.4.1}$$

is the *fluid vorticity*. The vorticity measures how much rotation a velocity field has (and its direction). Note that it is divergence free, which means that vortex lines cannot end within the fluid – they must either close on themselves (like a smoke ring) or intersect a boundary (like a tornado). Any fresh vortex lines that are made must be created as continuous curves that grow out of points or lines where the vorticity vanishes.

Assembling the above gives the *vorticity equation*,

$$\frac{\partial \boldsymbol{\omega}}{\partial t} - \boldsymbol{\nabla} \times (\boldsymbol{u} \times \boldsymbol{\omega}) = \frac{1}{\rho^2} \boldsymbol{\nabla}\rho \times \boldsymbol{\nabla} P. \tag{IV.4.2}$$

Note that the right-hand side of this equation vanishes if the pressure is *barotropic*, i.e., if $P = P(\rho)$, so that surfaces of constant density and constant pressure coincide. If these surfaces do not coincide, then the fluid is said to have "baroclinicity" or to be "baroclinic". I'll demonstrate below using mathematics what (IV.4.2) means physically, but you already know what the right-hand side means if you pay attention to the weather: areas of high atmospheric baroclinicity have frequent hurricanes and cyclones. In the parlance of fluid dynamics, this is called "baroclinic forcing". Now back to the math...

Dot (IV.4.2) into a differential surface element $\mathrm{d}\boldsymbol{\mathcal{S}}$ normal to the surface $\mathcal{S}$ of a fluid element, integrate over that surface, and use Stokes' theorem to replace the surface integral of a curl with a line integral over the surface boundary $\partial\mathcal{S}$:

$$\int_{\mathcal{S}} \frac{\partial \boldsymbol{\omega}}{\partial t} \cdot \mathrm{d}\boldsymbol{\mathcal{S}} - \oint_{\partial\mathcal{S}} (\boldsymbol{u} \times \boldsymbol{\omega}) \cdot \mathrm{d}\boldsymbol{\ell} = \oint_{\partial\mathcal{S}} \left(-\frac{1}{\rho} \boldsymbol{\nabla} P \right) \cdot \mathrm{d}\boldsymbol{\ell} = - \oint_{\partial\mathcal{S}} \frac{\mathrm{d}P}{\rho}.$$

Using (IV.3.4) to replace the left-hand side by the Lagrangian time derivative of $\boldsymbol{\omega} \cdot \mathrm{d}\boldsymbol{\mathcal{S}}$ yields

$$\frac{\mathrm{D}}{\mathrm{D}t} \int_{\mathcal{S}} \boldsymbol{\omega} \cdot \mathrm{d}\boldsymbol{\mathcal{S}} = - \oint_{\partial\mathcal{S}} \frac{\mathrm{d}P}{\rho}. \tag{IV.4.3}$$

The surface integral on the left-hand side of this equation may be expressed using Stokes' theorem as the *circulation* Γ:

$$\int_{\mathcal{S}} \boldsymbol{\omega} \cdot \mathrm{d}\boldsymbol{\mathcal{S}} = \oint_{\partial\mathcal{S}} \boldsymbol{u} \cdot \mathrm{d}\boldsymbol{\ell} \doteq \Gamma. \tag{IV.4.4}$$

The circulation around the boundary $\partial\mathcal{S}$ can be thought of as the number of vortex lines that thread the enclosed area S. Equation (IV.4.3) then states that the circulation is conserved if the fluid is barotropic – Kelvin's circulation theorem:[13]

$$\boxed{\frac{\mathrm{D}\Gamma}{\mathrm{D}t} = - \oint_{\partial\mathcal{S}} \frac{\mathrm{d}P}{\rho} = 0 \quad \text{if } P = P(\rho)} \tag{IV.4.5}$$

The figure below illustrates how baroclinic forcing generates vorticity.

[13]The above manipulations require that the surface is simply connected – that is, the region must be such that we can shrink the contour to a point without leaving the region. A region with a hole (like a bathtub drain) is not simply connected.

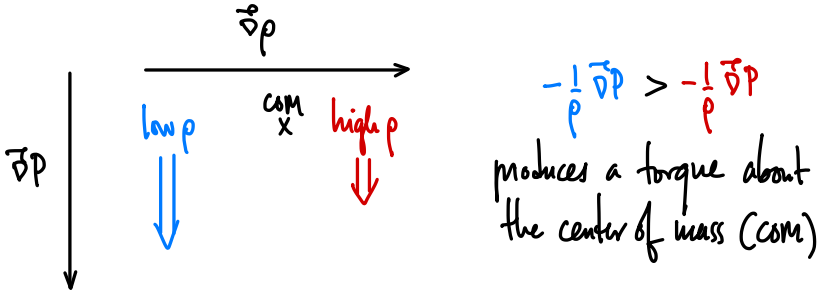

Another approach to proving (IV.4.5) is to work with $\Gamma = \oint_{\partial S} \boldsymbol{u} \cdot \mathrm{d}\boldsymbol{\ell}$ rather than $\int_S \boldsymbol{\omega} \cdot \mathrm{d}\boldsymbol{\mathcal{S}}$ and use the following for how an advected line element of ∂S changes in time:

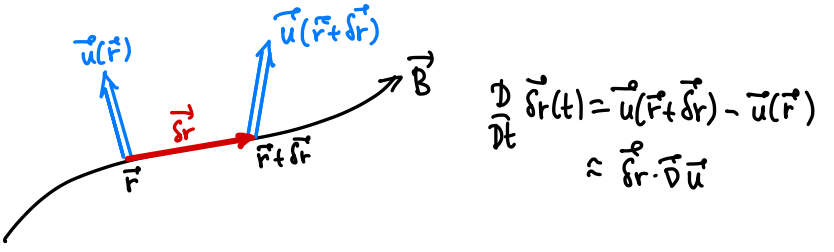

Exercise. The helicity of a region of fluid is defined to be $\mathcal{H} \doteq \int \boldsymbol{\omega} \cdot \boldsymbol{u} \, \mathrm{d}\mathcal{V}$, where the integral is taken over the volume of that region. Assume that $\Gamma = \text{const}$ and that $\boldsymbol{\omega} \cdot \hat{\boldsymbol{n}}$ vanishes when integrated over the surface bounding $\mathcal{V}$, where $\hat{\boldsymbol{n}}$ is the unit normal to that surface. Prove that the helicity $\mathcal{H}$ is conserved in a frame moving with the fluid, *viz.* $\mathrm{D}\mathcal{H}/\mathrm{D}t = 0$. Note that the fluid need not be incompressible for this property to hold.

The calculation leading to (IV.4.5) can be repeated in a reference frame rotating at a constant angular velocity $\boldsymbol{\Omega}$, in which the fluid velocity is measured to be $\boldsymbol{v} = \boldsymbol{u} - \boldsymbol{\Omega} \times \boldsymbol{r}$ (here, $\boldsymbol{u}$ is the fluid velocity in the inertial frame; see §IV.3). The associated vorticity in this rotating frame is

$$\boldsymbol{\omega}_{\mathrm{rot}} = \boldsymbol{\omega} - \boldsymbol{\nabla} \times (\boldsymbol{\Omega} \times \boldsymbol{r}) = \boldsymbol{\omega} - \boldsymbol{\Omega}(\boldsymbol{\nabla} \cdot \boldsymbol{r}) + (\boldsymbol{\Omega} \cdot \boldsymbol{\nabla})\boldsymbol{r} = \boldsymbol{\omega} - 3\boldsymbol{\Omega} + \boldsymbol{\Omega} = \boldsymbol{\omega} - 2\boldsymbol{\Omega}, \quad \text{(IV.4.6)}$$

where $\boldsymbol{\omega} = \boldsymbol{\nabla} \times \boldsymbol{u}$. The circulation in the rotating reference frame is then given by

$$\begin{aligned} \Gamma_{\mathrm{rot}} &= \int_{\mathcal{S}} \boldsymbol{\omega}_{\mathrm{rot}} \cdot \mathrm{d}\boldsymbol{\mathcal{S}} = \int_{\mathcal{S}} (\boldsymbol{\omega} - 2\boldsymbol{\Omega}) \cdot \mathrm{d}\boldsymbol{\mathcal{S}} \\ &= \oint_{\partial\mathcal{S}} \boldsymbol{u} \cdot \mathrm{d}\boldsymbol{\ell} - \int_{\mathcal{S}} 2\boldsymbol{\Omega} \cdot \mathrm{d}\boldsymbol{\mathcal{S}} \\ &= \Gamma - \int_{\mathcal{S}} 2\boldsymbol{\Omega} \cdot \mathrm{d}\boldsymbol{\mathcal{S}}. \end{aligned} \quad \text{(IV.4.7)}$$

Kelvin's circulation theorem in this rotating frame is therefore

$$\frac{\mathrm{D}\Gamma_{\mathrm{rot}}}{\mathrm{D}t} = -\oint_{\partial\mathcal{S}} \frac{\mathrm{d}P}{\rho} - 2\Omega \frac{\mathrm{D}\mathcal{S}_{\mathrm{n}}}{\mathrm{D}t}, \quad \text{(IV.4.8)}$$

where $\mathcal{S}_{\mathrm{n}}$ is component of the surface area oriented normally to $\boldsymbol{\Omega}$. In words, if the projected area of the vortex tube in the plane perpendicular to the rotation vector changes, then the circulation in the rotating frame must change to compensate. This is the origin of Rossby waves, something that will be discussed further in §IV.5.2.

IV.5. Rotating reference frames

The final calculation in the preceding section provides a natural segue into a discussion of fluid dynamics in rotating reference frames. To begin this discussion, let us first recall equation (IV.3.5), in which the nonlinearity $\boldsymbol{u}\cdot\boldsymbol{\nabla}\boldsymbol{u}$ was written out in cylindrical coordinates for a fluid velocity $\boldsymbol{u}$ consisting of a cylindrical rotation $R\Omega\hat{\boldsymbol{\varphi}}$ with angular velocity $\Omega = \Omega(R,z)$ and a residual velocity $\boldsymbol{v} \doteq \boldsymbol{u} - R\Omega\hat{\boldsymbol{\varphi}}$:

$$\boldsymbol{u}\cdot\boldsymbol{\nabla}\boldsymbol{u} = \left[\left(\boldsymbol{v}\cdot\boldsymbol{\nabla} + \Omega\frac{\partial}{\partial\varphi}\right)v_i\right]\hat{\boldsymbol{e}}_i + \left[2\Omega\hat{\boldsymbol{z}}\times\boldsymbol{v} - R\Omega^2\hat{\boldsymbol{R}} + R\hat{\boldsymbol{\varphi}}(\boldsymbol{v}\cdot\boldsymbol{\nabla})\Omega\right] + \left[\frac{v_R v_\varphi}{R}\hat{\boldsymbol{\varphi}} - \frac{v_\varphi^2}{R}\hat{\boldsymbol{R}}\right].$$

When this expansion was introduced in §IV.3, each of its components were described physically: 'The first term in brackets represents advection by the flow and the rotation. The second term in brackets contains the Coriolis force, the centrifugal force, and "tidal" terms due to the differential rotation... The third and final term in brackets captures curvature effects due to the cylindrical geometry.' Let's see these terms in action.

Using (IV.3.5), we may express the equations of hydrodynamics (IV.2.2) in cylindrical coordinates in a frame co-moving with the differential rotation. With

$$\frac{\mathrm{D}}{\mathrm{D}t} \to \frac{\partial}{\partial t} + \boldsymbol{v}\cdot\boldsymbol{\nabla} + \Omega\frac{\partial}{\partial\varphi} \tag{IV.5.1}$$

to include advection by the rotation, we have

$$\frac{\mathrm{D}\rho}{\mathrm{D}t} = -\rho\boldsymbol{\nabla}\cdot\boldsymbol{v}, \tag{IV.5.2a}$$

$$\frac{\mathrm{D}v_R}{\mathrm{D}t} = f_R + 2\Omega v_\varphi + R\Omega^2 + \frac{v_\varphi^2}{R}, \tag{IV.5.2b}$$

$$\frac{\mathrm{D}v_\varphi}{\mathrm{D}t} = f_\varphi - \frac{\kappa^2}{2\Omega}v_R - R\frac{\partial\Omega}{\partial Z}v_z - \frac{v_R v_\varphi}{R}, \tag{IV.5.2c}$$

$$\frac{\mathrm{D}v_z}{\mathrm{D}t} = f_z, \tag{IV.5.2d}$$

$$\frac{\mathrm{D}s}{\mathrm{D}t} = 0, \tag{IV.5.2e}$$

where

$$\boldsymbol{f} = -\frac{1}{\rho}\boldsymbol{\nabla}P - \boldsymbol{\nabla}\Phi \tag{IV.5.3}$$

and the combination

$$\boxed{\kappa^2 \doteq 4\Omega^2 + \frac{\partial\Omega^2}{\partial\ln R} = \frac{1}{R^3}\frac{\partial(R^4\Omega^2)}{\partial R}} \tag{IV.5.4}$$

is known as the (square of the) epicyclic frequency. Note that $R^4\Omega^2 = \ell^2$, the square of the specific angular momentum ℓ, and so κ^2 measures how much the specific angular momentum associated with the rotation increases or decreases outwards. For Keplerian rotation, $\kappa^2 = \Omega^2$.

In §VII.9, these equations will be modified for the presence and evolution of magnetic fields and used to look at linear waves and instabilities that rely on differential rotation. In the meantime, I'll close this portion of the notes by remarking on two useful applications of what you've learned here: the thermal wind equation (§IV.5.1) and Rossby waves (§IV.5.2).

IV.5.1. *Thermal wind equation*

In steady state with $\boldsymbol{v} = 0$, equations (IV.5.2*b*) and (IV.5.2*d*) become

$$0 = -\frac{1}{\rho}\frac{\partial P}{\partial R} - \frac{\partial \Phi}{\partial R} + R\Omega^2 \quad \text{and} \quad 0 = -\frac{1}{\rho}\frac{\partial P}{\partial z} - \frac{\partial \Phi}{\partial z}. \tag{IV.5.5}$$

Taking $\partial/\partial z$ of the first equation, using the second equation, and rearranging yields

$$R\frac{\partial \Omega^2}{\partial z} = \frac{\hat{\boldsymbol{\varphi}}}{\rho^2} \cdot (\boldsymbol{\nabla} P \times \boldsymbol{\nabla} \rho). \tag{IV.5.6}$$

This is the $\hat{\boldsymbol{\varphi}}$ component of the vorticity equation. Note that, if ρ is constant or if $P = P(\rho)$, then the angular velocity Ω must be constant on cylinders (this is related to *von Zeippel's theorem*). Now, let us recall the definition of the hydrodynamic entropy, $s = (\gamma - 1)^{-1} \ln P\rho^{-\gamma}$ and use it to replace $\boldsymbol{\nabla} \ln \rho$. The result is

$$R\frac{\partial \Omega^2}{\partial z} = \frac{\gamma - 1}{\gamma}\, \hat{\boldsymbol{\varphi}} \cdot \left(\boldsymbol{\nabla} s \times \frac{1}{\rho} \boldsymbol{\nabla} P \right) = \hat{\boldsymbol{\varphi}} \cdot \left(\frac{1}{\rho} \boldsymbol{\nabla} P \times \boldsymbol{\nabla} \ln T \right). \tag{IV.5.7}$$

In the Sun, $\boldsymbol{g} = (1/\rho)\boldsymbol{\nabla} P$ is an excellent approximation, with only a tiny angular component due to centrifugal effects. Adopting this simplification and working in spherical coordinates (r, θ, φ), equation (IV.5.7) becomes

$$\boxed{R\frac{\partial \Omega^2}{\partial z} = \frac{\gamma - 1}{\gamma} \frac{g}{r} \frac{\partial s}{\partial \theta}} \tag{IV.5.8}$$

where $g = GM/r^2$. [The right-hand side of (IV.5.8) can also be written as $-(g/r)\partial \ln T/\partial \theta$.] Equation (IV.5.8) is known as the *thermal wind equation*. It is used often in geophysical applications (e.g., longitudinal entropy gradients driven by temperature differences cause wind shear) and to understand the rotation profile in the convection zone of the Sun.

IV.5.2. *Rossby waves*

Consider a two-dimensional, incompressible fluid on the surface of uniformly rotating sphere (e.g., a planetary atmosphere). For a constant density or a barotropic equation of state, equation (IV.4.8) becomes

$$\frac{\mathrm{D}}{\mathrm{D}t}\left(\Gamma_{\mathrm{rot}} + 2\Omega \mathcal{S} \cos\theta \right) = 0, \tag{IV.5.9}$$

where θ is the angle between the rotation vector and the surface oriented normal to the fluid element. (Note that incompressibility assures $\mathcal{S} = \text{const.}$) This equation states that, as a fluid element makes its way from the equator northwards (*viz.*, from $\theta = \pi/2$ towards $\theta = 0$), its circulation as measured in the rotating frame must decrease. This means that the element must then rotate in the clockwise direction. Likewise, a fluid element that starts at the north pole and moves southwards towards the equator (*viz.*, from $\theta = 0$ towards $\theta = \pi/2$) increases its relative vorticity and thus rotates in the counterclockwise direction.

With this behavior in mind, let's now imagine a small-amplitude, wave-like disturbance at constant latitude (see diagram below). Northward displacements in this wave acquire negative relative vorticity and rotate clockwise; southward displacements acquire positive relative vorticity and rotate counterclockwise. These changes in the velocity of the disturbance actually feed back on the wave itself to make it travel westward; in effect, the wave is advecting itself to the west.

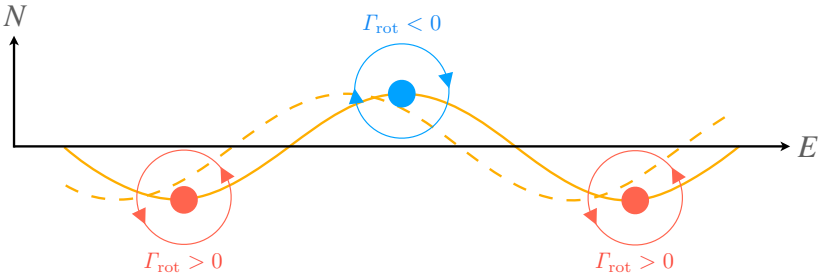

The relationship between the frequency ω and wavevector $\boldsymbol{k}$ for this wave – the *dispersion relation* – is given by

$$\omega = -\frac{k_y}{k_x^2 + k_y^2}\,\frac{2\Omega\sin\theta}{r}, \tag{IV.5.10}$$

where x denotes the local poloidal direction (pointing southward), y denotes the local azimuthal direction (pointing eastward), and r the spherical radial distance. With $\Omega > 0$ and $k_y > 0$, the phase velocity of the wave $\omega/k_y < 0$, i.e., the wave travels westward. Note that the group velocity, $\partial\omega/\partial k_y$, can be either positive or negative; in general, shorter wavelengths (higher k) have an eastward group velocity and longer wavelengths (smaller k) have a westward group velocity.

These waves are named after the meteorologist Carl Rossby, who derived the mathematics governing this phenomenon in 1939 while at MIT (after which he became assistant director of research at the U.S. Weather Bureau and then moved to University of Chicago as Chair of the Department of Meteorology).[14]

PART V
Ideal magnetohydrodynamics

V.1. The equations of ideal magnetohydrodynamics

Ideal magnetohydrodynamics (MHD) describes the hydrodynamics of a perfectly conducting fluid in the presence of electromagnetic fields. Mass is still conserved, so we still have the continuity equation:

$$\frac{\partial\rho}{\partial t} + \boldsymbol{\nabla}\cdot(\rho\boldsymbol{u}) = 0. \tag{V.1.1}$$

The first law of thermodynamics still holds, so we still have the internal energy equation:

$$\frac{\partial e}{\partial t} + \boldsymbol{\nabla}\cdot(e\boldsymbol{u}) = -P\boldsymbol{\nabla}\cdot\boldsymbol{u}. \tag{V.1.2}$$

And Newton's second law still governs the dynamics, so we still have the momentum equation:

$$\frac{\partial(\rho\boldsymbol{u})}{\partial t} + \boldsymbol{\nabla}\cdot(\rho\boldsymbol{u}\boldsymbol{u}) = \boldsymbol{f}. \tag{V.1.3}$$

But now we must supplement the force $\boldsymbol{f}$, which was equal to $-\boldsymbol{\nabla}P - \rho\boldsymbol{\nabla}\Phi$ in §IV, with the force due to the electromagnetic fields on the conducting fluid elements. To do so, let us view our conducting fluid elements as a coherent collection of ions (with charge $q_{\rm i} = Ze > 0$) and electrons (with charge $q_{\rm e} = -e < 0$), and ask how electric and magnetic fields influence each of these species.

[14] See https://elischolar.library.yale.edu/journal_of_marine_research/516.

The electromagnetic force per unit volume on a collection of charges of species α is given by

$$\boldsymbol{f}_{\rm EM} = q_\alpha n_\alpha \left(\boldsymbol{E} + \frac{\boldsymbol{u}_\alpha}{c} \times \boldsymbol{B} \right), \tag{V.1.4}$$

where n_α is the number density of the species and $\boldsymbol{u}_\alpha$ is that species' bulk velocity. You can think of this simply as the Lorentz force $q_\alpha(\boldsymbol{E} + \boldsymbol{v} \times \boldsymbol{B}/c)$ integrated over the ensemble of α charges in each fluid element and divided by the volume of said fluid element. Separating (V.1.3) into its charged constituent parts, we then have the momentum equation for species α,

$$\frac{\partial(\rho_\alpha \boldsymbol{u}_\alpha)}{\partial t} + \boldsymbol{\nabla} \cdot (\rho_\alpha \boldsymbol{u}_\alpha \boldsymbol{u}_\alpha) = -\boldsymbol{\nabla} P_\alpha - \rho_\alpha \boldsymbol{\nabla} \Phi + q_\alpha n_\alpha \left(\boldsymbol{E} + \frac{\boldsymbol{u}_\alpha}{c} \times \boldsymbol{B} \right). \tag{V.1.5}$$

At the moment, the trouble is that our continuity equation (V.1.1) and internal energy equation (V.1.2) make reference to the *total* mass density ρ, the *total* fluid velocity $\boldsymbol{u}$, the *total* pressure P, and the *total* internal energy e. The obvious thing to do, then, is to sum (V.1.5) over both species,

$$\sum_\alpha \left[\frac{\partial(\rho_\alpha \boldsymbol{u}_\alpha)}{\partial t} + \boldsymbol{\nabla} \cdot (\rho_\alpha \boldsymbol{u}_\alpha \boldsymbol{u}_\alpha) = -\boldsymbol{\nabla} P_\alpha - \rho_\alpha \boldsymbol{\nabla} \Phi + q_\alpha n_\alpha \left(\boldsymbol{E} + \frac{\boldsymbol{u}_\alpha}{c} \times \boldsymbol{B} \right) \right], \tag{V.1.6}$$

and simplify each of the sums one by one. The first term in (V.1.6) becomes familiar after introducing the center-of-mass fluid velocity,

$$\boldsymbol{u} \doteq \frac{1}{\rho} \sum_\alpha \rho_\alpha \boldsymbol{u}_\alpha, \quad \text{where} \quad \rho \doteq \sum_\alpha \rho_\alpha. \tag{V.1.7}$$

The second term in (V.1.6) requires a bit more work. Write $\boldsymbol{u}_\alpha = \boldsymbol{u} + \Delta\boldsymbol{u}_\alpha$, so that $\Delta\boldsymbol{u}_\alpha$ measures the difference between the bulk flow of species α and the center-of-mass velocity $\boldsymbol{u}$. Then

$$\sum_\alpha \rho_\alpha \boldsymbol{u}_\alpha \boldsymbol{u}_\alpha = \rho \boldsymbol{u}\boldsymbol{u} + \boldsymbol{u} \cancelto{0}{\left(\sum_\alpha \rho_\alpha \Delta\boldsymbol{u}_\alpha \right)} + \cancelto{0}{\left(\sum_\alpha \rho_\alpha \Delta\boldsymbol{u}_\alpha \right)} \boldsymbol{u} + \sum_\alpha \rho_\alpha \Delta\boldsymbol{u}_\alpha \Delta\boldsymbol{u}_\alpha.$$

The first term here ($\rho\boldsymbol{u}\boldsymbol{u}$) should look familiar: it's the flux of momentum density associated with the total fluid, the same as was seen in §IV. Moving the final term of the above expression to the right-hand side of (V.1.6) and writing $\sum_\alpha P_\alpha \doteq P$, we have a momentum equation that is starting to look more like (V.1.3):

$$\frac{\partial(\rho \boldsymbol{u})}{\partial t} + \boldsymbol{\nabla} \cdot (\rho \boldsymbol{u}\boldsymbol{u}) = -\boldsymbol{\nabla} P - \rho \boldsymbol{\nabla} \Phi - \sum_\alpha \rho_\alpha \Delta\boldsymbol{u}_\alpha \Delta\boldsymbol{u}_\alpha + \sum_\alpha q_\alpha n_\alpha \left(\boldsymbol{E} + \frac{\boldsymbol{u}_\alpha}{c} \times \boldsymbol{B} \right). \tag{V.1.8}$$

Now, this term involving $\Delta\boldsymbol{u}_\alpha$ has nothing really to do with MHD, and was in fact implicitly discarded in §IV.1.2, the reason being either that our fluid element is composed of a single species, or that collisions between different species keep their bulk flows very close to the center-of-mass velocity, or that the total mass density and total momentum density are completely dominated by a single species (e.g., the ions). In any of these cases, we may safely drop this term.

Almost there. All that remains to consider is

$$\sum_\alpha q_\alpha n_\alpha \left(\boldsymbol{E} + \frac{\boldsymbol{u}_\alpha}{c} \times \boldsymbol{B} \right).$$

In §I.5, we showed that the densities of the positive and negative charge carriers sur-

rounding a point charge Q in a weakly coupled plasma satisfies

$$\sum_\alpha q_\alpha n_\alpha = \cancelto{0}{\sum_\alpha q_\alpha n_\alpha} - \frac{Q}{4\pi\lambda_\mathrm{D}^3}\,\frac{\exp(-r/\lambda_\mathrm{D})}{r/\lambda_\mathrm{D}},$$

and therefore is extremely close to zero well outside of that charge's Debye sphere, i.e., the plasma is *quasi-neutral* on scales $r \gg \lambda_\mathrm{D}$. MHD concerns itself with just such scales, and so the total electric force on a fluid element in MHD vanishes under quasi-neutrality. This leaves the magnetic term, $(\sum_\alpha q_\alpha n_\alpha \boldsymbol{u}_\alpha) \times \boldsymbol{B}/c$. The sum in parentheses is equivalent to the *current density* of the plasma, $\boldsymbol{j}$, the amount of electric current flowing per unit cross-sectional area. We these principles implemented, our MHD momentum equation is finally here:

$$\boxed{\frac{\partial(\rho\boldsymbol{u})}{\partial t} + \boldsymbol{\nabla}\cdot(\rho\boldsymbol{u}\boldsymbol{u}) = -\boldsymbol{\nabla}P - \rho\boldsymbol{\nabla}\Phi + \frac{\boldsymbol{j}}{c}\times\boldsymbol{B}} \tag{V.1.9}$$

Another way to think of this additional term is by analogy with circuits: when a current $\boldsymbol{I}$ flows through a wire of length ℓ in the presence of a magnetic field $\boldsymbol{B}$, there is a force on the wire given by $\boldsymbol{I}\ell\times\boldsymbol{B}/c$. In the fluid context, the 'wire' is the conducting fluid element through which electrons and ions move differentially.

We now have our continuity equation, internal energy equation, and MHD momentum equation. However, in deriving the latter, we have introduced two new variables, $\boldsymbol{j}$ and $\boldsymbol{B}$. The remaining tasks are then to express the current density $\boldsymbol{j}$ in terms of the magnetic field $\boldsymbol{B}$ (since by summing over the momentum equations of each species, we've lost information about each species' bulk flow), and to provide an equation for how the magnetic field evolves. Both of these tasks are solved by Maxwell's equations:

$$\frac{\partial\boldsymbol{B}}{\partial t} = -c\boldsymbol{\nabla}\times\boldsymbol{E}, \quad \boldsymbol{\nabla}\cdot\boldsymbol{B} = 0, \quad \frac{\partial\boldsymbol{E}}{\partial t} = c\boldsymbol{\nabla}\times\boldsymbol{B} - 4\pi\boldsymbol{j}, \quad \boldsymbol{\nabla}\cdot\boldsymbol{E} = 4\pi\sum_\alpha q_\alpha n_\alpha,$$

with the important caveat that the final equation in red (Gauss' law) is rendered completely useless by the quasi-neutrality assumption, $\sum_\alpha q_\alpha n_\alpha \approx 0$. The other equations are (from left to right) Faraday's law of induction, Gauss' law for magnetism (no magnetic monopoles), and Maxwell's version of Ampère's law. No offense to Maxwell, but it turns out that the original Ampère's law,

$$\boldsymbol{j} = \frac{c}{4\pi}\boldsymbol{\nabla}\times\boldsymbol{B}, \tag{V.1.10}$$

is just fine our purposes. The displacement current, $(4\pi)^{-1}\partial\boldsymbol{E}/\partial t$, which mathematically and physically connects electromagnetism with the propagation of light, may be rigorously dropped if the fluid velocity satisfies $u^2 \ll c^2$. Why, you ask? Well, this brings us back to the first sentence of this section: we are interested in *perfect conductors*.

A perfect conductor is one that has exactly zero electrical resistance, and so by Ohm's law must have zero electrostatic field. But this doesn't necessarily mean that $\boldsymbol{E} = 0$, because an electric field can be induced by the motion of a conductor through a magnetic field (sometimes called the 'motional emf'). What we mean by a perfect conductor is then that the electric field vanishes *in the frame of the conductor*, or

$$\boldsymbol{E} + \frac{\boldsymbol{u}}{c}\times\boldsymbol{B} = 0. \tag{V.1.11}$$

Inserting this equation into the Maxwell–Ampère law and ordering $\partial/\partial t \sim u/\ell$ for some characteristic bulk flow velocity u and gradient lengthscale ℓ, we find that the

displacement current

$$\frac{\partial \boldsymbol{E}}{\partial t} \sim \frac{u^2}{c^2}\frac{cB}{\ell} \ll \frac{cB}{\ell} \sim c\boldsymbol{\nabla}\times\boldsymbol{B}$$

if the flow is non-relativistic. As claimed, the original Ampère's law is just fine.

Altogether then, we may close our MHD momentum equation with the following subset of Maxwell's equations:

$$\boxed{\frac{\partial \boldsymbol{B}}{\partial t} = \boldsymbol{\nabla}\times(\boldsymbol{u}\times\boldsymbol{B}), \quad \boldsymbol{\nabla}\cdot\boldsymbol{B} = 0, \quad \boldsymbol{j} = \frac{c}{4\pi}\boldsymbol{\nabla}\times\boldsymbol{B}} \tag{V.1.12}$$

These equations for the electromagnetic fields $\boldsymbol{B}$ and $\boldsymbol{j}$ – taken alongside (V.1.1), (V.1.2), and (V.2.2*b*) specifying the evolution of the hydrodynamics variables (ρ,$\rho\boldsymbol{u}$,e) – constitute the equations of ideal MHD.

V.1.1. *Ideal MHD induction equation*

Using a particular vector identity (see §IV.3.1), the ideal MHD induction equation may be written in the following form:

$$\frac{\partial \boldsymbol{B}}{\partial t} = \boldsymbol{\nabla}\times(\boldsymbol{u}\times\boldsymbol{B}) = -\boldsymbol{u}\cdot\boldsymbol{\nabla}\boldsymbol{B} + \boldsymbol{B}\cdot\boldsymbol{\nabla}\boldsymbol{u} - \boldsymbol{B}\boldsymbol{\nabla}\cdot\boldsymbol{u}. \tag{V.1.13}$$

Each of the terms on the right-hand side has a physical meaning. The first indicates that the magnetic field is advected (carried around by) the fluid flow; when placed on the left-hand side, we obtain the Lagrangian derivative of the magnetic field, $\mathrm{D}\boldsymbol{B}/\mathrm{D}t$, so that (V.1.13) becomes

$$\frac{\mathrm{D}\boldsymbol{B}}{\mathrm{D}t} = \boldsymbol{B}\cdot\boldsymbol{\nabla}\boldsymbol{u} - \boldsymbol{B}\boldsymbol{\nabla}\cdot\boldsymbol{u}. \tag{V.1.14}$$

In this Lagrangian frame, the magnetic field can evolve because of two effects. The first term on the right-hand side of (V.1.14), $\boldsymbol{B}\cdot\boldsymbol{\nabla}\boldsymbol{u}$, represents stretching of the magnetic field: if the fluid velocity has a gradient along the direction of the magnetic field, different parts of the field line will be carried along at different velocities, causing the field line to stretch. The final term, $-\boldsymbol{B}\boldsymbol{\nabla}\cdot\boldsymbol{u}$, corresponds to compression or rarefaction of the magnetic field. Indeed, with the continuity equation giving $-\boldsymbol{\nabla}\cdot\boldsymbol{u} = \mathrm{D}\ln\rho/\mathrm{D}t$, we see that co-moving increases (decreases) in the fluid density go hand-in-hand with increases (decreases) in the magnetic-field strength.

A rarely publicized but useful form of the induction equation (V.1.13) is obtained by defining the magnetic-field unit vector $\hat{\boldsymbol{b}} \doteq \boldsymbol{B}/B$ and writing separate equations for it and the magnetic-field strength B:

$$\frac{\mathrm{D}\ln B}{\mathrm{D}t} = \left(\hat{\boldsymbol{b}}\hat{\boldsymbol{b}} - \boldsymbol{I}\right) : \boldsymbol{\nabla}\boldsymbol{u} \quad \text{and} \quad \frac{\mathrm{D}\hat{\boldsymbol{b}}}{\mathrm{D}t} = \left(\boldsymbol{I} - \hat{\boldsymbol{b}}\hat{\boldsymbol{b}}\right) : \left(\hat{\boldsymbol{b}}\cdot\boldsymbol{\nabla}\boldsymbol{u}\right). \tag{V.1.15}$$

Just thought I'd throw that out there for you to chew on; we'll need the first of these in §§XII.5 and XIII.1.

V.1.2. *Flux freezing: Alfvén's theorem*

Arguably the most important prediction of the ideal MHD equations is that the magnetic flux Φ_B through the surface of any fluid element is exactly conserved as that element is advected and deformed by a flow $\boldsymbol{u} = \boldsymbol{u}(t,\boldsymbol{r})$. This is known as 'Alfvén's theorem' or, more colloquially, *flux freezing*. Given Leibniz's rule regarding the time derivatives of surface integrals whose integrations limits $\mathcal{S}(t)$ are time-dependent (eq. (IV.3.4)), the

proof itself is trivial:

$$\begin{aligned}\frac{\mathrm{D}\Phi_B}{\mathrm{D}t} \doteq \frac{\mathrm{D}}{\mathrm{D}t}\int_{\mathcal{S}(t)} \mathrm{d}\boldsymbol{\mathcal{S}}\cdot\boldsymbol{B} &= \int_{\mathcal{S}(t)} \mathrm{d}\boldsymbol{\mathcal{S}}\cdot\left[\frac{\partial \boldsymbol{B}}{\partial t} + (\boldsymbol{\nabla}\cdot\boldsymbol{B})\boldsymbol{u}\right] - \oint_{\partial\mathcal{S}(t)} \mathrm{d}\boldsymbol{\ell}\cdot(\boldsymbol{u}\times\boldsymbol{B}) \\ \text{(use equation (V.1.13))} &= \int_{\mathcal{S}(t)} \mathrm{d}\boldsymbol{\mathcal{S}}\cdot\left[\boldsymbol{\nabla}\times(\boldsymbol{u}\times\boldsymbol{B})\right] - \oint_{\partial\mathcal{S}(t)} \mathrm{d}\boldsymbol{\ell}\cdot(\boldsymbol{u}\times\boldsymbol{B}) \\ \text{(use Stokes' theorem)} &= \oint_{\partial\mathcal{S}(t)} \mathrm{d}\boldsymbol{\ell}\cdot(\boldsymbol{u}\times\boldsymbol{B}) - \oint_{\partial\mathcal{S}(t)} \mathrm{d}\boldsymbol{\ell}\cdot(\boldsymbol{u}\times\boldsymbol{B}) \\ &= 0. \end{aligned} \tag{V.1.16}$$

In words, the magnetic flux is conserved in a frame comoving with a fluid element. (This is analogous to Kelvin's circulation theorem governing the circulation; cf. (IV.4.5).)

An alternative description of flux freezing can be stated in terms of line tying: fluid elements that lie on a field line initially will remain on that field line (Lundquist 1951). Starting from the ideal induction equation (V.1.14), one may use the continuity equation to show that

$$\frac{\mathrm{D}}{\mathrm{D}t}\frac{\boldsymbol{B}}{\rho} = \frac{\boldsymbol{B}}{\rho}\cdot\boldsymbol{\nabla}\boldsymbol{u} - \frac{\boldsymbol{B}}{\rho}\boldsymbol{\nabla}\cdot\boldsymbol{u} + \frac{\boldsymbol{B}}{\rho}\boldsymbol{\nabla}\cdot\boldsymbol{u} = \frac{\boldsymbol{B}}{\rho}\cdot\boldsymbol{\nabla}\boldsymbol{u}. \tag{V.1.17}$$

This equation is formally equivalent to that describing the advection and stretching of a displacement vector $\boldsymbol{\xi}$ by a flow velocity $\boldsymbol{u}$, which is given by

$$\frac{\mathrm{D}\boldsymbol{\xi}}{\mathrm{D}t} = \boldsymbol{\xi}\cdot\boldsymbol{\nabla}\boldsymbol{u}.$$

Therefore, if two fluid elements are initially on the same field line, $\boldsymbol{\xi} = \text{const}\times(\boldsymbol{B}/\rho)$, then they will stay on that same field line.

V.1.3. *Lorentz force: Magnetic pressure and tension*

We now know that perfectly conducting fluids advect, stretch, and compress magnetic fields while conserving magnetic flux. What is the effect of that flux on the dynamics of the fluid element itself? For that, we revisit the Lorentz force in the MHD momentum equation (V.1.9), and use Ampère's law to cast the current density in terms of the magnetic field:

$$\boldsymbol{f}_{\mathrm{M}} = \frac{\boldsymbol{j}}{c}\times\boldsymbol{B} = \frac{(\boldsymbol{\nabla}\times\boldsymbol{B})\times\boldsymbol{B}}{4\pi} = -\boldsymbol{\nabla}\frac{B^2}{8\pi} + \frac{\boldsymbol{B}\cdot\boldsymbol{\nabla}\boldsymbol{B}}{4\pi}, \tag{V.1.18}$$

where to obtain the final equality we have used a well-known vector identity (see §IV.3.1). Because $\boldsymbol{\nabla}\cdot\boldsymbol{B} = 0$, this can also be written as

$$\boldsymbol{f}_{\mathrm{M}} = -\boldsymbol{\nabla}\cdot\left[\frac{B^2}{8\pi}\boldsymbol{I} - \frac{\boldsymbol{B}\boldsymbol{B}}{4\pi}\right] = -\boldsymbol{\nabla}\cdot\boldsymbol{M}, \tag{V.1.19}$$

which implicitly defines the 'Maxwell stress', $\boldsymbol{M}$. This form of the magnetic force suggests a kind of elasticity. To further see this, use the definition of the magnetic unit vector $\hat{\boldsymbol{b}} \doteq \boldsymbol{B}/B$ to write

$$\boldsymbol{B}\cdot\boldsymbol{\nabla}\boldsymbol{B} = B\hat{\boldsymbol{b}}\cdot\boldsymbol{\nabla}(B\hat{\boldsymbol{b}}) = B^2(\hat{\boldsymbol{b}}\cdot\boldsymbol{\nabla}\hat{\boldsymbol{b}}) + \hat{\boldsymbol{b}}\hat{\boldsymbol{b}}\cdot\boldsymbol{\nabla}\frac{B^2}{2}.$$

Using this in (V.1.18) and collecting terms yields

$$\boldsymbol{f}_{\mathrm{M}} = \frac{B^2}{4\pi}(\hat{\boldsymbol{b}}\cdot\boldsymbol{\nabla}\hat{\boldsymbol{b}}) - (\boldsymbol{I} - \hat{\boldsymbol{b}}\hat{\boldsymbol{b}})\cdot\boldsymbol{\nabla}\frac{B^2}{8\pi}. \tag{V.1.20}$$

The first term here corresponds to a curvature force, with $\hat{\boldsymbol{b}}\cdot\boldsymbol{\nabla}\hat{\boldsymbol{b}} \doteq \boldsymbol{\kappa}$ being the curvature of the field lines (see the diagram below). Note that $1/|\boldsymbol{\kappa}|$ is the radius of curvature. When a field line is bent, there is a force pointing towards the local center of curvature that is trying to un-bend the field line and push the plasma towards a lower-energy state in which the magnetic field is straight. The second term in (V.1.20) corresponds to a magnetic pressure force acting perpendicular to the field (thus the projection of the gradient onto $\boldsymbol{I} - \hat{\boldsymbol{b}}\hat{\boldsymbol{b}}$). This term causes the magnetic-field strength to evolve towards being uniform across itself, again seeking a lower-energy state. Magnetic fields like to be straight and evenly spaced, and they will coerce the fluid to adopt motions that drive them towards being straight and evenly spaced.

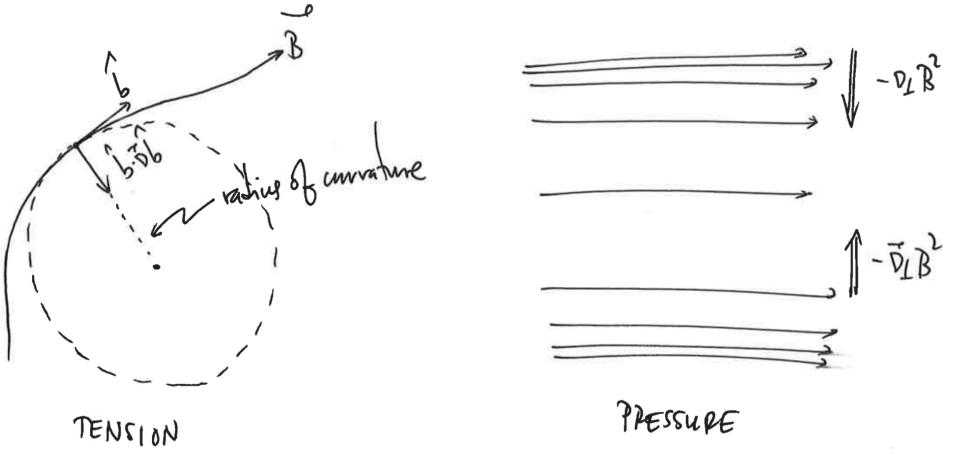

V.1.4. *MHD energy equation*

In §IV.1.3, we derived an evolution equation for the total energy of a neutral fluid (eq. (IV.1.20)). Here we augment that equation for a perfectly conducting fluid to include the energy of the magnetic field, $B^2/8\pi$. Take the ideal MHD induction equation (V.1.13) and dot it with $\boldsymbol{B}/4\pi$:

$$\begin{aligned}
\frac{\partial}{\partial t}\frac{B^2}{8\pi} &= \frac{\boldsymbol{B}}{4\pi}\cdot\boldsymbol{\nabla}\times(\boldsymbol{u}\times\boldsymbol{B}) = \frac{B_i}{4\pi}\,\epsilon_{ijk}\frac{\partial}{\partial x_j}(\boldsymbol{u}\times\boldsymbol{B})_k \\
&= \epsilon_{ijk}\frac{\partial}{\partial x_j}\left[\frac{B_i}{4\pi}(\boldsymbol{u}\times\boldsymbol{B})_k\right] - \epsilon_{ijk}(\boldsymbol{u}\times\boldsymbol{B})_k\frac{\partial}{\partial x_j}\frac{B_i}{4\pi} \\
&= \epsilon_{ijk}\frac{\partial}{\partial x_j}\left[\frac{B_i}{4\pi}(\boldsymbol{u}\times\boldsymbol{B})_k\right] - \epsilon_{ijk}\epsilon_{k\ell m}u_\ell B_m\frac{\partial}{\partial x_j}\frac{B_i}{4\pi} \\
&= \epsilon_{ijk}\frac{\partial}{\partial x_j}\left[\frac{B_i}{4\pi}(\boldsymbol{u}\times\boldsymbol{B})_k\right] - (\delta_{i\ell}\delta_{jm} - \delta_{im}\delta_{j\ell})u_\ell B_m\frac{\partial}{\partial x_j}\frac{B_i}{4\pi} \\
&= -\boldsymbol{\nabla}\cdot\left[\frac{\boldsymbol{B}\times(\boldsymbol{u}\times\boldsymbol{B})}{4\pi}\right] - \frac{\boldsymbol{uB}:\boldsymbol{\nabla B}}{4\pi} + \boldsymbol{u}\cdot\boldsymbol{\nabla}\frac{B^2}{8\pi}
\end{aligned}$$

$$\implies \quad \frac{\partial}{\partial t}\frac{B^2}{8\pi} + \boldsymbol{\nabla}\cdot\left[\frac{\boldsymbol{B}\times(\boldsymbol{u}\times\boldsymbol{B})}{4\pi}\right] = -\frac{\boldsymbol{uB}:\boldsymbol{\nabla B}}{4\pi} + \boldsymbol{u}\cdot\boldsymbol{\nabla}\frac{B^2}{8\pi}.$$

Note that the quantity inside the divergence on the left-hand side of this equation equals $(c/4\pi)\boldsymbol{E}\times\boldsymbol{B} \doteq \boldsymbol{\mathcal{S}}$... the Poynting flux! In words, magnetic energy (as measured in the lab frame; note the partial time derivative) is transported by the Poynting flux. Those two terms on the right-hand side corresponding to will be cancelled by two equal-and-

opposite terms found in the equation for the kinetic energy, obtained by dotting the momentum equation (V.1.9) with $\boldsymbol{u}$ and focusing on the Lorentz force:

$$\boldsymbol{u}\cdot\left(-\boldsymbol{\nabla}\frac{B^2}{8\pi}+\frac{\boldsymbol{B}\cdot\boldsymbol{\nabla}\boldsymbol{B}}{4\pi}\right).$$

Yep, they cancel. So, adding the total hydrodynamic energy equation including these Lorentz-force contributions to the magnetic energy equation leads to

$$\boxed{\frac{\partial}{\partial t}\left(\frac{1}{2}\rho u^2+e+\rho\Phi+\frac{B^2}{8\pi}\right)+\boldsymbol{\nabla}\cdot\left[\left(\frac{1}{2}\rho u^2+\gamma e+\rho\Phi\right)\boldsymbol{u}+\boldsymbol{\mathcal{S}}\right]=\rho\frac{\partial\Phi}{\partial t}.} \tag{V.1.21}$$

But for the impact of a time-varying gravitational potential, the total MHD energy $\mathcal{E}\doteq(1/2)\rho u^2+e+\rho\Phi+B^2/8\pi$ is conserved.

V.1.5. *Curvilinear coordinates and rotating reference frames revisited*

In §IV.3.3, we examined the nonlinear combination $\boldsymbol{u}\cdot\boldsymbol{\nabla}\boldsymbol{u}$ in curvilinear coordinates, finding additional terms that stemmed from differentiating unit vectors and which included Coriolis, centrifugal, and tidal accelerations. Here we take a similar look at the combination $\boldsymbol{u}\cdot\boldsymbol{\nabla}\boldsymbol{B}-\boldsymbol{B}\cdot\boldsymbol{\nabla}\boldsymbol{u}$ that features in the induction equation (V.1.13).

First, use $\partial\hat{\boldsymbol{\varphi}}/\partial\varphi=-\hat{\boldsymbol{R}}$ and $\partial\hat{\boldsymbol{R}}/\partial\varphi=\hat{\boldsymbol{\varphi}}$ in (V.1.13) to obtain

$$\frac{\partial\boldsymbol{B}}{\partial t}+\boldsymbol{B}\boldsymbol{\nabla}\cdot\boldsymbol{u}=(-\boldsymbol{u}\cdot\boldsymbol{\nabla}B_i)\hat{\boldsymbol{e}}_i+(\boldsymbol{B}\cdot\boldsymbol{\nabla}u_i)\hat{\boldsymbol{e}}_i+\frac{B_\varphi u_R-B_R u_\varphi}{R}\hat{\boldsymbol{\varphi}}.$$

As in §IV.5, if we then decompose the fluid velocity as $\boldsymbol{u}=\boldsymbol{v}+R\Omega(R,z)\hat{\boldsymbol{\varphi}}$, where Ω is an angular velocity, substitute this decomposition into the above equation, and re-group terms, we have

$$\frac{\mathrm{D}B_R}{\mathrm{D}t}=\boldsymbol{B}\cdot\boldsymbol{\nabla}v_R-B_R\boldsymbol{\nabla}\cdot\boldsymbol{v}, \tag{V.1.22a}$$

$$\frac{\mathrm{D}B_\varphi}{\mathrm{D}t}=\boldsymbol{B}\cdot\boldsymbol{\nabla}v_\varphi-B_\varphi\boldsymbol{\nabla}\cdot\boldsymbol{v}+B_R\frac{\partial\Omega}{\partial\ln R}+B_zR\frac{\partial\Omega}{\partial z}+\frac{B_\varphi v_R-B_R v_\varphi}{R}, \tag{V.1.22b}$$

$$\frac{\mathrm{D}B_z}{\mathrm{D}t}=\boldsymbol{B}\cdot\boldsymbol{\nabla}v_z-B_z\boldsymbol{\nabla}\cdot\boldsymbol{v}, \tag{V.1.22c}$$

with $\mathrm{D}/\mathrm{D}t\doteq\partial/\partial t+\boldsymbol{v}\cdot\boldsymbol{\nabla}+\Omega\,\partial/\partial\varphi$. Note that poloidal magnetic fields are sheared into the azimuthal direction by differential rotation. Likewise in cylindrical coordinates, the magnetic force becomes

$$\boldsymbol{f}_{\mathrm{M}}=-\boldsymbol{\nabla}\frac{B^2}{8\pi}+\frac{\boldsymbol{B}\cdot\boldsymbol{\nabla}B_i}{4\pi}\hat{\boldsymbol{e}}_i-\frac{B_\varphi^2}{4\pi R}\hat{\boldsymbol{R}}+\frac{B_RB_\varphi}{4\pi R}\hat{\boldsymbol{\varphi}} \tag{V.1.23}$$

Note the addition of an inwardly directed hoop stress caused by a magnetic field oriented in the azimuthal direction, and an azimuthally directed magnetic torque caused by $\partial\hat{\boldsymbol{R}}/\partial\hat{\boldsymbol{\varphi}}=\hat{\boldsymbol{\varphi}}$. The former guarantees that an azimuthal magnetic field satisfying $B_\varphi\propto 1/R$ is force free.

We'll revisit these equations when deriving the magnetorotational instability.

V.2. Summary: Adiabatic equations of ideal MHD

The adiabatic equations of MHD, written in conservative form, are:

$$\frac{\partial \rho}{\partial t} + \boldsymbol{\nabla} \cdot (\rho \boldsymbol{u}) = 0, \tag{V.2.1a}$$

$$\frac{\partial (\rho \boldsymbol{u})}{\partial t} + \boldsymbol{\nabla} \cdot (\rho \boldsymbol{u}\boldsymbol{u}) = -\boldsymbol{\nabla} \cdot \left[\left(P + \frac{B^2}{8\pi} \right) \boldsymbol{I} - \frac{\boldsymbol{B}\boldsymbol{B}}{4\pi} \right] - \rho \boldsymbol{\nabla} \Phi, \tag{V.2.1b}$$

$$\frac{\partial e}{\partial t} + \boldsymbol{\nabla} \cdot (e \boldsymbol{u}) = -P \boldsymbol{\nabla} \cdot \boldsymbol{u}, \tag{V.2.1c}$$

$$\frac{\partial \boldsymbol{B}}{\partial t} - \boldsymbol{\nabla} \times (\boldsymbol{u} \times \boldsymbol{B}) = 0. \tag{V.2.1d}$$

The left-hand sides of these equations express advection of, respectively, the mass density, the momentum density, the internal energy density, and the magnetic flux by the fluid velocity; the right-hand sides represents sources and sinks.

If we instead write these equations in terms of the density, fluid velocity, and entropy and make use of the Lagrangian derivative (IV.1.7), we have

$$\frac{\mathrm{D}\rho}{\mathrm{D}t} = -\rho \boldsymbol{\nabla} \cdot \boldsymbol{u}, \tag{V.2.2a}$$

$$\frac{\mathrm{D}\boldsymbol{u}}{\mathrm{D}t} = -\frac{1}{\rho} \boldsymbol{\nabla} \left(P + \frac{B^2}{8\pi} \right) + \frac{\boldsymbol{B} \cdot \boldsymbol{\nabla} \boldsymbol{B}}{4\pi\rho} - \boldsymbol{\nabla} \Phi, \tag{V.2.2b}$$

$$\frac{\mathrm{D}s}{\mathrm{D}t} = 0, \tag{V.2.2c}$$

$$\frac{\mathrm{D}\boldsymbol{B}}{\mathrm{D}t} = \boldsymbol{B} \cdot \boldsymbol{\nabla} \boldsymbol{u} - \boldsymbol{B} \boldsymbol{\nabla} \cdot \boldsymbol{u}, \tag{V.2.2d}$$

where $s \doteq (\gamma - 1)^{-1} \ln P \rho^{-\gamma}$.

PART VI
Linear theory of MHD waves

MHD waves and linear theory

Let us summarize our dissipationless "ideal MHD" eqns:

$$\frac{\partial \rho}{\partial t} + \vec{\nabla}\cdot(\rho\vec{u}) = 0$$

$$\rho\left(\frac{\partial}{\partial t} + \vec{u}\cdot\vec{\nabla}\right)\vec{u} = -\vec{\nabla}\left(P + \frac{B^2}{8\pi}\right) - \rho\vec{\nabla}\Phi + \frac{\vec{B}\cdot\vec{\nabla}\vec{B}}{4\pi}$$

$$\frac{P}{\gamma-1}\left(\frac{\partial}{\partial t} + \vec{u}\cdot\vec{\nabla}\right)\ln P\rho^{-\gamma} = 0$$

$$\frac{\partial \vec{B}}{\partial t} = \vec{\nabla}\times(\vec{u}\times\vec{B})$$

Now, let us consider a uniform, stationary MHD fluid, threaded by a uniform magnetic field. To orient our coordinate system, we will use $\vec{B} = B_0\hat{z}$, with the directions $\perp$ to the field being x and y. We perturb the fluid with small displacements, which we take (freely) to be sinusoidal:

$$\rho = \rho_0 + \delta\rho\, e^{i\vec{k}\cdot\vec{r} - i\omega t}$$
$$\vec{B} = B_0\hat{z} + \vec{\delta B}\, e^{i\vec{k}\cdot\vec{r} - i\omega t}$$
$$\vec{u} = \phi + \vec{\delta u}\, e^{i\vec{k}\cdot\vec{r} - i\omega t}$$
$$P = P_0 + \delta P\, e^{i\vec{k}\cdot\vec{r} - i\omega t}$$

Small? What's "small"? By "small", I mean that all nonlinearities ($\propto O(\delta^2)$) will be dropped. The result is linear theory.

Before we do this, note that, when computing actual observed quantities, we should take the real part (e.g. $e^{i\theta} \to \cos\theta$, $ie^{i\theta} \to -\sin\theta$, etc.)

First, let's do the simplest thing: $\vec{k} = k\hat{z}$. My notation is usually "$k_\parallel$" in this case, to remind me that k is parallel to the guide field. This notation is used in a lot of plasma physics, but less so in astronomy. Our linearized MHD eqns. are then

$$-i\omega \frac{\delta\rho}{\rho_0} + ik_\parallel \delta u_\parallel = 0$$

$$-i\omega \vec{\delta u} = -i\frac{k_\parallel \hat{z}}{\rho_0}\left(\delta p + \frac{B_0 \delta B_\parallel}{4\pi}\right) + \frac{ik_\parallel B_0}{4\pi\rho_0}\vec{\delta B}$$

$$-i\omega \frac{\vec{\delta B}}{B_0} = ik_\parallel \vec{\delta u} - \hat{z}\, ik_\parallel \delta u_\parallel \longrightarrow \delta B_\parallel = 0 \quad \text{(as is required by } \vec{k}\cdot\vec{\delta B} = 0\text{)}$$

Note that we don't need to know $\delta\rho$ or δp to solve for the perpendicular ($\perp$) dynamics:

$$\left.\begin{aligned} -i\omega \vec{\delta u}_\perp &= \frac{ik_\parallel B_0}{4\pi\rho_0}\vec{\delta B}_\perp \\ -i\omega \frac{\vec{\delta B}_\perp}{B_0} &= ik_\parallel \vec{\delta u}_\perp \end{aligned}\right\} \left(\omega^2 - k_\parallel^2 V_A^2\right)\frac{\vec{\delta B}_\perp}{B_0} = 0$$

$$\omega = \pm k_\parallel V_A \quad \text{with } V_A \equiv \frac{B_0}{\sqrt{4\pi\rho_0}}$$

These are "Alfvén waves", which are polarized across the guide field and which propagate at speed V_A, the "Alfvén speed". These waves are not associated with any motion along the field nor any changes in density.

Using $\frac{\delta p}{p_0} = \gamma\frac{\delta\rho}{\rho_0}$, the other modes are sound waves: $\boxed{\omega = \pm k_\parallel c_s}$, with $c_s \equiv \left(\frac{\gamma p_0}{\rho_0}\right)^{1/2}$ being the "sound speed".

The fifth mode is $\omega = 0$, and corresponds to a relabeling of fluid elements. It's called the "entropy mode"

Now, let's let $\vec{k} = k_\parallel \hat{z} + \vec{k}_\perp$ — a more general wavevector. Then our linearized equations are

(a) $$-i\omega \frac{\delta\rho}{\rho_0} + i k_\parallel \delta u_\parallel + i\vec{k}_\perp \cdot \delta\vec{u}_\perp = 0$$

$$-i\omega \delta\vec{u} = -\frac{i\vec{k}}{\rho_0}\left(\delta p + \frac{B_0 \delta B_\parallel}{4\pi}\right) + \frac{i k_\parallel B_0}{4\pi\rho_0}\delta\vec{B}$$

$$-i\omega \frac{\delta\vec{B}}{B_0} = i k_\parallel \delta\vec{u} - \hat{z}\left(i k_\parallel \delta u_\parallel + i\vec{k}_\perp \cdot \delta\vec{u}_\perp\right)$$

(b) $$-i\omega \frac{\delta\vec{B}_\perp}{B_0} = i k_\parallel \delta\vec{u}_\perp \quad \text{and} \quad (c)\ -i\omega \frac{\delta B_\parallel}{B_0} = -i\vec{k}_\perp \cdot \delta\vec{u}_\perp$$

(d) $$-i\omega \delta\vec{u}_\perp = -\frac{i\vec{k}_\perp}{\rho_0}\left(\delta p + \frac{B_0 \delta B_\parallel}{4\pi}\right) + \frac{i k_\parallel B_0}{4\pi\rho_0}\delta\vec{B}_\perp \quad \text{and}$$

(e) $$-i\omega \delta u_\parallel = -\frac{i k_\parallel}{\rho_0}\left(\delta p + \frac{B_0 \delta B_\parallel}{4\pi}\right) + \frac{i k_\parallel B_0}{4\pi\rho_0}\delta B_\parallel .$$

$\vec{k}_\perp \cdot$(d) + $k_\parallel$(e) $\Rightarrow$ $$-i\omega\left(\vec{k}_\perp \cdot \delta\vec{u}_\perp + k_\parallel \delta u_\parallel\right) = -\frac{i k^2}{\rho_0}\left(\delta p + \frac{B_0 \delta B_\parallel}{4\pi}\right) + \not{\phi}$$

use (a): $$+\frac{\not{i}\omega}{\not{k}}\left(\frac{\not{i}\omega \delta\rho}{\rho_0}\right) = +\frac{\not{i} k^2}{\rho_0}\left(\delta p + \frac{B_0 \delta B_\parallel}{4\pi}\right)$$

use $\frac{\delta p}{p_0} = \gamma \frac{\delta\rho}{\rho_0}$: $$\left(\omega^2 - k^2 c_s^2\right)\frac{\delta\rho}{\rho_0} = k^2 v_A^2 \frac{\delta B_\parallel}{B_0}$$

Now, (d) with (b) gives: $$\left(\omega^2 - k_\parallel^2 v_A^2\right)\frac{\delta\vec{B}_\perp}{B_0} = -k_\parallel \vec{k}_\perp\left(c_s^2 \frac{\delta\rho}{\rho_0} + v_A^2 \frac{\delta B_\parallel}{B_0}\right)$$

$$\left(\omega^2 - k_\parallel^2 v_A^2\right)\frac{\delta\vec{B}_\perp}{B_0} = -k_\parallel \vec{k}_\perp \frac{\delta B_\parallel}{B_0}\left[c_s^2 \frac{k^2 v_A^2}{\omega^2 - k^2 c_s^2} + v_A^2\right]$$

* here we've lost the entropy mode *

Note that the parallel and perpendicular components are now coupled!

$$\left(\omega^2 - k_\parallel^2 v_A^2\right)\frac{\delta B_\perp}{B_0} = -k_\parallel k_\perp v_A^2\left[\frac{\omega^2}{\omega^2 - k^2 c_s^2}\right]\frac{\delta B_\parallel}{B_0}$$

Before we go any further, note that, if $c_s^2/v_A^2 \gg 1$, then we have $\omega^2 - k_\parallel^2 v_A^2 \simeq 0$, so we get back something like an Alfvén wave in this limit. Proceeding by using $\frac{\delta B_\parallel}{B_0} = -\frac{\vec{k}_\perp \cdot \delta\vec{B}_\perp}{k_\parallel B_0}$ we have

$$\left[\overleftrightarrow{I}\left(\omega^2 - k_\parallel^2 v_A^2\right) - \vec{k}_\perp \vec{k}_\perp v_A^2 \frac{\omega^2}{\omega^2 - k^2 c_s^2}\right]\cdot\frac{\delta\vec{B}_\perp}{B_0} = 0.$$

Taking the determinant and setting it to zero gives the dispersion relation

$$\left(\omega^2 - k_\parallel^2 v_A^2\right)\left[\omega^2 - k_\parallel^2 v_A^2 - k_\perp^2 v_A^2 \frac{\omega^2}{\omega^2 - k^2 c_s^2}\right] = 0.$$

you'll often see this written as

$$\left[\omega^4 - \omega^2 k^2\left(c_s^2 + v_A^2\right) + k_\parallel^2 v_A^2 k^2 c_s^2\right]$$

But I like it like this because you can take β limits easier.

Note that we recover the Alfvén wave solution $\omega = \pm k_\parallel v_A$. Now we also have $\omega^2 = \frac{k^2\left(c_s^2 + v_A^2\right)}{2} \pm \sqrt{\frac{k^4\left(c_s^2 + v_A^2\right)^2}{4} - k_\parallel^2 v_A^2 k^2 c_s^2}$.

These are the "magnetosonic" modes — the ⊕ solution being the "fast wave" and the ⊖ solution being the "slow wave".

Note that, in the high-β limit, we have

$$\omega_+^2 \simeq k^2 c_s^2 \quad \text{and} \quad \omega_-^2 \simeq k_\parallel^2 v_A^2$$

(ω_+: sound!; ω_-: Alfvén!)

The difference between the slow mode here and an actual shear Alfvén wave is the latter involves no compressive fluctuations, being polarized with $\delta B_\parallel$ exactly $= 0$. This is sometimes called a "pseudo-Alfvén" wave.

Here are some pictures of these waves: ($\vec{\xi}$ is displacement)

Alfvén:

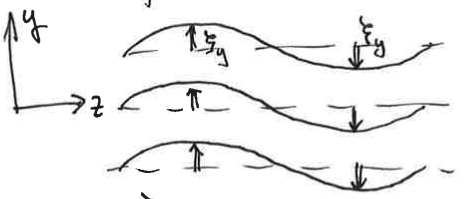

NB: can have $k_\perp \neq 0$

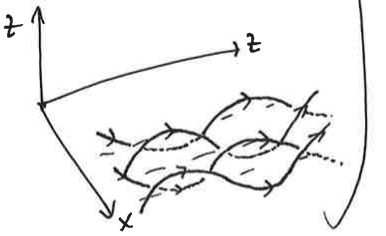

Sound:

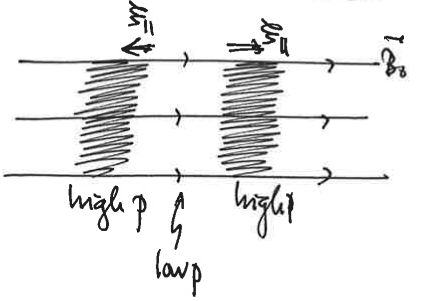

fast w/ $k_\parallel = 0$:

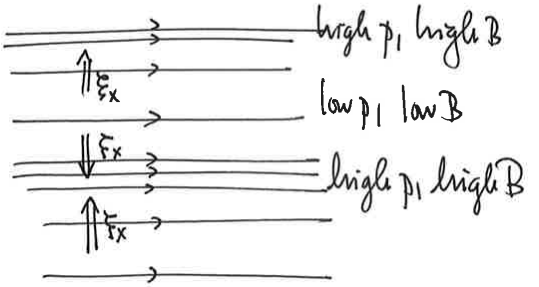

Fast:

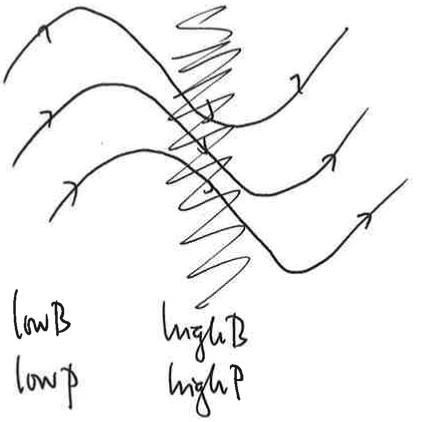

Slow:

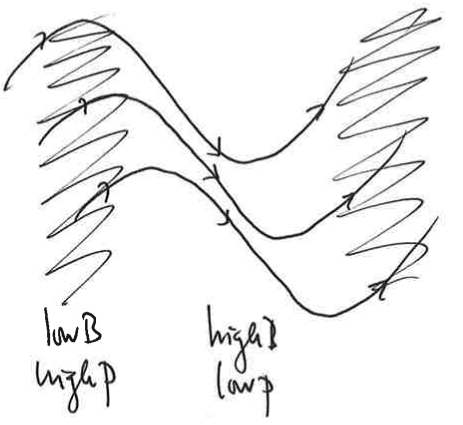

Slow with $k_\parallel/k_\perp \ll 1$:

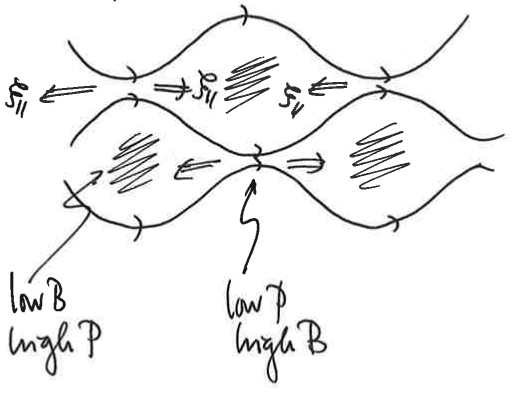

Now, this last limit, $k_\parallel/k_\perp \ll 1$, is quite useful for studies of Alfvénic turbulence. What are an waves in this limit? Alfvén is the same: $\pm k_\parallel V_A$. Magnetosonic waves become

$$\omega^2 \approx \frac{k_\perp^2 (C_s^2 + V_A^2)}{2}\left[1 \pm \left(1 - \frac{2 k_\parallel^2 V_A^2 k_\perp^2 C_s^2}{k_\perp^4 (C_s^2+V_A^2)^2}\right)\right]$$

$\oplus$ / FAST: $k_\perp^2 (C_s^2 + V_A^2)$

$\ominus$ / SLOW: $k_\parallel^2 V_A^2 \left(\frac{C_s^2}{C_s^2 + V_A^2}\right)$

· Let's look at the slow mode in this limit. Recall from our linear calculation that

$$\delta p = \delta\rho c_s^2 = \rho_0 c_s^2 \left(\frac{k^2 v_A^2}{\omega^2 - k^2 c_s^2}\right)\frac{\delta B_\parallel}{B_0} \Rightarrow \frac{\delta p}{p_0} + \left(\frac{k^2 v_A^2}{k^2 c_s^2 - \omega^2}\right)\frac{\delta B_\parallel}{B_0} = 0.$$

With $k_\perp \gg k_\parallel$ and $\omega^2 \approx k_\parallel^2 v_A^2 \left(\frac{c_s^2}{c_s^2 + v_A^2}\right)$, this becomes

$$\frac{\delta p}{p} + \frac{k_\perp^2 v_A^2 \left(\delta B_\parallel / B_0\right)}{k_\perp^2 c_s^2 - \frac{k_\parallel^2 v_A^2 c_s^2}{c_s^2 + v_A^2}} \approx \underbrace{\frac{\delta p}{p} + \frac{v_A^2}{c_s^2}\frac{\delta B_\parallel}{B_0} \approx 0}_{\text{pressure balance!}}$$

PART VII

Linear theory of MHD instabilities

Now let's do some MHD linear instabilities. The program is to set up some equilibria and then subject them to small-amplitude perturbations in the fluid and magnetic field. There are a few different ways of doing this and assessing whether the system is stable or unstable to these perturbations. There's something called the MHD energy principle, which will tell you whether a given set of perturbations about some equilibrium state will bring the system profitably to a lower energy state. There's something called Eulerian perturbation theory, where you subject the equilibrium state to small-amplitude perturbations, formulate those perturbations in the lab frame, and ask whether the perturbations oscillate, grow, or decay. And there's something called Lagrangian perturbation theory, which is same as Eulerian perturbation theory but is formulated in the frame of fluid. Each of these has its advantages depending on the equilibrium state, boundary conditions, and questions being asked. Eulerian perturbation theory is the most straightforward procedure, so we'll start there.

VII.1. A primer on instability

Before attacking the MHD equations, though, let's do something simpler to establish notation and learn the procedure. Consider the following ordinary differential equation:

$$\frac{\mathrm{d}^2x}{\mathrm{d}t^2} + 2\nu\frac{\mathrm{d}x}{\mathrm{d}t} + \Omega^2(x - x_0) = 0, \tag{VII.1.1}$$

where ν and $\Omega > 0$ are constants. You may recognize this as the equation for a damped simple harmonic oscillator of natural frequency Ω whose velocity along the x axis is damped at a rate $\nu > 0$. But let's not yet commit to any particular sign of ν. First, the equilibrium state. This is easy: the oscillator is at rest at $x = x_0$. We now displace the oscillator by a small amount ξ, so that $x(t) = x_0 + \xi(t)$. The equation governing this displacement is

$$\frac{\mathrm{d}^2\xi}{\mathrm{d}t^2} + 2\nu\frac{\mathrm{d}\xi}{\mathrm{d}t} + \Omega^2\xi = 0. \tag{VII.1.2}$$

This equation admits solutions $\xi \sim \exp(-\mathrm{i}\omega t)$, where ω is a complex frequency that satisfies the *dispersion relation*

$$\omega^2 + 2\mathrm{i}\omega\nu - \Omega^2 = 0 \quad \Longrightarrow \quad \omega = -\mathrm{i}\nu \pm \sqrt{\Omega^2 - \nu^2}. \tag{VII.1.3}$$

How do we assess stability? If the imaginary part of ω is positive, then $-\mathrm{i}\omega$ has a positive real part, and the displacements will grow exponentially in time. If the imaginary part of ω is negative, then $-\mathrm{i}\omega$ has a negative real part, and this corresponds to exponential decay of the perturbation. If ω additionally has a real part, then this represents a growing or decaying oscillator. It's clear from a cursory glance at the dispersion relation (VII.1.3) that the perturbations oscillate and decay exponentially if $\Omega > \nu > 0$. If $\nu > \Omega > 0$, then the perturbations decay without oscillating. But if $\nu < 0$, then there is always an exponentially growing solution. Thus, $\nu > 0$ is the *stability criterion* for this system.

Now, suppose the equation of interest were instead

$$\frac{\mathrm{d}^2x}{\mathrm{d}t^2} + 2\nu\frac{\mathrm{d}x}{\mathrm{d}t} + \Omega^2\sin(x - x_0) = 0. \tag{VII.1.4}$$

The equilibrium is still the same, but if we want simple harmonic oscillator solutions,

we're only go to get them if the displacement is small, i.e., $|\xi| \ll x_0$. In that case, we can Taylor expand $\sin(x - x_0) \approx \xi - \xi^3/6 + \ldots$. To leading order in ξ, we're back to where we started with (VII.1.2). This is *linear theory*: identify an equilibrium, perturb the system about that equilibrium, and drop all terms nonlinear in the perturbation amplitude.

Note that we are not solving an initial value problems. We are agnostic about the initial conditions and only ask whether some disturbance will ultimately grow or decay. In some situations (most notably, Landau damping), solving the initial value problem is absolutely essential to obtain the full solution and all the physics involved. But if you just want to calculate the wave-like response of a system to infinitesimally small perturbations and learn whether such a response grows or decays, you need only adopt solutions $\sim \exp(-\mathrm{i}\omega t)$, find the dispersion relation for ω vs $\boldsymbol{k}$, and examine the sign of its imaginary part. (The difference is related to a Laplace vs a Fourier transform in time.)

VII.2. Linearized MHD equations

Take (V.2.2) and write

$$\rho = \rho_0(\boldsymbol{r}) + \delta\rho(t,\boldsymbol{r}), \quad \boldsymbol{u} = \delta\boldsymbol{u}(t,\boldsymbol{r}), \quad P = P_0(\boldsymbol{r}) + \delta P(t,\boldsymbol{r}), \quad \boldsymbol{B} = \boldsymbol{B}_0(\boldsymbol{r}) + \delta\boldsymbol{B}(t,\boldsymbol{r});$$

i.e., consider a stratified, stationary equilibrium state threaded by a magnetic field and subject it to perturbations. Never mind how the equilibrium is set up – it is what it is, and we'll perturb it. Neglecting all terms quadratic in δ, equations (V.2.2) become

$$\frac{\partial\delta\rho}{\partial t} = -(\delta\boldsymbol{u}\cdot\boldsymbol{\nabla})\rho_0 - \rho_0(\boldsymbol{\nabla}\cdot\delta\boldsymbol{u}), \tag{VII.2.1}$$

$$\frac{\partial\delta\boldsymbol{u}}{\partial t} = -\frac{1}{\rho_0}\boldsymbol{\nabla}\left(\delta P + \frac{\boldsymbol{B}_0\cdot\delta\boldsymbol{B}}{4\pi}\right) + \frac{\delta\rho}{\rho_0^2}\boldsymbol{\nabla}\left(P_0 + \frac{B_0^2}{8\pi}\right) + \frac{(\boldsymbol{B}_0\cdot\boldsymbol{\nabla})\delta\boldsymbol{B}}{4\pi\rho_0} + \frac{(\delta\boldsymbol{B}\cdot\boldsymbol{\nabla})\boldsymbol{B}_0}{4\pi\rho_0} - \boldsymbol{\nabla}\delta\Phi, \tag{VII.2.2}$$

$$\frac{\partial\delta\boldsymbol{B}}{\partial t} = -(\delta\boldsymbol{u}\cdot\boldsymbol{\nabla})\boldsymbol{B}_0 + (\boldsymbol{B}_0\cdot\boldsymbol{\nabla})\delta\boldsymbol{u} - \boldsymbol{B}_0(\boldsymbol{\nabla}\cdot\delta\boldsymbol{u}), \tag{VII.2.3}$$

$$\frac{\partial}{\partial t}\left(\frac{\delta P}{P_0} - \gamma\frac{\delta\rho}{\rho_0}\right) = -\delta\boldsymbol{u}\cdot\boldsymbol{\nabla}\ln\frac{P_0}{\rho_0^\gamma}. \tag{VII.2.4}$$

(A quick way of getting these is to think of δ as a differential operator that commutes with partial differentiation.) Pretty much every gradient of an equilibrium quantity here will give an instability! (Otherwise, you just get back simple linear waves on a homogeneous background.) So let's not analyze this all at once. But I write this system of equations here for two important reasons: (i) it makes clear that we can adopt solutions $\delta \sim \exp(-\mathrm{i}\omega t)$ for the perturbations, since the equations are linear in the fluctuation amplitudes; (ii) we can only adopt full plane-wave solutions $\delta \sim \exp(-\mathrm{i}\omega t + \mathrm{i}\boldsymbol{k}\cdot\boldsymbol{r})$ if the fluctuations vary on length scales much smaller than that over which the background varies (the so-called WKB approximation). Otherwise, we have to worry about the exact structure of the background gradients and their boundary conditions.

So these are the themes of most linear stability analyses: a WKB approximation whereby plane-wave solutions are assumed on top of a background state that is slowly varying, and a focus only on whether fluctuations grow or decay rather than their specific spatio-temporal evolution from a set of initial conditions.

VII.3. Lagrangian versus Eulerian perturbations

There is one last thing worth discussing before proceeding with a linear stability analysis of the MHD equations. Just as there is an Eulerian time derivative and a Lagrangian time derivative, there is Eulerian perturbation theory and Lagrangian perturbation theory. The former, in which perturbations are denoted by a 'δ', measures the change in a quantity at a particular point in space. For example, if the equilibrium density at $\boldsymbol{r}$, $\rho(\boldsymbol{r})$, is changed at time t by some disturbance to become $\rho'(t,\boldsymbol{r})$, then we denote the Eulerian perturbation of the density by

$$\rho'(t,\boldsymbol{r}) - \rho(\boldsymbol{r}) \doteq \delta\rho \ll \rho(\boldsymbol{r}). \tag{VII.3.1}$$

Again, these perturbations are taken *at fixed position*. The latter – Lagrangian perturbation theory – concerns the evolution of small perturbations about a background state *within a particular fluid element* as it undergoes a displacement $\boldsymbol{\xi}$. For example, if a particularly fluid element is displaced from its equilibrium position $\boldsymbol{r}$ to position $\boldsymbol{r}+\boldsymbol{\xi}$, then the density of that fluid element changes by an amount

$$\rho'(t,\boldsymbol{r}+\boldsymbol{\xi}) - \rho(\boldsymbol{r}) \doteq \Delta\rho. \tag{VII.3.2}$$

This is a Lagrangian perturbation. To linear order, δ and Δ are related by

$$\Delta\rho \simeq \rho'(t,\boldsymbol{r}) + \boldsymbol{\xi}\cdot\boldsymbol{\nabla}\rho(\boldsymbol{r}) - \rho(\boldsymbol{r}) = \delta\rho + \boldsymbol{\xi}\cdot\boldsymbol{\nabla}\rho. \tag{VII.3.3}$$

There are many situations in which a Lagrangian approach is easier to use than an Eulerian approach; there are also some situations in which doing so is absolutely necessary (e.g., see §IIIe of Balbus (1988) and §Ic of Balbus & Soker (1989) for discussions of the perils of using Eulerian perturbations in the context of local thermal instability).

Question: It is possible to have zero Eulerian perturbation and yet have finite Lagrangian perturbation. What does this mean physically? Is there a physical change in the system?

The Lagrangian velocity perturbation $\Delta\boldsymbol{u}$ is given by

$$\Delta\boldsymbol{u} \doteq \frac{\mathrm{D}\boldsymbol{\xi}}{\mathrm{D}t} = \left(\frac{\partial}{\partial t} + \boldsymbol{u}\cdot\boldsymbol{\nabla}\right)\boldsymbol{\xi}, \tag{VII.3.4}$$

where $\boldsymbol{u}$ is the background velocity. It is the instantaneous time rate of rate of the displacement of a fluid element, taken relative to the unperturbed flow. Because $\Delta\boldsymbol{u} = \delta\boldsymbol{u} + \boldsymbol{\xi}\cdot\boldsymbol{\nabla}\boldsymbol{u}$, we have

$$\delta\boldsymbol{u} = \frac{\partial\boldsymbol{\xi}}{\partial t} + \boldsymbol{u}\cdot\boldsymbol{\nabla}\boldsymbol{\xi} - \boldsymbol{\xi}\cdot\boldsymbol{\nabla}\boldsymbol{u}. \tag{VII.3.5}$$

Note the additional $\boldsymbol{\xi}\cdot\boldsymbol{\nabla}\boldsymbol{u}$ term, representing a measurement of the background fluid gradients by the fluid displacement.

Exercise. Let $\boldsymbol{u} = R\Omega(R)\hat{\boldsymbol{\varphi}}$, as in a differentially rotating disk in cylindrical coordinates. Consider a displacement $\boldsymbol{\xi}$ with radial and azimuthal components ξ_R and ξ_φ, each depending upon R and φ. Show that

$$\frac{\mathrm{D}\xi_R}{\mathrm{D}t} = \delta u_R \quad \text{and} \quad \frac{\mathrm{D}\xi_\varphi}{\mathrm{D}t} = \delta u_\varphi + \xi_R\frac{\mathrm{d}\Omega}{\mathrm{d}\ln R}. \tag{VII.3.6}$$

The second term in the latter equation accounts for the stretching of radial displacements into

the azimuthal direction by the differential rotation. From the latter expression, show that

$$\frac{\Delta\Omega}{\Omega} = \frac{1}{R\Omega}\frac{\mathrm{D}\xi_\varphi}{\mathrm{D}t} \quad \text{and} \quad \frac{\Delta\ell}{\ell} = 2\frac{\xi_R}{R} + \frac{1}{R\Omega}\frac{\mathrm{D}\xi_\varphi}{\mathrm{D}t}, \tag{VII.3.7}$$

where $\ell \doteq \Omega R^2$ is the specific angular momentum.

You can think of δ and Δ as difference operators, since we're only working to linear order in the perturbation amplitude: e.g.,

$$\delta\left(\frac{1}{\rho}\right) = \frac{1}{\rho+\delta\rho} - \frac{1}{\rho} \simeq -\frac{\delta\rho}{\rho^2}.$$

But you must be very careful when mixing Eulerian and Lagrangian points of view. Prove the following commutation relations:

$$(i) \quad \left[\delta, \frac{\partial}{\partial t}\right] = 0;$$

$$(ii) \quad \left[\delta, \frac{\partial}{\partial x_i}\right] = 0;$$

$$(iii) \quad \left[\Delta, \frac{\partial}{\partial t}\right] = -\frac{\partial\xi_j}{\partial t}\frac{\partial}{\partial\xi_j};$$

$$(iv) \quad \left[\Delta, \frac{\partial}{\partial x_i}\right] = -\frac{\partial\xi_j}{\partial x_i}\frac{\partial}{\partial\xi_j};$$

$$(v) \quad \left[\Delta, \frac{\mathrm{D}}{\mathrm{D}t}\right] = 0;$$

$$(vi) \quad \left[\Delta, \frac{\mathrm{D}}{\mathrm{D}x_i}\right] = -\xi_j\frac{\partial}{\partial x_j}\frac{\mathrm{D}}{\mathrm{D}t};$$

$$(vii) \quad \left[\frac{\partial}{\partial x_i}, \frac{\mathrm{D}}{\mathrm{D}t}\right] = \frac{\partial u_j}{\partial x_i}\frac{\partial}{\partial x_j}.$$

You can use these to show that the linearized continuity equation, induction equation, and internal energy equation are

$$\frac{\Delta\rho}{\rho} = -\boldsymbol{\nabla}\cdot\boldsymbol{\xi}, \tag{VII.3.8}$$

$$\Delta\boldsymbol{B} = \boldsymbol{B}\cdot\boldsymbol{\nabla}\boldsymbol{\xi} - \boldsymbol{B}\boldsymbol{\nabla}\cdot\boldsymbol{\xi}, \tag{VII.3.9}$$

$$\frac{\Delta T}{T} = -(\gamma-1)\boldsymbol{\nabla}\cdot\boldsymbol{\xi}, \tag{VII.3.10}$$

respectively. These forms are particularly useful for linear analyses.

Now to calculate something... I'll start with two simple instabilities, the first of which (Jeans instability) will be analyzed using Eulerian perturbation theory, and the second of which (Kelvin–Helmholtz instability) will be analyzed using Lagrangian perturbation theory. Hopefully you'll see why one approach is sometimes easier than the other.

VII.4. Self-gravity: Jeans instability

One of the simplest hydrodynamical waves is a small-amplitude sound wave propagating on an infinite, homogeneous background. Take (V.2.2), set $\boldsymbol{B}_0 = 0$, and assume ρ_0

and P_0 to be constant. The resulting linearized equations are

$$\frac{\partial}{\partial t}\frac{\delta\rho}{\rho_0} = -\boldsymbol{\nabla}\cdot\delta\boldsymbol{u}, \quad \frac{\partial\delta\boldsymbol{u}}{\partial t} = -\frac{1}{\rho_0}\boldsymbol{\nabla}\delta P - \boldsymbol{\nabla}\delta\Phi, \quad \frac{\partial}{\partial t}\left(\frac{\delta P}{P_0} - \gamma\frac{\delta\rho}{\rho_0}\right) = 0. \tag{VII.4.1a}$$

I've retained the perturbed gravitational potential $\delta\Phi$ in the second equation, because we're going to assume that the fluid is self-gravitating with a potential that obey's Poisson's equation:[15]

$$\nabla^2\delta\Phi = 4\pi G\delta\rho. \tag{VII.4.1b}$$

These equations are linear in δ, and so we may adopt plane-wave solutions, $\delta \sim \exp(-\mathrm{i}\omega t + \mathrm{i}\boldsymbol{k}\cdot\boldsymbol{r})$. Substituting this form into (VII.4.1) gives

$$-\mathrm{i}\omega\frac{\delta\rho}{\rho_0} = -\mathrm{i}\boldsymbol{k}\cdot\delta\boldsymbol{u}, \quad -\mathrm{i}\omega\delta\boldsymbol{u} = -\mathrm{i}\boldsymbol{k}\frac{\delta P}{\rho_0} - \mathrm{i}\boldsymbol{k}\delta\Phi, \quad -\mathrm{i}\omega\left(\frac{\delta P}{P_0} - \gamma\frac{\delta\rho}{\rho_0}\right) = 0, \tag{VII.4.2a}$$

$$-k^2\delta\Phi = 4\pi G\delta\rho. \tag{VII.4.2b}$$

Taking $\boldsymbol{k}\cdot$ the second equation and using the other three yields the dispersion relation

$$\omega\left(\omega^2 - k^2a^2 + 4\pi G\rho_0\right) = 0, \tag{VII.4.3}$$

where $a^2 \doteq \gamma P_0/\rho_0$. The $\omega = 0$ root comes from the perturbed entropy equation, and corresponds to a isentropic relabelling of the fluid elements; its name is the 'entropy mode'. The other two roots correspond to forward- and backward-propagating sound waves under the influence of their own self-gravity:

$$\omega = \pm ka\sqrt{1 - \frac{4\pi G\rho_0}{k^2a^2}} \tag{VII.4.4}$$

Self-gravity reduces the speed of the wave for wavenumbers satisfying $ka > (4\pi G\rho_0)^{1/2}$, for which the (expansive) pressure force is greater than the (attractive) gravitational force. At $ka = (4\pi G\rho_0)^{1/2}$, these two forces balance exactly, and the mode is neutrally stable. But for $ka < (4\pi G\rho_0)^{1/2}$, the wavelength is long enough to include a sufficiently large amount of mass in the perturbation to overwhelm the pressure force. Instability ensues, and the mode grows without propagating. This is the *Jeans instability*, named after Sir James Jeans (although Sir Isaac Newton understood the concept over 200 years before the calculation).

The critical wavelength

$$\lambda_{\mathrm{J}} = a\sqrt{\frac{\pi}{G\rho_0}} \tag{VII.4.5}$$

is referred to as the *Jeans length*. For an isothermal ($\gamma = 1$) molecular cloud of temperature 10 K, number density 200 cm^{-3}, and mean mass per particle $2.33m_{\mathrm{p}}$, the Jeans length is $\simeq$1.5 pc. The corresponding *Jeans mass* enclosed within a spherical volume with λ_{J} as its diameter is

$$M_{\mathrm{J}} = \frac{\pi}{6}\rho_0\lambda_{\mathrm{J}}^3 = 20.3\left(\frac{T_0}{10\ \mathrm{K}}\right)^{3/2}\left(\frac{n}{200\ \mathrm{cm}^{-3}}\right)^{-1/2}\mathrm{M}_\odot. \tag{VII.4.6}$$

Giant molecular clouds with these parameters have typical masses $\gtrsim 10^4$ M$_\odot$, indicating

[15] Wouldn't an infinite, homogeneous, self-gravitating fluid collapse under its own weight? Indeed it would. Ignoring this inconvenience is known as the *Jeans swindle*. Following Binney & Tremaine (1987): 'it is a swindle because in general there is no formal justification for discarding the unperturbed gravitational field'.

that more must be going on than just thermal pressure support against self-gravity (see: magnetic fields and turbulence). Note that $M_{\rm J} = M_\odot$ at a density $n \simeq 8.2 \times 10^4$ cm^{-3}.

VII.5. Shear: Kelvin–Helmholtz instability

Consider two uniform fluids separated by a discontinuous interface at $z = 0$, as in the figure below:

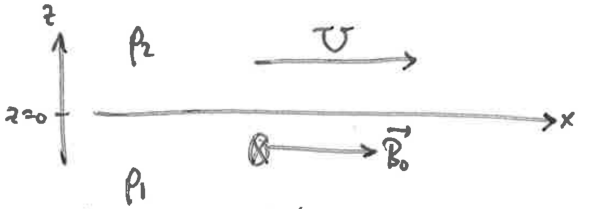

The fluid above the interface ($z > 0$) has density ρ_2 and equilibrium velocity $\boldsymbol{u}_0 = U\hat{\boldsymbol{x}}$. The fluid below the interface ($z < 0$) has density ρ_1 and is stationary. (We can always transform to a frame in which this fluid is stationary, so why not take advantage of that?) There is a uniform magnetic field $\boldsymbol{B}_0 = B_{0x}\hat{\boldsymbol{x}} + B_{0y}\hat{\boldsymbol{y}}$ oriented parallel to the interface that permeates all of the fluid, which we take to be perfectly conducting. For simplicity, take the fluid to be incompressible, *viz.* $\boldsymbol{\nabla}\cdot\boldsymbol{u} = 0$.

We seek the dispersion relation governing small-amplitude perturbations. It turns out that this problem is most easily analyzed using Lagrangian perturbations rather than Eulerian perturbations – the reason being that the interface and the interfacial pressure between the two fluids must remain continuous as the fluid is perturbed, and it's easier to measure this interface in the frame of the fluid element than in the lab frame.

Take the momentum equation in each of the fluids, above and below, and apply the difference operator $\Delta \doteq \delta + \boldsymbol{\xi}\cdot\boldsymbol{\nabla}$ while recalling that $[\Delta, \mathrm{D}/\mathrm{D}t] = 0$ and $\Delta\boldsymbol{u} = \mathrm{D}\boldsymbol{\xi}/\mathrm{D}t$:

$$\Delta\left[\rho\frac{\mathrm{D}\boldsymbol{u}}{\mathrm{D}t} = -\boldsymbol{\nabla}\left(P + \frac{B^2}{8\pi}\right) + \frac{\boldsymbol{B}\cdot\boldsymbol{\nabla}\boldsymbol{B}}{4\pi}\right]$$
$$\implies \rho\frac{\mathrm{D}^2\boldsymbol{\xi}}{\mathrm{D}t^2} = -\boldsymbol{\nabla}\delta\left(P + \frac{B^2}{8\pi}\right) + \frac{\boldsymbol{B}_0\cdot\boldsymbol{\nabla}\delta\boldsymbol{B}}{4\pi}, \tag{VII.5.1}$$

the form of the right-hand side following because $\boldsymbol{\nabla}B_0 = \boldsymbol{\nabla}P_0 = 0$. Use the linearized induction equation (VII.3.9) with $\boldsymbol{\nabla}B_0 = 0$, which reads $\delta\boldsymbol{B} = (\boldsymbol{B}_0\cdot\boldsymbol{\nabla})\boldsymbol{\xi}$, and rearrange to obtain

$$\left[\frac{\mathrm{D}^2}{\mathrm{D}t^2} - \frac{(\boldsymbol{B}_0\cdot\boldsymbol{\nabla})^2}{4\pi\rho}\right]\boldsymbol{\xi} = -\frac{1}{\rho}\boldsymbol{\nabla}\delta\left(P + \frac{B^2}{8\pi}\right) \doteq -\frac{1}{\rho}\boldsymbol{\nabla}\delta\Pi. \tag{VII.5.2}$$

Note that taking the divergence of this equation and using $\boldsymbol{\nabla}\cdot\boldsymbol{\xi} = 0$ (incompressibility) implies that the total perturbed pressure Π satisfies

$$\nabla^2\delta\Pi = 0. \tag{VII.5.3}$$

With the x and y directions being infinite in extent and the background state possessing no structure in those directions, we may write $\delta\Pi = \delta\Pi(z)\exp(\mathrm{i}k_x x + \mathrm{i}k_y y)$ to find

$$\left(-k^2 + \frac{\mathrm{d}^2}{\mathrm{d}z^2}\right)\delta\Pi(z) = 0 \quad\implies\quad \delta\Pi(z) \propto \exp(-|kz|), \quad k \equiv \sqrt{k_x^2 + k_y^2}. \tag{VII.5.4}$$

The absolute value in the argument of the exponential indicates that the perturbation must die off as $z \to \pm\infty$. We may now adopt solutions of the form $\exp(-\mathrm{i}\omega t)$ and evaluate

the z component of (VII.5.2) above and below the interface:

$$\left[(-\mathrm{i}\omega + \mathrm{i}k_x U)^2 + \frac{(\boldsymbol{k}\cdot\boldsymbol{B}_0)^2}{4\pi\rho_2}\right]\xi_{z2} = +\frac{1}{\rho_2}|k|\delta\Pi_2, \tag{VII.5.5a}$$

$$\left[(-\mathrm{i}\omega \qquad)^2 + \frac{(\boldsymbol{k}\cdot\boldsymbol{B}_0)^2}{4\pi\rho_1}\right]\xi_{z1} = -\frac{1}{\rho_1}|k|\delta\Pi_1, \tag{VII.5.5b}$$

respectively. At the interface, $\xi_{z1} = \xi_{z2}$ and $\Delta\Pi_1 = \Delta\Pi_2$, i.e., the two fluids must move together at the interface and their pressures must hold continuous as they are perturbed. Because $\boldsymbol{\nabla}B_0 = \boldsymbol{\nabla}P_0 = 0$, the latter implies $\delta\Pi_1 = \delta\Pi_2$. Using this information to match (VII.5.5a) and (VII.5.5b) leads to

$$(\omega - k_x U)^2\rho_2 + \omega^2\rho_1 = \frac{(\boldsymbol{k}\cdot\boldsymbol{B}_0)^2}{2\pi} \tag{VII.5.6}$$

$$\implies \quad \boxed{\omega = \frac{k_x U}{2}\frac{\overline{\rho}}{\rho_1}\left\{1 \pm \mathrm{i}\sqrt{\frac{\rho_1}{\rho_2}\left[1 - \frac{(\boldsymbol{k}\cdot\boldsymbol{B}_0)^2}{\pi\overline{\rho}k_x^2U^2}\right]}\right\}} \tag{VII.5.7}$$

where $\overline{\rho} \doteq 2\rho_1\rho_2/(\rho_1+\rho_2)$ is the reduced mass density. For

$$\frac{(\boldsymbol{k}\cdot\boldsymbol{B}_0)^2}{4\pi\overline{\rho}} < \left(\frac{k_x U}{2}\right)^2, \tag{VII.5.8}$$

the discriminant is positive and there is a growing (and propagating) mode whose growth rate is proportional to the wavenumber and the velocity shear across the interface. Note that, for $\rho_1 = \rho_2 = \rho$, we have $\overline{\rho} = \rho$, and then (VII.5.7) becomes

$$\omega = \frac{k_x U}{2}\left[1 \pm \mathrm{i}\sqrt{1 - \frac{(\boldsymbol{k}\cdot\boldsymbol{B}_0)^2}{\pi\rho k_x^2U^2}}\right];$$

for $U = 0$, this returns a stably propagating shear Alfvén wave, $\omega = \mp(\boldsymbol{k}\cdot\boldsymbol{v}_\mathrm{A})$. This indicates that it is the tension in the magnetic-field lines that is responsible for stabilizing the instability. That being said, if the magnetic field is oriented such that $B_{0x} = 0$, then (VII.5.8) can always be satisfied for small enough $|k_y/k_x|$, no matter how strong is B_{0y}.

The physics is as follows. An upwardly displaced distortion of the interface into region 2 causes a constriction of the velocity there, and the fluid must move faster to conserve its mass. But when it moves faster, the pressure must drop (Bernoulli!). The opposite happens below the interface. Now there is a pressure gradient pushing upwards, reinforcing the displacement, and the process runs away (unless the magnetic tension can stabilize the displacements and propagate them away as Alfvén waves). That's why pressure perturbations were vital in (VII.5.2).

Question: Does this instability occur in a simple linear shear flow, e.g., $\boldsymbol{u}_0 = Sz\hat{\boldsymbol{x}}$? No! The proof goes as follows. Drop the magnetic field for simplicity. With $\boldsymbol{u}_0 = u_0(z)\hat{\boldsymbol{x}}$, one can show using $\boldsymbol{\nabla}\cdot\boldsymbol{\xi} = 0$ and the momentum equation that

$$\frac{\mathrm{d}^2\xi_z}{\mathrm{d}z^2} - k_x^2\xi_z = \frac{ku_0''}{\omega - k_x u_0}\xi_z.$$

Multiply this by ξ_z^* (the '$*$' denotes the complex conjugate) and integrate between the upper

and lower boundaries $z = \pm L$ to obtain

$$\int_{-L}^{L} \mathrm{d}z \left(\xi_z^* \xi_z'' - k_x^2 |\xi_z|^2 \right) = \int_{-L}^{L} \mathrm{d}z \, \frac{k_x u_0''}{\omega - k_x u_0} |\xi_z|^2.$$

The first term on the left-hand side may be simplified using integration by parts and assuming either periodicity or that ξ_z or ξ_z' vanish at the boundaries. Then

$$\int_{-L}^{L} \mathrm{d}z \left(-|\xi_z'|^2 - k_x^2 |\xi_z|^2 \right) = \int_{-L}^{L} \mathrm{d}z \, \frac{k_x u_0''}{\omega - k_x u_0} |\xi_z|^2,$$

If the system is unstable, then ω must have an imaginary part, ω_I. Writing $\omega = \omega_\mathrm{R} + \mathrm{i}\omega_\mathrm{I}$, the imaginary part of the above equation is simply

$$\omega_\mathrm{I} \int_{-L}^{L} \mathrm{d}z \, \frac{k_x u_0''}{|\omega - k_x u_0|^2} |\xi_z|^2 = 0.$$

This states that u_0'' must be positive over part of the integration range, and negative over the remainder, i.e., u_0'' must pass through zero. Thus, instability requires an *inflection point* (Rayleigh 1880). (Note that the converse is not true: a velocity profile *with* an inflection point is not necessarily unstable.)

VII.6. Buoyancy: Rayleigh–Taylor instability

Using Lagrangian perturbation theory, it is easy to generalize the calculation in the previous section (§VII.5) to include gravity. Again, let the fluid above the interface ($z > 0$) have uniform density ρ_2, and the fluid below the interface ($z < 0$) have uniform density ρ_1. Include the same uniform background magnetic field as before, $\boldsymbol{B}_0 = B_{0x}\hat{\boldsymbol{x}} + B_{0y}\hat{\boldsymbol{y}}$. But now place these fluids in a constant gravitational field $\boldsymbol{g} = -g\hat{\boldsymbol{z}}$, with the gas pressure either side of the interface satisfying hydrostatic equilibrium in the vertical direction:

$$g = -\frac{1}{\rho_1}\frac{\mathrm{d}P_1}{\mathrm{d}z} = -\frac{1}{\rho_2}\frac{\mathrm{d}P_2}{\mathrm{d}z}.$$

The entire calculation goes through as before, but with the following additions and modifications. First, we must include the perturbed gravitational force in the momentum equation (VII.5.1), *viz.* $\Delta(\rho\boldsymbol{g}) = -(\Delta\rho)g\hat{\boldsymbol{z}}$. Secondly, because of the background pressure gradient in each of the fluids, we no longer have that $\Delta(\boldsymbol{\nabla}P) = \boldsymbol{\nabla}\delta P$, but rather that $\Delta(\boldsymbol{\nabla}P) = \boldsymbol{\nabla}\delta P + \boldsymbol{\xi}\cdot\boldsymbol{\nabla}(\boldsymbol{\nabla}P)$. Using hydrostatic equilibrium, this may equivalently be written as $\Delta(\boldsymbol{\nabla}P) = \boldsymbol{\nabla}\delta P - \boldsymbol{\xi}\cdot\boldsymbol{\nabla}(\rho g\hat{\boldsymbol{z}})$. Making these two changes in (VII.5.1) leads to

$$\rho\frac{\mathrm{D}^2\boldsymbol{\xi}}{\mathrm{D}t^2} = -\boldsymbol{\nabla}\delta\left(P + \frac{B^2}{8\pi}\right) + \frac{\boldsymbol{B}_0\cdot\boldsymbol{\nabla}\delta\boldsymbol{B}}{4\pi} - (\Delta\rho)g\hat{\boldsymbol{z}} + \boldsymbol{\xi}\cdot\boldsymbol{\nabla}(\rho g). \tag{VII.6.1}$$

Despite this extra work, however, those two additional terms cancel one another if the fluid is incompressible, since then $\Delta\rho - \boldsymbol{\xi}\cdot\boldsymbol{\nabla}\rho \doteq \delta\rho = 0$. As a result, the *only* difference between this calculation and the Kelvin–Helmholtz calculation in §VII.5 is that the imposition of pressure continuity at the perturbed interface does not imply that $\delta\Pi_1 = \delta\Pi_2$, but rather

$$\Delta\Pi_1 = \Delta\Pi_2 \implies \delta\Pi_1 - \xi_{z1}\rho_1 g = \delta\Pi_2 - \xi_{z2}\rho_2 g \implies \delta\Pi_2 - \delta\Pi_1 = \xi_z(\rho_2 - \rho_1)g.$$

We may then use this in (VII.5.5) to jump straight to the dispersion relation (cf. (VII.5.6))

$$(\omega - k_x U)^2\rho_2 + \omega^2\rho_1 = \frac{(\boldsymbol{k}\cdot\boldsymbol{B}_0)^2}{2\pi} + |k|g(\rho_1 - \rho_2), \tag{VII.6.2}$$

whose solutions are (cf. (VII.5.7))

$$\omega = \frac{k_x U}{2}\frac{\overline{\rho}}{\rho_1}\left\{1 \pm \mathrm{i}\sqrt{\frac{\rho_1}{\rho_2}\left[1 + \frac{2|k|g}{k_x^2 U^2}\frac{\rho_2 - \rho_1}{\overline{\rho}} - \frac{(\boldsymbol{k}\cdot\boldsymbol{B}_0)^2}{\pi\overline{\rho}k_x^2 U^2}\right]}\right\}. \tag{VII.6.3}$$

By design, this has both Kelvin–Helmholtz and Rayleigh–Taylor in it; let's set $U = 0$ to eliminate the former, in which case

$$\boxed{\omega = \pm\mathrm{i}\sqrt{|k|g\frac{\rho_2 - \rho_1}{\rho_1 + \rho_2} - \frac{(\boldsymbol{k}\cdot\boldsymbol{B}_0)^2}{2\pi(\rho_1 + \rho_2)}}} \tag{VII.6.4}$$

This equation states that linear instability requires $\rho_2 > \rho_1$ (heavy on top, light on the bottom), with the difference between the densities being large enough for the destabilizing pressure gradient (Bernoulli!) to overcome the stabilizing magnetic tension. Note that, if $\boldsymbol{B}_0$ is not oriented along the interface, no amount of magnetic field can stabilize the system.

Usually a physical explanation of the Rayleigh–Taylor instability isn't provided in derivations of its linear theory; indeed, the fact that heavy stuff falls down if given the opportunity to do so is fairly obvious. But it's worth thinking about the physics a little harder, and connecting this intuition back to the math. Let's return to (VII.6.1) with $U = 0$ and $\boldsymbol{B} = 0$ in order to isolate the Rayleigh–Taylor physics, and take curl of this equation:

$$\boldsymbol{\nabla}\times\left(\rho\frac{\mathrm{D}^2\boldsymbol{\xi}}{\mathrm{D}t^2}\right) = 0.$$

Chain-ruling the curl, dividing through by ρ, and using (VII.6.1) to eliminate $\mathrm{D}^2\boldsymbol{\xi}/\mathrm{D}t^2$ yields

$$\frac{\mathrm{D}^2}{\mathrm{D}t^2}\boldsymbol{\nabla}\times\boldsymbol{\xi} = \frac{1}{\rho^2}\boldsymbol{\nabla}\rho\times\boldsymbol{\nabla}\delta P.$$

If you read §IV.4, you'll recognize this as an equation for the vorticity, which is being baroclinically forced by the misalignment between the background density gradient and the *perturbed* pressure gradient. Because of the rippled interface, this perturbed pressure gradient has a component in the x direction, which points from regions where $\xi_z > 0$ towards regions where $\xi_z < 0$. With $\boldsymbol{\nabla}\rho$ pointing upwards (in the unstable situation), the baroclinic forcing is pointing in just the right direction to accentuate the vorticity in the original perturbation. See the figure below.

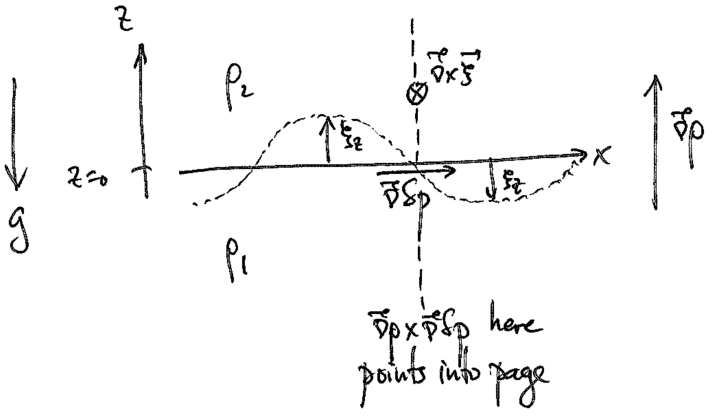

VII.7. Buoyancy: Convective (Schwarzschild) instability

Next up: stratification. Henceforth, ignore self-gravity. Suppose our plasma is immersed in a constant, externally imposed gravitational field $\boldsymbol{g} = -g\hat{\boldsymbol{z}}$ and that its thermal-pressure gradient balances the gravitational acceleration to produce a stationary, equilibrium state. Ignoring for the moment magnetic fields, this hydrostatic equilibrium is described by the equation

$$\frac{1}{\rho_0}\frac{\mathrm{d}P_0}{\mathrm{d}z} = g = \text{const}, \tag{VII.7.1}$$

where $\rho_0 = \rho_0(z)$. The hydrodynamic equations linearized about this equilibrium are

$$\frac{\partial}{\partial t}\frac{\delta\rho}{\rho_0} + \boldsymbol{\nabla}\cdot\delta\boldsymbol{u} + \delta u_z \frac{\mathrm{d}\ln\rho_0}{\mathrm{d}z} = 0, \tag{VII.7.2}$$

$$\frac{\partial\delta\boldsymbol{u}}{\partial t} = -\frac{1}{\rho_0}\boldsymbol{\nabla}\delta P - \frac{\delta\rho}{\rho_0}g\hat{\boldsymbol{z}}, \tag{VII.7.3}$$

$$\frac{\partial}{\partial t}\left(\frac{\delta P}{P_0} - \gamma\frac{\delta\rho}{\rho_0}\right) + \delta u_z \frac{\mathrm{d}}{\mathrm{d}z}\ln\frac{P_0}{\rho_0^\gamma} = 0. \tag{VII.7.4}$$

Solutions to this set of equations are $\propto \exp(-\mathrm{i}\omega t)$:

$$-\mathrm{i}\omega\frac{\delta\rho}{\rho_0} + \boldsymbol{\nabla}\cdot\delta\boldsymbol{u} + \delta u_z \frac{\mathrm{d}\ln\rho_0}{\mathrm{d}z} = 0, \tag{VII.7.5}$$

$$-\mathrm{i}\omega\delta\boldsymbol{u} = -\frac{1}{\rho_0}\boldsymbol{\nabla}\delta P - \frac{\delta\rho}{\rho_0}g\hat{\boldsymbol{z}}, \tag{VII.7.6}$$

$$-\mathrm{i}\omega\left(\frac{\delta P}{P_0} - \gamma\frac{\delta\rho}{\rho_0}\right) + \delta u_z \frac{\mathrm{d}}{\mathrm{d}z}\ln\frac{P_0}{\rho_0^\gamma} = 0. \tag{VII.7.7}$$

Continued on hand-written notes...

In general, we cannot Fourier transform these eqns. in z, because the coefficients in front of the perturbed quantities are z-dependent. But we can do so in the horizontal (say, x) direction:

$$-i\omega \frac{\delta\rho}{\rho_0} + ik_x \delta u_x + \frac{d\delta u_z}{dz} + \delta u_z \frac{d\ln\rho_0}{dz} = 0,$$

$$-i\omega \delta u_x = -ik_x \frac{\delta p}{\rho_0},$$

$$-i\omega \delta u_z = -\frac{1}{\rho_0}\frac{d\delta p}{dz} - \frac{\delta\rho}{\rho_0} g,$$

$$-i\omega \left(\frac{\delta p}{p_0} - \gamma \frac{\delta\rho}{\rho_0} \right) + \delta u_z \frac{d\ln p_0 \rho_0^{-\gamma}}{dz} = 0,$$

where now the fluctuations are z-dependent Fourier amplitudes. Denoting $\delta u = -i\omega \xi$, and dropping the equilibrium "0" subscripts for notational ease, we have

(A) $$\frac{\delta\rho}{\rho} + ik_x \xi_x + \xi_z' + \xi_z \frac{d\ln\rho}{dz} = 0,$$

(B) $$-\omega^2 \xi_x = -ik_x \frac{\delta p}{\rho},$$

(C) $$-\omega^2 \xi_z = -\frac{1}{\rho}\frac{d}{dz}\delta p - \frac{\delta\rho}{\rho} g,$$

(D) $$\frac{\delta p}{p} = \gamma \frac{\delta\rho}{\rho} - \xi_z \frac{d\ln p\rho^{-\gamma}}{dz}.$$

(B) and (D) $\Rightarrow$ $-\omega^2 \xi_x = -ik_x \frac{P}{\rho}\left[\gamma \frac{\delta\rho}{\rho} - \xi_z \frac{d\ln P\rho^{-\gamma}}{dz}\right]$

and (A) $\Rightarrow$ $-\omega^2 \xi_x = +ik_x \frac{P}{\rho}\gamma\left[+ik_x\xi_x + \xi_z' + \xi_z \frac{d\ln\rho}{dz}\right]$

$$+ ik_x \frac{P}{\rho}\xi_z \frac{d\ln P\rho^{-\gamma}}{dz}$$

$\Rightarrow \left(-\omega^2 + k_x^2 a^2\right)\xi_x = ik_x a^2 \xi_z' + \frac{ik_x a^2}{\gamma}\frac{d\ln\rho}{dz}\xi_z$,

where $a^2 \equiv \gamma P/\rho$. Note: $g = -\frac{a^2}{\gamma}\frac{d\ln\rho}{dz}$, so this is

(E) $\boxed{\left(-\omega^2 + k_x^2 a^2\right)\xi_x = ik_x a^2 \xi_z' - ik_x \xi_z g}$

(C) $\Rightarrow$ $\frac{\delta\rho}{\rho} = -\xi_z' - \xi_z \frac{d\ln\rho}{dz} - \frac{ik_x\left[ik_x a^2 \xi_z' - ik_x \xi_z g\right]}{-\omega^2 + k_x^2 a^2}$

$\Rightarrow$ $\boxed{\frac{\delta\rho}{\rho} = \frac{\omega^2 \xi_z' + \left[\left(\omega^2 - k_x^2 a^2\right)\frac{d\ln\rho}{dz} - k_x^2 g\right]\xi_z}{k_x^2 a^2 - \omega^2}}$ (G)

$\Rightarrow$ $\boxed{\frac{\delta P}{P} = \frac{1}{k_x^2 a^2 - \omega^2}\left[\gamma\omega^2 \xi_z' + \gamma\left(\left(\omega^2 - k_x^2 a^2\right)\frac{d\ln\rho}{dz} - k_x^2 g\right)\xi_z + \left(\omega^2 - k_x^2 a^2\right)\frac{d\ln P\rho^{-\gamma}}{dz}\xi_z\right]}$

$$= \frac{1}{k_x^2 a^2 - \omega^2}\left[\gamma\omega^2 \xi_z' + \omega^2 \frac{d\ln\rho}{dz}\xi_z\right]$$

$$= \frac{\omega^2}{k_x^2 a^2 - \omega^2}\left[\gamma\xi_z' + \frac{d\ln\rho}{dz}\xi_z\right]$$ (F)

into ⓒ:

$$+\omega^2\xi_z = +g\left[\frac{\omega^2\xi_x' + \left(\omega^2 - k_x^2a^2\right)\frac{d\ln\rho}{dz}\xi_z - k_x^2 g\,\xi_z}{k_x^2a^2-\omega^2}\right]$$

$$+\frac{1}{\rho}\frac{d}{dz}\left[\frac{\omega^2\rho}{k_x^2a^2-\omega^2}\left(\xi_z'\gamma + \xi_z\frac{d\ln p}{dz}\right)\right]$$

$$= \frac{\omega^2}{\rho}\frac{d\rho}{dz}\frac{\left(\xi_z'\gamma + \xi_z\frac{d\ln p}{dz}\right)}{k_x^2a^2-\omega^2} + \frac{\rho}{\rho}\frac{\omega^2}{k_x^2a^2-\omega^2}\left(\gamma\xi_z'' + \xi_z'\frac{d\ln p}{dz} + \xi_z\frac{d^2\ln p}{dz^2}\right)$$

$$-\frac{\omega^2\rho}{\rho}\frac{k_x^2}{\left(k_x^2a^2-\omega^2\right)^2}\frac{da^2}{dz}\left(\xi_z'\gamma + \xi_z\frac{d\ln p}{dz}\right)$$

$$\Rightarrow \omega^2\xi_z = \frac{g}{k_x^2a^2-\omega^2}\left[\omega^2\xi_x' - k_x^2 g\,\xi_z + \left(\omega^2 - k_x^2a^2\right)\frac{d\ln\rho}{dz}\xi_z\right]$$

$$+\frac{\omega^2}{k_x^2a^2-\omega^2}(-g)\left[\xi_z'\gamma + \xi_z\frac{d\ln p}{dz}\right]$$

$$+\left(\frac{a^2}{\gamma}\right)\frac{\omega^2}{k_x^2a^2-\omega^2}\left[\xi_z''\gamma + \xi_z'\frac{d\ln p}{dz} + \xi_z\frac{g\gamma}{a^2}\frac{d\ln T}{dz}\right]$$

$$-\frac{\omega^2}{\gamma}\frac{a^2k_x^2a^2}{\left(k_x^2a^2-\omega^2\right)^2}\frac{d\ln T}{dz}\left[\xi_z'\gamma + \xi_z\frac{d\ln p}{dz}\right]$$

Multiply by $\frac{k_x^2a^2-\omega^2}{\omega^2a^2}$ and group:

ξ_z'': 1.

ξ_z': $\cancel{\frac{g}{a^2}} - \frac{g\gamma}{a^2} + \cancel{\frac{1}{\gamma}\frac{d\ln p}{dz}} - \cancel{\frac{k_x^2 a^2}{\gamma}}\frac{1}{(k_x^2a^2-\omega^2)}\frac{d\ln T}{dz}\cancel{\gamma}$

$= \frac{d\ln p}{dz} - \left(\frac{k_x^2a^2}{k_x^2a^2-\omega^2}\right)\frac{d\ln T}{dz} = \frac{d\ln p/dz}{k_x^2a^2-\omega^2}\left[k_x^2a^2-\omega^2 - k_x^2a^2\frac{d\ln T}{d\ln p}\right]$

$= \frac{d\ln p/dz}{k_x^2a^2-\omega^2}\left[-\omega^2 + k_x^2a^2\frac{d\ln p}{d\ln p}\right] = \frac{\omega^2\frac{d\ln p}{dz} - k_x^2a^2\frac{d\ln p}{dz}}{\omega^2 - k_x^2a^2}$

ξ_z: $-\frac{(k_x^2a^2-\omega^2)}{a^2} - \frac{k_x^2g^2}{\omega^2a^2} - g\frac{d\ln p}{dz}\frac{k_x^2a^2-\omega^2}{\omega^2a^2}$

$-\cancel{\frac{g}{a^2}\frac{d\ln p}{dz}} + \frac{a^2}{\gamma}\cancel{\frac{1}{a^2}\frac{g\gamma}{a^2}\frac{d\ln T}{dz}} - \frac{k_x^2a^2}{\gamma(k_x^2a^2-\omega^2)}\frac{d\ln T}{dz}\frac{d\ln p}{dz}$

$= \frac{-1}{k_x^2a^2-\omega^2}\left[\frac{k_x^2a^2}{\gamma}\frac{d\ln T}{dz}\frac{d\ln p}{dz} + \frac{gk_x^2}{\omega^2}\frac{d\ln p}{dz}(k_x^2a^2-\omega^2) + \frac{k_x^2g^2}{a^2\omega^2}(k_x^2a^2-\omega^2) + \frac{(k_x^2a^2-\omega^2)^2}{a^2}\right]$

$= \frac{1}{\omega^2-k_x^2a^2}\left[\frac{\omega^4}{a^2} - 2\omega^2k_x^2 + k_x^4a^2 - \frac{k_x^2g^2}{a^2} - \cancel{gk_x^2\frac{d\ln p}{dz}} + \frac{k_x^2a^2}{\gamma}\frac{d\ln T}{dz}\frac{d\ln p}{dz} + \frac{gk_x^4a^2}{\omega^2}\frac{d\ln p}{dz} + \cancel{\frac{k_x^4a^2g^2}{a^2\omega^2}}\right]$

$-k_x^2g\left(\frac{d\ln T}{dz} - \cancel{\frac{d\ln p}{dz}}\right)$

So,

$$\xi_z'' + \xi_z' \left[\frac{\omega^2 \frac{d\ln\rho}{dz} - k_x^2 a^2 \frac{d\ln\rho}{dz}}{\omega^2 - k_x^2 a^2} \right]$$

$$+ \xi_z \frac{1}{\omega^2 - k_x^2 a^2} \left[\frac{\omega^4}{a^2} - 2\omega^2 k_x^2 + k_x^4 a^2 - k_x^2 g \frac{d\ln\rho}{dz}\left(1 - \frac{1}{\gamma}\right) \right.$$

$$\left. + g \frac{k_x^4 a^2}{\omega^2} \frac{d\ln\rho}{dz} + \frac{k_x^4 g^2}{\omega^2} \right] = 0.$$

This is UGLY!!! And we can't solve it analytically anyhow. It's just a stratified fluid — why is it so complicated?! The reason is twofold: (1) this equation mixes up buoyancy and sound waves — distinct physical effects; and (2) the sound and buoyancy frequencies are functions of height. Let's fix this by adopting an ordering: let

$$\frac{d\xi_z}{dz} \sim ik_z \xi_z = ik_z H \left(\frac{\xi_z}{H}\right) \gg \frac{\xi_z}{H},$$

where $H \equiv \left|\frac{dz}{d\ln\rho}\right| \sim \left|\frac{dz}{d\ln\rho}\right|$. In other words, we assume that ξ_z varies on a scale $\ll$ the scale of the background. This is a WKB approach. So...

Let $\epsilon \equiv \frac{1}{k_z H} \ll 1$. Also, $k_x \sim k_z$. Now, we must make a decision about the size of ω, by comparing it with

$\frac{a}{H} = \frac{\gamma_g}{a} = \sqrt{\frac{\gamma_g}{H}}$. There are two choices of interest:

(i) $\omega \sim a/H$

(ii) $\omega \sim ka \sim \underbrace{(a/H)}_{\epsilon} \gg \frac{a}{H}$.

First, write $\frac{d\xi_z}{dz} = ik_z \xi_z$ with $k_z H \equiv \frac{1}{\epsilon}$;  becomes

$$-k_z^2 \xi_z + ik_z \xi_z \left[\frac{\omega^2 \frac{d\ln\rho}{dz} - k_x^2 a^2 \frac{d\ln p}{dz}}{\omega^2 - k_x^2 a^2} \right]$$

$$+ \frac{\xi_z}{\omega^2 - k_x^2 a^2} \left[\frac{\omega^4}{a^2} - 2\omega^2 k_x^2 + k_x^4 a^2 - k_x^2 g \frac{d\ln p}{dz}\left(1 - \frac{1}{\gamma}\right) \right.$$

$$\left. + g\frac{k_x^4 a^2}{\omega^2} \frac{d\ln\rho}{dz} + \frac{k_x^4 g^2}{\omega^2} \right] = 0.$$

Now, (i) $\omega \sim a/H$ gives $k_x^2 a^2 \gg \omega^2$ and so the dominant terms are

$$-k_z^2 \xi_z + \xi_z(-k_x^2) - \xi_z g\frac{k_x^2}{\omega^2}\frac{d\ln\rho}{dz} - \xi_z \frac{k_x^2 g^2}{a^2\omega^2} = 0$$

$$\Rightarrow \quad k^2 + g\frac{k_x^2}{\omega^2}\left[\underbrace{\frac{d\ln\rho}{dz} + \frac{g}{a^2}}_{\frac{d\ln\rho}{dz} - \frac{1}{\gamma}\frac{d\ln p}{dz} = -\frac{1}{\gamma}\frac{d\ln \gamma p \rho^{-\gamma}}{dz}} \right] = 0.$$

$$\Rightarrow \boxed{\omega^2 = \frac{k_x^2}{k^2}\frac{g}{\gamma}\frac{d\ln p\rho^{-\gamma}}{dz} = -\frac{k_x^2}{k^2}\frac{1}{\gamma p}\frac{dp}{dz}\frac{d\ln p\rho^{-\gamma}}{dz} \equiv \frac{k_x^2}{k^2}N^2}$$

where N^2 is the square of the Brunt - Väisälä frequency.

If $N^2>0$, these are called <u>internal waves</u> or <u>g-modes</u>.

Note that different wavenumbers have different velocities (i.e., dispersion) and that ω depends on the direction of $\vec{k}$: $\frac{\partial\omega}{\partial\vec{k}} = \frac{\omega}{k^2}\frac{k_z}{k_x}\left(k_z\hat{x} - k_x\hat{z}\right)$, so that $\vec{k}\cdot\frac{\partial\omega}{\partial\vec{k}} = 0$.

We'll return to the physical cause of these waves later, after the "Boussinesq approximation" is introduced, but, for now, note that $N^2<0$ (i.e., upwardly decreasing entropy) gives instability. Go boil some water and think about it.

(ii) $\omega \sim ka >> a/H$. This gives the following dominant terms:

$$-k_z^2 + \frac{1}{\omega^2 - k_x^2a^2}\Bigg(\underbrace{\frac{\omega^4}{a^2} - 2\omega^2k_x^2 + k_x^4a^2}_{(\omega^2-k_x^2a^2)^2/a^2}\Bigg) = 0$$

$$\Rightarrow \boxed{\omega^2 = (k_x^2 + k_z^2)a^2}$$ <u>Sound waves!</u>

Now, sound waves are often a nuisance in many calculations. They mostly play a rather boring role, and often serve only to make the algebra more tedious. There is something called the Boussinesq approximation, which rigorously filters out sound waves. Let's see how this works in our convection problem...

Return to ✡ with $\omega \sim \epsilon ka$:

$$\frac{\delta p}{p} \simeq \frac{\omega^2}{k_x^2 a^2} ik_z \xi_z \gamma \quad \text{if} \quad k_z \neq 0;$$

$$\simeq \underbrace{\frac{\omega^2}{k_x^2 a^2}}_{\sim \epsilon^2 \ll 1} \frac{d\ln p}{dz} \xi_z \quad \text{otherwise.}$$

So, perhaps we should have dropped perturbations to the gas pressure at some point. Where? In the momentum equation? Hmm... careful. Consider Ⓑ with $\frac{\delta p}{p} \simeq \frac{\omega^2}{k_x^2 a^2} ik_z \xi_z \gamma$

$\Rightarrow \xi_x = -\xi_z \frac{k_z}{k_x}$, or $\vec{k} \cdot \vec{\xi} = 0$. Looks like pressure fluctuations are enforcing (near) incompressibility. Best not to drop them! And Ⓒ?

$$-\omega^2 \xi_z = -ik_z \frac{p}{\rho} \frac{\omega^2}{k_x^2 a^2} ik_z \xi_z \gamma - \frac{\delta p}{\rho} g$$

same order!

Okay. So, pressure fluctuations are small, but not so small that they can be dropped from the momentum eqn. What about the entropy eqn?

$$\textcircled{D} \Rightarrow \frac{\delta P}{P} = \gamma \frac{\delta \rho}{\rho} - \xi_z \frac{d \ln P \rho^{-\gamma}}{dz}$$

$\frac{\delta P}{P} \sim \frac{\xi_z}{H} \frac{\omega^2}{k_x^2 a^2}$; $\xi_z \frac{d \ln P\rho^{-\gamma}}{dz} \sim \frac{\xi_z}{H}$ 1 required for internal waves

or $\sim i k_z \xi_z \frac{\gamma \omega^2}{k_x^2 a^2}$, either way... it's small. So, drop δP from entropy equation! What does that leave us with?

$$\gamma \frac{\delta \rho}{\rho} \simeq \xi_z \frac{d \ln P \rho^{-\gamma}}{dz}$$

$\Rightarrow \frac{\delta \rho}{\rho} \sim \frac{\xi_z}{H}$. Ah! Look at $\textcircled{A}$: $\frac{\delta \rho}{\rho} + i k_z \xi_z + i k_x \xi_x + \xi_z \frac{d \ln \rho}{dz} = 0$

$\frac{\delta \rho}{\rho} \sim \frac{\xi_z}{H}$; $i k_z \xi_z \sim k \xi_z$; $\xi_z \frac{d \ln \rho}{dz} \sim \frac{\xi_z}{H}$

So, to leading order, we have $\vec{k} \cdot \vec{\xi} = 0$ — incompressibility! Okay, things are consistent, and we have the Boussinesq approx:

$$\frac{\delta P}{\bar{\rho}} \sim \frac{1}{kH}\frac{\delta\rho}{\bar{\rho}} \ll \frac{\delta\rho}{\bar{\rho}} \sim \frac{\delta u}{a} \ll \frac{k\delta u}{\omega} \sim k\xi \sim (kH)\frac{\delta u}{a}.$$

Or, defining the Mach number M and taking it to be small ($\sim \epsilon$),

$$\frac{\delta u}{a} \sim \frac{\delta\rho}{\bar{\rho}} \sim \frac{\delta T}{\bar{T}} \sim \frac{1}{M}\frac{\delta p}{\bar{p}} \sim \frac{1}{kH} \sim \epsilon \ll 1.$$

In practice, this means:

1) Assume (near) incompressibility ($\vec{\nabla}\cdot\vec{\delta u} = 0$)

2) Drop $\delta\rho$ everywhere EXCEPT the momentum eqn.
They are enforcing (near) incompressibility.

3) Keep $\delta\rho$ everywhere EXCEPT the continuity eqn.
They interact with gravity to give buoyancy.

Watch how much simpler this is...

Ⓐ → $ik_x\xi_x + ik_z\xi_z = 0$

Ⓑ → $-\omega^2\xi_x = -ik_x\frac{\delta p}{\bar{\rho}}$

Ⓒ → $-\omega^2\xi_z = -ik_z\frac{\delta p}{\bar{\rho}} - \frac{\delta\rho}{\bar{\rho}}g$

Ⓓ → $0 = \gamma\frac{\delta p}{\bar{p}} - \xi_z\frac{d\ln\bar{p}\,\bar{\rho}^{-\gamma}}{dz}$

Ⓑ, Ⓒ → $\frac{\delta\rho}{\bar{\rho}} = \frac{i\omega^2 k_z}{k_x^2}\xi_z$

Ⓒ → $\omega^2\xi_z = \frac{k_x^2}{k^2}g\frac{\delta\rho}{\bar{\rho}}$

Ⓓ → $\omega^2 = \frac{k_x^2}{k^2}N^2$. Done!

What we've done here is eliminated the restoring pressure forces that drive sound waves, essentially by assuming that a^2 is so large that sound waves propagate instantaneously. When the restoring force is purely external (e.g., gravity), the flow behaves as though it were incompressible (nearly). Physically, a slow-moving fluid element remains in pressure balance with its surroundings. This readjustment is what makes buoyancy waves and convection possible. Let us see that explicitly.

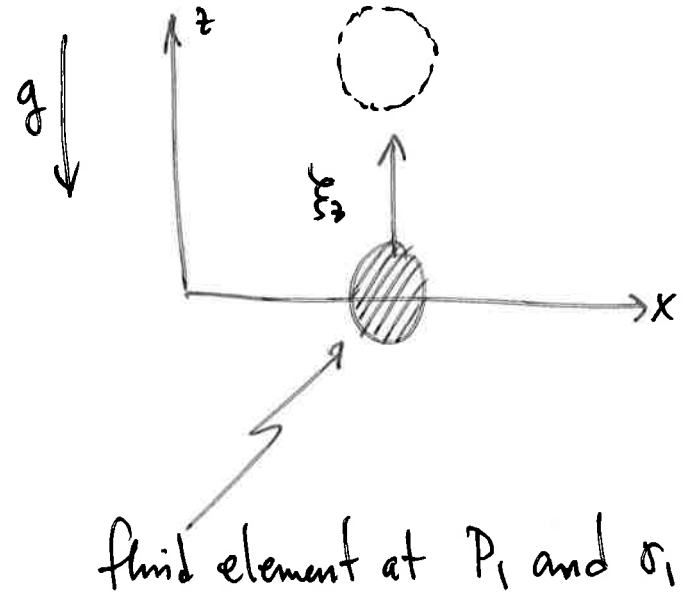

$P_2 < P_1$ $\quad \sigma_2 > \sigma_1$

P_1 $\quad \sigma_1$

where $\sigma \equiv P\rho^{-\gamma}$ is the entropy variable.

Displace fluid element upwards while conserving its entropy. Now it has less entropy than its surroundings. With pressure balance holding, this means that it is also denser than its surroundings. It must fall back to its equilibrium position. Overshooting, it will oscillate at frequency N. (Mathematically, $\Delta\sigma = 0 \Rightarrow \Delta p/p = \gamma \Delta\rho/\rho \Rightarrow \vec{\xi}\cdot\vec{\nabla}\ln p = \gamma\frac{\delta\rho}{\rho} + \gamma\vec{\xi}\cdot\vec{\nabla}\ln\rho \Rightarrow \frac{\delta\rho}{\rho} = \frac{N^2}{g}\xi_z$.)

Now, consider $\sigma_2 < \sigma_1$. Our upwardly displaced fluid element has more entropy than its surroundings, and it will continue to rise
$\longrightarrow$ convective instability. The (Karl) Schwarzschild criterion for convective stability is $\boxed{N^2 > 0}$.

Bonus: Exact solution to  for an isothermal atmosphere.

Suppose $\frac{d\ln\rho}{dz} = \frac{d\ln p}{dz}$ ($T = \text{const}$) Then $\frac{d\ln\rho}{dz} = -\frac{\gamma g}{a^2} = \text{const}$.

$\Rightarrow p = p_0 \exp(-z/H)$ with $H \equiv a^2/\gamma g$. Then we have

$$\xi_z'' - \frac{\xi_z'}{H} + \left[\frac{\omega^2 - k_x^2 a^2}{a^2} + \frac{k_x^2 g}{H}\left(1 - \frac{1}{\gamma}\right)\frac{1}{\omega^2}\right]\xi_z = 0.$$

let $\xi_z = f(z)\exp\left(\frac{z}{2H}\right)$. Then $\xi_z' = f' e^{z/2H} + \frac{f}{2H} e^{z/2H}$

$$= f' e^{z/2H} + \xi_z/2H$$

$$\xi_z'' = f'' e^{z/2H} + \frac{f'}{H} e^{z/2H} + \frac{\xi_z}{(2H)^2}$$

$$f'' + \frac{f'}{H} + \frac{f}{(2H)^2} - \frac{f'}{H} - \frac{f}{2H^2} + \left[\ldots\right] f = 0.$$

$$f'' + \left[-\frac{1}{4H^2} + \frac{\omega^2 - k_x^2 a^2}{a^2} + \frac{k_x^2 a^2}{\gamma H^2}\left(1 - \frac{1}{\gamma}\right)\frac{1}{\omega^2}\right] f = 0.$$

bracket

$= \text{const}$. $\Rightarrow f = \exp(\pm i k_z z)$ with $k_z^2 =$

$$\Rightarrow -k_z^2 - \frac{1}{4H^2} + \frac{\omega^2 - k_x^2 a^2}{a^2} + \frac{k_x^2 a^2}{\omega^2 H^2}\left(\frac{\gamma-1}{\gamma^2}\right) = 0.$$

Mult. by $\omega^2 a^2$ and regroup terms:

$$\omega^4 + \omega^2\left[-k_z^2 a^2 - \frac{a^2}{4H^2} - k_x^2 a^2\right] + k_x^2 a^2 \left(\frac{a^2}{H^2}\right)\left(\frac{\gamma-1}{\gamma^2}\right) = 0.$$

$$\Rightarrow \omega^2 = \frac{k^2 a^2 + \frac{a^2}{4H^2}}{2} \pm \frac{1}{2}\left[\left(k^2 a^2 + \frac{a^2}{4H^2}\right)^2 - 4k_x^2 a^2\left(\frac{a^2}{H^2}\right)\left(\frac{\gamma-1}{\gamma^2}\right)\right]^{1/2}.$$

Note that $N^2 \equiv \frac{g}{\gamma}\frac{d\ln P\rho^{-\gamma}}{dz} = \left(\frac{1-\gamma}{\gamma}\right) g \frac{d\ln\rho}{dz} = \frac{a^2}{H^2}\left(\frac{\gamma-1}{\gamma^2}\right)$.

So,

$$\boxed{\omega^2 = \frac{k^2 a^2 + \frac{a^2}{4H^2}}{2} \pm \frac{1}{2}\left[\left(k^2 a^2 + \frac{a^2}{4H^2}\right)^2 - 4k_x^2 a^2 N^2\right]^{1/2}.}$$

If $(kH)^2 \gg 1$, this becomes $\omega^2 = k^2 a^2$ for the sound wave (+ sign) and $\omega^2 = \frac{k_x^2 N^2}{k_z^2 + k_x^2}$ for the g-mode (- sign).

The final term in the square root captures the coupling between these modes.

VII.8. Buoyancy: Parker instability

Continued on hand-written notes...

- A related problem is the Parker Instability, or "magnetic Rayleigh-Taylor instability" (although it is different in detail from RTI and is closer to Schwarzschild Convection). Consider an atmosphere similar to that in our convective instability calculation, but with a magnetic field oriented perpendicularly to gravity with a z-dependence: $\vec{B}_0 = B_0(z)\hat{x}$. The force balance in the equilibrium state now includes a contribution from the magnetic pressure: $g = -\frac{1}{\rho}\left(\frac{dp}{dz} + \frac{dB_0^2}{dz}\right) = \text{const.}$, or

$$\frac{g}{a^2} = -\frac{1}{\gamma}\frac{d\ln p}{dz} - \frac{V_{A0}^2}{a^2}\frac{d\ln B_0}{dz}.$$

Our equations are almost the same:

$$\frac{\delta\rho}{\rho} + ik_x\xi_x + \xi_z' + \xi_z\frac{d\ln\rho}{dz} = 0,$$

$$-\omega^2\xi_x = -ik_x\left(\frac{\delta p}{\rho} + \frac{B_0\delta B_x}{4\pi\rho}\right) + \frac{ik_xB_0}{4\pi\rho}\delta B_x + \frac{\delta B_z}{4\pi\rho}\frac{dB_0}{dz},$$

$$-\omega^2\xi_z = -\frac{1}{\rho}\frac{d}{dz}\left(\delta p + \frac{B_0\delta B_x}{4\pi}\right) - \frac{\delta\rho}{\rho}g + \frac{ik_xB_0}{4\pi\rho}\delta B_z,$$

$$\frac{\delta p}{p} = \gamma\frac{\delta\rho}{\rho} - \xi_z\frac{d\ln p\rho^{-\gamma}}{dz},$$

but now with magnetic-field perturbations and gradients. The former are given by $\vec{\delta B} = \vec{\nabla}\times(\vec{\xi}\times\vec{B}_0) \Rightarrow \delta B_x = -\frac{d}{dz}(\xi_z B_0)$

$$\delta B_z = ik_x B_0\xi_z$$

First, note that $\frac{\delta p + B_0 \delta B_x / 4\pi}{\rho}$

$$= a^2 \frac{\delta\rho}{\rho} - \frac{a^2}{\gamma} \frac{d\ln p\rho^{-\gamma}}{dz} \xi_z + \frac{B_0}{4\pi\rho}\left(-\frac{d}{dz}\right)(\xi_z B_0)$$

$$= a^2\Big[-ik_x\xi_x - \xi_z' - \xi_z \frac{d\ln\rho}{dz} - \frac{1}{\gamma}\frac{d\ln p\rho^{-\gamma}}{dz}\xi_z - \frac{V_{A0}^2}{a^2}\left(\xi_z' + \xi_z \frac{d\ln B_0}{dz}\right)\Big]$$

$$= a^2\Big[-ik_x\xi_x - \xi_z'\left(1 + \frac{V_{A0}^2}{a^2}\right) + \frac{g}{a^2}\xi_z\Big].$$

Then

$$-\omega^2\xi_x = -ik_x a^2\Big[-ik_x\xi_x - \xi_z'\left(1 + \frac{V_{A0}^2}{a^2}\right) + \frac{g}{a^2}\xi_z\Big] + \frac{ik_x B_0}{4\pi\rho}\Big[-\xi_z' B_0 - \xi_z B_0 \frac{d\ln B_0}{dz}\Big] + \frac{ik_x B_0}{4\pi\rho}\xi_z \frac{dB_0}{dz}$$

$$\Rightarrow \left(-\omega^2 + k_x^2 a^2\right)\xi_x = ik_x a^2 \xi_z'\left(1 + \frac{V_{A0}^2}{a^2}\right) - ik_x g\xi_z - ik_x V_{A0}^2 \xi_z' - ik_x V_{A0}^2 \frac{d\ln B_0}{dz}\xi_z + ik_x V_{A0}^2 \frac{d\ln B_0}{dz}\xi_z$$

$$\Rightarrow \boxed{\left(-\omega^2 + k_x^2 a^2\right)\xi_x = ik_x a^2 \xi_z' - ik_x \xi_z g}$$

Same as (#) w/o B field!

$$\Rightarrow \frac{\delta\rho}{\rho} = -\xi_z' - \xi_z \frac{d\ln\rho}{dz} - ik_x \frac{\left[ik_x a^2 \xi_z' - ik_x \xi_z g\right]}{\left(-\omega^2 + k_x^2 a^2\right)}$$

$$\frac{\delta\rho}{\rho} = \frac{\omega^2 \xi_z' + \left[(\omega^2 - k_x^2 a^2)\frac{d\ln\rho}{dz} - k_x^2 g\right]\xi_z}{k_x^2 a^2 - \omega^2}$$

same as ◎ w/o B field!

Buoyancy is fundamentally the same as in the hydro case. Plugging all of this into the z-component of the momentum eqn. gives (with $\frac{\delta p + \delta B^2/8\pi}{\rho} = \frac{\omega^2}{\omega^2 - k_x^2 a^2}\left[\frac{\gamma g}{a^2}\xi_z - \gamma \xi_z'\right] - \frac{\gamma v_{A0}^2}{a^2}\xi_z'$)

$$-\omega^2 \xi_z = -\frac{1}{\rho}\frac{d}{dz}\left[\frac{\rho\omega^2}{\omega^2 - k_x^2 a^2}\left(\frac{\gamma g}{a^2}\xi_z - \gamma \xi_z'\right) - \frac{B_0^2}{4\pi}\xi_z'\right]$$

$$- g\left\{\frac{\omega^2 \xi_z' + \left[(\omega^2 - k_x^2 a^2)\frac{d\ln\rho}{dz} - k_x^2 g\right]\xi_z}{k_x^2 a^2 - \omega^2}\right\}$$

$$+ \frac{i k_x B_0}{4\pi\rho}\left(i k_x B_0 \xi_z\right)$$

$$\Rightarrow \left(-\omega^2 + k_x^2 v_{A0}^2\right)\xi_z = -\frac{a^2}{\gamma}\frac{d\ln\rho}{dz}\frac{\omega^2}{\omega^2 - k_x^2 a^2}\left(\frac{\gamma g}{a^2}\xi_z - \gamma \xi_z'\right)$$

$$- \frac{a^2}{\gamma}\frac{\omega^2 k_x^2 a^2}{(\omega^2 - k_x^2 a^2)^2}\frac{d\ln T}{dz}\left(\frac{\gamma g}{a^2}\xi_z - \gamma \xi_z'\right) + v_{A0}^2 \xi_z'' + \xi_z' v_{A0}^2 \frac{d\ln B_0^2}{dz}$$

$$- \frac{a^2}{\gamma}\frac{\omega^2}{\omega^2 - k_x^2 a^2}\left(\frac{\gamma g}{a^2}\xi_z' - \frac{\gamma g}{a^2}\xi_z \frac{d\ln T}{dz} - \gamma \xi_z''\right)$$

$$+ \frac{g}{\omega^2 - k_x^2 a^2}\left\{\omega^2 \xi_z' + \left[(\omega^2 - k_x^2 a^2)\frac{d\ln\rho}{dz} - k_x^2 g\right]\xi_z\right\}$$

After some straightforward algebra, we find

$$\xi_z''\left(V_{A0}^2+\frac{a^2\omega^2}{\omega^2-k_x^2a^2}\right)$$

$$+\xi_z'\left[V_{A0}^2\frac{d\ln B_0^2}{dz}+\frac{a^2\omega^2}{(\omega^2-k_x^2a^2)^2}\left(\omega^2\frac{d\ln p}{dz}-k_x^2a^2\frac{d\ln\rho}{dz}\right)\right]$$

$$+\xi_z\left[\frac{g}{\gamma}\frac{k_x^2a^2}{\omega^2-k_x^2a^2}\left(\frac{d\ln p\rho^{-\gamma}}{dz}+\frac{\gamma V_{A0}^2}{a^2}\frac{d\ln B_0}{dz}\right)-\frac{g\omega^2k_x^2a^2}{(\omega^2-k_x^2a^2)^2}\frac{d\ln T}{dz}\right.$$

$$\left.+\omega^2-k_x^2V_{A0}^2\right]$$

All extra terms $\propto V_{A0}^2$. For $k_z\to 0$, $k_x^2a^2\gg 1$, this becomes are

$$\boxed{\omega^2\simeq k_x^2V_{A0}^2+\frac{g}{\gamma}\left(\frac{d\ln p\rho^{-\gamma}}{dz}+\frac{1}{\beta}\frac{d\ln B_0^2}{dz}\right)} \quad \text{w/ } \beta=\frac{B_0^2}{8\pi p}.$$

magnetic tension — thermal buoyancy — magnetic buoyancy

Now, $\frac{d\ln p\rho^{-\gamma}}{dz}+\frac{1}{\beta}\frac{d\ln B_0^2}{dz}>0$ for stability. But the physics is the same as in Schwarzschild convection — just the pressure balance is different.

One can obtain an exact solution for an isothermal atmosphere, just like in the hydro case.

$$\frac{d\ln T}{dz} = 0 \quad ; \quad \frac{d\ln B^2}{dz} = \frac{d\ln\rho}{dz} = \frac{d\ln P}{dz} = -\frac{1}{H}$$

Write $\xi_z \propto e^{\pm i k_z z + z/2H}$ and set

$$k_z^2 \equiv -\frac{1}{4H^2} + \frac{(\omega^2 - k_x^2 V_A^2)(\omega^2 - k_x^2 a^2) + k_x^2 a^2 N_{ms}^2}{\omega^2(a^2 + V_A^2) - k_x^2 a^2 V_A^2}$$

w/ $N_{ms}^2 \equiv \frac{g}{\gamma}\left(\frac{d\ln p\rho^{-\gamma}}{dz} + \frac{1}{\beta}\frac{d\ln B^2}{dz}\right)$. Dispersion relation is then

$$\omega^4 - \omega^2\left(k^2 + \frac{1}{4H^2}\right)V_{ms}^2 + k_x^2 a^2\left[k_z^2 a^2 + \frac{V_A^2}{4H^2} + N_{ms}^2\right] = 0$$

with $V_{ms}^2 \equiv a^2 + V_A^2$ the magnetosonic speed (squared).

NB: A cold atmosphere ($a^2 \to 0$) with support only from $B(z)$ has

$$\omega^4 - \omega^2\left(k^2 + \frac{1}{4H^2}\right)V_A^2 - k_x^2 V_A^2 \frac{g}{H} = 0 \,,$$

which is unstable.

The idea is that the supporting magnetic pressure gradient wants to relax (B^2 likes being constant), and it can do so by offloading mass sinusoidally:

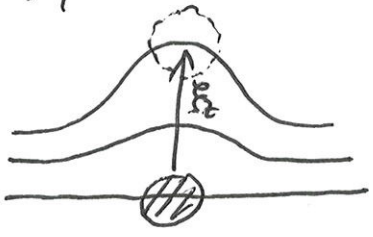

VII.9. Rotation

In §IV.5, we wrote down the equations of hydrodynamics in a rotating frame – see (IV.5.2). Here we do the same for the equations of MHD. With $\boldsymbol{v} = \boldsymbol{u} - R\Omega(R,z)\hat{\boldsymbol{\varphi}}$ and

$$\frac{\mathrm{D}}{\mathrm{D}t} \doteq \frac{\partial}{\partial t} + \boldsymbol{v}\cdot\boldsymbol{\nabla} + \Omega\frac{\partial}{\partial\varphi},$$

the continuity and force equations are the same,

$$\frac{\mathrm{D}\rho}{\mathrm{D}t} = -\rho\boldsymbol{\nabla}\cdot\boldsymbol{v}, \tag{VII.9.1}$$

$$\frac{\mathrm{D}v_R}{\mathrm{D}t} = f_R + 2\Omega v_\varphi + R\Omega^2 + \frac{v_\varphi^2}{R}, \tag{VII.9.2}$$

$$\frac{\mathrm{D}v_\varphi}{\mathrm{D}t} = f_\varphi - \frac{\kappa^2}{2\Omega}v_R - R\frac{\partial\Omega}{\partial z}v_z - \frac{v_R v_\varphi}{R}, \tag{VII.9.3}$$

$$\frac{\mathrm{D}v_z}{\mathrm{D}t} = f_z, \tag{VII.9.4}$$

but with the addition of the Lorentz force:

$$\boldsymbol{f} = -\frac{1}{\rho}\boldsymbol{\nabla}\left(P + \frac{B^2}{8\pi}\right) + \frac{\boldsymbol{B}\cdot\boldsymbol{\nabla}B_i}{4\pi\rho}\,\hat{\boldsymbol{e}}_i + \frac{B_R B_\varphi}{4\pi\rho R}\hat{\boldsymbol{\varphi}} - \frac{B_\varphi^2}{4\pi\rho R}\hat{\boldsymbol{R}} - \boldsymbol{\nabla}\Phi. \tag{VII.9.5}$$

Note the additional geometric terms $\propto B^2/R$; these are tension forces associated with the bend in the magnetic-field lines as they follow the azimuthal direction. To these equations we must append the induction equation:

$$\frac{\mathrm{D}B_R}{\mathrm{D}t} = -B_R\boldsymbol{\nabla}\cdot\boldsymbol{v} + \boldsymbol{B}\cdot\boldsymbol{\nabla}v_R, \tag{VII.9.6}$$

$$\frac{\mathrm{D}B_\varphi}{\mathrm{D}t} = -B_\varphi\boldsymbol{\nabla}\cdot\boldsymbol{v} + \boldsymbol{B}\cdot\boldsymbol{\nabla}v_\varphi + \frac{\partial\Omega}{\partial\ln R}B_R + R\frac{\partial\Omega}{\partial z}B_z, \tag{VII.9.7}$$

$$\frac{\mathrm{D}B_z}{\mathrm{D}t} = -B_z\boldsymbol{\nabla}\cdot\boldsymbol{v} + \boldsymbol{B}\cdot\boldsymbol{\nabla}v_z. \tag{VII.9.8}$$

With the exception of advection by the differential rotation, the only additions to the induction equation beyond its more customary Cartesian form appear in its azimuthal component: $+\,R\boldsymbol{B}\cdot\boldsymbol{\nabla}\Omega$ on the right-hand side. This corresponds to stretching of the flux-frozen magnetic field by the differential rotation.

In the hand-written pages that follow, these equations are used to describe the evolution of small fluctuations about a homogeneous, differentially rotating disk with $\Omega = \Omega(R)$, in which the centrifugal acceleration $R\Omega^2$ is balanced by gravity $-\partial\Phi/\partial R$. If the latter is dominated by that of a central point mass M, we have $\Phi = -GM/R$ and so $\Omega = (GM/R^3)^{1/2}$ – i.e., Keplerian rotation.

Before proceeding, I'll write down the linearized MHD equations written in cylindrical coordinates (R,φ,z) in a rotating frame with $\boldsymbol{\Omega} = \Omega(R,z)\hat{\boldsymbol{z}}$. The only assumptions here are that the background magnetic field is uniform, and that the equilibrium state arises from a balance between the centrifugal force and gravity plus thermal-pressure gradients (i.e., we allow for density and pressure stratification in the background state). We also neglect curvature terms of order $\sim(v_\mathrm{A}^2/R)(\delta B/B)$, as these are small compared to the other terms unless the toroidal magnetic field is super-thermal by a factor $\sim(R/H)^{1/2}$, where $H \sim c_\mathrm{s}/\Omega$ is the disk thickness and c_s is the sound speed – an atypical situation.

Without further ado...

$$\left(\frac{\partial}{\partial t}+\Omega\frac{\partial}{\partial\varphi}\right)\delta\rho=-(\delta\boldsymbol{v}\cdot\boldsymbol{\nabla})\rho-\rho(\boldsymbol{\nabla}\cdot\delta\boldsymbol{v}), \tag{VII.9.9}$$

$$\left(\frac{\partial}{\partial t}+\Omega\frac{\partial}{\partial\varphi}\right)\delta v_R=-\frac{1}{\rho}\frac{\partial}{\partial R}\left(\delta P+\frac{\boldsymbol{B}\cdot\delta\boldsymbol{B}}{4\pi}\right)+\frac{\delta\rho}{\rho^2}\frac{\partial P}{\partial R}+\frac{(\boldsymbol{B}\cdot\boldsymbol{\nabla})\delta B_R}{4\pi\rho}-\frac{\partial\delta\Phi}{\partial R}-2\Omega\delta v_\varphi, \tag{VII.9.10}$$

$$\left(\frac{\partial}{\partial t}+\Omega\frac{\partial}{\partial\varphi}\right)\delta v_\varphi=-\frac{1}{\rho R}\frac{\partial}{\partial\varphi}\left(\delta P+\frac{\boldsymbol{B}\cdot\delta\boldsymbol{B}}{4\pi}\right)+\frac{\delta\rho}{\rho}\frac{1}{\rho R}\frac{\partial P}{\partial\varphi}+\frac{(\boldsymbol{B}\cdot\boldsymbol{\nabla})\delta B_\varphi}{4\pi\rho}-\frac{1}{R}\frac{\partial\delta\Phi}{\partial\varphi}+\frac{\kappa^2}{2\Omega}\delta v_R+R\frac{\partial\Omega}{\partial z}\delta v_\varphi, \tag{VII.9.11}$$

$$\left(\frac{\partial}{\partial t}+\Omega\frac{\partial}{\partial\varphi}\right)\delta v_z=-\frac{1}{\rho}\frac{\partial}{\partial z}\left(\delta P+\frac{\boldsymbol{B}\cdot\delta\boldsymbol{B}}{4\pi}\right)+\frac{\delta\rho}{\rho^2}\frac{\partial P}{\partial z}+\frac{(\boldsymbol{B}\cdot\boldsymbol{\nabla})\delta B_z}{4\pi\rho}-\frac{\partial\delta\Phi}{\partial z} \tag{VII.9.12}$$

$$\left(\frac{\partial}{\partial t}+\Omega\frac{\partial}{\partial\varphi}\right)\delta B_R=(\boldsymbol{B}\cdot\boldsymbol{\nabla})\delta v_R-B_R(\boldsymbol{\nabla}\cdot\delta\boldsymbol{v}), \tag{VII.9.13}$$

$$\left(\frac{\partial}{\partial t}+\Omega\frac{\partial}{\partial\varphi}\right)\delta B_\varphi=(\boldsymbol{B}\cdot\boldsymbol{\nabla})\delta v_\varphi-B_\varphi(\boldsymbol{\nabla}\cdot\delta\boldsymbol{v})+\frac{\partial\Omega}{\partial\ln R}\delta B_R+R\frac{\partial\Omega}{\partial z}\delta B_z, \tag{VII.9.14}$$

$$\left(\frac{\partial}{\partial t}+\Omega\frac{\partial}{\partial\varphi}\right)\delta B_z=(\boldsymbol{B}\cdot\boldsymbol{\nabla})\delta v_z-B_z(\boldsymbol{\nabla}\cdot\delta\boldsymbol{v}), \tag{VII.9.15}$$

$$\left(\frac{\partial}{\partial t}+\Omega\frac{\partial}{\partial\varphi}\right)\delta\sigma=-\delta v_R\frac{\partial\ln P\rho^{-\gamma}}{\partial R}-\delta v_z\frac{\partial\ln P\rho^{-\gamma}}{\partial z}, \tag{VII.9.16}$$

where $\delta\sigma\doteq\delta P/P-\gamma\delta\rho/\rho$.

- Rotational and magnetorotational instability.

Accretion disks are ubiquitous in astrophysics, and they get their namesake by actually facilitating mass accretion onto compact objects like young protostars, neutron stars, black holes, etc. But for this to happen, angular momentum must be redistributed, and it turns out that this is frustratingly difficult in Keplerian disks. The problem is that, hydrodynamically, Keplerian flows are quite stable (we'll show below that they are linearly stable; there is no proof that they are nonlinearly stable, but experimental efforts to find nonlinear instability in hydrodynamic, differentially rotating flows have so far failed). Fluid elements do not like to give up their angular momentum. The culprit is the Coriolis force, a surprisingly strong stabilizing effect. (Indeed, planar shear flows without rotation quite easily disrupt so long as the viscosity is not too large.) Another issue is that the molecular viscosity, which might transport angular momentum purely by frictional means, is absolutely negligible in most all astrophysical fluids. One way out is to posit some anomalous viscosity via (unknown) turbulence. This is the route taken in the classic Shakura & Sunyaev

(1973) paper — assume turbulent transport, characterize it by a scalar viscosity, and take that viscous stress to be proportional to the gas pressure:

$$T_{R\phi} = \alpha_{SS} P$$

(P: gas pressure; α_{SS}: proportionality constant)

$T_{R\phi}$: R-ϕ component of the stress tensor, responsible for transporting ϕ momentum in the R direction.

This led to the "α-disk" framework of accretion disks, which has been extremely profitable, but woefully unsatisfying. This changed in 1991.

Let's pause here and explore the above claims a bit further. I said a Keplerian disk is hydrodynamically stable to small disturbances. Let's prove it. There are two ways to do this — using point masses in orbits, and using the full hydro eqns. in a rotating frame. Here's the first:

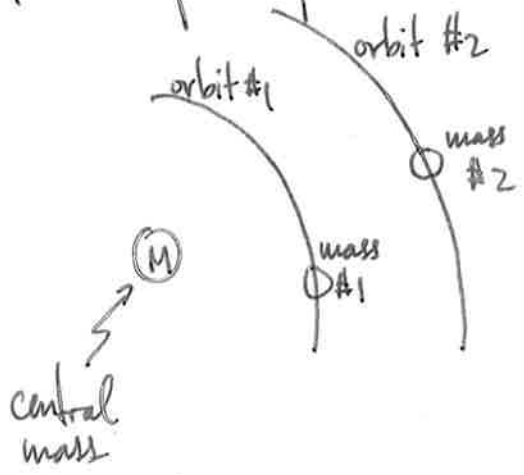

The eqns. of motion for these masses are

$$\ddot{x} - 2\Omega\dot{y} = -\frac{d\Omega^2}{d\ln R}\, x$$

$$\ddot{y} + 2\Omega\dot{x} = 0$$

These are called the "Hill equations" (Hill 1878). They include the Coriolis force and an extra term in the "radial" equation for the x displacement that accounts for the "tidal" force (the local difference between the centrifugal force and gravity). And they are local — note the Cartesian coordinate system with x pointing locally radial and y pointing locally azimuthal. Take solutions $x, y \sim e^{i\omega t}$ to compute the normal modes of this system:

$$\begin{bmatrix} -\omega^2 + \frac{d\Omega^2}{d\ln R} & 2\Omega i\omega \\ -2\Omega i\omega & -\omega^2 \end{bmatrix} \begin{bmatrix} x \\ y \end{bmatrix} = 0 \Rightarrow \omega^2\left(\omega^2 - \frac{d\Omega^2}{d\ln R}\right) = 4\Omega^2\omega^2$$

$$\Rightarrow \omega^2 - \underbrace{\left(4\Omega^2 + \frac{d\Omega^2}{d\ln R}\right)}_{\equiv \kappa^2} = 0 \Rightarrow \boxed{\omega = \pm\kappa}$$

κ: "epicyclic frequency"

These are epicyclic oscillations when $\kappa^2 > 0$, and exponentially growing disturbances when $\kappa^2 < 0$.

Note that $4\Omega^2 + \frac{d\Omega^2}{d\ln R} = \frac{1}{R^3}\frac{dl^2}{dR}$, where $l = \Omega R^2$ is the (specific) angular momentum. Thus,

$$\boxed{\frac{dl^2}{d\ln R} > 0 \iff \text{linear stability}}$$

"Rayleigh criterion"

The fluid way: Let's assume incompressibility for simplicity. Going back to our hydrodynamic eqns., with gravity from a central point mass and $\vec{u} = \vec{v} + R\Omega\hat{\varphi}$, we have

$$\left(\frac{\partial}{\partial t} + \Omega\frac{\partial}{\partial\varphi}\right)v_R + \vec{v}\cdot\vec{\nabla}v_R - 2\Omega v_\varphi - R\Omega^2 - \frac{v_\varphi^2}{R}$$

$$= -\frac{\partial p}{\partial R}\frac{1}{\rho} + g_R,$$

$$\left(\frac{\partial}{\partial t} + \Omega\frac{\partial}{\partial\varphi}\right)v_\varphi + \vec{v}\cdot\vec{\nabla}v_\varphi + 2\Omega v_R + v_R\frac{d\Omega}{d\ln R} + \frac{v_R v_\varphi}{R}$$

$$= -\frac{1}{R}\frac{\partial p}{\partial\varphi}\frac{1}{\rho},$$

where $g_R = -\frac{GM}{R^2}$. Our equilibrium state is $\vec{v}=0$, p = constant, and $g_R = -R\Omega^2 \Rightarrow \Omega^2 = \frac{GM}{R^3}$, a Keplerian orbit. Writing $\vec{v} = 0 + \vec{\delta v}$ and $p = p_0 + \delta p$, our equations to linear order in δ are

$$\left(\frac{\partial}{\partial t} + \Omega\frac{\partial}{\partial\varphi}\right)\delta v_R - 2\Omega\delta v_\varphi = -\frac{1}{\rho}\frac{\partial}{\partial R}\delta p,$$

$$\left(\frac{\partial}{\partial t} + \Omega\frac{\partial}{\partial\varphi}\right)\delta v_\varphi + 2\Omega\delta v_R + \frac{d\Omega}{d\ln R}\delta v_R = -\frac{1}{\rho}\frac{1}{R}\frac{\partial\,\delta p}{\partial\varphi}.$$

For simplicity, let us neglect the $\partial/\partial\varphi$ derivatives and let $\delta \sim \exp(-i\omega t + ik_R R + ik_z z)$. Then, with $\vec{\nabla}\cdot\delta\vec{v} = 0 \Rightarrow k_R \delta v_R = -k_z \delta v_z$ and $\frac{\partial}{\partial t}\delta v_z = -\frac{1}{\rho}\frac{\partial}{\partial z}\delta p$, we find $\frac{\delta p}{\rho} = -\frac{k_R}{k_z^2}\omega\,\delta v_R$ and so

$$\begin{bmatrix} -i\omega\frac{k^2}{k_z^2} & -2\Omega \\ \frac{k^2}{2\Omega} & -i\omega \end{bmatrix}\begin{bmatrix} \delta v_R \\ \delta v_\varphi \end{bmatrix} = 0 \Rightarrow \boxed{\omega^2 = \frac{k_z^2}{k^2}\kappa^2}$$

$\frac{k^2}{2\Omega} = 2\Omega + \frac{d\Omega}{d\ln R}$

Same stability criterion as before, $\kappa^2 > 0$.

Physically, what's going on? Take a fluid element at orbit #1 and displace it outwards to orbit #2 while maintaining a constant ang. momentum. Since $l_2 > l_1$, the fluid element cannot stay in its new orbit and must return back to orbit #1.

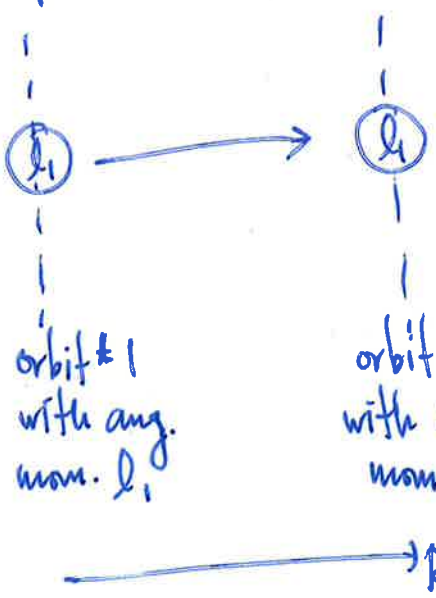

$\Rightarrow$ STABLE.

Now, back to 1991 ...

Steve Balbus and John Hawley, then both at Univ. of Virginia, found by a straightforward linear analysis and clever use of 90's supercomputers, that a small but finite magnetic field is all that is required to linearly destabilize Keplerian rotation. How could this be missed? The answer is complicated. The instability — at first known as the "Balbus-Hawley instability" but now goes by the moniker "magnetorotational instability" (MRI) — appeared in a little-known Russian paper by Velikhov in 1959, and 2 years later made its way into Chandrasekhar's classic text on "hydrodynamic and hydromagnetic stability". But there it appeared in a rather odd guise, at least to an astronomer thinking about accretion disks — Couette flow, i.e., rotational flow excited by placing a (conducting) fluid between two cylindrical walls rotating at different speeds. It wasn't until B&H rediscovered it and placed it in the astrophysical context that the instability became appreciated as a possible solution to the accretion problem. What followed was an industry of linear analysis and nonlinear numerical simulations aiming to characterize the MRI in a wide variety of disk systems. But let's go back to the beginning:

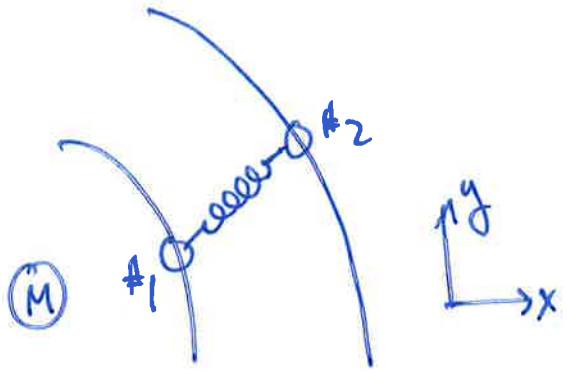

Take the Hill system but attach a spring between the two masses — magnetic fields act as springs, so you can imagine this being a field line threading two fluid elements. Add Hooke's law to the eqns. of motion:

$$\ddot{x} - 2\Omega\dot{y} = -\frac{d\Omega^2}{d\ln R}x - Kx$$

$$\ddot{y} + 2\Omega\dot{x} = -Ky$$

w/ K = spring constant

$$x, y \sim e^{-i\omega t} \Rightarrow \begin{bmatrix} -\omega^2 + \frac{d\Omega^2}{d\ln R} + K & 2\Omega i\omega \\ -2\Omega i\omega & -\omega^2 + K \end{bmatrix} \begin{bmatrix} x \\ y \end{bmatrix} = 0$$

$$\Rightarrow \left(\omega^2 - \frac{d\Omega^2}{d\ln R} - K\right)\left(\omega^2 - K\right) = 4\Omega^2\omega^2$$

$$\Rightarrow \left(\omega^2 - K\right)\left(\omega^2 - K - 4\Omega^2 - \frac{d\Omega^2}{d\ln R}\right) = 4\Omega^2 K$$

extra, extra, extra

Solutions are $\omega^2 - K = \frac{K^2}{2} \pm \sqrt{\left(\frac{K^2}{2}\right)^2 + 4\Omega^2 K}$,

whose (−) solution is unstable if $\boxed{K + \frac{d\Omega^2}{d\ln R} < 0}$

This is important, because Keplerian disks have $\frac{d\Omega^2}{d\ln R} < 0$! Note that the spring cannot be too strong here. Interestingly,

$$\frac{d\ell^2}{d\ln R} > 0 \text{ for hydro stability} \longrightarrow \frac{d\Omega^2}{d\ln R} > 0 \text{ for MHD stability}$$

One can show that the Lagrangian change in the ang. mom. of a fluid element as it is displaced is given by

$$\frac{\delta \ell}{\ell} = \frac{x}{R}\left(\frac{\kappa^2}{2\Omega^2} - \frac{i\omega}{\Omega}\frac{y}{x}\right)$$

$$= -\frac{x}{R}\left(\frac{2K}{\omega^2 - K}\right)$$ ← the spring broke conservation of angular momentum!

If $K \ll |\omega^2| \sim \Omega^2$, then outward displacements ($x > 0$) gain angular momentum as they are torqued by the spring (NB: $\omega^2 < 0$ corresponds to growth, so $\delta\ell \propto (x/R)$).

At max. growth (take $\frac{\partial}{\partial K}$ of disp. relation and find extrema of ω^2), the growth rate $-i\omega = \frac{1}{2}\left|\frac{d\Omega}{d\ln R}\right|$ and

$$\left.\frac{\delta\ell}{\ell}\right|_{max} = \frac{2x}{R}\left(1 - \frac{1}{4}\left|\frac{d\Omega}{d\ln R}\right|\right).$$

Now the fluid picture: (let $\vec{B}_0 = B_0\hat{z}$ for simplicity)

$$\left(\frac{\partial}{\partial t} + \Omega\frac{\partial}{\partial\varphi}\right)\delta v_R - 2\Omega\delta v_\varphi = -\frac{1}{\rho}\frac{\partial}{\partial R}\left(\delta p + \frac{\vec{B}_0\cdot\delta\vec{B}}{4\pi}\right) + \frac{\vec{B}_0\cdot\vec{\nabla}\,\delta B_R}{4\pi\rho},$$

$$\left(\frac{\partial}{\partial t} + \Omega\frac{\partial}{\partial\varphi}\right)\delta v_\varphi + \frac{\kappa^2}{2\Omega}\delta v_R = -\frac{1}{\rho}\frac{1}{R}\frac{\partial}{\partial\varphi}\left(\delta p + \frac{\vec{B}_0\cdot\delta\vec{B}}{4\pi}\right) + \frac{\vec{B}_0\cdot\vec{\nabla}\,\delta B_\varphi}{4\pi\rho}.$$

We need eqns. for δB_R and δB_φ (δB_z is determined from $\vec{\nabla}\cdot\delta\vec{B} = 0$). So, take the induction eqn. and write it in cylindrical coordinates w/ $\vec{u} = \vec{v} + R\Omega\hat{\varphi}$:

$$\left(\vec{B}\cdot\vec{\nabla}\vec{u} = \hat{e}_i\,\vec{B}\cdot\vec{\nabla}v_i + \frac{v_R B_\varphi}{R}\hat{\varphi} - \frac{v_\varphi B_\varphi}{R}\hat{R} - \Omega B_\varphi\hat{R} + \hat{\varphi}\,B_R\left(\Omega + \frac{d\Omega}{d\ln R}\right)\right)$$

$$\Rightarrow \left(\frac{\partial}{\partial t} + \Omega\frac{\partial}{\partial\varphi}\right)\delta B_R = \vec{B}_0\cdot\vec{\nabla}\,\delta v_R,$$

$$\left(\frac{\partial}{\partial t} + \Omega\frac{\partial}{\partial\varphi}\right)\delta B_\varphi = \vec{B}_0\cdot\vec{\nabla}\,\delta v_\varphi + \delta B_R\frac{d\Omega}{d\ln R}.$$

Again, take $\partial/\partial\varphi = 0$ and let $\delta \sim \exp\left(-i\omega t + ik_R R + ik_z z\right)$.

$$\left.\begin{aligned} \vec{\nabla}\cdot\delta\vec{v} = 0 &\rightarrow \delta v_z = -\frac{k_R}{k_z}\delta v_R \\ \vec{\nabla}\cdot\delta\vec{B} = 0 &\rightarrow \delta B_z = -\frac{k_R}{k_z}\delta B_R \end{aligned}\right\} \quad \frac{\partial}{\partial t}\delta v_z = -\frac{1}{\rho}\frac{\partial}{\partial z}\left(\delta p + \frac{\vec{B}_0\cdot\delta\vec{B}}{4\pi}\right) + \frac{\vec{B}_0\cdot\vec{\nabla}}{4\pi\rho}\delta B_z$$

$$\Rightarrow \frac{\delta p}{\rho} + \frac{\vec{B}_0\cdot\delta\vec{B}}{4\pi\rho} = \frac{-\omega k_R}{k_z^2}\delta v_R - \frac{\vec{k}\cdot\vec{B}_0}{4\pi\rho}\frac{k_R}{k_z^2}\delta B_R$$

$$\Rightarrow \begin{cases} -i\omega\delta v_R - 2\Omega\delta v_\varphi = -ik_R\left[-\dfrac{\omega k_R}{k_z^2}\delta v_R - \dfrac{\vec{k}\cdot\vec{B}_0}{4\pi\rho}\dfrac{k_R}{k_z^2}\delta B_R\right] + \dfrac{i\vec{k}\cdot\vec{B}_0}{4\pi\rho}\delta B_R \\ -i\omega\delta v_\varphi + \dfrac{\kappa^2}{2\Omega}\delta v_R = \dfrac{i\vec{k}\cdot\vec{B}_0}{4\pi\rho}\delta B_\varphi \end{cases}$$

$$\Rightarrow \begin{cases} -i\omega\dfrac{k^2}{k_z^2}\delta v_R - 2\Omega\delta v_\varphi = \dfrac{i\vec{k}\cdot\vec{B}_0}{4\pi\rho}\dfrac{k^2}{k_z^2}\delta B_R \\ \dfrac{\kappa^2}{2\Omega}\delta v_R - i\omega\delta v_\varphi = \dfrac{i\vec{k}\cdot\vec{B}_0}{4\pi\rho}\delta B_\varphi \end{cases}$$

and $\left\{\begin{aligned} -i\omega\delta B_R &= i\vec{k}\cdot\vec{B}_0\,\delta v_R \\ -i\omega\delta B_\varphi &= i\vec{k}\cdot\vec{B}_0\,\delta v_\varphi + \delta B_R\frac{d\Omega}{d\ln R}\end{aligned}\right\}$ solve these for $\delta\vec{v}$ and plug into these

$$\begin{cases} -i\omega \dfrac{k^2}{k_z^2}\left(\dfrac{-i\omega \delta B_R}{i\mathbf{k}\cdot\mathbf{B}_0}\right) - 2\Omega\left(\dfrac{-i\omega\delta B_\varphi - \delta B_R\, d\Omega/d\ln R}{i\mathbf{k}\cdot\mathbf{B}_0}\right) = \dfrac{i\mathbf{k}\cdot\mathbf{B}_0}{4\pi\rho}\dfrac{k^2}{k_z^2}\delta B_R \\ \dfrac{k^2}{2\Omega}\left(\dfrac{-i\omega\delta B_R}{i\mathbf{k}\cdot\mathbf{B}_0}\right) - i\omega\left(\dfrac{-i\omega\delta B_\varphi - \delta B_R\, d\Omega/d\ln R}{i\mathbf{k}\cdot\mathbf{B}_0}\right) = \dfrac{i\mathbf{k}\cdot\mathbf{B}_0}{4\pi\rho}\delta B_\varphi \end{cases}$$

Cleaning up...

$$\begin{bmatrix} -\omega^2 + (\mathbf{k}\cdot\mathbf{v}_A)^2 - \dfrac{k_z^2}{k^2}\dfrac{d\Omega^2}{d\ln R} & 2\Omega i\omega\dfrac{k_z^2}{k^2} \\ -2\Omega i\omega & -\omega^2 + (\mathbf{k}\cdot\mathbf{v}_A)^2 \end{bmatrix}\begin{bmatrix} \delta B_R \\ \delta B_\varphi \end{bmatrix} = 0.$$

Look familiar? $K \to (\mathbf{k}\cdot\mathbf{v}_A)^2$! Magnetic tension is a spring. Dispersion relation:

$$\left[\omega^2 - (\mathbf{k}\cdot\mathbf{v}_A)^2\right]\left[\omega^2 - (\mathbf{k}\cdot\mathbf{v}_A)^2 - \kappa^2\frac{k_z^2}{k^2}\right] = 4\Omega^2(\mathbf{k}\cdot\mathbf{v}_A)^2$$

$$\Rightarrow \quad \omega^2 - (\mathbf{k}\cdot\mathbf{v}_A)^2 = \frac{\kappa^2}{2} \pm \sqrt{\left(\frac{\kappa^2}{2}\right)^2 + 4\Omega^2(\mathbf{k}\cdot\mathbf{v}_A)^2}$$

unstable if $\boxed{(\mathbf{k}\cdot\mathbf{v}_A)^2 + \dfrac{d\Omega^2}{d\ln R} < 0}$

Note: Can write discriminant as $\left[\frac{\kappa^2}{2} + (\mathbf{k}\cdot\mathbf{v}_A)^2\right]^2 - (\mathbf{k}\cdot\mathbf{v}_A)^2\left[(\mathbf{k}\cdot\mathbf{v}_A)^2 + \kappa^2 - 4\Omega^2\right]$

$$= \left[\frac{\kappa^2}{2} + (\mathbf{k}\cdot\mathbf{v}_A)^2\right]^2 - (\mathbf{k}\cdot\mathbf{v}_A)^2\left[(\mathbf{k}\cdot\mathbf{v}_A)^2 + \frac{d\Omega^2}{d\ln R}\right]$$

This means Keplerian disks are linearly unstable, provided the magnetic field isn't so strong that all the wavenumbers $k_z = 2\pi/\lambda_z$ that can fit within the height of the disk satisfy $k_z^2 v_{Az}^2 > \left|\frac{d\Omega^2}{d\ln R}\right|$ — then tension stabilizes all relevant modes.

See Balbus & Hawley 1998 Rev. Mod. Phys. for more.

PART VIII

MHD discontinuities and shocks

Everything included in the last two Parts of these lecture notes focused solely on the linear evolution of perturbations, i.e., evolution in which nonlinearities affecting a single wave are ignored and any nonlinear couplings between different wave modes are ignored. This is usually justified by stating that the perturbation amplitudes are 'sufficiently small.' But there is actually more that is required. Even for small-amplitude perturbations, nonlinearities can accumulate over time and cause effects not described by linear theory. In the presence of multiple fluctuations, these nonlinearities can transfer energy amongst the modes, sending energy to smaller or larger scales in what is commonly referred to as a cascade. But even for single fluctuations, nonlinearities do interesting things. For example, nonlinearities can cause a fluctuation to steepen into a sawtooth-like, rather than sinusoidal, profile (§VIII.1). The resulting discontinuity at the front of the sawtooth profile triggers dissipative or dispersive effects whose job it is to smooth the profile over what is called a boundary layer. Nevertheless, there remains a relatively sharp transition between conditions just ahead of the boundary layer and just behind the boundary layer. Even though this transition often involves irreversible dissipation and the conversion of bulk flow energy into thermal energy, one may relate these two regions – upstream and downstream – via the conservation of mass, momentum, total energy, and, when magnetic fields are present, magnetic flux. These relations are called the Rankine–Hugoniot jump conditions, the topic of §VIII.2. But such discontinuities and the jump conditions that describe them apply more broadly than to the products of nonlinear wave steepening. Anything that generates a time-steady, discontinuous change in the state of the plasma can be described by the Rankine–Hugoniot jump conditions. The classic example of this is the shock, which occurs when an object or disturbance moves faster than information can propagate into the surrounding fluid or plasma. The lack of causal connection with the surrounding medium means that it cannot react and thus gets swept up and compressed. With multiple speeds characterizing a hot, magnetized plasma – sound, Alfvén, fast and slow magnetosonic – it is therefore not surprising that there are multiple types of shocks. Additional non-ideal physics, such as radiative cooling, anisotropic pressure, or two-fluid effects like ambipolar diffusion, make the study of MHD shocks all the more rich and rewarding.

VIII.1. Wave steepening

The process of wave steepening applies to a variety of linear waves, but for this presentation we focus solely on an adiabatic sound wave, in which case the only nonlinearity is from the Reynolds stress that provides the by-now-familiar $\boldsymbol{u}\cdot\boldsymbol{\nabla u}$ term. Estimating its size as $\sim k(\delta u)^2$ for a fluctuation of wavenumber k and amplitude δu, it is clear that this term becomes important when its time-integrated size becomes large enough to compete with the linear-in-δu inertial term:

$$\delta u \sim k(\delta u)^2 t_{\rm nl}, \tag{VIII.1.1}$$

where $t_{\rm nl}$ the nonlinear timescale over which such nonlinear effects accumulate. This is readily solved to find that

$$t_{\rm nl} \sim (k\delta u)^{-1}. \tag{VIII.1.2}$$

For a small-amplitude wave, this can be a long time, but the steepening is inevitable unless some self-organizational process acts to minimize the dot product between $\boldsymbol{u}$ and

its gradient $\boldsymbol{\nabla u}$. But why 'steepening'? The reason is that, as the sound wave propagates, the parts of the wave having larger density also have a larger sound speed, and vice versa for the parts with smaller density. With the sound speed being the characteristic speed at which the wave travels, this means that the peaks travel at a slightly larger speed than do the troughs. As those peaks advance ahead of the average wave speed, they gradually catch up to the troughs, causing the gradients in the density, and thus the flow, to get progressively larger. In a time $t_{\rm nl}$, those gradients become large enough for the 'linear' wave to no longer look like a linear wave: the sinusoidal variation of the density and flow has been replaced by a profile that is more like a sawtooth. Let us mathematize this physical reasoning.

Start with the continuity and momentum equations for the density and flow velocity:

$$\frac{\partial \varrho}{\partial t} + \boldsymbol{u}\cdot\boldsymbol{\nabla}\varrho = -\varrho\boldsymbol{\nabla}\cdot\boldsymbol{u} \quad \text{and} \quad \frac{\partial \boldsymbol{u}}{\partial t} + \boldsymbol{u}\cdot\boldsymbol{\nabla}\boldsymbol{u} = -c_{\rm s}^2\frac{\boldsymbol{\nabla}\varrho}{\varrho}. \tag{VIII.1.3}$$

Here we have taken the equation of state to be adiabatic, with the pressure $p = \varrho c_{\rm s}^2$ for an adiabatic sound speed $c_{\rm s} \doteq (\gamma p/\varrho)^{1/2}$. This adiabatic assumption will fail eventually, once the nonlinearity leads to gradients sharp enough to trigger dissipation, but let's run with it for now. Use this definition to replace ϱ in (VIII.1.3) with $c_{\rm s} = c_{\rm s0}(\varrho/\varrho_0)^{(\gamma-1)/2}$ for some background $c_{\rm s0}$ and ϱ_0:

$$\frac{2}{\gamma-1}\left(\frac{\partial c_{\rm s}}{\partial t} + \boldsymbol{u}\cdot\boldsymbol{\nabla}c_{\rm s}\right) = -c_{\rm s}\boldsymbol{\nabla}\cdot\boldsymbol{u} \quad \text{and} \quad \frac{\partial \boldsymbol{u}}{\partial t} + \boldsymbol{u}\cdot\boldsymbol{\nabla}\boldsymbol{u} = -\frac{2}{\gamma-1}c_{\rm s}\boldsymbol{\nabla}c_{\rm s}. \tag{VIII.1.4}$$

Restricting attention to the one-dimensional problem (without loss of generality) and re-arranging terms, we find

$$\frac{2}{\gamma-1}\frac{\partial c_{\rm s}}{\partial t} + c_{\rm s}\frac{\partial u}{\partial x} = -\frac{2}{\gamma-1}u\frac{\partial c_{\rm s}}{\partial x} \quad \text{and} \quad \frac{\partial u}{\partial t} + u\frac{\partial u}{\partial x} = -\frac{2}{\gamma-1}c_{\rm s}\frac{\partial c_{\rm s}}{\partial x}. \tag{VIII.1.5}$$

The symmetry of these equations is suggestive... add them and subtract them:

$$\frac{\partial}{\partial t}\left(u \pm \frac{2}{\gamma-1}c_{\rm s}\right) + (u \pm c_{\rm s})\frac{\partial}{\partial x}\left(u \pm \frac{2}{\gamma-1}c_{\rm s}\right) = 0. \tag{VIII.1.6}$$

This equation states that the quantities

$$J_\pm \doteq u \pm \frac{2}{\gamma-1}c_{\rm s} \tag{VIII.1.7}$$

are constant along the characteristics $v_\pm \doteq u \pm c_{\rm s}$. Given any initial conditions, we can compute $J_\pm$ and simply advect those quantities along $\mathrm{d}x/\mathrm{d}t = v_\pm$.

Consider initial conditions corresponding to the eigenvector of a linear sound wave having wavenumber k and propagating in the $+x$ direction:

$$\frac{\delta\varrho}{\varrho_0} = \frac{\delta u}{c_{\rm s0}} = \frac{2}{\gamma-1}\frac{\delta c_{\rm s}}{c_{\rm s0}}. \tag{VIII.1.8}$$

The corresponding values of $J_\pm$ are

$$J_+ = \delta u + \frac{2}{\gamma-1}(c_{\rm s0} + \delta c_{\rm s}) = 2\,\delta u + \frac{2}{\gamma-1}c_{\rm s0}, \tag{VIII.1.9}$$

$$J_- = \delta u - \frac{2}{\gamma-1}(c_{\rm s0} + \delta c_{\rm s}) = \quad - \frac{2}{\gamma-1}c_{\rm s0}. \tag{VIII.1.10}$$

With $\delta u = (1/2)(J_+ + J_-)$ and $c_{\rm s0} + \delta c_{\rm s} = [(\gamma-1)/4](J_+ - J_-)$, the characteristic velocity

expressed in terms of the invariants is

$$v = \frac{1}{2}(J_+ + J_-) + \frac{\gamma - 1}{4}(J_+ - J_-) = \frac{\gamma + 1}{4} J_+ + \frac{3 - \gamma}{4} J_-. \tag{VIII.1.11}$$

With J_- constant and independent of position, and J_+ constant along the characteristic, the characteristic velocity is constant along the characteristic. Substituting in the eigenvector $\delta u = A\, c_{s0} \cos kx$ with amplitude A, we have

$$v = c_{s0}\left(1 + A\,\frac{1+\gamma}{2}\cos kx\right) \quad \Longrightarrow \quad x(t, x_0) = c_{s0}\left(1 + A\,\frac{1+\gamma}{2}\cos kx_0\right) t + x_0. \tag{VIII.1.12}$$

The characteristics have different slopes depending on their origin x_0, and fluid elements issuing from different values of x_0 can end up at the same location. The condition for this to occur is that characteristics issuing from x_0 and $x_1 > x_0$ ultimately share the same $x(t_{nl})$ after the nonlinear time t_{nl}, or

$$c_{s0}\left(1 + A\,\frac{1+\gamma}{2}\cos kx_0\right) t_{nl} + x_0 = c_{s0}\left(1 + A\,\frac{1+\gamma}{2}\cos kx_1\right) t_{nl} + x_1 \tag{VIII.1.13}$$

$$\Longrightarrow \quad c_{s0} t_{nl} = \frac{2}{\gamma + 1}\,\frac{(x_1 - x_0)}{A(\cos kx_0 - \cos kx_1)} \approx \frac{2}{\gamma + 1}\,\frac{1}{Ak \sin kx_0} \tag{VIII.1.14}$$

when x_1 and x_0 are close. This matches our heuristic argument in (VIII.1.2). An example of such characteristics (for $A = 0.1$, $\gamma = 5/3$, $k = 2\pi$) is shown in the figure below, which an intersection of characteristics highlighted:

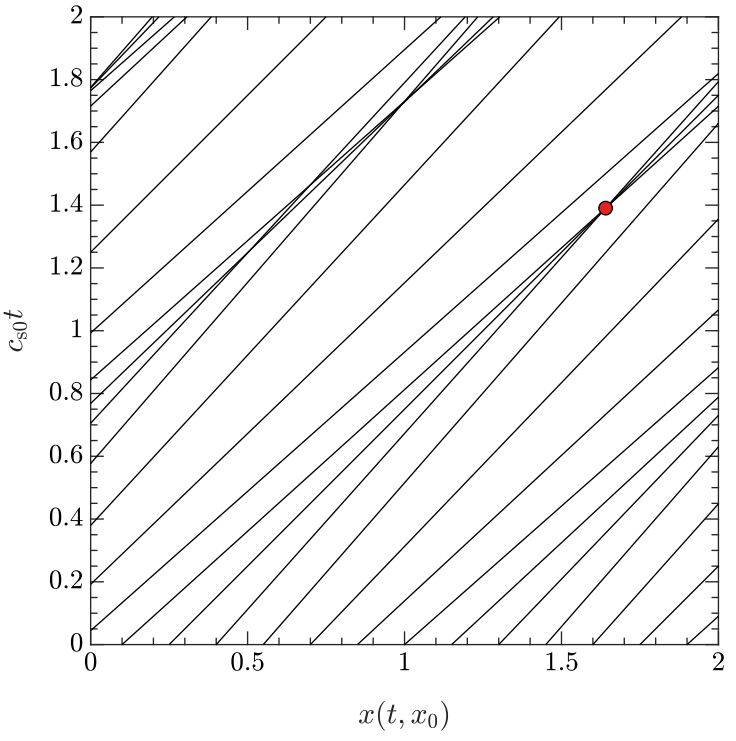

VIII.2. Rankine–Hugoniot jump conditions

Once a shock is established and evolves into a steady state, can the characteristics of the downstream plasma be expressed solely in terms of the conditions found upstream? The answer, supplied by the *Rankine–Hugoniot jump conditions*, is yes. For an MHD plasma, these conditions are obtained by taking the equations of mass continuity, momentum, total energy, and magnetic induction, setting their time derivatives equal to zero, and integrating the result across the shock front. When supplemented by the solenoidality constraint on the magnetic field, the result is a set of equations expressing continuity of the fluxes across the shock interface. This procedure is most easily done in the frame of the shock, such that the shock is a stationary boundary across which the fluid variables change discontinuously. The convention in what follows is that the upstream plasma enters from the shock front from the left, gets processed, and exits to the right. The calculation is also eased when the steady-state equations are written in conservative form:

$$\boldsymbol{\nabla}\cdot(\varrho\boldsymbol{u}) = 0, \tag{VIII.2.1}$$

$$\boldsymbol{\nabla}\cdot\left[\varrho\boldsymbol{u}\boldsymbol{u} + \left(p + \frac{B^2}{8\pi}\right)\boldsymbol{I} - \frac{\boldsymbol{B}\boldsymbol{B}}{4\pi}\right] = 0, \tag{VIII.2.2}$$

$$\boldsymbol{\nabla}\cdot\left[\left(\frac{1}{2}\varrho u^2 + \frac{\gamma p}{\gamma-1} + \frac{B^2}{4\pi}\right)\boldsymbol{u} - \frac{(\boldsymbol{B}\cdot\boldsymbol{u})\boldsymbol{B}}{4\pi}\right] = 0, \tag{VIII.2.3}$$

$$\boldsymbol{\nabla}\cdot(\boldsymbol{u}\boldsymbol{B} - \boldsymbol{B}\boldsymbol{u}) = 0, \tag{VIII.2.4}$$

$$\boldsymbol{\nabla}\cdot\boldsymbol{B} = 0. \tag{VIII.2.5}$$

Note that we are using here an equation for the total energy; the equation governing the internal energy (or the entropy) is useless here, because dissipation within the shock causes the fluid to jump to a different adiabat as it crosses through. Even though no time derivatives appear in the above equations, there is a sense of irreversibility, which in the fluid case is enabled by viscosity within the shock transition converting kinetic energy into internal energy.

VIII.2.1. *General derivation of the jump conditions*

To obtain the jump conditions, we integrate the above conservation laws over a volume centered about the shock front having infinitesimal thickness, and use Gauss' law to turn the divergences into surface integrals. Evaluating those surface integrals just upstream of the shock (subscript '1') and just downstream of the shock (subscript '2') leads to the following set of difference equations:

$$\left[\varrho u_n\right]_{12} = 0, \tag{VIII.2.6}$$

$$\left[\varrho u_n\boldsymbol{u} + \left(p + \frac{B^2}{8\pi}\right)\hat{\boldsymbol{n}} - \frac{B_n\boldsymbol{B}}{4\pi}\right]_{12} = 0, \tag{VIII.2.7}$$

$$\left[\left(\frac{1}{2}\varrho u^2 + \frac{\gamma p}{\gamma-1} + \frac{B^2}{4\pi}\right)u_n - \frac{(\boldsymbol{B}\cdot\boldsymbol{u})B_n}{4\pi}\right]_{12} = 0, \tag{VIII.2.8}$$

$$\left[u_n\boldsymbol{B} - B_n\boldsymbol{u}\right]_{12} = 0, \tag{VIII.2.9}$$

$$\left[B_n\right]_{12} = 0, \tag{VIII.2.10}$$

where $[\ldots]_{12}$ denotes the difference in the quantity in brackets between the two regions. A schematic is shown here with all quantities labeled:

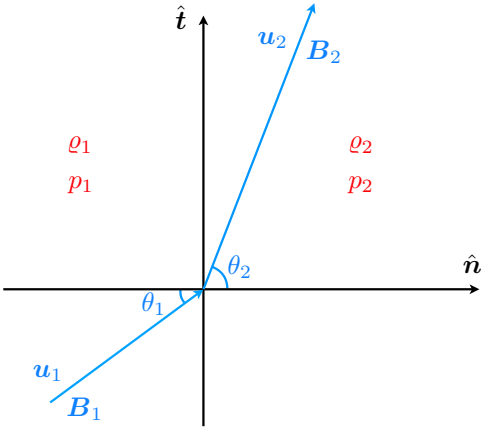

Equation (VIII.2.6) states that whatever mass flows into the shock must exit the shock in steady state:

$$\varrho_1 u_{n1} = \varrho_2 u_{n2} \quad \Longrightarrow \quad \frac{u_{n1}}{u_{n2}} = \frac{\varrho_2}{\varrho_1} \doteq R. \tag{VIII.2.11}$$

In the final line, we have followed standard practice in denoting the density ratio by R, a quantity that obviously must be >1 for there to be a shock. Our task is then to express the ratios of all other quantities (e.g., p_2/p_1, B_2/B_1) in terms of R, and then solve a polynomial equation for R to close the system.

The component of (VIII.2.7) along the shock normal is

$$\varrho_1 u_{n1}^2 + p_1 + \frac{B_1^2}{8\pi} - \frac{B_{n1}^2}{4\pi} = \varrho_2 u_{n2}^2 + p_2 + \frac{B_2^2}{8\pi} - \frac{B_{n2}^2}{4\pi} \tag{VIII.2.12}$$

With (VIII.2.10) guaranteeing that $B_{n2} = B_{n1}$, the only component of the magnetic field that enters this equation is the tangential component, B_t. Dividing this equation through by $\varrho_1 u_{n1}^2$ and defining the Mach number via $M^2 \doteq u_{\rm n1}^2/a_1^2$, where $a_1 \doteq (\gamma p_1/\varrho_1)^{1/2}$ is the adiabatic sound speed in the upstream fluid, we find that

$$1 + \frac{1}{\gamma M^2}\left(1 + \frac{B_{t1}^2}{8\pi p_1}\right) = \frac{1}{R} + \frac{1}{\gamma M^2}\left(\frac{p_2}{p_1} + \frac{B_{t2}^2}{8\pi p_1}\right) \tag{VIII.2.13}$$

Note that the magnetic field tangential to the shock front acts to enhance the pressure, making it more difficult for the shock to increase the density. At this point one might be tempted to introduce the plasma beta parameter in the upstream fluid, $\beta \doteq 8\pi p_1/B_1^2$, but it turns out to be more natural in shock problems to compare the magnetic energy not to the thermal pressure but rather to the ram pressure. So let us define the Alfvén Mach number $M_{\rm A} \doteq u_{n1}/v_{\rm A1}$, where $v_{\rm A1} \doteq B_1/(4\pi\varrho_1)^{1/2}$ is the upstream Alfvén speed. To indicate that only the tangential component of the magnetic field enters, we also define the geometric factor $T \doteq B_{t1}^2/B_1^2$, in which case (VIII.2.13) becomes

$$1 + \frac{1}{\gamma M^2} + \frac{T}{2M_{\rm A}^2} = \frac{1}{R} + \frac{1}{\gamma M^2}\frac{p_2}{p_1} + \frac{T}{2M_{\rm A}^2}\frac{B_{t2}^2}{B_{t1}^2}. \tag{VIII.2.14}$$

The next step is to eliminate B_{t2}/B_{t1} using the tangential component of the steady-state induction equation (VIII.2.9), which provides

$$u_{n1}\boldsymbol{B}_{t1} - B_{n1}\boldsymbol{u}_{t1} = u_{n2}\boldsymbol{B}_{t2} - B_{n2}\boldsymbol{u}_{t2} \quad \Longrightarrow \quad \frac{1}{R}\frac{\boldsymbol{B}_{t2}}{B_{n1}} - \frac{\boldsymbol{B}_{t1}}{B_{n1}} = \frac{\boldsymbol{u}_{t2}}{u_{n1}} - \frac{\boldsymbol{u}_{t1}}{u_{n1}}. \tag{VIII.2.15}$$

The right-hand side of this equation may be readily obtained from the tangential

component of the momentum equation (VIII.2.7):

$$\varrho_1 u_{n1}\boldsymbol{u}_{t1} - \frac{B_{n1}\boldsymbol{B}_{t1}}{4\pi} = \varrho_2 u_{n2}\boldsymbol{u}_{t2} - \frac{B_{n2}\boldsymbol{B}_{t2}}{4\pi} \quad \Longrightarrow \quad \frac{\boldsymbol{u}_{t2}}{u_{n1}} - \frac{\boldsymbol{u}_{t1}}{u_{n1}} = \frac{N}{M_{\rm A}^2}\left(\frac{\boldsymbol{B}_{t2}}{B_{n1}} - \frac{\boldsymbol{B}_{t1}}{B_{n1}}\right) \tag{VIII.2.16}$$

To obtain the final equality, we have used that $B_{n2} = B_{n1}$ and defined the geometric factor $N \doteq B_{n1}^2/B_1^2 = 1 - T$. Combining (VIII.2.15) and (VIII.2.16) then affords expressions for the tangential component of the magnetic field,

$$\boldsymbol{B}_{t2} = \left(\frac{R - RN/M_{\rm A}^2}{1 - RN/M_{\rm A}^2}\right)\boldsymbol{B}_{t1}, \tag{VIII.2.17}$$

and the tangential component of the velocity,

$$\frac{\boldsymbol{u}_{t2}}{u_{n1}} = \frac{\boldsymbol{u}_{t1}}{u_{n1}} + \frac{N}{M_{\rm A}^2}\left(\frac{R-1}{1 - RN/M_{\rm A}^2}\right)\frac{\boldsymbol{B}_{t1}}{B_{n1}}. \tag{VIII.2.18}$$

Note that $N = 0$ ensures $B_{t2}/B_{t1} = R$, so that the strength of the tangential field increases in proportion to the density (as expected from flux freezing). Note also the pole at $R = M_{\rm A}^2/N$, a feature to which we shall return in due course (§VIII.2.5). With (VIII.2.17) in hand, we can now revisit (VIII.2.14), eliminate B_{t2}^2/B_{t1}^2, and re-arrange to obtain an expression for the pressure ratio:

$$\frac{1}{\gamma M^2}\frac{p_2}{p_1} = 1 - \frac{1}{R} + \frac{1}{\gamma M^2} + \frac{T}{2M_{\rm A}^2}\left[1 - \left(\frac{R - RN/M_{\rm A}^2}{1 - RN/M_{\rm A}^2}\right)^2\right]. \tag{VIII.2.19}$$

With everything now expressed in terms of the unknown density enhancement R, we obtain our polynomial equation for R by substituting (VIII.2.11) and (VIII.2.17)–(VIII.2.19) into the total energy equation (VIII.2.8), or

$$\left(\frac{1}{2}\varrho_1 u_1^2 + \frac{\gamma p_1}{\gamma - 1} + \frac{B_{t1}^2}{4\pi}\right)u_{n1} - \frac{B_{n1}\boldsymbol{B}_{t1}\cdot\boldsymbol{u}_{t1}}{4\pi} = \left(\frac{1}{2}\varrho_2 u_2^2 + \frac{\gamma p_2}{\gamma - 1} + \frac{B_{t2}^2}{4\pi}\right)u_{n2} - \frac{B_{n2}\boldsymbol{B}_{t2}\cdot\boldsymbol{u}_{t2}}{4\pi}. \tag{VIII.2.20}$$

Writing $u_1^2 = u_{n1}^2 + u_{t1}^2$ and dividing through by $(1/2)\varrho_1 u_{n1}^3$ leads, after some straightforward algebra and re-organization, to the following equation for R:

$$\boxed{\begin{aligned}&\left(1 - \frac{RN}{M_{\rm A}^2}\right)^2\left[R^2\left(1 + \frac{2}{\gamma-1}\frac{1}{M^2}\right) - R\,\frac{2}{\gamma-1}\left(\gamma + \frac{1}{M^2}\right) + \frac{\gamma+1}{\gamma-1}\right]\\ &= \frac{RT}{M_{\rm A}^2}\left[-R^3\frac{N}{M_{\rm A}^2} + R^2\left(\frac{\gamma-2}{\gamma-1} + \frac{N}{M_{\rm A}^2}\frac{2\gamma}{\gamma-1}\right) - R\left(2 + \frac{N}{M_{\rm A}^2}\frac{\gamma+1}{\gamma-1}\right) + \frac{\gamma}{\gamma-1}\right]\end{aligned}} \tag{VIII.2.21}$$

The subsequent subsections analyze this equation in a variety of limits.

Before proceeding, however, it is instructive to take the limit $R \to 1$, in which case (VIII.2.21) returns

$$N = M_{\rm A}^2 \quad \text{and} \quad N = M^2 + M_{\rm A}^2 - M^2 M_{\rm A}^2. \tag{VIII.2.22}$$

Re-arranging these and casting them in more familiar variables, we find

$$u_{n1}^2 = v_{\rm A1}^2 N \quad \text{and} \quad u_{n1}^2 = \frac{a_1^2 + v_{\rm A1}^2}{2} \pm \sqrt{\left(\frac{a_1^2 + v_{\rm A1}^2}{2}\right)^2 - a_1^2 v_{\rm A1}^2 N}, \tag{VIII.2.23}$$

i.e., the squares of the Alfvén and (fast and slow) magnetosonic speeds. In this sense, one may consider the various MHD shocks that are analyzed below as nonlinear versions of

the usual MHD waves. It will turn out that $B_{t2} > B_{t1}$ for a fast shock, $B_{t2} < B_{t1}$ for a slow shock, and $B_{t2} \to -B_{t1}$ for an Alfvénic (sometimes called 'intermediate') shock in the limit. Let us proceed.

VIII.2.2. *HD and parallel MHD shocks*

Suppose there were no magnetic field (i.e., $M_\mathrm{A} \to \infty$). In this case, equation (VIII.2.21) reduces to

$$R^2\left(1+\frac{2}{\gamma-1}\frac{1}{M^2}\right)-R\,\frac{2}{\gamma-1}\left(\gamma+\frac{1}{M^2}\right)+\frac{\gamma+1}{\gamma-1}=0, \tag{VIII.2.24}$$

which may be readily solved to find

$$R=\frac{\gamma+1}{\gamma-1+2/M^2}. \tag{VIII.2.25}$$

This expression for R may then be substituted into the following expressions to obtain the jump ratios

$$\frac{\varrho_2}{\varrho_1}=\frac{u_{n1}}{u_{n2}}=R,\quad \frac{p_2}{p_1}=1+\gamma M^2\left(1-\frac{1}{R}\right)=1+\frac{2\gamma}{\gamma+1}(M^2-1),\quad \boldsymbol{u}_{t2}=\boldsymbol{u}_{t1}. \tag{VIII.2.26}$$

Note that M must be greater than unity, or else the pressure would have to decrease across the shock; doing so would violate the second law of thermodynamics, as it would imply that heat energy is converted into ordered kinetic energy, with the pressure gradient accelerating the flow. The case $M = 1$ is of course a trivial solution, in which there is no discontinuity in any of the flow variables. The Mach number downstream of the shock may be obtained from $u_2/u_1 = 1/R$ and $a_2/a_1 = (T_2/T_1)^{1/2} = (1/R)^{1/2}(p_2/p_1)^{1/2}$, or

$$M_2 \doteq \frac{u_2}{a_2}=\sqrt{\frac{(\gamma-1)+2/M^2}{2\gamma-(\gamma-1)/M^2}}<1. \tag{VIII.2.27}$$

The downstream flow is subsonic. Finally, it will be useful to have a general expression for the change in entropy $s \doteq \ln(p/\varrho^\gamma)$ across the shock front:

$$s_2-s_1=\ln\frac{p_2}{p_1}-\gamma\ln\frac{\varrho_2}{\varrho_1}=\ln\left[1+\frac{2\gamma}{\gamma+1}(M^2-1)\right]+\gamma\ln\left(\frac{\gamma-1+2/M^2}{\gamma+1}\right). \tag{VIII.2.28}$$

At $M = 1$, $s_2 - s_1 = 0$ because there is no shock. For $M > 1$, entropy increases and the fluid rapidly jumps to a different adiabat.

It is instructive to exam the two limiting cases of a strong shock ($M^2 \gg 1$) and a weak shock ($M^2 - 1 \ll 1$). The former can be easily read off:

$$\text{strong HD shock:}\quad R\approx\frac{\gamma+1}{\gamma-1},\quad \frac{p_2}{p_1}\approx\frac{2\gamma}{\gamma+1}M^2,\quad M_2\approx\sqrt{\frac{\gamma-1}{2\gamma}}. \tag{VIII.2.29}$$

Note that R asymptotes to a value that is independent of the Mach number (one that is worth committing to memory). For a monatomic gas with $\gamma = 5/3$, this implies a maximum compression ratio $R_\mathrm{max} = 4$, a pressure ratio $p_2/p_1 \approx (5/4)M^2$, a temperature ratio $T_2/T_1 \approx (5/16)M^2$, and a Mach number $M_2 \approx 0.45$. The reason for this asymptotic result is that the downstream pressure continues to increase as M^2, and so the fluid gets more and more difficult to compress as M increases. Despite the compression factor asymptoting to an order-unity number, the entropy increases without bound (see

(VIII.2.28)):

$$s_2 - s_1 \approx \ln \frac{2\gamma M^2}{\gamma+1} + \gamma \ln \frac{\gamma-1}{\gamma+1}. \tag{VIII.2.30}$$

This makes sense – more and more irreversible dissipation of the kinetic energy must occur as M increases in order keep the compression ratio fixed. In the opposite limit of a weak shock, we may expand (VIII.2.25) in $\epsilon \doteq M^2 - 1 \ll 1$ to find

$$\text{weak HD shock:} \quad R \approx 1 + \frac{2}{\gamma+1}\,\epsilon, \quad \frac{p_2}{p_1} \approx 1 + \frac{2\gamma}{\gamma+1}\,\epsilon, \quad M_2 \approx 1 - \frac{\epsilon}{2}. \tag{VIII.2.31}$$

Obtaining the entropy change in this case requires expanding (VIII.2.28) to $\mathcal{O}(\epsilon^3)$:

$$s_2 - s_1 \approx \frac{2\gamma(\gamma-1)}{3(\gamma+1)^2}\,\epsilon^3 \tag{VIII.2.32}$$

So, indeed, entropy increases (though barely!).

Let us restore the magnetic field, but take $N = 1$ ($T = 0$) so that the magnetic field is oriented along the shock normal. In this case, the entire right-hand side of (VIII.2.21) vanishes and we recover the hydrodynamic result (VIII.2.25) times an Alfvénic root at $R = M_{\rm A}^2$. This makes sense, because the shock occurs while sliding along an unperturbed magnetic field oriented parallel to the flow – a 'parallel MHD shock.'

VIII.2.3. *Perpendicular MHD shocks*

If the upstream magnetic field is instead oriented perpendicularly to the shock normal ($N = 0$, $T = 1$), then (VIII.2.21) becomes

$$R^2\left(1 + \frac{2}{\gamma-1}\frac{1}{M^2}\right) - R\,\frac{2}{\gamma-1}\left(\gamma + \frac{1}{M^2}\right) + \frac{\gamma+1}{\gamma-1} = \frac{R}{M_{\rm A}^2}\left(R^2\,\frac{\gamma-2}{\gamma-1} - 2R + \frac{\gamma}{\gamma-1}\right), \tag{VIII.2.33}$$

whose (cubic) solutions provide

$$\frac{p_2}{p_1} = 1 + \gamma M^2\left(1 - \frac{1}{R}\right) - \frac{1}{\beta}(R^2 - 1), \quad \boldsymbol{B}_{t2} = R\boldsymbol{B}_{t1}, \quad \boldsymbol{u}_{t2} = \boldsymbol{u}_{t1}. \tag{VIII.2.34}$$

The minus sign in the final $(1/\beta)$ term in the pressure ratio, combined with the need for $(R^2 - 1)$ to be positive, indicates that the magnetic pressure relieves some of the burden on the gas pressure in supporting the shock. But for that to be true, the incoming flow must be at least super-Alfvénic, so that any magnetic compression cannot be radiated away as a wave. In the hydrodynamic (or parallel MHD) case, we required $M > 1$ for there to be a shock. What is the criterion here? Rather than solve this cubic for R and demand that $R > 1$, a simpler route is to write $R = 1 + \epsilon$ with $|\epsilon| \ll 1$, demand that ϵ be positive, and solve for M in terms of $M_{\rm A}$. The result is that

$$1 > \frac{1}{M^2} + \frac{1}{M_{\rm A}^2} \quad \Longrightarrow \quad u_1^2 > a_1^2 + v_{\rm A1}^2; \tag{VIII.2.35}$$

i.e., the shock speed must exceed the fast magnetosonic speed ahead of the shock. Because of this, perpendicular shocks are often referred to as 'fast-mode shocks.'

Again without solving (VIII.2.33) exactly, we may determine the effect of the magnetic field on the shock by writing $R = R_{\rm HD}(1 + M_{\rm A}^{-2}\,\text{ɾ})$ with $R_{\rm HD}$ being the hydrodynamic solution (VIII.2.25), and solving perturbatively for the correction ɾ assuming that $M_{\rm A}^2 \gg 1$ (equivalently, $\beta M^2 \gg 1$). After some algebra and adroit consolidation of terms,

we find to $\mathcal{O}(M_{\rm A}^{-2})$ that

$$R = R_{\rm HD}\left\{1 - M_{\rm A}^{-2}\frac{2-(2-\gamma)/M^2-\gamma/M^4}{[(\gamma-1)+2/M^2][(\gamma-1)+(3-\gamma)/M^2-2/M^4]}\right\}. \quad \text{(VIII.2.36)}$$

In both the limits of $M^2 \gg 1$ and $(M^2-1) \ll 1$, the magnetic field acts to reduce the compression ratio:

$$\begin{aligned} \text{strong shock with } M_{\rm A}^2 \gg 1: \quad & R \approx R_{\rm HD}\left[1 - M_{\rm A}^{-2}\frac{2}{(\gamma-1)^2}\right], \\ \text{weak shock with } M_{\rm A}^2 \gg 1: \quad & R \approx R_{\rm HD}\left[1 - \frac{2}{\gamma\beta}\frac{\gamma+2}{(\gamma+1)^2}\right]. \end{aligned} \quad \text{(VIII.2.37)}$$

This makes sense physically, because some of the kinetic energy must go into compressing the magnetic field. More general solutions of (VIII.2.33) are obtained numerically and given in the figure below for different $\beta = (2/\gamma)(M_{\rm A}/M)^2$:

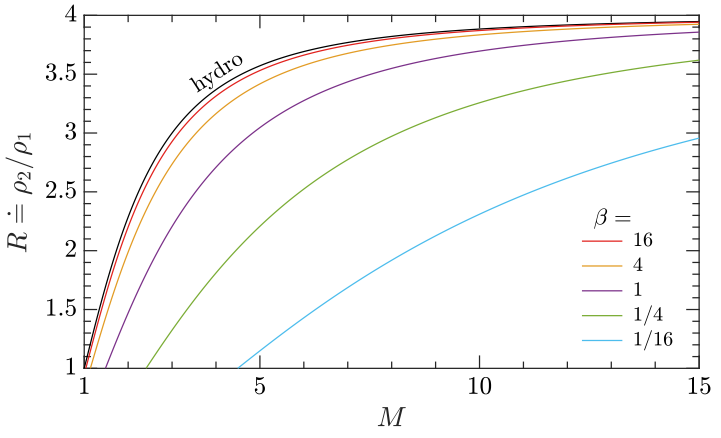

Stronger magnetic fields perpendicular to the shock normal reduce the compression ratio from its hydrodynamic value, while increasing the threshold Mach number for the shock to form.

VIII.2.4. *Oblique MHD shocks*

When the upstream magnetic field and/or the incoming flow is oriented at an oblique angle with respect to the shock front, the situation becomes more complex. The field and flow can be refracted by the shock, with the angle of incidence being different on either side of the interface. As a first pass through this calculation, let us first drop the magnetic field and ask what would happen in a hydrodynamic setting if the incoming flow were at an angle. Equation (VIII.2.16) states that $\boldsymbol{u}_{t2} = \boldsymbol{u}_{t1}$ in this case, and we know that $u_{n2} = u_{n1}/R$. Combining these, we see that $\tan\theta_2 \doteq u_{t2}/u_{n2} = R\,u_{t1}/u_{n1} \doteq R\tan\theta_1$, indicating that the flow changes direction in the downstream to become canted towards the plane of the shock. When an oblique magnetic field is also present, this increase in the angle θ across the shock is accompanied by a sharp bend in the magnetic-field lines, whose tension then affects the jump conditions by transferring momentum in the tangential direction.

An apparent complication from the conservation laws is that both $\boldsymbol{u}_{t1}$ and $\boldsymbol{B}_{t1}$ appear as initial conditions, implying that there are two independent angles to worry about, one related to u_{t1}^2/u_{n1}^2 and one related to $B_{t1}^2/B_{n1}^2 = T/N = 1/N - 1$. But the polynomial equation for R that we obtained (VIII.2.21) only makes reference to the latter. The

reason why is because one may boost to a frame in which $\boldsymbol{u}_1 \times \boldsymbol{B}_1 = \boldsymbol{0}$, in which the upstream flow and field are aligned. This frame is referred to as the *de Hoffmann–Teller frame* (De Hoffmann & Teller 1950). The idea is that, if $\boldsymbol{u}_1$ and $\boldsymbol{B}_1$ weren't aligned, then there would be a motional electric field corresponding to a conductor moving at the $\boldsymbol{E} \times \boldsymbol{B}$ drift velocity. By boosting to that $\boldsymbol{E} \times \boldsymbol{B}$-drifting frame, we can eliminate the electric field and have $\boldsymbol{u}_1 \times \boldsymbol{B}_1 = \boldsymbol{0}$ in that frame. It then follows from the jump condition (VIII.2.9) that $\boldsymbol{u}_2 \times \boldsymbol{B}_2 = \boldsymbol{0}$; i.e., if we work in a frame in which the upstream flow is parallel to the upstream magnetic field, then the downstream flow is also parallel to the downstream magnetic field. The velocity of this 'dH–T' frame is not unique; one can add any field-aligned vector to the $\boldsymbol{E} \times \boldsymbol{B}$ drift velocity without changing the physics:

$$\boldsymbol{u}_{\text{dH–T}} = \frac{\boldsymbol{B}_1 \times (\boldsymbol{u}_1 \times \boldsymbol{B}_1)}{B_1^2} + \lambda \boldsymbol{B}_1, \quad \lambda = \text{const.} \tag{VIII.2.38}$$

For example,

$$\boldsymbol{u}_{\text{dH–T}} = \hat{\boldsymbol{n}} \times \left(\boldsymbol{u}_1 \times \frac{\boldsymbol{B}_1}{B_{1n}} \right), \tag{VIII.2.39}$$

where $\hat{\boldsymbol{n}}$ denotes the shock normal, also works.

The figure below shows the compression ratio, calculated by solving (VIII.2.21) numerically, for a strong oblique shock with $\gamma = 5/3$, $M = 10$, and $\beta \in \{1/4, 1, 4\}$, at a variety of angles $\theta_1 \doteq \cos^{-1}(B_{n1}/B_1)$:

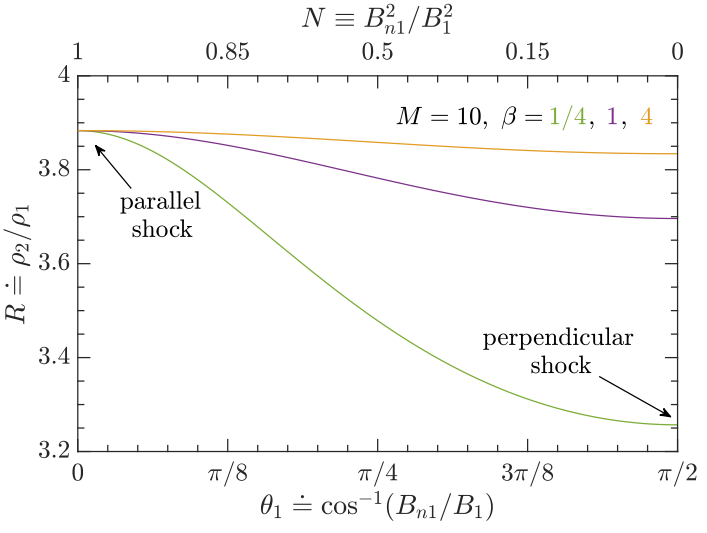

As expected (see (VIII.2.37)), the value of R decreases as the shock goes from parallel to perpendicular. Here is the angle $\theta_2 \doteq \cos^{-1}(B_{n2}/B_2)$ that the downstream magnetic field makes with respect to the shock normal:

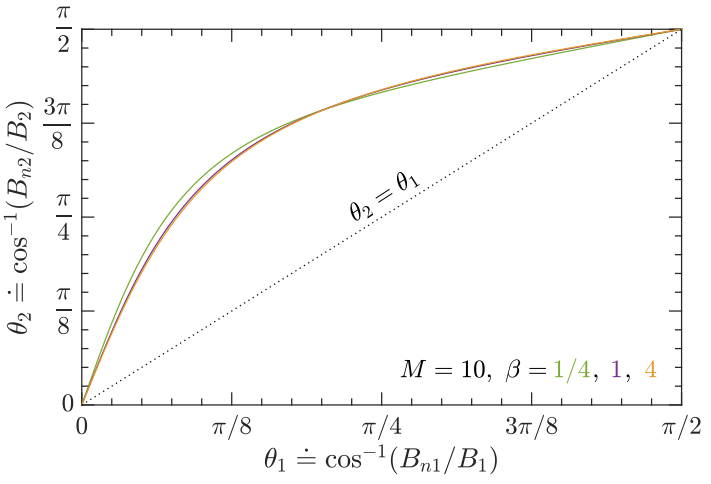

Note that $\theta_2 > \theta_1$ for $\theta_1 \in (0, \pi/2)$, indicating that the downstream magnetic field is canted upwards towards the shock interface in an oblique fast-mode shock. This makes physical sense: a super-Alfvénic shock can sweep up the tangential component of the magnetic field and compress it without the field having time to rarify to produce a magneto-sonic wave, thereby driving the orientation of the magnetic field towards the shock interface.

Here is the same set of plots but for a weak oblique shock with $M = 2$:

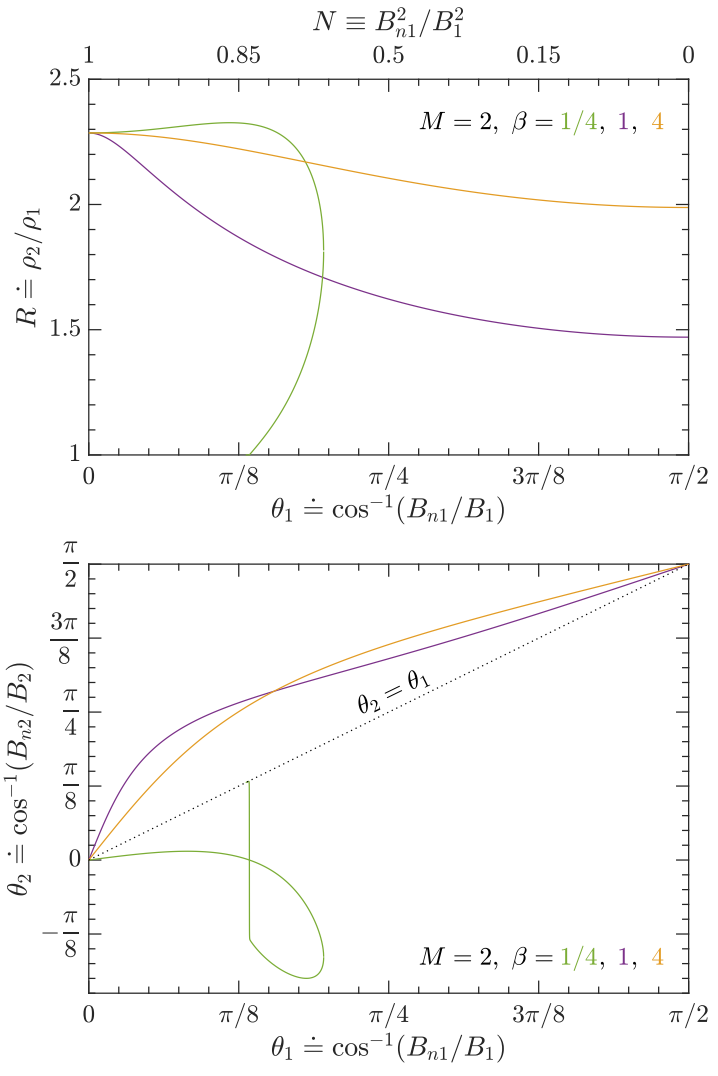

The behavior at $\beta = 1$ ($M_\mathrm{A} \simeq 1.8$) and $\beta = 4$ ($M_\mathrm{A} \simeq 3.7$) is qualitatively similar to what was seen for the strong shock: the compression ratio decreases as the shock becomes more perpendicular, and the angle of the magnetic field increases across the shock. But at $\beta = 1/4$ ($M_\mathrm{A} \simeq 0.9$), everything seems to change. The branch that starts at $N = 1$ where the parallel shocks live turns upwards towards larger compression factors, ultimately taking a dive towards small R and even becoming double-valued. To make this feature clearer, the following plots show R and θ_2 only for $\beta = 1/4$, but with the different branches traced in blue and red:

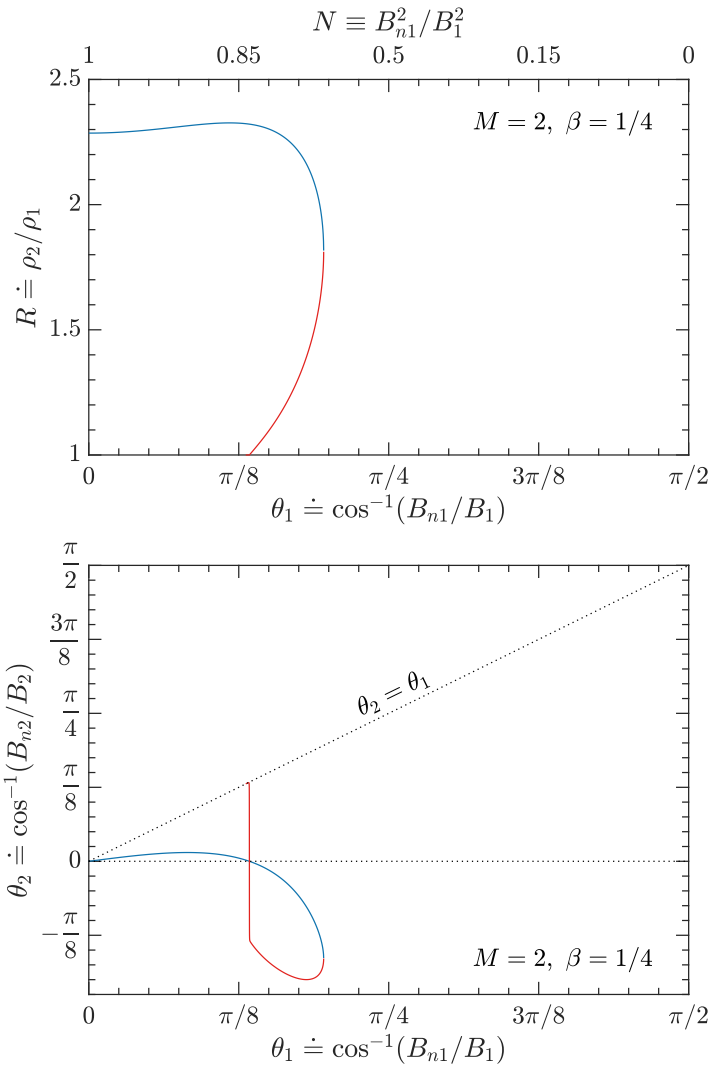

What's going on?

In general, R satisfies a fourth-order polynomial equation. Let's count the roots. One root is trivial, at $R = 1$. One root is the standard solution for a parallel and perpendicular shock, with a smooth interpolation between them at intermediate angles. The final two roots are the lines traced in blue and red. When the upstream magnetic field has a small tangential component, the blue root satisfies $\theta_2 < \theta_1$, indicating that the downstream magnetic field is oriented *closer* to the shock normal than in the upstream. The value of θ_2 actually passes through zero at $N = M_{\rm A}^2 = (\gamma\beta/2)M^2$, or $\theta_1 = \cos^{-1}(M\sqrt{\gamma\beta/2})$, and then goes negative (!), corresponding to B_{t2} having the opposite sign as B_{t1}. The red root does so as well, jumping off the trivial $R = 1$, $\theta_2 = \theta_1$ solution as N approaches $M_{\rm A}^2$ from above, and diving through zero and into negative territory for $N < M_{\rm A}^2$. This root ultimately connects to the blue root at the maximum value of θ_1 for which a shock solution exists.

The reason for this strange behavior is that the combination of $M = 2$ and $\beta = 1/4$ places the shock speed below the fast speed but above the slow speed for all N. As a result, the downstream magnetic field has the freedom to orient itself in different ways.

In particular, when $N < M_{\rm A}^2$, the shock speed is super-Alfvénic and the tangential component of the magnetic field can flip its sign. This flipping of signs is related to a phenomenon know as a 'switch-off' shock, our final stop on this tour of MHD shocks...

VIII.2.5. *Switch-off (and switch-on) shocks*

A 'switch-off' shock occurs when an oblique shock with $B_{t1}, u_{t1} \neq 0$ leads to a purely normal field and flow in the downstream, $B_{t2} = u_{t2} = 0$. Under these conditions, equations (VIII.2.15) and (VIII.2.16) demand that $N = M_{\rm A}^2 < 1$. In words, the incoming flow and magnetic field must be oriented with respect to the shock front at a precise angle that depends only on the Alfvén Mach number of the shock, and the incoming flow must be precisely Alfvénic (meaning that $u_{n1}^2 = v_{\rm A1}^2 N$ – see (VIII.2.23)). In this case, the compression ratio satisfies

$$R^2\left(\frac{2}{M^2}+\frac{\gamma-1}{M_{\rm A}^2}\right)-\gamma R\left(1+\frac{2}{\gamma M^2}+\frac{1}{M_{\rm A}^2}\right)+(\gamma+1)=0 \qquad \text{(VIII.2.40)}$$

for $M^2 < (2/\gamma)\beta^{-1}$. Being a quadratic, this equation admits two solutions for R, which are precisely the two (red and blue) solutions in the plot above at $\theta_2 = 0$ and $\theta_1 \simeq 0.13\pi$ ($N \simeq 0.83$). Graphically:

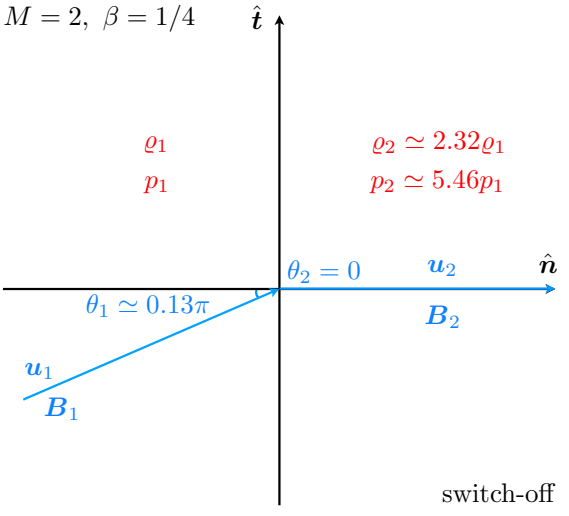

Solutions also allow for the reverse of this situation, called a 'switch-on shock.' In this case, a fluid with neither magnetic field nor flow velocity tangential to the shock front nevertheless acquires tangential components downstream of the shock, i.e., $B_{t2}, u_{t2} \neq 0$ even though $B_{t1}, u_{t1} = 0$. With $T = 0$ ($N = 1$), the momentum and induction equations provide

$$1+\frac{1}{\gamma M^2}=\frac{1}{R}+\frac{1}{\gamma M^2}\frac{p_2}{p_1}+\frac{1}{2M_{\rm A}^2}\frac{B_{t2}^2}{B_1^2},\quad \frac{\boldsymbol{B}_{t2}}{B_1}=R\frac{\boldsymbol{u}_{t2}}{u_1},\quad \text{and}\quad R=M_{\rm A}^2. \qquad \text{(VIII.2.41)}$$

Because R must be greater than one for a true shock solution, the shock must be super-Alfvénic for a switch-on solution to exist. The total energy equation in this situation may be solved for the pressure ratio:

$$\frac{p_2}{p_1}=(\gamma-1)\left[M_{\rm A}^2\left(\frac{M^2}{2}+\frac{1}{\gamma-1}\right)-\frac{M^2}{2M_{\rm A}^2}\left(1+\frac{B_{t2}^2}{B_1^2}\right)\right]. \qquad \text{(VIII.2.42)}$$

Substituting this expression back into (VIII.2.41) yields

$$\frac{B_{t2}^2}{B_1^2} = (M_{\rm A}^2 - 1)\left[(\gamma+1) - (\gamma-1)M_{\rm A}^2 - \frac{2M_{\rm A}^2}{M^2}\right]. \tag{VIII.2.43}$$

Note that the right-hand of this expression must be positive, corresponding to the tangential components 'switching on', if

$$(M_{\rm A}^2 - 1)\left[(\gamma+1) - (\gamma-1)M_{\rm A}^2 - \frac{2M_{\rm A}^2}{M^2}\right] > 0. \tag{VIII.2.44}$$

For $M^2 > 1$, this is satisfied provided that

$$1 < M_{\rm A}^2 < \frac{(\gamma+1)M^2}{(\gamma-1)M^2+2}, \quad \text{or} \quad \frac{2/\gamma}{M^2} < \beta < \frac{2(1+1/\gamma)}{(\gamma-1)M^2+2}. \tag{VIII.2.45}$$

For $\gamma = 5/3$, this is a fairly narrow range of Alfvén Mach numbers. An example of a switch-off shock is shown in the figure below for $\gamma = 5/3$, $M = 2$, and $\beta = 1/2$:

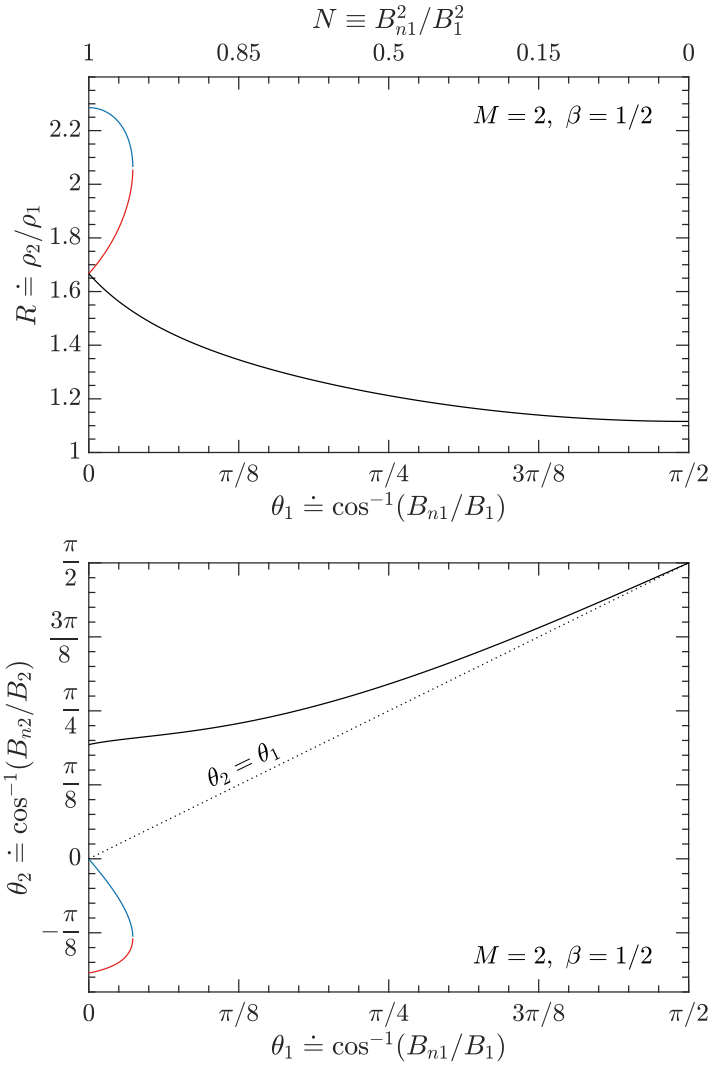

Notice that the roots traced by the black and red lines have non-zero θ_2 even when $\theta_1 = 0$, thus, switch-on shocks. These solutions stem from a degenerate root at $R = M_{\rm A}^2$, which separates as θ_1 becomes non-zero (as shown in the figure). Indeed, one may calculate a correction to the switch-off solution at small but non-zero $T = \epsilon \ll 1$ by writing $R = M_{\rm A}^2(1 + \epsilon^{1/2}\,\text{ɾ})$, expanding (VIII.2.21) out to $\mathcal{O}(\epsilon)$, and solving for ɾ. The result is that

$$R = M_{\rm A}^2\left(1 + T^{1/2}\,\text{ɾ}\right) \quad \text{with} \quad \text{ɾ} = \pm\sqrt{\frac{M_A^2 - 1}{\gamma + 1 - M_{\rm A}^2(\gamma - 1 + 2/M^2)}}. \tag{VIII.2.46}$$

With the factor in the square root being positive, R remains real and splits into two solutions, one $>M_{\rm A}^2$ and one $<M_{\rm A}^2$. Graphically:

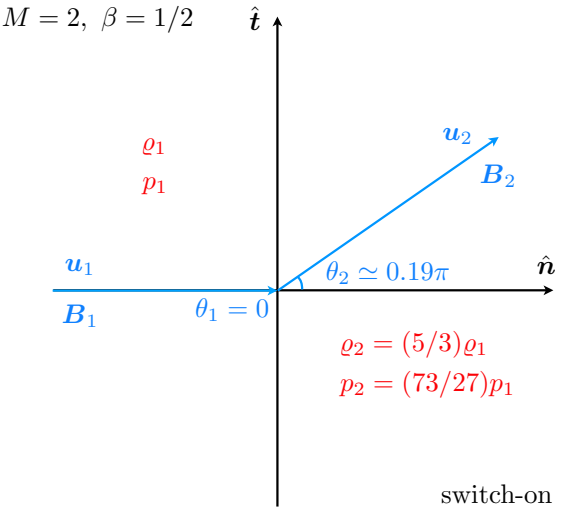

VIII.2.6. *Radiative shocks*

$$\boldsymbol{\nabla}\cdot\left[\left(\frac{1}{2}\varrho u^2 + \frac{\gamma p}{\gamma - 1} + \frac{B^2}{4\pi}\right)\boldsymbol{u} - \frac{(\boldsymbol{B}\cdot\boldsymbol{u})\boldsymbol{B}}{4\pi}\right] = -\varrho\mathcal{L} \tag{VIII.2.47}$$

in progress...

VIII.2.7. *Two-fluid shocks*

C-shocks via ambipolar diffusion. See problem set #4.

PART IX
Reduced MHD

Reduced MHD is a nonlinear system of fluid equations used to describe anisotropic fluctuations in magnetized plasmas at lengthscales $\ell \gg \varrho_{\rm i}$ and frequencies $\omega \ll \Omega_{\rm i}$. It was initially used to model elongated structures in tokamaks (Kadomtsev & Pogutse 1974; Strauss 1976, 1977), but has since become a standard paradigm in astrophysical contexts such as solar-wind turbulence (Zank & Matthaeus 1992*a*,*b*; Bhattacharjee *et al.* 1998) and the solar corona (Oughton *et al.* 2003; Perez & Chandran 2013).

While one may formulate different versions of RMHD, here I will confine the discussion solely to ideally conducting fluids whose equilibrium state is homogeneous ($\varrho_0 = \text{const}$, $p_0 = \text{const}$), stationary ($\boldsymbol{u}_0 = 0$), and threaded by a uniform mean magnetic field oriented along the z axis ($\boldsymbol{B}_0 = B_0\hat{\boldsymbol{z}}$). The fluid is perturbed with small displacements, which we take to satisfy the ordering

$$\frac{\delta\varrho}{\varrho_0} \sim \frac{\delta p}{p_0} \sim \frac{u_\perp}{c_\mathrm{s}} \sim \frac{u_\parallel}{c_\mathrm{s}} \sim \frac{\delta B_\perp}{B_0} \sim \frac{\delta B_\parallel}{B_0} \sim \frac{k_\parallel}{k_\perp} \doteq \epsilon \ll 1, \tag{IX.0.48}$$

where the sound speed $c_\mathrm{s} \doteq (\gamma p_0/\varrho_0)^{1/2}$ is of order the Alfvén speed $v_\mathrm{A} \doteq B_0/(4\pi\varrho_0)^{1/2}$. In other words, the plasma beta parameter

$$\beta \doteq \frac{8\pi p_0}{B_0^2} = \frac{2}{\gamma}\frac{c_\mathrm{s}^2}{v_\mathrm{A}^2} \tag{IX.0.49}$$

is taken to be of order unity; subsidiary limits in high and low β may be taken after the ϵ expansion is performed. The fluctuations are therefore sub-sonic, sub-Alfvénic, and spatially anisotropic with respect to the magnetic-field direction, with a characteristic length scale parallel to the field ($\sim k_\parallel^{-1}$) that is much larger than across the field ($\sim k_\perp^{-1}$). The characteristic frequency of the fluctuations $\omega \sim k_\parallel v_\mathrm{A}$, so that $\omega \sim \epsilon k_\perp v_\mathrm{A}$; as a result of this ordering, fast magnetosonic modes are ordered out of the equations. The ordering (IX.0.49) is applied to each of the ideal MHD equations and the result examined order by order in ϵ. Before doing so, note that the Lagrangian derivative

$$\frac{\mathrm{D}}{\mathrm{D}t} = \underbrace{\frac{\partial}{\partial t}}_{\sim\omega} + \underbrace{u_\parallel\nabla_\parallel}_{\sim\epsilon\omega} + \underbrace{\boldsymbol{u}_\perp\cdot\boldsymbol{\nabla}_\perp}_{\sim\omega} = \frac{\partial}{\partial t} + \boldsymbol{u}_\perp\cdot\boldsymbol{\nabla}_\perp + \mathcal{O}(\epsilon\omega),$$

so that fluctuations are nonlinearly advected to leading order by the $\boldsymbol{E}\times\boldsymbol{B}$ flow. This is important, as it indicates that, while the fluctuations are assumed small, they are *not* infinitesimally small. Let us proceed.

First, the continuity equation (V.2.2*a*):

$$\underbrace{\frac{\mathrm{D}}{\mathrm{D}t}\frac{\delta\varrho}{\varrho_0}}_{①} = \underbrace{-\nabla_\parallel u_\parallel}_{①} \underbrace{-\boldsymbol{\nabla}_\perp\cdot\boldsymbol{u}_\perp}_{⓪},$$

where the order in ϵ at which each term enters relative to ω is indicated. To leading order, we have

$$\boxed{\boldsymbol{\nabla}_\perp\cdot\boldsymbol{u}_\perp = 0} \tag{IX.0.50}$$

i.e., the perpendicular dynamics is incompressible. This implies that $\boldsymbol{u}_\perp$ can be written in terms of a stream function:

$$\boldsymbol{u}_\perp = \hat{\boldsymbol{z}}\times\boldsymbol{\nabla}_\perp\Phi. \tag{IX.0.51}$$

Likewise, the solenoidality constraint on the magnetic field allows us to write $\delta\boldsymbol{B}_\perp$ in terms of a flux function:

$$\frac{\delta\boldsymbol{B}_\perp}{\sqrt{4\pi\varrho_0}} = \hat{\boldsymbol{z}}\times\boldsymbol{\nabla}_\perp\Psi. \tag{IX.0.52}$$

Thus, the Alfvénic fluctuations can be described in terms of two scalar functions, Φ and Ψ. (The compressive fluctuations involve the higher-order terms in (V.2.2*a*), and are discussed below.)

The evolution equations for Φ and Ψ are obtained by applying the RMHD ordering (IX.0.49) to the induction equation (V.2.2*d*):

$$\underbrace{\frac{\mathrm{D}}{\mathrm{D}t}\frac{\delta\boldsymbol{B}}{B_0}}_{①} = \underbrace{\frac{\partial\boldsymbol{u}}{\partial z}}_{①} + \underbrace{\left(\frac{\delta\boldsymbol{B}_\perp}{B_0}\cdot\boldsymbol{\nabla}_\perp\right)\boldsymbol{u}}_{①} + \underbrace{\left(\frac{\delta B_\parallel}{B_0}\nabla_\parallel\right)\boldsymbol{u}}_{②} - \underbrace{\hat{\boldsymbol{z}}(\boldsymbol{\nabla}\cdot\boldsymbol{u})}_{①} - \underbrace{\frac{\delta\boldsymbol{B}}{B_0}(\boldsymbol{\nabla}\cdot\boldsymbol{u})}_{②}.$$

To leading order, the perpendicular magnetic-field fluctuations satisfy

$$\frac{\mathrm{D}}{\mathrm{D}t}\frac{\delta\boldsymbol{B}_\perp}{B_0} = \left(\frac{\partial}{\partial z} + \frac{\delta\boldsymbol{B}_\perp}{B_0}\cdot\boldsymbol{\nabla}_\perp\right)\boldsymbol{u}_\perp. \tag{IX.0.53}$$

The term in parentheses in (IX.0.53) is just $\hat{\boldsymbol{b}}\cdot\boldsymbol{\nabla}$ written out to $\mathcal{O}(\epsilon k_\perp)$, and so field-parallel gradients in the perpendicular flow drive (Lagrangian) changes in the perpendicular magnetic-field fluctuations. Using the expressions (IX.0.51) and (IX.0.52) for $\boldsymbol{u}_\perp$ and $\delta\boldsymbol{B}_\perp$, respectively, equation (IX.0.53) implies

$$\boxed{\frac{\partial\Psi}{\partial t} + \{\Phi,\Psi\} = v_\mathrm{A}\frac{\partial\Phi}{\partial z}} \tag{IX.0.54}$$

where the Poisson bracket

$$\{\Phi,\Psi\} \doteq \hat{\boldsymbol{z}}\cdot(\boldsymbol{\nabla}_\perp\Phi\times\boldsymbol{\nabla}_\perp\Psi) = \frac{\partial\Phi}{\partial x}\frac{\partial\Psi}{\partial y} - \frac{\partial\Phi}{\partial y}\frac{\partial\Psi}{\partial x}. \tag{IX.0.55}$$

The evolution equation for Φ is obtained from the perpendicular component of the momentum equation (V.2.2*b*):

$$\underbrace{\frac{\mathrm{D}\boldsymbol{u}_\perp}{\mathrm{D}t}}_{①} + \underbrace{(u_\parallel\nabla_\parallel)\boldsymbol{u}_\perp}_{②} + \underbrace{\frac{\delta\varrho}{\varrho_0}\frac{\mathrm{D}\boldsymbol{u}_\perp}{\mathrm{D}t}}_{②} + \underbrace{\frac{\delta\varrho}{\varrho_0}(u_\parallel\nabla_\parallel)\boldsymbol{u}_\perp}_{③} = \underbrace{-\boldsymbol{\nabla}_\perp\left(c_\mathrm{s}^2\frac{\delta p}{\gamma p_0} + v_\mathrm{A}^2\frac{\delta B_\parallel}{B_0}\right)}_{⓪}$$
$$\underbrace{- v_\mathrm{A}^2\boldsymbol{\nabla}_\perp\frac{|\delta\boldsymbol{B}|^2}{2B_0^2}}_{①} + \underbrace{v_\mathrm{A}^2\frac{\partial}{\partial z}\frac{\delta\boldsymbol{B}_\perp}{B_0}}_{①} + \underbrace{v_\mathrm{A}^2\left(\frac{\delta\boldsymbol{B}_\perp}{B_0}\cdot\boldsymbol{\nabla}_\perp\right)\frac{\delta\boldsymbol{B}_\perp}{B_0}}_{①} + \underbrace{v_\mathrm{A}^2\left(\frac{\delta B_\parallel}{B_0}\nabla_\parallel\right)\frac{\delta\boldsymbol{B}_\perp}{B_0}}_{②}, \tag{IX.0.56}$$

where the order in ϵ at which each term enters relative to ωc_s is indicated. At $\mathcal{O}(1)$, we have perpendicular pressure balance:

$$-\boldsymbol{\nabla}_\perp\left(c_\mathrm{s}^2\frac{\delta p}{\gamma p_0} + v_\mathrm{A}^2\frac{\delta B_\parallel}{B_0}\right) = 0 \quad\Longrightarrow\quad \frac{\delta p}{p_0} = -\frac{2}{\beta}\frac{\delta B_\parallel}{B_0} = -\gamma\frac{v_\mathrm{A}^2}{c_\mathrm{s}^2}\frac{\delta B_\parallel}{B_0}. \tag{IX.0.57}$$

At $\mathcal{O}(\epsilon)$,

$$\frac{\mathrm{D}\boldsymbol{u}_\perp}{\mathrm{D}t} = -\boldsymbol{\nabla}_\perp\left(c_\mathrm{s}^2\frac{\delta p_2}{\gamma p_0} + v_\mathrm{A}^2\frac{|\delta\boldsymbol{B}|^2}{2B_0^2}\right) + v_\mathrm{A}^2\frac{\partial}{\partial z}\frac{\delta\boldsymbol{B}_\perp}{B_0} + v_\mathrm{A}^2\left(\frac{\delta\boldsymbol{B}_\perp}{B_0}\cdot\boldsymbol{\nabla}_\perp\right)\frac{\delta\boldsymbol{B}_\perp}{B_0}, \tag{IX.0.58}$$

where δp_2 is the second-order pressure fluctuation. Fortunately, δp_2 need not be determined, since its only role is to enforce incompressibility, equation (IX.0.50). Indeed, taking the curl of (IX.0.58) eliminates the entire pressure term, leaving

$$\boldsymbol{\nabla}_\perp\times\left[\frac{\mathrm{D}\boldsymbol{u}_\perp}{\mathrm{D}t} = v_\mathrm{A}^2\frac{\partial}{\partial z}\frac{\delta\boldsymbol{B}_\perp}{B_0} + v_\mathrm{A}^2\left(\frac{\delta\boldsymbol{B}_\perp}{B_0}\cdot\boldsymbol{\nabla}_\perp\right)\frac{\delta\boldsymbol{B}_\perp}{B_0}\right] \tag{IX.0.59}$$

Noting that

$$\begin{aligned}
\boldsymbol{\nabla}_\perp \times (\hat{\boldsymbol{z}} \times \boldsymbol{\nabla}_\perp \Phi) &= \hat{\boldsymbol{z}}\, \nabla_\perp^2 \Phi, \\
\boldsymbol{\nabla}_\perp \times (\hat{\boldsymbol{z}} \times \boldsymbol{\nabla}_\perp \Psi) &= \hat{\boldsymbol{z}}\, \nabla_\perp^2 \Psi, \\
\boldsymbol{\nabla}_\perp \times \big[(\hat{\boldsymbol{z}} \times \boldsymbol{\nabla}_\perp \Phi) \cdot \boldsymbol{\nabla}_\perp (\hat{\boldsymbol{z}} \times \boldsymbol{\nabla}_\perp \Phi)\big] &= \hat{\boldsymbol{z}}\, \hat{\boldsymbol{z}} \cdot (\boldsymbol{\nabla}_\perp \Phi \times \boldsymbol{\nabla}_\perp \nabla_\perp^2 \Phi), \\
\boldsymbol{\nabla}_\perp \times \big[(\hat{\boldsymbol{z}} \times \boldsymbol{\nabla}_\perp \Psi) \cdot \boldsymbol{\nabla}_\perp (\hat{\boldsymbol{z}} \times \boldsymbol{\nabla}_\perp \Psi)\big] &= \hat{\boldsymbol{z}}\, \hat{\boldsymbol{z}} \cdot (\boldsymbol{\nabla}_\perp \Psi \times \boldsymbol{\nabla}_\perp \nabla_\perp^2 \Psi),
\end{aligned}$$

the $\hat{\boldsymbol{z}}$ component of (IX.0.59) may be written as

$$\boxed{\frac{\partial}{\partial t} \nabla_\perp^2 \Phi + \{\Phi, \nabla_\perp^2 \Phi\} = v_\mathrm{A} \frac{\partial}{\partial z} \nabla_\perp^2 \Psi + \{\Psi, \nabla_\perp^2 \Psi\}} \tag{IX.0.60}$$

This is essentially an equation for the flow vorticity.

Equations (IX.0.54) and (IX.0.60) form a closed set of equations for the Alfvénic fluctuations:

$$\frac{\mathrm{D}\Psi}{\mathrm{D}t} = v_\mathrm{A} \frac{\partial \Phi}{\partial z}, \tag{IX.0.61a}$$

$$\frac{\mathrm{D}}{\mathrm{D}t} \nabla_\perp^2 \Phi = v_\mathrm{A} \hat{\boldsymbol{b}} \cdot \boldsymbol{\nabla} \nabla_\perp^2 \Psi, \tag{IX.0.61b}$$

where

$$\frac{\mathrm{D}}{\mathrm{D}t} = \frac{\partial}{\partial t} + \{\Phi, \dots\} \quad \text{and} \quad \hat{\boldsymbol{b}} \cdot \boldsymbol{\nabla} = \frac{\partial}{\partial z} + \frac{1}{v_\mathrm{A}} \{\Psi, \dots\}. \tag{IX.0.62}$$

Note that the compressive fluctuations make no appearance in the equations for the Alfvénic fluctuations, and so the former exert no influence on the latter.

Finally, there is an advantageous combination of (IX.0.61) that makes clear the foundation of theories of Alfvén-wave turbulence. Define the Elsässer potentials

$$\zeta^\pm \doteq \Phi \pm \Psi. \tag{IX.0.63}$$

Then $\Phi = (\zeta^+ + \zeta^-)/2$ and $\Psi = (\zeta^+ - \zeta^-)/2$, and so (IX.0.61) may be written as

$$\frac{\partial}{\partial t} \left(\frac{\zeta^+ - \zeta^-}{2} \right) + \left\{ \frac{\zeta^+ + \zeta^-}{2}, \frac{\zeta^+ - \zeta^-}{2} \right\} = v_\mathrm{A} \frac{\partial}{\partial z} \left(\frac{\zeta^+ + \zeta^-}{2} \right) \tag{IX.0.64a}$$

$$\begin{aligned}
\frac{\partial}{\partial t} \nabla_\perp^2 \left(\frac{\zeta^+ + \zeta^-}{2} \right) + \left\{ \frac{\zeta^+ + \zeta^-}{2}, \nabla_\perp^2 \frac{\zeta^+ + \zeta^-}{2} \right\} &= v_\mathrm{A} \frac{\partial}{\partial z} \nabla_\perp^2 \left(\frac{\zeta^+ - \zeta^-}{2} \right) \\
&\quad + \left\{ \frac{\zeta^+ - \zeta^-}{2}, \nabla_\perp^2 \frac{\zeta^+ - \zeta^-}{2} \right\}.
\end{aligned} \tag{IX.0.64b}$$

Noting that $\{\zeta^\pm, \zeta^\pm\} = 0$ and taking $\nabla_\perp^2$ of (IX.0.64a), these become

$$\begin{aligned}
\frac{\partial}{\partial t} \nabla_\perp^2 (\zeta^+ - \zeta^-) + \frac{1}{2} \nabla_\perp^2 \Big(\{\zeta^-, \zeta^+\} - \{\zeta^+, \zeta^-\} \Big) &= v_\mathrm{A} \frac{\partial}{\partial z} \nabla_\perp^2 (\zeta^+ + \zeta^-), \\
\frac{\partial}{\partial t} \nabla_\perp^2 (\zeta^+ + \zeta^-) + \frac{1}{2} \Big(\{\zeta^+, \nabla_\perp^2 \zeta^-\} + \{\zeta^-, \nabla_\perp^2 \zeta^+\} \Big) &= v_\mathrm{A} \frac{\partial}{\partial z} \nabla_\perp^2 (\zeta^+ - \zeta^-) \\
&\quad - \frac{1}{2} \Big(\{\zeta^+, \nabla_\perp^2 \zeta^-\} + \{\zeta^-, \nabla_\perp^2 \zeta^+\} \Big),
\end{aligned}$$

which may be added to and subtracted from one another to obtain

$$\boxed{\frac{\partial}{\partial t} \nabla_\perp^2 \zeta^\pm \mp v_\mathrm{A} \frac{\partial}{\partial z} \nabla_\perp^2 \zeta^\pm = -\frac{1}{2} \Big(\{\zeta^+, \nabla_\perp^2 \zeta^-\} + \{\zeta^-, \nabla_\perp^2 \zeta^+\} \mp \nabla_\perp^2 \{\zeta^+, \zeta^-\} \Big)} \tag{IX.0.65}$$

The left-hand side of this equation captures the propagation of linear Alvén waves: $\zeta^{\pm} = f^{\pm}(x, y, z \mp v_{\mathrm{A}} t)$. What is notable is that these solutions are also exact *nonlinear* solutions if either $\zeta^{-} = 0$ or $\zeta^{+} = 0$, since the nonlinearities on the right-hand side of (IX.0.65) then vanish. In fact, in this case the fluctuation (or, indeed, wave packet) may be of arbitrary shape and magnitude, simply propagating along the mean magnetic field at the Alfvén speed. The key here is that only *counterpropagating* fluctuations can interact (Kraichnan 1965). They do so by scattering off each other without exchanging energy; indeed, it is easy to show by multiplying (IX.0.65) by $\varrho_0 \zeta^{\pm}$ and integrating by parts that the nonlinear Alfvén-wave energy

$$W^{\pm}_{\mathrm{AW}} \doteq \frac{1}{2} \int \mathrm{d}^3 \boldsymbol{r}\, \varrho_0 |\boldsymbol{\nabla}_{\perp} \zeta^{\pm}|^2 \tag{IX.0.66}$$

is conserved. This conservation law plays an important role in theories of Alfvén-wave turbulence, particularly the fact that, whatever the compressive fluctuations are doing, they are doing it independently of the Alfvén-wave cascade.

Now, the evolution equations for the compressive fluctuations will be derived and analyzed by you in a problem set. But let me state them here without proof:

$$\frac{\mathrm{D}}{\mathrm{D}t} \frac{\delta s}{s_0} = 0, \tag{IX.0.67}$$

$$\frac{\mathrm{D}}{\mathrm{D}t} \frac{\delta \varrho}{\varrho_0} = -\frac{1}{1 + c_{\mathrm{s}}^2 / v_{\mathrm{A}}^2} \hat{\boldsymbol{b}} \cdot \boldsymbol{\nabla} u_{\parallel}, \tag{IX.0.68}$$

$$\frac{\mathrm{D}}{\mathrm{D}t} \frac{\delta B_{\parallel}}{B_0} = \frac{1}{1 + v_{\mathrm{A}}^2 / c_{\mathrm{s}}^2} \hat{\boldsymbol{b}} \cdot \boldsymbol{\nabla} u_{\parallel}, \tag{IX.0.69}$$

$$\frac{\mathrm{D}}{\mathrm{D}t} u_{\parallel} = v_{\mathrm{A}}^2 \hat{\boldsymbol{b}} \cdot \boldsymbol{\nabla} \frac{\delta B_{\parallel}}{B_0}, \tag{IX.0.70}$$

where $s \doteq \ln p \varrho^{-\gamma}$ is the specific entropy. Equations (IX.0.68)–(IX.0.70) describe the slow-wave-polarized fluctuations, for which perpendicular pressure balance (equation (IX.0.57)) holds. Equation (IX.0.67) describes the zero-frequency entropy mode. Note that the only nonlinearities in these equations are via the derivatives defined in (IX.0.62). Questions: What does the imply about the relationship between the compressive fluctuations and the Alfvénic ones? Also, recall that MHD supports fast magnetosonic waves – where are they in RMHD?

More to follow in a problem set...

PART X
Non-ideal MHD

X.1. What is $\boldsymbol{u}$ in a poorly ionized plasma?

Let us revisit the ideal-MHD induction equation, repeated here for convenience:

$$\frac{\partial \boldsymbol{B}}{\partial t} = \boldsymbol{\nabla} \times (\boldsymbol{u} \times \boldsymbol{B}). \tag{X.1.1}$$

What is $\boldsymbol{u}$? Is it the ion velocity $\boldsymbol{u}_{\mathrm{i}}$? the electron velocity $\boldsymbol{u}_{\mathrm{e}}$? both? But if $\boldsymbol{u}_{\mathrm{i}} = \boldsymbol{u}_{\mathrm{e}}$, then where are the currents? You may be remembering that $\boldsymbol{u}$ is the $\boldsymbol{E} \times \boldsymbol{B}$ velocity. Fine, but all charged species drift with the same $\boldsymbol{E} \times \boldsymbol{B}$ velocity, so, again, where are the currents? Or, rather, is $\boldsymbol{u}$ the same center-of-mass velocity $\sum_\alpha m_\alpha n_\alpha \boldsymbol{u}_\alpha / \sum_\alpha m_\alpha n_\alpha$ that appears in the momentum equation? But if the plasma is primarily composed of neutrals

with, say, number density $n_\mathrm{n} \sim 10^7\, n_\mathrm{i}$, then the center-of-mass velocity is dominated by the velocity of the neutral fluid $\boldsymbol{u}_\mathrm{n}$. So the velocity in the induction equation is the neutral-fluid velocity? That's weird. Why would magnetic flux be frozen into a neutral fluid that doesn't conduct electricity?

In ideal MHD, all of these velocities are basically equivalent, because the interspecies drifts are small. For example, in a quasi-neutral ion–electron plasma,

$$\boldsymbol{u}_\mathrm{i} - \boldsymbol{u}_\mathrm{e} = \frac{\boldsymbol{j}}{e n_\mathrm{i}} = \frac{c\boldsymbol{\nabla}\times\boldsymbol{B}}{4\pi e n_\mathrm{i}} \quad\Longrightarrow\quad \left|\frac{u_\mathrm{i}-u_\mathrm{e}}{v_\mathrm{A}}\right| \sim \frac{d_\mathrm{i}}{\ell_B} \lll 1.$$

If there are charge-neutral particles around, then collisions keep them co-moving with the charged species. Let's go back to basics...

Consider a collisional plasma with neutrals, ions, and electrons. The momentum equations for these species are, respectively,

$$m_\mathrm{n} n_\mathrm{n} \frac{\mathrm{D}\boldsymbol{u}_\mathrm{n}}{\mathrm{D}t_\mathrm{n}} = -\boldsymbol{\nabla} p_\mathrm{n} + \boldsymbol{R}_\mathrm{ni} + \boldsymbol{R}_\mathrm{ne}, \tag{X.1.2}$$

$$m_\mathrm{i} n_\mathrm{i} \frac{\mathrm{D}\boldsymbol{u}_\mathrm{i}}{\mathrm{D}t_\mathrm{i}} = -\boldsymbol{\nabla} p_\mathrm{i} + \boldsymbol{R}_\mathrm{in} + \boldsymbol{R}_\mathrm{ie} + q_\mathrm{i} n_\mathrm{i}\left(\boldsymbol{E} + \frac{\boldsymbol{u}_\mathrm{i}}{c}\times\boldsymbol{B}\right), \tag{X.1.3}$$

$$m_\mathrm{e} n_\mathrm{e} \frac{\mathrm{D}\boldsymbol{u}_\mathrm{e}}{\mathrm{D}t_\mathrm{e}} = -\boldsymbol{\nabla} p_\mathrm{e} + \boldsymbol{R}_\mathrm{en} + \boldsymbol{R}_\mathrm{ei} - e n_\mathrm{e}\left(\boldsymbol{E} + \frac{\boldsymbol{u}_\mathrm{e}}{c}\times\boldsymbol{B}\right), \tag{X.1.4}$$

where $\mathrm{D}/\mathrm{D}t_\alpha \doteq \partial/\partial t_\alpha + \boldsymbol{u}_\alpha\cdot\boldsymbol{\nabla}$ is the Lagrangian time derivative in the frame of species α. The electric field here is what ensures $q_\mathrm{i} n_\mathrm{i} - e n_\mathrm{e} = 0$. Indeed, add (X.1.3) and (X.1.4):

$$\begin{aligned} m_\mathrm{i} n_\mathrm{i} \frac{\mathrm{D}\boldsymbol{u}_\mathrm{i}}{\mathrm{D}t_\mathrm{i}} + m_\mathrm{e} n_\mathrm{e} \frac{\mathrm{D}\boldsymbol{u}_\mathrm{e}}{\mathrm{D}t_\mathrm{e}} &= -\boldsymbol{\nabla}(p_\mathrm{i}+p_\mathrm{e}) + \boldsymbol{R}_\mathrm{in} + \cancel{\boldsymbol{R}_\mathrm{ie}} + \boldsymbol{R}_\mathrm{en} + \cancel{\boldsymbol{R}_\mathrm{ei}} \\ &\quad + \underbrace{(q_\mathrm{i} n_\mathrm{i} - e n_\mathrm{e})\,\boldsymbol{E}}_{=0 \text{ by quasi-neutrality}} + \frac{1}{c}\underbrace{(q_\mathrm{i} n_\mathrm{i}\boldsymbol{u}_\mathrm{i} - e n_\mathrm{e}\boldsymbol{u}_\mathrm{e})}_{=\boldsymbol{j} \text{ by def'n}}\times\boldsymbol{B} \end{aligned} \tag{X.1.5}$$

Now add (X.1.2) and (X.1.5):

$$\begin{aligned} m_\mathrm{n} n_\mathrm{n} \frac{\mathrm{D}\boldsymbol{u}_\mathrm{n}}{\mathrm{D}t_\mathrm{n}} + m_\mathrm{i} n_\mathrm{i} \frac{\mathrm{D}\boldsymbol{u}_\mathrm{i}}{\mathrm{D}t_\mathrm{i}} + m_\mathrm{e} n_\mathrm{e} \frac{\mathrm{D}\boldsymbol{u}_\mathrm{e}}{\mathrm{D}t_\mathrm{e}} &= -\boldsymbol{\nabla}(p_\mathrm{n}+p_\mathrm{i}+p_\mathrm{e}) \\ &\quad + \cancel{\boldsymbol{R}_\mathrm{ni}} + \cancel{\boldsymbol{R}_\mathrm{ne}} + \cancel{\boldsymbol{R}_\mathrm{in}} + \cancel{\boldsymbol{R}_\mathrm{en}} + \frac{\boldsymbol{j}}{c}\times\boldsymbol{B}. \end{aligned} \tag{X.1.6}$$

All the friction forces cancel by Newton's third law. Recalling (III.10.12)–(III.10.15), the left-hand side of (X.1.6) may be written as

$$\varrho\frac{\mathrm{D}\boldsymbol{u}}{\mathrm{D}t} + \boldsymbol{\nabla}\cdot\left(\sum_\alpha m_\alpha n_\alpha \Delta\boldsymbol{u}_\alpha \Delta\boldsymbol{u}_\alpha\right),$$

where $\Delta\boldsymbol{u}_\alpha \doteq \boldsymbol{u}_\alpha - \boldsymbol{u}$ are the species drifts relative to the center-of-mass velocity $\boldsymbol{u}$. Further using Ampère's law to write

$$\frac{\boldsymbol{j}}{c}\times\boldsymbol{B} = \boldsymbol{\nabla}\cdot\left(\frac{\boldsymbol{B}\boldsymbol{B}}{4\pi} - \boldsymbol{I}\frac{B^2}{8\pi}\right). \tag{X.1.7}$$

equation (X.1.6) becomes

$$\varrho\frac{\mathrm{D}\boldsymbol{u}}{\mathrm{D}t} = -\boldsymbol{\nabla}\cdot\left[\boldsymbol{I}\left(\sum_\alpha p_\alpha + \frac{B^2}{8\pi}\right) + \sum_\alpha m_\alpha n_\alpha \Delta\boldsymbol{u}_\alpha\Delta\boldsymbol{u}_\alpha - \frac{\boldsymbol{B}\boldsymbol{B}}{4\pi}\right]. \tag{X.1.8}$$

So, collisions between neutrals and charged species is what makes the neutrals see the Lorentz force. By virtue of their large mass and the low degree of ionization in many system, $\boldsymbol{u} \simeq \boldsymbol{u}_\mathrm{n}$, and so it *looks* like the neutrals are magnetized. Not true. They just need to collide often enough with the magnetized particles.

With that borne in mind, let us again return to the induction equation (X.1.1):

$$\frac{\partial \boldsymbol{B}}{\partial t} = \boldsymbol{\nabla} \times (\boldsymbol{u} \times \boldsymbol{B}).$$

Now, that $\boldsymbol{u}$ *cannot* be the neutral velocity; it would make no sense for the magnetic flux to be frozen into a neutral fluid! Let us instead write

$$\frac{\partial \boldsymbol{B}}{\partial t} = \boldsymbol{\nabla} \times (\boldsymbol{u}_\mathrm{f} \times \boldsymbol{B}), \tag{X.1.9}$$

where $\boldsymbol{u}_\mathrm{f}$ is the velocity of the field lines. This must be true: field lines are frozen into themselves (i.e., there exists a frame where the electric field vanishes). Now add zero:

$$\frac{\partial \boldsymbol{B}}{\partial t} = \boldsymbol{\nabla} \times \Bigg[\underbrace{(\boldsymbol{u}_\mathrm{f} - \boldsymbol{u}_\mathrm{e}) \times \boldsymbol{B}}_{\substack{\text{electron-}\boldsymbol{B}\\ \text{drift}\\ \text{(O)}}} + \underbrace{(\boldsymbol{u}_\mathrm{e} - \boldsymbol{u}_\mathrm{i}) \times \boldsymbol{B}}_{\substack{\text{ion-electron}\\ \text{drift}\\ \text{(H)}}} + \underbrace{(\boldsymbol{u}_\mathrm{i} - \boldsymbol{u}_\mathrm{n}) \times \boldsymbol{B}}_{\substack{\text{ion-neutral}\\ \text{drift}\\ \text{(A)}}} + \underbrace{\boldsymbol{u}_\mathrm{n} \times \boldsymbol{B}}_{\substack{\text{advection}\\ \text{by neutrals}\\ \text{(I)}}} \Bigg]. \tag{X.1.10}$$

(If that derivation of a generalized induction equation was wholly unsatisfactory for you, read §X.5 before proceeding to §X.2.)

The terms in (X.1.10) labelled (O) (Ohmic), (H) (Hall), and (A) (ambipolar) are formally zero in ideal MHD. Let us estimate their relative sizes:

$$\frac{\text{(O)}}{\text{(I)}} \sim \frac{1}{\mathrm{Rm}} \doteq \frac{\eta}{v_\mathrm{A} \ell_B} \sim \underbrace{\left(\frac{d_\mathrm{e}}{\ell_B}\right)}_{\text{small}} \underbrace{\left(\frac{d_\mathrm{e}}{v_\mathrm{A} \tau_\mathrm{en}}\right)}_{\substack{\text{could be}\\ \text{large}}} \tag{X.1.11}$$

$$\frac{\text{(H)}}{\text{(I)}} \sim \left|\frac{\boldsymbol{j}/e n_\mathrm{e}}{\boldsymbol{u}_\mathrm{n}}\right| \sim \underbrace{\left(\frac{d_\mathrm{i}}{\ell_B}\right)}_{\text{small}} \underbrace{\left(\frac{\varrho}{\varrho_\mathrm{i}}\right)^{1/2}}_{\substack{\sim 1\text{, but}\\ \text{could be}\\ \text{large}}} \underbrace{\left|\frac{v_\mathrm{A}}{u_\mathrm{n}}\right|}_{\sim 1} \tag{X.1.12}$$

$$\frac{\text{(A)}}{\text{(I)}} \sim \left|\frac{\boldsymbol{R}_\mathrm{ni} \tau_\mathrm{ni}}{\varrho_\mathrm{n} \boldsymbol{u}_\mathrm{n}}\right| \sim \left|\frac{\boldsymbol{j} \times \boldsymbol{B}}{c}\right| \frac{\tau_\mathrm{ni}}{\varrho_\mathrm{n} v_\mathrm{A}} \left|\frac{v_\mathrm{A}}{u_\mathrm{n}}\right| \sim \underbrace{\frac{v_\mathrm{A} \tau_\mathrm{ni}}{\ell_B}}_{\substack{\text{could be}\\ \sim 1}} \underbrace{\left(\frac{\varrho}{\varrho_\mathrm{n}}\right)^{1/2}}_{\gtrsim 1} \underbrace{\left|\frac{v_\mathrm{A}}{u_\mathrm{n}}\right|}_{\sim 1} \tag{X.1.13}$$

Note that (H)/(I) is the only ratio not involving collisions… we'll come back to this.

The next three sections focus on the above non-ideal effects in reverse order: ambipolar diffusion (§X.2), the Hall effect (§X.3), and Ohmic dissipation (§X.4). While Ohmic dissipation is certainly the easiest to handle of the three – not only because it's probably most familiar to you, but also because it acts isotropically – we'll postpone its discussion until after ambipolar diffusion and the Hall effect are elucidated. The reason is that a discussion of Ohmic dissipation will lead naturally into the topic of Part XI, magnetic reconnection.

In each of the sections below, astrophysical examples are provided for when each of these non-ideal MHD effects are important. But there is one particular system where all three non-ideal effects – ambipolar diffusion, the Hall effect, and Ohmic dissipation – are important: a protoplanetary disk. This is because the wide variety of ionization sources, temperatures, and densities give a wide variety of ionization fractions, collision rates, and Alfvén speeds:

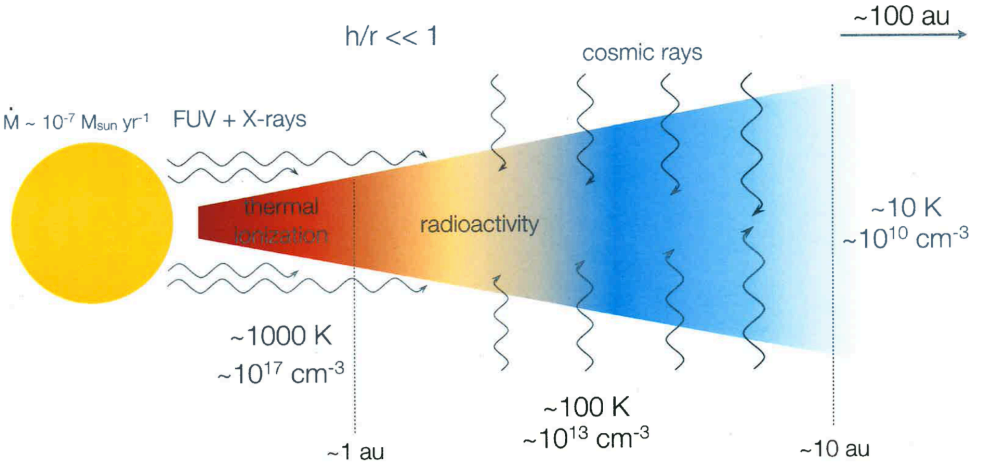

Using the estimates (X.1.11)–(X.1.13) with $v_A/c_s = 0.1$ in a model of the minimum-mass solar nebula (MMSN; Hayashi 1981) leads to the following figure, adapted from Kunz & Balbus (2004), which delineates the regimes in which different non-ideal effects dominate:

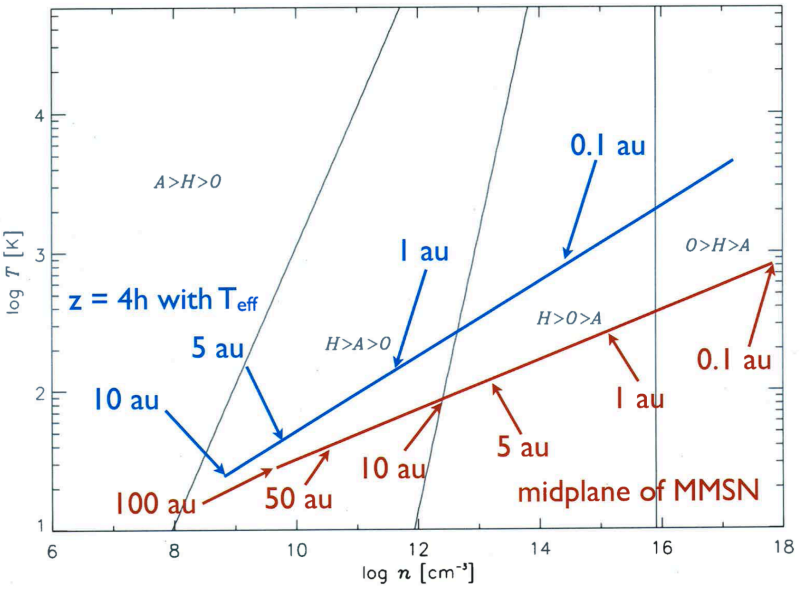

I show this particular plot not because it's the most accurate (it's not) or because it's mine (okay, maybe because it's mine), but because it demonstrates in a very simple way that – even without the myriad complications introduced by the consideration of dust grains, their size spectrum, and their spatial distribution – each non-ideal effect gets their

chance to affect the disk dynamics.[16] For more on this topic of "layered accretion", see Gammie (1996), Fromang *et al.* (2002), Wardle (2007), and Armitage (2011).

X.2. Ambipolar diffusion

X.2.1. *Astrophysical context and basic theory*

Imagine a poorly ionized gas of neutrals, ions, and electrons. Let us assume $\boldsymbol{u}_\mathrm{i} \simeq \boldsymbol{u}_\mathrm{e}$ (i.e., $d_\mathrm{i}/\ell_B \ll (\varrho_\mathrm{i}/\varrho)^{1/2}$) and negligible Ohmic dissipation on the scales of interest. To give some physical context for an astrophysical situation where these are fairly good assumptions, consider the cold ($T \sim 10$ K) plasma out of which stars form. Such gas is comprised primarily of neutral molecular hydrogen $\mathrm{H_2}$ ($n_{\mathrm{H_2}} \gtrsim 10^3$ cm^{-3}) with 20% He by number, along with trace ($\lesssim 10^{-7}$) amounts of electrons, molecular ions (primarily $\mathrm{HCO^+}$), and atomic ions (primarily $\mathrm{Na^+}$, $\mathrm{Mg^+}$, $\mathrm{K^+}$). There are also neutral, negatively charged, and positively charged dust grains, conglomerates of silicate and carbonaceous materials that are between a few molecules to 0.1 μm in size. While dust grains are of critical importance to interstellar chemistry, thermodynamics, and magnetic diffusion, we will ignore them for now.[17] (Sorry Bruce.) Molecular clouds are poorly ionized because their densities are large enough to screen the most potent sources of ionization (e.g., UV radiation) and their temperatures are low enough to render thermal ionization completely negligible. This leaves only infrequent cosmic rays of energy $\gtrsim$100 MeV (and extremely weak radioactive nuclides like ^{26}Al and ^{40}K) to ionize the plasma. So sad.

In molecular clouds, interspecies collisions are strong enough that $T_\mathrm{n} = T_\mathrm{i} = T_\mathrm{e}$. The friction forces are primarily due to elastic collisions and are accurately modeled by

$$\boldsymbol{R}_\mathrm{in} = \frac{m_\mathrm{n} n_\mathrm{n}}{\tau_\mathrm{ni}}(\boldsymbol{u}_\mathrm{n} - \boldsymbol{u}_\mathrm{i}) \quad \text{with} \quad \tau_\mathrm{ni} = \frac{m_\mathrm{n} n_\mathrm{n}}{m_\mathrm{i} n_\mathrm{i}}\,\tau_\mathrm{in} = 1.23\,\frac{m_\mathrm{i} + m_{\mathrm{H_2}}}{m_\mathrm{i} n_\mathrm{i} \langle \sigma w \rangle_{\mathrm{iH_2}}}, \tag{X.2.1}$$

$$\boldsymbol{R}_\mathrm{en} = \frac{m_\mathrm{n} n_\mathrm{n}}{\tau_\mathrm{ne}}(\boldsymbol{u}_\mathrm{n} - \boldsymbol{u}_\mathrm{e}) \quad \text{with} \quad \tau_\mathrm{ne} = \frac{m_\mathrm{n} n_\mathrm{n}}{m_\mathrm{e} n_\mathrm{e}}\,\tau_\mathrm{en} = 1.21\,\frac{m_\mathrm{e} + m_{\mathrm{H_2}}}{m_\mathrm{e} n_\mathrm{e} \langle \sigma w \rangle_{\mathrm{eH_2}}}, \tag{X.2.2}$$

$$\boldsymbol{R}_\mathrm{ie} = \frac{m_\mathrm{e} n_\mathrm{e}}{\tau_\mathrm{ei}}(\boldsymbol{u}_\mathrm{e} - \boldsymbol{u}_\mathrm{i}) \quad \text{with} \quad \tau_\mathrm{ei} = \frac{3\sqrt{m_\mathrm{e}}(k_\mathrm{B} T_\mathrm{e})^{3/2}}{4\sqrt{2\pi} q_\mathrm{i}^2 e^2 n_\mathrm{i} \ln \lambda_\mathrm{ei}}, \tag{X.2.3}$$

where $\langle \sigma w \rangle_{\alpha \mathrm{H_2}}$ is the mean collisional rate between species α and hydrogen molecules of mass $m_{\mathrm{H_2}}$; the pre-factors of 1.23 and 1.21 account for the presence of He lengthening the slowing-down time relative to the value it would have if only α-$\mathrm{H_2}$ collisions were considered. The mass ratios worth knowing in this context are $m_\mathrm{i}/m_\mathrm{p} = 29$ for $\mathrm{HCO^+}$, $m_\mathrm{i}/m_\mathrm{p} = 23$ for $\mathrm{Na^+}$, $m_\mathrm{i}/m_\mathrm{p} = 24$ for $\mathrm{Mg^+}$, and $m_\mathrm{p}/m_\mathrm{e} = 1836$; the mean mass per particle in molecular clouds is

$$\mu \doteq \frac{\varrho}{n} = 2.33 m_\mathrm{p}. \tag{X.2.4}$$

With $\langle \sigma w \rangle_{\mathrm{iH_2}} = 1.69 \times 10^{-9}$ cm^3 s^{-1} for $\mathrm{HCO^+}$–$\mathrm{H_2}$ collisions (similar values hold for

[16] . . . and they do. For linear stability analyses, see Blaes & Balbus (1994), Wardle (1999), Balbus & Terquem (2001), Kunz & Balbus (2004), Desch (2004), Salmeron & Wardle (2003, 2005, 2008), Kunz (2008), and Wardle & Salmeron (2012). For nonlinear numerical simulations, see Hawley & Stone (1998), Sano & Stone (2002*a*,*b*), Bai & Stone (2011, 2013), Simon *et al.* (2013*a*,*b*), Kunz & Lesur (2013), Lesur *et al.* (2014), Bai (2013, 2014, 2015), Simon *et al.* (2015), Gressel *et al.* (2015), Béthune *et al.* (2016), Bai & Stone (2017), Béthune *et al.* (2017), and Bai (2017).

[17] Interstellar grains comprise about 1% of the mass in the interstellar medium (Spitzer 1978). Baker (1979), Elmegreen (1979), and Nakano & Umebayashi (1980) suggested that charged grains may couple to the magnetic field and thereby play a role in ambipolar diffusion and star formation (see also Ciolek & Mouschovias (1993, 1994)).

Na^+ and Mg^+) and $\langle\sigma w\rangle_{\mathrm{eH_2}} = 1.3\times10^{-9}\,(T/10\ \mathrm{K})^{1/2}\ \mathrm{cm^3\ s^{-1}}$ for e–$\mathrm{H_2}$ collisions, the above collision timescales become

$$\tau_{\mathrm{ni}} = 0.23\left(1+\frac{m_{\mathrm{H_2}}}{m_{\mathrm{i}}}\right)\left(\frac{10^{-7}}{x_{\mathrm{i}}}\right)\left(\frac{10^3\ \mathrm{cm^{-3}}}{n_{\mathrm{n}}}\right)\ \mathrm{Myr}, \tag{X.2.5}$$

$$\tau_{\mathrm{ne}} = 0.29\,\frac{m_{\mathrm{H_2}}}{m_{\mathrm{e}}}\left(\frac{10^{-7}}{x_{\mathrm{e}}}\right)\left(\frac{10^3\ \mathrm{cm^{-3}}}{n_{\mathrm{n}}}\right)\left(\frac{10\ \mathrm{K}}{T}\right)^{1/2}\ \mathrm{Myr}, \tag{X.2.6}$$

$$\tau_{\mathrm{ei}} = 1.2\left(\frac{10^{-7}}{x_{\mathrm{i}}}\right)\left(\frac{10^3\ \mathrm{cm^{-3}}}{n_{\mathrm{n}}}\right)\left(\frac{T}{10\ \mathrm{K}}\right)^{3/2}\ \mathrm{hr}, \tag{X.2.7}$$

where $x_{\mathrm{i}} \doteq n_{\mathrm{i}}/n_{\mathrm{n}}$ is the degree of ionization. Because $m_{\mathrm{H_2}}/m_{\mathrm{e}} \gg 1$, $\boldsymbol{R}_{\mathrm{in}} + \boldsymbol{R}_{\mathrm{en}} \simeq \boldsymbol{R}_{\mathrm{in}}$.

To give the above timescales some context, dynamical timescales in star-forming molecular clouds are $\tau_{\mathrm{dyn}} \sim 0.1$–$10$ Myr. Magnetic-field strengths are $\sim$10–100 μG, giving an ion cyclotron frequency $\sim$0.1 Hz and an Alfvén speed $\sim$1 km $\mathrm{s^{-1}}$. Every astrophysicist should know that 1 km $\mathrm{s^{-1}} \simeq 1$ pc $\mathrm{Myr^{-1}}$, and so an Alfvén wave crosses a typical molecular cloud of size $\sim$10 pc in $\sim$10 Myr and a typical pre-stellar core of size $\sim$0.1 pc in $\sim$0.1 Myr. Sound travels slower at $\simeq$0.2 km $\mathrm{s^{-1}}$, and so the plasma $\beta \sim 0.01$ or so. The gravitational free-fall time is roughly $\tau_{\mathrm{ff}} \sim 1$ Myr at the mean density of a molecular cloud, although support against gravitational collapse provided by magnetic tension renders this timescale almost meaningless (Mestel 1965; Mouschovias 1976*a*,*b*).

Under these conditions, equation (X.1.5) becomes

$$m_{\mathrm{i}} n_{\mathrm{i}} \frac{\mathrm{D}\boldsymbol{u}_{\mathrm{i}}}{\mathrm{D}t_{\mathrm{i}}} = -\boldsymbol{\nabla}(p_{\mathrm{i}} + p_{\mathrm{e}}) + \boldsymbol{R}_{\mathrm{in}} + \frac{\boldsymbol{j}}{c}\times\boldsymbol{B}. \tag{X.2.8}$$

Next we make a number of simplifying assumptions, which are certainly not true in all cases of interest but hold rather well in molecular clouds (again, ignoring grains). The left-hand side of (X.2.8) is typically small, $\sim x_{\mathrm{i}}\varrho v_{\mathrm{A}}/\tau_{\mathrm{dyn}}$. Comparing that to the Lorentz force on the right-hand side, $\boldsymbol{j}\times\boldsymbol{B}/c \sim \varrho v_{\mathrm{A}}^2/\ell_B$, the inertial term is indeed smaller by a factor $\sim x_{\mathrm{i}}\ell_B/(v_{\mathrm{A}}\tau_{\mathrm{dyn}})$, which is at most $\sim 10^{-8}(1\ \mathrm{Myr}/\tau_{\mathrm{dyn}})$ in molecular cloud cores. The pressure-gradient terms on the right-hand side of (X.2.8) are $\sim x_{\mathrm{i}}\beta\varrho v_{\mathrm{A}}^2/\ell$ and so, as long as the pressure-gradient scales do not differ from the magnetic-gradient scales by more than a factor $\sim x_{\mathrm{i}}\beta \lesssim 10^{-8}$ (unlikely), the pressure-gradient terms are completely negligible. This leaves the friction force, $\boldsymbol{R}_{\mathrm{in}}$, and so the dominant balance in (X.2.8) is

$$\boldsymbol{R}_{\mathrm{in}} = \frac{\varrho_{\mathrm{n}}}{\tau_{\mathrm{ni}}}(\boldsymbol{u}_{\mathrm{n}} - \boldsymbol{u}_{\mathrm{i}}) \simeq -\frac{\boldsymbol{j}}{c}\times\boldsymbol{B} \quad\Longrightarrow\quad \boldsymbol{u}_{\mathrm{i}} \simeq \boldsymbol{u}_{\mathrm{n}} + \frac{\tau_{\mathrm{ni}}}{\varrho_{\mathrm{n}}}\frac{\boldsymbol{j}}{c}\times\boldsymbol{B}. \tag{X.2.9}$$

Substituting (X.2.9) into the non-ideal induction equation (X.1.10) with the Ohmic and Hall terms neglected, we find

$$\frac{\partial\boldsymbol{B}}{\partial t} = \boldsymbol{\nabla}\times(\boldsymbol{u}_{\mathrm{i}}\times\boldsymbol{B}) = \boldsymbol{\nabla}\times\left[\boldsymbol{u}_{\mathrm{n}}\times\boldsymbol{B} + \frac{(\boldsymbol{j}\times\boldsymbol{B})\times\boldsymbol{B}}{c\varrho_{\mathrm{n}}\nu_{\mathrm{ni}}}\right], \tag{X.2.10}$$

where $\nu_{\mathrm{ni}} \doteq \tau_{\mathrm{ni}}^{-1}$ is the neutral-ion collision frequency. Thus, there is an electric field in the frame of the neutrals, generated as the field lines slip through the bulk neutral plasma. Note that

$$\frac{(\boldsymbol{j}\times\boldsymbol{B})\times\boldsymbol{B}}{c\varrho_{\mathrm{n}}\nu_{\mathrm{ni}}} = -\frac{B^2}{4\pi\varrho_{\mathrm{n}}\nu_{\mathrm{ni}}}\boldsymbol{j}_\perp = -\frac{v_{\mathrm{A}}^2}{\nu_{\mathrm{ni}}}\boldsymbol{j}_\perp$$

only targets perpendicular currents; i.e., ambipolar diffusion is *anisotropic* diffusion. It is also *non-linear* diffusion, in that the magnetic-diffusion coefficient is proportional to B^2. (Note that better coupling, $\nu_{\mathrm{ni}} \to \infty$, returns the ideal-MHD case.)

Finally, with (X.2.9) specifying the ion-neutral drift, we have

$$\sum_\alpha m_\alpha n_\alpha \Delta\boldsymbol{u}_\alpha \Delta\boldsymbol{u}_\alpha \simeq m_\mathrm{i} n_\mathrm{i} |\Delta\boldsymbol{u}_\mathrm{i}|^2 \simeq m_\mathrm{i} n_\mathrm{i} \left| \frac{\boldsymbol{j}\times\boldsymbol{B}\tau_\mathrm{ni}}{c\varrho_\mathrm{n}} \right|^2 \sim \frac{m_\mathrm{i} n_\mathrm{i}}{\varrho_\mathrm{n}} \left| \frac{v_\mathrm{A}\tau_\mathrm{ni}}{\ell_B} \right|^2 \frac{B^2}{4\pi} \ll \frac{B^2}{4\pi},$$

and so the single-fluid momentum equation (X.1.8) becomes

$$\varrho \frac{\mathrm{D}\boldsymbol{u}}{\mathrm{D}t} \simeq m_\mathrm{n} n_\mathrm{n} \frac{\mathrm{D}\boldsymbol{u}_\mathrm{n}}{\mathrm{D}t_\mathrm{n}} = -\boldsymbol{\nabla} p_\mathrm{n} + \frac{\boldsymbol{j}}{c}\times\boldsymbol{B}. \tag{X.2.11}$$

Therefore, the only substantive change from ideal MHD is an additional (anisotropic) diffusive term in the induction equation.

X.2.2. *Wave-driven ambipolar diffusion*

Ambipolar diffusion is now recognized to be important in a wide range of astrophysical plasmas, many of which are extremely complex, both dynamically and chemically. Let's curb our ambition and simply investigate how ambipolar diffusion affects linear waves in a static, homogeneous background. As usual, separate the fields into their background (adorned by a "0") and fluctuating parts:

$$\boldsymbol{B} = \boldsymbol{B}_0 + \delta\boldsymbol{B}, \quad \boldsymbol{u}_\mathrm{n} = \delta\boldsymbol{u}, \quad p_\mathrm{n} = p_0 + \delta p, \quad \varrho_\mathrm{n} = \varrho_0 + \delta\varrho, \tag{X.2.12}$$

with $\delta \sim \exp(-\mathrm{i}\omega t + \mathrm{i}\boldsymbol{k}\cdot\boldsymbol{r})$. Working to $\mathcal{O}(\delta)$, our MHD equations including ambipolar diffusion become

$$-\mathrm{i}\omega\delta\varrho = -\mathrm{i}\varrho_0 \boldsymbol{k}\cdot\delta\boldsymbol{u}, \tag{X.2.13}$$

$$-\mathrm{i}\omega\delta\boldsymbol{u} = -\mathrm{i}\boldsymbol{k}\left(\frac{\delta p}{\varrho_0} + \frac{\boldsymbol{B}_0\cdot\delta\boldsymbol{B}}{4\pi\varrho_0}\right) + \frac{\mathrm{i}\boldsymbol{k}\cdot\boldsymbol{B}_0}{4\pi\varrho_0}\delta\boldsymbol{B}, \tag{X.2.14}$$

$$-\mathrm{i}\omega\delta\boldsymbol{B} = \mathrm{i}\boldsymbol{k}\cdot\boldsymbol{B}_0\delta\boldsymbol{u} - \boldsymbol{B}_0\mathrm{i}\boldsymbol{k}\cdot\delta\boldsymbol{u} + \mathrm{i}\boldsymbol{k}\times\left[\frac{(\delta\boldsymbol{j}\times\boldsymbol{B}_0)\times\boldsymbol{B}_0}{c\varrho_0\nu_\mathrm{ni}}\right]. \tag{X.2.15}$$

The final (ambipolar) term may be recast using two vector identities and the linearized Ampére's law, $\delta\boldsymbol{j} = (c/4\pi)(\mathrm{i}\boldsymbol{k}\times\delta\boldsymbol{B})$:

$$\begin{aligned}
\mathrm{i}\boldsymbol{k}\times\left[\frac{(\delta\boldsymbol{j}\times\boldsymbol{B}_0)\times\boldsymbol{B}_0}{c\varrho_0\nu_\mathrm{ni}}\right] &= -\mathrm{i}\boldsymbol{k}\times\left[\frac{B_0^2}{c\varrho_0\nu_\mathrm{ni}}\left(\boldsymbol{I} - \frac{\boldsymbol{B}_0\boldsymbol{B}_0}{B_0^2}\right)\cdot\delta\boldsymbol{j}\right] \\
&= \boldsymbol{k}\times\left[\frac{B_0^2}{4\pi\varrho_0\nu_\mathrm{ni}}\left(\boldsymbol{I} - \frac{\boldsymbol{B}_0\boldsymbol{B}_0}{B_0^2}\right)\cdot(\boldsymbol{k}\times\delta\boldsymbol{B})\right] \\
&= -\frac{k^2 v_\mathrm{A}^2}{\nu_\mathrm{ni}}\left[\boldsymbol{I} - \frac{(\boldsymbol{k}\times\boldsymbol{B}_0)(\boldsymbol{k}\times\boldsymbol{B}_0)}{k^2 B_0^2}\right]\cdot\delta\boldsymbol{B},
\end{aligned}$$

where $v_\mathrm{A}^2 = B_0^2/4\pi\varrho_0$ refers only to the zeroth-order quantities. Equation (X.2.15) may then be written as

$$\left[\left(-\mathrm{i}\omega + \frac{k^2 v_\mathrm{A}^2}{\nu_\mathrm{ni}}\right)\boldsymbol{I} - \frac{(\boldsymbol{k}\times\boldsymbol{v}_\mathrm{A})(\boldsymbol{k}\times\boldsymbol{v}_\mathrm{A})}{\nu_\mathrm{ni}}\right]\cdot\delta\boldsymbol{B} = \mathrm{i}\boldsymbol{k}\cdot\boldsymbol{B}_0\delta\boldsymbol{u} - \boldsymbol{B}_0\mathrm{i}\boldsymbol{k}\cdot\delta\boldsymbol{u}. \tag{X.2.16}$$

Note that, if $\boldsymbol{k} \parallel \boldsymbol{B}_0$, equation (X.2.16) is the standard linearized induction equation but with $\omega \to \omega + \mathrm{i}k_\parallel^2 v_\mathrm{A}^2/\nu_\mathrm{ni}$. In this case, if you remember the linear dispersion relation for ideal MHD with $\boldsymbol{k} = k_\parallel\hat{\boldsymbol{b}}_0$, you can skip right to the end by simply replacing ω with

$\omega + \mathrm{i}k_\parallel^2 v_\mathrm{A}^2/\nu_\mathrm{ni}$. The result is

$$\omega\left(\omega + \mathrm{i}\frac{k_\parallel^2 v_\mathrm{A}^2}{\nu_\mathrm{ni}}\right) = k_\parallel^2 v_\mathrm{A}^2 \quad \Longrightarrow \quad \omega = -\mathrm{i}\frac{k_\parallel^2 v_\mathrm{A}^2}{2\nu_\mathrm{ni}} \pm \sqrt{k_\parallel^2 v_\mathrm{A}^2 - \left(\frac{k_\parallel^2 v_\mathrm{A}^2}{2\nu_\mathrm{ni}}\right)^2}. \tag{X.2.17}$$

Easy… damped shear-Alfvén waves. Physically, as the field lines oscillate with the effectively inertialess, flux-frozen ions, the inertia-bearing neutrals get left behind (if $k \gtrsim 2\nu_\mathrm{ni}/v_\mathrm{A}$) and frictionally drag on the ions, damping the oscillation. Put differently, if an Alfvénic disturbance in the magnetic field has wavelength $\lambda \lesssim \lambda_\mathrm{AD} \doteq \pi v_\mathrm{A}\tau_\mathrm{ni}$, it diffuses before collisions between neutrals and ions have time to transmit to the neutrals the magnetic force (e.g., Kulsrud & Pearce 1969, Appendix; also, Mouschovias 1991).

To give you a feeling for the numbers involved here,

$$\lambda_\mathrm{AD} \doteq \pi v_\mathrm{A}\tau_\mathrm{ni} \simeq \left(\frac{B}{10\ \mu\mathrm{G}}\right)\left(\frac{n_{\mathrm{H}_2}}{10^3\ \mathrm{cm}^{-3}}\right)^{-1/2}\left(\frac{n_\mathrm{i}}{3.3\times10^{-5}\ \mathrm{cm}^{-3}}\right)^{-1}\ \mathrm{pc}, \tag{X.2.18}$$

using $m_\mathrm{i} = 29m_\mathrm{H}$, $\varrho_\mathrm{n} = 2.33m_\mathrm{H}n_\mathrm{n} = 1.4m_{\mathrm{H}_2}n_{\mathrm{H}_2}$, and $\langle\sigma w\rangle_{\mathrm{iH}_2} = 1.69\times10^{-9}\ \mathrm{cm}^3\ \mathrm{s}^{-1}$ (see (X.2.1)). To obtain n_i in terms of n_{H_2}, a customary simplification in used in molecular cloud research is to assume a balance between cosmic-ray ionization and dissociative recombination:

$$\zeta_\mathrm{cr}n_{\mathrm{H}_2} = \alpha_\mathrm{dr}n_\mathrm{i}n_\mathrm{e} = \alpha_\mathrm{dr}n_\mathrm{i}^2, \tag{X.2.19}$$

where ζ_cr is the cosmic-ray ionization rate and α_dr is the dissociative recombination rate. Using $\zeta_\mathrm{cr} = 5\times10^{-17}\ \mathrm{s}^{-1}$ and $\alpha_\mathrm{dr} = 2.5\times10^{-6}\,(T/10\ \mathrm{K})^{-3/4}\ \mathrm{cm}^3\ \mathrm{s}^{-1}$ (Umebayashi & Nakano 1990) to replace n_i in (X.2.18) by $(\zeta_\mathrm{cr}n_{\mathrm{H}_2}/\alpha_\mathrm{dr})^{1/2}$, we find

$$\lambda_\mathrm{AD} \simeq 0.23\left(\frac{B}{10\ \mu\mathrm{G}}\right)\left(\frac{n_{\mathrm{H}_2}}{10^3\ \mathrm{cm}^{-3}}\right)^{-1}\ \mathrm{pc}, \tag{X.2.20}$$

a suggestive number given that prestellar cores in molecular clouds are observed to be quiescent with thermalized linewidths (e.g. Goodman *et al.* 1998; Bacmann *et al.* 2000; Caselli *et al.* 2002; Tafalla *et al.* 2004).

The general case is more interesting physically. Take $\mathrm{i}\boldsymbol{k}\cdot$(X.2.14):

$$\begin{aligned}
&\underbrace{\omega\boldsymbol{k}\cdot\delta\boldsymbol{u}}_{\substack{=\omega^2\delta\varrho/\varrho_0\\ \text{using}\\ \text{(X.2.13)}}} = k^2\left(\frac{\delta p}{\varrho_0} + \frac{\boldsymbol{B}_0\cdot\delta\boldsymbol{B}}{4\pi\varrho_0}\right) - \frac{\boldsymbol{k}\cdot\boldsymbol{B}_0}{4\pi\varrho_0}\cancel{\boldsymbol{k}\cdot\delta\boldsymbol{B}}^{\,0}\\
\Longrightarrow\quad &\omega^2\frac{\delta\varrho}{\varrho_0} = k^2\left(\frac{\delta p}{\varrho_0} + \frac{\boldsymbol{B}_0\cdot\delta\boldsymbol{B}}{4\pi\varrho_0}\right) = k^2a^2\frac{\delta\varrho}{\varrho_0} + k^2\frac{\boldsymbol{B}_0\cdot\delta\boldsymbol{B}}{4\pi\varrho_0}\\
&\Longrightarrow\quad \frac{\delta\varrho}{\varrho_0} = \frac{1}{a^2}\frac{\delta p}{\varrho_0} = \frac{k^2}{\omega^2 - k^2a^2}\frac{\boldsymbol{B}_0\cdot\delta\boldsymbol{B}}{4\pi\varrho_0}.
\end{aligned} \tag{X.2.21}$$

Substituting (X.2.21) back into (X.2.14) and re-arranging leads to

$$-\mathrm{i}\omega\delta\boldsymbol{u} = -\mathrm{i}\boldsymbol{k}\frac{\boldsymbol{B}_0\cdot\delta\boldsymbol{B}}{4\pi\varrho_0}\frac{\omega^2}{\omega^2 - k^2a^2} + \frac{\mathrm{i}\boldsymbol{k}\cdot\boldsymbol{B}_0}{4\pi\varrho_0}\delta\boldsymbol{B}, \tag{X.2.22}$$

which may then be fed into (X.2.16) to obtain

$$\boldsymbol{M}\cdot\delta\boldsymbol{B} \doteq \left\{\left[\omega^2 + \mathrm{i}\omega\frac{k^2 v_{\mathrm{A}}^2}{\nu_{\mathrm{ni}}} - (\boldsymbol{k}\cdot\boldsymbol{v}_{\mathrm{A}})^2\right]\boldsymbol{I} - \mathrm{i}\omega\frac{(\boldsymbol{k}\times\boldsymbol{v}_{\mathrm{A}})(\boldsymbol{k}\times\boldsymbol{v}_{\mathrm{A}})}{\nu_{\mathrm{ni}}} + \frac{\omega^2}{\omega^2 - k^2a^2}\left(\boldsymbol{k}\cdot\boldsymbol{v}_{\mathrm{A}}\boldsymbol{k}\boldsymbol{v}_{\mathrm{A}} - k^2\boldsymbol{v}_{\mathrm{A}}\boldsymbol{v}_{\mathrm{A}}\right)\right\}\cdot\delta\boldsymbol{B} = 0. \tag{X.2.23}$$

Taking the determinant of $\boldsymbol{M}$ and setting it to zero gives the dispersion relation. The algebra is aided greatly by a good choice of coordinate system:

$$\boldsymbol{B}_0 = B_0\hat{\boldsymbol{z}}, \quad \boldsymbol{k} = k_\parallel\hat{\boldsymbol{z}} + k_\perp\hat{\boldsymbol{x}}, \quad \delta\boldsymbol{B} = \delta B_\parallel\hat{\boldsymbol{z}} + \delta B_x\hat{\boldsymbol{x}} + \delta B_y\hat{\boldsymbol{y}}. \tag{X.2.24}$$

Then we have

$$\boldsymbol{k}\times\boldsymbol{v}_{\mathrm{A}} = -\hat{\boldsymbol{y}}k_\perp v_{\mathrm{A}} \quad\text{and}\quad \delta\boldsymbol{v}_{\mathrm{A}}\cdot\delta\boldsymbol{B} = -v_{\mathrm{A}}\frac{k_\perp}{k_\parallel}\delta B_x. \tag{X.2.25}$$

Introducing

$$\widetilde{\omega}^2 \doteq \omega^2 - (\boldsymbol{k}\cdot\boldsymbol{v}_{\mathrm{A}})^2, \tag{X.2.26}$$

equation (X.2.23) may be written as

$$\begin{bmatrix} \widetilde{\omega}^2 + \mathrm{i}\omega\dfrac{k^2v_{\mathrm{A}}^2}{\nu_{\mathrm{ni}}} - \dfrac{\omega^2k_\perp^2v_{\mathrm{A}}^2}{\omega^2 - k^2a^2} & 0 \\ 0 & \widetilde{\omega}^2 + \mathrm{i}\omega\dfrac{k_\parallel^2v_{\mathrm{A}}^2}{\nu_{\mathrm{ni}}} \end{bmatrix}\begin{bmatrix} \delta B_x \\ \delta B_y \end{bmatrix} = 0. \tag{X.2.27}$$

The dispersion relation is thus

$$\underbrace{\left(\omega^2 + \mathrm{i}\omega\frac{k_\parallel^2v_{\mathrm{A}}^2}{\nu_{\mathrm{ni}}} - k_\parallel^2v_{\mathrm{A}}^2\right)}_{\text{damped Alfvén waves}}\underbrace{\left(\omega^2 + \mathrm{i}\omega\frac{k^2v_{\mathrm{A}}^2}{\nu_{\mathrm{ni}}} - k_\parallel^2v_{\mathrm{A}}^2 - \frac{\omega^2k_\perp^2v_{\mathrm{A}}^2}{\omega^2 - k^2a^2}\right)}_{\text{damped magnetosonic waves}} = 0, \tag{X.2.28}$$

where the two branches have been labelled. For the Alfvén-wave branch, we recover (X.2.17) – damped Alfvén waves. But for the magnetosonic branch, we have

$$\underbrace{\omega^4 - \omega^2k^2\left(a^2 + v_{\mathrm{A}}^2\right) + k^2a^2k_\parallel^2v_{\mathrm{A}}^2}_{\text{fast and slow modes}} = \underbrace{-\mathrm{i}\omega\frac{k^2v_{\mathrm{A}}^2}{\nu_{\mathrm{ni}}}\left(\omega^2 - k^2a^2\right)}_{\substack{\text{damping by}\\ \text{ambipolar diffusion}}}. \tag{X.2.29}$$

Notice that the magnetosonic modes are damped at a different rate than the Alfvén waves! This is because ambipolar diffusion affects only *perpendicular* currents, a feature that is particularly important in the context of planar shear flows and differentially rotating accretion disks (Kunz & Balbus 2004; Kunz 2008).

X.2.3. *Gravitationally driven ambipolar diffusion*

In the previous section, ambipolar diffusion – ion-neutral drift and the consequent frictional damping of MHD fluctuations – occurred because the tension in the field lines drives the ions through the neutral gas. Another way ambipolar diffusion can occur, particularly important in the context of star formation, is when the neutrals contract under their own self-gravity as they slip through the magnetic-field lines. You'll do a problem on this for homework, but it's worth some foreshadowing.

Consider a self-gravitating, infinite slab of poorly ionized, isothermal gas, threaded by a uniform magnetic field and embedded in a hot gas with external pressure $p_{\rm ext}$:

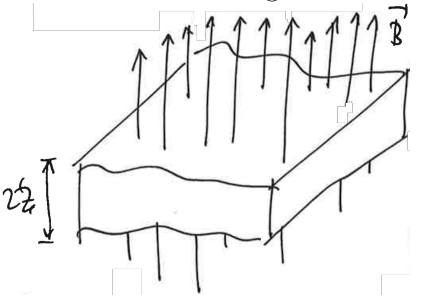

Force balance along field lines is

$$-\frac{\mathrm{d}p}{\mathrm{d}z} = \varrho_{\rm n} g = 4\pi G \varrho_{\rm n}^2 z. \tag{X.2.30}$$

Integrating (X.2.30) from $z = 0$ to the surface $z = Z$ yields

$$-\int_0^Z \mathrm{d}z \frac{\mathrm{d}p}{\mathrm{d}z} = \int_0^Z \mathrm{d}z\, 4\pi G \varrho_{\rm n}^2 z \quad \Longrightarrow \quad -p_{\rm ext} + \varrho_n C^2 = 4\pi G \varrho_{\rm n}^2 \frac{Z^2}{2} = \frac{\pi}{2} G \sigma_{\rm n}^2, \tag{X.2.31}$$

where C is the isothermal sound speed and $\sigma_{\rm n} = \varrho_{\rm n} 2Z$ is the column density of the neutrals. In molecular clouds, $p_{\rm ext}/\varrho_{\rm n} C^2 \sim 0.1$, so let's drop it for this simple exercise. Thus, $\sigma_{\rm n} = (2\varrho_{\rm n} C^2/\pi G)^{1/2}$.

A particular important quantity in star-formation theory and observation is the *mass-to-flux ratio*, i.e., the amount of self-gravitating mass loaded onto magnetic field lines enclosed within a flux surface. In the case above,

$$\frac{M}{\Phi_B} = \frac{\pi R^2 \sigma_{\rm n}}{B \pi R^2} = \frac{\sigma_{\rm n}}{B} = \left(\frac{2\varrho_{\rm n} C^2}{B^2 \pi G}\right)^{1/2}. \tag{X.2.32}$$

Now, there is a critical value of $(M/\Phi_B) = (M/\Phi_B)_{\rm crit}$, beyond which the tension in the magnetic-field lines cannot support the cloud against self-gravitationally driven fragmentation and contraction. For a slab geometry, it is (Nakano & Nakamura 1978)

$$\left(\frac{M}{\Phi_B}\right)_{\rm crit} = \frac{1}{2\pi\sqrt{G}} \quad \text{(slab)}. \tag{X.2.33}$$

For a perhaps more realistic configuration in which a spherical distribution of mass is allowed to flatten self-consistently along field lines into an oblate spheroid (Mouschovias & Spitzer 1976),

$$\left(\frac{M}{\Phi_B}\right)_{\rm crit} \simeq \frac{0.126}{\sqrt{G}} \quad \text{(oblate spheroid)}. \tag{X.2.34}$$

In the central flux tube threading the mass, the critical mass-to-flux ratio is 3/2 times this value.

Thus, in our model cloud,

$$\frac{(M/\Phi_B)}{(M/\Phi_B)_{\rm crit}} = \left(\frac{8\pi\varrho_{\rm n} C^2}{B^2}\right)^{1/2} \simeq 0.65 \left(\frac{n_{\rm H_2}}{10^3\ {\rm cm}^{-3}}\right)^{1/2} \left(\frac{B}{10\ \mu{\rm G}}\right)^{-1}. \tag{X.2.35}$$

Such a cloud would be magnetically supported against fragmentation. That is, unless the mass-bearing neutrals slip through the magnetic field (Mestel & Spitzer 1956). Ambipolar diffusion can lead to a redistribution of (neutral) mass in the central flux tubes of the

cloud, leaving the magnetic field behind with the ions (Mouschovias 1979).[18] This idea formed the basis for early theories of star formation, which attributed the inefficiency of star formation in the Galaxy to magnetic support of clouds on large scales and ambipolar diffusion leading to fragmentation and contraction on small scales (Mouschovias 1976*a*,*b*, 1978, 1979). A lineage of numerical calculations following the contraction of a magnetized, protostellar core – accounting for myriad effects such as ambipolar diffusion, Ohmic dissipation, rotation, chemistry, dust grains, radiative transport – have made this into a quantitative theory (e.g., Fiedler & Mouschovias 1993; Ciolek & Mouschovias 1993, 1994; Basu & Mouschovias 1994, 1995*a*,*b*; Ciolek & Mouschovias 1995; Ciolek & Königl 1998; Desch & Mouschovias 2001; Tassis & Mouschovias 2005*a*,*b*, 2007*a*,*b*,*c*; Mellon & Li 2009; Kunz & Mouschovias 2009, 2010; Dapp & Basu 2010; Li *et al.* 2011; Dapp *et al.* 2012). More recent calculations have ventured into three-dimensional geometry to investigate fragmentation (Basu & Ciolek 2004; Li & Nakamura 2004; Nakamura & Li 2005; Basu *et al.* 2009*a*,*b*) and the formation of rotationally supported protostellar accretion disks (Machida & Matsumoto 2012; Tomida *et al.* 2013; Machida *et al.* 2014; Tomida *et al.* 2015; Zhao *et al.* 2018), with varying degrees of sophistication in their treatment of the non-ideal MHD.

Effects like ambipolar diffusion aid in the resolution of one of the most fundamental, heretofore-unsolved problems of theoretical astrophysics: the magnetic flux problem of star formation. Babcock & Cowling (1953, p. 373) state it as follows:

> Suppose that a star is formed by condensation from the interstellar material in a region where the magnetic field is sensibly uniform in direction. During the condensation the density increases by a factor of, say, 10^{24}; thus, assuming the same degree of contraction in all directions, the linear dimensions of the mass forming the star are reduced in the ratio $10^8 : 1$. The contraction squeezes the lines of force together, the total magnetic induction through the mass remaining constant; thus the magnetic field increases in the ratio $10^{16} : 1$. Hence, if one were to begin with a field of order 10^{-5} gauss, such as is quoted by some theoretical workers to explain the polarization of starlight, the contraction would increase this to 10^{11} gauss. So high a figure is altogether impossible, since the mechanical effects of a field of 10^{11} gauss would be so strong as altogether to prevent gravitational forces from pushing the material together.

Put differently, take a 1 $M_\odot$ spherical blob from the interstellar medium and compute

[18] Mestel & Spitzer (1956) actually proposed ambipolar diffusion as a means by which an interstellar cloud as a whole would reduce its magnetic flux and thereby collapse. Some further history, if you're interested: Pneuman & Mitchell (1965) undertook a detailed calculation of the collapse of such (spherical) cloud. Spitzer (1968) calculated the ambipolar-diffusion time scale by assuming that the magnetic force on the ions is balanced by the (self-)gravitational force on the neutrals. Nakano (1979) followed the quasistatic (i.e., negligible acceleration) contraction of a cloud due to ambipolar diffusion using a sequence of the Mouschovias (1976*b*) equilibrium states, each one of which had a smaller magnetic flux than the previous one. A new solution for ambipolar diffusion by Mouschovias (1979) showed that the essence of this process is a redistribution of mass in the central flux tubes of a molecular cloud, rather than a loss of magnetic flux by the cloud as a whole. He found the ambipolar-diffusion timescale to be typically 3 orders of magnitude smaller in the interior of a cloud than in the outermost envelope, where there is a much better coupling between neutral particles and the magnetic field because of the much greater degree of ionization. This suggested naturally a self-initiated fragmentation of (or core formation in) molecular clouds on the ambipolar-diffusion timescale $\tau_{\rm AD} \simeq 1.8 \times 10^6\,(x_{\rm i}/10^{-7})$ yr. Time-dependent solutions for gravitationally driven ambipolar diffusion in slab geometries were obtained by Mouschovias & Paleologou (1981) and Shu (1983). See Shu *et al.* (1987) and Mouschovias & Ciolek (1999) for more.

the magnetic flux threading it:

$$\Phi_B = B\pi\lambda^2 = B\pi\left(\frac{3M_\odot}{4\pi\varrho}\right)^{2/3} \simeq 5.8\times10^{32}\left(\frac{B}{5\ \mu G}\right)\left(\frac{n_H}{1\ \mathrm{cm}^{-3}}\right)\underbrace{\mathrm{Mx}}_{\substack{\approx10^{31}\\ \mu\mathrm{G\ pc}^2}}. \tag{X.2.36}$$

The flux of a typical Ap star[19] is $\sim3\times10^{26}$ Mx. Thus, at least five orders of magnitude of magnetic flux must be redistributed on the path towards building a star. Want to solve the problem? A lot of non-ideal radiation magnetohydrodynamics plus chemistry is needed along the way (see, e.g., Kunz & Mouschovias 2009).

X.2.4. *Ambipolar diffusion heats plasma*

As ambipolar diffusion relaxes perpendicular currents and allows the redistribution of mass in magnetic flux tubes, heat is generated equivalent to the work done by the ion-neutral friction force:

$$(\boldsymbol{u}_n-\boldsymbol{u}_i)\cdot\boldsymbol{R}_{in} = \frac{\tau_{ni}}{\varrho_n}\frac{\boldsymbol{j}}{c}\times\boldsymbol{B}\cdot\frac{\boldsymbol{j}}{c}\times\boldsymbol{B} = \frac{4\pi}{c^2}v_A^2\tau_{ni}|\boldsymbol{j}_\perp|^2 \doteq \eta_A|\boldsymbol{j}_\perp|^2, \tag{X.2.37}$$

where η_A is the ambipolar resistivity. Note that $\eta_A\propto(n_n n_i)^{-1}$ – denser gas gets heated less. This heating was first considered in the context of magnetic star formation by Scalo (1977) to put constraints on how the magnetic-field strength scales with density during protostellar core contraction. Zweibel & Josafatsson (1983) considered what constraints heating by wave damping (including ambipolar diffusion) places on the properties of the turbulent fluctuations observed in molecular clouds (see also Arons & Max (1975)). Draine *et al.* (1983) considered heating by ambipolar diffusion occurring in so-called "*C*-type shock waves" in turbulent molecular clouds (see HW04).

X.3. The Hall effect

X.3.1. *Astrophysical context and basic theory*

Now suppose that $|\boldsymbol{u}_i-\boldsymbol{u}_n|\ll u_n$, so that ambipolar diffusion is ignorable, but that $(d_i/\ell_B)(\varrho/\varrho_i)^{1/2}\sim1$ (recall (X.1.12)). That is, the ions appreciably drift with respect to the electrons on the scales of interest. (In what follows, we will also ignore Ohmic dissipation, postponing its discussion to §X.4.) In a fully ionized plasma, this is only true if the magnetic field has structure on scales ℓ_B comparable to the ion skin depth d_i. But in a poorly ionized plasma, the ion skin depth is effectively larger by a factor of $(\varrho/\varrho_i)^{1/2}$, which is potentially huge in protostellar cores and protoplanetary disks. This is an inertial effect: as a magnetic fluctuation oscillates in a plasma, for the ions to be responsive to that fluctuation they must cope with the sluggishness of not only their inertial mass but also the inertial mass of the more abundant neutrals to which they are collisionally coupled. This makes for a larger *Hall length scale*,

$$\ell_H \doteq d_i\left(\frac{\varrho}{\varrho_i}\right)^{1/2} = \frac{v_A}{\omega_H}, \tag{X.3.1}$$

[19] a type of star believed to avoid the convective stage as a protostar and thus avoid appreciable dynamo amplification of any fossil field. A typical Ap star is θ Aurigae, which is young ($\sim$200 Myr) and has a radius 4.5 $R_\odot$ and magnetic-field strength $\sim$1 kG (van Rensbergen *et al.* 1984).

where

$$\omega_{\rm H} \doteq \frac{q_{\rm i} B}{\mu c} \frac{n_{\rm i}}{n} \tag{X.3.2}$$

is the *Hall frequency* (e.g., Kunz & Lesur 2013). (Recall the definition of μ, the mean mass per particle: (X.2.4)). Note that $\ell_{\rm H}$ is independent of the magnetic-field strength. At scales $\ell_B \lesssim \ell_{\rm H}$, the Hall effect is important.

An example of an astrophysical system in which the Hall effect is very important is a protoplanetary disk, ∼1–10 au from the central protostar in particular. While such systems are chemically rich, for the sake of obtaining a simple estimate let us assume the customary balance between cosmic-ray ionization and dissociative recombination, equation (X.2.19). Setting $m_{\rm i} = 39 m_{\rm p}$ (appropriate for K^+ being the dominant ion) and $\mu = 2.33 m_{\rm p}$, and using $\zeta_{\rm cr} = 5 \times 10^{-17}$ s^{-1} and $\alpha_{\rm dr} = 2.5 \times 10^{-6} \, (T/10 \text{ K})^{-3/4}$ cm^3 s^{-1} as in §X.2.2, equation (X.3.1) becomes

$$\ell_{\rm H} \simeq 2.5 \times 10^{-6} \frac{n_{\rm H_2}^{1/2}}{n_{\rm i}} \text{ au} \simeq 0.24 \left(\frac{T}{100 \text{ K}} \right)^{-3/8} \text{ au}, \tag{X.3.3}$$

independent of density. Comparing this to the disk scale height in the minimum-mass solar nebula (MMSN; Hayashi 1981),

$$h \simeq 0.033 \left(\frac{R}{1 \text{ au}} \right)^{5/4} \text{ au} \quad \text{with} \quad T \simeq 280 \left(\frac{R}{1 \text{ au}} \right)^{-1/2} \text{ K},$$

we have

$$\frac{\ell_{\rm H}}{h} \approx 5 \left(\frac{R}{1 \text{ au}} \right)^{-17/16} \quad \Longrightarrow \quad \ell_{\rm H} \approx H \text{ at } R \approx 5 \text{ au}. \tag{X.3.4}$$

Given the uncertainties in these numbers, the radial location in a protoplanetary disk at which scales comparable to the disk scale height are subject to Hall electromotive forces likely ranges between ∼1–10 au. (Within ∼1 au, cosmic rays are attenuated, the ionization fraction drops precipitously, and Ohmic dissipation becomes the dominant diffusion mechanism.) Dust grains complicate this estimate greatly, especially since they tend to be the dominant charge carriers around $n_{\rm H_2} \gtrsim 10^{12}$ cm^{-3} (e.g., Umebayashi & Nakano 1990; Desch & Mouschovias 2001; Kunz & Mouschovias 2010).

Under these conditions, and again specializing to a quasi-neutral ion-electron-neutral plasma devoid of dust grains, the non-ideal induction equation (X.1.10) becomes

$$\frac{\partial \boldsymbol{B}}{\partial t} = \boldsymbol{\nabla} \times \left(\boldsymbol{u} \times \boldsymbol{B} - \frac{\boldsymbol{j} \times \boldsymbol{B}}{e n_{\rm e}} \right), \tag{X.3.5}$$

where $\boldsymbol{u} \simeq \boldsymbol{u}_{\rm n} \simeq \boldsymbol{u}_{\rm i}$ and $\boldsymbol{j} = e n_{\rm e} (\boldsymbol{u}_{\rm i} - \boldsymbol{u}_{\rm e})$.

X.3.2. *Wave-driven Hall diffusion*

As in §X.2.2, let us temper our ambition and focus first on the linear theory of waves in a static, homogeneous plasma, subject to Hall diffusion. The linearized continuity and momentum equations are identical to (X.2.13) and (X.2.14), respectively. The linearized induction equation (X.3.5) becomes

$$-\mathrm{i}\omega \delta \boldsymbol{B} = \mathrm{i} \boldsymbol{k} \cdot \boldsymbol{B}_0 \delta \boldsymbol{u} - \boldsymbol{B}_0 \mathrm{i} \boldsymbol{k} \cdot \delta \boldsymbol{u} - \mathrm{i} \boldsymbol{k} \times \left(\frac{\delta \boldsymbol{j} \times \boldsymbol{B}_0}{e n_{\rm e0}} \right). \tag{X.3.6}$$

The final (Hall) term may be recast using two vector identities and the linearized Ampére's law, $\delta\boldsymbol{j} = (c/4\pi)(\mathrm{i}\boldsymbol{k}\times\delta\boldsymbol{B})$:

$$\begin{aligned}\mathrm{i}\boldsymbol{k}\times\left(\frac{\delta\boldsymbol{j}\times\boldsymbol{B}_0}{en_{\mathrm{e}0}}\right) &= \mathrm{i}\boldsymbol{k}\cdot\boldsymbol{B}_0\left(\frac{\delta\boldsymbol{j}}{en_{\mathrm{e}0}}\right) - \mathrm{i}\boldsymbol{k}\cdot\left(\frac{\delta\boldsymbol{j}}{en_{\mathrm{e}0}}\right)\boldsymbol{B}_0\\ &= \mathrm{i}\boldsymbol{k}\cdot\boldsymbol{B}_0\left(\frac{c\mathrm{i}\boldsymbol{k}\times\delta\boldsymbol{B}}{4\pi en_{\mathrm{e}0}}\right) - \cancelto{0}{\mathrm{i}\boldsymbol{k}\cdot\left(\frac{c\mathrm{i}\boldsymbol{k}\times\delta\boldsymbol{B}}{4\pi en_{\mathrm{e}0}}\right)\boldsymbol{B}_0}\\ &= -\frac{c\boldsymbol{k}\cdot\boldsymbol{B}_0}{4\pi en_{\mathrm{e}0}}(\boldsymbol{k}\times\delta\boldsymbol{B})\end{aligned}$$

Equation (X.3.6) may then be written as

$$-\mathrm{i}\omega\delta\boldsymbol{B} - \frac{c\boldsymbol{k}\cdot\boldsymbol{B}_0}{4\pi en_{\mathrm{e}0}}(\boldsymbol{k}\times\delta\boldsymbol{B}) = \mathrm{i}\boldsymbol{k}\cdot\boldsymbol{B}_0\delta\boldsymbol{u} - \boldsymbol{B}_0\mathrm{i}\boldsymbol{k}\cdot\delta\boldsymbol{u}. \tag{X.3.7}$$

Before using the linearized continuity and momentum equations in (X.3.7) to obtain the dispersion relation, let's do something extremely simple yet incredibly enlightening. Set $\delta\boldsymbol{u} = 0$, i.e., stationary ions and neutrals. Using $\boldsymbol{k}\cdot\delta\boldsymbol{B} = 0$, equation (X.3.7) then becomes

$$-\mathrm{i}\omega\delta\boldsymbol{B} - \left(\frac{c\boldsymbol{k}\cdot\boldsymbol{B}_0}{4\pi en_{\mathrm{e}0}}\right)^2\frac{k^2}{\mathrm{i}\omega}\delta\boldsymbol{B} = 0 \quad\Longrightarrow\quad \omega = \pm\frac{ck\boldsymbol{k}\cdot\boldsymbol{B}_0}{4\pi en_{\mathrm{e}0}}. \tag{X.3.8}$$

This is the linear dispersion relation for a *whistler wave*. Note that is it a *dispersive* wave, in that different wavelengths travel at different speeds. Note further that there is no dissipation involved. Why? For $\boldsymbol{k}\parallel\boldsymbol{B}_0$ and $\boldsymbol{B}_0 = B_0\hat{\boldsymbol{z}}$, equation (X.3.7) with $\delta\boldsymbol{u} = 0$ may be written as

$$-\mathrm{i}\omega\begin{bmatrix}\delta B_x\\ \delta B_y\end{bmatrix} - \frac{ckk_\parallel B_0}{4\pi en_{\mathrm{e}0}}\begin{bmatrix}0 & -1\\ 1 & 0\end{bmatrix}\begin{bmatrix}\delta B_x\\ \delta B_y\end{bmatrix} = 0. \tag{X.3.9}$$

The Hall effect is just rotating the perpendicular magnetic-field fluctuations about the guide field! Indeed, eigenvector corresponding to (X.3.8) is $\delta B_y/\delta B_x = \pm\mathrm{i}$. That there is a rotation involved should have been clear from the $(\boldsymbol{k}\times\delta\boldsymbol{B})$ in (X.3.7).

Now let's restore the ion/neutral motion:

$$\begin{aligned}-\mathrm{i}\omega\delta\boldsymbol{B} - \frac{c\boldsymbol{k}\cdot\boldsymbol{B}_0}{4\pi en_{\mathrm{e}0}}(\boldsymbol{k}\times\delta\boldsymbol{B}) &= \mathrm{i}\boldsymbol{k}\cdot\boldsymbol{B}_0\left(\frac{\omega\boldsymbol{k}}{\omega^2-k^2a^2}\frac{\boldsymbol{B}_0\cdot\delta\boldsymbol{B}}{4\pi\varrho_0} - \frac{1}{\omega}\frac{\boldsymbol{k}\cdot\boldsymbol{B}_0}{4\pi\varrho_0}\delta\boldsymbol{B}\right)\\ &\quad - \boldsymbol{B}_0\mathrm{i}\boldsymbol{k}\cdot\left(\frac{\omega\boldsymbol{k}}{\omega^2-k^2a^2}\frac{\boldsymbol{B}_0\cdot\delta\boldsymbol{B}}{4\pi\varrho_0} - \frac{1}{\omega}\frac{\boldsymbol{k}\cdot\boldsymbol{B}_0}{4\pi\varrho_0}\delta\boldsymbol{B}\right).\end{aligned} \tag{X.3.10}$$

Multiplying by $-\mathrm{i}\omega$, using $\boldsymbol{k}\cdot\delta\boldsymbol{B} = 0$, and rearranging (X.3.10),

$$\left\{\left[\omega^2 - (\boldsymbol{k}\cdot\boldsymbol{v}_{\mathrm{A}})^2\right]\boldsymbol{I} + \frac{\omega^2}{\omega^2-k^2a^2}\left(\boldsymbol{k}\cdot\boldsymbol{v}_{\mathrm{A}}\boldsymbol{k}\boldsymbol{v}_{\mathrm{A}} - k^2\boldsymbol{v}_{\mathrm{A}}\boldsymbol{v}_{\mathrm{A}}\right)\right\}\cdot\delta\boldsymbol{B} = \frac{\mathrm{i}\omega c\boldsymbol{k}\cdot\boldsymbol{B}_0}{4\pi en_{\mathrm{e}0}}\boldsymbol{k}\times\delta\boldsymbol{B}. \tag{X.3.11}$$

Using the same coordinate system as in (X.2.24), the dispersion relation emerges after a few lines of algebra:

$$\left(\omega^2 + \omega\frac{ckk_\parallel B_0}{4\pi en_{\mathrm{e}0}} - k_\parallel^2 v_{\mathrm{A}}^2\right)\left(\omega^2 - \omega\frac{ckk_\parallel B_0}{4\pi en_{\mathrm{e}0}} - k_\parallel^2 v_{\mathrm{A}}^2\right) = \frac{\omega^2 k_\perp^2 v_{\mathrm{A}}^2}{\omega^2-k^2a^2}\left(\omega^2 - k_\parallel^2 v_{\mathrm{A}}^2\right) \tag{X.3.12}$$

Let us focus on incompressible fluctuations, which may be extracted by taking $a^2\to\infty$

(i.e., pressure fluctuations propagate instantaneously). The right-hand side of (X.3.12) then drops out and we find that the positive-frequency solutions satisfy

$$\omega = \mp\frac{ckk_\parallel B_0}{8\pi e n_{e0}} + \frac{ckk_\parallel B_0}{8\pi e n_{e0}}\sqrt{1+\frac{16\pi e^2 n_{e0}^2}{c^2k^2\varrho_0}} = \frac{1}{2}k_\parallel v_A k\ell_H\left[\mp 1+\sqrt{1+\left(\frac{2\omega_H}{kv_A}\right)^2}\right] \tag{X.3.13a}$$

$$\to \begin{cases} k_\parallel v_A & (\mp,\ \text{Alfvén wave}) & \text{if } kd_i \ll 1 \\ \dfrac{k_\parallel}{k}\omega_H & (-,\ \text{left-handed ion-cyclotron wave}) & \text{if } kd_i \gg 1 \\ k_\parallel v_A k\ell_H & (+,\ \text{right-handed whistler wave}) & \text{if } kd_i \gg 1, \end{cases} \tag{X.3.13b}$$

where $\mu \doteq \varrho/n$.

For $k = k_\parallel$, the dispersion relation looks like this:

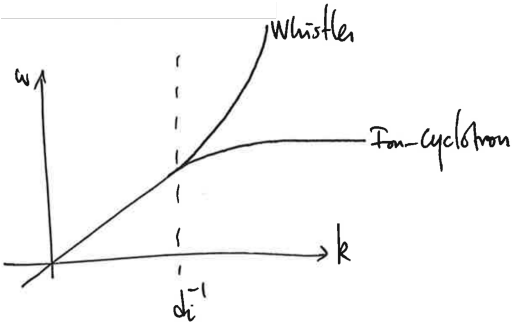

with the long-wavelength Alfvén waves bifurcating at $kd_i \sim 1$ according to their handedness. The ion-cyclotron wave gets "cut off" at the Hall frequency, at which the rotating electric field associated with the left-handed wave resonates with the ion gyro-motion. At this resonance, wave energy is converted into perpendicular kinetic energy of the ions. (The right-handed whistler wave gets cut off at the electron Larmor frequency for a similar reason.) This difference in handedness of can be obtained from (X.3.11) in the $k\ell_H \gg 1$ limit:

$$\frac{\delta B_y}{\delta B_x} \approx \pm\frac{\mathrm{i}}{\omega}k^2 v_A \ell_H. \tag{X.3.14}$$

For an ion-cyclotron wave, $\delta B_y/\delta B_x \approx -\mathrm{i}(k/k_\parallel)(k\ell_H)^2$, whereas for a whistler wave, $\delta B_y/\delta B_x \approx \mathrm{i}(k/k_\parallel)$. Graphically,

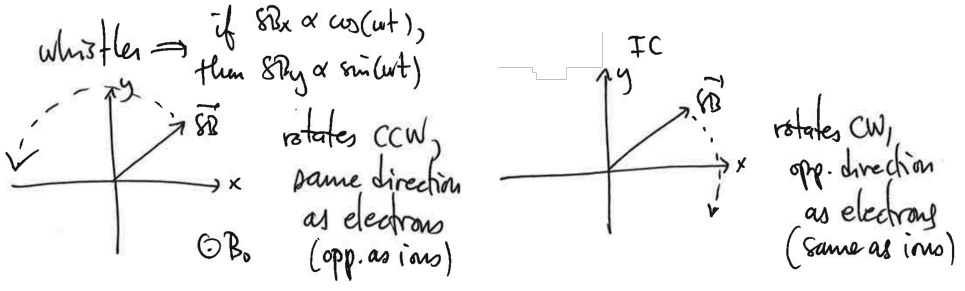

Whistler waves have been studied in the magnetosphere for more than 100 years, starting with passive ground observations of very-low-frequency radio waves from the ionosphere. (The following historical tidbits are taken from Stenzel (1999).) Preece (1894) reported that operators on the Liverpool-Hamburg telephone lines heard strange

rumblings. Barkhausen (1919) described observations of "Pfeiftöne" (whistling tones) on long wire antennas and related their occurrence to lighting and auroral activity. After World War II, a lot of research into whistler waves started (not surprisingly). Whistlers have a distinct pattern in observed frequency versus time:

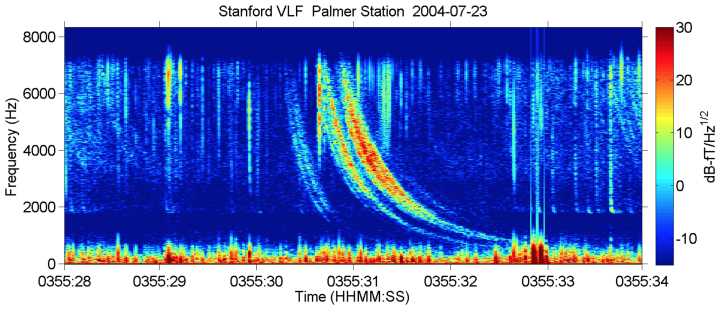

Because $\omega \propto k^2$ implies a phase velocity $\propto k$, the highest-wavenumber/frequency waves arrive first, leading to the descending tone. Such observations can be used to measure the electron density of the ionosphere.

X.3.3. *The Hall effect does not heat plasma*

From (X.3.13), it is clear that the Hall effect results in wave dispersion but *not* wave dissipation. Indeed, the electromagnetic work done by the Hall electric field, $\boldsymbol{j}\cdot\boldsymbol{E}_{\rm H} \propto \boldsymbol{j}\cdot(\boldsymbol{j}\times\boldsymbol{B}) = 0$. This makes sense from the physical discussion in the previous section: the Hall effect only *rotates* magnetic-field fluctuations; it does not damp their energy. Because of this, it is a bit of a misnomer to refer to "Hall diffusion", as it's not really diffusion in the usual dissipative sense of the word. Because collisions are not involved, there is nothing irreversible about the Hall effect (despite the $\eta_{\rm H}$ notation used in §X.5). It is simply a result of differences in the field-perpendicular fluid motion of oppositely charged species caused by their disparate inertia.[20]

X.3.4. *Lorentz force, Hall effect, and canonical vorticity*

Those differences result in an interesting change to Kelvin's circulation theorem. In HW02 #3, you showed that, for $p = p(\rho)$, the fluid vorticity $\boldsymbol{\omega} = \boldsymbol{\nabla}\times\boldsymbol{u}$ satisfies

$$\frac{\partial\boldsymbol{\omega}}{\partial t} = \boldsymbol{\nabla}\times\left(\boldsymbol{u}\times\boldsymbol{\omega} + \frac{\boldsymbol{j}\times\boldsymbol{B}}{c\rho}\right), \tag{X.3.15}$$

so that the circulation $\Gamma \doteq \int_S \boldsymbol{\omega}\cdot\mathrm{d}\boldsymbol{S}$ within a fluid element is conserved but for the rotational influence of the Lorentz force:

$$\frac{\mathrm{D}\Gamma}{\mathrm{D}t} = \oint_{\partial S}\left(\frac{\boldsymbol{j}\times\boldsymbol{B}}{c\rho}\right)\cdot\mathrm{d}\boldsymbol{\ell}. \tag{X.3.16}$$

Now, when the Hall effect is important, the induction equation (X.3.5) reads

$$\frac{\partial\boldsymbol{B}}{\partial t} = \boldsymbol{\nabla}\times\left(\boldsymbol{u}\times\boldsymbol{B} - \frac{\boldsymbol{j}\times\boldsymbol{B}}{en_{\rm e}}\right). \tag{X.3.17}$$

Compare (X.3.15) and (X.3.17). Clearly there is some special symmetry here that is saying something important. Just as the Lorentz force changes the number of vortex lines threading a fluid element, the Hall effect changes the number of magnetic-field lines

[20] Disparate inertia is key. There is no Hall effect in a pair plasma.

threading a fluid element. Indeed, the origin of the Hall term is the differential motion between the electrons, to which the magnetic-field lines are tied (modulo Ohmic losses), and the drifting ions, which we take to be collisionally well coupled to the bulk neutral fluid.

Since the divergences of both the vorticity and the magnetic field are zero, any new vortex and magnetic-field lines that are made must be created as continuous curves that grow out of points or lines where the vorticity and magnetic field, respectively, vanish. Put simply, just as the effect of the Lorentz force on the vorticity is non-dissipative, so too is the Hall effect on the magnetic field; vorticity and magnetic flux can only be *redistributed* by these processes. We now prove that they must be redistributed in a specific way.

Consider the canonical momentum

$$\boldsymbol{\wp}_{\rm can} \doteq m\boldsymbol{u} + \frac{e\boldsymbol{A}}{c}\frac{n_{\rm e}}{n}, \tag{X.3.18}$$

and the associated *canonical vorticity*

$$\boldsymbol{\omega}_{\rm can} \doteq \frac{1}{m}\boldsymbol{\nabla}\times\boldsymbol{\wp}_{\rm can} = \boldsymbol{\omega} + \frac{e\boldsymbol{B}}{mc}\frac{n_{\rm e}}{n}, \tag{X.3.19}$$

where $\boldsymbol{A}$ is the vector potential satisfying $\boldsymbol{B} = \boldsymbol{\nabla}\times\boldsymbol{A}$. The final term in (X.3.19) should look familiar. Combining (X.3.15) and (X.3.17), we find that the canonical vorticity satisfies

$$\frac{\partial\boldsymbol{\omega}_{\rm can}}{\partial t} = \boldsymbol{\nabla}\times(\boldsymbol{u}\times\boldsymbol{\omega}_{\rm can}). \tag{X.3.20}$$

This equation states that, in the absence of dissipative sinks[21], the canonical vorticity is frozen into the fluid. As a result, the combined number of vortex and magnetic-field lines threading a material surface is conserved; i.e., the *canonical circulation*

$$\mathit{\Gamma}_{\rm can} \doteq \oint_{\partial S}\boldsymbol{\wp}_{\rm can}\cdot{\rm d}\boldsymbol{\ell} \quad \left(= \frac{1}{m}\int_S \boldsymbol{\omega}_{\rm can}\cdot{\rm d}\boldsymbol{S}\right) \tag{X.3.21}$$

around a simple closed contour $\partial\boldsymbol{S}$ bounding a material surface S is a constant. This is simply Kelvin's (1869) circulation theorem generalized for Hall-MHD. An important consequence is that *a local increase in magnetic flux must be accompanied by a local decrease in vorticity flux and vice versa*.

Such behavior is absent in ideal MHD, in which the magnetic flux is conserved for each fluid element independent of how the vorticity is advected. The difference is due to the fact that, in Hall-MHD, the ion-neutral fluid drifts relative to the field lines and, as such, has its momentum augmented by the magnetic field through which it travels. One may think of this as a consequence of Lenz's law. This property received special attention in work by Kunz & Lesur (2013) on the magneto-rotational instability in poorly ionized protostellar accretion disks, with surprising consequences for its saturation and the global self-organization of the magnetic field.

X.4. Ohmic dissipation

X.4.1. *Astrophysical context and basic theory*

Up to now, we've assumed that there is always at least one a species that is infinitely conducting, i.e., there is a species into whose fluid velocity the magnetic field is frozen. We now relax that assumption and, in so doing, introduce a finite conductivity σ that

[21] ... which add $\nabla^2(\nu\boldsymbol{\omega} + \eta\boldsymbol{\omega}_{\rm H})$ to the right-hand side of (X.3.20).

relates the current density $\boldsymbol{j}$ to the electric field $\boldsymbol{E}'$ in the rest frame of the plasma:

$$\boldsymbol{j} = \sigma \boldsymbol{E}'. \tag{X.4.1}$$

I speak of a "plasma rest frame", as I am no longer distinguishing between the fluid velocity of the neutrals and that of the charged species. Finite σ implies finite resistivity η, which in a collisional plasma is driven primarily by the friction force between the ions and electrons (see (X.1.4) with (X.2.3)):

$$\begin{aligned} 0 \approx \boldsymbol{R}_{\mathrm{ei}} - e n_{\mathrm{e}} \boldsymbol{E}' = \frac{m_{\mathrm{e}} n_{\mathrm{e}}}{\tau_{\mathrm{ei}}} (\boldsymbol{u}_{\mathrm{i}} - \boldsymbol{u}_{\mathrm{e}}) - e n_{\mathrm{e}} \boldsymbol{E}' = \frac{m_{\mathrm{e}} n_{\mathrm{e}}}{\tau_{\mathrm{ei}}} \frac{\boldsymbol{j}}{e n_{\mathrm{e}}} - e n_{\mathrm{e}} \boldsymbol{E}' \\ \implies \quad \boldsymbol{j} = \frac{e^2 n_{\mathrm{e}} \tau_{\mathrm{ei}}}{m_{\mathrm{e}}} \boldsymbol{E}' \doteq \sigma \boldsymbol{E}' \doteq \frac{1}{\eta} \boldsymbol{E}'. \end{aligned} \tag{X.4.2}$$

Using Ampére's law, the non-ideal induction equation then reads

$$\frac{\partial \boldsymbol{B}}{\partial t} = \boldsymbol{\nabla} \times (\boldsymbol{u} \times \boldsymbol{B}) - \boldsymbol{\nabla} \times \left(\frac{c^2 \eta}{4\pi} \boldsymbol{\nabla} \times \boldsymbol{B} \right). \tag{X.4.3}$$

The first term is the familiar advection term. The second term might look more familiar to you if we take the resistivity to be spatially uniform and use $\boldsymbol{\nabla} \times (\boldsymbol{\nabla} \times \boldsymbol{B}) = -\nabla^2 \boldsymbol{B}$ to obtain

$$\frac{\partial \boldsymbol{B}}{\partial t} = \boldsymbol{\nabla} \times (\boldsymbol{u} \times \boldsymbol{B}) + \frac{c^2 \eta}{4\pi} \nabla^2 \boldsymbol{B},$$

in which case the resistive term leads to a diffusion equation with diffusion coefficient $c^2\eta/4\pi$. Because this factor of $c^2/4\pi$ is often a nuisance to carry around, I will henceforth absorb this factor into the definition of the resistivity and regard η as a diffusion coefficient (with units of length^2 per time).

The relative importance of the advection and diffusion terms in (X.4.3) is quantified using the dimensionless *magnetic Reynolds number*,

$$\mathrm{Rm} \doteq \frac{UL}{\eta}, \tag{X.4.4}$$

where U and L are characteristic scales for the flow velocity and spatial gradients, respectively. For example,

$$\begin{aligned} \text{liquid metals in industrial contexts:} \quad & \mathrm{Rm} \sim 10^{-3} \ldots 10^{-1}, \\ \text{laboratory plasma-astrophysics experiments:} \quad & \mathrm{Rm} \sim 1 \ldots 100 \text{ (and growing)}, \\ \text{planetary interiors:} \quad & \mathrm{Rm} \sim 100 \ldots 300, \\ \text{solar convective zone:} \quad & \mathrm{Rm} \sim 10^{6} \ldots 10^{9}, \\ \text{warm phase of the interstellar medium:} \quad & \mathrm{Rm} \sim 10^{18}, \\ \text{intracluster medium of galaxy clusters:} \quad & \mathrm{Rm} \sim 10^{29}. \end{aligned}$$

But be careful: even in situations with $\mathrm{Rm} \ggg 1$ on the macroscopic scales, resistivity may still be important if sufficiently small spatial scales are produced, say, by a turbulent cascade or in a forming current sheet. Both of these topics – turbulence and reconnection – will be covered in Parts XI and XII. For now, let's take a quick look at linear theory.

X.4.2. *Wave-driven Ohmic dissipation*

Regarding the linear theory of waves on a static, homogeneous background, there is nothing particularly special about the Ohmic decay of Alfvén waves versus the Ohmic decay of magnetosonic waves. Because the diffusion operator is isotropic, all modes

suffer the same rate of magnetic diffusion, dependent only upon the magnitude of the wavenumber. Indeed, the linearized induction equation is

$$-\mathrm{i}\omega\delta\boldsymbol{B} = \mathrm{i}\boldsymbol{k}\cdot\boldsymbol{B}_0\delta\boldsymbol{u} - \boldsymbol{B}_0\mathrm{i}\boldsymbol{k}\cdot\delta\boldsymbol{u} - k^2\eta\delta\boldsymbol{B}. \tag{X.4.5}$$

In the final term, there is no projection onto the plane perpendicular to $\boldsymbol{k}\times\boldsymbol{B}_0$ (as in ambipolar diffusion), nor is there a $\boldsymbol{k}$-dependent rotation of the magnetic perturbation (as in the Hall effect). There is only a simple, isotropic decay at a rate $k^2\eta$. For a shear Alfvén wave with $\delta\boldsymbol{u} = -(\boldsymbol{k}\cdot\boldsymbol{B}_0/\omega)(\delta\boldsymbol{B}/4\pi\varrho)$, equation (X.4.5) becomes

$$\left[\omega(\omega + \mathrm{i}k^2\eta) - k_\parallel^2 v_\mathrm{A}^2\right]\delta\boldsymbol{B} = 0, \tag{X.4.6}$$

whose solutions satisfy

$$\omega = -\mathrm{i}\frac{k^2\eta}{2} \pm k_\parallel v_\mathrm{A}\sqrt{1 - \left(\frac{k^2\eta}{2k_\parallel v_\mathrm{A}}\right)^2}. \tag{X.4.7}$$

For $\mathrm{Rm} \sim v_\mathrm{A}/(k\eta) \gg 1$, these solutions become $\omega \approx \pm k_\parallel v_\mathrm{A} - \mathrm{i}k^2\eta/2$, i.e., weakly damped shear-Alfvén waves. Magnetic-field fluctuations produce currents, currents are associated with drifts between the charged species, and these interspecies drifts are damped by collisional friction.

X.4.3. *Ohmic dissipation heats plasma*

Think back to grade-school physics when you played with circuits... power is current squared times resistance, $P = RI^2$. In the language of non-ideal MHD, $\boldsymbol{j}\cdot\boldsymbol{E}' = \eta|\boldsymbol{j}|^2$. It is straightforward to show by dotting (X.4.3) with $\boldsymbol{B}/4\pi$ that this is precisely the rate at which the total magnetic energy decays:

$$\frac{\mathrm{d}}{\mathrm{d}t}\int \mathrm{d}V\,\frac{B^2}{8\pi} = \underbrace{-\int \mathrm{d}V\,\boldsymbol{u}\cdot\left(\frac{\boldsymbol{j}}{c}\times\boldsymbol{B}\right)}_{\substack{\text{minus the work of the}\\ \text{Lorentz force on the flow}}} - \underbrace{\frac{c}{4\pi}\oint \mathrm{d}\boldsymbol{S}\cdot(\boldsymbol{E}\times\boldsymbol{B})}_{\text{Poynting flux}} - \underbrace{\int \mathrm{d}V\,\eta|\boldsymbol{j}|^2}_{\substack{\text{Ohmic}\\ \text{dissipation}}}. \tag{X.4.8}$$

This liberated magnetic energy must go somewhere, of course, and it does:

$$\frac{p}{\gamma-1}\frac{\mathrm{D}}{\mathrm{D}t}\ln\frac{p}{\varrho^\gamma} = \eta|\boldsymbol{j}|^2, \tag{X.4.9}$$

Voila. Joule heating.

X.5. A more rigorous derivation of a generalized Ohm's law

This is **optional** material detailing a more rigorous derivation of the non-ideal induction equation.

Consider the (inertia- and pressure-less) force equation for the charged species:

$$0 = q_\alpha n_\alpha\left(\boldsymbol{E} + \frac{\boldsymbol{u}_\alpha}{c}\times\boldsymbol{B}\right) + \boldsymbol{R}_{\alpha\mathrm{n}}, \tag{X.5.1}$$

where $\alpha = \mathrm{i}, \mathrm{e}, \mathrm{g}_+, \mathrm{g}_-$. With the friction force due to collisions with the neutrals given by

$$\boldsymbol{R}_{\alpha\mathrm{n}} = \frac{\varrho_\mathrm{n}}{\tau_{\mathrm{n}\alpha}}(\boldsymbol{u}_\mathrm{n} - \boldsymbol{u}_\alpha) = \frac{\varrho_\alpha}{\tau_{\alpha\mathrm{n}}}(\boldsymbol{u}_\mathrm{n} - \boldsymbol{u}_\alpha),$$

equation (X.5.1) becomes

$$0 = q_\alpha n_\alpha\left(\boldsymbol{E} + \frac{\boldsymbol{u}_\alpha}{c}\times\boldsymbol{B}\right) + \frac{\varrho_\alpha}{\tau_{\alpha\mathrm{n}}}(\boldsymbol{u}_\mathrm{n} - \boldsymbol{u}_\alpha). \tag{X.5.2}$$

We are going to use this system of equations to obtain $\boldsymbol{E}$. We'll only consider elastic collisions with the neutrals, since these are the dominant collisions in most of the parameter space in molecular clouds and their cores. The collision time scales for ion–neutral and electron–neutral collisions were already provided in (X.2.1) and (X.2.2); for collisions between grains with radius $a_{\rm gr}$ and neutrals,

$$\tau_{\rm ng} = \frac{m_{\rm n} n_{\rm n}}{m_{\rm g} n_{\rm g}} \tau_{\rm gn} = 1.09 \, \frac{m_{\rm g} + m_{\rm H_2}}{m_{\rm g} n_{\rm g} \langle \sigma w \rangle_{\rm gH_2}}, \tag{X.5.3}$$

where the mean collisional rate between the grain species and H_2 is

$$\langle \sigma w \rangle_{\rm gH_2} = \pi a_{\rm gr}^2 \left(\frac{8 k_{\rm B} T}{\pi m_{\rm H_2}} \right)^{1/2} \quad \text{for } |\boldsymbol{u}_{\rm n} - \boldsymbol{u}_{\rm g}| < C. \tag{X.5.4}$$

Collisions between, say, ions and electrons can be readily incorporated at the expense of algebraic discomfort. For an inclusion of inelastic grain-grain collisions, see the Appendix of Kunz & Mouschovias (2009).

The derivation begins by shifting to the frame of the neutrals by introducing $\boldsymbol{w}_\alpha \doteq \boldsymbol{u}_\alpha - \boldsymbol{u}_{\rm n}$ and $\boldsymbol{E}_{\rm n} \doteq \boldsymbol{E} + \boldsymbol{u}_{\rm n} \times \boldsymbol{B}/c$, so that (X.5.2) becomes

$$0 = q_\alpha n_\alpha \left(\boldsymbol{E}_{\rm n} + \frac{\boldsymbol{w}_\alpha}{c} \times \boldsymbol{B} \right) - \frac{\varrho_\alpha}{\tau_{\alpha {\rm n}}} \boldsymbol{w}_\alpha. \tag{X.5.5}$$

Using quasi-neutrality, the current density $\boldsymbol{j} = \sum_\alpha q_\alpha n_\alpha \boldsymbol{u}_\alpha = \sum_\alpha q_\alpha n_\alpha \boldsymbol{w}_\alpha$. Thus, if we can write $\boldsymbol{w}_\alpha$ in terms of the electric field $\boldsymbol{E}$, we can invert this equation to obtain $\boldsymbol{E} = \boldsymbol{E}(\boldsymbol{j})$ – a generalized Ohm's law.

To solve (X.5.5) for the relative species velocities $\boldsymbol{w}_\alpha$, start by taking its cross product with $\boldsymbol{B}$ and multiplying by $q_\alpha \tau_{\alpha {\rm n}}/m_\alpha c$ to find

$$0 = \frac{q_\alpha^2 n_\alpha \tau_{\alpha {\rm n}}}{m_\alpha c} \left(\boldsymbol{E}_{\rm n} \times \boldsymbol{B} - \frac{\boldsymbol{w}_{\alpha\perp}}{c} B^2 \right) - q_\alpha n_\alpha \frac{\boldsymbol{w}_\alpha}{c} \times \boldsymbol{B}. \tag{X.5.6}$$

Adding (X.5.6) to (X.5.5) and multiplying by $\tau_{\alpha {\rm n}}/\varrho_\alpha$,

$$0 = \frac{q_\alpha \tau_{\alpha {\rm n}}}{m_\alpha} \boldsymbol{E}_{\rm n} + (\Omega_\alpha \tau_{\alpha {\rm n}})^2 \left(\frac{c}{B} \boldsymbol{E}_{\rm n} \times \hat{\boldsymbol{b}} - \boldsymbol{w}_{\alpha\perp} \right) - \boldsymbol{w}_\alpha. \tag{X.5.7}$$

Note that if the entire plasma is well magnetized, *viz.* $(\Omega_\alpha \tau_{\alpha {\rm n}})^2 \gg 1$ for each α, then the leading-order motion of all species consists of the same $\boldsymbol{E} \times \boldsymbol{B}$ drift.

We solve (X.5.7) by examining its parallel and perpendicular components separately. The former gives

$$\boldsymbol{w}_{\alpha\parallel} = \frac{q_\alpha \tau_{\alpha {\rm n}}}{m_\alpha} \boldsymbol{E}_{{\rm n}\parallel} \quad \Longrightarrow \quad \boldsymbol{j}_\parallel = \left(\sum_\alpha \frac{q_\alpha^2 n_\alpha \tau_{\alpha {\rm n}}}{m_\alpha} \right) \boldsymbol{E}_{{\rm n}\parallel} \doteq \left(\sum_\alpha \sigma_\alpha \right) \boldsymbol{E}_{{\rm n}\parallel} \doteq \sigma_\parallel \boldsymbol{E}_{{\rm n}\parallel}, \tag{X.5.8}$$

where the parallel conductivity $\sigma_\parallel$ has been defined *in situ*. The perpendicular component of (X.5.7) may be rearranged to obtain

$$\boldsymbol{w}_{\alpha\perp} = \frac{q_\alpha \tau_{\alpha {\rm n}}}{m_\alpha} \left[\frac{1}{1 + (\Omega_\alpha \tau_{\alpha {\rm n}})^2} \boldsymbol{E}_{{\rm n}\perp} + \frac{\Omega_\alpha \tau_{\alpha {\rm n}}}{1 + (\Omega_\alpha \tau_{\alpha {\rm n}})^2} \boldsymbol{E}_{\rm n} \times \hat{\boldsymbol{b}} \right]$$

$$\Longrightarrow \quad \boldsymbol{j}_\perp = \left[\sum_\alpha \frac{\sigma_\alpha}{1 + (\Omega_\alpha \tau_{\alpha {\rm n}})^2} \right] \boldsymbol{E}_{{\rm n}\perp} + \left[\sum_\alpha \frac{\sigma_\alpha \Omega_\alpha \tau_{\alpha {\rm n}}}{1 + (\Omega_\alpha \tau_{\alpha {\rm n}})^2} \right] \boldsymbol{E}_{\rm n} \times \hat{\boldsymbol{b}}$$

$$\doteq \sigma_\perp \boldsymbol{E}_{{\rm n}\perp} - \sigma_{\rm H} \boldsymbol{E}_{\rm n} \times \hat{\boldsymbol{b}}, \tag{X.5.9}$$

where the perpendicular conductivity $\sigma_\perp$ and Hall conductivity σ_H have been defined *in situ*. Combining (X.5.8) and (X.5.9), the total current density

$$\boldsymbol{j} = \sigma_\parallel \boldsymbol{E}_{\mathrm{n}\parallel} + \sigma_\perp \boldsymbol{E}_{\mathrm{n}\perp} - \sigma_\mathrm{H} \boldsymbol{E}_\mathrm{n} \times \hat{\boldsymbol{b}}, \tag{X.5.10}$$

which may be inverted to find

$$\boldsymbol{E}_\mathrm{n} = \eta_\parallel \boldsymbol{j}_\parallel + \eta_\perp \boldsymbol{j}_\perp + \eta_\mathrm{H} \boldsymbol{j} \times \hat{\boldsymbol{b}}, \tag{X.5.11}$$

where the parallel, perpendicular, and Hall resistivities are

$$\eta_\parallel \doteq \frac{1}{\sigma_\parallel}, \quad \eta_\perp \doteq \frac{\sigma_\perp}{\sigma_\perp^2 + \sigma_\mathrm{H}^2}, \quad \eta_\mathrm{H} \doteq \frac{\sigma_\mathrm{H}}{\sigma_\perp^2 + \sigma_\mathrm{H}^2}, \tag{X.5.12}$$

respectively. Knowing that Ohmic dissipation affects the total current while ambipolar diffusion affects only the perpendicular component, the Ohmic (O) and ambipolar (A) resistivities are

$$\eta_\mathrm{O} \doteq \eta_\parallel \quad \text{and} \quad \eta_\mathrm{A} \doteq \eta_\perp - \eta_\parallel, \tag{X.5.13}$$

respectively. Thus,

$$\boldsymbol{E} = -\frac{\boldsymbol{u}_\mathrm{n}}{c} \times \boldsymbol{B} + \eta_\mathrm{O} \boldsymbol{j} + \eta_\mathrm{A} \boldsymbol{j}_\perp + \eta_\mathrm{H} \boldsymbol{j} \times \hat{\boldsymbol{b}} \tag{X.5.14}$$

is the generalized Ohm's law. Note that an arbitrary number of species may be included in this expression, so long as their abundance is small enough that they may be considered inertia- and pressure-less and so long as the dominant collisional processes affecting their dynamics involve only the neutrals. (Regarding this final point, the inclusion of inelastic collisions between charged grains, neutral grains, ions, and electrons does not change the basic form of (X.5.14).)

PART XI
Reconnection

Magnetic reconnection refers to the topological rearrangement of magnetic-field lines that converts magnetic energy to plasma energy. In these lecture notes, we will assume that such a rearrangement is facilitated by a spatially constant Ohmic resistivity, as might occur in a well-ionized collisional fluid:

$$\frac{\partial \boldsymbol{B}}{\partial t} = \boldsymbol{\nabla} \times (\boldsymbol{u} \times \boldsymbol{B}) + \eta \nabla^2 \boldsymbol{B}.$$

This assumption is obviously not warranted in hot, dilute astrophysical systems, such as the collisionless solar wind, or in poorly ionized systems, like molecular clouds and pre-stellar cores. But let us assume this anyhow, knowing that (i) the physics of reconnection in even the simplest of systems is surprisingly rich and complex, and (ii) there is a huge amount of literature on all aspects of magnetic reconnection in a wide variety of environments. This part of the lecture notes is not intended as a replacement of that literature, nor a synopsis of current research in the field (particularly in the laboratory and the Earth's magnetosheath). What follows is an incomplete presentation of a few key highlights in the theory of magnetic reconnection, which will hopefully provide enough pedagogical value and inspiration to encourage you to dig into the literature further. For that, I recommend that you start with the excellent review articles by Zweibel & Yamada (2009), Yamada *et al.* (2010), and Loureiro & Uzdensky (2016).

XI.1. Tearing instability

XI.1.1. *Formulation of the problem*

We begin by analyzing the stability of a simple stationary equilibrium in which the magnetic field reverses across $x = 0$:

$$\boldsymbol{B}_0 = B_y(x)\hat{\boldsymbol{y}} + B_{\rm g}\hat{\boldsymbol{z}}, \tag{XI.1.1}$$

where $B_y(x)$ is an odd function and $B_{\rm g} = \text{const}$ denotes the guide field. A oft-employed profile for $B_y(x)$ is the Harris (1962) sheet:

$$B_y(x) = B_{\rm r}\tanh\Big(\frac{x}{a}\Big), \tag{XI.1.2}$$

where $B_{\rm r}$ is the asymptotic value of the reconnecting field and a is the characteristic scale length of the current sheet. Its profile, and the associated current density $j_z = (B_{\rm r}/a)\,\mathrm{sech}^2(x/a)$, are shown in the figure below:

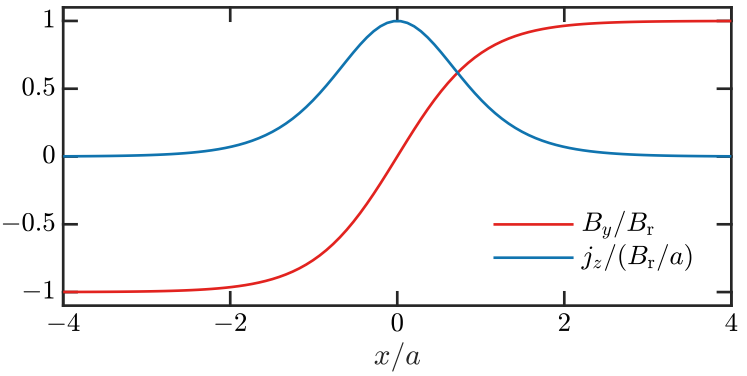

To have a stationary equilibrium, we require something to balance the magnetic pressure gradient implied by (XI.1.1). One option is to allow the thermal pressure in the background to vary so that $P(x) + B_y^2(x)/8\pi = \text{const}$. Another option is to make the guide field also depend upon x and arrange for the total magnetic-field strength to be constant; for example, if the reconnecting field satisfies (XI.1.2), then the guide field should satisfy $B_{\rm g}(x) = B_{\rm r}\,\mathrm{sech}(x/a)$. Either way, the total pressure $P + B^2/8\pi$ in the equilibrium should be constant. We might consider allowing the background magnetic pressure gradient to be unbalanced, which would be fine if the tearing instability were to grow much faster than the current sheet would evolve globally from being initialized out of equilibrium. But the latter would occur on the Alfvén-crossing time of the sheet, $\sim a/v_{\rm A,r}$, which we will find is actually *shorter* than the characteristic growth time of the fastest-growing tearing mode. Many presentations of the tearing instability conveniently omit this point.

We start by linearizing the momentum and non-ideal induction equations about the x-dependent, pressure-balanced equilibrium (cf. (VII.2.1)):

$$\rho\frac{\partial\delta\boldsymbol{u}}{\partial t} = -\boldsymbol{\nabla}\bigg(\delta P + \frac{B_{\rm g}\delta B_z}{4\pi} + \frac{B_y\delta B_y}{4\pi}\bigg) + \frac{B_{\rm g}}{4\pi}\frac{\partial\delta\boldsymbol{B}}{\partial z} + \frac{B_y}{4\pi}\frac{\partial\delta\boldsymbol{B}}{\partial y} + \frac{\mathrm{d}B_y}{\mathrm{d}x}\frac{\delta B_x}{4\pi}\hat{\boldsymbol{y}}, \tag{XI.1.3a}$$

$$\frac{\partial\delta\boldsymbol{B}}{\partial t} = -\delta u_x\frac{\mathrm{d}B_y}{\mathrm{d}x}\hat{\boldsymbol{y}} + B_{\rm g}\frac{\partial\delta\boldsymbol{u}}{\partial z} + B_y\frac{\partial\delta\boldsymbol{u}}{\partial y} + \eta\nabla^2\delta\boldsymbol{B}. \tag{XI.1.3b}$$

Here we have taken the plasma to be incompressible, $\boldsymbol{\nabla}\cdot\delta\boldsymbol{u} = 0$; note further that the mass density ρ in (XI.1.3*a*) refers only to its time-independent background value. As a result, we don't need the continuity equation to close our system of equations, and the energy equation is replaced by the requirement that the divergence of $(1/\rho)\times$ (XI.1.3*a*)

vanish (which constrains δP). We have also ignored resistive diffusion of the background current-sheet profile, which should be fine as long as the growth rate of the tearing mode is $\gg \eta B_\mathrm{r}/a^2$; this will amount to the condition that the Lundquist number of the current sheet, $S_a \doteq v_{\mathrm{A,r}} a/\eta$ where $v_{\mathrm{A,r}} \doteq B_\mathrm{r}/\sqrt{4\pi\rho_0}$ is the Alfvén speed associated with the reconnecting field and ρ_0 is the mass density at the center of the reconnecting layer ($x = 0$), satisfies $S_a^{1/2} \gg 1$.

The next step, which is not at all necessary but is standard and simplifies this first pass through the analysis, is to assume that the perturbations have no z component and do not vary in the z direction, thereby reducing the problem completely to 2D. In this case, the guide field B_g disappears from the analysis, and incompressibility and the solenoidality constraint on the magnetic field allow us to write the perturbed velocity and magnetic field in terms of scalar potentials whose gradients lie in the x-y plane:

$$\delta\boldsymbol{u} = \hat{\boldsymbol{z}} \times \boldsymbol{\nabla}\phi, \quad \frac{\delta\boldsymbol{B}}{\sqrt{4\pi\rho_0}} = \hat{\boldsymbol{z}} \times \boldsymbol{\nabla}\psi, \tag{XI.1.4}$$

Likewise, we may associate the background reconnecting field B_y with a scalar potential: $B_y(x)/\sqrt{4\pi\rho_0} = \Psi'(x)$, where the prime denotes differentiation with respect to x. For example, if B_y is taken to be the Harris-sheet profile (XI.1.2), then $\Psi(x) = v_{\mathrm{A,r}} a \ln[\cosh(x/a)]$. Making these simplifications in (XI.1.3), substituting in (XI.1.4), and simplifying leads to

$$\frac{\partial}{\partial t}\left(\frac{\rho}{\rho_0}\hat{\boldsymbol{z}} \times \boldsymbol{\nabla}\phi\right) = -\boldsymbol{\nabla}\left(\frac{\delta P}{\rho_0} + \Psi'\frac{\partial\psi}{\partial x}\right) + \Psi'\frac{\partial}{\partial y}\hat{\boldsymbol{z}} \times \boldsymbol{\nabla}\psi - \Psi''\frac{\partial\psi}{\partial y}\hat{\boldsymbol{y}}, \tag{XI.1.5a}$$

$$\hat{\boldsymbol{z}} \times \boldsymbol{\nabla}\frac{\partial}{\partial t}\psi = \hat{\boldsymbol{z}} \times \boldsymbol{\nabla}\left(\Psi'\frac{\partial\phi}{\partial y} + \eta\nabla^2\psi\right). \tag{XI.1.5b}$$

We may remove the $\hat{\boldsymbol{z}} \times \boldsymbol{\nabla}$ from both sides of the latter equation without consequence. Finally, to eliminate $\boldsymbol{\nabla}\delta P$ from (XI.1.5a), we take the curl of (XI.1.5a) and use $\boldsymbol{\nabla} \times \boldsymbol{\nabla} = 0$. After the use of some vector identities and rearranging, our final equations are

$$\frac{\rho}{\rho_0}\frac{\partial}{\partial t}\left(\nabla^2\phi + \frac{\mathrm{d}\ln\rho}{\mathrm{d}x}\frac{\mathrm{d}\phi}{\mathrm{d}x}\right) = \Psi'\frac{\partial}{\partial y}\nabla^2\psi - \Psi'''\frac{\partial\psi}{\partial y}, \tag{XI.1.6a}$$

$$\frac{\partial\psi}{\partial t} - \Psi'\frac{\partial\phi}{\partial y} = \eta\nabla^2\psi. \tag{XI.1.6b}$$

The former equation describes the evolution of the fluid vorticity, $\boldsymbol{\nabla} \times \boldsymbol{u} = \hat{\boldsymbol{z}}\nabla^2\psi$.

Because (XI.1.6) are linear in the perturbation amplitudes, and because the background only depends upon x, we are allowed to adopt the solutions

$$\psi(t,x,y) = \psi(x)\,\mathrm{e}^{\mathrm{i}ky+\gamma t} \qquad \text{and} \qquad \phi(t,x,y) = \phi(x)\,\mathrm{e}^{\mathrm{i}ky+\gamma t}, \tag{XI.1.7}$$

where k is the wavenumber and γ is the rate at which the perturbations will grow or decay. In this case, $\partial/\partial t \to \gamma$ and $\partial/\partial y \to \mathrm{i}k$, leaving us with

$$\gamma\frac{\rho}{\rho_0}\left(\frac{\mathrm{d}^2}{\mathrm{d}x^2} - k^2 + \frac{\mathrm{d}\ln\rho}{\mathrm{d}x}\frac{\mathrm{d}}{\mathrm{d}x}\right)\phi = \mathrm{i}k\Psi'\left(\frac{\mathrm{d}^2}{\mathrm{d}x^2} - k^2\right)\psi - \mathrm{i}k\Psi'''\psi, \tag{XI.1.8a}$$

$$\gamma\psi - \mathrm{i}k\Psi'\phi = \eta\left(\frac{\mathrm{d}^2}{\mathrm{d}x^2} - k^2\right)\psi. \tag{XI.1.8b}$$

The trick to solving this set of equations is to realize that, as η tends towards zero, the derivative on the right-hand side of (XI.1.8b) must grow to balance the terms on the left-hand side. In other words, a boundary layer forms about $x = 0$, outside of which the system satisfies the ideal-MHD equations and inside of which the resistivity is important.

The width of this boundary layer is customarily denoted $\delta_{\rm in}$, and much of reconnection theory rests on determining its size given the various attributes of the host plasma. To do so, we will first solve (XI.1.8*a*) and (XI.1.8*b*) in the "outer region", where the resistivity is negligible and the system behaves as though it were ideal. Then they will be solved in the "inner region", where the resistivity dominates and $k \sim a^{-1} \ll \mathrm{d}/\mathrm{d}x \sim \delta_{\rm in}^{-1}$. The two solutions must asymptotically join onto one another; this matching, along with boundary conditions at $x = 0$ and $\pm\infty$, will determine the full solution.

Before proceeding with this program, it will be advantageous to define the resistive and Alfvén timescales,

$$\tau_\eta \doteq \frac{a^2}{\eta} \quad \text{and} \quad \tau_{\rm A} \doteq \frac{1}{ka\Psi_0''(0)} = \frac{1}{kv_{\rm A,r}}, \tag{XI.1.9}$$

respectively. We further assume $\tau_\eta^{-1} \ll \gamma \ll \tau_{\rm A}^{-1}$, i.e. the tearing mode grows faster than it takes for the entirety of the current sheet to resistively diffuse but slower than it takes for an Alfvén wave to cross k^{-1}. Physically, this implies that the outer solution results from neglecting the plasma's inertia and Ohmic resistivity.

XI.1.2. *Outer equation*

Adopting the ordering $\tau_\eta^{-1} \ll \gamma \ll \tau_{\rm A}^{-1}$, equations (XI.1.8*a*) and (XI.1.8*b*) reduce to

$$0 = \left(\frac{\mathrm{d}^2}{\mathrm{d}x^2} - k^2 - \frac{\Psi'''}{\Psi'}\right)\psi_{\rm out} \quad \text{and} \quad \phi_{\rm out} = \frac{\gamma}{\mathrm{i}k\Psi'}\psi_{\rm out}. \tag{XI.1.10}$$

Note that $\Psi'''/\Psi' = B_y''/B_y$ measures the gradient of the current density, and so different current-sheet profiles will result in different solutions to (XI.1.10). Regardless of the exact current-sheet profile, however, both $\phi_{\rm out}$ and $\psi_{\rm out}$ must tend to zero as $x \to \pm\infty$. Also, since the y-component of the perturbed magnetic field must reverse direction at $x = 0$, $\psi_{\rm out}$ must have a discontinuous derivative there, corresponding to a singular current. Indeed, it is this discontinuity that characterizes the free energy available to reconnect, quantified by the tearing-instability parameter

$$\Delta' \doteq \frac{1}{\psi_{\rm out}(0)}\frac{\mathrm{d}\psi_{\rm out}}{\mathrm{d}x}\bigg|_{-0}^{+0}, \tag{XI.1.11}$$

and that ultimately warrants consideration of a resistive inner layer.

XI.1.3. *Inner equation*

In the inner region where $k \ll \mathrm{d}/\mathrm{d}x \sim \delta_{\rm in}^{-1}$, the dominant terms in (XI.1.8*a*) and (XI.1.8*b*) are

$$\gamma\frac{\rho}{\rho_0}\frac{\mathrm{d}^2\phi_{\rm in}}{\mathrm{d}x^2} = \mathrm{i}k\Psi'\frac{\mathrm{d}^2\psi_{\rm in}}{\mathrm{d}x^2}, \tag{XI.1.12}$$

$$\gamma\psi_{\rm in} - \mathrm{i}k\phi_{\rm in}\Psi' = \eta\frac{\mathrm{d}^2\psi_{\rm in}}{\mathrm{d}x^2}. \tag{XI.1.13}$$

Note that ρ, whose gradient length scale is a, may be taken as constant over the inner-layer thickness $\delta_{\rm in} \ll a$, and so the pre-factor ρ/ρ_0 in (XI.1.12) is $\simeq$1. These equations may be solved analytically provided some amenable form of Ψ'. Because we are deep within the current sheet, the leading-order term in a Taylor expansion will suffice, *viz.*, $\Psi' \approx \Psi''(0)x = v_{\rm A,r}(x/a)$. Then (XI.1.12) and (XI.1.13) may be straightforwardly combined

to obtain

$$\frac{\mathrm{d}^2\psi_{\rm in}}{\mathrm{d}x^2} = -\left[\frac{\gamma}{k\Psi''(0)}\right]^2 \frac{1}{x}\frac{\mathrm{d}^2}{\mathrm{d}x^2}\left[\frac{1}{x}\left(1-\frac{\eta}{\gamma}\frac{\mathrm{d}^2}{\mathrm{d}x^2}\right)\psi_{\rm in}\right]. \tag{XI.1.14}$$

With some effort, this equation can actually be solved for $\psi_{\rm in}$ analytically. I'll show you how below. But even without that effort, equation (XI.1.14) may be used to estimate the width of the boundary layer, $\delta_{\rm in}$:

$$1 \sim (\gamma a \tau_{\rm A})^2 \frac{\eta}{\gamma \delta_{\rm in}^4} \quad \Longrightarrow \quad \frac{\delta_{\rm in}}{a} \sim \left(\frac{\gamma \tau_{\rm A}^2}{\tau_\eta}\right)^{1/4}. \tag{XI.1.15}$$

Note that $\delta_{\rm in}$ depends on k – each tearing mode k has a different boundary-layer width; because of this, each k will correspond to a different Δ'.

Normalizing lengthscales to $\delta_{\rm in}$ by introducing $\xi \doteq x/\delta_{\rm in}$, equation (XI.1.14) may be written as

$$\frac{\mathrm{d}^2\psi_{\rm in}}{\mathrm{d}\xi^2} = -\frac{1}{\xi}\frac{\mathrm{d}^2}{\mathrm{d}\xi^2}\left[\frac{1}{\xi}\left(\Lambda - \frac{\mathrm{d}^2}{\mathrm{d}\xi^2}\right)\psi_{\rm in}\right], \tag{XI.1.16}$$

where the eigenvalue $\Lambda \doteq \gamma^{3/2}\tau_{\rm A}\tau_\eta^{1/2} = \gamma\delta_{\rm in}^2/\eta$ is the growth rate of the tearing mode normalized by the rate of resistive diffusion across a layer of width $\delta_{\rm in}$. Provided we can solve (XI.1.16), the solution $\psi_{\rm in}$ must be matched onto the outer solution $\psi_{\rm out}$. This is done by equating the discontinuity in $\psi_{\rm out}$, quantified by Δ' (see (XI.1.11)), to the total change in $\mathrm{d}\psi_{\rm in}/\mathrm{d}x$ across the inner region, *viz.*,

$$\Delta' = \frac{2}{\delta_{\rm in}}\int_0^1 \mathrm{d}\xi\, \frac{1}{\psi_{\rm in}(0)}\frac{\mathrm{d}^2\psi_{\rm in}}{\mathrm{d}\xi^2}.$$

(The factor of 2 is because the solution is odd, and so the total change across the $x = 0$ surface is twice the change measured for $x > 0$.) The upper limit on the integral can be extended to $+\infty$ by committing only a $\sim$10% error:

$$\Delta' = \frac{2}{\delta_{\rm in}}\int_0^\infty \mathrm{d}\xi\, \frac{1}{\psi_{\rm in}(0)}\frac{\mathrm{d}^2\psi_{\rm in}}{\mathrm{d}\xi^2}. \tag{XI.1.17}$$

So, find $\psi(\xi)$ by solving the inner equation (XI.1.16), compute the integral in (XI.1.17), and invert the answer to obtain the growth rate in terms of Δ'.

Before carrying out that program, it will be useful to further simply (XI.1.16) by introducing

$$\chi(\xi) \doteq \xi^2 \frac{\mathrm{d}}{\mathrm{d}\xi}\left[\frac{\psi_{\rm in}(\xi)}{\xi}\right], \tag{XI.1.18}$$

so that

$$\frac{\mathrm{d}}{\mathrm{d}\xi}\left[\frac{\mathrm{d}}{\mathrm{d}\xi}\left(\frac{1}{\xi^2}\frac{\mathrm{d}\chi}{\mathrm{d}\xi}\right) - \left(1+\frac{\Lambda}{\xi^2}\right)\chi\right] = 0. \tag{XI.1.19}$$

Integrating this equation once and, for reasons that will eventually become apparent, setting the integration constant to $-\chi_\infty$, we find

$$\xi^2\frac{\mathrm{d}}{\mathrm{d}\xi}\left(\frac{1}{\xi^2}\frac{\mathrm{d}\chi}{\mathrm{d}\xi}\right) - \left(\xi^2+\Lambda\right)\chi = -\chi_\infty\xi^2. \tag{XI.1.20}$$

Once this equation is solved, the inner solution is obtained using (cf. (XI.1.18))

$$\psi_{\rm in}(\xi) = -\xi\int_\xi^\infty \mathrm{d}x\,\frac{\chi(x)}{x^2} = -\xi\int_\xi^\infty \mathrm{d}x\,\frac{\chi'(x)}{x} - \chi(\xi), \tag{XI.1.21}$$

which may then be plugged into (XI.1.17) to compute Δ'.

XI.1.4. *Approximate solutions*

There are a few ways to solve (XI.1.10) and (XI.1.20), none of which are particularly obvious. However, it's possible to obtain scaling laws for Δ' and the tearing-mode growth rate γ without actually doing so. In fact, the answers obtained in this way differ from those obtained by a more mathematically rigorous solution (see §XI.1.5) by only order-unity coefficients. Nice.

We start with (XI.1.10), the outer equation. With some knowledge that the fastest-growing modes occur at long wavelengths ($ka \ll 1$), we can make some progress by simply dropping the middle term in (XI.1.10). Then, so long as B_y varies faster within $|x| \lesssim a$ than it does at $|x| \gg a$, we can estimate

$$\Delta' \sim \frac{1}{ka^2}. \tag{XI.1.22}$$

(This scaling is exact for the Harris-sheet profile, solved for in §XI.1.5.) One may formalize this estimate somewhat (Loureiro *et al.* 2007, 2013) by quantifying what "varies faster within $|x| \lesssim a$ than it does at $|x| \gg a$" means, but not much is gained intuitively by going that route, and the estimate (XI.1.22) will suffice.

As for the inner equation (XI.1.16), we know from (XI.1.20) that, whatever its solution, $\psi_{\rm in}(\xi)$ only depends on the parameter Λ. Thus, equation (XI.1.17) may be written as

$$\Delta' \delta_{\rm in} = f(\Lambda) \tag{XI.1.23}$$

for some function $f(\Lambda)$. Combining (XI.1.22) and (XI.1.23) yields an expression for the growth rate, provided we can invert $f(\Lambda)$. Fortunately, we can, at least in certain limits.

The first limit is the so-called "constant-ψ approximation" or "FKR regime", which corresponds to $f(\Lambda) \sim \Lambda \ll 1$ (Furth *et al.* 1963). Then (XI.1.23) gives $\Delta' \delta_{\rm in} \sim \Lambda$, so that

$$\boxed{\gamma_{\rm FKR} \sim \tau_{\rm A}^{-2/5} \tau_\eta^{-3/5} (\Delta' a)^{4/5}, \quad \frac{\delta_{\rm in}}{a} \sim \left(\frac{\tau_{\rm A}}{\tau_\eta}\right)^{2/5} (\Delta' a)^{1/5}} \tag{XI.1.24}$$

With $\Delta' \sim 1/ka^2$ (see (XI.1.22)), these become

$$\frac{\gamma_{\rm FKR}}{v_{\rm A,r}/a} \sim (ka)^{-2/5} S_a^{-3/5}, \quad \frac{\delta_{\rm in}}{a} \sim (ka)^{-3/5} S_a^{-2/5}, \tag{XI.1.25}$$

where we have introduced the *Lundquist number*

$$S_a \doteq \frac{a v_{\rm A,r}}{\eta}. \tag{XI.1.26}$$

Note that longer wavelengths have faster growth rates (the divergence as $k \to 0$ will be cured in the "Coppi" regime, in which the small-Δ' assumption breaks down – see below). This approximation results from setting $\psi_{\rm in} = \psi_{\rm in}(0)$ on the left-hand side of (XI.1.13), so that the inner equation (XI.1.13) becomes

$$\gamma \psi_{\rm in}(0) - {\rm i} k \phi_{\rm in} \Psi_0''(0) x = \eta \frac{{\rm d}^2 \psi_{\rm in}}{{\rm d}x^2}, \tag{XI.1.27}$$

and so (cf. (XI.1.20))

$$\xi^2 \frac{\rm d}{{\rm d}\xi} \left(\frac{1}{\xi^2} \frac{{\rm d}\chi}{{\rm d}\xi} \right) - \xi^2 (\chi - \chi_\infty) = -\Lambda \psi_{\rm in}(0). \tag{XI.1.28}$$

In effect, we are assuming that the resistive diffusion time across the inner-layer thickness is much shorter than the instability growth time, i.e., $\gamma \ll \eta/\delta_{\rm in}^2$, so that $\psi_{\rm in}$ can be

approximated as constant on the dynamical time scale. Using (XI.1.25) in this inequality requires $S_a \gg (\Delta' a)^4$. This is sometimes called the "small-Δ' regime".

The second limit is the "Coppi regime" or "large-Δ' regime", in which the constant-ψ approximation breaks down and $\gamma \sim \eta/\delta_{\rm in}^2$. This occurs for $\Lambda \sim 1^-$, at which $f(\Lambda) \to \infty$. The growth rate then becomes independent of Δ' and we have

$$\boxed{\gamma_{\rm Coppi} \sim \tau_{\rm A}^{-2/3}\tau_\eta^{-1/3}\,, \quad \frac{\delta_{\rm in}}{a} \sim \left(\frac{\tau_{\rm A}}{\tau_\eta}\right)^{1/3}} \tag{XI.1.29}$$

In terms of the tearing-mode wavenumber k and the Lundquist number S_a,

$$\frac{\gamma_{\rm Coppi}}{v_{\rm A,r}/a} \sim (ka)^{2/3} S_a^{-1/3}\,, \quad \frac{\delta_{\rm in}}{a} \sim (ka)^{-1/3} S_a^{-1/3}. \tag{XI.1.30}$$

In this limit, the shorter wavelengths have faster growth rates, opposite to the FKR scaling (XI.1.25). This suggests a maximally growing mode, whose growth rate $\gamma_{\rm max}$ and wavenumber $k_{\rm max}$ may be estimated by matching the FKR solution (XI.1.25) to the Coppi one (XI.1.30):

$$\gamma_{\rm FKR} \sim \gamma_{\rm Coppi} \quad \Longrightarrow \quad k_{\rm max} a \sim S_a^{-1/4}\,, \quad \frac{\gamma_{\rm max}}{v_{\rm A,r}/a} \sim S_a^{-1/2}\,, \quad \frac{\delta_{\rm in}}{a} \sim S_a^{-1/4}. \tag{XI.1.31}$$

Note that the FKR (Coppi) regime corresponds to $k > k_{\rm max}$ ($k < k_{\rm max}$).

Of course, all of these scalings make sense only if the modes can fit into the current sheet, i.e., $kL \gtrsim 1$, where L is the length of the current sheet. For the maximally growing mode to be viable thus requires a current-sheet aspect ratio of $L/a \gtrsim S_a^{1/4}$. If this inequality is not satisfied, then the fastest-growing mode will be the FKR mode (XI.1.25) with the smallest possible allowed wavenumber, $kL \sim 1$. Thus, low-aspect-ratio sheets with $L/a \ll S_a^{1/4}$ will develop tearing perturbations comprising just one or two islands; the high-aspect-ratio sheets, in which the Coppi regime is accessible, will instead spawn whole chains comprising $\sim k_{\rm max} L$ islands.

XI.1.5. *Exact solution for a Harris sheet*

This is **optional** material detailing a more rigorous derivation of the tearing-mode dispersion relation.

The solutions obtained in the last section should suffice for this course. But with some (read: a lot of) effort, one can be more precise. For that task, let us adopt the equilibrium flux function $\Psi_0 = a v_{\rm A,r} \ln[\cosh(x/a)]$, corresponding to the Harris-sheet profile (XI.1.2). Then (XI.1.10) becomes

$$\left[\frac{{\rm d}^2}{{\rm d}x^2} - k^2 + \frac{2}{a^2}\,{\rm sech}^2\!\left(\frac{x}{a}\right)\right]\psi_{\rm out} = 0 \quad \text{and} \quad \phi_{\rm out} = -{\rm i}\gamma\tau_{\rm A}\coth\!\left(\frac{x}{a}\right)\psi_{\rm out}. \tag{XI.1.32}$$

The former equation can be solved by changing variables to $\mu = \tanh(x/a)$, so that ${\rm sech}^2(x/a) = (1-\mu^2)^{-1}$ and

$$\frac{\rm d}{{\rm d}x} = \frac{1-\mu^2}{a}\frac{\rm d}{{\rm d}\mu}, \quad \frac{{\rm d}^2}{{\rm d}x^2} = \frac{1-\mu^2}{a}\frac{\rm d}{{\rm d}\mu}\frac{1-\mu^2}{a}\frac{\rm d}{{\rm d}\mu}.$$

Then (XI.1.32) becomes

$$\left[\frac{\rm d}{{\rm d}\mu}(1-\mu^2)\frac{\rm d}{{\rm d}\mu} + 2 - \frac{k^2a^2}{1-\mu^2}\right]\psi_{\rm out} = 0 \quad \text{and} \quad \phi_{\rm out} = -{\rm i}\gamma\tau_{\rm A}\frac{\psi_{\rm out}}{\mu}, \tag{XI.1.33}$$

the first of which you might recognize as the associated Legendre equation

$$\left[\frac{\mathrm{d}}{\mathrm{d}\mu}(1-\mu^2)\frac{\mathrm{d}}{\mathrm{d}\mu}+\ell(\ell+1)-\frac{m^2}{1-\mu^2}\right]P_\ell^m(\mu)=0$$

with $\ell=1$ and $m=ka$. Transforming the boundary conditions $\psi(\pm\infty)=0$ into $\psi(\mu=\pm1)=0$ and enforcing $\psi(\mu)=\psi(-\mu)$, the solution to (XI.1.33) is thus

$$\psi_{\rm out}=C_{1m}P_1^m(\mu), \tag{XI.1.34}$$

with $C_{1m}=$ const. If you can't picture in your head what the first associated Legendre polynomial with non-integer m looks like – I know I can't – you may like to know that the outer solution may be equivalently written as

$$\psi_{\rm out}(x)=C'_{1m}\mathrm{e}^{-kx}\left[1+\frac{1}{ka}\tanh\left(\frac{x}{a}\right)\right] \tag{XI.1.35}$$

for $\xi\geqslant0$, where $C'_{1m}=$ const. (Note that $\psi_{\rm out}(-\xi)=\psi_{\rm out}(\xi)$.) Visually:

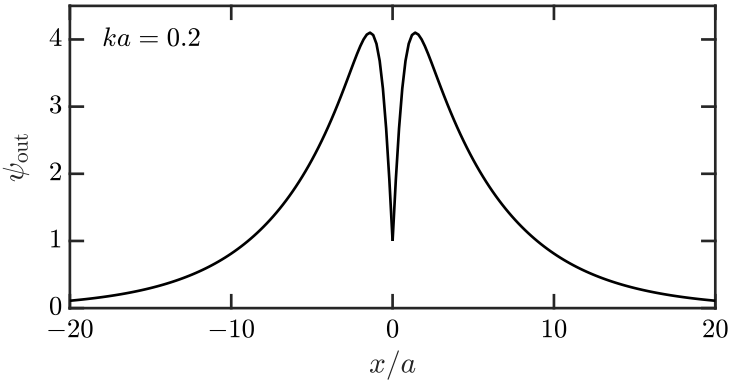

Recall that Δ' measures the discontinuity of $\mathrm{d}\psi_{\rm out}/\mathrm{d}x$ at $x=0$ (see (XI.1.11)). Restoring the $\cos(ky)$ dependence of $\psi_{\rm out}$ provides the following isocontours of $\psi_{\rm out}$, which are equivalently the magnetic-field lines:

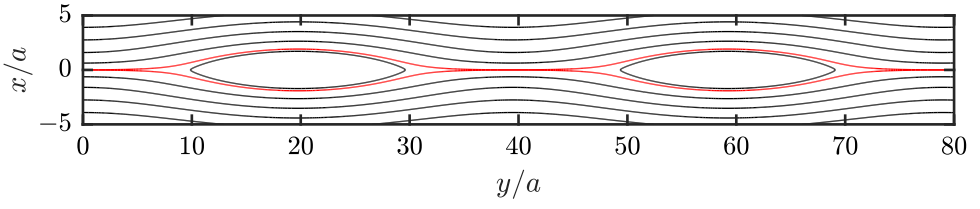

For ease of visualization, I plotted two y wavelengths using $ka=(2\pi)^{-1}$ and set the tearing-mode amplitude to 0.2 (which in a realistic system would be well outside of the linear regime). The red line is called the *separatrix*; it serves as the boundary between the inside of each magnetic island and the surrounding field lines, and runs through the "X-points" that lie at $y=0,2\pi/k,4\pi/k$, etc. To determine the island width w, we follow the isocontour that starts from the X-point at, say, $(x,y)=(0,0)$ and set its x location when $y=\pi/k$ equal to the half-width $w/2$:

$$\cancel{\Psi(0)}^{0}+\underbrace{\psi(0,0)}_{=\psi_{\rm out}(0)}=\Psi(w/2)+\psi(w/2,\pi/k)\approx\frac{1}{2}\Psi''(0)\frac{w^2}{4}+\underbrace{\psi(w/2,\pi/k)}_{=-\psi_{\rm out}(w/2)},$$

where we've used $\cos(\pi) = -1$ and approximated $\Psi(x)$ a distance x away from the neutral line by its Taylor expansion, $(1/2)\Psi''(0)x^2$. If we then take ψ to be approximately constant within the island, *viz.* $\psi_{\rm out}(w/2) \approx \psi_{\rm out}(0)$, we find that island width satisfies

$$w \approx 4\sqrt{\frac{\psi(0)}{\Psi''(0)}}.$$

Note that $\Psi''(0) = v_{\rm A,r}/a$ for the Harris-sheet profile. Solving for the mode amplitude C_{1m} (or C'_{1m}) requires matching onto the inner solution, but even before doing that we can compute Δ' using $\psi_{\rm out} \propto P_1^m(\mu)$ in (XI.1.11):[22]

$$\begin{aligned}\Delta' a &= \frac{1}{P_1^m(0)}\frac{\mathrm{d}P_1^m}{\mathrm{d}\mu}\bigg|_{-0}^{+0} = \frac{2}{P_1^m(0)}\frac{\mathrm{d}P_1^m}{\mathrm{d}\mu}\bigg|_{\mu=0} = 2\left(\frac{1}{m} - m\right)\\ &= 2\left(\frac{1}{ka} - ka\right).\end{aligned} \tag{XI.1.36}$$

Note that $\Delta' > 0$ requires $ka < 1$ – any unstable mode must have an extent at least as large as the current-sheet thickness. This places an upper limit on the wavenumber of the FKR modes (XI.1.25).

As for the inner equation, let us use its compact form (XI.1.20), repeated here for convenience:

$$\xi^2\frac{\mathrm{d}}{\mathrm{d}\xi}\left(\frac{1}{\xi^2}\frac{\mathrm{d}\chi}{\mathrm{d}\xi}\right) - \Big(\xi^2 + \Lambda\Big)\chi = -\chi_\infty\xi^2, \tag{XI.1.37}$$

where $\Lambda \doteq \gamma^{3/2}\tau_{\rm A}\tau_\eta^{1/2}$. There are a few ways to solve (XI.1.37), none of which are particularly obvious. One way, explained in Appendix A of Ara *et al.* (1978), is as follows. Write

$$\chi = \chi_\infty\sum_{n=0}^{\infty} a_n L_n^{(-3/2)}(\xi^2)\,\mathrm{e}^{-\xi^2/2}, \tag{XI.1.38}$$

where $L_n^\alpha(z)$ are the associated Laguerre (or "Sonine") polynomials satisfying

$$z\frac{\mathrm{d}^2L_n^{(\alpha)}}{\mathrm{d}z^2} + (\alpha + 1 - z)\frac{\mathrm{d}L_n^{(\alpha)}}{\mathrm{d}z} + nL_n^{(\alpha)} = 0. \tag{XI.1.39}$$

Substitute this decomposition into (XI.1.20) and use the recursion relations

$$\begin{aligned}\frac{\mathrm{d}L_n^\alpha}{\mathrm{d}z} &= -L_{n-1}^{\alpha+1}(z) \text{ if } 1 \leqslant n \ (= 0 \text{ otherwise}),\\ nL_n^{(-3/2)}(z) &= -\left(z + \frac{1}{2}\right)L_{n-1}^{(-1/2)}(z) - zL_{n-2}^{(1/2)}(z),\end{aligned}$$

to obtain

$$\sum_{n=0}^{\infty} a_n\,\xi^{-2}\,\mathrm{e}^{-\xi^2/2}L_n^{(-3/2)}(\xi^2)\big(4n + \Lambda - 1\big) = 1. \tag{XI.1.40}$$

Multiply this by $\mathrm{e}^{-\xi^2/2}\xi^{-1}L_m^{-3/2}$, integrate, and use the orthogonality relation

$$\int_0^\infty \mathrm{d}z\,\mathrm{e}^{-z}z^\alpha L_m^\alpha L_n^\alpha = \delta_{mn}\frac{\Gamma(n+\alpha+1)}{\Gamma(n+1)}$$

[22] See https://dlmf.nist.gov/14.5 for information on $P_\ell^m(0)$ and $\mathrm{d}P_\ell^m/\mathrm{d}\mu|_{\mu=0}$.

to find that

$$\begin{aligned} a_n \frac{(n-3/2)!}{n!}(4n+\Lambda-1) &= \int_0^\infty \mathrm{d}z\, z^{-1/2}\mathrm{e}^{-z/2} L_n^{-3/2} \\ &= \int_0^\infty \mathrm{d}z\, z^{-1/2}\mathrm{e}^{-z/2}(L_n^{-1/2} - L_{n-1}^{-1/2}) \\ &= \sqrt{2}(-1)^n \left[\frac{\Gamma(n+1/2)}{\Gamma(n+1)} + \frac{\Gamma(n-1/2)}{\Gamma(n)}\right] \\ \implies \quad a_n &= \frac{(-1)^n}{\sqrt{2}} \frac{4n-1}{4n+\Lambda-1}. \end{aligned}$$

Thus, equation (XI.1.38) becomes[23]

$$\chi = \frac{\chi_\infty}{\sqrt{2}}\,\mathrm{e}^{-\xi^2/2} \sum_{n=0}^{\infty} (-1)^n L_n^{-3/2}(\xi^2) \frac{4n-1}{4n+\Lambda-1} = \xi^2 \frac{\mathrm{d}}{\mathrm{d}\xi}\frac{\psi_{\mathrm{in}}}{\xi}, \tag{XI.1.41}$$

which may be solved for ψ_{in} following (XI.1.21).

Actually doing so and plugging the solution into (XI.1.17) to compute Δ' ain't easy, as it involves a lot of non-standard math. I may LaTeX those steps up one day, but, for now, I'll just skip to the answer:

$$\Delta'\delta_{\mathrm{in}} = f(\Lambda) \doteq \frac{\pi}{2}\frac{\Gamma[(\Lambda+3)/4]}{\Gamma[(\Lambda+5)/4]}\frac{\Lambda}{1-\Lambda}. \tag{XI.1.42}$$

This is an implicit equation for Γ, which may be solved numerically (see figure below). But it's possible to recover our approximate results (XI.1.24) and (XI.1.29) in their respective limits. For $\Lambda \ll 1$,

$$f(\Lambda) \approx \frac{\pi}{2}\frac{\Gamma(3/4)}{\Gamma(5/4)}\Lambda \simeq 2.124\,\Lambda \quad \implies \quad \gamma \approx 0.547\,\tau_{\mathrm{A}}^{-2/5}\tau_\eta^{-3/5}(\Delta' a)^{4/5}. \tag{XI.1.43}$$

Our approximate result for this FKR regime, equation (XI.1.24), is off by only a factor of 0.547 – not too bad. For $\Lambda = 1^-$,

$$f(\Lambda) \approx \frac{\pi}{2}\frac{\Gamma(1)}{\Gamma(3/2)}\frac{1}{1-\Lambda} = \frac{\sqrt{\pi}}{1-\Lambda} \quad \implies \quad \gamma \approx \tau_{\mathrm{A}}^{-2/3}\tau_\eta^{-1/3} - \mathcal{O}\left(\frac{k v_{\mathrm{A,r}}}{\Delta' a}\right). \tag{XI.1.44}$$

This matches our Coppi-regime estimate, (XI.1.29). These asymptotic solutions actually do rather well across the full range of wavenumbers:

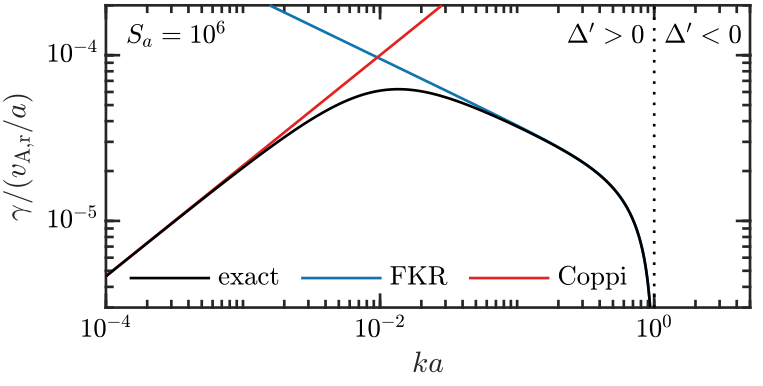

[23] Note that we cannot use the expansion (XI.1.38) if $\Lambda = 1$.

It also appears that we are well justified in estimating the maximally growing mode by matching the FKR and Coppi expressions (as in (XI.1.31)). These regimes also occur where we anticipated, with $f(\Lambda) = \Delta'\delta_{\rm in}$ being $\ll 1$ ($\gg 1$) in the FKR (Coppi) regime:

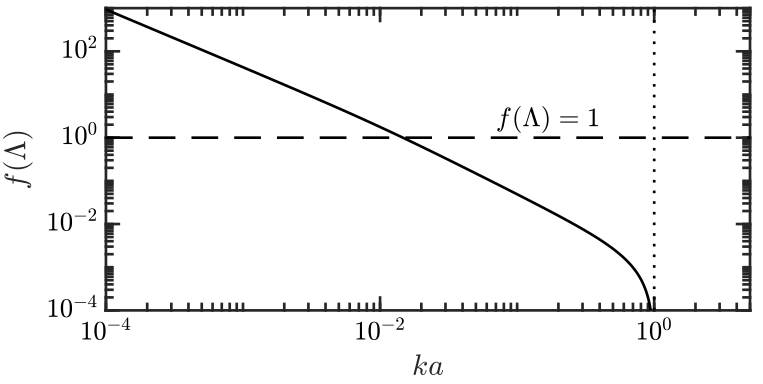

Thus the "small-Δ'" / "large-Δ'" phraseology.

XI.1.6. *Nonlinear evolution and X-point collapse*

How long does this linear phase, in which the tearing modes grow exponentially, last? That depends on the Δ' of the mode. If the Coppi regime is accessible – i.e., if the maximally growing wavenumber $k_{\rm max}$ (see (XI.1.31)) that results in $\Delta'\delta_{\rm in} \gtrsim 1$ also satisfies $k_{\rm max}a < 1$ – then X-point collapse is essentially instantaneous once the width $w = 4\sqrt{-\psi(0)/\Psi_0''(0)}$ of the exponentially growing island reaches $\delta_{\rm in}$. At this moment, $w\Delta'$ is also $\sim$1, and so the deformations of the current sheet by the nonlinear islands have driven the regions between the X-points to marginal stability. If the fastest-growing available modes are instead FKR-like, then there is a gap between when the nonlinear regime begins ($w \sim \delta_{\rm in}$) and when it ends ($w\Delta' \sim 1$). In between occurs a period of secular growth called the Rutherford (1973) stage, in which $\dot{w} \sim \eta\Delta'(w)$, the argument of Δ' indicating that the logarithmic derivative of $\psi_{\rm out}$ is to be taken across the island (rather than across the inner-layer width).[24] During this slow growth stage, the initially unstable current profile flattens and conditions are set up for the collapse of the inter-island X points (Waelbroeck 1993; Loureiro *et al.* 2005). The figure below, adapted from Loureiro *et al.* (2005), shows contours of ψ at the beginning of X-point collapse (left) and the formation of an embedded, high-aspect ratio current sheet (right):

[24] Rutherford (1973) did not predict a saturation amplitude for the algebraically growing nonlinear tearing mode. Subsequent papers by Militello & Porcelli (2004) and Escande & Ottaviani (2004) ("POEM") derived a modified equation for the Rutherford stage, $\dot{w} \sim \eta(\Delta' - \alpha w/a^2)$ with α being a constant dependent upon the initial current-sheet geometry, thus predicting a saturated amplitude $w \sim \Delta' a^2$.

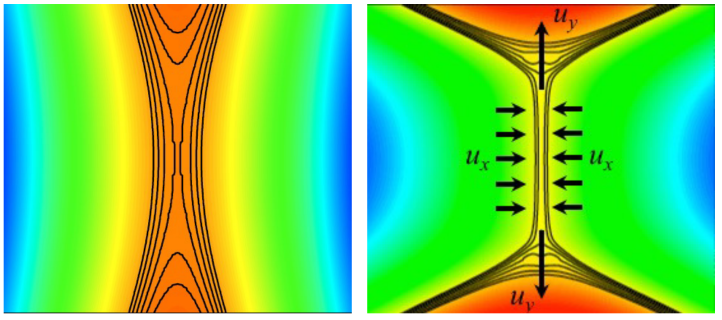

This current sheet is reminiscent of the now-famous Sweet–Parker configuration.

XI.2. Sweet–Parker reconnection

Peter Sweet (Sweet 1958) and Eugene Parker (Parker 1957) provided the first quantitative model of magnetic reconnection, envisioning it to be a steady-state process in which a two-dimensional, incompressible flow advects magnetic flux into a current sheet of length L and thickness $\delta_{\rm SP} \ll L$. It is through the latter dimension that plasma, accelerated in the direction along the current sheet by magnetic tension, is expelled in the form of an outflow:

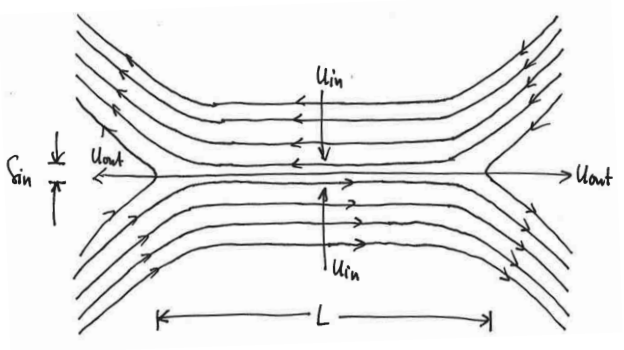

Steady state is achieved by (i) balancing the inflow velocity $u_{\rm in}$ and the outflow velocity $u_{\rm out}$ using mass conservation, $u_{\rm in}L \sim u_{\rm out}\delta_{\rm SP}$; (ii) balancing the advective and resistive electric fields so that all the inflowing magnetic flux is resistively destroyed, $u_{\rm in}v_{\rm A,r} \sim \eta j_z \sim \eta v_{\rm A,r}/\delta_{\rm SP}$; and (iii) stipulating that the outflows are Alfvénic, $u_{\rm out} \sim v_{\rm A,r}$. (This final ingredient follows from conservation of energy, with the magnetic energy flux into the sheet balancing the kinetic energy flux out of the sheet.) The result is

$$\frac{u_{\rm in}}{v_{\rm A,r}} \sim \frac{\delta_{\rm SP}}{L} \sim \left(\frac{v_{\rm A,r}L}{\eta}\right)^{-1/2} \doteq S^{-1/2}, \qquad \text{(XI.2.1)}$$

where S is the Lundquist number (using the current-sheet length L as the normalizing lengthscale). In the solar corona, $S \sim 10^{12}$–10^{14}; in the Earth's magnetotail, $S \sim 10^{15}$–10^{16}; and in a modern tokamak like JET, $S \sim 10^{6}$–10^{8}. You can see that $S^{-1/2}$ is typically a very small number, and so Sweet–Parker (SP) reconnection is *slow* – not as slow as pure resistive diffusion, but slow in the sense that the reconnection rate $\tau_{\rm r}^{-1} \doteq u_{\rm in}/L \sim (v_{\rm A,r}/L)\, S^{-1/2}$ tends towards zero as $S \to \infty$. For example, the SP model predicts that a reconnection-driven solar flare in a $S \sim 10^{14}$ part of the solar corona should last ∼2 mths; instead, flares are observed to last between 15 min and 1 hr. Not good.

This mismatch between theory and observation was immediately appreciated, and

spawned several attempts to formulate a model in which fast reconnection occurs. The culprit is the smallness of the resistive layer: the fact that it must be thin enough to make the current density large also means that the outflowing mass must pass through too small of an opening. One particularly notorious attempt to circumvent this constraint was proposed by Petschek (1964) (later revisited and amended by Kulsrud (2001)), in which the current-sheet length L was shortened at the expense of introducing four standing slow-mode shocks emanating from a central diffusion region:

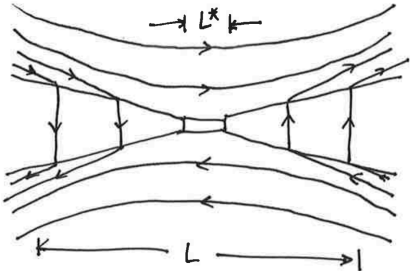

The result is a logarithmic dependence of the reconnection rate on S, $\tau_{\rm r}^{-1} \sim (v_{\rm A,r}/L)\ln S$. Unfortunately, no convincing evidence for this type of reconnection has been found (Park *et al.* 1984; Biskamp 1986; Uzdensky & Kulsrud 2000; Malyshkin *et al.* 2005; Loureiro *et al.* 2005), even when Petschek's solution is used as an initial condition (Uzdensky & Kulsrud 2000).[25]

It is worth emphasizing that the failure of the SP model to explain magnetic reconnection as it occurs in nature is not due to any shortcoming of the theory itself. There are no obvious mistakes in the theory, which has been put on a rigorous footing (e.g., Uzdensky & Kulsrud 2000). Indeed, both numerical simulations (e.g., see figure 4(b) of Loureiro *et al.* 2005) and laboratory experiments (e.g., Ji *et al.* 1998) have measured reconnection rates in excellent agreement with the SP scalings (XI.2.1). What, then, is the issue?

XI.3. Plasmoid instability

Let us suspend judgement for the meantime and suppose that the SP model is correct. With tearing-mode theory in hand, let us ask the intriguing question of whether or not the steady-state SP current sheet is stable to tearing instabilities. One could of course go the route of rigorously doing the linear tearing theory using the SP solution as the background state, as Loureiro *et al.* (2007) did in a now-classic paper, but for our purposes it will be sufficient to simply replace the current-sheet thickness a in the tearing-mode theory of §XI.1 with $\delta_{\rm SP} \sim S^{-1/2}L$ (Tajima & Shibata 1997; Bhattacharjee *et al.* 2009; Loureiro *et al.* 2013). Focusing on the maximally growing tearing mode (XI.1.31),

$$k_{\max}L \sim \frac{L}{a}S_a^{-1/4} \longrightarrow \frac{L}{\delta_{\rm SP}}\left(\frac{v_{\rm A,r}\delta_{\rm SP}}{\eta}\right)^{-1/4} \sim S^{3/8}, \tag{XI.3.1a}$$

$$\frac{\gamma_{\max}}{v_{\rm A,r}/L} \sim \frac{L}{a}S_a^{-1/2} \longrightarrow \frac{L}{\delta_{\rm SP}}\left(\frac{v_{\rm A,r}\delta_{\rm SP}}{\eta}\right)^{-1/2} \sim S^{1/4}, \tag{XI.3.1b}$$

$$\frac{\delta_{\rm in}}{L} \sim \frac{a}{L}S_a^{-1/4} \longrightarrow \frac{\delta_{\rm SP}}{L}\left(\frac{v_{\rm A,r}\delta_{\rm SP}}{\eta}\right)^{-1/4} \sim S^{-5/8}. \tag{XI.3.1c}$$

[25] Petschek-like configurations do emerge when strongly localized (anomalous) resistivity profiles are used (Malyshkin *et al.* 2005; Sato & Hayashi 1979; Ugai 1995; Scholer 1989; Erkaev *et al.* 2000, 2001; Biskamp & Schwarz 2001), as might occur under collisionless conditions.

This is the *plasmoid instability* – essentially, the tearing instability of a SP current layer. Of course, the situation in question is very different than that obtained using the stationary equilibrium Harris sheet, perhaps most obviously because the former has background flows. These flows can be stabilizing in the tearing calculation, a possibility we have ignored in making the estimates in (XI.3.1). This may be circumvented, however, by demanding that $\gamma \gg v_{\rm A,r}/L$, $k_{\rm max}L \gg 1$, and $\delta_{\rm in}/\delta_{\rm SP} \ll 1$ – demands that may be satisfied if $S \gtrsim 10^4$. Indeed, it is at this critical Lundquist number that the plasmoid instability is (now routinely) observed to occur in numerical simulations of reconnection (e.g., Samtaney *et al.* 2009; Daughton *et al.* 2009; Bhattacharjee *et al.* 2009; Ni *et al.* 2010; Huang & Bhattacharjee 2010; Loureiro *et al.* 2012, 2013). The example below is taken from a resistive-MHD numerical simulation by Samtaney *et al.* (2009), showing the evolution of the current density (color) in the central $x = [-\delta_{\rm SP}, \delta_{\rm SP}]$ region of a SP current sheet with $S = 10^7$:

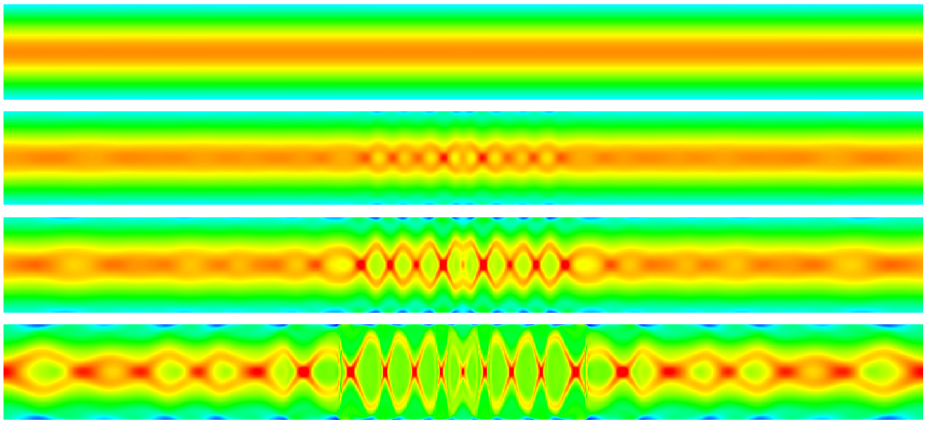

Below is another example, taken from Bhattacharjee *et al.* (2009) using $S = 2\pi \times 10^5$:

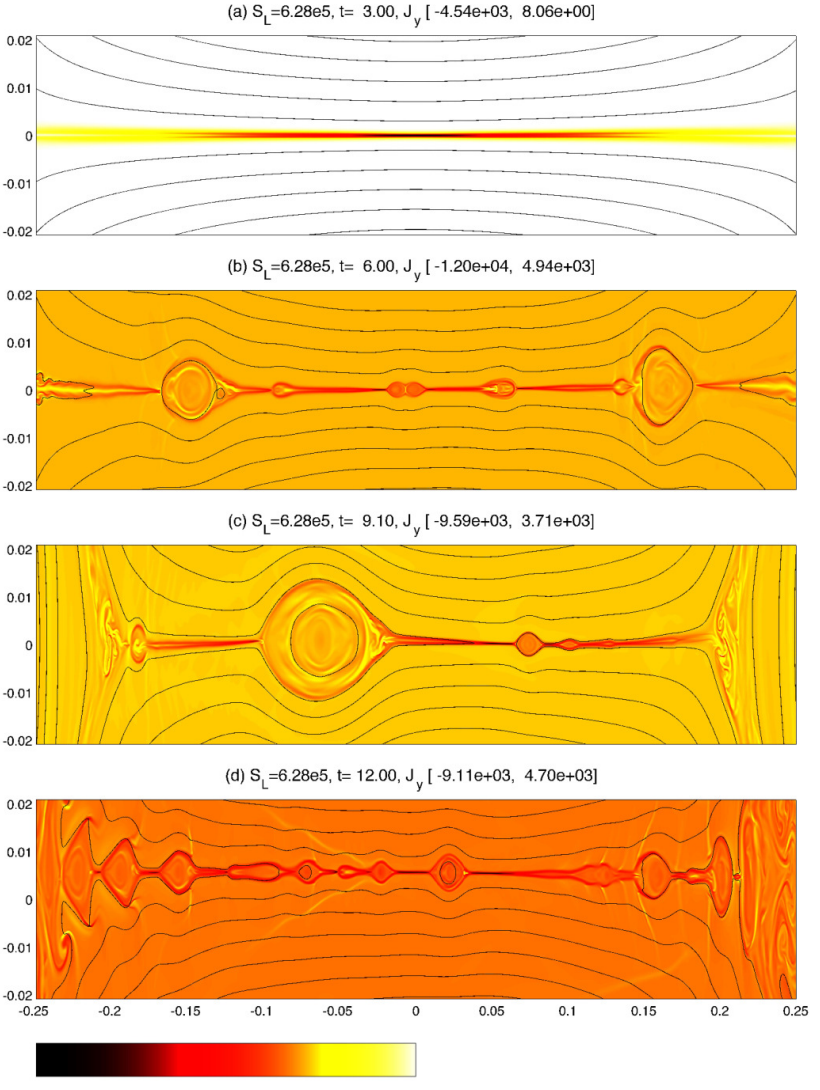

Since then, simulations of plasmoid-dominated reconnection has become an industry.

Given that large-aspect-ratio SP current sheets are violently unstable to the plasmoid instability, it is worth asking whether we should expect them to exist in nature at all. Indeed, Lundquist numbers of typical space and astrophysical plasmas are absurdly large, with $S \sim 10^{13}$ or so in the solar corona implying a plasmoid-instability time scale less than 0.06% of the dynamical time scale. Why would a nice SP current sheet ever be realized under these conditions? Good question (Pucci & Velli 2014; Uzdensky & Loureiro 2016); there's a problem set question on this topic.[26]

[26] You may also wish to see Alt & Kunz (2019) and Winarto & Kunz (2022) for reasons why a relatively large-scale, smoothly varying current layer (e.g., a Harris sheet) should not be expected to occur in a weakly collisional, high-β plasma.

PART XII

Turbulence and dynamo

> The breaking of a wave cannot explain the whole sea.
>
> Vladimir Nabokov
> *The Real Life of Sebastian Knight* (1941)

Before starting this (unfinished) chapter, let me note one big reason that it remains unfinished: Schekochihin (2022). Once that excellent and comprehensive review of scaling theories of MHD turbulence was published in the Journal of Plasma Physics, it seemed to me unnecessary to finish this chapter; I have nothing to say, nor means of saying it more eloquently, than what can already be found in, and readily absorbed from, Alex's review. What follows in the next section are some brief notes of my own from an early set of lecture notes, which traces the story from Kolmogorov to Iroshnikov–Kraichnan, then to Goldreich–Sridhar and Boldyrev, and finally to recent ideas by Alfy Mallet, Ben Chandran, and Alex Schekochihin. Thereafter follows some notes on dynamo theory, though there again can be found another recent Journal of Plasma Physics review, this time by Francois Rincon (Rincon 2019). My hope is that there's just enough here to set the stage and stimulate you to read those expert reviews and explore more ideas your own.

XII.1. Kolmogorov–Obukhov theory of hydrodynamic turbulence

This is simple. Like all simple things, it resulted from a stroke of genius (Kolmogorov 1941; Obukhov 1941), one which everyone now says is obvious. It's *just* dimensionless analysis!

Suppose energy is being pumped into some fluid at large scales at a rate ε, which is fixed. At scales small enough that the system is locally homogeneous but not so small that viscosity (or whatever dissipative effect there are) is unimportant – the so-called "inertial range" – this ε is passed along conservatively, scale by scale: a constant energy flux. Assuming this "passing" of energy is local, the energy spectrum is, by dimensional analysis,

$$\boxed{E(k) \sim \varepsilon^{2/3} k^{-5/3}} \tag{XII.1.1}$$

It cannot be any different under these assumptions:

$$[\varepsilon] = \frac{U^3}{L} \qquad \left[\int \mathrm{d}k\, E(k)\right] = U^2,$$

and that's it. There is one timescale – L/U, the eddy turnover time at the outer scale L where the velocity is U. (Density is taken to be constant, which becomes a better assumption the further down the cascade you go where the motions become more and more subsonic.) This also implies that the typical velocity increment between points separated by a distance λ is

$$\boxed{\delta u_\lambda \sim (\varepsilon\lambda)^{1/3}} \tag{XII.1.2}$$

The corresponding scale-dependent rate of strain is $\delta u_\lambda/\lambda \sim \epsilon^{1/3}\lambda^{-2/3}$. Thus, the fastest eddies are the ones at the viscous scale, $\delta u_{\lambda_\nu}/\lambda_\nu \propto \lambda_\nu^{-2/3}$, where the kinetic energy is ultimately thermalized as heat.

One could go on from here to some other Kolmogorovian things, but I won't.

XII.2. Iroshnikov–Kraichnan theory of MHD turbulence

Now suppose that fluid were conducting and threaded by a magnetic field. The problem with just using Kolmogorov may be stated in two ways. First, the homogeneous assumption in the Kolmogorov treatment is similar to saying that, at sufficiently small scales (but still those above the dissipative scales), the fluctuations on those scales are independent of any large-scale structure or features of the "background" in which they reside. This is obviously *not* true when there is a magnetic field: all scales feel that magnetic field, even if it is only at large scales.[27] Secondly, dimensional analysis is no longer enough, as now there are two speed, U and $v_\mathrm{A} \doteq B/\sqrt{4\pi\varrho}$, and a directionality imposed by $\boldsymbol{B}$. One way of dealing with the latter – the route taken by Iroshnikov (1963) and Kraichnan (1965) – is to assume isotropy in the Kolmogorovian way, even at small scales: there is no $k_\parallel$ and $k_\perp$, there is only k. Their way of dealing with the former was to give special prominence to the Alfvén time, $\tau_\mathrm{A} \sim \lambda/v_\mathrm{A}$ – the time for an Alfvén wave to cross the scale λ. The nonlinear cascade time that goes into $\varepsilon = \text{const} \sim \delta u_\lambda^2/\tau_\lambda$ is obtained by asking how long must one wait for a wave packet to be sufficiently distorted. You see, MHD turbulence has Alfvén-wave packets as its building blocks, not hydrodynamic eddies. From the RMHD equations written in terms of Elsässer potentials (IX.0.65), it is clear that only oppositely propagating Alfvén-wave packets interact, and that the change in δu_λ of one packet due to the nonlinear interaction with another in a crossing time τ_A is $\sim(\delta u_\lambda^2/\lambda) \times (\lambda/v_\mathrm{A})$ – the nonlinearity times the characteristic timescale. In "weak" turbulence, this gives only a small change. So, one requires many collisions to distort a wave packet by an amount equal to itself. If these collisions add up randomly, we get the random-wave scaling

$$N_\mathrm{collisions}^{1/2} \Delta(\delta u_\lambda) \sim \delta u_\lambda \quad \Longrightarrow \quad N_\mathrm{collisions} \sim \left[\frac{\delta u_\lambda}{\Delta(\delta u_\lambda)}\right]^2 \sim \left(\frac{v_\mathrm{A}}{\delta u_\lambda}\right)^2.$$

The energy transfer time is then $N_\mathrm{collisions}\tau_\mathrm{A} \sim \tau_\lambda$, so

$$\tau_\lambda \sim \left(\frac{v_\mathrm{A}}{\delta u_\lambda}\right)^2 \frac{\lambda}{v_\mathrm{A}} \sim \frac{v_\mathrm{A}\lambda}{\delta u_\lambda^2}.$$

Combining these relations yields

$$\varepsilon \sim \frac{\delta u_\lambda^2}{\tau_\lambda} \sim \delta u_\lambda^2 \frac{\delta u_\lambda^2}{v_\mathrm{A}\lambda} = \text{const} \quad \Longrightarrow \quad \boxed{\delta u_\lambda \sim (\varepsilon v_\mathrm{A}\lambda)^{1/4}} \tag{XII.2.1}$$

Accordingly,

$$\int_{1/\lambda}^{\infty} \mathrm{d}k\, E(k) \sim \delta u_\lambda^2 \quad \Longrightarrow \quad E(k) \sim (\varepsilon v_\mathrm{A})^{1/2} k^{-3/2} \tag{XII.2.2}$$

(Note: Since $\tau_\lambda \gg \lambda/v_\mathrm{A}$, a wave packet must undergo many uncorrelated interactions with oppositely moving wave packets before energy is transferred to small scales.)

This picture held for 30 years.[28]

XII.3. Goldreich–Sridhar theory of MHD turbulence

Isotropy can't be right. Again, a simple statement that is obvious in retrospect. (This was realized relatively early on from tentative experimental and numerical evidence,

[27] Equivalently, a uniform magnetic field cannot be removed by a Galilean transform.

[28] I learned from Alex Schekochihin that Iroshnikov (1963) was largely unnoticed at the time and "he disappeared into Soviet obscurity." Apparently, he worked at the Institute of Oceanology in later years and died in 1991 at the age of 54.

e.g., Montgomery & Turner (1981) and Shebalin *et al.* (1983).) But it took until 1995 to be worked into a predictive theory (Goldreich & Sridhar 1995). The idea is that perturbations with $k_\parallel \ll k_\perp$ are more natural in a magnetic field that is hard to bend but has little qualms with small-scale structure perpendicular to itself. The problem is to determine how $k_\parallel/k_\perp$ scales. This is provided by *critical balance*: the linear and nonlinear timescales are comparable at all scales.[29] Thus,

$$\tau_\mathrm{A} = \frac{\ell}{v_\mathrm{A}} \sim \tau_\lambda \sim \frac{\lambda}{\delta u_\lambda}, \tag{XII.3.1}$$

where now λ denotes a perpendicular scale and ℓ denotes a parallel scale. Proceeding as in Kolmogorov,

$$\varepsilon \sim \frac{\delta u_\lambda^2}{\tau_\lambda} \sim \frac{\delta u_\lambda^3}{\lambda} \quad \Longrightarrow \quad E(k_\perp) \sim \varepsilon^{2/3} k_\perp^{-5/3}. \tag{XII.3.2}$$

A Kolmogorov spectrum, but one in the direction across the field. Along the field,

$$\ell \sim \lambda \frac{v_\mathrm{A}}{\delta u_\lambda} \quad \Longrightarrow \quad \frac{\ell}{\lambda} \sim v_\mathrm{A} (\varepsilon\lambda)^{-1/3}, \tag{XII.3.3}$$

and so the anisotropy *increases* at smaller scales. We have

$$\delta u_\lambda \sim (\varepsilon\lambda)^{1/3} \quad \text{and} \quad \delta u_\ell \sim (\varepsilon\ell/v_\mathrm{A})^{1/2},$$

so that $E(k_\parallel) = E(k_\perp)(\mathrm{d}k_\perp/\mathrm{d}k_\parallel) \propto k_\parallel^{-2}$. Physically, the critical balance ban be argued from causality (e.g. Boldyrev 2005; Nazarenko & Schekochihin 2011): ℓ is the distance an Alfvénic pulse travels along the field at speed v_A in a time τ_λ – this is the maximum distance over which the fluctuation can remain correlated.

These (predicted!) scalings have been since measured in numerical simulations and in the solar wind. For the latter, the figure on the left below shows the parallel ($P_\parallel$) and perpendicular ($P_\perp$) spectra (Fourier and wavelet) of the magnetic fluctuations in the solar wind, measured by the *Ulysses* spacecraft and computed by Wicks *et al.* (2010). (The spacecraft-measured frequencies have been converted to wavenumbers k using the Taylor hypothesis.) An earlier (and first ever) result – the spectral index as a function of the angle to the local mean magnetic field θ_B – is shown on the right (Horbury *et al.* 2008). Note that both are in agreement with the GS scalings, $E(k_\perp) \propto k_\perp^{-5/3}$ and $E(k_\parallel) \propto k_\parallel^{-2}$.

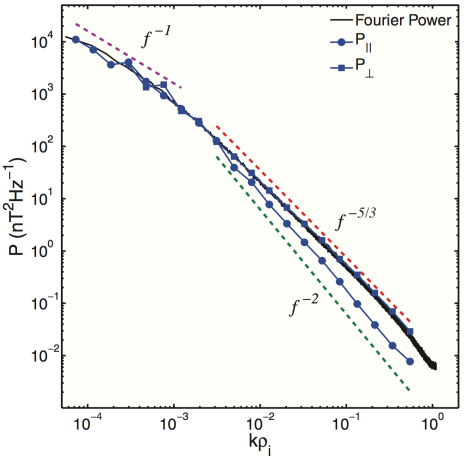

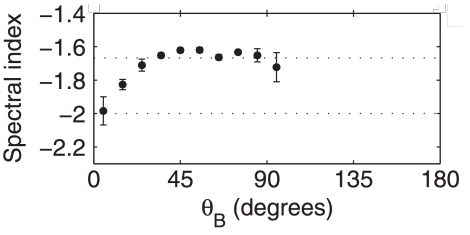

[29] That $\tau_\mathrm{A}/\tau_\lambda$ is scare invariant has only been found recently by Mallet *et al.* (2015), who dubbed this "refined critical balance".

One slight issue is that simulations, while confirming the $\ell \sim \lambda^{2/3}$ scaling (e.g., Cho & Vishniac 2000; Maron & Goldreich 2001), instead find a $-3/2$ spectrum (rather than $-5/3$). This led Boldyrev (2006) to propose a correction to the theory dubbed *dynamical alignment*.

XII.4. Boldyrev's dynamical alignment

[in preparation]

Argued that the filament-like eddies implied by the GS95 picture are not realizable; that, instead, fluctuations are three-dimensionally anisotropic. This anisotropy is due to an angular alignment of magnetic-field and velocity-field polarizations – essentially, the turbulence wants to be as "Alfvénic" as possible, with $\boldsymbol{u}_\perp$ and $\boldsymbol{B}_\perp$ the same. ((Matthaeus *et al.* 2008) identified the dynamical tendency for the velocity and magnetic field to align locally in patches in numerical simulations.) Of course, this alignment cannot be precise, or else the nonlinear interaction between counterpropagating Alfvén-wave packets would be turned off. Instead, Boldyrev (2006) argued that, at each scale λ, the alignment of fluctuations should attain the maximal level consistent with a constant energy flux through that scale. This implies an alignment angle $\theta_\lambda \propto \lambda^{1/4}$, so that the magnetic-field and velocity-field fluctuations become increasingly aligned at smaller and smaller scales, i.e., the dynamic alignment is *scale dependent*. This progressively weakens the nonlinear interaction. The end result is a perpendicular energy spectrum $E(k_\perp) \propto k_\perp^{-3/2}$, consistent with multiple numerical simulations of MHD turbulence.

rephrased: minimal degree of misalignment is set by a kind of uncertainty principle: direction of local magnetic field can only be defined with a small angle $\theta_\lambda \sim \delta B_\lambda / B_0 \ll 1$, and so the fluctuations cannot be aligned any more precisely than this.

Boldyrev:

$$\boldsymbol{z}_\perp^\pm \cdot \boldsymbol{\nabla} \boldsymbol{z}_\perp^\mp \sim \theta_\lambda \frac{\delta u_\lambda^2}{\lambda} \quad \Longrightarrow \quad \ell \sim \frac{v_\mathrm{A} \lambda}{\theta_\lambda \delta u_\lambda}$$

$$\tau_\lambda \sim \frac{\ell}{v_\mathrm{A}} \sim \frac{\lambda}{\theta_\lambda \delta u_\lambda}$$

$$\frac{\delta u_\perp^2}{\tau_\lambda} = \text{const} \quad \Longrightarrow \quad \delta u_\lambda \propto (\lambda/\theta_\lambda)^{1/3} \sim (\varepsilon v_\mathrm{A} \lambda)^{1/4} \quad \Longrightarrow \quad E(k_\perp) \sim (\varepsilon v_\mathrm{A})^{1/2} k_\perp^{-3/2}.$$

Looks like IK spectrum but is anisotropic with critical balance: $\ell \sim v_\mathrm{A}^{3/2} \varepsilon^{-1/2} \lambda^{1/2}$. Parallel spectrum is the same as in GS95.

adapted from Boldyrev (2006):

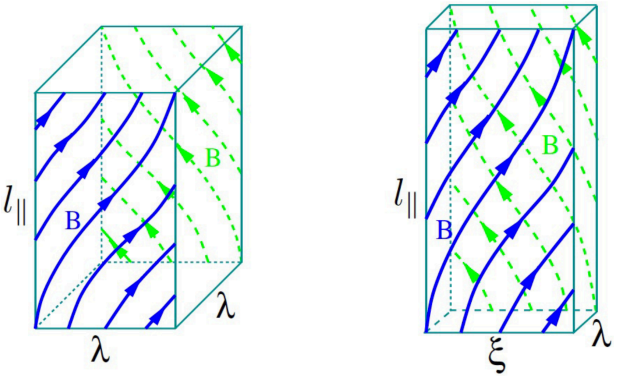

See Mason *et al.* (2006, 2008, 2011, 2012); Perez *et al.* (2012, 2014)

Beresnyak (2011): in RMHD limit, $\delta B_\lambda/B_0$ is an arbitrarily small quantity and thus so must be θ_λ. This means nonlinearity would disappear from RMHD ordering. Only way to keep nonlinearity is to order $\theta_\lambda \sim 1$ wrt RMHD ordering, i.e., it cannot scale with ϵ. Thus, you can't have $\ell/v_\mathrm{A} \propto \lambda^{1/2}$. This, even though aligned MHD turbulence has been measured in RMHD simulations.

Chandran *et al.* (2015); Mallet *et al.* (2015); Mallet & Schekochihin (2017): alignment between $\boldsymbol{u}_\perp$ and $\boldsymbol{B}_\perp$ not, mathematically, the same as alignment between $\boldsymbol{z}^+_\perp$ and $\boldsymbol{z}^-_\perp$. Found that alignment angle between the Elsasser fields at any given scale is *anticorrelated* with their amplitudes. Intermittency matters: how is λ, ξ, and ℓ distributed in a turbulent MHD system?

For many more details (especially concerning weak turbulence and the most recent explorations of the connection between turbulence and the disruption of current sheets by tearing instability), see the excellent recent review of MHD turbulence by Alex Schekochihin (Schekochihin 2022).

XII.5. Zel'dovich's fluctuation dynamo

What if we now have hydrodynamic turbulence sitting in a conducting fluid hosting a weak zero-net-flux magnetic field (i.e., no imposed field)? Let us set aside the question of what the turbulence looks like and ask a simpler question: under what conditions will this "seed" magnetic field be amplified? This is the problem of *small-scale* or *fluctuation dynamo*. It's not easy, and has only been solved under specific conditions.

As a first step, suppose we have a planar flow field $\boldsymbol{u} = u_x(t,x,y,z)\hat{\boldsymbol{x}} + u_y(t,x,y,z)\hat{\boldsymbol{y}}$, with $\boldsymbol{\nabla}\cdot\boldsymbol{u} = 0$ but otherwise arbitrary. The z-component of the resistive-MHD induction equation with constant η,

$$\frac{\partial \boldsymbol{B}}{\partial t} = \boldsymbol{\nabla}\times(\boldsymbol{u}\times\boldsymbol{B}) + \eta\nabla^2\boldsymbol{B}, \tag{XII.5.1}$$

is then

$$\frac{\partial B_z}{\partial t} + \boldsymbol{u}\cdot\boldsymbol{\nabla}B_z = \eta\nabla^2 B_z. \tag{XII.5.2}$$

Multiplying (XII.5.2) by $2B_z$ and integrating over the volume of the plasma, we find

$$\frac{\partial\langle B_z^2\rangle}{\partial t} = -2\eta\langle|\boldsymbol{\nabla}B_z|^2\rangle, \tag{XII.5.3}$$

and so B_z resistively decays to 0. If $B_z = 0$, then the solenoidality constraint on the magnetic field becomes $\partial B_x/\partial x + \partial B_y/\partial y = 0$ and so the planar components of the magnetic field may be written in terms of a vector potential, $\boldsymbol{B} = \boldsymbol{\nabla}\times(A\hat{\boldsymbol{z}})$. The latter satisfies the un-curled induction equation,

$$\frac{\partial A}{\partial t} + \boldsymbol{u}\cdot\boldsymbol{\nabla}A = \eta\nabla^2 A \quad\Longrightarrow\quad \frac{\mathrm{d}}{\mathrm{d}t}\langle A^2\rangle = -2\eta\langle|\boldsymbol{\nabla}A|^2\rangle. \tag{XII.5.4}$$

Again, the magnetic field decays resistively. Thus, no dynamo can be maintained by a planar flow (Zel'dovich 1957). This is referred to as *Zel'dovich's anti-dynamo theorem*. There are other "anti-dynamo theorems", one of which will be proven below (§XII.7), but let us explore the fluctuation dynamo a bit further.

The simplest approach is to consider the zero-net-flux magnetic field to be so weak energetically that it exerts no dynamical effect on the fluid flow, i.e., the Lorentz force is negligible on all scales of interest. This is the *kinematic* limit, in which the velocity field can be prescribed without regard for the evolution of the magnetic field. Also, we'll take

$\mathrm{Pm} \doteq \nu/\eta = \mathrm{Rm}/\mathrm{Re} \gg 1$.[30] This causes the viscous scale λ_ν, at which $\boldsymbol{u}\cdot\boldsymbol{\nabla u} \sim \nu\nabla^2\boldsymbol{u}$, to be much larger than the resistive scale λ_η, at which $\boldsymbol{B}\cdot\boldsymbol{\nabla u} \sim \eta\nabla^2\boldsymbol{B}$. The former may be estimated using

$$\boldsymbol{u}\cdot\boldsymbol{\nabla u} \sim \frac{\delta u_{\lambda_\nu}^2}{\lambda_\nu} \sim \varepsilon^{2/3}\lambda_\nu^{-1/3} \quad \text{and} \quad \nu\nabla^2\boldsymbol{u} \sim \nu\frac{\delta u_{\lambda_\nu}}{\lambda_\nu^2} \sim \nu\varepsilon^{1/3}\lambda_\nu^{-5/3}.$$

Matching these gives

$$\lambda_\nu \sim \nu^{3/4}\varepsilon^{-1/4} \sim L\,\mathrm{Re}^{-3/4} \quad \text{and} \quad \delta u_{\lambda_\nu} \sim \nu^{1/4}\varepsilon^{1/4} \sim U\,\mathrm{Re}^{-1/4}, \tag{XII.5.5}$$

where $\mathrm{Re} \doteq UL/\nu$. To estimate the latter (the resistive scale), note that

$$\frac{\partial\boldsymbol{B}}{\partial t} = \boldsymbol{\nabla}\times(\boldsymbol{u}\times\boldsymbol{B}) \quad\Longrightarrow\quad \frac{\mathrm{d}B^2}{\mathrm{d}t} = 2\boldsymbol{BB}:\boldsymbol{\nabla u} \quad\Longrightarrow\quad \frac{\mathrm{d}\ln B}{\mathrm{d}t} = \hat{\boldsymbol{b}}\hat{\boldsymbol{b}}:\boldsymbol{\nabla u} \tag{XII.5.6}$$

for an incompressible velocity field. Thus, because velocity gradients are what grow the field, the viscous-scale eddies, where the stretching rate $\delta u_\lambda/\lambda \sim \varepsilon^{1/3}\lambda^{-2/3}$ is fastest, will be the most important. Accordingly, $\boldsymbol{\nabla u} \sim \delta u_{\lambda_\nu}/\ell_\nu \sim (U/L)\,\mathrm{Re}^{1/2}$; balancing this with $\eta\lambda_\eta^2$ at the resistive scale leads to

$$\lambda_\eta \sim L\,\mathrm{Re}^{-1/4}\,\mathrm{Rm}^{-1/2} \sim \lambda_\nu\,\mathrm{Pm}^{-1/2} \ll \lambda_\nu. \tag{XII.5.7}$$

Graphically,

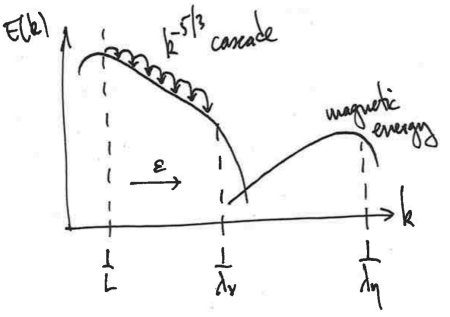

Now then, because $\delta u_{\lambda_\nu} \sim (\varepsilon/\nu)^{1/2}\lambda_\nu \propto \lambda_\nu$, the viscous-scale motions are smooth and Taylor-expandable. The turbulence looks like a succession of random-in-time linear shears, and the magnetic field becomes arranged in folds with field reversals on the resistive scale (see Schekochihin & Cowley 2007, for a review):

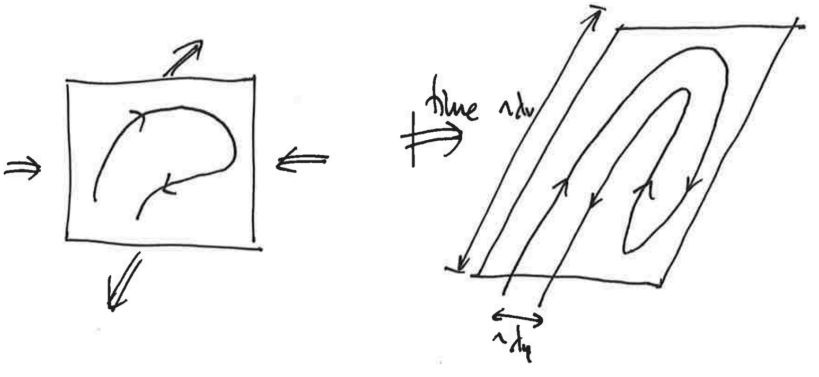

It is in this configuration that the mean magnetic-field strength becomes amplified by the chaotic flows, a point we now prove following the arguments in Zel'dovich *et al.* (1984).

[30] $\mathrm{Pm} \simeq 2.6\times10^{-5}T^4/n$ in fully ionized plasmas, which is $\sim10^{29}$ in the ICM and $\sim10^{11}$ in the warm phase of the ISM.

Because the viscous-scale velocity fluctuations $\delta u_{\ell_\nu} \propto \ell_\nu$ are smooth, we can write the velocity field as a Taylor expansion about some point $\boldsymbol{r} = \boldsymbol{0}$:

$$u^\ell(t,\boldsymbol{r}) = u^\ell(t,\boldsymbol{0}) + \sigma^\ell_m(t) r^m + \ldots, \tag{XII.5.8}$$

where summation over repeated indices is implied. Of course, we have the freedom to set $u^i(t,\boldsymbol{0}) = 0$ by moving to that frame of reference. Then, the jth component of the resistive-MHD induction equation (XII.5.1) is

$$\frac{\partial B^j}{\partial t} + \sigma^\ell_m(t) r^m \frac{\partial B^j}{\partial r^\ell} = B^m \sigma^j_m(t) + \eta \nabla^2 B^j. \tag{XII.5.9}$$

We seek a solution as a sum of plane waves with time-dependent wavevector $\boldsymbol{k} = \boldsymbol{k}(t)$:

$$B^j(t,\boldsymbol{r}) = \int \mathrm{d}^3\boldsymbol{k}_0\, B^j(t,\boldsymbol{k}_0) \exp\bigl[\mathrm{i} k_n(t,\boldsymbol{k}_0) r^n\bigr], \tag{XII.5.10}$$

where $\boldsymbol{k}(t,\boldsymbol{k}_0)$ is the time-dependent wavenumber whose value at $t = 0$ is $\boldsymbol{k}_0$. (Thus, $k_n(0,\boldsymbol{k}_0) = k_{0n}$.) This works nicely because (XII.5.9) is linear, so that each $\boldsymbol{k}$ is a solution. Substituting (XII.5.10) into (XII.5.9) and examining each Fourier component independently,

$$\begin{aligned}\frac{\partial}{\partial t}\Bigl[B^j(t,\boldsymbol{k}_0)\mathrm{e}^{\mathrm{i}k_n(t,\boldsymbol{k}_0)r^n}\Bigr] &= \mathrm{e}^{\mathrm{i}k_n(t,\boldsymbol{k}_0)r^n}\left[\frac{\partial B^j(t,\boldsymbol{k}_0)}{\partial t} + \mathrm{i}B^j(t,\boldsymbol{k}_0) r^m \frac{\partial k_m(t,\boldsymbol{k}_0)}{\partial t}\right] \\ &= \mathrm{e}^{\mathrm{i}k_n(t,\boldsymbol{k}_0)r^n}\Bigl[-\sigma^\ell_m(t) r^m\, \mathrm{i}k_\ell(t,\boldsymbol{k}_0) B^j(t,\boldsymbol{k}_0) \\ &\qquad + B^m(t,\boldsymbol{k}_0)\sigma^i_m(t) - \eta k^2(t,\boldsymbol{k}_0) B^j(t,\boldsymbol{k}_0)\Bigr],\end{aligned} \tag{XII.5.11}$$

Equation (XII.5.11) must be satisfied at each $\boldsymbol{r}$, and so

$$\frac{\partial B^j(t,\boldsymbol{k}_0)}{\partial t} = -\eta k^2(t,\boldsymbol{k}_0) B^j(t,\boldsymbol{k}_0) + B^m(t,\boldsymbol{k}_0)\sigma^j_m(t), \tag{XII.5.12a}$$

$$\frac{\partial k_m(t,\boldsymbol{k}_0)}{\partial t} = -k_\ell(t,\boldsymbol{k}_0)\sigma^\ell_m(t), \tag{XII.5.12b}$$

with the initial conditions $B^j(0,\boldsymbol{k}_0) = B^j_0(\boldsymbol{k}_0)$ and $k_m(0,\boldsymbol{k}_0) = k_{0m}$.

To go any further, we require a model $\sigma^\ell_m(t)$ tensor. There are a few options, but the following is the simplest:

$$\boldsymbol{\sigma} = \begin{bmatrix} \lambda_1 & 0 & 0 \\ 0 & \lambda_2 & 0 \\ 0 & 0 & \lambda_3 \end{bmatrix} \tag{XII.5.13}$$

with $\mathrm{tr}(\boldsymbol{\sigma}) = \lambda_1 + \lambda_2 + \lambda_3 = 0$ (incompressibility). We may arrange the coordinate system such that

$$\underbrace{\lambda_1}_{\text{stretching}} \;>\; \underbrace{\lambda_2}_{\text{“null”}} \;>\; \underbrace{\lambda_3}_{\text{compression}} \qquad \text{and} \quad \lambda_1 > 0,\ \lambda_3 < 0. \tag{XII.5.14}$$

Then (XII.5.12) becomes

$$\frac{\partial B^j(t,\boldsymbol{k}_0)}{\partial t} = -\eta k^2(t,\boldsymbol{k}_0) B^j(t,\boldsymbol{k}_0) + B^j(t,\boldsymbol{k}_0)\lambda_j, \tag{XII.5.15a}$$

$$\frac{\partial k_m(t,\boldsymbol{k}_0)}{\partial t} = -k_\ell(t,\boldsymbol{k}_0)\lambda^\ell, \tag{XII.5.15b}$$

whose solutions are

$$B^j(t,\boldsymbol{k}_0) = B_0^j(\boldsymbol{k}_0)\,\mathrm{e}^{\lambda_j t - \eta\int_0^t \mathrm{d}t'\,k^2(t',\boldsymbol{k}_0)}, \tag{XII.5.16a}$$

$$k_m(t,\boldsymbol{k}_0) = k_{0m}\,\mathrm{e}^{-\lambda_m t}. \tag{XII.5.16b}$$

Note that some components of $\boldsymbol{k}(t,\boldsymbol{k}_0)$ decay (k_1) while others grow (k_3); thus, stretching (along $\hat{\boldsymbol{e}}_1$) and compression (along $\hat{\boldsymbol{e}}_3$). We now ask whether or not this leads to a net amplification of the mean magnetic energy:

$$\begin{aligned}
\langle B^2\rangle &\doteq \int \mathrm{d}^3\boldsymbol{r}\,|\boldsymbol{B}(t,\boldsymbol{r})|^2 \\
&= \int \mathrm{d}^3\boldsymbol{r}\int \mathrm{d}^3\boldsymbol{k}_0\int \mathrm{d}^3\boldsymbol{k}_0'\,B_j(t,\boldsymbol{k}_0)B^j(t,\boldsymbol{k}_0')\,\mathrm{e}^{\mathrm{i}[k_n(t,\boldsymbol{k}_0)+k_n(t,\boldsymbol{k}_0')]r^n} \\
&= \int \mathrm{d}^3\boldsymbol{k}_0\int \mathrm{d}^3\boldsymbol{k}_0'\,B_j(t,\boldsymbol{k}_0)B^j(t,\boldsymbol{k}_0')\,(2\pi)^3\underbrace{\delta\big[\boldsymbol{k}(t,\boldsymbol{k}_0)+\boldsymbol{k}(t,\boldsymbol{k}_0')\big]}_{\substack{=\delta\left[(\boldsymbol{k}_0+\boldsymbol{k}_0')_n\,\mathrm{e}^{-\lambda_n t}\right]\\ =\delta(\boldsymbol{k}_0+\boldsymbol{k}_0')\left[\det\left(\mathrm{e}^{-\boldsymbol{\sigma}t}\right)\right]^{-1}\\ =\delta(\boldsymbol{k}_0+\boldsymbol{k}_0')\,\mathrm{e}^{-\mathrm{tr}(\boldsymbol{\sigma})t}\\ =\delta(\boldsymbol{k}_0+\boldsymbol{k}_0')\text{ since }\mathrm{tr}(\boldsymbol{\sigma})=0}}, \\
&= \int \mathrm{d}^3\boldsymbol{k}_0\,(2\pi)^3\,B_j(t,\boldsymbol{k}_0)B^j(t,-\boldsymbol{k}_0), \\
&= \int \mathrm{d}^3\boldsymbol{k}_0\,(2\pi)^3\,|\boldsymbol{B}(t,\boldsymbol{k}_0)|^2,
\end{aligned}$$

which is just Parseval's theorem, i.e., the energy of the field is the sum of the energies of the plane waves. So we must calculate the energy of each mode using (XII.5.16):

$$\begin{aligned}
|\boldsymbol{B}(t,\boldsymbol{k}_0)|^2 &= \mathrm{e}^{-2\eta\int_0^t \mathrm{d}t'\,k^2(t',\boldsymbol{k}_0)}\Big[\underbrace{|B_{01}(\boldsymbol{k}_0)|^2\,\mathrm{e}^{2\lambda_1 t}}_{\substack{\text{exponentially larger}\\ \text{than the rest,}\\ \text{since }\lambda_1>\lambda_2>\lambda_3}} + |B_{02}(\boldsymbol{k}_0)|^2\,\mathrm{e}^{2\lambda_2 t} + |B_{03}(\boldsymbol{k}_0)|^2\,\mathrm{e}^{2\lambda_3 t}\Big] \\
&\approx |B_{01}(\boldsymbol{k}_0)|^2\,\mathrm{e}^{2\lambda_1 t - 2\eta\int_0^t \mathrm{d}t'\,k^2(t',\boldsymbol{k}_0)}.
\end{aligned}$$

The time integral in the exponential is

$$\begin{aligned}
\int_0^t \mathrm{d}t'\,k^2(t',\boldsymbol{k}_0) &= \int_0^t \mathrm{d}t'\left(k_{01}^2\,\mathrm{e}^{-2\lambda_1 t} + k_{02}^2\,\mathrm{e}^{-2\lambda_2 t} + k_{03}^2\,\mathrm{e}^{-2\lambda_3 t}\right) \\
&= \frac{k_{01}^2}{2\lambda_1}(1-\mathrm{e}^{-2\lambda_1 t}) + \frac{k_{02}^2}{2\lambda_2}(1-\mathrm{e}^{-2\lambda_2 t}) - \underbrace{\frac{k_{03}^2}{2|\lambda_3|}(1-\mathrm{e}^{2|\lambda_3|t})}_{\text{since }\lambda_3<0} \\
&\approx \frac{k_{01}^2}{2\lambda_1} + \frac{k_{02}^2}{2\lambda_2} + \frac{k_{03}^2}{2|\lambda_3|}\mathrm{e}^{2|\lambda_3|t},
\end{aligned}$$

with the final line following after assuming $\lambda_2 > 0$ (as it usually is in real turbulence). Thus,

$$|\boldsymbol{B}(t,\boldsymbol{k}_0)|^2 \approx |\boldsymbol{B}_{01}(\boldsymbol{k}_0)|^2\,\exp\left[2\lambda_1 t - \eta\left(\frac{k_{01}^2}{\lambda_1} + \frac{k_{02}^2}{\lambda_2} + \frac{k_{03}^2}{|\lambda_3|}\,\mathrm{e}^{2|\lambda_3|t}\right)\right]. \tag{XII.5.17}$$

For most modes, the energy decays super-exponentially. But there is a subset of modes,

those satisfying

$$\frac{k_{01}^2}{2\lambda_1^2 t/\eta} + \frac{k_{02}^2}{2\lambda_1\lambda_2 t/\eta} + \frac{k_{03}^2}{2\lambda_1|\lambda_3|t\,\mathrm{e}^{-2|\lambda_3|t}/\eta} \lesssim 1, \tag{XII.5.18}$$

which actually grows. Within this ellipsoidal volume of size

$$\sim \lambda_1^2(\lambda_2|\lambda_3|)^{1/2}\left(\frac{t}{\eta}\right)^{3/2}\mathrm{e}^{-|\lambda_3|t},$$

the mean magnetic energy satisfies

$$\begin{aligned}\frac{\langle B^2\rangle}{(2\pi)^3} &= \int \mathrm{d}^3\boldsymbol{k}_0\,|\boldsymbol{B}(t,\boldsymbol{k}_0)|^2 \\ &\sim \lambda_1^2(\lambda_2|\lambda_3|)^{1/2}\left(\frac{t}{\eta}\right)^{3/2}|B_{01}(\boldsymbol{k}_0)|^2\ \underbrace{\mathrm{e}^{2\lambda_1 t-|\lambda_3|t}}_{\substack{=\mathrm{e}^{(\lambda_1-\lambda_2)t}\\ \text{since } \mathrm{tr}(\boldsymbol{\sigma})=0}} \\ &\propto t^{3/2}\,\mathrm{e}^{(\lambda_1-\lambda_2)t},\end{aligned} \tag{XII.5.19}$$

which increases in time because $\lambda_1 > \lambda_2$. Therefore, dynamo works in 3D for certain $\boldsymbol{k}_0$.

What if $\lambda_2 < 0$? In this case, the growing modes occur within the volume

$$\frac{k_{01}^2}{2\lambda_1^2 t/\eta} + \frac{k_{02}^2}{2\lambda_1|\lambda_2|t\,\mathrm{e}^{-2|\lambda_2|t}/\eta} + \frac{k_{03}^2}{2\lambda_1|\lambda_3|t\,\mathrm{e}^{-2|\lambda_3|t}/\eta} \lesssim 1,$$

and one can show that

$$\langle B^2\rangle \sim \lambda_1^2(|\lambda_2||\lambda_3|)^{1/2}\left(\frac{t}{\eta}\right)^{3/2}B_{02}^2\ \underbrace{\mathrm{e}^{(\lambda_1-2|\lambda_2|)t}}_{=\mathrm{e}^{(|\lambda_3|-|\lambda_2|)t}}.$$

Thus, the mean magnetic energy grows at rate set by $|\lambda_3| - |\lambda_2|$.

Physically, what's going on is the following. During stretching, the magnetic field aligns with $\hat{\boldsymbol{e}}_1$ (i.e., $\boldsymbol{B} \sim B_{01}\,\mathrm{e}^{\lambda_1 t}\hat{\boldsymbol{e}}_1$). The wavevector mostly wants to align with the compression direction (i.e., $\boldsymbol{k} \sim k_{03}\,\mathrm{e}^{|\lambda_3|t}\hat{\boldsymbol{e}}_3$), which makes most modes decay super-exponentially. The only modes that don't decay are those that had $\boldsymbol{k}_0$ almost perpendicular to $\hat{\boldsymbol{e}}_3$ to begin with (i.e., $k_{03} \lesssim (\dots)\,\mathrm{e}^{-|\lambda_3|t}$ – see (XII.5.18)). Since $\boldsymbol{k}_0 \perp \boldsymbol{B}_0$, this means that the growing modes mostly have $\boldsymbol{k}_0 \sim k_{02}\hat{\boldsymbol{e}}_2$. Again, the picture is

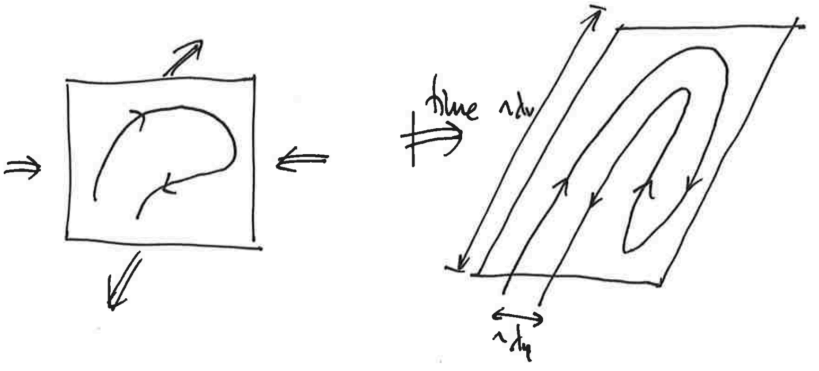

And the winning configuration is

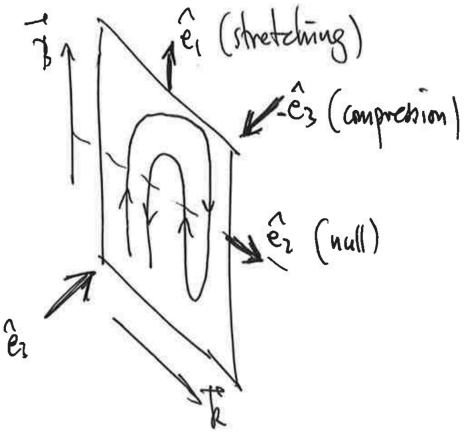

Any other configuration means that each time you stretch, you also compress – then antiparallel field lines are brought together and B^2 decays resistively.[31]

Zel'dovich showed that such a dynamo won't work in 2D. Can we show that using his model? First, in 2D we have $\lambda_1 + \lambda_2 = 0$. Without loss of generality, assume $\lambda_1 > 0$, so that $\hat{\boldsymbol{e}}_1$ is the "stretching" direction and $\hat{\boldsymbol{e}}_2$ is the "compressing" direction. Equations (XII.5.16) then imply

$$\begin{aligned} |\boldsymbol{B}(t,\boldsymbol{k}_0)|^2 &= \mathrm{e}^{-2\eta\int_0^t \mathrm{d}t'\, k^2(t',\boldsymbol{k}_0)}\left[|B_{01}(\boldsymbol{k}_0)|^2\mathrm{e}^{2\lambda_1 t} + |B_{02}(\boldsymbol{k}_0)|^2\mathrm{e}^{-2\lambda_1 t}\right], \\ &\approx |B_{01}(\boldsymbol{k}_0)|^2\,\mathrm{e}^{2\lambda_1 t - 2\eta\int_0^t \mathrm{d}t'\, k^2(t',\boldsymbol{k}_0)}, \end{aligned} \tag{XII.5.20}$$

where the time integral in the exponential is

$$\begin{aligned} \int_0^t \mathrm{d}t'\, k^2(t',\boldsymbol{k}_0) &= \int_0^t \mathrm{d}t'\left(k_{01}^2\,\mathrm{e}^{-2\lambda_1 t} + k_{02}^2\,\mathrm{e}^{2\lambda_1 t}\right) \\ &= \frac{k_{01}^2}{2\lambda_1}(1-\mathrm{e}^{-2\lambda_1 t}) - \frac{k_{02}^2}{2\lambda_1}(1-\mathrm{e}^{2\lambda_1 t}) \\ &\approx \frac{k_{01}^2}{2\lambda_1} + \frac{k_{02}^2}{2\lambda_1}\mathrm{e}^{2\lambda_1 t}. \end{aligned} \tag{XII.5.21}$$

Thus, growth is only possible for those modes satisfying

$$\frac{k_{01}^2}{2\lambda_1^2 t/\eta} + \frac{k_{02}^2}{2\lambda_1^2 t\,\mathrm{e}^{-2\lambda_1 t}/\eta} \lesssim 1, \tag{XII.5.22}$$

which constitutes an ellipsoidal area of size

$$\sim \lambda_1^2\left(\frac{t}{\eta}\right)\mathrm{e}^{-\lambda_1 t}. \tag{XII.5.23}$$

The problem is that, with $k_2(t)$ increasing exponentially, the only modes with the potential for growth must have $\boldsymbol{k}_0$ almost perpendicular to $\hat{\boldsymbol{e}}_2$. But, because $\boldsymbol{k}_0 \cdot \boldsymbol{B}_0(\boldsymbol{k}_0) = 0$ via the divergence-free constraint on the magnetic field, the initial field must then be largely in the $\hat{\boldsymbol{e}}_2$ direction:

$$B_{01}(\boldsymbol{k}_0) = -\frac{k_{02}}{k_{01}}B_{02}(\boldsymbol{k}_0) \sim -\mathrm{e}^{-\lambda_1 t}B_{02}(\boldsymbol{k}_0), \tag{XII.5.24}$$

[31] I learned all this stuff from Alex Schekochihin.

the final step following from (XII.5.22). Then the mean magnetic energy satisfies

$$\begin{aligned}\frac{\langle B^2\rangle}{(2\pi)^2} &= \int \mathrm{d}^2\boldsymbol{k}_0\,|\boldsymbol{B}(t,\boldsymbol{k}_0)|^2 \\ &\sim \lambda_1^2\left(\frac{t}{\eta}\right)\mathrm{e}^{-\lambda_1 t}\,|B_{01}(\boldsymbol{k}_0)|^2\,\mathrm{e}^{2\lambda_1 t} \\ &\sim \lambda_1^2\left(\frac{t}{\eta}\right)|B_{02}(\boldsymbol{k}_0)|^2\,\mathrm{e}^{-\lambda_1 t}. \end{aligned} \tag{XII.5.25}$$

Thus, the fluctuation dynamo is impossible in 2D. Physically, the difficulty is that the only way to avoid bringing oppositely oriented magnetic fields together in a 2D incompressible flow, and thereby avoid super-exponential resistive damping, is to orient the initial magnetic field across the stretching direction rather than along it. But this stretching then dilutes (rather than increases) the field strength, leading to exponential decay. The difference between 2D and 3D is that, in the latter case, the compression direction, to which the wavevector would want to align exponentially, can be avoided by starting with modes whose $\boldsymbol{k}_0$ initially lies in the third ("null") direction. Otherwise, every time you stretch, you also compress, and antiparallel field lines are brought together.

XII.6. Kazantsev–Kraichnan model of the fluctuation dynamo

This is **optional** material and is not written pedagogically.

We start with the evolution equations (XII.5.12), repeated here for convenience:

$$\begin{aligned}\frac{\partial B^i(t,\boldsymbol{k}_0)}{\partial t} &= -\eta k^2(t,\boldsymbol{k}_0)B^i(t,\boldsymbol{k}_0) + B^m(t,\boldsymbol{k}_0)\sigma^i_m(t), \\ \frac{\partial k_m(t,\boldsymbol{k}_0)}{\partial t} &= -k_i(t,\boldsymbol{k}_0)\sigma^i_m(t).\end{aligned}$$

The first step is to split the magnetic field into its scalar strength and its unit-vector direction: $\boldsymbol{B} = B\hat{\boldsymbol{b}}$, so that $B^i = Bb^i$. Substituting this decomposition into the above equations, and henceforth suppressing the argument $(t,\boldsymbol{k}_0)$, yields

$$\begin{aligned}\frac{\partial B}{\partial t} &= -\eta k^2 B + b^i b^m \sigma^i_m B, \\ \frac{\partial b^i}{\partial t} &= b^m\sigma^i_m - b^\ell b^m \sigma^\ell_m b^i, \\ \frac{\partial k_m}{\partial t} &= -k_i\sigma^i_m\end{aligned}$$

The next step is to adorn all of these variables with tildes, which will denote that they are *random* variables. We are about to engage in a statistical calculation, which is quite different than what was done in the previous section. In this case, all random variables are distributed according to a joint probability density function, $\mathcal{P}(t;B,\boldsymbol{k},\hat{\boldsymbol{b}})$, and the tildes will remind us that the field strength, field direction, and wavenumber that we are carrying around in our equations are not *the* field strength, field direction, and

wavenumber. So,

$$\frac{\partial \tilde{B}}{\partial t} = -\eta \tilde{k}^2 \tilde{B} + \tilde{b}^i \tilde{b}^m \tilde{\sigma}^i_m \tilde{B}, \tag{XII.6.1a}$$

$$\frac{\partial \tilde{b}^i}{\partial t} = \tilde{b}^m \tilde{\sigma}^i_m - \tilde{b}^\ell \tilde{b}^m \tilde{\sigma}^\ell_m \tilde{b}^i, \tag{XII.6.1b}$$

$$\frac{\partial \tilde{k}_m}{\partial t} = -\tilde{k}_i \tilde{\sigma}^i_m \tag{XII.6.1c}$$

The rate-of-strain tensor $\tilde{\sigma}^\ell_m \doteq \partial_m \tilde{u}^\ell$ is taken to have the two-time correlation function

$$\overline{\tilde{\sigma}^i_m(t)\tilde{\sigma}^j_n(t')} = \mathit{\Gamma}^{ij}_{mn}(t)\delta(t-t'), \tag{XII.6.2}$$

where the overline denotes the statistical ensemble average and

$$\mathit{\Gamma}^{ij}_{mn}(t) = \kappa_2 \Big[\delta^{ij}\delta_{mn} + a(\delta^i_m \delta^j_n + \delta^i_n \delta^j_m)\Big]. \tag{XII.6.3}$$

Here, κ_2 is the second-order coefficient in the Taylor expansion of the velocity correlation tensor

$$\overline{\tilde{u}^i(t,\boldsymbol{r})\tilde{u}^j(t',\boldsymbol{r}')} = \delta(t-t')\kappa^{ij}(\boldsymbol{r}-\boldsymbol{r}'), \tag{XII.6.4}$$

where

$$\kappa^{ij}(\boldsymbol{y}) = \kappa_0 \delta^{ij} - \frac{1}{2}\kappa_2 \Big[y^2 \delta^{ij} + 2a y^i y^j\Big] + \ldots. \tag{XII.6.5}$$

The constant a parametrizes the rate of strain; its value is fixed by assuming an incompressible flow, $\mathit{\Gamma}^{ij}_{in} = 0$ and $\mathit{\Gamma}^{ij}_{mj} = 0$, giving

$$a = -\frac{1}{1+d} \tag{XII.6.6}$$

in d dimensions. The tensors $\mathit{\Gamma}^{ij}_{mn}$ and κ^{ij} are related in Fourier space by

$$\mathit{\Gamma}^{ij}_{mn}(t) = \int \frac{\mathrm{d}^d \boldsymbol{k}}{(2\pi)^d}\, k_m k_n \kappa^{ij}(\boldsymbol{k}). \tag{XII.6.7}$$

Our ultimate goal here is to obtain an evolution equation for the magnetic-energy spectrum $M(k)$. This can be done by first deriving an evolution equation for the joint probability density function of the magnetic field $\boldsymbol{B}$ and its wavenumber $\boldsymbol{k}$,

$$\mathcal{P}(t; B, \boldsymbol{k}, \hat{\boldsymbol{b}}) = \overline{\tilde{\mathcal{P}}} \doteq \overline{\delta(B - \tilde{B}(t))\delta(k_m - \tilde{k}_m(t))\delta(b^i - \tilde{b}^i(t))}, \tag{XII.6.8}$$

and then taking the appropriate moments; to wit,

$$M(t,k) = \int \mathrm{d}\Omega_{\boldsymbol{k}}\, k^2 \int \mathrm{d}^3\hat{\boldsymbol{b}} \int \mathrm{d}B\, B^2 \mathcal{P}(t; B, \boldsymbol{k}, \hat{\boldsymbol{b}}), \tag{XII.6.9}$$

where $\mathrm{d}\Omega_{\boldsymbol{k}}$ is an element of solid angle in wavenumber space. Taking the time derivative

of (XII.6.8) and using (XII.6.1), we get

$$\begin{aligned}\frac{\partial \mathcal{P}}{\partial t} &= \overline{\frac{\partial \tilde{\mathcal{P}}}{\partial t}} = \overline{\left[-\frac{\partial \tilde{B}(t)}{\partial t}\frac{\partial}{\partial B} - \frac{\partial \tilde{k}_m(t)}{\partial t}\frac{\partial}{\partial k_m} - \frac{\partial \tilde{b}^i(t)}{\partial t}\frac{\partial}{\partial b^i}\right]\tilde{\mathcal{P}}} \\ &= -\overline{\left[\tilde{b}^i(t)\tilde{b}^m(t)\tilde{\sigma}^i_m(t)\tilde{B}(t)\frac{\partial}{\partial B} - \eta\tilde{k}^2(t)\tilde{B}(t)\frac{\partial}{\partial B} - \tilde{\sigma}^i_m(t)\tilde{k}_i(t)\frac{\partial}{\partial k_m}\right.} \\ &\quad \overline{\left. + \tilde{\sigma}^i_m(t)\tilde{b}^m(t)\frac{\partial}{\partial b^i} - \tilde{\sigma}^l_m(t)\tilde{b}^l(t)\tilde{b}^m(t)\tilde{b}^i(t)\frac{\partial}{\partial b^i}\right]\tilde{\mathcal{P}}} \\ &= -\hat{L}^m_i\overline{\tilde{\sigma}^i_m(t)\tilde{\mathcal{P}}} + \eta k^2\frac{\partial}{\partial B}B\mathcal{P}, \end{aligned} \tag{XII.6.10}$$

where

$$\hat{L}^m_i \doteq \frac{\partial}{\partial B}Bb^ib^m - \frac{\partial}{\partial k_m}k_i + \frac{\partial}{\partial b^i}b^m - \frac{\partial}{\partial b^l}b^lb^ib^m. \tag{XII.6.11}$$

To arrive at the final line of (XII.6.10), the identity $a\,\delta(a-b) = b\,\delta(a-b)$ was used. Note that everything in the square brackets in the final line is non-random. To perform the remaining ensemble average, we make use of the Furutsu–Novikov formula (Furutsu 1963; Novikov 1965), which generalizes Gaussian splitting to functions:

$$\overline{\tilde{\sigma}^i_m(t)\tilde{\mathcal{P}}(t)} = \int_0^t \mathrm{d}t'\,\overline{\tilde{\sigma}^i_m(t)\tilde{\sigma}^j_n(t')}\,\overline{\frac{\delta\tilde{\mathcal{P}}(t)}{\delta\tilde{\sigma}^j_n(t')}}. \tag{XII.6.12}$$

The functional derivative with respect to $\tilde{\sigma}^j_n(t')$ can be calculated by formally integrating $\partial\tilde{\mathcal{P}}(t)/\partial t$ with respect to time:

$$\begin{aligned}\frac{\delta\tilde{\mathcal{P}}(t)}{\delta\tilde{\sigma}^j_n(t')} &= -\hat{L}^m_i\int_0^t \mathrm{d}t''\,\frac{\delta\tilde{\sigma}^i_m(t'')}{\delta\tilde{\sigma}^j_n(t')}\tilde{\mathcal{P}}(t'') - \int_0^t \mathrm{d}t''\,\left(\hat{L}^m_i\tilde{\sigma}^i_m(t'') - \eta k^2\frac{\partial}{\partial B}B\right)\frac{\delta\tilde{\mathcal{P}}(t'')}{\delta\tilde{\sigma}^j_n(t')} \\ &= -\hat{L}^n_j\int_0^t \mathrm{d}t''\,\delta(t'-t'')\tilde{\mathcal{P}}(t'') = -\hat{L}^n_j\tilde{\mathcal{P}}(t'). \end{aligned} \tag{XII.6.13}$$

The last term in first line is dropped because it disappears when $t = t'$, owing to causality (i.e., $\tilde{\mathcal{P}}$ cannot depend on future values of $\tilde{\sigma}$). Using this result in (XII.6.12) alongside (XII.6.2), we find

$$\overline{\tilde{\sigma}^i_m(t)\tilde{\mathcal{P}}(t)} = -\frac{1}{2}\hat{L}^n_j\Gamma^{ij}_{mn}\overline{\tilde{\mathcal{P}}(t)} = -\frac{1}{2}\hat{L}^n_j\Gamma^{ij}_{mn}\mathcal{P}(t). \tag{XII.6.14}$$

The result of these manipulations is a closed equation for the joint probability density function:

$$\frac{\partial\mathcal{P}}{\partial t} = \frac{1}{2}\hat{L}^m_i\hat{L}^n_j\Gamma^{ij}_{mn}\mathcal{P} + \eta k^2\frac{\partial}{\partial B}B\mathcal{P}. \tag{XII.6.15}$$

Equation (XII.6.15) can be greatly simplified by noting that $\mathcal{P}(B, \boldsymbol{k}, \hat{\boldsymbol{b}})$ must have the following factorization:

$$\mathcal{P}(B, \boldsymbol{k}, \hat{\boldsymbol{b}}) = \delta(|\hat{\boldsymbol{b}}|^2 - 1)\delta(\hat{\boldsymbol{b}}\cdot\boldsymbol{k})\widehat{P}(B, k). \tag{XII.6.16}$$

The two delta functions result, respectively, from $\hat{\boldsymbol{b}}$ being a unit vector and from the solenoidality constraint $\hat{\boldsymbol{b}}\cdot\boldsymbol{k} = 0$. The remaining factor in (XII.6.16), $\widehat{P}(B, k)$, is a result of the statistics being homogeneous and the relative alignment of $\hat{\boldsymbol{b}}$ and $\boldsymbol{k}$ being fixed.[32]

[32] $\widehat{P}(B, k)$ receives proper normalization below in (XII.6.24), after which its ornamental hat is dropped.

In order to express (XII.6.15) in terms of $\widehat{P}$, we use the chain rule to write

$$\hat{L}_j^n = -k_j \frac{\partial}{\partial k_n} + \left(b^n \frac{\partial}{\partial b^j} - b^j b^n b^q \frac{\partial}{\partial b^q} \right) + b^j b^n \left(\frac{\partial}{\partial B} B - d - 2 \right), \tag{XII.6.17}$$

where d is the dimensionality of the system, and then calculate the combination $\hat{L}_j^n \Gamma_{mn}^{ij} \mathcal{P}(B, \boldsymbol{k}, \hat{\boldsymbol{b}})$. For any function f,

$$\begin{aligned} \hat{L}_j^n \delta(\hat{\boldsymbol{b}} \cdot \boldsymbol{k}) f &= \delta(\hat{\boldsymbol{b}} \cdot \boldsymbol{k}) \hat{L}_j^n f - k_j b^n \delta'(\hat{\boldsymbol{b}} \cdot \boldsymbol{k}) f + (b^n k_j - b^j b^n \hat{\boldsymbol{b}} \cdot \boldsymbol{k}) \delta'(\hat{\boldsymbol{b}} \cdot \boldsymbol{k}) f \\ &= \delta(\hat{\boldsymbol{b}} \cdot \boldsymbol{k}) \hat{L}_j^n f - b^j b^n (\hat{\boldsymbol{b}} \cdot \boldsymbol{k}) \delta'(\hat{\boldsymbol{b}} \cdot \boldsymbol{k}) f \\ &= \delta(\hat{\boldsymbol{b}} \cdot \boldsymbol{k}) (\hat{L}_j^n + b^n b^j) f, \end{aligned} \tag{XII.6.18}$$

where we have used $x\delta'(x) = -\delta(x)$ to obtain the final equality. Similarly,

$$\hat{L}_j^n \delta(|\hat{\boldsymbol{b}}|^2 - 1) f = \delta(|\hat{\boldsymbol{b}}|^2 - 1)(\hat{L}_j^n + 2 b^n b^j) f. \tag{XII.6.19}$$

Combining (XII.6.18) and (XII.6.19) leads to

$$\begin{aligned} \hat{L}_j^n \Gamma_{mn}^{ij} \mathcal{P} &= \delta(\hat{\boldsymbol{b}} \cdot \boldsymbol{k}) \delta(|\hat{\boldsymbol{b}}|^2 - 1)(\hat{L}_j^n + 3 b^n b^j) \Gamma_{mn}^{ij} \widehat{P}(B, k) \\ &= \delta(\hat{\boldsymbol{b}} \cdot \boldsymbol{k}) \delta(|\hat{\boldsymbol{b}}|^2 - 1) \left[-\frac{k_j k_n}{k^2} \Gamma_{mn}^{ij} k \frac{\partial}{\partial k} + b^j b^n \Gamma_{mn}^{ij} \left(\frac{\partial}{\partial B} B - d + 1 \right) \right] \widehat{P}(B, k). \end{aligned} \tag{XII.6.20}$$

Taking into account the solenoidality constraint $\hat{\boldsymbol{b}} \cdot \boldsymbol{k} = 0$ imposed by the prefactor in (XII.6.20), the following combinations in (XII.6.20) may be calculated:

$$\frac{k_j k_n}{k^2} \Gamma_{mn}^{ij} = \kappa_2 \left[a \delta_m^i + (a+1) \frac{k_i k_m}{k^2} \right], \tag{XII.6.21a}$$

$$b^j b^n \Gamma_{mn}^{ij} = \kappa_2 \left[a \delta_m^i + (1+a) b^i b^m \right]. \tag{XII.6.21b}$$

Using these formulae in (XII.6.20) gives

$$\begin{aligned} \hat{L}_j^n \Gamma_{mn}^{ij} \mathcal{P} = \kappa_2 \delta(\hat{\boldsymbol{b}} \cdot \boldsymbol{k}) \delta(|\hat{\boldsymbol{b}}|^2 - 1) \Bigg\{ &- \left[a \delta_m^i + (a+1) \frac{k_i k_m}{k^2} \right] k \frac{\partial}{\partial k} \\ &+ \left[a \delta_m^i + (1+a) b^i b^m \right] \frac{\partial}{\partial B} B - a(d-1) \delta_m^i - (1+a)(d-1) b^i b^m \Bigg\} \widehat{P}(B, k). \end{aligned} \tag{XII.6.22}$$

Further applying the operator $\hat{L}_i^m$ and expending much effort along the same lines gives us the expression for the first term in (XII.6.15):

$$\begin{aligned} \hat{L}_i^m \hat{L}_j^n \Gamma_{mn}^{ij} \mathcal{P} = \Bigg\{ &(2a+1) k^2 \frac{\partial^2}{\partial k^2} + (1+2a) \frac{\partial}{\partial B} B \frac{\partial}{\partial B} B \\ &- 2a \frac{\partial}{\partial B} B k \frac{\partial}{\partial k} + \left[d + (3d-1)a \right] k \frac{\partial}{\partial k} \\ &- (1+3a)(d-1) \frac{\partial}{\partial B} B + a(d-1)^2 \Bigg\} \widehat{P}(B, k). \end{aligned} \tag{XII.6.23}$$

Normalizability of the PDF requires that

$$\begin{aligned} 1 &= \int \mathrm{d}^d \hat{\boldsymbol{b}}\, \delta(|\hat{\boldsymbol{b}}|^2 - 1) \int \mathrm{d}^d \boldsymbol{k}\, \delta(\hat{\boldsymbol{b}} \cdot \boldsymbol{k}) \int \mathrm{d}B\, \widehat{P}(B, k) \\ &= \frac{S_{d-1} S_{d-2}}{2} \int_0^\infty \mathrm{d}k\, k^{d-2} \int \mathrm{d}B\, \widehat{P}(B, k), \end{aligned} \tag{XII.6.24}$$

where S_n is the surface area of unit n-sphere (e.g., $S_1 = 2\pi$, $S_2 = 4\pi$). Taking this normalization into consideration, we define $P(B,k) \doteq S_{d-1}S_{d-2}k^{d-2}\widehat{P}(B,k)/2$ and use

$$k^{d-2}k\frac{\partial}{\partial k}\frac{1}{k^{d-2}}P = \left[k\frac{\partial}{\partial k} - (d-2)\right]P, \tag{XII.6.25a}$$

$$k^{d-2}k^2\frac{\partial^2}{\partial k^2}\frac{1}{k^{d-2}}P = \left[k^2\frac{\partial^2}{\partial k^2} - 2(d-2)k\frac{\partial}{\partial k} + (d-2)(d-1)\right]P \tag{XII.6.25b}$$

to turn (XII.6.15) into

$$\begin{aligned}\frac{\partial P}{\partial t} = \frac{1}{2}\kappa_2\Big\{&(1+2a)\frac{\partial}{\partial k}k^2\frac{\partial}{\partial k} + (1+2a)\frac{\partial}{\partial B}B\frac{\partial}{\partial B}B\\ &- 2a\frac{\partial}{\partial B}B\frac{\partial}{\partial k}k - \big[(d-2)+(d-3)a\big]\frac{\partial}{\partial k}k\\ &- (1+a)(d-1)\frac{\partial}{\partial B}B\Big\}P + \eta k^2\frac{\partial}{\partial B}BP.\end{aligned} \tag{XII.6.26}$$

We now enforce incompressibility. Substituting (XII.6.6) into (XII.6.26) leads to the final form of the evolution equation of the joint PDF:

$$\begin{aligned}\frac{\partial P}{\partial t} = \frac{\kappa_2}{2(d+1)}\Big[&(d-1)\frac{\partial}{\partial k}k^2\frac{\partial}{\partial k} + (d-1)\frac{\partial}{\partial B}B\frac{\partial}{\partial B}B + 2\frac{\partial}{\partial B}B\frac{\partial}{\partial k}k\\ &- (d-1)^2\frac{\partial}{\partial k}k - d(d-1)\frac{\partial}{\partial B}B\Big]P + \eta k^2\frac{\partial}{\partial B}BP.\end{aligned} \tag{XII.6.27}$$

The magnetic-energy spectrum is $M(k) = (1/2)\int_0^\infty \mathrm{d}B\, B^2 P(B,k)$. Taking the B^2 moment of (XII.6.27) leads to

$$\frac{\partial M}{\partial t} = \frac{\overline{\gamma}}{d+2}\frac{\partial}{\partial k}\left[k^2\frac{\partial}{\partial k} - \left(\frac{4}{d-1}+d-1\right)k\right]M + 2\overline{\gamma}M - 2\eta k^2 M, \tag{XII.6.28}$$

where

$$\overline{\gamma} \doteq \kappa_2\frac{(d-1)(d+2)}{2(d+1)}. \tag{XII.6.29}$$

It is straightforward to show by changing variables using $z = \ln k$ that equation (XII.6.28) is a diffusion equation with constant coefficients. In fact, it is in the form of a Fokker–Planck equation, with diffusion of the magnetic energy through k-space (the term in brackets), growth of the magnetic energy via stretching at a rate $2\overline{\gamma}$, and diffusion of the magnetic field via resistivity at a rate $2\eta k^2$.

In three dimensions ($d = 3$), equation (XII.6.28) becomes

$$\frac{\partial M}{\partial t} = \frac{\overline{\gamma}}{5}\frac{\partial}{\partial k}\left(k^2\frac{\partial}{\partial k} - 4k\right)M + 2\overline{\gamma}M - 2\eta k^2 M, \quad \text{with} \quad \overline{\gamma} = \kappa_2\frac{5}{4}. \tag{XII.6.30}$$

This equation has the following solution when $\eta = 0$:

$$M(t,k) = \mathrm{e}^{(3/4)\overline{\gamma}t}\int_0^\infty \frac{\mathrm{d}k'}{k'}\,M_0(k')\frac{1}{\sqrt{\pi\kappa_2 t}}\left(\frac{k}{k'}\right)^{3/2}\mathrm{e}^{-[\ln(k/k')]^2/\kappa_2 t}, \tag{XII.6.31}$$

which you can verify by substitution; here, $M_0(k)$ is the initial spectrum of the magnetic energy. Thus, the magnetic energy grows exponentially and exhibits a power spectrum $\propto k^{3/2}$ – the *Kazantsev spectrum*. The peak wavenumber moves exponentially fast towards smaller scales until resistivity becomes important, at which time the following

approximate solution holds:

$$M(k) \approx k^{3/2} \mathrm{e}^{(3/4)\overline{\gamma}t} K_0(k/k_\eta), \tag{XII.6.32}$$

where K_0 is the zeroth-order modified Bessel function of the second kind ("MacDonald function") and $k_\eta = \sqrt{\overline{\gamma}/10\eta} \gg k_\nu$ is the resistive scale. Such a spectrum is shown in the figure below:

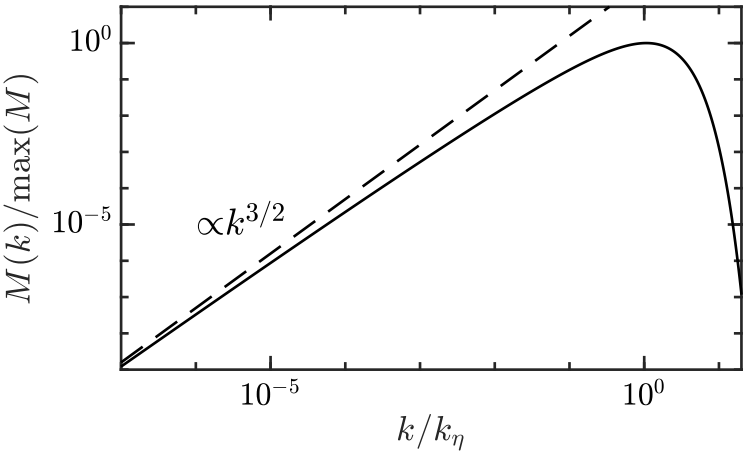

Read more in Kulsrud & Anderson (1992) and Schekochihin *et al.* (2002).

XII.7. Cowling's anti-dynamo theorem

Zel'dovich's anti-dynamo theorem is just one of many anti-dynamo theorems, all of which involve some constraints on the allowed symmetries of the velocity fields that can act as dynamos or of the magnetic fields that can be generated by dynamo action. Their essence can be summarized in three words: "symmetry is bad". (There is another type of constraint on dynamo action concerning the minimum Rm below which field amplification is hampered by resistivity, but I won't cover that here.) Perhaps the most well-known of these is the Cowling (1933) anti-dynamo theorem, which states that an axisymmetric magnetic field (that vanishes at infinity) cannot be maintained by dynamo action. (Wikipedia adds "by an axially symmetric current", but this qualifier is unnecessary. A non-axisymmetric flow always creates a non-axisymmetric field. The converse is not true, however: an axisymmetric flow can create a non-axisymmetric magnetic field, e.g., the Ponomarenko dynamo.) From Cowling's seminal paper on magnetic fields in sunspots:

> A similar argument shows that a field which resembles an axially symmetric field in certain respects cannot, in general, be maintained by the currents it itself sets up. For example, suppose that the lines of force are closed curves all threading a limiting closed curve, and threading it in the same direction. Then the currents required to maintain the field will, near the limit curve, have a component in the direction of the curve which is at all points directed in the same sense round the curve. This component is not due to electrostatic fields, which can only make currents flow from points of high potential to points of low potential, and cannot cause them to flow round a circuit: equally it cannot be due to electromagnetic induction, by an argument similar to the above. Hence such a field cannot be self-maintained...
>
> Since, then, fields possessing a general similarity to an axially symmetric field cannot be self-maintained, we are led to conclude that the magnetic field of a

sunspot is not self-maintained. For the same reason the general magnetic fields of the Sun and the Earth cannot be self-maintained, as was suggested by Larmor.[33]

The proof goes as follows. Consider an axisymmetric magnetic field in cylindrical coordinates (R, φ, Z) of the form $\boldsymbol{B} = B_\varphi(R,Z)\hat{\boldsymbol{\varphi}} + \boldsymbol{B}_\mathrm{p}(R,Z)$, where B_φ is the toroidal (azimuthal) component and $\boldsymbol{B}_\mathrm{p} = \boldsymbol{\nabla}\times(A\hat{\boldsymbol{\varphi}})$ is the poloidal (radial and axial) component. The fluid flow is, by necessity, axisymmetric as well: $\boldsymbol{u} = u_\varphi(R,Z)\hat{\boldsymbol{\varphi}} + \boldsymbol{u}_\mathrm{p}(R,Z)$, with $\boldsymbol{\nabla}\cdot\boldsymbol{u}_\mathrm{p} = 0$ assumed. Substituting these fields into the resistive-MHD induction equation (XII.5.1) leads to

$$\frac{\partial B_\varphi}{\partial t} + R\boldsymbol{u}_\mathrm{p}\cdot\boldsymbol{\nabla}\frac{B_\varphi}{R} = \eta\left(\nabla^2 - \frac{1}{R^2}\right)B_\varphi + R\boldsymbol{B}_\mathrm{p}\cdot\boldsymbol{\nabla}\frac{u_\varphi}{R}, \tag{XII.7.1}$$

$$\frac{\partial A}{\partial t} + \frac{1}{R}\boldsymbol{u}_\mathrm{p}\cdot\boldsymbol{\nabla}(RA) = \eta\left(\nabla^2 - \frac{1}{R^2}\right)A. \tag{XII.7.2}$$

These are the cylindrical analogues of (XII.5.2) and (XII.5.4), respectively. The important term here is the final one in (XII.7.1); with $u_\varphi = R\Omega(R,Z)$, it constitutes a source term that produces a toroidal magnetic field by the shearing of a poloidal one – the so-called "Ω effect". While this can transiently make a strong toroidal field, it does not constitute a dynamo. The reason why is that this term relies on the longevity of the poloidal field, whose evolution is governed through (XII.7.2). It is this equation that dooms the poloidal field to resistive decay. To see this, define the flux function $\psi \doteq RA$; then (XII.7.2) may be written as

$$\frac{\partial\psi}{\partial t} + \boldsymbol{u}_\mathrm{p}\cdot\boldsymbol{\nabla}\psi = \eta R\left(\nabla^2 - \frac{1}{R^2}\right)\frac{\psi}{R}.$$

Multiplying this equation through by 2ψ and re-arranging terms,

$$\frac{\partial\psi^2}{\partial t} + \boldsymbol{\nabla}\cdot(\boldsymbol{u}_\mathrm{p}\psi^2) = 2\eta\boldsymbol{\nabla}\cdot\left(\psi^2\,\boldsymbol{\nabla}\ln\frac{\psi}{R}\right) - 2\eta|\boldsymbol{\nabla}\psi|^2.$$

Integrating over space leaves

$$\frac{\mathrm{d}\langle\psi^2\rangle}{\mathrm{d}t} = -2\eta\langle|\boldsymbol{\nabla}\psi|^2\rangle,$$

and so the poloidal component of the magnetic field decays resistively. With no source term in (XII.7.1), the toroidal component shares the same fate.

XII.8. Mean-field dynamos

In the fluctuation dynamo, a zero-net-flux magnetic field is amplified by a chaotic flow. The resulting field generally has its power on the smallest available scales. There is another kind of dynamo in which both the magnetic and velocity fields have mean components – one which generically leads to the growth of large-scale magnetic fields. While

[33] Sir Joseph Larmor (1919) at a meeting of the British Association for the Advancement of Science asked "How could a rotating body such as the Sun become a magnet? ... Such internal motion induces an electric field acting on the moving matter: and if any conducting path around the Solar axis happens to be open, an electric current will flow round it, which may in turn increase the inducing magnetic field. In this way it is possible for the internal cyclic motion to act after the manner of the cycle of a self-exciting dynamo, and maintain a permanent magnetic field from insignificant beginnings, at the expense of some of the energy of the internal circulation."

an active topic of research concerns the interplay between the small-scale fluctuation dynamo and this "mean-field dynamo", here I will focus exclusively on the latter.[34]

The basic idea is to split the magnetic and velocity fields into their mean and fluctuating parts:

$$\boldsymbol{B} = \langle \boldsymbol{B} \rangle + \delta \boldsymbol{B} \quad \text{and} \quad \boldsymbol{u} = \langle \boldsymbol{u} \rangle + \delta \boldsymbol{u}. \tag{XII.8.1}$$

Note that $\langle \delta \boldsymbol{B} \rangle = \langle \delta \boldsymbol{u} \rangle = 0$ by definition. The evolution of the volume-averaged quantities $\langle \boldsymbol{B} \rangle$ and $\langle \boldsymbol{u} \rangle$ will depend upon quantities quadratic in the fluctuations, *viz.* $\langle \delta \boldsymbol{B}\, \delta \boldsymbol{B} \rangle$, $\langle \delta \boldsymbol{B}\, \delta \boldsymbol{u} \rangle$, $\langle \delta \boldsymbol{u}\, \delta \boldsymbol{B} \rangle$, and $\langle \delta \boldsymbol{u}\, \delta \boldsymbol{u} \rangle$. These quadratic quantities will then depend on cubic terms, and the cubic terms on quartic terms, and on. It is the business of mean-field theory to close this hierarchy and thereby obtain a closed equation for the time evolution of $\langle \boldsymbol{B} \rangle$ and $\langle \boldsymbol{u} \rangle$. This proceeds as follows.

Assuming that our averaging procedure commutes with differentiation, the averaged resistive-MHD induction equation (see (XII.5.1)) is

$$\frac{\partial \langle \boldsymbol{B} \rangle}{\partial t} = \boldsymbol{\nabla} \times \langle \boldsymbol{u} \times \boldsymbol{B} \rangle + \eta \nabla^2 \langle \boldsymbol{B} \rangle. \tag{XII.8.2}$$

The term of interest is, of course, the inductive term, which may be expanded using (XII.8.1):

$$\langle \boldsymbol{u} \times \boldsymbol{B} \rangle = \langle \boldsymbol{u} \rangle \times \langle \boldsymbol{B} \rangle + \langle \delta \boldsymbol{u} \times \delta \boldsymbol{B} \rangle \doteq \langle \boldsymbol{u} \rangle \times \langle \boldsymbol{B} \rangle + \boldsymbol{\mathcal{E}}, \tag{XII.8.3}$$

where we have defined the *mean electro-motive force* (emf) $\boldsymbol{\mathcal{E}}$. Equation (XII.8.2) then becomes

$$\boxed{\frac{\partial \langle \boldsymbol{B} \rangle}{\partial t} = \boldsymbol{\nabla} \times \big(\langle \boldsymbol{u} \rangle \times \langle \boldsymbol{B} \rangle \big) + \boldsymbol{\nabla} \times \boldsymbol{\mathcal{E}} + \eta \nabla^2 \langle \boldsymbol{B} \rangle} \tag{XII.8.4}$$

It is this mean emf that spoils Cowling's theorem. As I foreshadowed, one cannot write down a closed-form expression for $\boldsymbol{\mathcal{E}}$ without approximation, but let us feign ignorance and carry on regardless.

The equation governing the magnetic-field fluctuations may be obtained by further subtracting (XII.8.4) from (XII.5.1). Introducing the vector $\boldsymbol{\mathcal{G}} \doteq \delta \boldsymbol{u} \times \delta \boldsymbol{B} - \langle \delta \boldsymbol{u} \times \delta \boldsymbol{B} \rangle$ and re-arranging terms, the result is

$$\frac{\partial \delta \boldsymbol{B}}{\partial t} - \boldsymbol{\nabla} \times \big(\langle \boldsymbol{u} \rangle \times \delta \boldsymbol{B} \big) - \boldsymbol{\nabla} \times \boldsymbol{\mathcal{G}} - \eta \nabla^2 \delta \boldsymbol{B} = \boldsymbol{\nabla} \times \big(\delta \boldsymbol{u} \times \langle \boldsymbol{B} \rangle \big). \tag{XII.8.5}$$

Note that all terms on the left-hand side of this equation are linear in $\delta \boldsymbol{B}$, at least to the extent that $\boldsymbol{u}$ is independently prescribed. The right-hand side, however, is a source term; physically, it represents the creation of a fluctuating magnetic field by the fluctuating velocity shearing and tangling the mean magnetic field. It is at this point that most discussions state that the resulting linear relation between $\delta \boldsymbol{B}$ and $\langle \boldsymbol{B} \rangle$ implies a linear relation between $\boldsymbol{\mathcal{E}}$ and $\langle \boldsymbol{B} \rangle$, and that relation is simply written down as if it fell from heaven above. I don't buy it, so perhaps it is worthwhile to actually calculate the

[34] You can find a nice review article on mean-field dynamos and their history here: http://www.aip.de/People/khraedler/HIST_MHD_06_Rae.pdf

contribution to $\boldsymbol{\mathcal{E}}$ from that source term:

$$\begin{aligned}
\boldsymbol{\mathcal{E}}_{\text{source}}(t) &= \left\langle \delta\boldsymbol{u}(t) \times \int^t \mathrm{d}t' \left.\frac{\partial \delta\boldsymbol{B}(t')}{\partial t'}\right|_{\text{source}} \right\rangle \\
&= \left\langle \delta\boldsymbol{u}(t) \times \int^t \mathrm{d}t' \, \boldsymbol{\nabla} \times \big[\delta\boldsymbol{u}(t') \times \langle \boldsymbol{B}(t')\rangle\big] \right\rangle \\
&= \int^t \mathrm{d}t' \left\langle \big[\boldsymbol{\nabla}(\delta\boldsymbol{u}(t') \times \langle \boldsymbol{B}(t')\rangle)\big] \cdot \delta\boldsymbol{u}(t) - \delta\boldsymbol{u}(t) \cdot \boldsymbol{\nabla}\big[\delta\boldsymbol{u}(t') \times \langle \boldsymbol{B}(t')\rangle\big] \right\rangle \\
\implies \quad \mathcal{E}^i_{\text{source}}(t) &= \int^t \mathrm{d}t' \, (\epsilon_{j\ell m}\delta_{ik} - \epsilon_{jim}\delta_{\ell k}) \\
&\quad \times \left[\left\langle \delta u^\ell(t) \frac{\partial \delta u^m(t')}{\partial r^k} \right\rangle \langle B^j(t')\rangle + \langle \delta u^\ell(t) \delta u^m(t')\rangle \frac{\partial \langle B^j(t')\rangle}{\partial r^k} \right] \\
&\doteq \int^t \mathrm{d}t' \left[\alpha_{ij}(t-t') \langle B^j(t')\rangle + \beta_{ijk}(t-t') \frac{\partial \langle B^j(t')\rangle}{\partial r^k} \right].
\end{aligned} \tag{XII.8.6}$$

In the final step, we have introduced the $\boldsymbol{\alpha}(\tau)$ and $\boldsymbol{\beta}(\tau)$ tensors, which are related to correlations between the velocity fluctuations separated in time by an interval τ. Notably, $\boldsymbol{\alpha}$ says something about the correlation between the velocity fluctuations and their vorticity, $\delta\boldsymbol{\omega} \doteq \boldsymbol{\nabla} \times \delta\boldsymbol{u}$. If the turbulence is homogeneous and isotropic, then $\alpha_{ij}(\tau) = \alpha(\tau)\delta_{ij}$ and $\beta_{ijk}(\tau) = \beta(\tau)\epsilon_{ijk}$, and (XII.8.6) becomes

$$\boldsymbol{\mathcal{E}}_{\text{source}} = \int^t \mathrm{d}t' \left[\alpha(t-t') \langle \boldsymbol{B}(t')\rangle - \beta(t-t') \boldsymbol{\nabla} \times \langle \boldsymbol{B}(t')\rangle \right], \tag{XII.8.7}$$

where

$$\alpha(t-t') = -\frac{1}{3}\langle \delta\boldsymbol{u}(t) \cdot \delta\boldsymbol{\omega}(t')\rangle \quad \text{and} \quad \beta(t-t') = \frac{1}{3}\langle \delta\boldsymbol{u}(t) \cdot \delta\boldsymbol{u}(t')\rangle. \tag{XII.8.8}$$

The combination $\boldsymbol{u} \cdot \boldsymbol{\omega}$ is known as the *kinetic helicity*; it is zero if the velocity field is on the average mirror symmetric. If the flow has a vanishing correlation time relative to the growth/decay time of the magnetic field, then it is said to be "delta-correlated" and (XII.8.7) becomes

$$\boldsymbol{\mathcal{E}}_{\text{source}} \simeq \alpha\langle \boldsymbol{B}\rangle - \beta \boldsymbol{\nabla} \times \boldsymbol{B}. \tag{XII.8.9}$$

In this case, the final (β) term acts as a turbulent diffusivity, supplementing the resistive diffusivity: $\eta\nabla^2\langle \boldsymbol{B}\rangle$ in (XII.8.4) becomes $(\eta + \beta)\nabla^2\langle \boldsymbol{B}\rangle$.

The α and β terms are usually argued to represent not only the source term on the right-hand side of (XII.8.5) but also all the other emf-like terms on its left-hand side. Let us follow this assumption and adopt (XII.8.9) as an approximation for the total mean emf and see what it implies for dynamo action. Equation (XII.8.4) then reads

$$\frac{\partial \langle \boldsymbol{B}\rangle}{\partial t} = \boldsymbol{\nabla} \times \big(\langle \boldsymbol{u}\rangle \times \langle \boldsymbol{B}\rangle\big) + \alpha \boldsymbol{\nabla} \times \langle \boldsymbol{B}\rangle + (\eta + \beta)\nabla^2\langle \boldsymbol{B}\rangle. \tag{XII.8.10}$$

We consider two limits of this equation. First, assume $\langle \boldsymbol{u}\rangle = 0$, so that the mean-field inductive term vanishes and we have

$$\frac{\partial \langle \boldsymbol{B}\rangle}{\partial t} = \alpha \boldsymbol{\nabla} \times \langle \boldsymbol{B}\rangle + (\eta + \beta)\nabla^2\langle \boldsymbol{B}\rangle.$$

Adopting plane-wave solutions $\sim \exp(\gamma t + \mathrm{i}\boldsymbol{k} \cdot \boldsymbol{r})$, it is straightforward to show that the growth/decay rate γ satisfies

$$\gamma = \pm k\alpha - k^2(\eta + \beta), \tag{XII.8.11}$$

where the upper (lower) sign corresponds to negative (positive) magnetic helicity. The growing solution is called an "α^2 dynamo". For $k > 0$, the α term generates $\langle B_y \rangle$ from $\langle B_x \rangle$, and then further uses that $\langle B_y \rangle$ to amplify the original $\langle B_x \rangle$. Note that the signs of the kinetic and magnetic helicities must be alike. If, for some reason α were to depend on $\langle \boldsymbol{B} \rangle$ in such a way that it decreases as the mean magnetic-field strength increases (e.g., via back-reaction from the Lorentz force), then this dynamo will eventually shut off – an effect referred to as "α quenching".

Now restore the $\langle \boldsymbol{u} \rangle \times \langle \boldsymbol{B} \rangle$ term and suppose $\langle \boldsymbol{u} \rangle = -\omega x \hat{\boldsymbol{y}}$, where $\omega > 0$ is the characteristic frequency of the flow shear. Then (XII.8.10) becomes

$$\left(\frac{\partial}{\partial t} - \omega x \frac{\partial}{\partial y} \right) \langle \boldsymbol{B} \rangle = -\omega \langle B_x \rangle \hat{\boldsymbol{y}} + \alpha \boldsymbol{\nabla} \times \langle \boldsymbol{B} \rangle + (\eta + \beta) \nabla^2 \langle \boldsymbol{B} \rangle .$$

Note that the gradient in the fluid flow generates $\langle B_y \rangle$ by shearing $\langle B_x \rangle$ into the streamwise direction. If the α term is such that this generated field is re-oriented into the x direction, then the mean field will grow – a process known as the "α-ω dynamo". So long as $\boldsymbol{k} \cdot \hat{\boldsymbol{y}} = 0$, plane-wave solutions satisfy

$$\gamma = \pm \sqrt{k_z \alpha (\mathrm{i}\omega + k_z \alpha)} - k^2 (\eta + \beta). \tag{XII.8.12}$$

Clearly, there must be a component of $\boldsymbol{k}$ in the $\hat{\boldsymbol{y}} \times \boldsymbol{\nabla} |\langle \boldsymbol{u} \rangle|$ direction. But it also must have the correct sign for growth. This is complicated by the i that accompanies ω: the growth rate is complex, and so these *dynamo waves* propagate. To figure this out, let us assume $|k_z \alpha| \ll \omega$, so that the α^2 component of the dynamo expressed in (XII.8.12) is sub-dominant to the α-ω component. Then

$$\gamma \approx \pm \sqrt{\mathrm{i} k_z \alpha \omega} - k^2 (\eta + \beta).$$

Suppose that $\mathrm{Re}(\gamma) > 0$, so that we have growth. Recalling $\sqrt{\mathrm{i}} = \pm (1 + \mathrm{i})/\sqrt{2}$, we require $k_z \alpha \omega = \boldsymbol{k} \cdot (\hat{\boldsymbol{y}} \times \boldsymbol{\nabla} |\langle \boldsymbol{u} \rangle|) > 0$. In this case, $\gamma \approx k_z \alpha \omega (1 + \mathrm{i})/\sqrt{2}$ and so the mode grows and propagates along the trajectory $\dot{z} = -\alpha \omega / \sqrt{2}$, i.e., in the $-\alpha \hat{\boldsymbol{y}} \times \boldsymbol{\nabla} |\langle \boldsymbol{u} \rangle|$ direction. Note further that the fastest-growing mode has $\boldsymbol{k}$ exactly parallel to $\hat{\boldsymbol{y}} \times \boldsymbol{\nabla} |\langle \boldsymbol{u} \rangle|$.

This kind of mean-field dynamo is important in the differentially rotating solar convective zone, in which the resulting dynamo waves have been conjectured to cause the observed 22-year period of sunspot activity (Parker 1955). (In spherical geometry with φ replacing y and (r, θ) replacing (x, z), the growing dynamo mode propagates in the $-\alpha \hat{\boldsymbol{\varphi}} \times \boldsymbol{\nabla} \Omega$ direction, where $\Omega(r, \theta)$ is the angular velocity.) The idea is that the Solar dynamo is of the α-ω type, with $\alpha > 0$ (< 0) in the northern (southern) hemisphere and $\partial \Omega / \partial r < 0$ throughout the convection zone. This combination gives the correct equator-ward migration of sunspots (e.g. Moffatt 1978; Parker 1979; Krause & Raedler 1980).

One could write a lot more about dynamo theory, experiment, and observation, but these course notes are not really the place for that. If you'd like to learn more, you can start with the excellent reviews by Childress & Gilbert (1995), Gilbert (2003), and Rincon (2019).

PART XIII

Braginskii: MHD in a magnetized plasma

XIII.1. Chapman–Enskog, Braginskii, and magnetized transport

By now you've spent a great deal of time playing with various versions and applications of the MHD equations. So now it's time to formulate some new equations! Go all the way back to the end of Part III where general "fluid" equations were obtained by taking moments of the Vlasov–Landau equation. So that you don't have to go digging through this PDF or your notes, I'll repeat them here:

$$\frac{\mathrm{D}n_\alpha}{\mathrm{D}t_\alpha} + n_\alpha \boldsymbol{\nabla\cdot} \boldsymbol{u}_\alpha = 0, \tag{XIII.1.1}$$

$$m_\alpha n_\alpha \frac{\mathrm{D}\boldsymbol{u}_\alpha}{\mathrm{D}t_\alpha} - q_\alpha n_\alpha \left(\boldsymbol{E} + \frac{\boldsymbol{u}_\alpha}{c}\times\boldsymbol{B}\right) - m_\alpha n_\alpha \boldsymbol{g} + \boldsymbol{\nabla} p_\alpha = -\boldsymbol{\nabla\cdot}\boldsymbol{\Pi}_\alpha + \boldsymbol{R}_\alpha, \tag{XIII.1.2}$$

$$\frac{3}{2} p_\alpha \frac{\mathrm{D}}{\mathrm{D}t_\alpha} \ln \frac{p_\alpha}{n_\alpha^{5/3}} = -\boldsymbol{\nabla\cdot}\boldsymbol{q}_\alpha - \boldsymbol{\Pi}_\alpha : \boldsymbol{\nabla}\boldsymbol{u}_\alpha + Q_\alpha. \tag{XIII.1.3}$$

You should recognize that everything on the left-hand sides of these equations ultimately gave us ideal MHD after summing over species and using quasi-neutrality,

$$\sum_\alpha q_\alpha n_\alpha = 0,$$

and Ampère's law,

$$\sum_\alpha q_\alpha n_\alpha \boldsymbol{u}_\alpha = \boldsymbol{j} = \frac{c}{4\pi}\boldsymbol{\nabla}\times\boldsymbol{B}.$$

Remember: in ideal MHD, the distribution function of the plasma particles is locally Maxwellian (exactly!) and thus the plasma can be described entirely in terms of the density n_α, the flow velocity $\boldsymbol{u}_\alpha$, and the pressure p_α of each constituent species α. So what remains on the right-hand sides? These additional terms come in two flavors.

First, $\boldsymbol{R}_\alpha$ and Q_α are the first and second moments of the collision operator, and thus capture the collisional exchange of momentum and entropy between species. (There is no corresponding term in the continuity equation, because we have adopted a collision operator that preserves the total particle number of each species, e.g., recombination is not allowed.) These terms did not appear in single-fluid MHD because $\sum_\alpha \boldsymbol{R}_\alpha = \sum_\alpha Q_\alpha = 0$: Newton's third and energy conservation. But there's nothing particularly "non-MHD" about them: each species could be locally Maxwellian and these terms would still be non-zero, so long as each species' flow velocities and/or temperatures were different. Thus, these terms are important for establishing a *global* thermodynamic equilibrium: through inter-species collisions, all species should eventually take on the same flow velocity, and all species should eventually have the same temperature. The second flavor of non-ideal terms – those involving the viscous stress tensor $\boldsymbol{\Pi}_\alpha \doteq \boldsymbol{P}_\alpha - p_\alpha \boldsymbol{I}$ and the heat flux $\boldsymbol{q}_\alpha$ – are entirely due to non-Maxwellian features in the plasma and are only related to collisions insofar as collisions between species help to regulate departures from local thermodynamic equilibrium. Most importantly, they appear inside divergences and thus represent fluxes of momentum and entropy from one fluid element to the next; in the limit where collisions are important (what "important" means here will be defined below), they capture the diffusive transport of momentum and entropy that occurs locally

between neighboring fluid elements as the system tries to achieve global thermodynamic equilibrium through collisions. Pictorially:

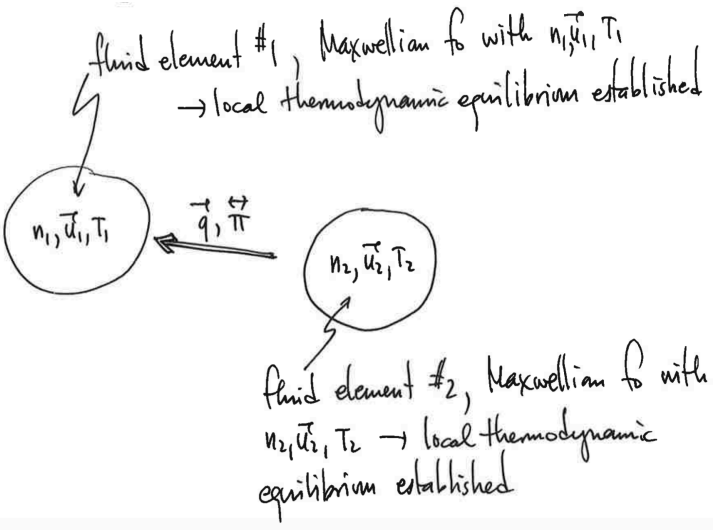

The following excerpt from the review article by Hinton (1983) on classical transport provides this illustration's caption:

> When the transport processes are local, the plasma may be considered to be made up of many approximately closed subsystems, with slightly different densities, mean velocities and temperatures. Charged-particle collisions tend to force each subsystem to local thermodynamic equilibrium, with the subsystem entropies being maximized, subject to the constraints imposed by particle, momentum and energy conservation. Because of the small differences between subsystems, the velocity distributions for these subsystems depart slightly from Maxwellians. For example, the distribution of the velocity component in the direction of the temperature gradient is skewed somewhat in the direction of motion of those particles coming from the hotter region. As a result, there are small fluxes of particles, momentum and energy between subsystems, which are approximately linear in the thermodynamic forces (e.g. the density and temperature gradients). The resulting entropy fluxes between subsystems then make the plasma as a whole tend towards a state of global thermal equilibrium. Because of the boundary conditions and other external constraints, such as applied electromotive forces, the plasma generally is not able to reach this equilibrium state but remains in a nonequilibrium steady state. The charged particles and energy are lost from the plasma at the same rate that they are produced in the plasma in this steady state. It is the goal of transport theory to calculate these loss rates, assuming they are due to Coulomb collisions.

Now, this is *not* a course on transport theory due to Coulomb collisions – that is AST554, which I also teach and invite you to attend – and so it's not appropriate to go through the details here. But you should be made aware that the procedure of calculating these (diffusive) "loss rates" and writing them in terms of the "fluid" variables (i.e., the zeroth, first, and second moments of the distribution function) is called the *Chapman–Enskog expansion*. One assumes that collisions occur frequently enough to maintain the plasma *near* (but not exactly) Maxwellian, and then discovers that the viscous stress and heat flux are diffusive, i.e., they have coefficients $\sim v_{\rm th}\lambda_{\rm mfp}$) and are linearly proportional to the flow-velocity and temperature gradients. Namely, when the ratio of the collisional mean free path $\lambda_{\rm mfp} = v_{\rm th}/\nu$ and the characteristic gradient lengthscale L – the so-called

"Knudsen number" – satisfies

$$\mathrm{Kn} \doteq \frac{\lambda_{\mathrm{mfp}}}{L} \ll 1, \tag{XIII.1.4}$$

then the viscous stress and heat flux take on the following forms:

$$\boldsymbol{\Pi} \propto -\frac{p}{\nu}\boldsymbol{W} \quad \text{and} \quad \boldsymbol{q} \propto -\frac{p}{\nu}\boldsymbol{\nabla}\frac{T}{m}, \tag{XIII.1.5}$$

respectively, where

$$\boldsymbol{W} \doteq \boldsymbol{\nabla}\boldsymbol{u} + (\boldsymbol{\nabla}\boldsymbol{u})^T - \frac{2}{3}(\boldsymbol{\nabla}\cdot\boldsymbol{u})\boldsymbol{I}. \tag{XIII.1.6}$$

is the (traceless, symmetric) rate-of-strain tensor and $\boldsymbol{I}$ is the unit dyadic. The proportionalities in (XIII.1.5) cover up order-unity coefficients that depend on the exact form of the collision operator being employed. Those coefficients need not concern us here; in fact, you'll probably never see them explicitly unless you go digging, as they're usually wrapped up into the definitions of the viscous and heat diffusion coefficients, μ and κ (both $\propto v_{\mathrm{th}}^2/\nu$), so that

$$\boldsymbol{\Pi} = -mn\mu\boldsymbol{W} \quad \text{and} \quad \boldsymbol{q} = -n\kappa\boldsymbol{\nabla}T. \tag{XIII.1.7}$$

Then you just look up μ and κ in the NRL formulary (or consult my publicly available AST554 notes if you want the details). The fact that these fluxes are proportional to $\mathrm{Kn} = \lambda_{\mathrm{mfp}}/L \ll 1$ means that the departures from local thermodynamic equilibrium are, indeed, small.

The 1916–17 contributions of Chapman and Enskog have now been honored. So then where does Braginskii enter into all of this? In a now-classic 1965 article in *Reviews of Plasma Physics*, Braginskii applied the Chapman–Enskog procedure to determine the collisional transport in a *magnetized* plasma.[35] It's a beautiful piece of mathematics and physics, and the article itself offers a good blend of rigorous presentation and pedagogical discussion. In this Part, I'll provide a brief overview of Braginskii's theory, favoring a discussion of the physical processes involved and their dynamical consequences over a formal derivation (which can be found in my AST554 notes). We'll then build our intuition by applying this theory to linear waves (§XIII.5) and elucidating some instabilities of astrophysical interest (§XIII.6).

The basic idea can be gathered by returning to the illustration of local transport shown above, condensed here:

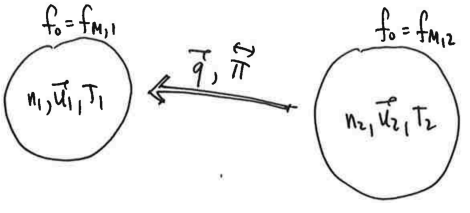

If we put a magnetic field with $\rho/\lambda_{\mathrm{mfp}} \ll 1$ perpendicular to the white arrow, then those heat and momentum fluxes will be stifled because the particles cannot travel a collisional

[35] Everyone now cites this 1965 review article, but Braginskii laid down the main results in 1958 in the then-Soviet *Journal of Experimental and Theoretical Physics*.

mean free path across the magnetic field. In other words, when $\rho/L \ll 1$, charged particles can only sample a Larmor's radius worth of the gradients perpendicular to the magnetic field about which they gyrate; when $\rho/\lambda_{\rm mfp} \ll 1$, this constraint means that gyrating particles within fluid elements on neighboring field lines barely communicate collisionally. If instead we orient the magnetic field along the white arrow, then heat and momentum fluxes can readily proceed since the particles can stream along the magnetic field unimpeded but for collisions. Thus, transport in a magnetized plasma is fundamentally *anisotropic*. Visually,

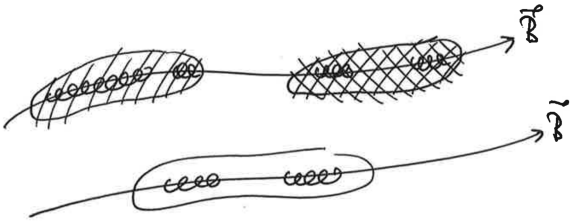

and can viscously transport momentum and conductively transport heat between one another. But these two cannot easily do so with , because of the smallness of the particles' Larmor radii. Let us see what this means for $\boldsymbol{\Pi}$ and $\boldsymbol{q}$.

XIII.2. Pressure anisotropy and anisotropic viscosity

We first return to the idea of particle motion used in §II.4. Decompose each particle's velocity in the bulk flow of the fluid element in which that particle resides and the random (thermal) velocity of the particle:

$$\boldsymbol{v} = \boldsymbol{u}(t, \boldsymbol{r}) + \boldsymbol{w}. \tag{XIII.2.1}$$

As in §II.4, we split the latter into its components parallel and perpendicular to the local magnetic-field direction $\hat{\boldsymbol{b}}$:

$$\boldsymbol{w} = w_\parallel \hat{\boldsymbol{b}} + \boldsymbol{w}_\perp = w_\parallel \hat{\boldsymbol{b}} + w_\perp \big(\hat{\boldsymbol{e}}_1 \cos\vartheta + \hat{\boldsymbol{e}}_2 \sin\vartheta\big), \tag{XIII.2.2}$$

where ϑ is the gyrophase:

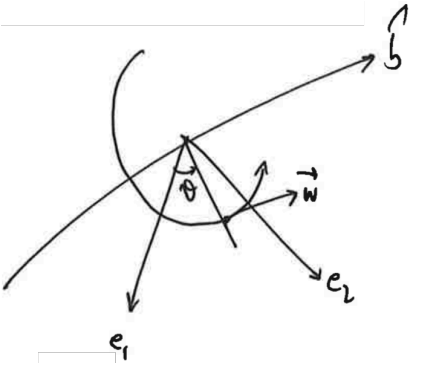

To see what this decomposition means for the transport of momentum, let us calculate explicitly the thermal pressure tensor $\boldsymbol{P} \doteq \int \mathrm{d}\boldsymbol{w}\, m\boldsymbol{w}\boldsymbol{w} f$:

$$\begin{aligned}\boldsymbol{P} &= \int \mathrm{d}\boldsymbol{w}\, m\big[w_\parallel \hat{\boldsymbol{b}} + w_\perp\big(\hat{\boldsymbol{e}}_1\cos\vartheta + \hat{\boldsymbol{e}}_2\sin\vartheta\big)\big]\big[w_\parallel \hat{\boldsymbol{b}} + w_\perp\big(\hat{\boldsymbol{e}}_1\cos\vartheta + \hat{\boldsymbol{e}}_2\sin\vartheta\big)\big] f \\ &= \int \mathrm{d}\boldsymbol{w}\, m w_\parallel^2 \hat{\boldsymbol{b}}\hat{\boldsymbol{b}}\, f + \int \mathrm{d}\boldsymbol{w}\, m w_\perp^2 \big(\cos^2\vartheta \hat{\boldsymbol{e}}_1\hat{\boldsymbol{e}}_1 + \sin^2\vartheta \hat{\boldsymbol{e}}_2\hat{\boldsymbol{e}}_2\big) f \\ &\quad + \int \mathrm{d}\boldsymbol{w}\, \frac{1}{2} m w_\perp^2 \sin 2\vartheta (\hat{\boldsymbol{e}}_1\hat{\boldsymbol{e}}_2 + \hat{\boldsymbol{e}}_2\hat{\boldsymbol{e}}_1) f \\ &\quad + \int \mathrm{d}\boldsymbol{w}\, m w_\parallel w_\perp \big[\cos\vartheta(\hat{\boldsymbol{e}}_1\hat{\boldsymbol{b}} + \hat{\boldsymbol{b}}\hat{\boldsymbol{e}}_1) + \sin\vartheta(\hat{\boldsymbol{e}}_2\hat{\boldsymbol{b}} + \hat{\boldsymbol{b}}\hat{\boldsymbol{e}}_2)\big] f. \end{aligned} \tag{XIII.2.3}$$

Now, if ρ is much smaller than any other lengthscale of interest L, and if Ω is much larger than any other frequency of interest ω, then the largest term in the kinetic equation governing the distribution function f is that which describes Larmor motion:

$$\frac{q}{m}\frac{\boldsymbol{w}\times\boldsymbol{B}}{c}\cdot\frac{\partial f}{\partial \boldsymbol{w}} = 0. \tag{XIII.2.4}$$

In our $(w_\parallel, w_\perp, \vartheta)$ coordinate system, the velocity-space gradient may be written as

$$\frac{\partial}{\partial \boldsymbol{w}} = \hat{\boldsymbol{b}}\frac{\partial}{\partial w_\parallel} + \frac{\boldsymbol{w}_\perp}{w_\perp}\frac{\partial}{\partial w_\perp} + \frac{(\boldsymbol{w}\times\hat{\boldsymbol{b}})}{w_\perp}\frac{\partial}{\partial\vartheta},$$

and so (XIII.2.4) implies that $\partial f/\partial\vartheta = 0$ to leading order in ρ/L, ω/Ω – that is, f is *gyrotropic* to leading order. Let us therefore write f as the sum of a dominant gyrotropic piece ($\overline{f}$) and the remaining small gyro-phase-dependent piece ($\widetilde{f}$),

$$f(w_\parallel, w_\perp, \vartheta) = \overline{f}(w_\parallel, w_\perp) + \widetilde{f}(w_\parallel, w_\perp, \vartheta),$$

and substitute this decomposition into (XIII.2.3). After performing the gyrophase integration, we find that

$$\begin{aligned}\boldsymbol{P} &= \underbrace{\int \mathrm{d}\boldsymbol{w}\, m w_\parallel^2\, \overline{f}}_{\doteq p_\parallel}\, \hat{\boldsymbol{b}}\hat{\boldsymbol{b}} + \underbrace{\int \mathrm{d}\boldsymbol{w}\, \frac{1}{2} m w_\perp^2\, \overline{f}}_{\doteq p_\perp}\, \underbrace{\big(\hat{\boldsymbol{e}}_1\hat{\boldsymbol{e}}_1 + \hat{\boldsymbol{e}}_2\hat{\boldsymbol{e}}_2\big)}_{=(\boldsymbol{I}-\hat{\boldsymbol{b}}\hat{\boldsymbol{b}})} + \underbrace{\int \mathrm{d}\boldsymbol{w}\, m\boldsymbol{w}\boldsymbol{w}\, \widetilde{f}}_{\doteq \boldsymbol{\pi}} \\ &= p_\parallel \hat{\boldsymbol{b}}\hat{\boldsymbol{b}} + p_\perp(\boldsymbol{I} - \hat{\boldsymbol{b}}\hat{\boldsymbol{b}}) + \boldsymbol{\pi}. \end{aligned} \tag{XIII.2.5}$$

In other words, in a frame aligned with $\hat{\boldsymbol{b}} = \hat{\boldsymbol{z}}$, the pressure tensor is predominantly diagonal:

$$\boldsymbol{P} \simeq \begin{pmatrix} p_\perp & 0 & 0 \\ 0 & p_\perp & 0 \\ 0 & 0 & p_\parallel \end{pmatrix}. \tag{XIII.2.6}$$

In this course, I will make no further comments about the gyro-phase-dependent piece of the pressure tensor ($\boldsymbol{\pi}$), other than to say that it captures suppressed collisional transport across magnetic-field lines [at a level $\sim(\rho/\lambda_{\mathrm{mfp}})^2$ times the parallel transport] and a finite-Larmor-radius effect called "gyro-viscosity" [at a level $\sim(\rho/\lambda_{\mathrm{mfp}})$ times the parallel transport]. Henceforth,

$$\boldsymbol{P} = p_\parallel \hat{\boldsymbol{b}}\hat{\boldsymbol{b}} + p_\perp(\boldsymbol{I} - \hat{\boldsymbol{b}}\hat{\boldsymbol{b}}) = p\boldsymbol{I} - \left(\hat{\boldsymbol{b}}\hat{\boldsymbol{b}} - \frac{\boldsymbol{I}}{3}\right)(p_\perp - p_\parallel) \doteq p\boldsymbol{I} + \boldsymbol{\Pi}, \tag{XIII.2.7}$$

where we have used $p = (2/3)p_\perp + (1/3)p_\parallel$ to obtain the second equality.

Thus, the viscous stress tensor in a magnetized plasma is anisotropic with respect to the local magnetic field and has a magnitude that is related to the difference between the field-perpendicular and -parallel pressures. But why would a plasma have $p_\perp \neq p_\parallel$? Go all the way back to §§II.5–II.7:

$$\mu \doteq \frac{1}{2} m \frac{w_\perp^2}{B} \simeq \text{const} \quad \text{and} \quad J \doteq m \oint \mathrm{d}\ell \, w_\parallel \simeq \text{const},$$

the first and second adiabatic invariants. What is the mean value of the magnetic moment μ in a plasma?

$$\langle \mu \rangle = \frac{\int \mathrm{d}\boldsymbol{w} \, \mu f}{\int \mathrm{d}\boldsymbol{w} \, f} = \frac{\frac{1}{B} \int \mathrm{d}\boldsymbol{w} \, \frac{1}{2} m w_\perp^2 f}{\int \mathrm{d}\boldsymbol{w} \, f} = \frac{p_\perp / B}{n} \simeq \text{const} \quad \Longrightarrow \quad T_\perp \propto B. \tag{XIII.2.8}$$

If the magnetic-field strengths changes in a magnetized plasma, then the perpendicular temperature must change as well. (This can be thought of as a macroscopic consequence of Lenz's law.) What is the mean value of the bounce invariant J? For that, we need an estimate of the "extension" ℓ of a fluid element along the magnetic-field line. Quoting Kulsrud (1983):

> The quantity ℓ has an amount of uncertainty in its definition since the particles are dispersing at a considerable rate. However, it is known that even in free expansion of a one-dimensional gas the mean square dispersion of velocities decreases as the density does and moreover is inversely proportional to the length of the element of gas squared... For our case the length ℓ is proportional to B/n since the volume of a tube of force is inversely proportional to n, while the cross sectional area is inversely proportional to B.

Adopting this argument (which is formalized later in these notes),

$$\langle J^2 \rangle = \frac{\int \mathrm{d}\boldsymbol{w} \, J^2 f}{\int \mathrm{d}\boldsymbol{w} \, f} \propto \frac{\frac{B^2}{n^2} \int \mathrm{d}\boldsymbol{w} \, m w_\parallel^2 f}{\int \mathrm{d}\boldsymbol{w} \, f} = \frac{(B/n)^2 \, p_\parallel}{n} \simeq \text{const} \quad \Longrightarrow \quad T_\parallel \propto \frac{n^2}{B^2}. \tag{XIII.2.9}$$

If the ratio of magnetic-field strength and density changes in a magnetized plasma, then the parallel temperature must change as well. Now, while $T_\perp / B \simeq \text{const}$ is usually pretty well satisfied, $T_\parallel B^2 / n^2 \simeq \text{const}$ is not – it is often spoiled by the rapid flow of heat along magnetic-field lines. But let us ignore that complication and carry on to obtain the *double-adiabatic equations of state*:

$$\frac{\mathrm{D}}{\mathrm{D}t} \left(\frac{T_\perp}{B} \right) = \frac{\mathrm{D}}{\mathrm{D}t} \left(\frac{p_\perp}{nB} \right) \simeq 0 \quad \text{and} \quad \frac{\mathrm{D}}{\mathrm{D}t} \left(\frac{T_\parallel B^2}{n^2} \right) = \frac{\mathrm{D}}{\mathrm{D}t} \left(\frac{p_\parallel B^2}{n^3} \right) \simeq 0. \tag{XIII.2.10}$$

(The $\mathrm{D}/\mathrm{D}t$ are here because these changes are measured in the co-moving frame of the fluid element.) These equations state that the thermal energy of particles is redistributed in the directions perpendicular and parallel to the local magnetic field when certain macroscopic properties of the magnetized plasma change on time- and lengthscales much larger than those associated with Larmor motion and bounce motion.

In this Part of the lecture notes, we are concerned with collisional, magnetized plasmas, and so it stands to reason that the double-adiabatic equations (XIII.2.10) ought to be modified to account for the collisional relaxation of the plasma back towards an isotropic Maxwellian. (Physically, this would correspond to particles getting kicked off their μ-

conserving Larmor orbits or J-conserving bounce orbits via Coulomb interactions with other particles.) Again, this physics is mathematically formalized later in these notes, but for now let us use this motivation to simply append some collisional terms to the right-hand sides of (XIII.2.10):

$$\frac{\mathrm{D}p_\perp}{\mathrm{D}t} \simeq p_\perp \frac{\mathrm{D}}{\mathrm{D}t} \ln Bn - \nu(p_\perp - p),$$
$$\frac{\mathrm{D}p_\parallel}{\mathrm{D}t} \simeq p_\parallel \frac{\mathrm{D}}{\mathrm{D}t} \ln \frac{n^3}{B^2} - \nu(p_\parallel - p).$$

Subtracting these two equations and stipulating that the collisions are sufficiently strong so as to maintain the plasma near (but not at!) local thermodynamic equilibrium, an equation for the *pressure anisotropy* of the plasma results:

$$\frac{\mathrm{D}}{\mathrm{D}t}(p_\perp - p_\parallel) \simeq p \frac{\mathrm{D}}{\mathrm{D}t} \ln \frac{B^3}{n^{2/3}} - \nu(p_\perp - p_\parallel). \tag{XIII.2.11}$$

This equation states that pressure anisotropy in a fluid element is generated by adiabatic invariance and relaxed by collisional isotropization. Now we enact Braginskii's magnetized, collisional ordering:

$$\Omega \gg \nu \gg T^{-1} \quad \text{and} \quad L \gg \lambda_{\mathrm{mfp}} \gg \rho, \tag{XIII.2.12}$$

where T and L are some fiducial macroscopic time- and lengthscales on which the fluid dynamically evolves. In practice, this ordering means that the left-hand side of (XIII.2.11) is small compared to the final term on its right-hand side, leaving

$$p_\perp - p_\parallel \simeq \frac{3p}{\nu} \frac{\mathrm{D}}{\mathrm{D}t} \ln \frac{B}{n^{2/3}}. \tag{XIII.2.13}$$

This is Braginskii's closure for the pressure anisotropy, which figures into the anisotropic viscosity (see (XIII.2.7)). It represents an instantaneous balance between adiabatic production and collisional relaxation of pressure anisotropy, and reveals that the departures from an isotropic distribution function the correspond to pressure anisotropy are $\sim(\nu T)^{-1} \ll 1$.

One more thing. Let us use the continuity equation and the induction equation in the forms

$$\frac{\mathrm{D} \ln n}{\mathrm{D}t} = -\boldsymbol{\nabla \cdot u} \quad \text{and} \quad \frac{\mathrm{D} \ln B}{\mathrm{D}t} = \left(\hat{\boldsymbol{b}}\hat{\boldsymbol{b}} - \boldsymbol{I}\right) : \boldsymbol{\nabla u}$$

(recall (**??**)) to write (XIII.2.13) as

$$p_\perp - p_\parallel \simeq \frac{3p}{\nu} \left(\hat{\boldsymbol{b}}\hat{\boldsymbol{b}} - \frac{\boldsymbol{I}}{3}\right) : \boldsymbol{\nabla u}. \tag{XIII.2.14}$$

Why is this useful? Substitute Braginskii's viscous stress tensor into the momentum equation:

$$mn \frac{\mathrm{D}\boldsymbol{u}}{\mathrm{D}t} + \cdots = -\boldsymbol{\nabla \cdot \Pi} = \boldsymbol{\nabla \cdot} \left[\frac{3p}{\nu} \left(\hat{\boldsymbol{b}}\hat{\boldsymbol{b}} - \frac{\boldsymbol{I}}{3}\right) \left(\hat{\boldsymbol{b}}\hat{\boldsymbol{b}} - \frac{\boldsymbol{I}}{3}\right) : \boldsymbol{\nabla u}\right].$$

Other than the appearance of the tensor projection onto $(\hat{\boldsymbol{b}}\hat{\boldsymbol{b}} - \boldsymbol{I}/3)$, this looks just like a viscosity: there are two gradients of the fluid velocity, and a coefficient $p/\nu \propto mnv_{\mathrm{th}}\lambda_{\mathrm{mfp}}$. Thus, Braginskii's pressure anisotropy endows the magnetized, collisional fluid with an *anisotropic viscosity*. In the language of (XIII.1.5),

$$\boldsymbol{\Pi} = -mn\mu \boldsymbol{W} \longrightarrow -mn\mu \left(\hat{\boldsymbol{b}}\hat{\boldsymbol{b}} - \frac{\boldsymbol{I}}{3}\right) \left(\hat{\boldsymbol{b}}\hat{\boldsymbol{b}} - \frac{\boldsymbol{I}}{3}\right) : \boldsymbol{W}. \tag{XIII.2.15}$$

Note that, because $\mu \propto v_{\rm th}^2/\nu$ and $\nu \propto m^{-1/2}$, the heavier species (ions) dominate the viscous transport. Remember this.

Finally, note that the term on the right-hand side of the entropy equation (XIII.1.3) that involves the viscous stress may be simplified using Braginskii's closure:

$$-\boldsymbol{\Pi} : \boldsymbol{\nabla u} = (p_\perp - p_\parallel)\left(\hat{\boldsymbol{b}}\hat{\boldsymbol{b}} - \frac{\boldsymbol{I}}{3}\right) : \boldsymbol{\nabla u} = \frac{3p}{\nu}\left[\left(\hat{\boldsymbol{b}}\hat{\boldsymbol{b}} - \frac{\boldsymbol{I}}{3}\right) : \boldsymbol{\nabla u}\right]^2 \geqslant 0. \qquad \text{(XIII.2.16)}$$

This equation states that the entropy increases due to anisotropic viscous damping of fluid motions. On a microphysical level, departures from local thermodynamic equilibrium are shaped by the particles' allegiance to the magnetic-field direction, promoted by adiabatic invariance, and relaxed by collisions; this last step leads to irreversible heating.

The most important thing to note in going forward is that the anisotropic viscosity only targets those motions whose rate of strain has a projection onto the field-aligned tensor $(\hat{\boldsymbol{b}}\hat{\boldsymbol{b}} - \boldsymbol{I}/3)$. In §XIII.5, we will show that, as a consequence, linear shear Alvén waves are not damped. Nonlinear circularly polarized Alfvén waves are not damped. Neither of these produce any adiabatic change in the form of the distribution function, because neither of these change the magnetic-field strength and density of the plasma. Magnetosonic waves, on the other hand, do produce pressure anisotropy, and thus are viscously damped.

XIII.3. Anisotropic conduction

The notion that collisional transport is affected by the presence of a magnetic field holds true as well for the transport of heat. We begin by examining the form of the thermal heat flux $\boldsymbol{q} \doteq \int \mathrm{d}\boldsymbol{w}\,(1/2)mw^2\boldsymbol{w}f$ (recall (III.10.22)) when $f = f(w_\parallel, w_\perp)$ is gyrotropic:

$$\begin{aligned}\boldsymbol{q} &= \int \mathrm{d}\boldsymbol{w}\,\frac{1}{2}mw^2\left[w_\parallel\hat{\boldsymbol{b}} + w_\perp\left(\hat{\boldsymbol{e}}_1\cos\vartheta + \hat{\boldsymbol{e}}_2\sin\vartheta\right)\right]f \\ &= \int \mathrm{d}\boldsymbol{w}\,\frac{1}{2}mw^2 w_\parallel\hat{\boldsymbol{b}}\,f \doteq q\hat{\boldsymbol{b}}.\end{aligned} \qquad \text{(XIII.3.1)}$$

If you've followed the story so far, then there should be no surprises here: the transport of heat flows along the local magnetic field. To formally calculate the scalar q for a magnetized, collisional plasma requires a Chapman–Enskog–Braginskii treatment, but we may combine our qualitative argument that particles have difficulty sampling gradients across field lines with some knowledge of the isotropic result $\boldsymbol{q} = -n\kappa\boldsymbol{\nabla}T$ to guess that

$$\boldsymbol{q} = -n\kappa\boldsymbol{\nabla}T \;\longrightarrow\; -n\kappa\hat{\boldsymbol{b}}\hat{\boldsymbol{b}}\cdot\boldsymbol{\nabla}T. \qquad \text{(XIII.3.2)}$$

This turns out to be correct. There's the familiar projection of a free-energy gradient (here $\boldsymbol{\nabla}T$) onto a tensor composed of magnetic-field unit vectors, just as with the anisotropic viscous stress. Note that, because $\kappa \propto v_{\rm th}^2/\nu$ and $\nu \propto m^{-1/2}$, the lighter species (electrons) dominate the conductive transport.

If the distribution function is not exactly gyrotropic, there are additional contributions to the heat flux that account for cross-field transport. As with the viscous stress, these are small when ρ/L, $\rho/\lambda_{\rm mfp} \ll 1$. Namely, there is a term that captures suppressed collisional transport across magnetic-field lines [at a level $\sim(\rho/\lambda_{\rm mfp})^2$ times the parallel transport] and a term dependent on the finite size of the Larmor radius called the "diamagnetic heat flux" [at a level $\sim(\rho/\lambda_{\rm mfp})$ times the parallel transport]. These will not be discussed in this course.

XIII.4. Braginskii-MHD equations

When (XIII.2.12) are satisfied, the viscous stress tensor and the heat flux take on the following field-anisotropic forms:

$$\boldsymbol{\Pi}_\alpha = -\left(\hat{\boldsymbol{b}}\hat{\boldsymbol{b}} - \frac{\boldsymbol{I}}{3}\right)(p_{\perp\alpha} - p_{\parallel\alpha}) = -m_\alpha n_\alpha \mu_\alpha \left(\hat{\boldsymbol{b}}\hat{\boldsymbol{b}} - \frac{\boldsymbol{I}}{3}\right)\left(\hat{\boldsymbol{b}}\hat{\boldsymbol{b}} - \frac{\boldsymbol{I}}{3}\right) : \boldsymbol{\nabla}\boldsymbol{u}_\alpha, \tag{XIII.4.1}$$

$$\boldsymbol{q}_\alpha = \hat{\boldsymbol{b}} q_\alpha = -n_\alpha \kappa_\alpha \hat{\boldsymbol{b}}\hat{\boldsymbol{b}} \cdot \boldsymbol{\nabla} T_\alpha, \tag{XIII.4.2}$$

where the viscous and thermal diffusion coefficients for ions ($\alpha = \mathrm{i}$) and electrons ($\alpha = \mathrm{e}$) are given by

$$\mu_\mathrm{i} = 0.96 \times \frac{3}{2} v_{\mathrm{thi}}^2 \tau_\mathrm{i}, \quad \mu_\mathrm{e} = 0.73 \times \frac{3}{2} v_{\mathrm{the}}^2 \tau_\mathrm{e},$$
$$\kappa_\mathrm{i} = 1.56 \times \frac{5}{4} v_{\mathrm{thi}}^2 \tau_\mathrm{i}, \quad \kappa_\mathrm{e} = 1.26 \times \frac{5}{4} v_{\mathrm{the}}^2 \tau_\mathrm{e}.$$

The multiplicative prefactors here are specific to the Landau collision operator (they all equal 1 for a Krook operator). The ion and electron collision timescales are

$$\tau_\mathrm{i} = \frac{3\sqrt{m_\mathrm{i}} T_\mathrm{i}^{3/2}}{4\sqrt{\pi} n \lambda_\mathrm{i} e^4} = 0.67 \, \frac{T_\mathrm{i}^2}{n\lambda_\mathrm{i}} \text{ yr}, \qquad \tau_\mathrm{e} = \frac{3\sqrt{m_\mathrm{e}} T_\mathrm{e}^{3/2}}{4\sqrt{2\pi} n \lambda_\mathrm{e} e^4} = 0.011 \, \frac{T_\mathrm{e}^2}{n\lambda_\mathrm{e}} \text{ yr};$$

where λ_α is the Coulomb logarithm of species α; in the final numerical expressions, T is measured in eV and n in cm^{-3}. Note that particle collisional mean free paths are all comparable, $\lambda_\mathrm{e} \sim \lambda_\mathrm{i}$, despite the collision timescales being different.

Two further assumptions in the Braginskii model are that (i) the Mach number M of the bulk flows is of order unity with respect to the square root of the mass ratio, $\sqrt{m_\mathrm{i}/m_\mathrm{e}}$, and (ii) the ions and electrons have comparable temperatures differing by no more than $\sim\sqrt{m_\mathrm{i}/m_\mathrm{e}}$. The former assumption is called a "high-flow" ordering: subsonic and supersonic flows are allowed, so long as they do not interfere with various mass-ratio expansions that occur in Braginskii's calculation.[36] A consequence of this ordering is that the perpendicular flow velocity of the ions and electrons are very nearly the same and are equal to the $\boldsymbol{E} \times \boldsymbol{B}$ drift velocity.

Under these conditions, the single-fluid Braginskii-MHD equations for a quasi-neutral ion-electron plasma are:

$$\frac{\mathrm{D}\varrho}{\mathrm{D}t} = -\varrho \boldsymbol{\nabla} \cdot \boldsymbol{u}, \tag{XIII.4.3}$$

$$\varrho \frac{\mathrm{D}\boldsymbol{u}}{\mathrm{D}t} = \boldsymbol{g} - \boldsymbol{\nabla}\left(p_\perp + \frac{B^2}{8\pi}\right) + \boldsymbol{\nabla} \cdot \left[\hat{\boldsymbol{b}}\hat{\boldsymbol{b}}\left(\frac{B^2}{4\pi} + p_\perp - p_\parallel\right)\right]$$
$$= \boldsymbol{g} - \boldsymbol{\nabla}\left(p + \frac{B^2}{8\pi}\right) + \frac{\boldsymbol{B}\cdot\boldsymbol{\nabla}\boldsymbol{B}}{4\pi} + \boldsymbol{\nabla} \cdot \left[\varrho\mu\left(\hat{\boldsymbol{b}}\hat{\boldsymbol{b}} - \frac{\boldsymbol{I}}{3}\right)\left(\hat{\boldsymbol{b}}\hat{\boldsymbol{b}} - \frac{\boldsymbol{I}}{3}\right) : \boldsymbol{\nabla}\boldsymbol{u}\right], \tag{XIII.4.4}$$

$$\frac{\mathrm{D}\boldsymbol{B}}{\mathrm{D}t} = \boldsymbol{B}\cdot\boldsymbol{\nabla}\boldsymbol{u} - \boldsymbol{B}\boldsymbol{\nabla}\cdot\boldsymbol{u}, \tag{XIII.4.5}$$

$$p\frac{\mathrm{D}s}{\mathrm{D}t} = \boldsymbol{\nabla} \cdot \left(n\kappa\hat{\boldsymbol{b}}\hat{\boldsymbol{b}} \cdot \boldsymbol{\nabla} T_\mathrm{e}\right) + \varrho\mu\left[\left(\hat{\boldsymbol{b}}\hat{\boldsymbol{b}} - \frac{\boldsymbol{I}}{3}\right) : \boldsymbol{\nabla}\boldsymbol{u}\right]^2, \tag{XIII.4.6}$$

where $p = p_\mathrm{i} + p_\mathrm{e}$, $s = (3/2)\ln p\varrho^{-5/3}$, $\mu \simeq \mu_\mathrm{i}$, $\kappa \simeq \kappa_\mathrm{e}$, and $T_\mathrm{e} \simeq T_\mathrm{i}$. Recall that we

[36] "Low-flow" orderings with flow velocities of order the diamagnetic drift velocity introduce additional physics of relevance to tokamak plasmas; see Catto & Simakov (2004), which follows Mikhailovskii & Tsypin (1971, 1984).

have only retained the leading-order contributions to the viscous momentum flux and the conductive heat flux, which correspond to field-aligned transport.

XIII.5. Linear waves in Braginskii-MHD

To obtain some intuition for the physics captured by (XIII.4.3), it helps to calculate the linear theory using a simple equilibrium state: a uniform, stationary, pressure-isotropic plasma threaded by a uniform magnetic field. Ignore gravity. As usual, write $\varrho \to \varrho + \delta\varrho$, $\boldsymbol{u} \to \delta\boldsymbol{u}$, $p \to p + \delta p$, $\boldsymbol{B} \to \boldsymbol{B} + \delta\boldsymbol{B}$, and retain only those terms linear in the fluctuation amplitude. The resulting set of equations support plane-wave solutions $\propto \exp(-\mathrm{i}\omega t + \mathrm{i}\boldsymbol{k}\cdot\boldsymbol{r})$ with $\boldsymbol{k} = k_\parallel \hat{\boldsymbol{b}} + \boldsymbol{k}_\perp$ and ω a complex frequency. The linear theory is as before (in ideal MHD) except for the addition of the linearized viscous stress to the right-hand side of the momentum equation,

$$+\mathrm{i}\boldsymbol{k}\cdot\left[\varrho\mu\left(\hat{\boldsymbol{b}}\hat{\boldsymbol{b}} - \frac{\boldsymbol{I}}{3}\right)\left(\hat{\boldsymbol{b}}\hat{\boldsymbol{b}} - \frac{\boldsymbol{I}}{3}\right) : \mathrm{i}\boldsymbol{k}\delta\boldsymbol{u}\right] = -\varrho\mu\left(k_\parallel\hat{\boldsymbol{b}} - \frac{\boldsymbol{k}}{3}\right)\left(k_\parallel\delta u_\parallel - \frac{\boldsymbol{k}\cdot\delta\boldsymbol{u}}{3}\right),$$

and the addition of the linearized heat flux to the right-hand side of the entropy equation,

$$+\mathrm{i}\boldsymbol{k}\cdot\left(n\kappa\hat{\boldsymbol{b}}\hat{\boldsymbol{b}}\cdot\mathrm{i}\boldsymbol{k}\delta T_e\right) = -nk_\parallel^2\kappa\delta T_e.$$

Unless otherwise explicitly stated, we shall assume that the ions and electrons maintain the same temperature $T = p/2n$ (recall that $p = p_\mathrm{i} + p_\mathrm{e} = 2p_\mathrm{i}$). Note that the parallel-viscous heating is quadratic in the perturbations and thus does not enter the analysis.

One might be tempted to keep things "simple" and retain the effects of just one additional term at a time (e.g., $\nu \neq 0$ but $\kappa = 0$). But the incorporation of the heat-flux term into the linearized entropy equation is surprisingly straightforward, and there is a pain-free way to carry the influence of this heat flux through the entire calculation. To see this, note that the linearized heat-flux term may be written as

$$-nT_e k_\parallel^2\kappa\left(\frac{\delta p}{p} - \frac{\delta\varrho}{\varrho}\right) = -\frac{p}{2}k_\parallel^2\kappa\left(\frac{\delta p}{p} - \frac{\delta\varrho}{\varrho}\right),$$

so that the linearized entropy equation

$$\frac{3}{2}\mathrm{i}\omega\left(\frac{\delta p}{p} - \frac{5}{3}\frac{\delta\varrho}{\varrho}\right) = \frac{1}{2}k_\parallel^2\kappa\left(\frac{\delta p}{p} - \frac{\delta\varrho}{\varrho}\right) \quad\Longrightarrow\quad \frac{\delta p}{p} = \frac{\delta\varrho}{\varrho}\left(\frac{5\mathrm{i}\omega - k_\parallel^2\kappa}{3\mathrm{i}\omega - k_\parallel^2\kappa}\right) \doteq \frac{\delta\varrho}{p}\,a_\mathrm{eff}^2.$$

When conduction is unimportant ($k_\parallel^2\kappa \ll \omega$), $a_\mathrm{eff}^2 \to a^2 \doteq (5/3)p/\varrho$, the square of the usual adiabatic sound speed. The perturbations are adiabatic. When conduction is strong ($k_\parallel^2\kappa \gg \omega$), we find that $a_\mathrm{eff}^2 = p/\varrho$. The perturbations are isothermal, because rapid conduction along field lines causes magnetically tethered fluid elements to behave isothermally as they are displaced. Thus, everywhere we see an a^2 in our linear theory, we simply replace it with a_eff^2 and use that as a tag to follow the influence of conduction.

Our linearized equations are then:

$$-\mathrm{i}\omega\frac{\delta\varrho}{\varrho} = -\mathrm{i}\boldsymbol{k}\cdot\delta\boldsymbol{u}, \tag{XIII.5.1}$$

$$-\mathrm{i}\omega\delta\boldsymbol{u} = -\mathrm{i}\boldsymbol{k}\left(\frac{\delta p}{\varrho} + v_\mathrm{A}^2\frac{\delta B_\parallel}{B}\right) + \mathrm{i}k_\parallel v_\mathrm{A}^2\frac{\delta\boldsymbol{B}}{B} - \mu\left(k_\parallel\hat{\boldsymbol{b}} - \frac{\boldsymbol{k}}{3}\right)\left(k_\parallel\delta u_\parallel - \frac{\boldsymbol{k}\cdot\delta\boldsymbol{u}}{3}\right), \tag{XIII.5.2}$$

$$-\mathrm{i}\omega\frac{\delta\boldsymbol{B}}{B} = \mathrm{i}k_\parallel\delta\boldsymbol{u} - \hat{\boldsymbol{b}}\,\mathrm{i}\boldsymbol{k}\cdot\delta\boldsymbol{u}, \tag{XIII.5.3}$$

with $\delta p = a_{\rm eff}^2 \delta\varrho$. Solving this set is straightforward. First, use (XIII.5.1) to replace $\boldsymbol{k}\cdot\delta\boldsymbol{u}$ everywhere by $\omega(\delta\varrho/\varrho)$. Then solve (XIII.5.3) for $\delta\boldsymbol{u}$ in terms of $\delta\boldsymbol{B}$ and $\delta\varrho$, and substitute the result into (XIII.5.2). Multiply through by $\mathrm{i}k_\parallel$ and rearrange to find

$$\left(\omega^2 - k_\parallel^2 v_{\rm A}^2\right)\frac{\delta\boldsymbol{B}}{B} + \left[\boldsymbol{k}k_\parallel v_{\rm A}^2 + \mathrm{i}\mu\omega k_\parallel\left(k_\parallel\hat{\boldsymbol{b}} - \frac{\boldsymbol{k}}{3}\right)\right]\frac{\delta B_\parallel}{B}$$
$$= \left[\omega^2\hat{\boldsymbol{b}} - \boldsymbol{k}k_\parallel a_{\rm eff}^2 + \frac{2\mathrm{i}}{3}\mu\omega k_\parallel\left(k_\parallel\hat{\boldsymbol{b}} - \frac{\boldsymbol{k}}{3}\right)\right]\frac{\delta\varrho}{\varrho}. \tag{XIII.5.4}$$

Dot this equation with $\boldsymbol{k}/k_\parallel$ and use $\boldsymbol{k}\cdot\delta\boldsymbol{B} = 0$ to obtain an expression for the density fluctuation in terms of the magnetic-field-strength fluctuation:

$$\left[\omega^2 - k^2 a_{\rm eff}^2 + \frac{2\mathrm{i}}{3}\mu\omega\left(k_\parallel^2 - \frac{k^2}{3}\right)\right]\frac{\delta\varrho}{\varrho} = \left[k^2 v_{\rm A}^2 + \mathrm{i}\mu\omega\left(k_\parallel^2 - \frac{k^2}{3}\right)\right]\frac{\delta B_\parallel}{B}.$$

This is then substituted back into (XIII.5.4) to obtain an equation involving only $\delta\boldsymbol{B}$:

$$\left(\omega^2 - k_\parallel^2 v_{\rm A}^2\right)\frac{\delta\boldsymbol{B}}{B} + \left[\boldsymbol{k}k_\parallel v_{\rm A}^2 + \mathrm{i}\mu\omega k_\parallel\left(k_\parallel\hat{\boldsymbol{b}} - \frac{\boldsymbol{k}}{3}\right)\right]\frac{\delta B_\parallel}{B}$$
$$= \left[\omega^2\hat{\boldsymbol{b}} - \boldsymbol{k}k_\parallel a_{\rm eff}^2 + \frac{2\mathrm{i}}{3}\mu\omega k_\parallel\left(k_\parallel\hat{\boldsymbol{b}} - \frac{\boldsymbol{k}}{3}\right)\right]\left[\frac{k^2 v_{\rm A}^2 + \mathrm{i}\mu\omega\left(k_\parallel^2 - \frac{k^2}{3}\right)}{\omega^2 - k^2 a_{\rm eff}^2 + \frac{2\mathrm{i}}{3}\mu\omega\left(k_\parallel^2 - \frac{k^2}{3}\right)}\right]\frac{\delta B_\parallel}{B}. \tag{XIII.5.5}$$

This equation may be split into two decoupled branches by first dotting it with $\boldsymbol{k}\times\hat{\boldsymbol{b}}$ to eliminate all terms proportional to $\delta B_\parallel$. The resulting dispersion relation

$$\omega^2 - k_\parallel^2 v_{\rm A}^2 = 0 \tag{XIII.5.6}$$

describes undamped Alfvén waves whose magnetic-field fluctuations are perpendicular to both $\boldsymbol{k}$ and $\hat{\boldsymbol{b}}$. Anisotropic viscosity and conduction play no role, which shouldn't be surprising: such waves do not change density or magnetic-field strength to linear order in the fluctuation amplitudes, thus they do not produce any pressure anisotropy, thus they are not subject to collisional damping. To obtain the other branch, dot (XIII.5.5) with $\hat{\boldsymbol{b}}$. After some rearrangement, the dispersion relation governing these magnetosonic modes is

$$\omega^2 + \mathrm{i}\mu\omega k_\parallel^2\frac{k_\perp^2}{k^2} - k_\parallel^2 v_{\rm A}^2 = \frac{\omega\left(\omega + \frac{2\mathrm{i}}{3}\mu k_\parallel^2\right)\left[k_\perp^2 v_{\rm A}^2 + \mathrm{i}\mu\omega\frac{k_\perp^2}{k^2}\left(k_\parallel^2 - \frac{k^2}{3}\right)\right]}{\omega^2 - k^2 a_{\rm eff}^2 + \frac{2\mathrm{i}}{3}\mu\omega\left(k_\parallel^2 - \frac{k^2}{3}\right)}. \tag{XIII.5.7}$$

The advantage to writing this equation in this form is that we make readily take the limit $k^2 a^2 \to \infty$ to eliminate sound waves (and thus the fast mode) and find the dispersion relation for the slow mode:

$$\omega^2 + \mathrm{i}\mu\omega k_\parallel^2\frac{k_\perp^2}{k^2} - k_\parallel^2 v_{\rm A}^2 = 0. \tag{XIII.5.8}$$

Now this mode *is* viscously damped, and it's no wonder: slow modes have $\delta B_\parallel \neq 0$, which drives pressure anisotropy, which results in viscous damping of the wave.

XIII.6. Magneto-viscous and magneto-thermal instabilities

[in progress – see Balbus (2000, 2001, 2004); Kunz (2011)]

PART XIV
Magnetokinetics

> We can know only that we know nothing. And that is the highest degree of human wisdom.
>
> Leo Tolstoy
> *War and Peace* (1869)

See my hand-written lecture notes.

REFERENCES

Alt, Andrew & Kunz, Matthew W. 2019 Onset of magnetic reconnection in a collisionless, high-β plasma. *J. Plasma Phys.* **85** (1), 764850101.

Ara, G., Basu, B., Coppi, B., Laval, G., Rosenbluth, M. N. & Waddell, B. V. 1978 Magnetic reconnection and m = 1 oscillations in current carrying plasmas. *Annals of Physics* **112**, 443–476.

Armitage, P. J. 2011 Dynamics of Protoplanetary Disks. *Ann. Rev. Astron. Astrophys.* **49**, 195–236.

Arons, J. & Max, C. E. 1975 Hydromagnetic Waves in Molecular Clouds. *Astrophys. J. Lett.* **196**, L77.

Babcock, H. W. & Cowling, T. G. 1953 General magnetic fields in the Sun and stars (Report on progress of astronomy). *Mon. Not. R. Astron. Soc.* **113**, 357–381.

Bacmann, A., André, P., Puget, J.-L., Abergel, A., Bontemps, S. & Ward-Thompson, D. 2000 An ISOCAM absorption survey of the structure of pre-stellar cloud cores. *Astron. Astrophys.* **361**, 555–580.

Bai, X.-N. 2013 Wind-driven Accretion in Protoplanetary Disks. II. Radial Dependence and Global Picture. *Astrophys. J.* **772**, 96.

Bai, X.-N. 2014 Hall-effect-Controlled Gas Dynamics in Protoplanetary Disks. I. Wind Solutions at the Inner Disk. *Astrophys. J.* **791**, 137.

Bai, X.-N. 2015 Hall Effect Controlled Gas Dynamics in Protoplanetary Disks. II. Full 3D Simulations toward the Outer Disk. *Astrophys. J.* **798**, 84.

Bai, X.-N. 2017 Global Simulations of the Inner Regions of Protoplanetary Disks with Comprehensive Disk Microphysics. *Astrophys. J.* **845**, 75.

Bai, X.-N. & Stone, J. M. 2011 Effect of Ambipolar Diffusion on the Nonlinear Evolution of Magnetorotational Instability in Weakly Ionized Disks. *Astrophys. J.* **736**, 144.

Bai, X.-N. & Stone, J. M. 2013 Wind-driven Accretion in Protoplanetary Disks. I. Suppression of the Magnetorotational Instability and Launching of the Magnetocentrifugal Wind. *Astrophys. J.* **769**, 76.

Bai, X.-N. & Stone, J. M. 2017 Hall Effect-Mediated Magnetic Flux Transport in Protoplanetary Disks. *Astrophys. J.* **836**, 46.

Baker, P. L. 1979 On the magnetic field in interstellar molecular clouds. *Astron. Astrophys.* **75**, 54–60.

Balbus, Steven A. 1988 On Thermal Instability and Hydrostatic Equilibrium in Cooling Flows. *Astrophys. J.* **328**, 395.

Balbus, S. A. 2000 Stability, Instability, and "Backward" Transport in Stratified Fluids. *Astrophys. J.* **534**, 420–427.

Balbus, S. A. 2001 Convective and Rotational Stability of a Dilute Plasma. *Astrophys. J.* **562**, 909–917.

Balbus, Steven A. 2004 Viscous Shear Instability in Weakly Magnetized, Dilute Plasmas. *Astrophys. J.* **616** (2), 857–864.

Balbus, Steven A. & Soker, Noam 1989 Theory of Local Thermal Instability in Spherical Systems. *Astrophys. J.* **341**, 611.

Balbus, S. A. & Terquem, C. 2001 Linear Analysis of the Hall Effect in Protostellar Disks. *Astrophys. J.* **552**, 235–247.

Balescu, R. 1960 Irreversible Processes in Ionized Gases. *Physics of Fluids* **3**, 52–63.

Basu, S. & Ciolek, G. E. 2004 Formation and Collapse of Nonaxisymmetric Protostellar Cores in Planar Magnetic Molecular Clouds. *Astrophys. J. Lett.* **607**, L39–L42.

Basu, S., Ciolek, G. E., Dapp, W. B. & Wurster, J. 2009*a* Magnetically-regulated fragmentation induced by nonlinear flows and ambipolar diffusion. *New Astronomy* **14**, 483–495.

Basu, S., Ciolek, G. E. & Wurster, J. 2009*b* Nonlinear evolution of gravitational fragmentation regulated by magnetic fields and ambipolar diffusion. *New Astronomy* **14**, 221–237.

Basu, S. & Mouschovias, T. C. 1994 Magnetic braking, ambipolar diffusion, and the formation of cloud cores and protostars. 1: Axisymmetric solutions. *Astrophys. J.* **432**, 720–741.

Basu, S. & Mouschovias, T. C. 1995*a* Magnetic Braking, Ambipolar Diffusion, and the Formation of Cloud Cores and Protostars. II. A Parameter Study. *Astrophys. J.* **452**, 386.

Basu, S. & Mouschovias, T. C. 1995*b* Magnetic Braking, Ambipolar Diffusion, and the Formation of Cloud Cores and Protostars. III. Effect of the Initial Mass-to-Flux Ratio. *Astrophys. J.* **453**, 271.

Beresnyak, A. 2011 Spectral Slope and Kolmogorov Constant of MHD Turbulence. *Physical Review Letters* **106** (7), 075001.

Béthune, W., Lesur, G. & Ferreira, J. 2016 Self-organisation in protoplanetary discs. Global, non-stratified Hall-MHD simulations. *Astron. Astrophys.* **589**, A87.

Béthune, W., Lesur, G. & Ferreira, J. 2017 Global simulations of protoplanetary disks with net magnetic flux. I. Non-ideal MHD case. *Astron. Astrophys.* **600**, A75.

Bhattacharjee, A., Huang, Y.-M., Yang, H. & Rogers, B. 2009 Fast reconnection in high-Lundquist-number plasmas due to the plasmoid Instability. *Phys. Plasmas* **16** (11), 112102.

Bhattacharjee, A., Ng, C. S. & Spangler, S. R. 1998 Weakly Compressible Magnetohydrodynamic Turbulence in the Solar Wind and the Interstellar Medium. *Astrophys. J.* **494**, 409–418.

Biskamp, D. 1986 Magnetic reconnection via current sheets. *Physics of Fluids* **29**, 1520–1531.

Biskamp, D. & Schwarz, E. 2001 Localization, the clue to fast magnetic reconnection. *Physics of Plasmas* **8**, 4729–4731.

Blaes, O. M. & Balbus, S. A. 1994 Local shear instabilities in weakly ionized, weakly magnetized disks. *Astrophys. J.* **421**, 163–177.

Boldyrev, S. 2005 On the spectrum of magnetohydrodynamic turbulence. *Astrophys. J.* **626**, L37.

Boldyrev, Stanislav 2006 Spectrum of magnetohydrodynamic turbulence. *Phys. Rev. Lett.* **96**, 115002.

Braginskii, S. I. 1958 Transport Phenomena in a Completely Ionized Two-Temperature Plasma. *Soviet Journal of Experimental and Theoretical Physics* **6**, 358.

Braginskii, S. I. 1965 Transport Processes in a Plasma. *Rev. Plasma Phys.* **1**, 205.

Caselli, P., Benson, P. J., Myers, P. C. & Tafalla, M. 2002 Dense Cores in Dark Clouds. XIV. N_2H^+ (1-0) Maps of Dense Cloud Cores. *Astrophys. J.* **572**, 238–263.

Catto, P. J. & Simakov, A. N. 2004 A drift ordered short mean free path description for magnetized plasma allowing strong spatial anisotropy. *Physics of Plasmas* **11**, 90–102.

Chandran, B. D. G., Schekochihin, A. A. & Mallet, A. 2015 Intermittency and Alignment in Strong RMHD Turbulence. *Astrophys. J.* **807**, 39.

Childress, S. & Gilbert, A. D. 1995 *Stretch, Twist, Fold: The Fast Dynamo*. Springer-Verlag.

Cho, J. & Vishniac, E. T. 2000 The Anisotropy of Magnetohydrodynamic Alfvénic Turbulence. *Astrophys. J.* **539**, 273–282.

Ciolek, G. E. & Königl, A. 1998 Dynamical Collapse of Nonrotating Magnetic Molecular Cloud Cores: Evolution through Point-Mass Formation. *Astrophys. J.* **504**, 257–279.

Ciolek, G. E. & Mouschovias, T. C. 1993 Ambipolar Diffusion, Interstellar Dust, and the Formation of Cloud Cores and Protostars. I. Basic Physics and Formulation of the Problem. *Astrophys. J.* **418**, 774.

Ciolek, G. E. & Mouschovias, T. C. 1994 Ambipolar diffusion, interstellar dust, and the formation of cloud cores and protostars. 3: Typical axisymmetric solutions. *Astrophys. J.* **425**, 142–160.

Ciolek, G. E. & Mouschovias, T. C. 1995 Ambipolar Diffusion, Interstellar Dust, and the Formation of Cloud Cores and Protostars. IV. Effect of Ultraviolet Ionization and Magnetically Controlled Infall Rate. *Astrophys. J.* **454**, 194.

Cowling, T. G. 1933 The magnetic field of sunspots. *Mon. Not. R. Astron. Soc.* **94**, 39–48.

Dapp, W. B. & Basu, S. 2010 Averting the magnetic braking catastrophe on small scales: disk formation due to Ohmic dissipation. *Astron. Astrophys.* **521**, L56.

Dapp, W. B., Basu, S. & Kunz, M. W. 2012 Bridging the gap: disk formation in the Class 0 phase with ambipolar diffusion and Ohmic dissipation. *Astron. Astrophys.* **541**, A35.

Daughton, W., Roytershteyn, V., Albright, B. J., Karimabadi, H., Yin, L. &

Bowers, K. J. 2009 Transition from collisional to kinetic regimes in large-scale reconnection layers. *Physical Review Letters* **103** (6), 065004.

De Hoffmann, F. & Teller, E. 1950 Magneto-hydrodynamic shocks. *Phys. Rev.* **80**, 692–703.

Desch, S. J. 2004 Linear Analysis of the Magnetorotational Instability, Including Ambipolar Diffusion, with Application to Protoplanetary Disks. *Astrophys. J.* **608**, 509–525.

Desch, S. J. & Mouschovias, T. C. 2001 The Magnetic Decoupling Stage of Star Formation. *Astrophys. J.* **550**, 314–333.

Draine, B. T., Roberge, W. G. & Dalgarno, A. 1983 Magnetohydrodynamic shock waves in molecular clouds. *Astrophys. J.* **264**, 485–507.

Elmegreen, B. G. 1979 Magnetic diffusion and ionization fractions in dense molecular clouds - The role of charged grains. *Astrophys. J.* **232**, 729–739.

Erkaev, N. V., Semenov, V. S., Alexeev, I. V. & Biernat, H. K. 2001 Rate of steady-state reconnection in an incompressible plasma. *Physics of Plasmas* **8**, 4800–4809.

Erkaev, N. V., Semenov, V. S. & Jamitzky, F. 2000 Reconnection Rate for the Inhomogeneous Resistivity Petschek Model. *Physical Review Letters* **84**, 1455–1458.

Escande, D. F. & Ottaviani, M. 2004 Simple and rigorous solution for the nonlinear tearing mode. *Physics Letters A* **323**, 278–284.

Fiedler, R. A. & Mouschovias, T. C. 1993 Ambipolar Diffusion and Star Formation: Formation and Contraction of Axisymmetric Cloud Cores. II. Results. *Astrophys. J.* **415**, 680.

Fromang, S., Terquem, C. & Balbus, S. A. 2002 The ionization fraction in α models of protoplanetary discs. *Mon. Not. R. Astron. Soc.* **329**, 18–28.

Furth, H. P., Killeen, J. & Rosenbluth, M. N. 1963 Finite-Resistivity Instabilities of a Sheet Pinch. *Physics of Fluids* **6**, 459–484.

Furutsu, K. 1963 On the statistical theory of electromagnetic waves in a fluctuating medium (I). *J. Res. NBS* **67D**, 303.

Gammie, C. F. 1996 Layered Accretion in T Tauri Disks. *Astrophys. J.* **457**, 355.

Gilbert, A. D. 2003 Dynamo theory. In *Handbook of mathematical fluid dynamics, Volume 2* (ed. S. Friedlander & D. Serre), pp. 355–441. Elsevier Science BV.

Goldreich, P. & Sridhar, S. 1995 Toward a theory of interstellar turbulence. 2: Strong alfvenic turbulence. *Astrophys. J.* **438**, 763–775.

Goodman, A. A., Barranco, J. A., Wilner, D. J. & Heyer, M. H. 1998 Coherence in Dense Cores. II. The Transition to Coherence. *Astrophys. J.* **504**, 223–246.

Gressel, O., Turner, N. J., Nelson, R. P. & McNally, C. P. 2015 Global Simulations of Protoplanetary Disks With Ohmic Resistivity and Ambipolar Diffusion. *Astrophys. J.* **801**, 84.

Harris, E. G. 1962 On a plasma sheath separating regions of oppositely directed magnetic field. *Il Nuovo Cimento* **23**, 115–121.

Hawley, J. F. & Stone, J. M. 1998 Nonlinear Evolution of the Magnetorotational Instability in Ion-Neutral Disks. *Astrophys. J.* **501**, 758–771.

Hayashi, C. 1981 Structure of the Solar Nebula, Growth and Decay of Magnetic Fields and Effects of Magnetic and Turbulent Viscosities on the Nebula. *Progress of Theoretical Physics Supplement* **70**, 35–53.

Helander, P. & Sigmar, D. J. 2005 *Collisional Transport in Magnetized Plasmas*. Cambridge: Cambridge University Press.

Hinton, F. L. 1983 Collisional Transport in Plasma. In *Basic Plasma Physics: Selected Chapters, Handbook of Plasma Physics, Volume 1* (ed. A. A. Galeev & R. N. Sudan), p. 147.

Horbury, T. S., Forman, M. & Oughton, S. 2008 Anisotropic Scaling of Magnetohydrodynamic Turbulence. *Physical Review Letters* **101** (17), 175005.

Huang, Y.-M. & Bhattacharjee, A. 2010 Scaling laws of resistive magnetohydrodynamic reconnection in the high-Lundquist-number, plasmoid-unstable regime. *Physics of Plasmas* **17** (6), 062104–062104.

Ichimaru, S. 2004 *Statistical Plasma Physics: Volume I*. Boulder, CO: Westview Press.

Iroshnikov, P. S. 1963 Turbulence of a Conducting Fluid in a Strong Magnetic Field. *Astronomicheskii Zhurnal* **40**, 742.

Ji, H., Yamada, M., Hsu, S. & Kulsrud, R. 1998 Experimental Test of the Sweet-Parker Model of Magnetic Reconnection. *Physical Review Letters* **80**, 3256–3259.

Kadomtsev, B. B. & Pogutse, O. P. 1974 Nonlinear helical perturbations of a plasma in the tokamak. *Soviet Journal of Experimental and Theoretical Physics* **38**, 283–290.

Kolmogorov, A. 1941 The Local Structure of Turbulence in Incompressible Viscous Fluid for Very Large Reynolds' Numbers. *Akademiia Nauk SSSR Doklady* **30**, 301–305.

Kraichnan, R. H. 1965 Inertial-Range Spectrum of Hydromagnetic Turbulence. *Physics of Fluids* **8**, 1385–1387.

Krall, N. A. & Trivelpiece, A. W. 1973 *Principles of plasma physics*. New York: McGraw-Hill.

Krause, F. & Raedler, K.-H. 1980 *Mean-field magnetohydrodynamics and dynamo theory*. Pergamon.

Kruskal, M. 1962 Asymptotic Theory of Hamiltonian and other Systems with all Solutions Nearly Periodic. *Journal of Mathematical Physics* **3**, 806–828.

Kruskal, M. D. 1958 The Gyration of a Charged Particle. *Project Matterhorn Publications and Reports* .

Kulsrud, R. & Pearce, W. P. 1969 The Effect of Wave-Particle Interactions on the Propagation of Cosmic Rays. *Astrophys. J.* **156**, 445.

Kulsrud, R. M. 1983 MHD description of plasma. In *Basic Plasma Physics: Selected Chapters, Handbook of Plasma Physics, Volume 1* (ed. A. A. Galeev & R. N. Sudan), p. 1.

Kulsrud, R. M. 2001 Magnetic reconnection: Sweet-Parker versus Petschek. *Earth, Planets, and Space* **53**, 417–422.

Kulsrud, R. M. 2005 *Plasma physics for astrophysics*. Princeton University Press.

Kulsrud, Russell M. & Anderson, Stephen W. 1992 The Spectrum of Random Magnetic Fields in the Mean Field Dynamo Theory of the Galactic Magnetic Field. *Astrophys. J.* **396**, 606.

Kunz, M. W. 2008 On the linear stability of weakly ionized, magnetized planar shear flows. *Mon. Not. R. Astron. Soc.* **385**, 1494–1510.

Kunz, M. W. 2011 Dynamical stability of a thermally stratified intracluster medium with anisotropic momentum and heat transport. *Mon. Not. R. Astron. Soc.* **417**, 602–616.

Kunz, M. W. & Balbus, S. A. 2004 Ambipolar diffusion in the magnetorotational instability. *Mon. Not. R. Astron. Soc.* **348**, 355–360.

Kunz, M. W. & Lesur, G. 2013 Magnetic self-organization in Hall-dominated magnetorotational turbulence. *Mon. Not. R. Astron. Soc.* **434**, 2295–2312.

Kunz, M. W. & Mouschovias, T. C. 2009 The Nonisothermal Stage of Magnetic Star Formation. I. Formulation of the Problem and Method of Solution. *Astrophys. J.* **693**, 1895–1911.

Kunz, M. W. & Mouschovias, T. C. 2010 The non-isothermal stage of magnetic star formation - II. Results. *Mon. Not. R. Astron. Soc.* **408**, 322–341.

Landau, L. 1937 Transport equation in the case of Coulomb interaction. *Zh. Eksper. i Teoret. Fiz.* **7**, 203.

Lenard, A. 1960 On Bogoliubov's kinetic equation for a spatially homogeneous plasma. *Annals of Physics* **10**, 390–400.

Lesur, G., Kunz, M. W. & Fromang, S. 2014 Thanatology in protoplanetary discs. The combined influence of Ohmic, Hall, and ambipolar diffusion on dead zones. *Astron. Astrophys.* **566**, A56.

Li, Z.-Y., Krasnopolsky, R. & Shang, H. 2011 Non-ideal MHD Effects and Magnetic Braking Catastrophe in Protostellar Disk Formation. *Astrophys. J.* **738**, 180.

Li, Z.-Y. & Nakamura, F. 2004 Magnetically Regulated Star Formation in Turbulent Clouds. *Astrophys. J. Lett.* **609**, L83–L86.

Loureiro, N. F., Cowley, S. C., Dorland, W. D., Haines, M. G. & Schekochihin, A. A. 2005 X-Point Collapse and Saturation in the Nonlinear Tearing Mode Reconnection. *Phys. Rev. Lett.* **95** (23), 235003.

Loureiro, N. F., Samtaney, R., Schekochihin, A. A. & Uzdensky, D. A. 2012 Magnetic reconnection and stochastic plasmoid chains in high-Lundquist-number plasmas. *Physics of Plasmas* **19** (4), 042303–042303.

Loureiro, N. F., Schekochihin, A. A. & Cowley, S. C. 2007 Instability of current sheets and formation of plasmoid chains. *Phys. Plasmas* **14** (10), 100703–100703.

Loureiro, N. F., Schekochihin, A. A. & Uzdensky, D. A. 2013 Plasmoid and Kelvin-Helmholtz instabilities in Sweet-Parker current sheets. *Phys. Rev. E* **87** (1), 013102.

Loureiro, N. F. & Uzdensky, D. A. 2016 Magnetic reconnection: from the Sweet-Parker model to stochastic plasmoid chains. *Plasma Phys. Controlled Fusion* **58** (1), 014021.

Lundquist, S. 1951 On the stability of magneto-hydrostatic fields. *Phys. Rev.* **83**, 307.

Machida, M. N., Inutsuka, S.-i. & Matsumoto, T. 2014 Conditions for circumstellar disc formation: effects of initial cloud configuration and sink treatment. *Mon. Not. R. Astron. Soc.* **438**, 2278–2306.

Machida, M. N. & Matsumoto, T. 2012 Impact of protostellar outflow on star formation: effects of the initial cloud mass. *Mon. Not. R. Astron. Soc.* **421**, 588–607.

Mallet, A. & Schekochihin, A. A. 2017 A statistical model of three-dimensional anisotropy and intermittency in strong Alfvénic turbulence. *Mon. Not. R. Astron. Soc.* **466**, 3918–3927.

Mallet, A., Schekochihin, A. A. & Chandran, B. D. G. 2015 Refined critical balance in strong Alfvénic turbulence. *Mon. Not. R. Astron. Soc.* **449**, L77.

Malyshkin, L. M., Linde, T. & Kulsrud, R. M. 2005 Magnetic reconnection with anomalous resistivity in two-and-a-half dimensions. I. Quasistationary case. *Physics of Plasmas* **12** (10), 102902–102902.

Maron, J. & Goldreich, P. 2001 Simulations of Incompressible Magnetohydrodynamic Turbulence. *Astrophys. J.* **554**, 1175–1196.

Mason, J., Cattaneo, F. & Boldyrev, S. 2006 Dynamic Alignment in Driven Magnetohydrodynamic Turbulence. *Physical Review Letters* **97** (25), 255002.

Mason, J., Cattaneo, F. & Boldyrev, S. 2008 Numerical measurements of the spectrum in magnetohydrodynamic turbulence. *Phys. Rev. E* **77** (3), 036403.

Mason, J., Perez, J. C., Boldyrev, S. & Cattaneo, F. 2012 Numerical simulations of strong incompressible magnetohydrodynamic turbulence. *Physics of Plasmas* **19** (5), 055902–055902.

Mason, J., Perez, J. C., Cattaneo, F. & Boldyrev, S. 2011 Extended Scaling Laws in Numerical Simulations of Magnetohydrodynamic Turbulence. *Astrophys. J. Lett.* **735**, L26.

Matthaeus, W. H., Pouquet, A., Mininni, P. D., Dmitruk, P. & Breech, B. 2008 Rapid Alignment of Velocity and Magnetic Field in Magnetohydrodynamic Turbulence. *Physical Review Letters* **100** (8), 085003.

Mellon, R. R. & Li, Z.-Y. 2009 Magnetic Braking and Protostellar Disk Formation: Ambipolar Diffusion. *Astrophys. J.* **698**, 922–927.

Mestel, L. 1965 Problems of Star Formation - II. *Quarterly J. R. Astron. Soc.* **6**, 265.

Mestel, L. & Spitzer, Jr., L. 1956 Star formation in magnetic dust clouds. *Mon. Not. R. Astron. Soc.* **116**, 503.

Mikhailovskii, A. B. & Tsypin, V. S. 1971 Transport equations and gradient instabilities in a high pressure collisional plasma. *Plasma Physics* **13**, 785–798.

Mikhailovskii, A. B. & Tsypin, V. S. 1984 Transport equations of plasma in curvilinear magnetic field. *Beiträge aus der Plasmaphysik* **24**, 335–354.

Militello, F. & Porcelli, F. 2004 Simple analysis of the nonlinear saturation of the tearing mode. *Physics of Plasmas* **11**, L13–L16.

Moffatt, H. K. 1978 *Magnetic field generation in electrically conducting fluids*. Cambridge University Press.

Montgomery, D. & Turner, L. 1981 Anisotropic magnetohydrodynamic turbulence in a strong external magnetic field. *Phys. Fluids* **24**, 825.

Mouschovias, T. C. 1976*a* Nonhomologous contraction and equilibria of self-gravitating, magnetic interstellar clouds embedded in an intercloud medium: Star formation. I Formulation of the problem and method of solution. *Astrophys. J.* **206**, 753–767.

Mouschovias, T. C. 1976*b* Nonhomologous contraction and equilibria of self-gravitating, magnetic interstellar clouds embedded in an intercloud medium: Star formation. II - Results. *Astrophys. J.* **207**, 141–158.

Mouschovias, T. C. 1978 Formation of stars and planetary systems in magnetic interstellar

clouds. In *IAU Colloq. 52: Protostars and Planets* (ed. T. Gehrels & M. S. Matthews), pp. 209–242.

Mouschovias, T. C. 1979 Ambipolar diffusion in interstellar clouds - A new solution. *Astrophys. J.* **228**, 475–481.

Mouschovias, T. C. 1991 Magnetic braking, ambipolar diffusion, cloud cores, and star formation - Natural length scales and protostellar masses. *Astrophys. J.* **373**, 169–186.

Mouschovias, T. C. & Ciolek, G. E. 1999 Magnetic Fields and Star Formation: A Theory Reaching Adulthood. In *NATO Advanced Science Institutes (ASI) Series C* (ed. C. J. Lada & N. D. Kylafis), *NATO Advanced Science Institutes (ASI) Series C*, vol. 540, p. 305.

Mouschovias, T. C. & Paleologou, E. V. 1981 Ambipolar diffusion in interstellar clouds - Time-dependent solutions in one spatial dimension. *Astrophys. J.* **246**, 48–64.

Mouschovias, T. C. & Spitzer, Jr., L. 1976 Note on the collapse of magnetic interstellar clouds. *Astrophys. J.* **210**, 326.

Nakamura, F. & Li, Z.-Y. 2005 Quiescent Cores and the Efficiency of Turbulence-accelerated, Magnetically Regulated Star Formation. *Astrophys. J.* **631**, 411–428.

Nakano, T. 1979 Quasistatic Contraction of Magnetic Protostars due to Magnetic Flux Leakage - Part One - Formulation and an Example. *Pub. Astron. Soc. Japan* **31**, 697.

Nakano, T. & Nakamura, T. 1978 Gravitational Instability of Magnetized Gaseous Disks 6. *Pub. Astron. Soc. Japan* **30**, 671–680.

Nakano, T. & Umebayashi, T. 1980 Behavior of Grains in the Drift of Plasma and Magnetic Field in Dense Interstellar Clouds. *Pub. Astron. Soc. Japan* **32**, 613.

Nazarenko, S. V. & Schekochihin, A. A. 2011 Critical balance in magnetohydrodynamic, rotating and stratified turbulence: towards a universal scaling conjecture. *J. Fluid Mech.* **677**, 134.

Ni, L., Germaschewski, K., Huang, Y.-M., Sullivan, B. P., Yang, H. & Bhattacharjee, A. 2010 Linear plasmoid instability of thin current sheets with shear flow. *Physics of Plasmas* **17** (5), 052109.

Nicholson, D. 1983 *Introduction to plasma theory*. New York: John Wiley & Sons, Inc.

Northrop, T. G. 1963*a* Adiabatic Charged-Particle Motion. *Reviews of Geophysics and Space Physics* **1**, 283–304.

Northrop, T. G. 1963*b* *The adiabatic motion of charged particles*. New York: Interscience Publishers.

Novikov, E. A. 1965 Functionals and the random-force method in turbulence theory. *J. Exp. Theor. Phys.* **20**, 1290.

Obukhov, A. M. 1941 On the distribution of energy in the spectrum of turbulent flow. *Akademiia Nauk SSSR Doklady* **32**, 19.

Oughton, S., Dmitruk, P. & Matthaeus, W. H. 2003 Coronal Heating and Reduced MHD. In *Turbulence and Magnetic Fields in Astrophysics* (ed. E. Falgarone & T. Passot), *Lecture Notes in Physics, Berlin Springer Verlag*, vol. 614, pp. 28–55.

Park, W., Monticello, D. A. & White, R. B. 1984 Reconnection rates of magnetic fields including the effects of viscosity. *Physics of Fluids* **27**, 137–149.

Parker, E. N. 1955 Hydromagnetic Dynamo Models. *Astrophys. J.* **122**, 293.

Parker, E. N. 1957 Sweet's Mechanism for Merging Magnetic Fields in Conducting Fluids. *J. Geophys. Res.* **62**, 509–520.

Parker, E. N. 1979 *Cosmical magnetic fields: Their origin and their activity*. Oxford University Press.

Perez, J. C. & Chandran, B. D. G. 2013 Direct Numerical Simulations of Reflection-driven, Reduced Magnetohydrodynamic Turbulence from the Sun to the Alfvén Critical Point. *Astrophys. J.* **776**, 124.

Perez, J. C., Mason, J., Boldyrev, S. & Cattaneo, F. 2012 On the Energy Spectrum of Strong Magnetohydrodynamic Turbulence. *Physical Review X* **2** (4), 041005.

Perez, J. C., Mason, J., Boldyrev, S. & Cattaneo, F. 2014 Scaling Properties of Small-scale Fluctuations in Magnetohydrodynamic Turbulence. *Astrophys. J. Lett.* **793**, L13.

Petschek, H. E. 1964 Magnetic Field Annihilation. *NASA Special Publication* **50**, 425.

Pneuman, G. W. & Mitchell, T. P. 1965 Evolution of the Solar Magnetic Field. *Icarus* **4**, 494–505.

Pucci, F. & Velli, M. 2014 Reconnection of Quasi-singular Current Sheets: The "Ideal" Tearing Mode. *Astrophys. J. Lett.* **780**, L19.

Rayleigh, J. W. S. 1880 On the stability, or instability, of certain fluid motions. *Proc. London Math. Soc.* **11**, 57.

Rincon, François 2019 Dynamo theories. *Journal of Plasma Physics* **85** (4), 205850401.

Rutherford, P. H. 1973 Nonlinear growth of the tearing mode. *Phys. Fluids* **16**, 1903–1908.

Salmeron, R. & Wardle, M. 2003 Magnetorotational instability in stratified, weakly ionized accretion discs. *Mon. Not. R. Astron. Soc.* **345**, 992–1008.

Salmeron, R. & Wardle, M. 2005 Magnetorotational instability in protoplanetary discs. *Mon. Not. R. Astron. Soc.* **361**, 45–69.

Salmeron, R. & Wardle, M. 2008 Magnetorotational instability in protoplanetary discs: the effect of dust grains. *Mon. Not. R. Astron. Soc.* **388**, 1223–1238.

Samtaney, R., Loureiro, N. F., Uzdensky, D. A., Schekochihin, A. A. & Cowley, S. C. 2009 Formation of Plasmoid Chains in Magnetic Reconnection. *Physical Review Letters* **103** (10), 105004.

Sano, T. & Stone, J. M. 2002*a* The Effect of the Hall Term on the Nonlinear Evolution of the Magnetorotational Instability. I. Local Axisymmetric Simulations. *Astrophys. J.* **570**, 314–328.

Sano, T. & Stone, J. M. 2002*b* The Effect of the Hall Term on the Nonlinear Evolution of the Magnetorotational Instability. II. Saturation Level and Critical Magnetic Reynolds Number. *Astrophys. J.* **577**, 534–553.

Sato, T. & Hayashi, T. 1979 Externally driven magnetic reconnection and a powerful magnetic energy converter. *Physics of Fluids* **22**, 1189–1202.

Scalo, J. M. 1977 Heating of dense interstellar clouds by magnetic ion slip - A constraint on cloud field strengths. *Astrophys. J.* **213**, 705–711.

Schekochihin, Alexander A. 2022 MHD turbulence: a biased review. *J. Plasma Phys.* **88** (5), 155880501.

Schekochihin, Alexander A., Boldyrev, Stanislav A. & Kulsrud, Russell M. 2002 Spectra and Growth Rates of Fluctuating Magnetic Fields in the Kinematic Dynamo Theory with Large Magnetic Prandtl Numbers. *Astrophys. J.* **567** (2), 828–852.

Schekochihin, A. A. & Cowley, S. C. 2007 Turbulence and Magnetic Fields in Astrophysical Plasmas. In *Magnetohydrodynamics: Historical Evolution and Trends* (ed. S. Molokov, R. Moreau & H. K. Moffatt), p. 85. Springer.

Scholer, M. 1989 Undriven magnetic reconnection in an isolated current sheet. *J. Geophys. Res.* **94**, 8805–8812.

Shebalin, J. V., Matthaeus, W. H. & Montgomery, D. 1983 Anisotropy in MHD turbulence due to a mean magnetic field. *J. Plasma Phys.* **29**, 525–547.

Shu, F. H. 1983 Ambipolar diffusion in self-gravitating isothermal layers. *Astrophys. J.* **273**, 202–213.

Shu, F. H., Adams, F. C. & Lizano, S. 1987 Star formation in molecular clouds - Observation and theory. *Ann. Rev. Astron. Astrophys.* **25**, 23–81.

Simon, J. B., Bai, X.-N., Armitage, P. J., Stone, J. M. & Beckwith, K. 2013*a* Turbulence in the Outer Regions of Protoplanetary Disks. II. Strong Accretion Driven by a Vertical Magnetic Field. *Astrophys. J.* **775**, 73.

Simon, J. B., Bai, X.-N., Stone, J. M., Armitage, P. J. & Beckwith, K. 2013*b* Turbulence in the Outer Regions of Protoplanetary Disks. I. Weak Accretion with No Vertical Magnetic Flux. *Astrophys. J.* **764**, 66.

Simon, J. B., Lesur, G., Kunz, M. W. & Armitage, P. J. 2015 Magnetically driven accretion in protoplanetary discs. *Mon. Not. R. Astron. Soc.* **454**, 1117–1131.

Spitzer, L. 1968 *Diffuse matter in space*. Interscience Publication.

Spitzer, L. 1978 *Physical processes in the interstellar medium*. Wiley-Interscience.

Stenzel, R. L. 1999 Whistler waves in space and laboratory plasmas. *J. Geophys. Res.* **104**, 14379–14396.

Strauss, H. R. 1976 Nonlinear, three-dimensional magnetohydrodynamics of noncircular tokamaks. *Phys. Fluids* **19**, 134–140.

Strauss, H. R. 1977 Dynamics of high beta Tokamaks. *Phys. Fluids* **20**, 1354–1360.

Sweet, P. A. 1958 The Neutral Point Theory of Solar Flares. In *Electromagnetic Phenomena in Cosmical Physics* (ed. B. Lehnert), *IAU Symposium*, vol. 6, p. 123.

Tafalla, M., Myers, P. C., Caselli, P. & Walmsley, C. M. 2004 On the internal structure of starless cores. I. Physical conditions and the distribution of CO, CS, N_2H^+, and NH_3 in L1498 and L1517B. *Astron. Astrophys.* **416**, 191–212.

Tajima, T. & Shibata, K., ed. 1997 *Plasma astrophysics*.

Tassis, K. & Mouschovias, T. C. 2005*a* Magnetically Controlled Spasmodic Accretion during Star Formation. I. Formulation of the Problem and Method of Solution. *Astrophys. J.* **618**, 769–782.

Tassis, K. & Mouschovias, T. C. 2005*b* Magnetically Controlled Spasmodic Accretion during Star Formation. II. Results. *Astrophys. J.* **618**, 783–794.

Tassis, K. & Mouschovias, T. C. 2007*a* Protostar Formation in Magnetic Molecular Clouds beyond Ion Detachment. I. Formulation of the Problem and Method of Solution. *Astrophys. J.* **660**, 370–387.

Tassis, K. & Mouschovias, T. C. 2007*b* Protostar Formation in Magnetic Molecular Clouds beyond Ion Detachment. II. Typical Axisymmetric Solution. *Astrophys. J.* **660**, 388–401.

Tassis, K. & Mouschovias, T. C. 2007*c* Protostar Formation in Magnetic Molecular Clouds beyond Ion Detachment. III. A Parameter Study. *Astrophys. J.* **660**, 402–417.

Tomida, K., Okuzumi, S. & Machida, M. N. 2015 Radiation Magnetohydrodynamic Simulations of Protostellar Collapse: Nonideal Magnetohydrodynamic Effects and Early Formation of Circumstellar Disks. *Astrophys. J.* **801**, 117.

Tomida, K., Tomisaka, K., Matsumoto, T., Hori, Y., Okuzumi, S., Machida, M. N. & Saigo, K. 2013 Radiation Magnetohydrodynamic Simulations of Protostellar Collapse: Protostellar Core Formation. *Astrophys. J.* **763**, 6.

Ugai, M. 1995 Computer studies on powerful magnetic energy conversion by the spontaneous fast reconnection mechanism. *Physics of Plasmas* **2**, 388–397.

Umebayashi, T. & Nakano, T. 1990 Magnetic flux loss from interstellar clouds. *Mon. Not. R. Astron. Soc.* **243**, 103–113.

Uzdensky, D. A. & Kulsrud, R. M. 2000 Two-dimensional numerical simulation of the resistive reconnection layer. *Physics of Plasmas* **7**, 4018–4030.

Uzdensky, D. A. & Loureiro, N. F. 2016 Magnetic Reconnection Onset via Disruption of a Forming Current Sheet by the Tearing Instability. *Phys. Rev. Lett.* **116** (10), 105003.

van Rensbergen, W., Hensberge, H. & Adelman, S. J. 1984 General study of the apparently average magnetic AP star Theta Aurigae. II - Model. *Astron. Astrophys.* **136**, 31–36.

Waelbroeck, F. L. 1993 Onset of the sawtooth crash. *Phys. Rev. Lett.* **70**, 3259–3262.

Wardle, M. 1999 The Balbus-Hawley instability in weakly ionized discs. *Mon. Not. R. Astron. Soc.* **307**, 849–856.

Wardle, M. 2007 Magnetic fields in protoplanetary disks. *Astrophys. Space Sci.* **311**, 35–45.

Wardle, M. & Salmeron, R. 2012 Hall diffusion and the magnetorotational instability in protoplanetary discs. *Mon. Not. R. Astron. Soc.* **422**, 2737–2755.

Wicks, R. T., Horbury, T. S., Chen, C. H. K. & Schekochihin, A. A. 2010 Power and spectral index anisotropy of the entire inertial range of turbulence in the fast solar wind. *Mon. Not. R. Astron. Soc.* **407**, L31–L35.

Winarto, Himawan W. & Kunz, Matthew W. 2022 Triggering tearing in a forming current sheet with the mirror instability. *J. Plasma Phys.* **88** (2), 905880210.

Yamada, M., Kulsrud, R. & Ji, H. 2010 Magnetic reconnection. *Rev. Mod. Phys.* **82**, 603–664.

Zank, G. P. & Matthaeus, W. H. 1992*a* The equations of reduced magnetohydrodynamics. *J. Plasma Phys.* **48**, 85.

Zank, G. P. & Matthaeus, W. H. 1992*b* Waves and turbulence in the solar wind. *J. Geophys. Res.* **97**, 17189.

Zel'dovich, Ya. B. 1957 The Magnetic Field in the Two-Dimensional Motion of a Conducting Turbulent Liquid. *Soviet Journal of Experimental and Theoretical Physics* **4**, 460.

Zel'dovich, Y. B., Ruzmaikin, A. A., Molchanov, S. A. & Sokolov, D. D. 1984 Kinematic dynamo problem in a linear velocity field. *Journal of Fluid Mechanics* **144**, 1–11.

Zhao, B., Caselli, P., Li, Z.-Y. & Krasnopolsky, R. 2018 Decoupling of magnetic fields in collapsing protostellar envelopes and disc formation and fragmentation. *Mon. Not. R. Astron. Soc.* **473**, 4868–4889.

Zweibel, E. G. & Josafatsson, K. 1983 Hydromagnetic wave dissipation in molecular clouds. *Astrophys. J.* **270**, 511–518.

Zweibel, E. G. & Yamada, M. 2009 Magnetic Reconnection in Astrophysical and Laboratory Plasmas. *Ann. Rev. Astron. Astrophys.* **47**, 291–332.